Integrated Active Control Strategies and Licensing Approaches for Urban Wastewater Systems

Submitted by Biniam Biruk Ashagre to the University of Exeter

as a thesis for the degree of

Doctor of Engineering (EngD) in Water Engineering

In July 2018

I certify that all material in this thesis which is not my own work has been identified and that no material has previously been submitted and approved for the award of a degree by this or any other University.

Signature: ……..

Abstract

The wastewater sector in the UK and other EU member states are facing stringent regulatory standards. The environmental water quality standards such as the EU-WFD, on the one hand, require a higher level of wastewater treatment which can result in increased GHG emissions and operational cost through higher energy use, chemical consumption, and capital investment. On the other hand, the Carbon Reduction Commitment Energy Efficiency scheme requires the water industries to reduce their GHG emission significantly. The research assesses the advantage of integrated active control of existing WWTPs, their optimisation and dynamic licensing approach to tackle this challenge while maintaining the quality of the receiving river. The dynamic licensing approach focuses on the design of control strategies based on the receiving river's assimilative capacity.

A simulation approach is used to test control strategies and their optimisation, interventions, and dynamic licensing approaches. The study developed an integrated UWWS model that fully integrate WWTP, sewer network, and receiving river, which enables the assessment of the advantage of integrated control strategies and dynamic licensing approach. The hybrid modelling approach uses mechanistic, conceptual and data-driven models in order to reduce computational cost while maintaining the model accuracy.

Initially, the WWTP model was set up using average values of model parameters from the literature. However, this did not give a model with good accuracy. Hence, through, a careful design and identification of key parameters, a data campaign was designed to characterise influent wastewater, flow pattern, and biological processes of a real-world case study. The model accuracy was further improved using auto-calibration processes using a sensitivity analysis, identifying influential parameters to which the final effluent and oxidation ditch quality indicators are sensitive to. The sensitivity and auto-calibration were done using statistical measures that compare simulated and measured data points. Nash-Sutcliff coefficient (NSE) and root-mean-square-error (RMSE) measures show consistency in the sensitivity analysis, but correlation coefficient R^2 showed a slight difference as it focusses on pattern similarity than values closeness. The combined use of NSE and RMSE gave the best result in model accuracy using fewer generation in the multi-objective optimisation using NSGA-II.

Further local sensitivity analysis is used to identify the effect of varying control handles on GHG emissions (as equivalent CO_2 emission), operational cost and effluent quality. The GHG emissions both from direct and indirect sources are considered in this study. The indirect GHG emissions consider the major GHG emissions (CO_2, N_2O, and CH_4) associated with the use of electricity, sludge transport, and offsite degradation of sludge and final effluent. Similarly, the direct GHG emissions consider the emission of these major gases from different biological processes within the WWTP such as substrate utilisation, denitrification and biomass decay. This knowledge helps in the development of control strategies by indicating influential control handles and aids the selection of control strategies for optimisation purposes.

It is found that multi-objective optimisation can reduce GHG emissions, operational cost while operating under the effluent quality standards. Multi-objective optimisation of control loops coupled with integrated active control of oxygen using final effluent ammonia concentration showed the highest reduction in GHG emissions and reduction in operational cost without violating the current effluent quality standard. Through dynamic licensing approach, the oxygen level in the oxidation ditch is controlled based on the assimilative capacity of the receiving river, which reduces the operational cost and effluent quality index without increased GHG emissions. However, to benefit from the dynamic licensing approach, a trade-off needs to be considered further between final effluent NO_3 concentration and reduction in oxygen level in the oxidation ditch to reduce biomass decay which is responsible for higher GHG emission in this scenario.

Acknowledgement

I am grateful to the EPSRC and Scottish Water for their financial support through the STREAM-IDC programme.

The successful completion of this thesis is a testimony to the professional support, guidance, encouragement and patience from my supervisors Professor Guangtao Fu and Professor David Butler. Besides my supervisors, I appreciate Miranda Jacques-Turner and Kerry Davidson from Scottish Water (SW) for their support in making this study as real-world focused as possible. My sincere appreciation goes Syed Abbas partner project manager at SW, process scientists and operative teams at Cupar and Selkirk WWTP (although Selkirk is not included in this thesis) for sharing data and detailed responses. I am grateful to project partners from the University of Sheffield for their continuous effort and cooperation towards the development of an integrated urban wastewater model.

I am thankful to Professor Gustaf Olsson, Professor Peter Vanrolleghem, Dr Lorenzo Benedetti, and Dr Chris Sweetapple for their invaluable advice and support. I would also like to thank colleagues and friends at the Centre for Water Systems at the University of Exeter and those at the Safe & Sure project for the stimulating discussions, creating such a wonderful working environment and all the fun we had.

Most of all I would like to thank my family, without their great support, unlimited love and patience, it would have been impossible to reach the completion of this thesis. Thanks for coping with me in the ups and downs of this EngD journey. I am especially grateful to my wife Emma who encourages me in all my pursuits and helping me to have such resilience that I never thought I would have otherwise. The unlimited love and everyday smiles from Liya and Alazar was the fuel that helped me going throughout the entire EngD process and more.

I want to thank my mum for her big role in making me the person I am now. You are the most resilient and rational person I have ever known, and I am lucky to have you. All my family and friends who have been supporting me in the entire process, please accept my deepest thanks. I want to thank you for your advice, encouragement and listening. It would be an enormous list to mention, but you know who you are and thanks for being with me throughout my EngD journey.

Table of contents

List of Figures

List of Tables

List of Abbreviations

ADALINE	Adaptive Linear Neuron
AE	Aeration Energy
ANC	Acid Neutralising Capacity
ANN	Artificial Neural Network
AOB	Ammonia Oxidising Bacteria
ASM1	Activated Sludge Model no. 1
ASMN	Activated Sludge Model for Nitrogen
BSM2	Benchmark Simulation Model no. 2
BSM-e	Benchmark Simulation Model with emission
CAR	Controlled Activities Regulations
CC	Climate Change
CFD	Computational Fluid Dynamics
CHP	Combined Heat Power
CO_2	Carbon Dioxide
CO_{2e}	Carbon Dioxide equivalent
CPS	Control Pressure Set-point
CRC	Carbon Reduction Commitment
CSO	Combined Sewer Overflow
DDMs	Data-Driven Models
DEM	Digital Elevation Model
DOsat	Saturated Dissolved Oxygen [mg L^{-1}]
DSM	Demand Side Management
DWF	Dry Weather Flow [$m^3 d^{-1}$]
EPSRC	Engineering and Physical Sciences Research Council
EQI	Effluent Quality Index
EQS	Environmental Quality Standards
GA	Genetic Algorithm
GHG	Greenhouse Gas
GWP	Global Warming Potential
HH	Household
HRT	Hydraulic Retention Time [hr]
ICBMs	Integrated Component-based Models
IPCC	Intergovernmental Panel for Climate Change
IUDMs	Integrated Urban Drainage Models
IUWCMs	Integrated Urban Water Cycle Models
IUWSMs	Integrated Urban Water Systems Models
IWA	International Water Association
KTP	Knowledge Transfer Programme
LB	Lower Bound
LQG	Linear Quadratic-Gaussian
MLSS	Mixed Liquor Suspended Solid [mg L^{-1}]
MOCI	Modified Operational Cost
MPC	Model Predictive Control
N_2O	Nitrous Oxide

NARX	Non-linear Autoregressive with eXogenous input
NOB	Nitrate-Oxidising Bacteria
NSE	Nash-Sutcliffe Coefficient
NSGA	Non-dominated Sorting in Genetic Algorithms
OAT	One-At-a-Time
OC	Organic Carbon
OCI	Operational Cost
OD	Oxidation Ditch
OTE	Oxygen Transfer Efficiency
OTR	Oxygen Transfer Rate
PE	Population Equivalent
PESA	Pareto Envelope-based Selection Algorithm
PID	Proportional Integral Derivative
PLC	Programmable Logic Controller
RAS	Return Activated Sludge [m^3 d^{-1}]
RBMP	River Basin Management Plans
RICT	River Invertebrate Classification Tool
RMSE	Root-Mean-Square-Error
ROC	Renewables Obligation Certificate
RPM	Revolution Per Minute
SAS	Surplus Activated Sludge [m^3 d^{-1}]
SCADA	Supervisory Control And Data Acquisition
SEPA	Scottish Environment Protection Agency
SME	Small Medium size Enterprise
SRBDD	Scotland River Basin District Direction
SRT	Solid Retention Time
SUDs	Sustainable Urban Drainage Systems
SWAT	Soil and Water Assessment Tool
SWS	Scottish Water Scientific
TSP	Total Sludge Production
UB	Upper Bound
UKAS	United Kingdom Accreditation Service
UNFCC	United Nations Framework Convention on Climate Change
UWWS	Urban Wastewater System
UWWTD	Urban Wastewater Treatment Directive
WFD	Water Framework Directive
WFD-UKTAG	Water framework Directive United Kingdom Advisory Group
WHPT	Whalley, Hawkes, Paisley and Trigg
WIA	Water Industry Act
WICS	Water Industry Commission for Scotland
WWT	Wastewater Treatment
WWTP	Wastewater Treatment Plant

List of Wastewater Characterising and Model Parameters

BOD	Biochemical Oxygen Demand [mg L^{-1}]
CBOD	Carbonaceous Biochemical Oxygen Demand [mg L^{-1}]
COD	Chemical Oxygen Demand [mg L^{-1}]
COD_f	Filtered Chemical Oxygen Demand [mg L^{-1}]
COD_{ff}	Filtered and Flocculated Chemical Oxygen Demand [mg L^{-1}]
DO	Dissolved Oxygen [mg L^{-1}]
NBOD	Nitrogenous Biochemical Oxygen Demand [mg L^{-1}]
S_{ALK}	Alkalinity
SBCOD	Slowly Biodegradable Chemical Oxygen Demand [mg L^{-1}]
S_I	Soluble inert organic matter [mg L^{-1}]
S_{ND}	Soluble biodegradable organic nitrogen [mg L^{-1}]
S_{NH}	Ammonia-nitrogen [mg L^{-1}]
S_{NO}	Nitrate and nitrite nitrogen [mg L^{-1}]
S_s	Readily biodegradable substrate
TKN	Total Kjeldahl Nitrogen [mg L^{-1}]
TN	Total Nitrogen [mg L^{-1}]
TON	Total Oxidised Nitrogen [mg L^{-1}]
TSS	Total Suspended Solid [mg L^{-1}]
VSS	Volatile Suspended Solid [mg L^{-1}]
$X_{B,A}$	Active autotrophic biomass [mg L^{-1}]
$X_{B,H}$	Active heterotrophic biomass [mg L^{-1}]
X_I	Particulate inert organic matter [mg L^{-1}]
X_{ND}	Particulate biodegradable organic nitrogen [mg L^{-1}]
X_P	Particulate products arising from biomass decay [mg L^{-1}]
X_S	Slowly biodegradable substrate [mg L^{-1}]

1. Introduction

The wastewater sector is facing an inherent tension between the increased associated costs to improve effluent quality and operating in a regulatory framework that demands reductions in Greenhouse Gas (GHG) emissions. On the one hand, stringent environmental water quality standards require higher levels of wastewater treatment, which needs significant capital investment to upgrade existing operation systems or/and treatment processes. These changes can increase operational costs through higher energy use, chemical consumption, greenhouse gas emissions associated with high energy consumption and direct emissions. On the other hand, the Carbon Reduction Commitment Energy Efficiency scheme requires the water industry to reduce their GHG emissions significantly to meet the target of 80 % GHG emission reduction by 2050, relative to the 1990 baseline. This poses great challenges to the water industry in the UK and other EU countries. The next two sub-sections, to gain an in-depth understanding of these challenges, presents the gradual change in legislation and wastewater treatment technology development, focusing on the UK, in particular, Scotland.

1.1. Water Environment Related Regulations and the Wastewater Sector in the UK

To assess the current regulatory framework and legislation, understanding its historical development is necessary. One of the most important pieces of legislation to impact on the waste water sector, 'The Royal Commission Standard', came into force in 1912, which was later adopted by other countries (Lens et al., 2001). This legislation was driven by public health and hygiene issues and set a quality standard on sewage discharge to rivers, for the first time, specifying physiochemical water quality indicators (Lens et al., 2001). It set a limit of 20 mg L^{-1} of biochemical oxygen demand (BOD) and 30 mg L^{-1} of total suspended solids (TSS) (Smith, 2005). Such standards resulted in the invention of new wastewater treatment methods such as Activated Sludge processes which became and remain as the main secondary wastewater treatment process in the UK (Lens et al., 2001).

In the 1970s, increasing attention was paid to improving the quality of the water environment. This resulted in the formulation of different legislation across Europe, such as Surface Water Directions 1975, Bathing Water Directives 1976, Drinking Water Directives 1980, and Urban Wastewater Treatment Directives (UWWTD) 1991. For example, the UWWTD had a significant impact on EU member countries by setting stringent standards on the level of treatment and removal of nutrients from wastewater treatment plants' (WWTP) effluent; such as nitrogen and phosphorus. The European Union Water Framework Directive (EU-WFD 2000) in line with the UWWTD (1991) (CEC, 1991) promoted a sustainable and holistic approach in managing the water-environment by setting out more stringent standards that affect the urban wastewater systems (UWWS).

1.2. Climate Change Regulations in the UK, with Reference to Scotland

It is not only water environment focused legislation that has shaped the wastewater sector in the UK and other European countries. An understanding of climate change and its strong correlation with the increase in the world population and industrialisation has driven new legislation which has had an impact on urban wastewater systems, in addition to other industries.

International conventions and regulations have been developed as a response to the increased understanding of the earth's natural greenhouse effect and the causes for it as well as the monitoring and measurement of increased emissions of greenhouse gases (GHG). Using the work of the IPCC (1990), the Kyoto Protocol was introduced in 1997 to reduce GHG emissions of 37 countries by 5 % below their 1990 emissions for the period 2008 – 2012 (IPCC, 2013). Later in 2015, the Paris Agreement brought 160 members of the United Nations Framework Convention on Climate Change (UNFCCC) to agree on the reduction of their GHG by 2030.

The UK government has not produced new legislation based on the Paris Agreement (CCP, 2018), but they gave priority to take action to meet the targets set in the CC-Act (2008) and CC-Scotland-Act (2009). The Climate Change Act, 2008 and Climate Change Act (Scotland), 2009 commits the UK government to reduce GHG emissions to at least 80 % of the 1990 level by 2050. This included reducing emissions from the devolved administrations (Scotland, Wales and

Northern Ireland, which currently account for about 22 % of the UK's emissions, and Scotland accounted for 9 % of the UK's emission) (CCC, 2017).

This legislation uses a five-yearly 'carbon budgets' approach as a stepping stone to reach the 2050 target. Although the UK is on track in meeting its target in the second and third budget periods (2013 – 2019, and 2018 – 2022), it is not on track to meet the fourth target. The fourth target is reducing the GHG emissions by 51 % by 2025 compared to the 1990 level (CCP, 2018). To reach to this target, Scotland has further set a more stringent target, which is to reduce emissions by at least 30 % compared to the 2015 level (CCP, 2018). Due to the need for further reduction of GHG and uncertainty in the wastewater GHG emission levels, CCP (2018) indicated that further policy strengthening is required in the wastewater sector to meet the fourth and the sixth (2030) carbon budgets. The wastewater sector in Scotland, as a public body, is affected by the Carbon Reduction Commitment (CRC) energy efficiency scheme which sets similar targets as the Climate Change Act (Scotland), 2009.

The wastewater sector in the UK is not only subjected to stringent regulation already set out in the Climate Change Act, 2008, but it is also expecting a more stringent target within the interim periods to make sure the 2050 target is achieved (CCC, 2017; CCP, 2018).

1.3. Challenges from Climate Change and Population Increase

The UUWS faces a number of challenges, not least a set of competing and disparate regulatory imperatives as detailed in Section 1.2. For example, in the EU, the Water Framework Directive is driving stricter discharge standards, leading to increased compliance costs, energy use, and carbon emissions at WWTPs; while simultaneously climate change regulation requires the reduction of GHG emissions.

Additional pressures also come from climate change, urban population growth and aging assets making it more difficult for the water industry in the UK to maintain compliance within the current operational and regulatory paradigms (Astaraie-Imani et al., 2012).

Although the UK government aims to reduce water consumption from 150 L d^{-1} per person to 120 L d^{-1} per person by 2030, the increase in urban population directly increases the total water demand which ultimately increases the total wastewater flow reaching WWTPs. In addition, this increase in an urban population usually results in the need for new developments, which increase impervious surfaces, ultimately increasing the storm water entering the sewer network unless a careful planning is put in places such as separate sewer networks and SUDs options. Urbanisation can also alter the per-capita water consumption due to change in the way of life in the urban areas, which can lead to increased water demand and domestic wastewater. Also, Butler and Davies (2010) argued that an increase in population can strongly influence the quality of dry weather flow and the increase in sewage flow to WWTPs. The increase in total flow entering sewer networks can ultimately increase the energy demand for pumping (both in the sewer network and in within WWTP) and the cost of treatment. The combined effect of both increases in population and change in water use behaviour imposes a significant stress on the wastewater water.

Climate change can result in a change in rainfall pattern, i.e., the change in seasonality of rainfall, rainfall depth and rainfall intensity. For example, Astaraie-Imani et al. (2012) showed that increases in rainfall depth could result in the deterioration of rivers quality, mainly due to increased combined sewer overflow (CSO) and storm tanks' overflow.

These pressures combined with the need to reduce energy costs while maintaining the quality of receiving water bodies provide a challenge in managing the UWWS.

1.4. Integrated Urban Wastewater System Management

The urban wastewater system (UWWS) has three important elements:

- the sewer network sub-system (which includes the rainfall-runoff process in the urban areas, the collection of storm water and municipal waste and associated assets Peters et al. (2007),
- wastewater treatment plants,
- and, the recipient water body

These elements are conventionally designed and managed independently, but there is a need to treat them as an integrated urban wastewater system and

manage these elements integrally (Fu et al., 2008; Butler and Schütze, 2005). Greater integration in UWWS is mainly being driven by the holistic approach of the CEC (2000), and the need to address the challenges outlined in Section 1.3.

For any system, to be environmentally sustainable, including UWWSs, they should be able to overcome both the current challenges that exist and should be robust enough to cope with future changes.

If a system cannot manage to cope with changes and extreme events, it fails to meet regulatory limits, which can affect the receiving water quality, ultimately affecting ecosystems and public health which rely on water. Both Schilling et al. (1996), and Butler and Schütze (2005) emphasised the potential benefit of using active control of the sewer sub-system to tackle both current and future environmentally related challenges. Active control, as defined in Section 2.1.1, it is a real-time control system commonly focusing on a unit process or system. For example, the benefit of active control strategies in regulating flow within the sewer networks is demonstrated clearly over other measures in the case-study by Cembrano et al. (2004). Such approaches have demonstrated benefit in managing the dynamic nature of the nutrient load to WWTPs. For example, Kishida et al. (2008) showed the possibility of achieving the stable removal of nitrogen and phosphorus through careful design of active control strategies.

A well-designed active control system can be used to achieve different operational objectives and provide efficient operations that can reduce operational energy use and associated GHG emissions (Hamilton et al., 2006). The potential of the active control approach can be increased by integrating the components of the UWWS and by using a holistic approach (Vanrolleghem et al., 2005; Fu et al., 2008; Butler and Schütze, 2005; Schütze et al., 2004).

An integrated approach coupled with the implementation of active control systems is not only able to achieve environmental sustainability, but it can also deliver economic sustainability by helping to get the best out of the existing infrastructures in the UWWSs. Expensive construction or expansion of the existing systems with high capital investment can be avoided by prudent utilisation of the existing capacity, which can maintain cost efficiency (Zacharof et al., 2004). Schütze et al. (2004) showed the benefit of active control systems compared to that of capital investment for the static expansion of sewer networks.

For example, in the Quebec urban community, Canada, the estimated cost of the design and construction of a conventional infrastructure to control CSO was reduced from USD 15.5 million to USD 2.6 million with a 70% reduction in overflow through design and implementation of active control systems.

Regarding management, it is also important to consider the combination of the current fixed licensing approach implemented in the UK wastewater sector and the commonly used process-focused control systems in most of the existing WWTPs as this does not help to utilise the receiving capacity of the water environment. One hypothesis is that a dynamic licensing approach that uses variable effluent standards based on the receiving capacity of the river can help to ensure that receiving water quality is maintained across a range of flow, load and environmental conditions. A dynamic licensing approach seeks to utilise the assimilative capacity of rivers which can reduce the need for higher effluent quality and increase effluent quality whenever the assimilative capacity is low, and thus potentially reduce GHG emissions and operational costs of treatment while maintaining environmental targets.

1.5. Aims and Objectives

This research project aims to investigate the benefits of integrated active control of existing WWTPs through the development of control strategies, interventions and licensing approaches to find out the best trade-off among the reduction in energy use, GHG gas emissions and maintaining the quality of the water environment. It also assesses the benefit and challenges of using the receiving river's assimilative capacity by varying the statistical-based fixed licensing approach that is widely used in the UK and other European countries.

A set of specific objectives were identified to achieve the aim of this project:

1. Identify the main research gaps regarding modelling GHG emissions and integrating modelling approaches.
2. Characterise influent wastewater, collect further data based on the need identified in the model calibration process and perform further calibration using the new dataset where necessary.
3. Set up models for each UWWS components; WWTP model to represent the case-study, an influent generator to simulate influent to WWTP from the sewer network, river flow and quality model. Moreover, integrate each

sub-system models for the selected site for testing integrated control strategies and licensing approaches.

4. Test different control strategies using a case study. This objective will focus on understanding the case-study's current (baseline) unit processes and their interaction, i.e. the layout of the plant, operational procedures, and regulations and licenses by which the WWTP needs to abide.
5. Investigate the possibility, potential benefits and drawbacks of the application of different control and licensing approaches regarding reducing operational cost, energy consumption, and GHG emission while maintaining the quality of the environment. Upon result from this investigation, develop new control strategies and licensing approaches.
6. Suggest a guideline to select and apply the suggested control strategies based on the complexity of implementation and capital investment. Moreover, highlighting the overall benefit of this project and how the outputs from this work can be implemented in a wider context on a company scale.

1.6. Thesis Structure

This thesis comprises nine chapters; their interdependency is shown in Figure 1-1.

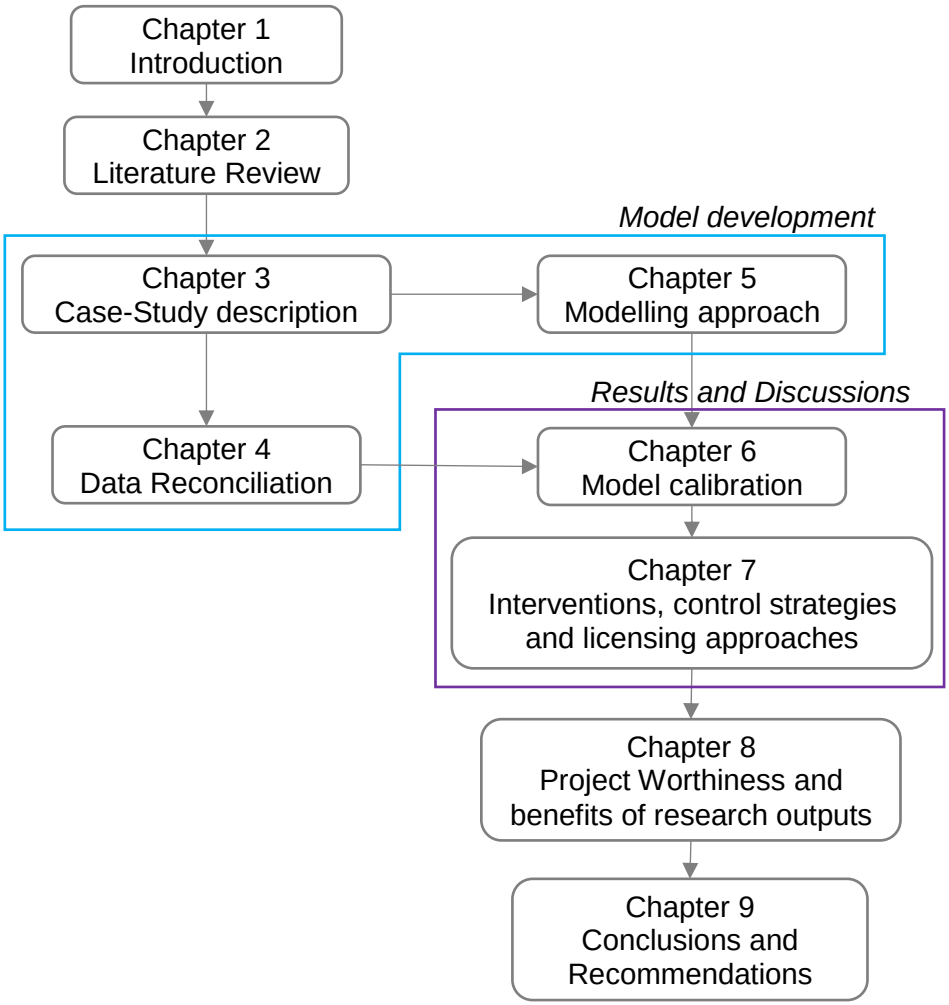

Figure 1-1 Thesis structure and chapter interplay

Chapter 1 covers the background information on the challenges of the urban wastewater systems and their management, and the aim and objectives of the project.

Chapter 2 provides a literature review on three topics; control strategies, modelling tools and the legislations and guidance that influence the water industry in the UK, Scotland. It gives an in-depth discussion on control design in WWTPs and the role of simulation in evaluating control strategies. The chapter provides a detailed discussion on models for estimating GHG emissions from WWTPs, influent generator and sewer modelling approach that take process control and optimisation into account, and river quality modelling approaches with a focus on integrating them with WWTP models. Finally, the chapter gives background information on existing regulations and identifies their contradictions.

Chapter 3 outlines the major components of the case-study WWTP, their operational procedures and unit process-based model block development. This

chapter shows how current operational procedures control each process unit and the implementation of unit processes and associated operational procedure within the model.

Chapter 4 illustrates the step-by-step procedure used to characterise the influent wastewater. The wastewater characterisation is done with the aim of quantifying each state variables in the activated sludge model no. 1 (ASM1). It covers the identification of data requirement, the design of monitoring campaign, and the analysis and validation of monitored dataset. This chapter contains the research work published at the European Wastewater Management Conference 2015, (Ashagre et al., 2015):

Ashagre, B., Fu, G., Davidson, K. & Butler, D. The Impact of data availability on the predictive accuracy of wastewater treatment works models. 9th European Waste Water Management Conference, 12/10/2015, Manchester, UK.

Chapter 5 describes the GHG emission modelling approach at WWTP scale with an in-depth explanation of the methods used to estimate the direct and indirect GHG emissions from WWTPs. The chapter covers the methods used for WWTP performance assessment that reflect on operational energy consumption, GHG emissions and effluent quality. Additionally, the chapter gives a detailed description of the modelling approach for the sewer network and the river model. Finally, a comprehensive explanation on the integration of the three components of the integrated UWWS is given.

Chapter 6 covers the model calibration process and results for the WWTP and influent generator after integration. Statistical goodness-to-fit measures were used to assess how close the simulated quality indicators are to the measured ones and the results are presented in this chapter. These measures were used for the execution of sensitivity analysis and auto-calibration of WWTP model with the view to increase the model accuracy.

Chapter 7 assesses different interventions, control strategies, and innovative regulatory approaches. The chapter presents the direct application of control strategies and identifies the benefit accrued by optimisation of control strategies. The assessment of interventions and control strategies was assisted using One-At-a-Time OAT sensitivity analysis. The initial assessment was done using the sensitivity result as guidance. Those with potential in meeting system-wide

objectives are further assessed by implementing multi-objective optimisation. The chapter suggests innovative regulatory approaches and investigates their benefit through an integrated active control loop.

Chapter 8 explores the contribution of this project and the Engineering Doctorate scheme from a water company point of view. The chapter covers how the results of this study can be implemented on a wider scale and the potential benefits to the wastewater industry.

1.7. Originality and Contribution to Knowledge

This thesis demonstrates originality in that is has modified and integrated a selection of different modelling approaches to result in a positive trade-off between GHG emissions, operational cost and effluent quality. Moreover, this was done using a real-world case study, and this thesis demonstrates how to overcome the associated challenges in doing so. It outlines a step by step approach for influent wastewater characterisation, data reconciliation and their impact on model accuracy by assessing them through a statistical measure through model calibration processes. The thesis highlighted the potential of control strategy optimisation and innovative regulatory approaches.

The following points show the main contributions and originality of the work presented in this thesis.

- The study developed a new integrated model by integrating WWTP model, influent generator model, and a hybrid purpose-built receiving river model that uses both a deterministic and empirical approach to simulate real case-study of an integrated UWWS. Modelling integrated UWWS on real world case-study level to test control strategies at the WWTP, is still in its early stages and this study has contributed to a better understanding of the possibilities, challenges and potential advantages. *(Chapter 3 and 5)*
- A step by step procedure is developed to identify the minimum data that is required in modelling WWTPs for the design of control strategies. It demonstrates that through careful design and identification of key datasets to characterise influent wastewater and mimic hydraulic and biological processes, it is possible to increase overall WWTP model accuracy. This procedure can be used as a guideline for integrated model calibration and data monitoring campaign design. *(Chapter 4 and 6)*

- The study identified influential parameters for model calibration to which final effluent total suspended solid, NO_3, NO_2, and mixed liquor suspended solid and dissolved oxygen level in the oxidation ditch are sensitive. The variation in each parameter and the resulting direction of change in the model accuracy indicators was determined using a one-at-a-time (OAT) sensitivity analysis. This knowledge will aid future calibration works as it provides the key parameters that have the greatest influence on model accuracy, which can reduce a significant time for optimisation runs in autocalibration processes. *(Chapter 6)*
- The study demonstrates the role of multi-objective optimisation in improving control strategies and integrated active control strategies in trading-off the reduction in GHG emissions from WWTPs, reduction of operational costs, and maintaining effluent quality standards. The thesis showed that it is possible to trade-off these objectives without the need to implement new treatment technology or the need for a major upgrade. *(Chapter 7)*
- The study contributes to the understanding and utilisation of the assimilative capacity of receiving rivers to trade-off strict and sometimes contradicting regulations to which the wastewater sector needs to abide. Innovative regulatory approaches such as a dynamic licensing approach presented here (varying the fixed effluent quality standard based on the assimilative capacity of the river) demonstrate that there is great potential to reduce GHG emissions without affecting river quality or status as defined in the EU Water Framework Directives 2000/60/EC, CEC (2000). *(Chapter 7)*
- Develops a guideline for selecting and implementing interventions, control strategies and innovative regulatory schemes by considering the simplicity and complexity of the implementation and the associated capital investment. *(Chapter 7)*

2. Literature Review

The literature review section is divided into three sections covering control strategies, modelling tools and the legislations and guidance that influence the water industry in the UK, Scotland.

In Section 2.1 the detail of control design, its application in the wastewater sector and the benefit of active control and integrated active control are discussed. In Section 2.2 covers modelling approaches. The discussion is set up first by discussing the modelling advancement in WWTP modelling and capabilities in simulating GHG emissions. To assess the benefit of integrated active control strategies, Section 2.2 investigates different sewer and river quality modelling approaches that can easily integrate with WWTP models and suitable for application in real-time control and optimisation problems. Section 2.3 covers the current regulatory approaches that influence the water industry, specifically for wastewater treatment plants in Scotland, UK. It assesses the current fixed licensing approaches and river assimilative-capacity-based variable licensing approaches.

2.1. Wastewater Treatment Control strategies

2.1.1. Introduction to Control Systems

The definition of ‘system’ can be very ambiguous. In this study, we define a system based on the definition given by Distefano et al. (1997) as an arrangement or set of elements connected to form or act as an entirety. Control systems can be defined as the arrangement or connection of units in such a way that they regulate, direct or command themselves or another system. For example, dart players control the movement of the darts. The player can throw the dart without any pre-calculation and hit anywhere on the board; this is still a control system. Alternatively, the player can judge the distance between him and the dart board and adjust the angle and the speed of throwing to hit the exact point he is intended to, this also control. Again, doing all this the player’s accuracy (in this case both the sensor and the actuator are the player) determine whether he hits the target or not. Hence, control systems can be simple or sophisticated. Simple controls are cheaper and easier to setup while sophisticated, for example, closed loop control systems can be more complex and expensive but can decrease system sensitivity to a variable load, reduce operational cost, and enable adjustment of

unit processes without affecting system performance. In wastewater systems, the advantages of feedback control over its cons are demonstrated in the literature (Lukasse, 1999; Olsson and Newell, 1999; Olsson et al., 2005; Olsson, 2012; Dirckx et al., 2011)

In wastewater engineering, systems are usually dynamic, and therefore the term control is associated with dynamically or actively regulating, commanding or directing the system.

A control system normally has an input and output. The input is the stimulus applied to the control system to produce a response from the control system, and the actual response from the control system is the output. The control system output may not be equal to the response expected based on the magnitude or nature of the input. For example, in the above example of the dart, the input is the signal (location of the dart board and the dart itself) send by the player's eyes to his brain (eyes can be considered as sensors). The signal from the eyes goes to the brain where the control action is decided, and the signal goes to the arm (the muscles on the arms are the actuators) to throw the dart to the intended location on the dart board.

Control systems can be classified into open-loop and closed-loop control systems. In open-loop (feed-forward) control systems, the control action is independent of the output (Jacobs, 1974), see Figure 2-1. In contrary, in a closed-loop, commonly referred to as feedback control system, the control action is dependent on the output, i.e. check output post-activity and adjust offsets accordingly, see Figure 2-2. The above dart example can be taken as an open-loop control since no control action can be taken based on the direction of the dart once it left the player's hand. However, if we take a closed-loop example, a girl picking up a cup, her arm and hand positions (outputs in this case) are continuously sensed by her eyes and position of arm continuously adjusted (output) using arm muscles (actuators). The continuous checking of inputs and/or outputs to adjust control variables concurrently is commonly termed as real-time control, active control or dynamic control. In this study, we refer to such type of controls as active control systems.

The definition of feedback given by Distefano et al. (1997) is used in this study. *"Feedback is the property of a closed-loop system which permits the output (or*

some other controlled variable of the system) to be compared with the input to the system (or an input to some other internally situated component or subsystem of the system) so that the appropriate control action may be formed as some function of the output and input."

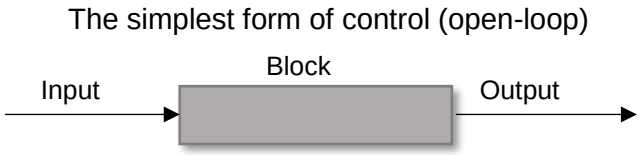

Figure 2-1 Open-loop control (the simplest form of a control system)

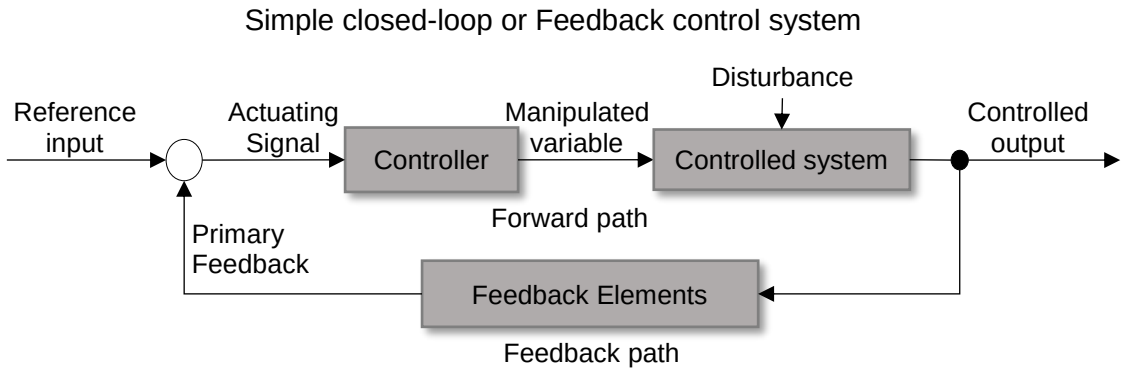

Figure 2-2 Closed-loop control (feedback control system)

Feedforward control systems are early warnings by identifying potential disturbances and prevent the problem from happening. In wastewater systems, this necessarily requires monitoring and understanding pattern of flow and nutrient load coming into the WWTPs (Santín et al., 2015b) or forecasting of rainfall to forecast sewer and river flow and quality (Yan et al., 2013; Jing et al., 2015)

From the WWTP perspective, controlled systems in activated sludge processes can be different components of the system that can be controlled to influence the effluent quality, energy use, and so on (Răducan et al., 2006; Lukasse, 1999; Chen and Beck, 2001). Referring to Figure 2-2; the controller is the element in the controlled system that generates the appropriate values of the variables manipulated, e.g. Programmable Logic Controller (PLC) or Supervisory Control And Data Acquisition (SCADA) that generates the change to the actuators. The feedback elements are the ones that establish a relationship between the primary feedback signal and controlled output, e.g. algorithms used to relate oxygen concentration in activated sludge reactors to the requirement of blower speed.

The actuating signal usually referred to as error or control action is the algebraic sum of the primary feedback signal and the reference input (Jacobs, 1974; Distefano et al., 1997). The manipulated variable is the quantity of change that should be applied to the controlled system as determined by the controller. The disturbance is undesirable inputs or conditions that affect the controlled output.

2.1.2. Control of WWTPs: Past and Present

Control systems in urban wastewater systems can vary from as simple as turning a pump on/off manually to as complex as using complex algorithms with real-time control approaches. The benefit of advanced control and automation in the wastewater sector has been identified since the ’70s (Olsson et al., 2005). However, its application faced challenges, especially due to the inconvenient design of existing wastewater treatment plants (WWTPs) for advanced control, limited capability of sensors, actuators, and computers and their robustness in a hazardous environment (Hreiz et al., 2015; Hamilton et al., 2006; Olsson, 2006). Although the sector faces these challenges, due to the rapid growth of processing speed of computers, and online instrumentation advanced control and automation of existing systems had become possible (Olsson, 2012).

Olsson (2012) analysed the focus given to instrumentation, control and automation since 1970 by academia and industries by analysing the percentage of papers submitted to the ICA international conference over the years. The participation of academia increased from 10 % to 60 % while the contribution of industries and utilities reduced from 80 % to 25 % by 2009. The pattern in the reduction of participation of industries was mainly due to the different challenges at different times. For example, instrumentation was the crucial limitation in the 70s and 80s hence the highest contribution from industries and utilities to address this issue. In recent years, the advancement in instrumentation was significant, and it is not the main bottleneck anymore, which was one of the reasons for the reduction in ICA conference participation from industries over the years (Olsson et al., 2005). Instead, modelling and simulations of wastewater systems became crucial mostly for comparing different control strategies and optimising the wastewater system (García et al., 2015; Gernaey et al., 2014). Although data acquisition and monitoring technologies have developed massively, still more work needs to ensure data quality through screening and also lots of room for further data monitoring (Benedetti et al., 2013).

Future demand for integrated active control of WWTPs is expected to increase due to stricter regulations, the need for higher efficiency to mitigate climate change, reduction of operational cost, equalisation of peak flow and pollutant load to effectively use spare capacity, etc. (Schütze et al., 2011; Astaraie-Imani et al., 2012). Testing and designing control strategies is convenient and inexpensive to be performed initially on a model scale before application (Olsson and Newell, 1999). In Europe, including the UK, models were mostly a research subject whereas in other parts of the world, like North America, WWTP models are predominantly used as an engineering tool in practice (Hauduc et al., 2009). Since then, the use of WWTP models, system automation, and control are now changing in the UK (UKWIR, 2013b). Water utilities have started to incorporate WWTP models in decision making, process control, and optimisation. According to UKWIR (2013b), WWTP models are now being used for advanced process control and this practice is expected to increase significantly in the future due to tighter regulations and the potential of advanced control systems to save energy, chemical usage, and greenhouse gas emissions.

2.1.3. The Need for Control

There are various reasons for the need for process control. However, commonly, processes are controlled for the following three reasons; reduce variability, increase efficiency, and ensure safety (Li and Zheng, 2015; Lindberg, 1997; Olsson and Newell, 1999; Schilling et al., 1996; Svrcek et al., 2014). Safety can refer to the safety of the environment, staff on site, or the asset. Below are some of the reasons that Engineers have used control systems in the past:

- The need to reduce the impact of disturbances within the system such as variations in flow, the proportion of nutrients, temperature, biomass concentration and other factors.
- To cope with the increased load to WWTPs due to increased urbanisation or industrialisation.
- The need to increase WWTPs capacity or the need to adopt complex processes due to increased load or tighter regulation but without a high capital investment
- Protect the environment, this necessary includes the reduction of GHG emissions from WWTP and maintain desired effluent quality.
- Protect assets from acute failure and reduce deterioration

- Reliable service with a consistent and high quality of output, for example, ensuring consistent effluent quality.
- Reduction of capital investment and operational cost
- Increasing system efficiency through reduction of operational energy consumption
- Monitoring and diagnosing

2.1.4. Control Design

In simpler terms, the design of control systems consists of establishing the system goals or defining the control problem, identifications of variables to be controlled through real performance measurement or simulations and preparing the control algorithm. Control design is not a one-off exercise. Rather, as in the case with wastewater control systems, it needs several iterations for tuning and performance evaluation with simulation and full-scale physical tests (Mahmoud and Xia, 2012; Olsson et al., 2005).

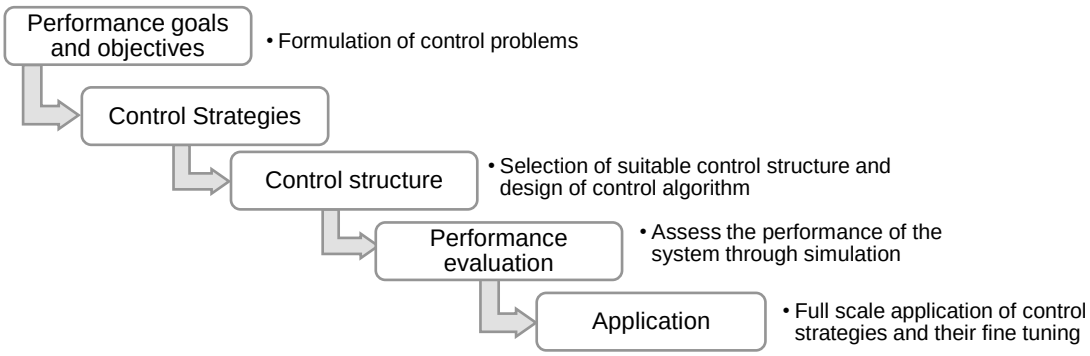

Figure 2-3 Control design procedures suggested by Olsson et al. (2005)

2.1.4.1. Performance Goals and Objectives

In wastewater treatment control systems, the main drivers are the goals. Goals specifically refer to finding out what do we want to achieve; reduce disturbance, raising standards or maximising efficiency, and so on. These goals may be brought about because of caring for the environment, the employee and customers, because of stricter regulations. Similarly, they may be brought about as a result of corporate goals such as reduction of capital investment and operational cost. Olsson and Newell (1999) referred to them as community/societal goals. Societal goals are met by specific goals at a WWTP scale or a process scale, usually referred to as a process or plant goals (Olsson and Newell, 1999; Schütze et al., 2004). Process/plant goals can be, for example,

meeting effluent quality requirements, reduce dry weather spills to receiving water bodies, system optimisation to reduce cost, minimise control actions (Ocampo-Martinez, 2010; Schütze et al., 2002). Olsson and Newell (1999) manifested that the process goal can be even more specific, referred to as operational objectives, and designed so that a specific treatment plant can meet the plant or process goals. A water utility can have the same plant or process goal for several WWTPs, but this goal might be achieved through different operational objectives based on site conditions and schemes.

Figure 2-4 Interlink between different goals and objectives that drives control designs at WWTPs (based on Olsson and Newell (1999))

2.1.4.2. Control Strategies

Schütze et al. (2011) defined control strategy as the identification of the vector of parameters (strategy parameters) describing the control strategy framework. The authors define control strategy framework in simple terminologies, a procedure describing how the settings of identified process units to be controlled (referred as actuators, e.g. pumps, blowers, valves, and so on) is determined from the available sensor information. Strategy parameters include settings of actuators, controller parameters, setpoints or set-point determining algorithms, and so on. Hence, a strategy framework portrays the general idea of a strategy without allocating values to its parameters. *"A control strategy represents an instantiation of a framework, with defined values of its parameters"* (Schütze et al., 2011).

Olsson et al. (2005) described control strategy development as the difficult step in control system design due to the requirement of a thorough understanding of control engineering and the process under consideration. Due to this reason, the complexity and dynamic nature of wastewater processes and other uncertainties, different control strategies have been used in wastewater control systems.

This includes:

Adaptive control strategy: "An adaptive control system measures a certain performance index of the control system using the inputs, the states, the outputs and the known disturbances. From the comparison of the measured performance index and a set of given ones, the adaptation mechanism modifies the parameters of the adjustable controller and/or generates an auxiliary control to maintain the performance index of the control system close to the set of given ones"(Landau et al., 2011). Adaptive control structures have been applied in the WWTPs control exercise since Sasaki et al. (1994). Adaptive controls have been applied for different control purposes in the wastewater system., including; control of hydraulics, dissolved oxygen level, and anaerobic digestion (Jonelis et al., 2009; Kandare et al., 2012; Lin and Luo, 2015; Luo et al., 2014; Monroy et al., 1996; Nejjari et al., 1999; Petre et al., 2013; Qiao et al., 2013; Repšyte et al., 2009).

Hierarchal control strategy **-** is a strategy where a higher-level or supervisory control identifies the set-point of the lower-level controllers (Suescun et al., 2001). These control strategies have been used for WwTPs and integrated wastewater systems to control nitrification and ammonia concentration, denitrification and nitrate concentration, MLSS and DO in aerators, sludge blanket in final settlement tanks, etc. (Brdys et al., 2008; Holubar et al., 2002; Piotrowski et al., 2008; Sanchez et al., 2001; Suescun et al., 2001).

Optimal control strategy - Fu et al. (2008) defined an optimal control strategy as a control strategy that aims to achieve the best system performance on several operational objectives. There are various optimal control structures that has been used in wastewater systems such as genetic algorithm (Fu et al., 2008), Model Predictive Control (MPC)(Li and Zheng, 2015; Ocampo-Martinez, 2010; Wahab et al., 2011), and Linear-Quadratic-Gaussian control (LQG) (Johnson and Sanchez, 2003).

Robust control strategy - Bhattacharyya et al. (1995) defined robust control strategies as control systems that are designed to secure the stability of systems confronting uncertainty and the worst case performance over the uncertainties fall in the acceptable range. This approach helps systems to cope with uncertainties arise from modelling, measurement and limited knowledge of the process (Petre and Selişteanu, 2013). Robust control strategies have been used

in the past to design control systems for wastewater systems (Aguilar-López, 2008; Schaper et al., 1990; Serhani et al., 2009; Song et al., 2012).

Due to the complex non-linear nature of the systems, poor understanding of their dynamics and lack of cheap, and reliable online-sensors, various control strategies have been suggested and used in the past (Petre and Selişteanu, 2013). This includes linearizing strategy (Dochain and Perrier, 1993; Carlsson and Milocco, 2001; Torres Zúñiga et al., 2012), robust and optimal control (Fu et al., 2008; Suescun et al., 2001; Wik et al., 2003; Logist et al., 2011), neural strategies (Hayakawa et al., 2008; Petre et al., 2010), and so on.

2.1.4.3. Control Structure

Control structure can be as simple as a heuristic algorithm where control systems are designed purely based on experience without any dynamic modelling (Kokash, 2005). Alternatively, it can be as complex as a model predictive control that uses a prediction of the system response to identifying the appropriate control action (Venkat et al., 2008; Toro et al., 2011). Hence, to meet the operational objectives, the control structure should be designed based on system complexity, model availability and other features of the control system (Francisco et al., 2015). For example, control structure that uses convectional feedback can be implemented first by measuring the controlled variables, then by comparing the measurements with the set point and by feeding the difference into the controller which will generate the appropriate control (Landau et al., 2011). However, the conventional feedback control may not be adequate to secure stability in some non-linear systems that go through parameter disturbances. These disturbances can affect the performance of the system and a control structure that monitors the performance of the system for better rejection of the disturbances, e.g. disturbance rejection feedforward controller (Landau et al., 2011; Olsson et al., 2005).

2.1.4.4. Performance Evaluation Through Simulation and Application

A good control strategy is the one that can ensure acceptable performance in most operational conditions (Olsson et al., 2005). Hence, it is important to assess the performance of a control system under various conditions. Modelling and simulation play a significant role in providing a platform where these

performances can be evaluated, and the controller can be tuned (Gernaey et al., 2004; Dochain and Vanrolleghem, 2001; Andrews, 1993; Andrews, 1974).

Since models cannot fully replicate the real system, there is always a difference between the response of models and real systems. Thus, it is important to test the suggested control strategies at full-scale to ensure that the control system does not bring unexpected adverse effect on system performance (Olsson et al., 2005; Olsson and Newell, 1999).

2.1.5. Comparing/Benchmarking of Control Strategies

In previous sections, it has been said that WWTPs are complex non-linear systems experiencing large disturbances and uncertainties, e.g. the composition of the influent wastewater. Many control strategies at a different scale and a different unit of processes have been proposed in the literature to ensure a stable operation regardless of these factors (Concepcion et al., 2013; Ye et al., 2013; Piotrowski et al., 2008). However, their performance evaluation and comparison approach used in the past was difficult and inconsistent which was mainly due to the lack of standard evaluation criteria (Gernaey et al., 2014). In 1998, the EU research programme COST 624 (http://apps.ensic.inpl-nancy.fr/COSTWWTP/) was initiated to address this issue by developing a methodology through benchmarking simulations, influent loads, test procedures and performance evaluation criteria.

Gernaey et al. (2014) stated that the benchmarking of control strategies had been a topic for academia and the technique has been limited to this sector due to its objectivity. They also manifest that this approach may not guarantee that a control strategy that showed a good performance using the benchmark test to show similar performance in real cases. Mainly, because, the approach compares strategies objectively without considering location-specific conditions. They also suggested that the modelling tools and the evaluation criteria can be used to assess the suitability of objectively tested control strategies in the process of solving problems on a real plant.

In addition to this, it can be difficult to quantify the impact of the suggested control strategy on the performance of a WWTP since the baseline situation is hardly optimal (Vrecko et al., 2006), considering that the baseline situation of many WWTPs is not optimal.

Gernaey et al. (2014) strongly recommended that new or innovative control strategies need to be evaluated thoroughly by developing a reasonably accurate model of the plant, the influent load, sensors, controllers and performance criteria

2.1.6. Active Control and Integrated Active Control

As defined in Section 2.1.1 active control is a type of control where continuous checking of inputs and/or outputs are performed to adjust control variables concurrently and commonly limited to one process unit/system. However, integrated active control refers to the application of active control approach to two or more systems that operate in coalesce. Integrate active control approach can have single or multiple objectives with a capacity in delivering a wider goal (societal goals) than the active control approach objectives (plant wide or process-based goals).

In urban wastewater systems, most of the studies in the literature focus on plant wide control or process level control, e.g. Li and Zheng (2015); De Gussem et al. (2014). They are either unit process controls with the objective to optimise the unit process within the WWTP, or they are plant wide process controls without the integration of other systems. Active control (real-time) control of sewer networks were widely tested without considering the WWTP e.g. (Cembrano et al., 2004; Lacour and Schütze, 2011), in other cases plant wide control was done without considering the sewer network (Samuelsson, 2005), and in most cases without considering the capacity of the receiving water (Wu and Luo, 2012; Hreiz et al., 2015).

Before proceeding discussing further on integrated active-control approach, it is essential to define the urban wastewater system. In this study, the urban wastewater is defined as domestic wastewater (wastewater discharged from residential settlements predominantly originates from household activities or human metabolism) or the mixture of domestic wastewater with industrial wastewater (wastewater discharge from premises used for carrying on trade or industry) and/or storm water (CEC, 1991). ‘Urban area’ in this study is equivalent to ‘agglomeration’ as defined in CEC (1991); it is an area where the population is sufficiently concentrated so that urban wastewater can be collected through a sewer network and conducted to the wastewater treatment plant. The appropriately treated wastewater from the wastewater treatment plant (WWTP) is discharged to the receiving water. Integrated urban wastewater system refers

to the consideration of the three systems, the sewer network, the wastewater treatment, and the receiving water, as an integrated one system, Figure 2-5.

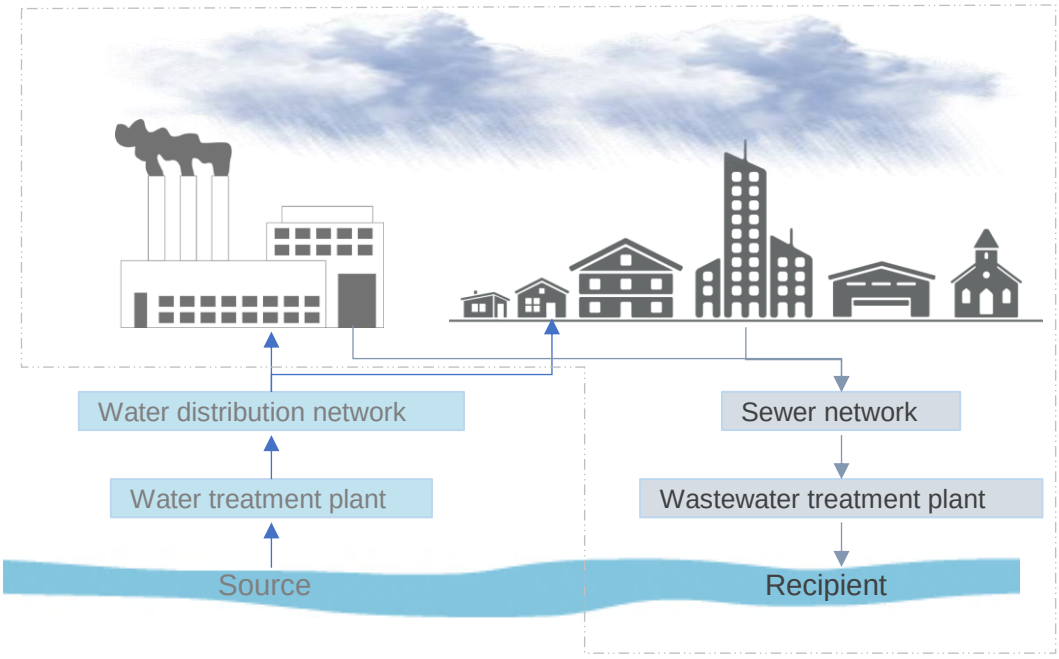

Figure 2-5 Interlink among the main components of a typical urban water and wastewater system. The dotted line showing the boundry of an uban wastewater system

Integrated active-control of urban wastewater system presents opportunities both in design and operation of the system with different objectives (Benedetti et al., 2013; Vanrolleghem et al., 2005). However, the objectives can be different and the resulting degree of complexity as well. For example, most studies in control of wastewater treatment plants focus on the control aeration systems with the goal of reducing energy consumption (Xu and Cheng, 2016; Wu and Luo, 2012; Yang et al., 2016; Rieger et al., 2014; Åmand and Carlsson, 2014). Some studies showed the reduction of energy by considering other options than controlling the aeration systems, for example, De Gussem et al. (2014) presented control of impellers in aerators resulting in a reduction of energy use up to 2.3 %.

The objective of reducing energy consumption usually go along with meeting effluent standards, and several studies explicitly discuss and test different control strategies to reduce operational energy consumption and meeting effluent standards (Zhang et al., 2008; Yong et al., 2006). Others looked at control strategies for only meeting effluent quality standards (Vrečko et al., 2011; Vrečko et al., 2006; Traoré et al., 2005).

The wastewater sector in the EU and the US is under strict regulation regarding effluent standards (Maere et al., 2016; Meng et al., 2016). Some literature focuses on meeting only effluent quality standards and give less emphasis to the energy used or systems efficiency. For example, Santín et al. (2015a) and Santín et al. (2015b) focused on avoiding violations of effluent pollution limits, however giving a lesser emphasis on reducing the operational energy consumption of the system.

However, regulations such as the EU Water Framework Directive (WFD) requires a holistic approach to improve the status of water bodies which was the main driver to look at wastewater systems as an integrated system and broaden objectives beyond meeting effluent quality standard (Rauch et al., 1998; Fu et al., 2008). The scale of integration and the objectives that are assessed so far in the literature varies significantly. On the one hand, Langeveld et al. (2002) clearly showed the necessity of an integrated approach to assess sewer systems and WWTPs as an integral unit but not emphasise the need of integrating the receiving water. On the other hand, Benedetti et al. (2007) focused on integrating only the WWTP and the receiving river. Erbe and Schütze (2005) presented an integrated approach that allows a holistic pollution-based control of the drainage system as a function of state variables in the WWTP and the receiving water but focusing mainly on managing the drainage network. In contrast, Meirlaen et al. (2002) integrated the three subsystems (urban drainage network, WWTP, and receiving water) and used the river's ammonia concentration to influence the total flow to the WWTP without influencing processes within the WWTP.

Although the integrated control approach presented in Meirlaen et al. (2002); Vanrolleghem et al. (2005), has been accepted by many researchers, the approach was used with different objectives. As discussed in previous paragraphs, several objectives can be sought while using integrated active-control approaches. Flores-Alsina et al. (2014b) use a hypothetical benchmark WWTP to assess the trade-off effluent quality, reduction of operational cost and reduction of greenhouse gas (GHG) emissions. The trade-off among these objectives is further discussed in Section 2.3.

There are no studies in the literature that uses the receiving water quality as an objective and uses an integrated approach to balance receiving water quality, reduction of GHG emissions, and reduction of operational energy or operational

cost. Some of the studies on integrated active-control of UWWS that includes influencing WWTPs processes with the objective to trade-off reduction of cost, GHG emission and meet effluent quality (without considering the receiving water body) were done either on hypothetical plants or semi-hypothetical systems (Flores-Alsina et al., 2014b). Those that use a case study (full-scale) system failed to show the accuracy of the models used in the assessment of control strategies (Katebi and Graells, 2005; Muschalla, 2008).

2.2. Modelling Tools for Urban Wastewater Systems

The urban wastewater system is part of the big hydrological cycle where the receiving water takes discharge from surface runoff from the urban catchments, effluent from the wastewater treatment plants, and overflow from combined sewer networks. The sewer network, the wastewater treatment plant, and the receiving water body form the urban wastewater system (Schütze et al., 2011).

Urban wastewater system has been considered as part of the urban water system. The urban water system consists of the source of water, water treatment or purification plants, drinking water distribution, the consumers (urban catchment which includes households and industries), sewer system, wastewater treatment plant and recipient water bodies. The urban wastewater and the water supply system can be seen separately unless the recipient is also used as raw water sources (Butler and Schütze, 2005; Schütze et al., 2004).

These elements of the urban wastewater system commonly treated and managed independently, but in some cases, integrated urban wastewater management is implemented (Fu et al., 2008; Butler and Schütze, 2005). To assess the impact of alterations, interventions, control strategies and so on, on these systems, modelling and simulation of the processes is a preliminary step to implementation (Erbe and Schütze, 2005; Olsson and Newell, 1999). Various simulation tools focus on system components either as a separate unit or holistically as part of a bigger unit (Gernaey et al., 2004; García et al., 2015). The following subsections will look at their capabilities and suitability for an integrated urban wastewater system modelling specifically looking at GHG emission modelling capability and suitability for integrated active (real-time) control.

2.2.1. Wastewater Treatment Plant Modelling and GHG

There are several simulation tools available to model the different components of the wastewater systems. It is important not to confuse activated sludge model with wastewater treatment plant model. WWTP models consist of different components of the system such as primary clarifier and secondary clarifier requiring clarifier models in addition to activated sludge model to simulate biological transformation processes (Gernaey et al., 2004). On the other hand, activated sludge model refers to the mathematical models that simulate the transformation process with a reactor in the WWTP (Jeppsson and Pons, 2004).

2.2.1.1. Modelling of GHG Emissions from WWTPs

Greenhouse Gas (GHG) emissions from WWTPs can be classified as 'direct' or 'indirect' emissions. Direct emissions are the GHG produced onsite due to biochemical processes within the boundary of the WWTP (Sweetapple, 2014). The indirect emissions are the GHG produced outside the premise but as a result of activities/processes within the WWTP (for example, GHG emissions due to energy use with the WWTP) or outside the WWTP (for example, GHG emissions due to sludge transportation) (Sweetapple, 2014).

Direct GHG emissions include the production of carbon dioxide (CO_2), and the more potent gases such as nitrous oxide (N_2O) and methane (CH_4). Methane can only be produced in anaerobic process/condition; however, it can be emitted from aeration tanks, most likely due to the formation of CH_4 in earlier processes or the sewer network (Foley et al., 2015). Studies suggested that there is methane production by methanogens in aeration tanks but very limited, 0.01 – 0.02 % of the carbon removed (Gray et al., 2002). Due to this limited contribution and the uncertainties in the estimation of its production from aerobic systems methane production from aerobic systems is not discussed here. Also, since the study focuses on aerobic systems the methane production from anaerobic processes is not disused either.

The CO_2 production from aerobic processes is due to two processes; the breakdown of organic matter in the presence of oxygen to produce energy or CO_2 emissions associated with either biosynthesis (building of new tissue) or auto-oxidation or endogenous respiration during the shortage of oxygen (Sweetapple, 2014). Monteith et al. (2005) put forward a steady state CO_2 emission estimation from these processes, based on carbonaceous biochemical oxygen demand

(CBOD) converted to biomass and based on the oxygen requirement. This approach is later adopted by various studies (Sweetapple, 2014; Flores-Alsina et al., 2011). The approach uses a ratio procedure to apportion BOD conversion by oxidation, biosynthesis, and auto-oxidation processes coupled with a stoichiometry approach to estimate the emission factors. The emission actors for the oxidation process, based on 0.8 moles of CO_2 production for every mole of oxygen, leads to a conversion factor of 1.1 kg CO_2 per kg O_2 (Monteith et al., 2005). There is no CO_2 emission during biosynthesis processes; however, during auto-oxidation processes, 1 mole of biomass production results in the production of 5 moles of CO_2 leading to a conversion factor of 1.947 kg CO_2 per kg VSS (Monteith et al., 2005).

In addition to direct CO_2 emissions from the utilisation of BOD, nutrient removal may also generate GHG emissions (Sweetapple, 2014). For example, the CO_2 emissions from denitrification processes in the activated sludge reactors can be estimated similarly, by assuming complete denitrification, using a stoichiometry approach (Shahabadi et al., 2010). The emission factor based on the stoichiometry approach is 2.62 kg CO_2 per kg N-nitrate and 2.81 kg CO_2 per kg N-nitrite from the denitrification processes (Shahabadi et al., 2010).

The other potent GHG emitted directly from wastewater treatment is nitrous oxide (N_2O) (Foley et al., 2015). The degradation of nitrogen components within the wastewater results in the formation of N_2O (IPCC, 2013). However, the emission of N_2O from WWTPs reported so far is highly variable, for example, based on site measurement the N_2O emission can vary from 0.0001 to 0.112 kg N_2O per kg of the influent Total Kjeldahl Nitrogen (TKN) (Foley et al., 2015). There is variation not only in the measured amount of N_2O but also a source of N_2O. Most researchers agree on the fact that most of the N_2O emission comes from aerobic zones and the production of N_2O from anoxic zones is still unclear (Ahn et al., 2010; Campos et al., 2016). Foley et al. (2015), based on their pilot scale monitoring, argues that N_2O production is mainly from aerobic zones because of nitrification processes compared to the N_2O production from denitrification. Accumulation of NO_2^- in the aeration zone results in the formation of N_2O mainly due to the following three reasons; low oxygen level in aeration zones, sudden changes in ammonia load, and higher temperature (Foley et al., 2015). On the other hand, Boiocchi et al. (2017) argue that, in addition to poor aeration in the

aerobic zones, high oxygen supply can also result in N_2O emission through the inhibition of heterotrophic denitrification resulting in an incomplete deduction of NO_x. In contrast, Gupta and Singh (2012) argue that N_2O is mostly associated with denitrification process in the anoxic zone.

Recently various attempts have been made to estimate the emission of N_2O from WWTPs (Hiatt and Grady, 2008; Flores-Alsina et al., 2011). However, not all considered all the possible N_2O production paths. Ni et al. (2013) reviewed four existing models (Ni et al., 2011; Mampaey et al., 2013; Law et al., 2012; Yu et al., 2010) in simulating N_2O by ammonia-oxidising bacteria (AOB). They found out that none-of these models could reproduce the measured N_2O, suggesting the need for a consensus and a unified model to capture the interaction between different N_2O production pathways. For example, the Activated Sludge Model for Nitrogen (ASMN) (Hiatt and Grady, 2008) N_2O emission model, which was integrated into the BSM2 (Flores-Alsina et al., 2011) only considers the denitrification process as a source of N_2O emissions. Samie et al. (2011) modified the ASMN model from a one-step process into a four-step denitrification process to enable the production of N_2O at different stages, which is latter adopted by Sweetapple (2014).

Indirect GHG emissions include emissions associated with the use of energy, chemicals or embodied carbon, reactor effluent, and sludge transportation or solid waste disposal (Sweetapple, 2014).

One of the obvious sources of indirect GHG is the use of energy within the WWTPs. The estimation of CO_2 emissions from power generation depends on the source of energy; however, electricity power generation can have various sources which can have different emission conversion factor. Regardless of this variation, the common approach used to estimate this emission is the use of a fixed emission factor, (kg CO_2 kWh^{-1}) (Monteith et al., 2005; Shahabadi et al., 2010; Sweetapple, 2014). For simplicity, these emission factors are taken as the national average, (Sweetapple, 2014). For example, based on typical UK power generation mix the emission factor is suggested to be 0.4622 kg CO_2 kWh^{-1} (DEFRA, 2015).

Estimation of individual processes within the WWTP is essential in the evaluation of control strategies and selection of interventions (Shahabadi et al., 2010;

Lindblom et al., 2016; Magnus et al., 2016; de Faria et al., 2015). One of the most energy intensive processes within activated sludge WWTPs is aeration (Sharma et al., 2011; Mamais et al., 2015; Stenstrom and Rosso, 2008). Cakir and Stenstrom (2005) and Jeppsson et al. (2007) assumes a linear relationship between oxygen requirement in the reactor and the energy demand. They used an aeration efficiency kg O_2 kWh^{-1}, which is later adopted in BSM-e model (Sweetapple et al., 2014). Rosso et al. (2008) gave a detailed analysis of aeration efficiency for fine and coarse bubble diffusers and showed that this efficiency declines through aging and bacterial fouling.

Other energy uses within the WWTP includes pumping and mixing which can be estimated using their operational conditions, the operating power, and efficiency (De Keyser et al., 2014; Ragazzo et al., 2013; Hreiz et al., 2015). Sweetapple et al. (2014) and Jeppsson et al. (2007) presented a surrogate model for estimating energy is by pumps which deploy a linear relationship between energy use and flowrate of wastewater pumped. The approach assumes pump efficiency to be constant and independent of the flowrate. However, pump efficiency varies based on flowrate, and their efficiency considerably deteriorates if loading is reduced by 25 % or lower (Henderson and Reardon, 2004; Monteith et al., 2007) cited in (De Keyser et al., 2014). Since pumping is mostly the second energy intensive process in WWTPs, a less-simplified and non-linear approach can help in accurately estimating the energy saving that can be done through operational changes and pump replacements (De Keyser et al., 2014).

There are other commercial WWTP models available developed for various purposes. The BSM2e suits this study due to its consideration of various GHG emissions including N_2O. The source code is open for users which gives significant flexibility in modifying model blocks and implementing control strategies. Although some of the commercial models such as GPS-X, WEST and SIMBA can be used for testing control strategies, the activated sludge model included within these simulators does not consider the four-step denitrification process for an accurate modelling of GHG emissions (Makinia, 2010). Other simulators such as STOAT and AQUASIM, unlike BSM2, are close models where only pre-defined compartment models within the simulator can be used (Schütze et al., 2011).

2.2.1.2. BSM2-e for Modelling GHG Emissions

Recently, due to increased awareness and stricter regulations, GHG emissions from WWTP various modelling tools have been proposed; however, most of them are associated with a degree of uncertainty (Sweetapple et al., 2013; Mannina et al., 2016). These uncertainties mostly come from lack of accuracy in characterising the influent wastewater (for example biodegradable organic matters or C/N ratio) (Corominas et al., 2012), not-fully-understood N_2O emission mechanisms (Mannina et al., 2016; Foley et al., 2015; Flores-Alsina et al., 2014a), and accuracy in representing temporal variation (Corominas et al., 2012).

Generally, the trend shows that GHG emissions modelling is moving from an empirical approach towards comprehensive and more complex process-based models (Mannina et al., 2016). Corominas et al. (2012) showed the advantage of using process-based GHG emissions modelling approaches, especially to evaluate better and reduce uncertainty.

One of the most commonly used WWTP GHG emission modelling tools is BSM2G. BSM2G is a version of the Bench Mark Simulation Model No. 2 (BSM2) where the International Water Association (IWA) task group activated sludge model (ASM1) is replaced with Activated sludge model for nitrogen (ASMN) (Hiatt and Grady, 2008). ASMN includes simulation of N_2O production in addition to direct CO_2 emissions (Corominas et al., 2012). ASMN considers two nitrifying populations Ammonia-nitrifying bacteria (AOB) and Nitrite-oxidising bacteria (NOB). The approach is based on the theory that AOB utilises free ammonia and NOB utilises nitrous acid (Hiatt and Grady, 2008).

Extending the ASM1 to ASMN (Hiatt and Grady, 2008) for modelling production of N_2O formation suffers from errors within the model structure as identified by Corominas et al. (2012); Ni et al. (2013), and Snip et al. (2014). Sweetapple (2014) modifies the BSM2 (Jeppsson et al., 2007) and developed BSM2-e to simulate the production of N_2O from a four-step denitrification process based on the approach outlined by Samie et al. (2011). Unlike the BSM2G, BSM2-e incorporates four-step denitrification and stripping of N_2O using Henry's law. BSM2-e has been adopted by Sweetapple et al. (2014) for assessing multi-objective optimisation for implementing plant wide control strategies. The model is setup within the BSM2 environment using the layout of the Ludzack-Ettinger configuration of the activated sludge system (Jeppsson et al., 2007). The plant

wide BSM2-e model has shown promising results in trading of objectives through optimisation of control strategies, but this modelling is not yet applied to real case scenarios, and its simulation performance is not tested using measured dataset.

2.2.2. Sewer Network, WWTP Influent, and Influent Generators

GHG emissions from integrated urban wastewater systems are generated from the WWTP, the sewer network and the receiving water body. Although there are attempts to estimate GHG from WWTP, the estimation of GHG emissions from sewer networks and receiving water body is still not well understood (Mannina et al., 2018). Some studies showed that there is a considerable amount of CH_4 production/emission in the sewer network which usually correlates with the hydraulic retention time (Guisasola et al., 2008). To fully understand such processes, it is required to develop a detailed model which can be simplified later for integration and simulation speed (Mannina et al., 2018). Estimating GHG emission from sewer networks and rivers is out of the scope of this project but understanding the interaction of these UWWSs' components with WWTPs is essential to estimate GHG emissions from the WWTPs accurately. For example, Activated Sludge Models have been used for simulation-based studies of WWTPs without considering the sewer network (Gernaey et al., 2011), which means usually the simulations run for a short period of time due to the demanding data campaigning to get a continuous measurement of influent flow and pollutant concentrations for a long period (Rieger et al., 2010; Gernaey et al., 2011).

There is a consensus that one or two weeks' data is not sufficient to evaluate wastewater treatment plant performances in assessing control strategies. The main reason has been the existence of slow actuators which take a long time to respond, e.g. control of sludge waste flowrate (Gernaey et al., 2005a). In integrated control approaches, the receiving water response can be very slow and seasonally varying control strategies may be of interest. In such situations, it is important to assess strategies for at least for one year (Olsson et al., 2005; Butler and Schütze, 2005).

This high cost (both regarding workload and financial resources) related to the need for an extended dynamic influent data monitoring is one of the main reasons in limiting the application of WWTP models for an extended (Martin and Vanrolleghem, 2014). However, by using a sewer network models capable of generating influent to the WWTP for an extended period, at least for a year, is

desirable. The general approach in generating influent data for WWTP modelling is to perform a data monitoring campaign, usually for two weeks or more to characterise the influent wastewater, and develop typical patters and generating new dataset on that basis (Martin and Vanrolleghem, 2014).

Martin and Vanrolleghem (2014) classified existing solutions for characterising wastewater influent in situations where there is no complete quantity and quality data available. The first solution was based on the use of existing/literature data interpretations to create typical patterns (De Keyser et al., 2010; Devisscher et al., 2006). The second solution was the use of harmonic series or Fourier-based models to describe wastewater patterns especially in the dry season (Mannina et al., 2011; Langergraber et al., 2008). The third solution was based on the analysis of the wastewater generation mechanism. This can mean, using physically-based or mechanistic models, by considering the influence of rainfall, soil/infiltration, catchment area and type, population activity, industrial discharge, sewer length, and so on, but this can be challenging and costly to be accurately simulated using process-based or deterministic models. Instead, simplified models such as the phenomenological models (Gernaey et al., 2011), which can represent the observed wastewater patterns without going into the detail of the underlying generating mechanism is an alternative solution (Martin and Vanrolleghem, 2014).

There are several techniques used to characterise, estimate and generate wastewater flow and pollutant load; some at the source of the wastewater (Butler, 1991; Butler, 1993; Butler et al., 1995; Friedler et al., 1996; Friedler and Butler, 1996; Almeida et al., 1999), some within the sewer network (Ort et al., 2005; Rodríguez et al., 2013), and some at the influent point of WWTPs (Bott and Parker, 2011; Mhlanga and Brouckaert, 2013; Schilperoort, 2011). The patterns observed at the source may experience considerable change due to either retention or biological processes within the sewer network and/or due to different pumping schedules within the sewer network. A literature search showed that most recent studies coming out focuses on characterisation of the influent wastewater at the inlet of WWTPs (Wang et al., 2017; Mhlanga and Brouckaert, 2013).

Gernaey et al. (2011) developed an influent generator with the objective in balancing the trade-off among reducing the number of measured parameters,

reducing empirical approaches (increasing number of parameters with physical meanings), and flexibility regarding integration and modification by users. The approach uses a typical flowrate and pollutant concentration from domestic and industrial wastewater over a typical week. It uses a simple capacity-based surface runoff generation process coupled with a water-balance approach to estimate sub-surface flows and infiltration into sewer networks. It assumes no biological processes occur in the sewer network due to the less-understood biochemical processes in these sub-systems (Baban and Talinli, 2009).

Flores-Alsina et al. (2014c) demonstrate the full-scale feasibility of the phenomenological influent generator developed by Gernaey et al. (2011) through calibrating and validating the approach for two Scandinavian WWTPs for two years. Although they did not use a statistical measure to show the accuracy or predictive capability of the approach, their graphical analysis showed a good prediction capability and a reliable flow, temperature, and pollutant concentration generation. They also showed the ability of the model to assess different scenarios such as a change in rainfall pattern because of climate change and change in the composition of domestic and industrial wastewater, i.e. uncertainty in the fractionation of organic matter in the influent wastewater.

Later, Snip et al. (2016) use the BSM2 influent generator (Gernaey et al., 2011) to create realistic dynamic influent pollutant disturbance scenarios to understand the fate of micropollutants (three pharmaceutical compounds) in WWTPs. They showed that the BSM2 influent generator could simulate the dynamics of both the common BSM2 variables and the three additional micropollutants as well. Similar to Flores-Alsina et al. (2014c), the graphical analysis (Snip et al., 2016) showed that the influent generator simulates the temperature, NH_4, and COD concentration close to the measured values although the capability at higher COD and NH_4 values was not as good as it is at lower values.

The phenomenological wastewater generator model for BSM2 (Gernaey et al., 2011) is developed taking into account process control and optimisation and showed a good compromise between cost and model accuracy. It is an ‘open source’, i.e. users can modify the original structure to customise the model for a specific study area in hand without limitation. This approach is flexible, near-to-reality, and can easily be linked to BSM2 (Jeppsson et al., 2007).

2.2.3. River water quality models as part of an integrated UWWS

Several studies have been conducted to assess and understand the impact of point sources such as effluent from WWTPs and CSOs on the quality of receiving water bodies, mainly rivers (Ferreira et al., 2011; Candela et al., 2012; Brion et al., 2015; Riechel et al., 2016; König et al., 2017). To fully assess and understand the interactions among the components of urban wastewater systems (UWWS), Figure 2-5, it is essential to treat the entire system in an integrated manner (Rauch et al., 2002; Freni et al., 2011; Schütze et al., 2011; Benedetti et al., 2013; Bach et al., 2014). Peña-Guzmán et al. (2017) showed how complex the UWWS can be and that some of the models suggested so far differs significantly depending on their scopes and boundaries. Bach et al. (2014) give a clear definition and classification of integrated UWWS models based on their scope:

- Integrated Component-based Models (ICBMs): covers the integration of process units within components of the UWWS (e.g. WWTP wide models)
- Integrated Urban Drainage Models (IUDMs): system-wide models that cover urban drainage systems and receiving water
- Integrated Urban Water Cycle Models (IUWCMs); Links the urban drainage systems with the water supply system that shares the same receiving water body or water supply river.
- Integrated Urban Water Systems models (IUWSMs): the highest level of integration where the total water system is integrated on a basin-scale and at a multi-disciplinary level

The scope of the project in this study focuses on the urban wastewater system, and the next paragraphs will focus on IUDMs that integrate WWTPs, sewer systems (storm and wastewater), and the receiving river (simulation of catchment drainage to quantify runoff and pollution) (Bach et al., 2014).

IUDMs can be complex and, depending on their application; their modelling approach varies from complex mechanistic/physically-based models to simple conceptual or empirical models (Freni et al., 2011). The main driver for the need towards simplified conceptual models is the need to reduce the demanding computational nature of mechanistic models and due to their costly need for data to cover both spatial and temporal variations while reducing uncertainties (Fu et al., 2009; Asher et al., 2015). Conceptual models simplify the complex model either by using a hierarchical approach that simplifies the physical process

(ignoring or aggregating processes) or through reducing the number of parameters and their space through projection or using data-driven approximation (Asher et al., 2015). Since one of the objectives of this project is to investigate the advantage of system optimisation, which requires running several simulations, it is essential to choose modelling approaches that are not computationally demanding. The next section assesses the suitability of data-driven models for such applications.

2.2.3.1. Data-driven models

Data-driven models (DDMs) are those that are structured, built and updated based on available data/information about the system (García et al., 2015). In modelling practice, data reconciliation and identification of parameters is an important step to represent the modelled system as accurately as possible (Solomatine and Ostfeld, 2008). However, in the UWWS, in most cases, parameters that are monitored by different stakeholders within the systems do not match and mostly not sufficient to the requirement of a mechanistic model (Sharma and Kansal, 2012). For example, Kannel et al. (2011) compared mechanistic water quality models, such as QUAL2Kw, QUAL2EU, QUASAR, and WASP7, with conceptual models such as SIMCAT (Warn, 1987) and TOMCAT (Brown, 1986). They pointed out that these conceptual DDMs can run with limited data but much quicker than that of the mechanistic ones but with the cost of over-simplification, in this case.

The application of process-based models in real-time control studies is limited mainly due to their set-up and the computationally intensive simulation to be used in multiple simulation problems such as optimisation (Bermúdez et al., 2018). One suggestion is to use data-driven models. Data-driven modelling techniques include; Artificial Neural Networks (ANN), genetic programming, evolutionary polynomial regression, support vector machines, linear regression, and so on. The most commonly used DDMs are ANNs both with in the UWWSs and other disciplines (Corzo et al., 2009; Duncan et al., 2013; Srivastava and Singh, 2014; Kalantar et al., 2017; Amita et al., 2016). For example, within the UWWS, ANNs has been used in early warning systems for prediction of combined sewer overflow (CSO), urban flooding, and river quality hazards (Mounce et al., 2014; Duncan et al., 2013; ten Veldhuis and Tait, 2011). These models showed good accuracy and flexibility, for example, under 5 % of error in model accuracy is

reported in Mounce et al. (2014) in their ANN model that simulates sewer overflow.

DDMs have also been used to increase the performance of process-based models. For example, Corzo et al. (2009) used the IHMS-HBV hydrological model, which is mainly used for forecasting and modelling data-scarce catchments, and replaced the sub-basin model component with ANN in order to increase overall model accuracy. In another case, Mekonnen et al. (2015) fused the process-based model Soil and Water Assessment Tool (SWAT) with ANN so that the ANN model can deal with non-contributing areas and improve overall model capabilities.

Similarly, Dickinson (2018) used a single layer ANN to simulate CSOs integrated with a more complex auto regression based multi-layer ANN to simulate rainfall-runoff generation coupled with a mechanistic (process-based) river water quality and routing model. Dickinson (2018)'s approach gave an accurate model by utilising existing dataset and by designing additional monitoring the CSOs water level upstream of weir, river ammonia concentration, and river dissolved oxygen level. The approach used measured rainfall data as an input but can be replaced with radar data for forecasting capability. The approach can be linked to the ASM1 based WWTP scale model, such as BSM2, by converting the BOD based state variables used in Dickinson (2018). The model outputs include the assimilative capacity of receiving river, an optimisation approach to estimate the available capacity for WWTP effluent, and river flow and quality indicators, such as nitrogenous BOD, BOD, DO, and temperature.

The river model presented by Dickinson (2018) uses a fixed high constant flow rate for the WWTP final effluent to calculate the allowable pollutant concentration without violating NBOD, BOD and DO. Such an approach does not consider the fluctuation of flow in the final effluent and under estimate the assimilative capacity of the river. It is evident that this section of the river model should be modified during the integration process, for example, by directly estimating the river quality downstream of the final effluent point. Hence, instead of calculating the allowable pollutant load from the final effluent, it is recommended to consider the river as an integral part of the UWWS and control WWT processes based on the river quality downstream of the final effluent point.

2.3. Wastewater Treatment Regulations

There are various legislations and regulations governing the water/wastewater industry in the UK. The sector is under stringent and contradicting regulations. The main drivers of these legislations can be classified as the water environment quality and quantity, water use or demand management, GHG emissions, and economic point of view (Georges et al., 2009).

Reduction of GHG emission is one of the ways to mitigate the changing climate since the human factor is the major reason for the recent increase in global surface temperature (IPCC, 2013). Carbon Reduction Commitment (CRC) announced in Energy White Paper of 2007: Emission reduction target 4 Mt CO_2 per year by 2020 from large non-energy intensive businesses, which are classified based on their half-hourly monitored consumption >6,000 MWh per year; Water companies fall into this category. The Climate Change Act for Scotland (CC-Scotland-Act, 2009) sets an overall target of 42 % reduction in CO_2 emission by 2020 and 80 % reduction in GHG emissions by 2050 against the 1990 baseline.

Also, a renewable energy source is encouraged, and an incentive is put in place. However, the five-year financial plan of the water industry in the UK made this incentive impracticable. For example, rising energy prices and the CRC are both encouraging reductions in energy use and hence may help reduce carbon emissions. However, without sufficient cost savings, the capital investment in renewable energy sources may not be recouped within the five-year asset management plan/periodic review period (Georges et al., 2009).

The other legislation driven by the economy and sustainable use of resources is the Renewables Obligation Certificate (ROC), which is a certificate issued to operators, in the UK, of accredited renewable electricity projects for the eligible renewable electricity they generate (Woodman and Mitchell, 2011). The order requires all electricity suppliers to provide a percentage of their electricity from renewable sources. This percentage is incremental to encourage continued growth. Where the supplier does not generate sufficient renewable energy, a 'buy out' payment is made; it is this fund of money that is made available for the purchase of ROCs. The income generated, in addition to any value, is for the sale of electricity (Woodman and Mitchell, 2011). The electricity generated from

sewage gas is combined heat and power (CHP) with a ROC value of 0.5 ROC MWh^{-1} (Georges et al., 2009). Other forms of renewable energy sources that can be used by the wastewater industry include advanced anaerobic digestion, co-digestion of food from local food waste, hydropower, wind power, solar energy, and so on.

In addition to the Renewables Obligation, the demand management side of things focuses on the reduction of consumption, tackling pollutants at source, and promotion of Sustainable Urban Drainage systems (SUDS). For example, in England and Wales (DEFRA, 2008) with an emphasis on climate change and mitigation targets the reduction of water consumption 150 to 130 litres per capita per day by 2030. It also promotes the use of SUDs to reduce storm flows entering into sewer networks and ultimately the receiving water (DEFRA, 2008).

The main driver of regulations in the water sector in the UK is the reduction of pollution to the water environment (Meng et al., 2016) and is governed by number of directives; Urban Waste Water Treatment Directive (UWWTD), Bathing Water Directive (BWD), the Water Framework Directive (WFD), Water Industry Act (WIA) which is amended by Water Act 2014 for England and Wales, Water Industry Commission for Scotland (WICS), Habitat Directives (HD), Natural England, Natural Resource Wales, Scottish Natural Heritage, English Heritage, and so on.

The EU WFD, (2000/60/E), is the most influential water legislation produced by the European Commission, for achieving sustainable management of the water environment in the UK and the other Member States. The Directive requires the member states to aim to achieve at least a ‘good’ environmental status by defining and implementing the necessary measures. It establishes a framework where state members obliged to adopt to assure:

- Avoidance of long-term deterioration of freshwater quality and groundwater pollution through progressive reduction of emissions of hazardous substances to water
- Environmental damage is a priority and polluters should pay approach to apply at source solutions
- Integration of water environment management with other policy areas such as energy, agriculture, fisheries, transport, regional policies and tourism

- Protection of aquatic ecosystems near the cost and estuaries or in gulfs which are strongly influenced by the quality of inland waters and so on

The WFD (CEC, 2000) entered into force in 2000 giving three years for member states to get prepared such as interpreting requirements to national legislations and define river basin districts and authorities. It gives further six years to analyse issues and prepare the River Basin Management Plans (RBMP), and an additional three years for implementation of measures based on RBMPs, i.e. until 2012. After the implementation of measures, the framework gives three years to achieve objectives. After 2015 the member states should have a six years' planning, consultation and implementation cycles until 2027 to make sure environmental objectives defined in the RBMPs are met.

2.3.1. Implementation of WFD in Scotland: Focusing on Wastewater

The Scotland River Basin District Direction (SRBDD) is a direction produced by the Scottish Government to the Scottish Environmental Protection Agency (SEPA) which came to force in 2013. The Direction has two section standards and status. The standards direction outlines criteria for classifying the type of a body of water to determine the required environmental standards, condition limits, threshold values for different pollutants and hazardous substances (SRBDD, 2014a). The status direction, on the other hand, outlines how the status of a water body should be identified including surface water, artificial or heavily modified water body, and groundwater (SRBDD, 2014b).

Based on the SRBDD Scottish River Basin Management Plan is a basin management plan that specifies environmental objectives, identify pressure on the water environment (both water quality and physical conditions), how to tackle these pressures, and assess status in the previous cycle.

Scottish Environment Protection Agency (SEPA) is the body that regulates different activities that may pollute the water environment, air and land. The duties of this regulatory body include:

i. assign a Type/Types to each river
ii. apply environmental standards to each river
iii. calculate morphological condition values for the relevant features of each river

iv. provide condition limits

v. apply spatial environmental standards for assessing the ecological status of surface water

vi. apply the environmental standards for certain dangerous chemicals

SEPA issues the water environment Controlled Activities Regulations (CAR) to make sure discharges from sewer networks and WWTPs to surface water do not deteriorate the water environment. CAR licenses are issued for each WWTP based on the standards of the receiving river and the target status, which includes setting effluent pollutant concentration limits, minimum flowrate to bypass flow during storm events. These licenses are prepared by integrating the SRBDD and the UWWTD. UWWTD (CEC, 1991) is put in place to ensure the appropriate treatment of wastewater before discharging to the environment to protect human health and the environment (Maere et al., 2016). The directive sets out EU-wide rules for collection, treatment and wastewater discharge. The next section covers how the standards for receiving rivers is determined based on the SRBDD.

2.3.2. Receiving Water Body Standards

The standards for surface water is the target for estimating the assimilative capacity of the receiving water to accept pollutants, which is later used in this thesis for controlling operations in WWTPs.

2.3.2.1. *Criteria for Classifying River Types*

Rivers to which DO, BOD, and ammonia standards apply to are classified into seven types, Table 2-1, based on site altitude and alkalinity of the river (mg L^{-1} $CaCO_3$) (SRBDD, 2014). For example, for the case study used in this study, the River Eden, it has alkalinity, on average, varying from 110 to 134 mg L^{-1} of $CaCO_3$, (ECN, 2005). The average elevation of the Eden Catchment is below 80 m above mean sea level, based on Digital Elevation Model (DEM) data [source]. Hence, based on these information and classification table below the River Eden is classified as type 5. Note, this classification is not cross-checked with SEPA.

Table 2-1 Criteria for identifying the types of river to which DO, BOD and ammonia standards for river apply: Source (SRBDD, 2014a)

<table>
<tr><td rowspan="2"></td><td colspan="5">Alkalinity (mg L^{-1} $CaCO_3$)</td></tr>
<tr><td>Site altitude</td><td>≤ 10</td><td>>10 to ≤50</td><td>>50 to ≤100</td><td>>100 to ≤200</td><td>>200</td></tr>
<tr><td>≤ 80m above mean sea level</td><td rowspan="2">Type 1</td><td rowspan="2">Type 2</td><td>Type 3</td><td>Type 5</td><td rowspan="2">Type 7</td></tr>
<tr><td>> 80m above mean sea level</td><td>Type 4</td><td>Type 6</td></tr>
</table>

Table 2-2 Annual average alkalinity of the River Eden: Source (ECN, 2005)

Year	1994	1995	1996	1997	1998	1999	2000	2001	2002	2003
Annual mean Alkalinity ($CaCO_3$) [mg L^{-1}]	117.7	124.8	114.3	119.1	114.6	121.7	121	126.7	110.1	133.8

If the river supports salmon fish species, it should be classified as 'Salmonid', and if it supports cyprinid fish, but not salmonid fish, it should be classified as 'Cryprind'. In addition to classifying rivers based on species they support, the environmental standards for river flow apply based on average annual rainfall, base flow index and, and catchment area. Based on this classification there are six types of rivers (A1, A2, B1, B2, C2, and D2). Rivers to which the morphological condition limits apply to are classified into five types (A, B, C, D, and F) mainly based on channel characteristics, valley form, channel slope, sinuosity (ratio of stream length to valley length), dominant geologic formation and channel bed characteristics. In addition, if acidity environmental standard is applied, based on dissolved Organic Carbon (OC) concentration, the river can be classified as 'clear' water (< 10 mg L^{-1} of OC) or 'humic' water (≥ 10 mg L^{-1} of OC).

2.3.2.2. Biological Environmental-Standards

The environmental standards are classified as biological environmental-standards, hydro-morphological environmental standards, and chemical and physicochemical environmental standards (SRBDD, 2014a).

The biological environmental standards classify rivers as 'high', 'good', 'moderate' or 'poor' based on the benthic zone invertebrate fauna standards using both the Water Framework Directive - United Kingdom Technical Advisory Group (WFD-UKTAG) classification method known as "Invertebrates (General Degradation): Whalley, Hawkes, Paisley and Trigg (WHPT) metric in River Invertebrate Classification Tool (RICT) and the WFD Acid Water Indicator Community method", aquatic macrophyte standards, phytobenthic standards, impact on the phytobenthic community, and fish fauna standards.

2.3.2.3. Hydromorphological Environmental Standards

Hydromorphological environmental standards classify rivers as 'high', 'good', 'moderate', or 'poor' for those river types to which DO, BOD, and ammonia standards apply to and for those classified based on the presence of macrophyte communities as well; A1, A2, B1, B2, C1, C2, D1 and D2. The hydro-

morphological environmental standards are defined mainly based on the river types, the maximum permitted total abstraction per day as a proportion of daily natural flow, and the location of the stream; either headwater or downstream (SRBDD, 2014a).

2.3.2.4. Chemical and Physicochemical Environmental Standards for Rivers

SRBDD (2014a) classifies a river as 'high', 'good', 'moderate' and 'poor' for each physiochemical characteristic indicator; DO, BOD, phosphorus, temperature, pH, and acid neutralising capacity (ANC).

If a river is classified based on its altitude and alkalinity concentration as shown in Table 2-1, the river must be classified as 'high', 'good', 'moderate', or 'poor' based on the dissolved oxygen level. The percentage oxygen saturation is defined as the ratio of the concentration of dissolved oxygen in the water to the maximum amount of oxygen that can dissolve in the water at that temperature, pressure and ionic concentration of the water. Since the ability of oxygen to dissolve in water depends on these factors, the percentage saturation is used as a quality indicator instead of the dissolved oxygen concentration in the river. Supersaturation can occur when the water holds more oxygen molecules than usual for a given temperature, i.e. percentage saturation is higher than100 %. For example, sunny days with abundant photosynthesis or turbulent water conditions can result in a supersaturation. The 10-percentile value refers to the value of the percentage oxygen saturation which is exceeded by 90 % of the data points, Table 2-3.

Table 2-3 Dissolved oxygen standards for rivers (SRBDD, 2014a)

Percentage oxygen saturation as 10-percentile values				
River type	High	Good	Moderate	Poor
1, 2, 4, and 6 and Salmonid	80	75	64	50
3, 5, and 7	70	**60**	54	45

Biochemical Oxygen Demand (BOD) concentration are used together with the river type to classify the river as 'high', 'good', 'moderate', and 'poor', Table 2-4 and Table 2-5. This approach is used for chemical status classification, and the directive suggests not to use this classification for the ecological status of the river.

Table 2-4 Standards for BOD (mg L^{-1})for rivers (SRBDD, 2014a)

Biochemical oxygen demand (BOD) 90-percentile values (mg L^{-1})				
River type	High	Good	Moderate	Poor
1, 2, 4, and 6 and Salmonid	3	4	6	7.5
3, 5, and 7	4	**5**	6.5	9

Table 2-5 Standards for BOD (mg L^{-1}) in rivers for short-term and intermittent changes in BOD (SRBDD, 2014a)

Biochemical oxygen demand (BOD) 99-percentile values (mg L^{-1})				
River type	High	Good	Moderate	Poor
1, 2, 4, and 6	7	9	14	16
3, 5, and 7	9	**11**	14	19

Reactive phosphorus concentration, the concentration of phosphorus determined using the phosphor-molybdenum blue colorimetric method, is used to classify the river as ‘high’, ‘good’, ‘moderate’, or ‘poor’ regarding phosphorus concentration. However, phosphorous is out of the scope of the project and is not discussed further.

Specific pollutant environmental-standards include ammonia concentration, which limit is defined based on the type of the receiving water body, Table 2-6. The 99-percentile limit is 0.4 mg L^{-1} regardless of the river type (SRBDD, 2014a).

Table 2-6 Standards for total ammonia (mg L^{-1}) in river as 90 percentile values (SRBDD, 2014a)

Total ammonia (NH_3-N) mg L^{-1} as 90 - percentile values				
River type	High	Good	Moderate	Poor
1, 2, 4, and 6	0.2	0.3	0.75	1.1
3, 5, and 7	0.3	**0.6**	1.1	2.5

Due to their quantitative approach of current regulatory systems and the fact that physiochemical parameters can be monitored/sampled and analysed more quickly than the biotic or response-based parameter they are used as the main quality indicators (Abbasi and Abbasi, 2012). They can be monitored continuously, which make them convenient to be used in the design and implementation of integrated active control strategies. In addition, the physiochemical quality approach can identify the cause or pollutant that causes stress in the biological system of the water body (Abbasi and Abbasi, 2011). This study uses the physiochemical quality indices for estimation the assimilative capacity of the river and determining the maximum load available for wastewater discharges.

2.3.3. Stringent Regulations and GHG Emissions

The tightening of licenses under the WFD due to higher environment quality standards (EQS) will make significant investment necessary at the WWTP unless effective measures are put in place (Guo et al., 2016). Water companies managing urban wastewater systems discharging to a receiving water body with a low assimilative capacity may end up investing more and end up contributing more GHG emission due to the higher EQS (Stamatelatou and Tsagarakis, 2015). Previously suggested measures include source control measures, investing in new and innovative technologies, and consumption management. WFD will inevitably increase GHG emissions from WWTPs, if alternative law-carbon treatment methods or catchment based solutions could be used to reduce or offset these emissions (Maere et al., 2016; Flores-Alsina et al., 2014a).

Georges et al. (2009) suggested strategies for the water companies to mitigate the potential carbon impact of legislations specifically WFD. They put forward the following strategies; source control of pollutants, the addition of least carbon processes, improved energy efficiency, redeveloping existing WWTPs, and generation of renewable energy. Georges et al. (2009) argue that greater carbon saving can be achieved through control of pollutants at the source; however, the water industry does not have direct control over these such as agricultural runoff and domestic sewage.

Greater operational efficiencies can reduce energy demand through optimisation of operations and managements in the UWWS and a better design of catchments at a wider scale. For example, Sweetapple et al. (2014) show the benefit of optimisation of operation procedures at WWTP to in reducing GHG emissions. Similarly, Thornton et al. (2010) show the benefit of automation and real-time control of WWTPs in reducing operational energy and chemical use.

Redeveloping existing treatment processes require switching conventional processes to lower energy alternatives (Castro-Barros et al., 2015) and a more cost-effective approach such as resource recovery and recycling schemes (Guest et al., 2009). Can reduce the effluent concentration to meet WFD and can reduce GHG emission as well but their capital investment is much higher than for example system optimisation and automation of processes control (Ocampo-Martinez, 2010).

2.3.4. Dynamic Licensing

Although the WFD promotes an integrated approach and the legislation is designed based on a holistic view, as discussed in Section 2.3.3, their interpretation and implementation are achieved through standards, licenses, permits, and compliance methods which resulted in separate management of each UWWS components (Maere et al., 2016). The current fixed licensing approach does not help the integration of these components. The fixed licensing approach tries to achieve the target 'status' of the receiving water by setting an effluent standard for WWTP discharges, regardless of the assimilative capacity of the river (Maere et al., 2016). The assimilative capacity of a river, in this study, is defined as the ability of the river to take pollutants without losing its 'good' status or any other desired status for that particular pollutant as defined in different directives such as SRBDD (2014b). The definition of the river's status and the maximum allowable pollutant concentration limit may vary based on the river classification as defined in directives such as SRBDD (2014a). However, to maintain the pollutant level in the receiving river below the maximum limit or even to use the assimilative capacity of the river with the aim of reducing GHG emissions from the WWTP, it is essential to revise the current fixed licensing approach (Meng et al., 2016).

Maere et al. (2016) assess the regulatory approaches that are in place in Europe, USA, and Canada focusing on the inhibition of innovation as a result of the local regulation structures. The study pointed out that the current discharge permit structures for nutrients should consider variability in the quality of receiving waters and reliability of the removal performance of WWTPs. The tight deadlines and inflexible local regulation structure inhibit the freedom in achieving the environmental goals through innovative approaches.

Similarly, Meng et al. (2016) assess the current fixed-license (end-of-pipe permitting) approach and recommends a receiving water quality based regulatory approach. Although such approaches are already in place in the UK, they are limited to the regulation of CSOs (Meng et al., 2016), i.e. the derivation of operational strategies to meet the receiving water quality standards. For such approaches to come into practice both the regulatory body and the water sector need to be engaged and committed to an integrated UWWS management and

use of comprehensive models. For example, Severn Trent Limited in the UK, through their carbon balancing and ecology programme, investigates the benefit of variable licensing, i.e. varying the effluent quality standard based on the seasonal variation of flow of the receiving river. Similarly, Scottish Water investigates the benefit of this approach through two trials by working closely with the regulatory body Scottish Environment Protection Agency (SEPA) to determine effluent standard based on river water level.

3 Cupar WWTP Modelling and Operation

Cupar wastewater treatment plant (WWTP) is located in the Eastern part of Cupar town, Fife, Scotland. The plant has a design capacity of 15,000 P.E. with the current load of 16,000 P.E or a dry weather flow (DWF) of 30 L s^{-1}. The treatment plant receives water from combined and separate sewer networks of Cupar town with different sub-catchments listed below, see Figure 3-1.

- South east area with a combined sewer system
- Barony area (south west) majority with only foul sewer serves mainly residential areas
- The area of Bonnygate in Cupar along St. Catherine Street in the west is fully combined and serves a mixed residential and commercial area
- The area of Lebanon with a partially separate system in the upstream part of the catchment lying to the north, although some areas are combined
- Braehead, a small residential area, located in the north east of Cupar have a combined sewer network
- Cupar Trading Estate (East of Cupar) commercial/industrial area with a separate sewer network

As the sewage passes through the works, it is treated using preliminary (screening and grit removal) and secondary treatment (activated sludge process) before the final effluent is discharged to the River Eden. The bypassed storm flow is diverted to two storm tanks on site. Any surplus sludge from the treatment process (together with sludge imported from other sites) is dewatered and thickened before being removed by road tanker to Drumshangie, located 57miles from Cupar wastewater treatment plant near Glasgow (per onsite recorded datasheet as of August 2014).

The incoming flow of sewage from Cupar sewer network enters the WWTP through an inlet chamber and passes to a band-screen. The screen can be bypassed via a bar hand raked screen during maintenance or emergency cases. The screenings are removed from the band screen by a wash compactor and transferred to the skip. Screened sewage passes under a weir and flows below 2.3 $\times$ DWF (69 L s^{-1}) flow to a grit trap. Following screening and de-gritting, the sewage gravitates into a wet-well from where it is pumped by three

duty/standby/assist pumps to the oxidation ditch for secondary treatment.

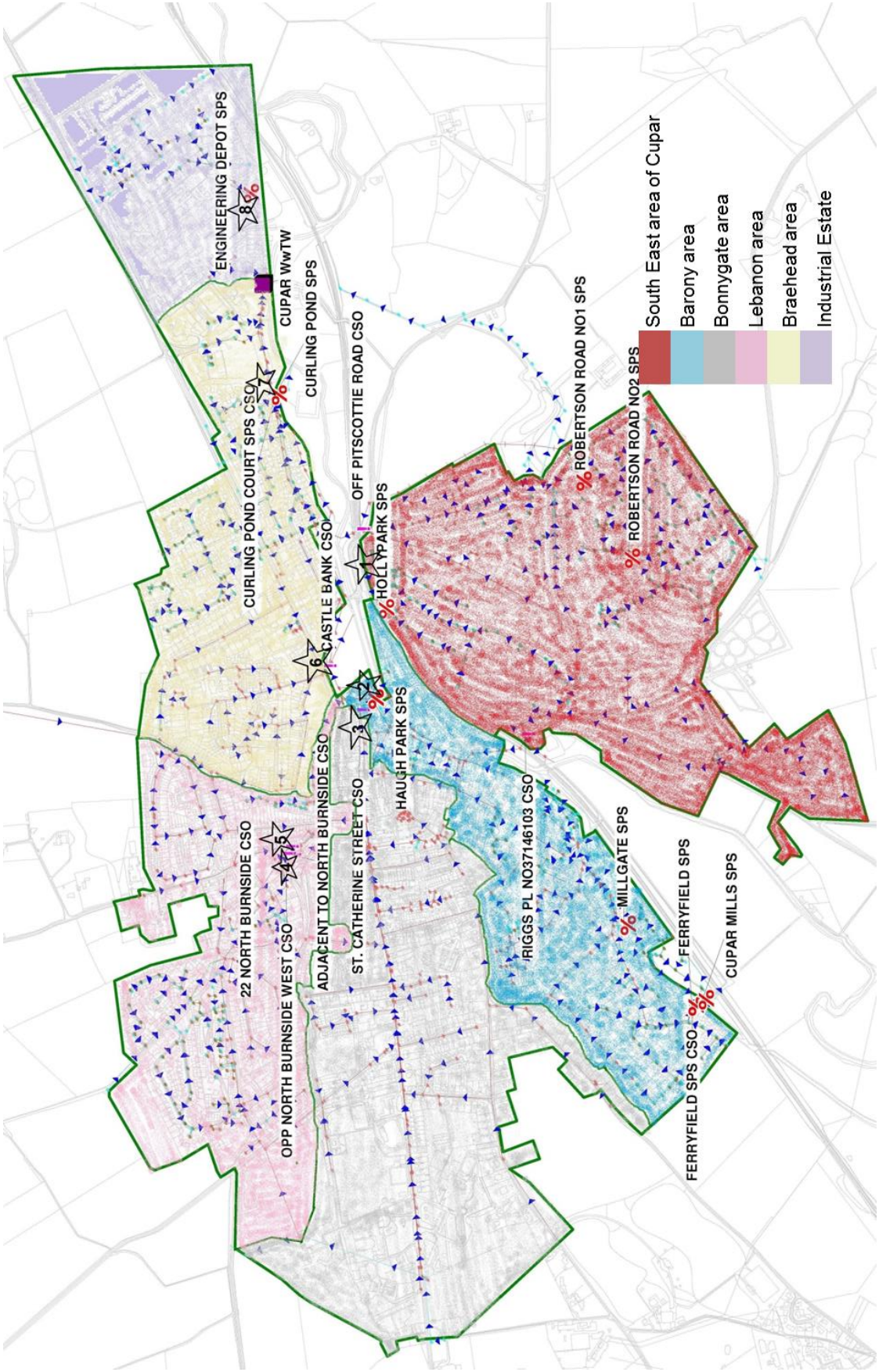

Figure 3-1 Cupar WWTP sewer catchment

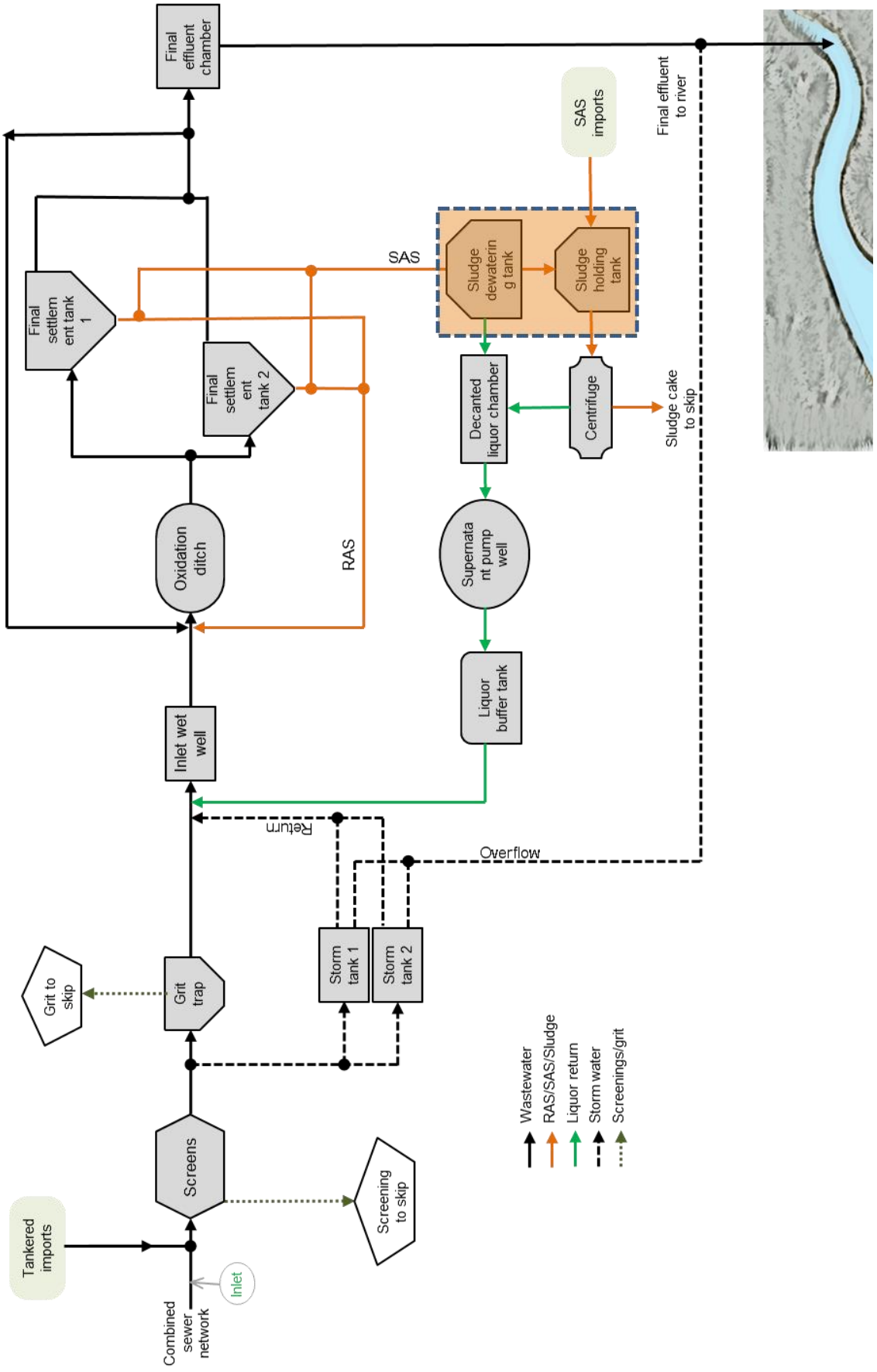

Figure 3-2 Cupar WWTP layout

Flow to full treatment through the works is limited to 69 L s^{-1} (2.3 $\times$ DWF) overflow at the inlet works. Excess storm flow passes into two horizontal storm tanks. Based on the water level in the inlet wet-well pumping station, the storm water in the tanks returns to the main treatment line.

The inlet wastewater combined with supernatant return and scum return flow is pumped from the inlet wet-well to the oxidation ditch. From the oxidation ditch, the biologically treated sewage (activated effluent) passes into the final settlement tanks. The final effluent from the settlement tank overflows a weir into an outlet channel from where it gravitates to a sampling chamber and is discharged into the River Eden. If the storm tanks are full, any overflow is combined with the final effluent and discharged into the River Eden.

Surplus Activated Sludge (SAS) is drawn off the final tank manually by a single SAS pump which discharges to the sludge dewatering tank on site. From the sludge dewatering tank, the sludge is pumped to the sludge-holding tank. The settled sludge passes to a centrifuge for dewatering. To aid dewatering, the sludge is dosed with a polyelectrolyte solution in the sludge centrifuge the dewatered sludge is deposited into a skip prior to being removed to a landfill. The supernatant from the sludge dewatering tank drains back into the inlet wet-well and combines with the incoming sewage.

In addition to treating sludge generated on site, Cupar WWTP also accepts sludge from tankers from Garbridge WWTP and occasionally from Strathmiglo WWTP and Bowhouse WWTP.

3.1. Preliminary Treatment: Component Description and Model Development

Large solids and grit can interfere with wastewater treatment (WWT) processes or cause undue mechanical wear. These solids are separated using a preliminary treatment such as screening, grit removal, flow equalisation and so on (US-EPA, 2003). The preliminary treatment at Cupar WWTP consists of screening, grit removal, inlet wet-well, and storm bypass penstock and tanks.

The transported wastewater from other WWTPs is discharged at the inlet, upstream of screening. Due to the unknown nature of the imported wastewater

and relatively smaller volume compared to the influent flow to Cupar WWTP, these import flows are not considered in the modelling approach.

Table 3-1 Intermittent wastewater import to Cupar WWTP for a typical month

Date	Sludge source Site	Discharge point	Type of wastewater	Volume (m^3)
03/01/2014	Pitscottie	Inlet	Top water	13
06/01/2014	Largoward	Inlet	co settled Humus or primary effluent	13
06/01/2014	Leuchars	Inlet	co settled Humus or primary effluent	13
06/01/2014	Valleyfield	Inlet	Grit	13
07/01/2014	Brunton	Inlet	Septic tank	26
13/01/2014	Leuchars	Inlet	co settled Humus or primary effluent	13
15/01/2014	Pumping Station	Inlet	Grit	1 tonne
16/01/2014	Pumping Station	Inlet	Rags	2 tonnes
20/01/2014	Leuchars	Inlet	co settled Humus or primary effluent	13
20/01/2014	Largoward	Inlet	co settled Humus or primary effluent	13
21/01/2014	Luthrie	Inlet	Septic tank	13
22/01/2014	Dairsie	Inlet	co settled Humus or primary effluent	13
23/01/2014	Pumping Station	Inlet	Grit	2.5 tonnes
27/01/2014	Leuchars	Inlet	co settled Humus or primary effluent	13
28/01/2014	Strathmiglo	Inlet	SAS	26
30/01/2014	Peat Inn	Inlet	Humus tank effluent	13
31/01/2014	Balmerino	Inlet	Septic tank	26
03/02/2014	Leuchars	Inlet	co settled Humus or primary effluent	13
03/02/2014	Largoward	Inlet	co settled Humus or primary effluent	13
04/02/2014	Pitscottie	Inlet	Top water	13
05/02/2014	Pumping Station	Inlet	Grit	0.25 tonnes
06/02/2014	Pitscottie	Inlet	Top water	26
10/02/2014	Leuchars	Inlet	co settled Humus or primary effluent	13
11/02/2014	Brunton	Inlet	Septic tank	26
12/02/2014	Pumping Station	Inlet	Grit	1 tonne

3.1.1 Screening


a)

b)

Figure 3-3: Screens at Cupar WWTP a) Online fine screen b) emergency bar screen

There is one online band-screen with a screen size of 6 mm equipped with wash compactor. There is an emergency bypass bar screen, see Figure 3-3. From the inlet chamber, the incoming flow passes through a band-screen where the separation of solids is carried out. To avoid clogging there is a subsequent washing and dewatering of the extracted screenings.

If the automatic screen fails, the incoming wastewater will be directed to a bypass channel containing a bar hand raked screen with a screen size of 25 mm. The larger solids and rags which become trapped on the bypass screen are removed manually by the operator. The screened wastewater drains into the main flow of sewage to the grit extraction unit.

3.1.1.1 Processes Control and Modelling

Under normal operation, the screen wash cycle operates automatically under a feedback loop from a differential level created by the ultrasonic level sensors upstream and downstream of the screens. The screenings from the emergency bypass screen are removed manually by the site operator.

Screening is not modelled as it does not involve biological processes or flow attenuation and the modelled influent does not include large solids.

3.1.2 Grit Extraction

Following the screening, only the 2.3 × DWF sewage is directed into a Pista Grit Detritor. As the sewage passes through the grit trap, sufficient retention time is given to allow the grit to settle, the settlement being assisted by the slowly rotating paddle. The settlement action is such that it permits only the heavier grit particles to settle, the lighter organic solids remaining in suspension and continuing for further treatment.

The settled grit retained in the base of the hopper is removed automatically by a timer initiating operation of the grit trap air compressor and wash-water. The compressor operates an air lift device, which draws up the settled grit from the base of the hopper and discharges it into an adjacent classifier. Prior to removal from the trap, the grit is partially cleaned by injecting it with a mixture of backwash water and compressed air. The washed grit is compressed and deposited into a waste skip.

3.1.2.1 Process Control and Modelling

The grit extractor controlled automatically, i.e. under normal operation, the settled grit is removed automatically by a timer initiating operation of the grit trap air blower. The grit classifier also controlled automatically on a timed basis to coincide with the operation of the air blower. The grit skip is removed by the disposal contractor as required.

Grit removals are usually put in place to remove heavy solids which may ultimately weir and damage processing units like pumps. Since there is no biological process or significant retention of sewage, the grit removal process was not modelled in this study.

3.1.3 Storm Bypass

Figure 3-4: Onsite storm tanks at Cupar WWTP

Following the online flow meter, the screened sewage before grit extractor passes through a 2.3 × DWF storm overflow weir. The Water Environment Controlled Activities Regulations (CAR) 2007 for Cupar WWTP in their authorisation notice stated that the bypass to the storm tanks could only consist of flow more than the pass-forward flow rate. Tha CAR license set the pass-forwared flow rate to 89 L s^{-1}, which consists of the maximum pass-forward flow to the inlet wet-well, 69 L s^{-1} (2.3 × DWF) and an average scum and supernatant return flow rate of 20 L s^{-1}. At the inlet penstoke, flows below 69 L s^{-1} will continue forward to the grit extractor. Whereas inlet flow more than 69 L s^{-1} passes over a weir into two onsite rectangular storm tanks, each with a maximum capacity of 686 m^3 (L × W × D = 30.5 m × 7.5 m × 3 m) (preliminary data sheet of Cupar WWTP prepared by Scottish Water Solutions). However, on days that the storm tanks observed to be overflowing, telemetry data showed that the storm tank level varies from 1.70 m to 1.76 m. This was crossed checked and confirmed during a site visit in August 2014 by physical measurement, and the current maximum depth of the storm tanks is 1.7 m. Hence, the current operating capacity of each storm tank is 389 m^3 (L × W × D = 30.5 m × 7.5 m × 1.7 m), with a total storm storage capacity of 778 m^3, two storm tanks.

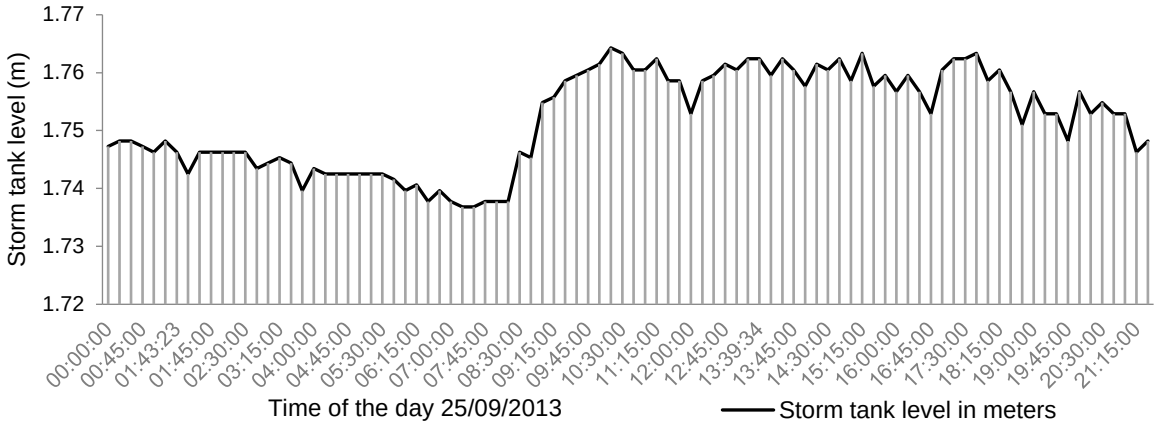

Figure 3-5: Storm tank level on a day that over-flow was observed (15 minutes dataset with some additional intermediate data points)

Based on the water level in the inlet wet-well pumping station, storm water will return from the storm tanks to the main treatment line. If the storm conditions persist and both storm tanks fill, the settled flow from the tanks will overflow into an outlet channel to be mixed with the final effluent and discharge by outfall into the River Eden.

3.1.3.1 Process Control

Control of the return flow from the storm tanks to the inlet wet-well structure is actuated as follows, based on Scottish-Water (2008). The valves controlling flow from the storm tanks to the inlet wet-well open when the assist pump in the inlet well is not operating, and sewage flows through gravity from the storm tanks to the wet-well. However, it was not possible to confirm actual set points either from operational manuals or the dependency of this flowrate on pump state from SCADA screens. Hence, during modelling, the control strategy is setup in such a way that the storm return flow occurs whenever the inlet-flow to the WWTP is below the capacity of the duty pump minus return flows to wet-well, i.e. whenever the inlet flow is below 35 L s^{-1}.

3.1.3.2 Storm Bypass Modelling

The by-pass storm flow is modelled using a BSM2 'flowsplitter' s-function (type 2) (Alex et al., 2008). When the influent flow rate is less than 2.3 × DWF (69 L s^{-1}), the flow continues to the next treatment stage; otherwise, the excess flow is bypassed to the storm tanks, and the flow rate is determined below.

$$If \quad Q_{in} < Q_{toStormtank,ctrl};$$
$$Q_{ww} = Q_{in}$$
$$Q_{ST,bypass} = 0 \qquad \textit{Eq. 3-1}$$

$$If \quad Q_{in} \geq Q_{toStormtank,ctrl};$$
$$Q_{ww} = Q_{toStormtank,ctrl}$$
$$Q_{ST,bypass} = Q_{in} - Q_{toStormtank,ctrl} \qquad \textit{Eq. 3-2}$$

Where:

Q_{in}	=	Inlet flow to treatment plant [m^3d^{-1}]
$Q_{toStormtank,ctrl}$	=	Set-point for bypass to storm tanks [m^3d^{-1}]
Q_{ww}	=	Flow to wet-wet well from inlet structure after bypass to storm tanks [m^3d^{-1}]
$Q_{ST,bypass}$	=	Total storm flow bypassed to storm tanks [m^3d^{-1}]

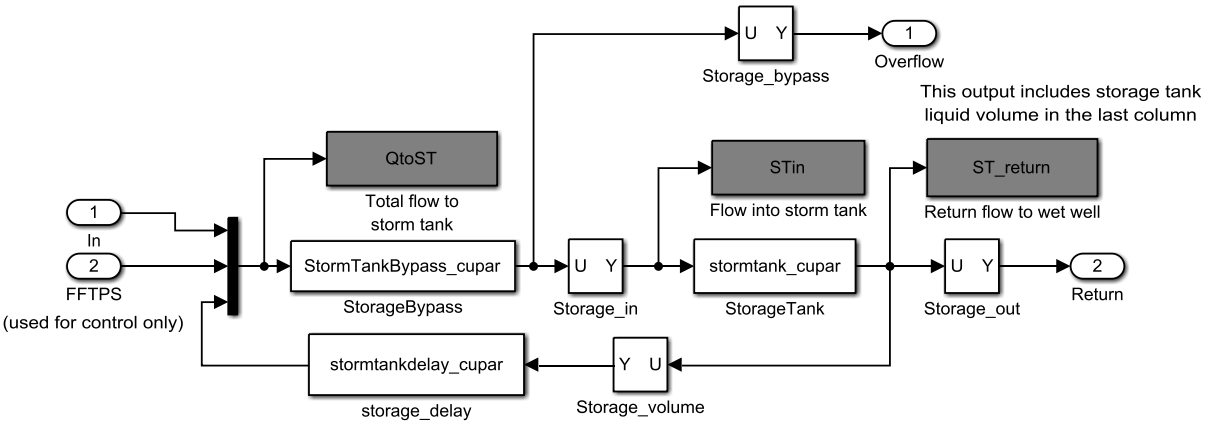

Figure 3-6: Simulink implementation of the storm tank model

The two storm tanks, to improve the model efficiency, are modelled as one shown in Figure 3-6, with a total combined storage volume of 778 m^3 (based on a depth of 2 m before overflows occur). The storm tanks overflow, filling and return-flow to wet-well are calculated by modifying the BSM2 'storagebypass_bsm2' block in which the filling and overflow rate is determined based on the capacity of the storm tank, and the outflow rate is determined based on the inlet flow rate. The use of inlet flow rate to control the return flow was found to be computationally efficient while mimicking the current control philosophy. Hence, instead of using the inlet wet-well pumps' operational state, the return flow from storm tanks is instigated whenever the inlet flowrate is below 20 L s^{-1} as follows.

First, the storm tank return-flow rate ($Q_{ST,return}$) is estimated based on the inlet flow rate using Eq. 3-3 and Eq. 3-4.

$$If \quad Q_{in} < Q_{FFTPS,ctrl}\ ;$$
$$Q_{ST,return} = Q_{return} \qquad \textit{Eq. 3-3}$$
$$If \quad Q_{in} \geq Q_{FFTPS,ctrl}\ ;$$
$$Q_{ST,return} = 0 \qquad \text{Eq. 3-4}$$

When the tanks are not full and not empty, there will be no overflow, and all the storm bypass, if any, will enter the storm tanks, see Eq. 3-5.

$$If \quad V_{ST} < V_{ST,max}\ \&\ V_{ST} > V_{ST,min}\ ;$$
$$Q_{ST,in} = Q_{ST,bypass}$$
$$Q_{ST,overflow} = 0 \qquad \text{Eq. 3-5}$$

When the tanks are full, the storm bypass flow will not enter the storm tanks rather it will overflow to combine with the final effluent, Eq. 3-6.

$$If \quad V_{ST} \geq V_{ST,max}\ ;$$
$$Q_{ST,in} = 0$$
$$\mathrm{Q_{ST,overflow}} = \mathrm{Q_{ST,bypass}} \qquad \textit{Eq. 3-6}$$

When the tank is empty, there is no return flow to the wet-well, and all flow to the tank enters the tank, with no overflow, Eq. 3-7.

$$\text{If} \quad V_{ST} \leq V_{ST,min}\ ;$$
$$Q_{ST,in} = Q_{ST,bypass}$$
$$Q_{ST,overflow} = 0$$
$$Q_{ST,return} = 0 \qquad \textit{Eq. 3-7}$$

where:

Q_{in} = Inlet flowrate to WWTP [$m^3\ d^{-1}$]

$Q_{FFTPS,ctrl}$ = Flowrate set-point to control return-flow from storm tanks [$m^3\ d^{-1}$]

$Q_{ST,return}$ = Return flowrate from storm tanks to wet well [$m^3\ d^{-1}$]

Q_{return} = Average return flowrate whenever there is a return flow [$m^3 d^{-1}$]

V_{ST} = Volume of storm water in the storm tanks [m^3]

$V_{ST,max}$ = Maximum vol. of storm tanks (99 % of maximum capacity) [m^3]

$V_{ST,min}$ = Minimum vol. of storm tanks (1 % maximum capacity) [m^3]

$Q_{ST,in}$ = Actual storm water flow into the storm tanks [$m^3\ d^{-1}$]

$Q_{ST,bypass}$ = Total storm flow bypassed to storm tanks [$m^3\ d^{-1}$]

$Q_{ST,overflow}$ = Storm tanks overflow [$m^3\ d^{-1}$]

There are two submerged pumps in each tank to avoid settlement, and the tanks have a small capacity with short retention time. Hence, it is assumed, for modelling purpose, that no settling of sediment and no reactions occur in the storm tanks; wastewater composition is uniform throughout the tanks and equal to the outflow composition. Variations of storm water volume and concentrations in the storm tanks due to influent and effluent flows are modelled as in BSM2, 'stormtank_cupar' block.

3.1.4 Inlet Wet-well

The inlet well in Cupar WWTP is one of the most important components regarding controlling flow to the oxidation ditch, and flow from the supernatant return, storm tank return and scum return from the settlement tanks, see Figure 3-7. There are three pumps, duty assist and stand-by, which are working at a constant speed with a current capacity of 45 L s^{-1} each (based on measured flow data, see Section 6.2). The pumps are suited in a dry section of the pump station connected to the wet-well as shown in Figure 3-8. The assist and the duty pumps are turned on and off based on the water level in the inlet well. The wet-well level is also used in controlling the flows from the storm tanks as well.

The wet-well has a maximum depth of 4.6m, but an overflow/backflow occurs above 3m. Hence the capacity is limited to a maximum depth of 3m with a cross-sectional area of 17.11 m^2 ((4.8 m + 4.45 m) × 1.85 m), see Figure 3-9.

The detail of the pumps, their operation, and modelling approach is presented in Sections 5.2.1.4 and 6.2.

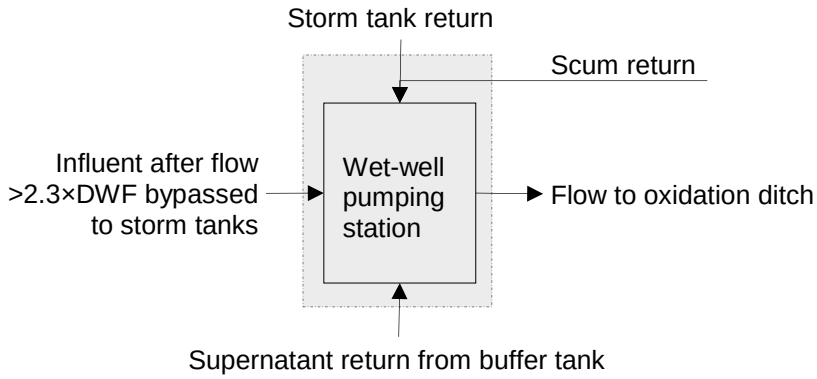

Figure 3-7: Flow diagram of the inlet wet-well

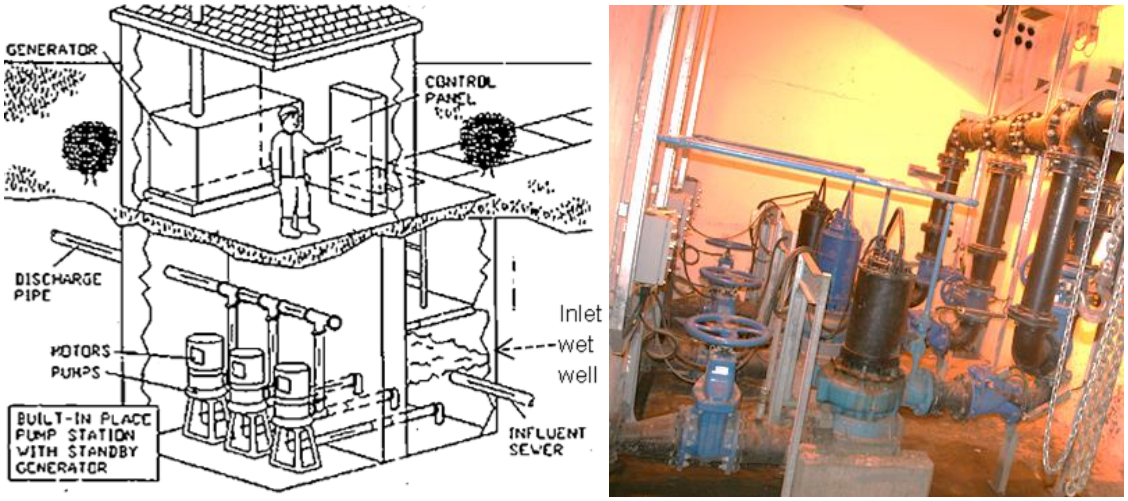

Figure 3-8: Inlet wet-well - Left: demonstration of the wet-well pumping station at Cupar WWTP (Source: http://www.electric-technologies.com/pumps_history.html) Right: inlet wet-well pumps at Cupar WWTP

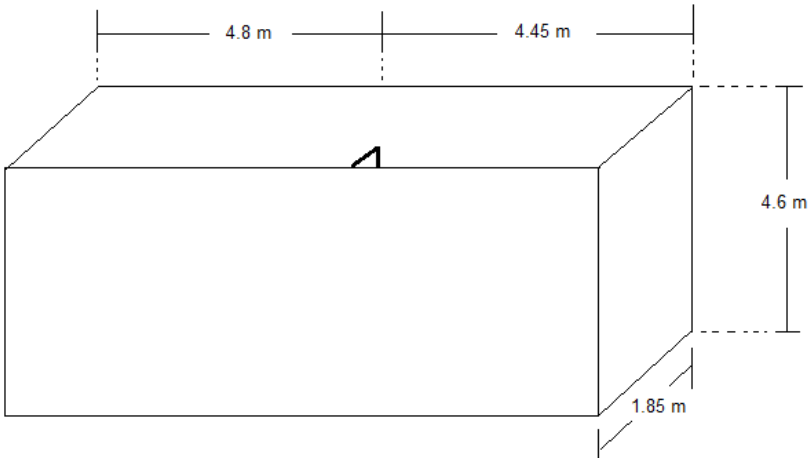

Figure 3-9: Two inlet wells of Cupar WWTP operating as a combined one wet-well

Process control

The wet-well received online flow less than 2.3DWF (69 L s^{-1}) from the inlet works, see Section 3.1.1. The return-flow from the storm tanks is controlled based on the wet-well level, the details on current practice and the modelling approach used in this study are discussed in Section 3.1.3. The return flow from the sludge buffer tank (supernatant flow) is continuous and depends on the operation schedule for sludge treatment and supernatant level in the buffer tank, see Section 3.2.3. The scum return-flow from the two final settlement tanks flows into the wet-well and controlled in an ad hoc manner by the operators depending on the scum level in the final settlement tanks, for the detail see Section 3.2.2. The

site drainage also flows into the inlet wet-well, but this flow is relatively small, and it is not considered in this study.

The flow out from the wet-well to the oxidation ditch is controlled based on the status (on/off) of the duty and the assist pumps. The status of these pumps is controlled based on the wet-well level as shown in Table 3-2. If the duty pump is off at the start, whenever the wet well level is above 1.2m the duty pumps start operating. If inflow is higher than outflow and wet well level keep on increasing and reaches to 1.6m, the assist pump will start operating, i.e. duty and assist-pump operate together. While both pumps are operating, and the outflow is higher than inflow resulting in the reduction in the wet-well level, the assist pump will turn off when the wet well level reaches to 1.0m. If wet well level reduces to be below 0.7m, then the duty pump will stop operating.

Table 3-2: Cupar WWTP inlet wet-well pumps status control set-points

Wet-well set points based on SCADA screen at Cupar WWTP (09/22/2013)	
Inlet wet-well pumps status	Wet well level set points (m)
Duty pump starting level	1.2
Duty pump stop level	0.7
Assist pump starting level	1.6
Assist pump stop level	1

3.1.4.1 Wet-well Modelling

The wet-well is modelled as a tank, using a modified version of the BSM2 'storage' s-function in which calculation of the outflow is dependent on the states of the two pumps, which in turn are dependent on the water level in the wet-well. The third pump is a standby which is used to replace the duty pump when needed and, in the model, its state is always off.

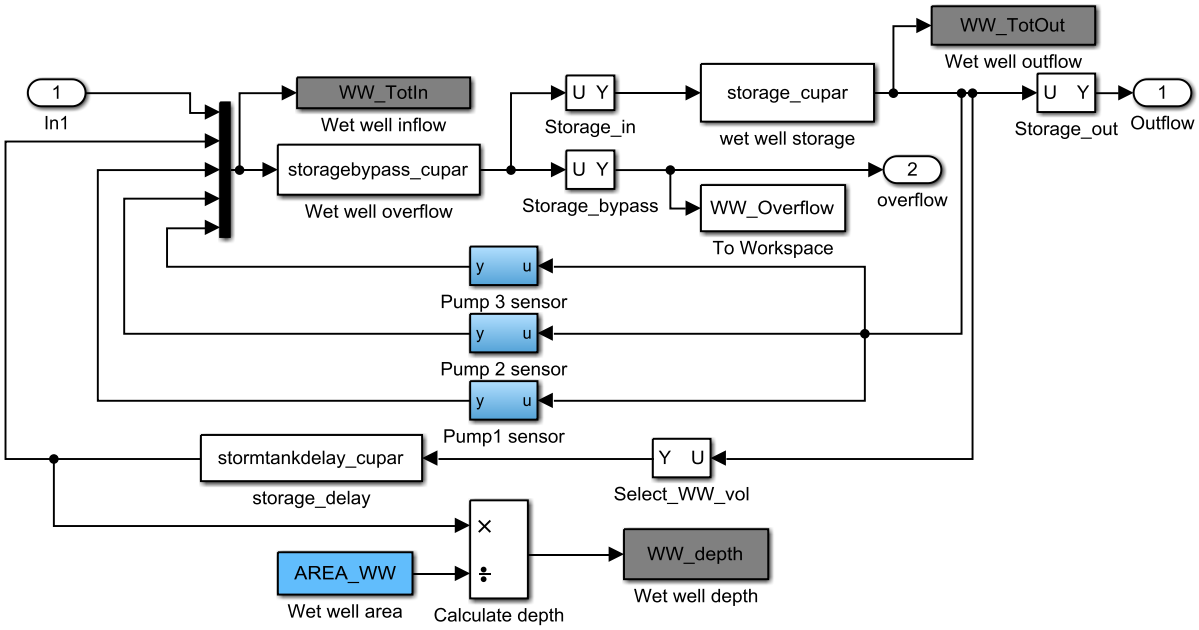

Figure 3-10: Simulink model for inlet wet-well

The Simulink implementation of the wet-well tank model is shown in Figure 3-10**Error! Reference source not found.**. The feedback loops shown are required since knowledge of pump states at the previous time-step (t-1) is required to calculate pumps' state at the current time-step (t-1) in the 'storagebypass_cupar' block, see Eq. 3-8, Eq. 3-9, Eq. 3-10, and Eq. 3-11.

The duty pump's state:

If the previous state of the duty pump was ON, i.e.

$$If \quad State_{ww,P1(t-1)} = 1, \quad then$$
$$If \quad h_{ww(t)} > h_{ww,P1,stop};$$
$$State_{ww,P1(t)} = 1$$
$$If \quad h_{ww(t)} \leq h_{ww,P1,stop};$$
$$State_{ww,P1(t)} = 0 \qquad \text{Eq. 3-8}$$

If the previous state of the duty pump was OFF, i.e.

$$If \quad State_{ww,P1(t-1)} = 0, \quad then$$
$$If \quad h_{ww(t)} > h_{ww,P1,start};$$
$$State_{ww,P1(t)} = 1$$
$$If \quad h_{ww(t)} \leq h_{ww,P1,start};$$
$$State_{ww,P1(t)} = 0 \qquad \text{Eq. 3-9}$$

The assist pump's state:

If the previous state of the assist pump was ON, i.e.

$$If \quad State_{ww,P2(t-1)} = 1, \quad then$$
$$If \quad h_{ww(t)} > h_{ww,P2,stop};$$
$$State_{ww,P2(t)} = 1$$
$$If \quad h_{ww(t)} \leq h_{ww,P1,stop};$$
$$State_{ww,P1(t)} = 1 \qquad \text{Eq. 3-10}$$

If the previous state of the assist pump was OFF, i.e.

$$If \quad State_{ww,P2(t-1)} = 0, \quad then$$
$$If \quad h_{ww(t)} > h_{ww,P2,start};$$
$$State_{ww,P2(t)} = 1$$
$$If \quad h_{ww(t)} \leq h_{ww,P2,start};$$
$$State_{ww,P2(t)} = 0 \qquad \text{Eq. 3-11}$$

Where:

$State_{ww,P1(t)}$	=	The current state of duty pump; 1=ON and 0=OFF
$State_{ww,P1(t-1)}$	=	Previous time-step sate of duty pump
$State_{ww,P2(t)}$	=	The current state of assist pump; 1=ON and 0=OFF
$State_{ww,P2(t-1)}$	=	Previous time-step sate of assist pump
$h_{ww(t)}$	=	Current height we wet-well [m]
$h_{ww,P1,start}$	=	Duty pump starting wet-well level [m]
$h_{ww,P1,stop}$		Duty pump stopping wet-well level [m]
$h_{ww,P2,start}$	=	Assist pump starting wet-well level [m]
$h_{ww,P2,stop}$	=	Assist pump stopping wet-well level [m]

The outflow from the wet-well $Q_{ww,out}$ is calculated based on the current capacity of the pumps and an empirical linear equation based on the wet-well depth as described in Eq. 3-12, Eq. 3-13, and Eq. 3-14. The derivation of the linear equation is presented in Section 6.2.

$$If \quad State_{ww,P2(t)} = 1 \quad \& \quad State_{ww,P1(t)} = 1 \quad then$$
$$Q_{ww,out} = (a_1 h_{ww} + b_1) \times 86.4 \qquad \text{Eq. 3-12}$$
$$If \quad State_{ww,P2(t)} = 0 \quad \& \quad State_{ww,P1(t)} = 1 \quad then$$
$$Q_{ww,out} = (a_2 h_{ww} + b_2) \times 86.4 \qquad \text{Eq. 3-13}$$
$$If \quad State_{ww,P2(t)} = 0 \quad \& \quad State_{ww,P1(t)} = 0 \quad then$$
$$Q_{ww,out} = 0 \qquad \text{Eq. 3-14}$$

Where:

$State_{ww,P1(t)}$	=	The current state of duty pump; 1=ON and 0=OFF

$State_{ww,P2(t)}$ = The current state of assist pump; 1=ON and 0=OFF
$Q_{ww,out}$ = Flow out from wet-well to oxidation ditch [m^3d^{-1}]
a_1 = Empirical constant for both pumps operating (slope of the linear trendline) [14.53]
b_1 = Empirical constant for both pumps operating (intercept of linear trendline) [48.8]
a_2 = Empirical constant only duty pump operating (slope of the linear trendline) [18.1]
b_2 = Empirical constant only duty pump operating (intercept of linear trendline) [23.9]
h_{ww} = Current height of wet-well [m]
86.4 = Factor for unit conversion from L s^{-1} to m^3 d^{-1}

For modelling the wet-well, a water-balance approach is used, similar to the model block 'storagebypass_BSM2' in BSM2. In this instance, the modified version, 'storagebypass_Cupar' is used to determine the actual flow of wastewater into the wet-well, and overflow, if any, but with modifications as described below.

When the wet-well is not full and not empty, there will be no overflow, and all the flow towards the wet-well will enter the inlet wet-well:

$$If \quad V_{ww} < V_{ww,max} \;\&\; V_{ww} > V_{ww,min} \quad then$$
$$Q_{ww,in} = Q_{ww} + Q_{scum} + Q_{ST,return} + Q_{supernatant}$$
$$Q_{ww,overflow} = 0 \qquad \text{Eq. 3-15}$$

If the wet-well is near to its maximum capacity, i.e. if the volume of wastewater in the wet well is equal or above 99 % of the wet-well capacity then the actual flow entering the wet-well and the overflow will depend on the incoming flow towards wet-well and outflow calculated in Eq. 3-16, and Eq. 3-17.

$$If \quad V_{ww} \geq V_{ww,max} \;\&\; \left(Q_{ww} + Q_{scum} + Q_{ST,return} + Q_{supernatant}\right) \geq Q_{ww,out} \; then$$
$$Q_{ww,in} = Q_{ww,out}$$
$$Q_{ww,overflow} = \left(Q_{ww} + Q_{scum} + Q_{ST,return} + Q_{supernatant}\right) - Q_{ww,out} \qquad \text{Eq. 3-16}$$

$$If \quad V_{ww} \geq V_{ww,max} \;\&\; \left(Q_{ww} + Q_{scum} + Q_{ST,return} + Q_{supernatant}\right) < Q_{ww,out} \; then$$
$$Q_{ww,in} = \left(Q_{ww} + Q_{scum} + Q_{ST,return} + Q_{supernatant}\right) \qquad \text{Eq. 3-17}$$

$$Q_{ww,overflow} = 0$$

If wet-well is near to empty, i.e. volume of wastewater is less than or equal to 1 % of the maximum capacity of the wet-well, the actual flow into the wet well and the overflow is calculated using Eq. 3-18.

$$If \qquad V_{ww} \leq V_{ww,min} \qquad then$$
$$Q_{ww,in} = \left(Q_{ww} + Q_{scum} + Q_{ST,return} + Q_{supernatant}\right)$$
$$Q_{ww,overflow} = 0 \qquad \text{Eq. 3-18}$$

3.2 Secondary Treatment: Component Description and Model Development

According to EU-UWWTD secondary treatment is defined as the wastewater treatment processes involving a biological treatment with a secondary settlement or another process to reduce the BOD, COD, and TSS of the final effluent to the required level (CEC, 1991). Cupar WWTP uses an activated sludge process followed by two final settlement tanks in parallel. The activated sludge process in this case study uses an oxidation ditch (OD) that uses a longer solid retention time where the activated sludge flows in a continuous circuitous path while aeration is provided at fixed points along the path. In oxidation ditches, the anoxic condition is achieved as oxygen depleted between the aerators (Shammas and Wang, 2009), i.e. high DO concentrations near the aerators and gradually decreasing DO concentration until the activated sludge reaches to the next aerator in the OD.

Figure 3-11: Oxidation ditch at Cupar WWTP

3.2.1 Oxidation Ditch

From the inlet wet-well, where the wastewater from inlet structure is mixed with the supernatant return-flow, storm tank return-flow, and scum return-flow the wastewater is pumped to the aerobic selector zone positioned along the side of the oxidation ditch. The system was designed so that the incoming wastewater in the selector zone is pre-aerated and mixed using the two mixers to create favourable condition for aerobic bacteria. However, in practice, both mixers and the aerators in the selector zone are not operative. During all the site visits and as we informed by the process scientist and operators, the blowers have not been functioning since 2012. Hence, the supposedly aerobic selector zone is serving as an anoxic zone. The selector zone has a volumetric capacity of 90 m^3; 1 m × 20 m × 4 m (width × length × depth). This zone is connected to the oxidation ditch as shown in Figure 3-12.

The oxidation ditch has a capacity of 2980 m^3 with a surface area of 744.9 m^2 and maximum activated sludge depth of 4 m; details of the layout is shown in Figure 3-12. Wastewater from selector zone enters the oxidation ditch.

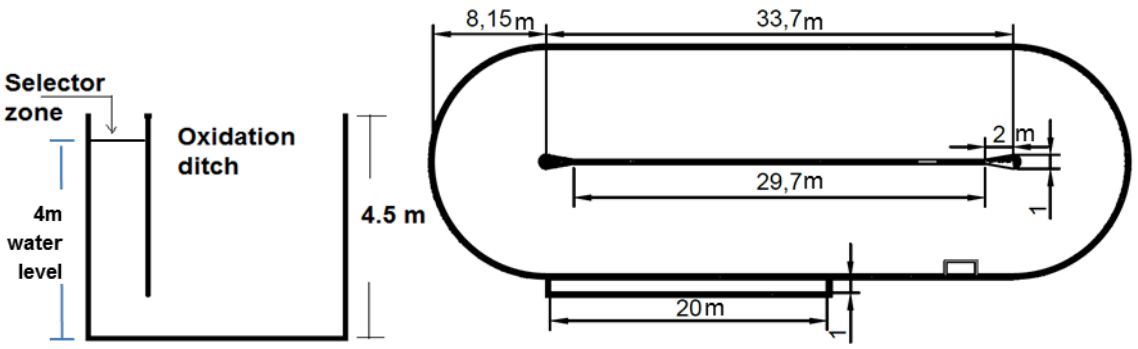

Figure 3-12: Oxidation ditch and selector zone at Cupar WWTP (Left: Longitudinal section and right: a plan view of the oxidation ditch and selector zone)

From the aerobic selector zone, the mixed liquor passes into the main oxidation ditch. Flow velocity around the oxidation ditch is maintained by four submerged continuously operating flow inducers which are located at two different places in the oxidation ditch. The actual flow velocity of the activated sludge in oxidation ditch is not known, but according to the design parameter, it is 0.33 m s^{-1}. This information was obtained from the operational team leader. Oxidation ditch horizontal velocity can typically vary between 0.25 - 0.35 m s^{-1} (Metcalf & Eddy, 2004).

There is no chemical addition to the oxidation ditch.

Aeration is one of the important processes in activated sludge WWT processes, and it is commonly the major energy consumer in WWTPS (Henze et al., 2008). At the study site, the subsurface aeration system delivers oxygen into the mixed liquor in the oxidation ditch by compressing air and pumping it through fine-bubble diffusers. There are three identical positive displacement blowers on site (duty, assist and standby). The blowers, AERZEN®, Delta Blower GM 60 S/ 280S, can operate at a variable speed of 950-2850 revolution per minute (RPM), with an inlet volume of 14.5-55.8 m^3/minute, the differential press of 470 mbar, and power consumption of 16.8-56 kW (motor power 75KW).

Oxygen is transferred into liquid in several ways; shearing the liquid surface with mixers (surface aerators), releasing air through porous media (coarse or fine-bubble diffusers), or through direct contact of air and water over a large surface area (Henze et al., 2008). At this site, oxygen is transferred into the mixed liquor by releasing fine-bubbles through a fine-bubble aeration grid system installed at the bottom of the oxidation ditch. The fine-pore diffusers are made of oval

membrane tube diffusers forming the aeration grid system, the details of which is shown in Figure 3-13 and Figure 3-14.

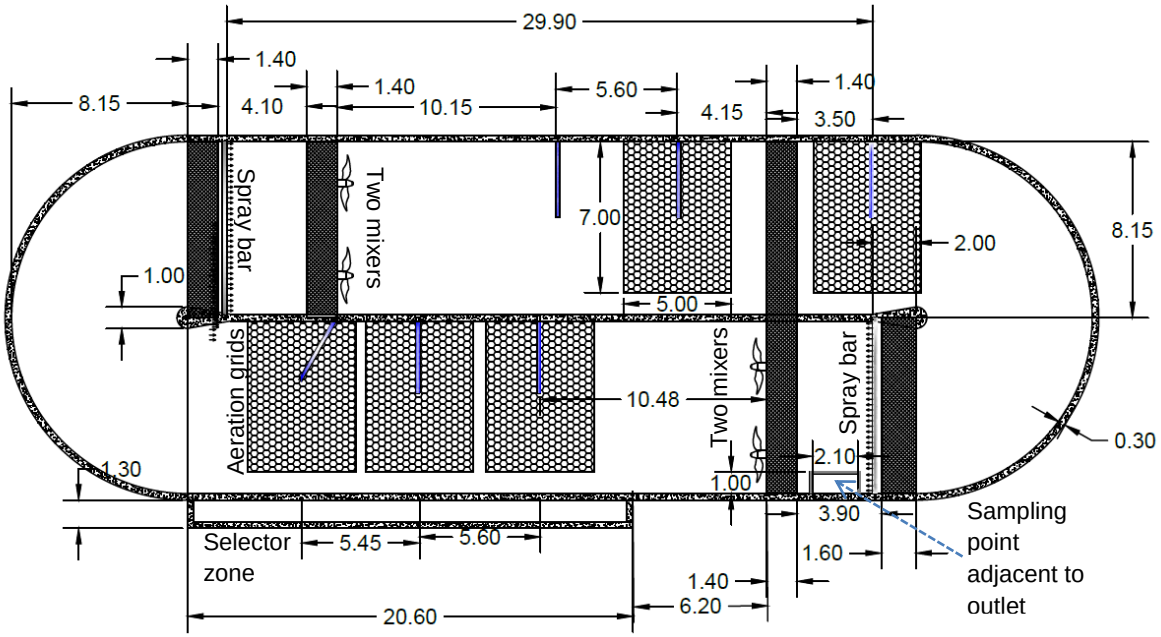

Figure 3-13: Layout of aeration grid, mixers, spray-bars and other details at Cupar WWTP (dimensions are in meters)

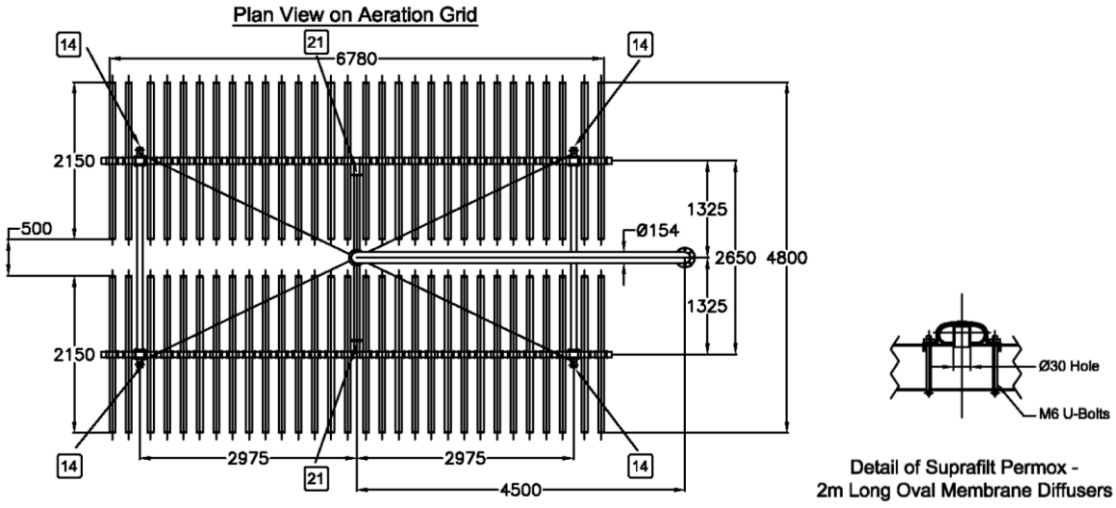

Figure 3-14: Details of one of the five aeration grids and diffusers at Cupar WWTP

Aeration systems can serve both for supplying oxygen to create an aerobic condition for microorganisms metabolism and mixing the liqour so that microorganisms can have closer contact with nutrients and organic matter (Mcgee and Pearson, 1999). Surface aerator have the benefit of both; however, fine-pore diffusers require a separate mixing system (Stenstrom and Rosso, 2008). The mixing at Cupar WWTP is achieved using four propeller type subsurface mixers situated at two different locations in the oxidation ditch, see Figure 3-13. The mixers in the oxidation ditch have two-fold purposes; first is

blending the liqour to reduce concentration variation including a dispersion of oxygen, and the second is to induce flow accelaration and give the required horizontal flow in the oxidation ditch.

Cupar WWTP used to suffer from a foaming problem in the oxidation ditch. Foaming is a persistent viscous brown foam (Soddell and Seviour, 1990) that can be caused due to several reasons:

- presences of surfactants such as household detergents
- excess prodcution of extracelluar polymeric substances by the biomass in the acivated sludge
- existance of flimentous bacteria and favouring condition for their growth (de los Reyes, 2010)

One of the most common solutions for foaming or scum formation is the use of water spray bars (Soddell and Seviour, 1990). Cupar WWTP uses water sprays to control foaming in the oxidation ditch. On average, based on measured data, 22 L s^{-1} of final effluent is returned to the oxidation ditch spray bar for this purpose. The spray bars are located at two different points in the oxidatin ditch as shown in Figure 3-13.

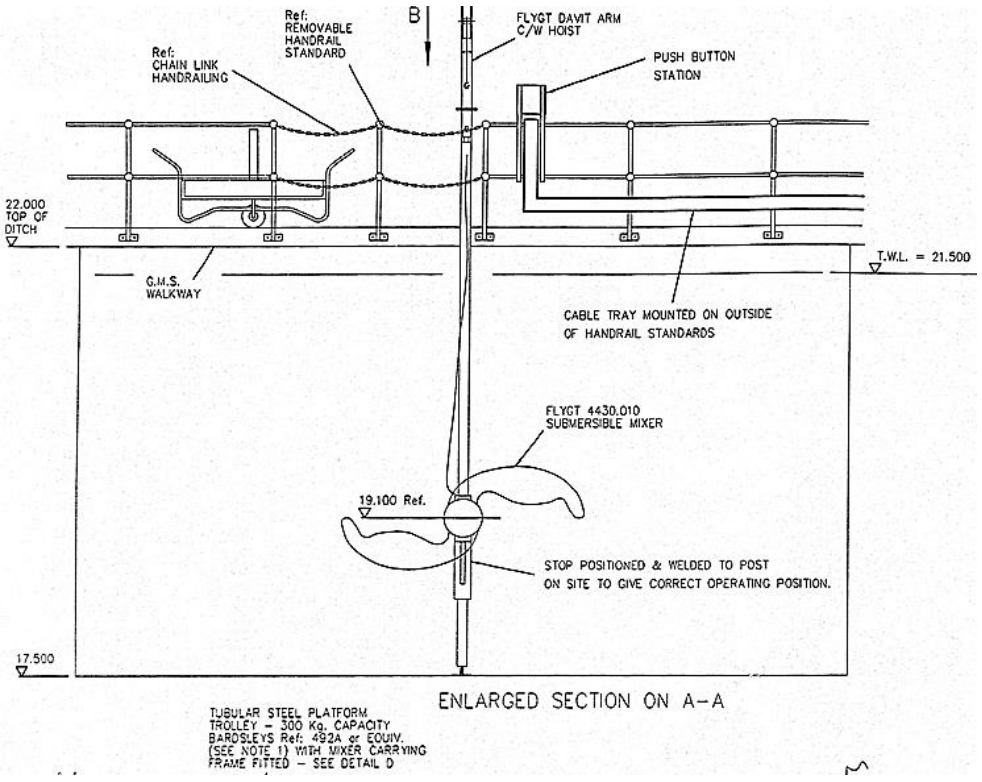

Figure 3-15: Details of one of the impellers in the oxidation ditch at Cupar WWTP

The returned activated sludge (RAS) is pumped using two pumps with a capacity of 45 L s^{-1} from the final settlement tanks back to the selector zone. The RAS pumps operate automatically on a continuous basis. According to the operation manual, if only the duty pump in the wet-well is operating, then only one RAS pump is required. If both duty and assist pump at the inlet wet-well are operating, then both RAS pumps are required to maintain the proportional flow through the plant. However, analysing measured data on RAS and SAS at the WWTP, showed that only the duty pumps at each settler are running continuously and the assist RAS pumps are off all the time. As described in Section 4.1.5, the RAS is retuned at a constant rate of, on average, 35 L s^{-1}. The crossover valves allow the duties of the RAS pumps and the SAS pump to be substituted when required. The SAS off-take to the sludge treatment is done only to one of the settlement tanks at a time.

The surplus activated sludge (SAS) is pumped from the final settlement tanks, on average at a constant rate of 30 L s^{-1}, see Section 4.1.5. The SAS pump is operated manually to suit the required level of Mixed Liquor Suspended Solids (MLSS) in the oxidation ditch. In other words, the MLSS in the oxidation ditch is controlled by varying the frequency of the SAS pumps operation. However, according to the operator, this is not religiously followed; instead, the SAS pump is turned on once in three days to pump a volume of 200 m^3 of activated sludge. Whenever the MLSS is tested, and if the MLSS is higher than 3250 mg L^{-1}, then the SAS removal may take place every day.

Operators have a significant role in WWTP control (Olsson et al., 2005). However, there is a great need for better education and awareness in control technology and documentation of process control operations. In this study, it was observed that, based on the operators' experience, some process control procedures were not consistent with documented control philosophies. Although in most cases, the control procedures were based on good intentions, they are hardly recorded and documented. Furthermore, in some cases, practicing process engineers did not appreciate how documenting changes in control procedures can benefit the assessment of integrated active control systems or indeed any control strategy. Hence, emphasis should be given to training, operational data collection and documentation of control procedures as they are key in creating robust WWTP processes, and thus resilient systems.

3.2.1.1 Oxidation Ditch DO Level Control Philosophy

The dissolved oxygen (DO) level in the oxidation ditch is controlled by measuring the DO concentration at the outlet point of the oxidation ditch, see Figure 3-13. A proportional-integral-derivative (PID) controller is used to bring the measured DO concentration as close as possible to the reference DO concentration. The reduction or increase in DO achieved by varying the speed of the displacement blowers, the actuators, as follows. The blowers have two operational modes: constant aeration and intermittent aeration. Under constant aeration, the DO set-point is 0.75 mg L^{-1}, and blower speed is increased or decreased to bring the DO concentration as close as the reference DO concentration. Since the blower's minimum speed is limited to 950 rpm, it is possible not to close the gap between the actual DO concentration and the reference DO concentration even if the blower works at a minimum speed. Hence, the need for the intermittent operational phase. Whenever the DO exceeds 2.25 mg L^{-1}, an intermittent aeration phase triggers, where the duty blower runs for 10 minutes and then turned off for 20 minutes until the DO concentration drops to 1.5 mg L^{-1}, upon which continuous aeration is resumed. To ensure both duty and standby blowers are regularly exercised, their role is alternated automatically every 24 hours.

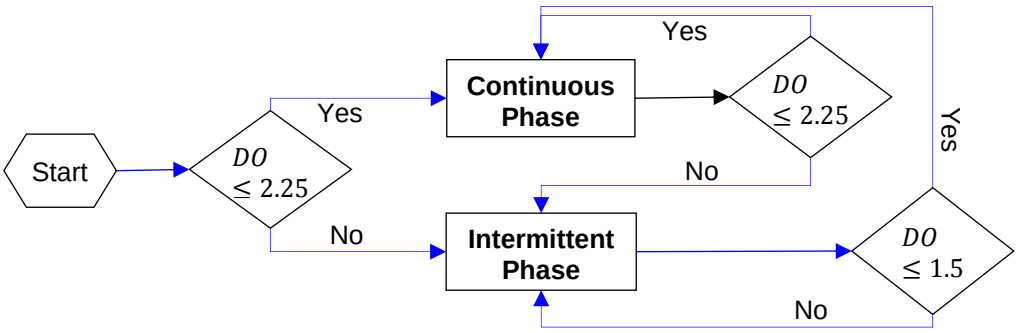

Figure 3-16 Flow diagram showing the switching between continuous phase (PID controller, set-point 0.75 mg L^{-1}) and intermittent phase (one blower operating at minimum speed for 10 minutes and resting for 20 minutes)

During the continuous DO control phase, the compressed airflow valve on the main air duct is used to vary the pressure at the throat, as shown in Figure 3-17. For example, if the DO reading is less than the set-point (0.75 mg L^{-1}), the valve opens proportionally, and if the DO level is above the set-point (0.75 mg L^{-1}), then the valve closes proportionally. In this control approach, the DO concentration in the oxidation ditch directly dictates the valve, not the blowers. The actuator uses the concept of a Venturi meter so that the pressure at the throat is used to control the blowers' speed as shown in Figure 3-17.

If air pressure is less than the start set point (1.00 bars), the duty blower starts at the minimum speed, 1200 rpm. The blower speed will increase gradually to the required speed which is controlled by PID to achieve the control pressure set-point (CPS) of 0.55 bars. If the actual pressure in the air pipe is less than the CPS and duty blower is running at its maximum speed (2400 rpm) then, after two minutes of delay, the assist blower will start at a minimum speed of 1200 rpm. If DO is less than the set-point, then the valve opens further increasing the pressure at the throat, and as a result, the assist blower will gradually ramp up its speed controlled by the PID controller. If the air pressure in the air duct is equal to the CPS (0.55 bars) then there won't be any speed change, i.e. DO is the same as the DO set-point and blowers continue operating at the same rate. If DO concentration increases and the valve starts closing, the air pressure will be lower than the CPS then the assist blower speed will reduce to increase the pressure on the valve. If the condition persists and the assist blower reaches its minimum speed, it stops after a delay time of two minutes. If the actual pressure transmitter is still less than the CPS, then the duty pump starts to ramp down to minimum speed but will not stop. If the condition persists and DO concentration increases to 2.25 mg L^{-1}, the continuous phase will change to intermittent phase.

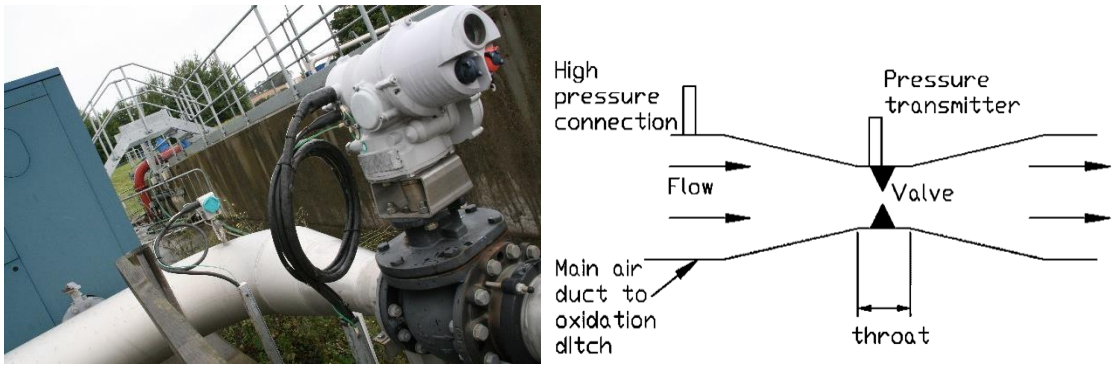

Figure 3-17: Pressure control on the main air duct to the oxidation ditch

3.2.1.2 Modelling the Oxidation Ditch

Biochemical processes in oxidation ditches have previously been modelled using ASM1 for example, Abusam et al. (2001); Abusam and Keesman (1999); Abusam et al. (2003), Stamou (1997). There is no consensus on the modelling of the hydraulic behaviour of oxidation ditches (Ghermandi et al., 2005). Some other suggested approaches, e.g. Alex et al. (1999); Von Sperling and Lumbers (1989a); Dudley (1995), are sophisticated and computationally demanding (Ghermandi et al., 2005). Simpler but computationally less demanding approaches suggested by De Clercq et al. (1999), and Derco et al. (1994) showed

that is possible to produce good results using a series of continuously stirred tanks.

It has been suggested that ten completely stirred reactors (or the minimum number required for adequate representation of the aeration configuration) are sufficient to model an oxidation ditch (Abusam and Keesman, 1999). In this instance, it is found that twelve reactors are required to represent the configuration of blowers, the average measured DO variation across the oxidation ditch (Figure 3-18), and the influent and effluent flow from the oxidation ditch, with an additional reactor for the selector zone. These are arranged as shown in Figure 3-18 with their volumes listed.

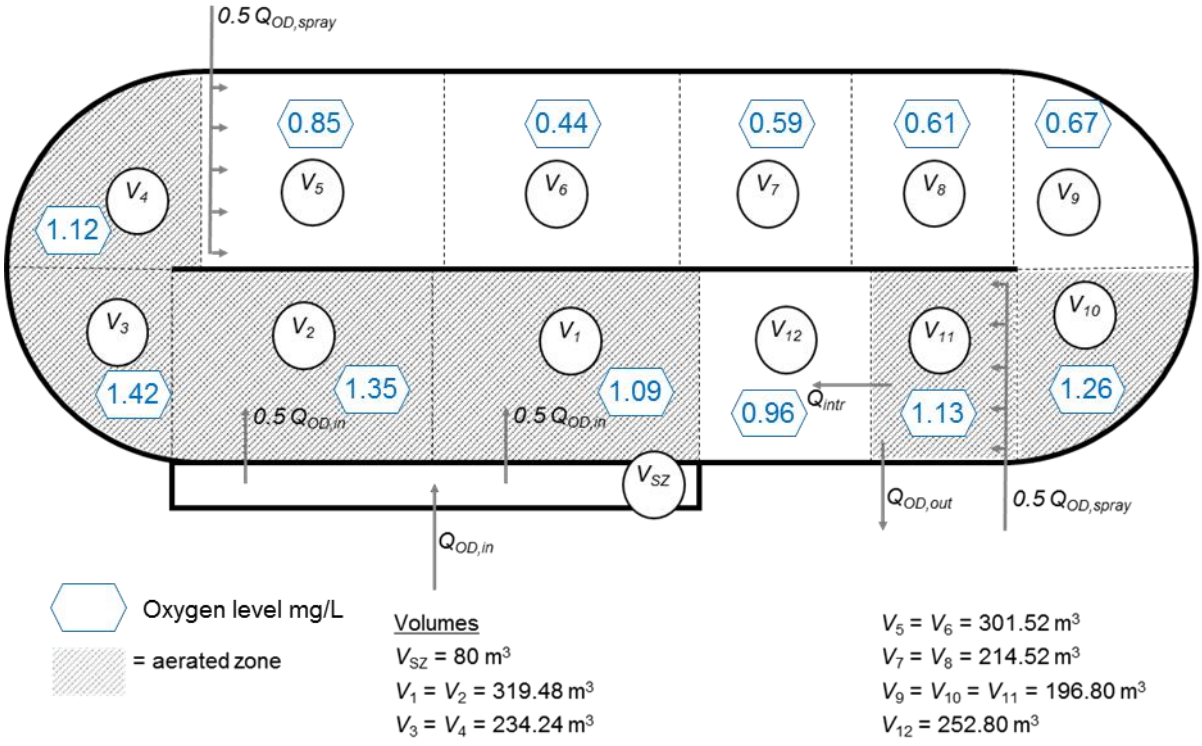

Figure 3-18: Divisions of oxidation ditch into series of continuously stirred tanks for modelling, showing inflows, return flows, outflows and aeration zones

Biochemical processes in each reactor are modelled using the modified ASM1, as detailed in the BSM2-e model by Sweetapple (2014); this enables calculation of dynamic N_2O emissions in addition to water quality parameters.

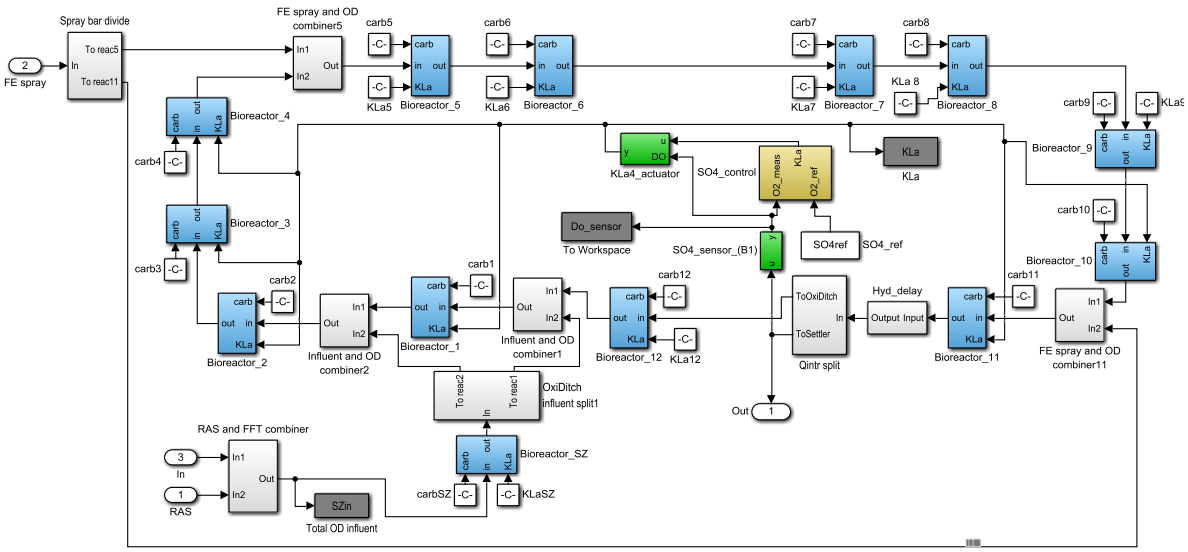

Figure 3-19: Simulink implementation of the oxidation ditch model

The Simulink implementation of the selector zone and oxidation ditch model is shown in Figure 3-19**Error! Reference source not found.**. The selector zone receives flow from the wet-well pumping station and the RAS feed, and this is distributed evenly between the first two reactors in the oxidation ditch model. Reactors 5 and 11 receive flow from the final effluent (representing the spray bars) – as this flow rate is unknown, it is provisionally set to 20 L s^{-1} (combined total flow). Flow leaves the oxidation ditch following reactor 11, and the flow rate is calculated by mass balance, assuming that there is no change in the volume of mixed liquor stored in each reactor. Based on the horizontal speed the internal circulation is estiamted to be 5280 L s^{-1} (456,192 m^3 d^{-1}), Q_{intr}. However, since the horizontal speed is not measured in this study, this parameter is left for calibration, see Section 6.2.

The model requires carbon source addition to each reactor to be specified; this is set to zero in all instances. Each reactor block also requires input for aeration intensity. For the non-aerated zones, this is set to zero, while the DO sensor, PID controller and actuator from BSM2 are used to set aeration intensity for reactors 1, 2, 3, 4, 10 and 11. The selection of the aerated zones is mainly done with guidance from the measured DO concentration along the oxidation ditch. These zones do not exactly overlap with the orientation of the aeration grid due to the internal circulation flow rate and the location of the mixers.

The DO control modelling approach used in the BSM2 is a simplified model, which uses the oxygen transfer coefficient (kLa, [h^{-1}]) to estimate the energy use directly. A mechanistic method is developed here to relate the kLa factor to the

change in speed of blowers, which later used in the calculation of energy use and indirect greenhouse gas (GHG) emissions, see Section 5.2.1.4. For modelling purposes, the speed variation of the blower is assumed to be continuous. Hence, a PID controller in the BSM2 model is used to vary the kLa values continuously while the DO control is in a continuous phase. When DO level rises and DO control goes to intermittent phase, PID controller is by passed and a minimum kLa value, $kLa_{min,2}$ is used until the DO level is below 2.25 mg L^{-1}. This modification is done to reduce sophistication and maximise modelling speed. Hence, for modelling purposes, it is specified that the minimum aeration intensity achievable from the blowers is 72 h^{-1} during continuous operation and 24 h^{-1} during the intermittent operational phase. For simplicity, it is assumed that implementation of near-zero aeration intensities provides an equivalent effect of the intermittent aeration. The Simulink model showing the representation of the controller is shown in Figure 3-20.

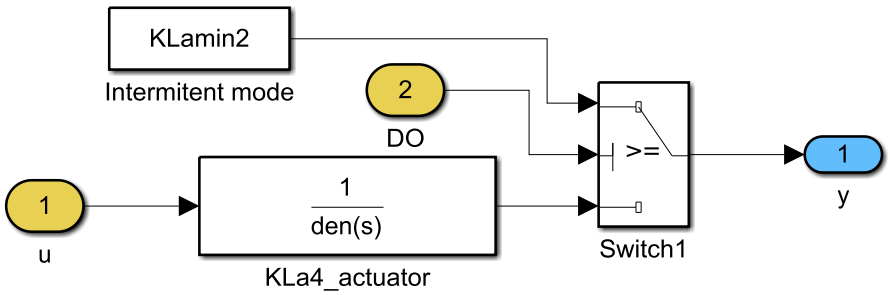

Figure 3-20: Simulink model showing switching between intermittent and continuous phase

The relation between change in kLa and the need for the change in blower speed discussed below. This approach is used to estimate the minimum kLa value during the continuous phase (kLa_{min}), the minimum kLa during the intermittent phase, ($kLa_{min,2}$), and the maximum kLa value the two blowers operate at the same time, kLa_{max}. This approach is later used to estimate the change in blower speed, which is used to calculate the operational cost and associated CO_2 emissions.

The estimation of air flow rate based on the rotational speed of the pumps is formulated by simplifying the numerical approaching suggested in Huang and Liu (2009). The theoretical capacity of the air blowers, regarding flow rate, is estimated in Eq. 3-19.

$$Q_0 = \frac{n \times q_0}{1000} \qquad \text{Eq. 3-19}$$

Where Q_0 is the theoretical flow rate capacity of an air blower [m^3/min], q_0 is the scoop volume of the blower per revolution [L/r], and n is the rotational speed of the motor [rpm].

The air blowers at Cupar are AERZEN GM 60 S / DN 200 motor size 280 S, which are positive displacement pumps. Positive displacement pumps commonly do not pump the full displacement or scoop volume due to slipping of air between the clearance provided between the rotors and the case, which requires re-pumping. This phenomenon will decrease the blower volumetric efficiency, η_v, see Eq. 3-21, (McDougald et al., 1974). The slipping back factor or the volumetric efficiency for root blowers can be as low as 0.4 and can be as high as 0.85 (McDougald et al., 1974). The scoop volume of the AERZEN GM 60 S / DN 200 model with a pressure differential of 470 mbar, the scoop volume is 20 L (AERZEN, 2014). The volumetric flow rate of oxygen is calculated using Eq. 3-22 and Eq. 3-20.

$$Q_{n,O_2} = \frac{n \times q_0}{1000} \times \eta_v \times f_{O_2} \qquad \text{Eq. 3-20}$$

$$\eta_v = \frac{Q_n}{Q_0} \qquad \text{Eq. 3-21}$$

$$Q_n = \frac{n \times q_0}{1000} \times \eta_v \qquad \text{Eq. 3-22}$$

Where, Q_n is the actual flow rate of the blower and Q_0 is the theoretical flow rate. Q_{n,O_2} is the volumetric flow rate of O_2 supplied by the blower and f_{O_2} is the volume fraction of O_2 in the air pumped by the blower. According to the Earths System Research Laboratory (www.esrl.noaa.gov), the volumetric percentage of oxygen in the earth's dry atmosphere, as of 2009, was 20.9 %. The mass of oxygen pumped by the blowers can be estimated using the above equation and the density of oxygen at that temperature and pressure. For simplicity, the impact of temperature and pressure were not considered, and the density of O_2 at standard temperature (0 ^oC) and pressure (1 atmosphere) is assumed to be 1.43 kg m^{-3} (Weast, 1972).

Based on the specification, the actual maximum air flow rate is specified to be 58.2 m^3/min, at a motor speed of 2970 rpm. The scoop volume (q_0) of the rotor at Cupar, using this information, was estimated to be 19.5 L per revolution.

The DO control available in the BSM2 is a surrogate model which is based on the liquid-side oxygen transfer coefficient (kLa, [h^{-1}]) and does not reflect on the change in air flow rate or speed of the blower. Cupar WWTP's DO control system is designed by manipulating the air flow rate. Hence, it was necessary to develop a way to link the amount of air supplied to the biomass in the aerator and the amount of oxygen dissolved into the mixed liquor, i.e. relating air flowrate and kLa. The oxygen transfer rate (OTR) can be expressed as below (Henze et al., 2008).

$$OTR = kLa\,(DO_{sat} - DO) \times V \qquad \text{Eq. 3-23}$$

Where DO is the dissolved oxygen level in the mixed liquor, and DO_{sat} is the dissolved oxygen in the mixed liquor at saturation, in kg of O_2 m^{-3}. V is the volume of the mixed liquor in each zone in m^3. For subsurface aerators, such as fine bubble diffusers, the oxygen transfer efficiency (OTE, %) can be calculated below (Henze et al., 2008)

$$OTE = \frac{O_{2,in} - O_{2,out}}{O_{2,in}} \qquad \text{Eq. 3-24}$$

Where $O_{2,\,in}$ and $O_{2,\,out}$ representing mass fluxes of oxygen in and out of the mixed liquor in each aeration zone. The difference between the two is the amount of oxygen transferred to a liquid state at a given time which is equivalent to the average rate of oxygen transfer and $O_{2,in}$ would be the average rate of oxygen supplied by the blower. Hence;

$$OTE \times Q_{n,O_2} \times \rho_{O_2} = kLa\,(DO - DO_{sat}) \times V \qquad \text{Eq. 3-25}$$

By combining Eq. 3-20 and Eq. 3-25 the kLa factor was expressed as shown in Eq. 3-26.

$$kLa = \frac{OTE \times \frac{n \times q_0}{1000} \times \eta_v \times f_{O_2} \times \rho_{O_2}}{(DO - DO_{sat}) \times V} \qquad \text{Eq. 3-26}$$

Groves et al. (1992) assessed the OTE of 65 different diffused aeration basins at 20 different WwTPs and showed that the OTE depends on different factors such as the type of diffuser, diffuser density, submergence, layout, and age. Operation factors also affect OTE such as solid retention time (SRT), food to microorganism ratio, air flowrate per diffuser and the dissolved oxygen level in the mixed liquor. Their result showed that the following factors increase the OTE; fine bubble

diffuser over coarse ones, new diffusers over old ones, grid layout over the spiral roll, and higher SRT. Cupar WWTP uses fine bubble diffusers, with a grid layout installed in 2005 and a solid retention time of 13 hours. Due to the dependency of OTE on different factors, it is not possible to estimate actual OTE accurately without continuous monitoring at the WWTP. For simplicity, the OTE in this instance is assumed to be constant through the simulation period and assumed to be 10% based on the matching characteristics Cupar with some of the WWTP assessed in Groves et al. (1992). Due to the surrounding uncertainties, the above equation is not used in modelling the DO control, but it is used to estimate the energy required by the blowers to achieve a specific kLa.

The impact of mixers on the internal circulation of the liquor and the estimation of energy use and the associated GHG emission are detailed in Section 5.2.1.4.

3.2.2 Final Settlement Tanks

Figure 3-21: One of the final settlement tanks at Cupar WWTP

The mixed liquors from the Oxidation Ditch flow, through gravity, to two circular conical basin final settlement tanks, see Figure 3-21, each with a capacity of 1458m^3 and surface area of 464m^2. The top zone of the tank with volume V_1 is cylinder whereas the lower two zones with volume V_2 and V_3 are truncated cones. The details of these zones and their volume are shown in Figure 3-22. These two identical final settlement tanks with radial flow path have a central inlet and a rotating bridge from which submerged scrapers are suspended. These submerged scrapers directed the settled sludge at the bottom of the tank to a

central sludge well in the tank. An upper scraper fitted to the half bridge directs any surface scum to two trap scum boxes on the periphery of the tank.

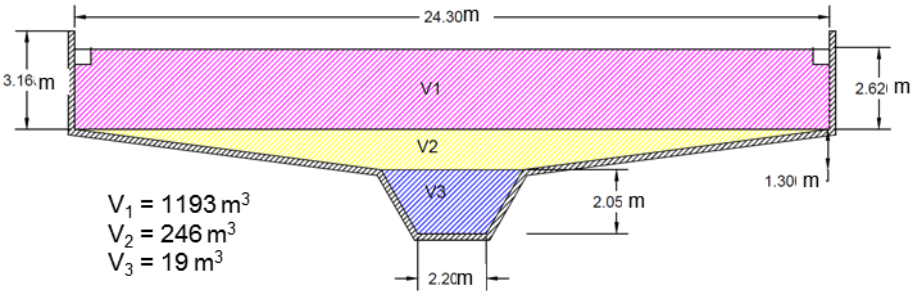

Figure 3-22: Cross section of final settlement tanks

An essential feature of the activated sludge treatment process is that most of the activated sludge is returned to the oxidation ditch to maintain the necessary population of micro-organisms (Haandel and Lubbe, 2011). In this instance, the return activated sludge is continually pumped to the oxidation ditch via the selector zone from the final settlement tank settled sludge. Three pumps (duty/assist and standby) with a capacity of 45 L s^{-1} for each settlement tanks. The RAS pumps' operation and control philosophy are detailed in Section 3.2.1.

The Surplus Activated Sludge (SAS) is pumped from the final tanks to the sludge dewatering tank. The pump used for SAS removal is the same as the RAS pump where it is manually controlled by the crossover valve, i.e. when there is a SAS flow, there won't be a RAS flow from that settlement. At a time, the SAS is pumped only from one of the final settlement tanks. The details of the control philosophy for the SAS is given in Section 3.2.1.

The final effluent from the settlement tank overflows a weir into an outlet channel on the periphery of the tank. From this channel, the effluent gravitates to a sampling chamber (where SEPA took samples of the final effluent) and flows by outfall into the River Eden. Before the effluent gravitates to the sampling chamber 30 – 35 L s^{-1} of effluent water will be returned and sprayed over the mixed liquor in the oxidation ditch.

3.2.2.1 Final Settlement Tanks Modelling

The two final settlement tanks, each with a surface area of 464 m^2 and volume of 1458 m^3, are modelled as a single tank with a surface area of 928 m^2 and volume of 2916 m^3, using the BSM2 model (a ten-layer model), based on (Takács et al.,

1991). This assumes no biological activity occurs and the shape of the settlement tanks were assumed to be cylindrical all the way through with the above volume and surface area.

The two duty RAS pumps are modelled combined to operate at a constant flow rate of 70 L s^{-1}, based on measured data. The RAS flow reduced to 35 L s^{-1} whenever the SAS crossover valve is open. The SAS crossover pump is opened once in every three days only if the MLSS in the oxidation ditch is greater than the MLSS set-point, $MLSS_{ctrl}$, 3250 mg L^{-1} and delivers sludge at a rate of 30 L s^{-1}, Q_{SAS}, for 1.85 hours, T_{SAS}. If these conditions are not met the SAS will be zero. The SAS control philosophy is modelled as shown below, Eq. 3-27.

If the simulation day is an even number (i.e. SAS is removed every other day) and:

$$If \quad (t_{sim} - day) \geq t_{SAS,start} \quad and \quad (t_{sim} - day) \leq t_{SAS,stop}$$

$$If \quad MLSS \geq MLSS_{ctrl}$$

$$Q_{SAS,t} = Q_{SAS}$$

Otherwise:

$$Q_{SAS,t} = 0 \qquad \text{Eq. 3-27}$$

Where:

t_{sim}	=	Current simulation day considering time of the day [d]
day	=	Current simulation day without considering the time of the day [d]
$t_{SAS,start}$	=	Time the SAS pump instigated manually (7:00 a.m.), expressed as a fraction of the day [d]
$t_{SAS,stop}$	=	Time the SAS pump stops, as a fraction of the day [d]
$MLSS$	=	Mixed liquor concentration in the oxidation ditch [mg L^{-1}]
$MLSS_{ctrl}$	=	Set-point for the MLSS in the oxidation ditch [mg L^{-1}]
$Q_{SAS,t}$	=	SAS flow rate at the current time step [m^3 d^{-1}]
Q_{SAS}	=	SAS flow rate whenever it is instigated (30 L s^{-1}) [m^3 d^{-1}]

3.2.3 Sludge Treatment

The Sludge Treatment process within the WWTP is carried out by using sludge dewatering tank, sludge-holding tank, sludge thickener (Centrifuge), liquor buffer tank, and two supernatant return pumps.

In addition to treating the surplus activated sludge generated onsite, Cupar WWTP accepts sludge from nearby wastewater treatment works.

The sludge dewatering tank and the sludge holding tanks are identical in size and shape as shown in Figure 3-23.

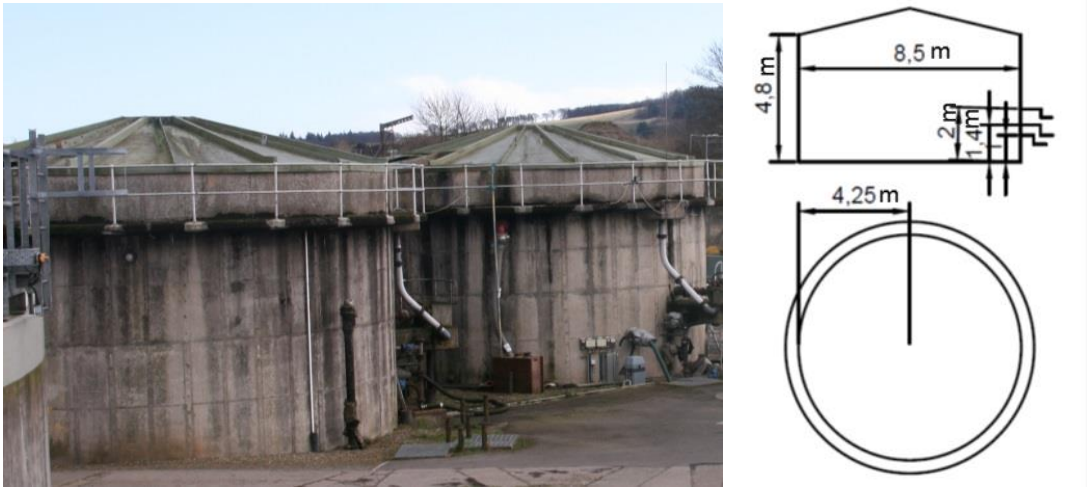

Figure 3-23: Left to right sludge holding tank (in some documents referred as sludge holding tank 1), sludge dewatering tank (in some documents referred as sludge holding tank 2), and longitudinal and plan view of the sludge dewatering/holding tanks; dimensions in meters

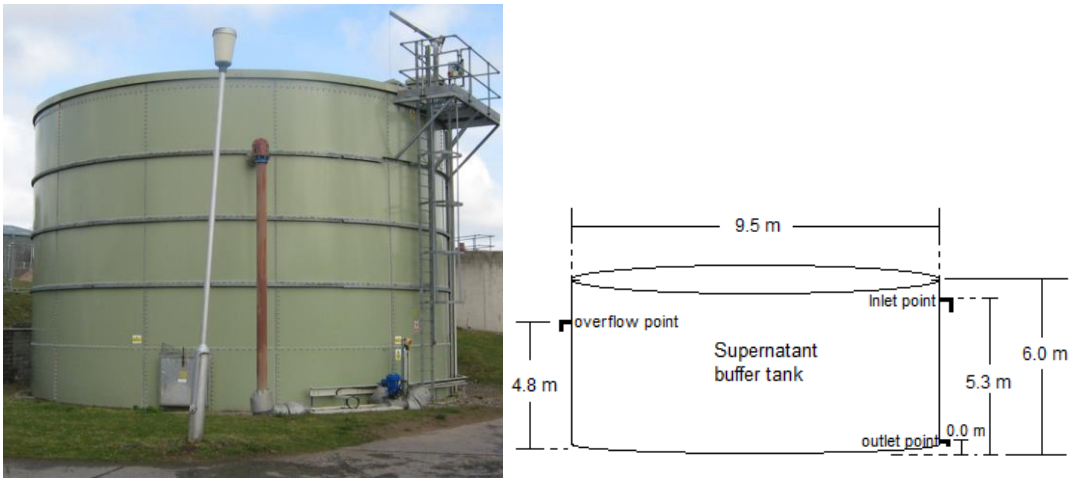

Figure 3-24: Details of the liquor buffer tank

SAS initially gravitates to the first holding tank on site. In the first tank, the SAS can settle, and any supernatant can be decanted. Following decantation, the sludge remaining in the dewatering tank is then pumped into the sludge holding tank where it combines with sludge from other facilities. The settled sludge in the sludge-holding tank is transferred to the centrifuge sludge processor.

SAS from the final settlement tanks enters a sludge dewatering tank with a total storage capacity of 272.4 m^3 (8.50 m diameter, 4.80 m depth), in which settling occurs. This process is manually operated, and after settling a valve is opened to enable supernatant to flow to the supernatant wet well, via the decanted liquor

chamber. The supernatant wet well measures 2.10 m in diameter and 2.92 m in depth, and has two pumps which operate alternately to transfer supernatant to the 340.2 m^3 liquor buffer tank (9.50 m diameter, 4.80 m depth), see Figure 3-24.

Sludge from the dewatering tank is pumped to the sludge holding tank, which is of equal size, approximately 24 hours after activation of the SAS pump or when the supernatant has been removed. The sludge-holding tank also receives imported sludge from three WWTPs in addition to that generated on site. No sludge import data is available for the time span covered by other data sets, but the volume and date of sludge imports during the period 03/01/2014 – 12/02/2014 is known. Individual imports range from 13 to 39 m^3, yielding an overall mean flow rate of 11.05 $m^3\ d^{-1}$ (0.13 L s^{-1}). Mixers in the sludge-holding tank are operated manually and run continuously.

Settled sludge from the sludge-holding tank is dried using a Hiller Decapress centrifuge, which gives sludge with 18 – 20 % dry solid. Based on recorded values for the sludge cake, an average of 19.77 % dry solids is achieved. Polyelectrolyte dosing is used to aid the dewatering. The centrifuge is a batch process, operates when the WWTP is manned, i.e. the centrifuge sludge processor turned on in the morning and ran on average for 7hrs, five days a week. Sludge cake from the centrifuge is transported 57 miles by road to a landfill disposal point three times a week.

Liquor from the centrifuge flows to liquor chamber, where it combines with the liquor return flow from the sludge dewatering tank. The return liquor (supernatant return flow) flows through gravity to the supernatant wet-well and is pumped to the liquor buffer tank automatically, based on liquor level in the supernatant wet-well. The set-points for supernatant pumps control are given in Table 3-3. There are two submerged pumps in the supernatant wet-well working in rotation, and the state of the pumps (ON/OFF) is determined based on the set-points.

Table 3-3: Set-points for supernatant wet-well pumps control

Set-points for Supernatant pump well SCADA screen shot 07/03/2014 12:28:14	
Unit/variable	**Set point**
Supernatant pump duty rotation time	24 hrs
Supernatant duty pump start level	0.9m
Supernatant duty pump stop level	0.5m
Supernatant pump wet-well high level	1.8m
Return liquor buffer tank high level	4.5m

3.2.3.1 Sludge Treatment Modelling

The gravity thickening in the sludge dewatering tank is modelled as in the BSM2 thickener block; this assumes 98 % solids removal efficiency with no biological activity. The centrifuge is modelled using the BSM2 'dewatering' block, with a specified dewatered sludge TSS content of 19.77 % (based on site records). As in BSM2, 98 % of solids entering the unit is concentrated in the sludge stream, and both the sludge and supernatant contain equal concentrations of soluble components. Sludge processing units represented by the 'thickener' and 'dewatering' blocks are shown in Figure 3-25.

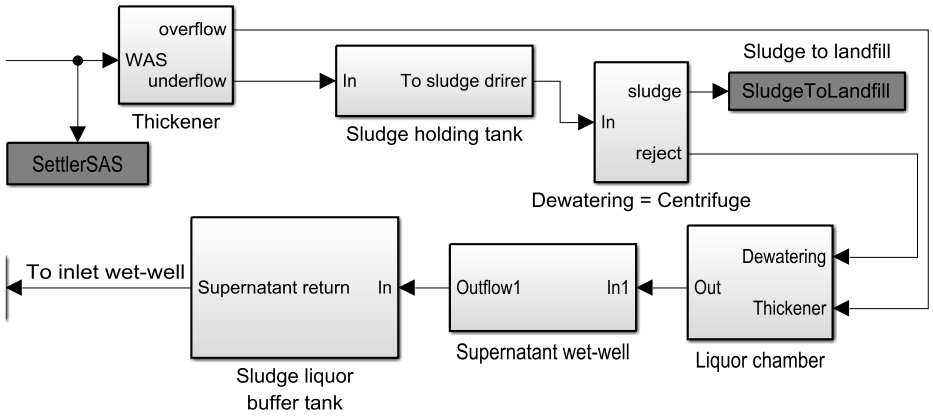

Figure 3-25: Sludge processing units represented by the 'thickener', 'sludge holding tank', and 'dewatering' model blocks

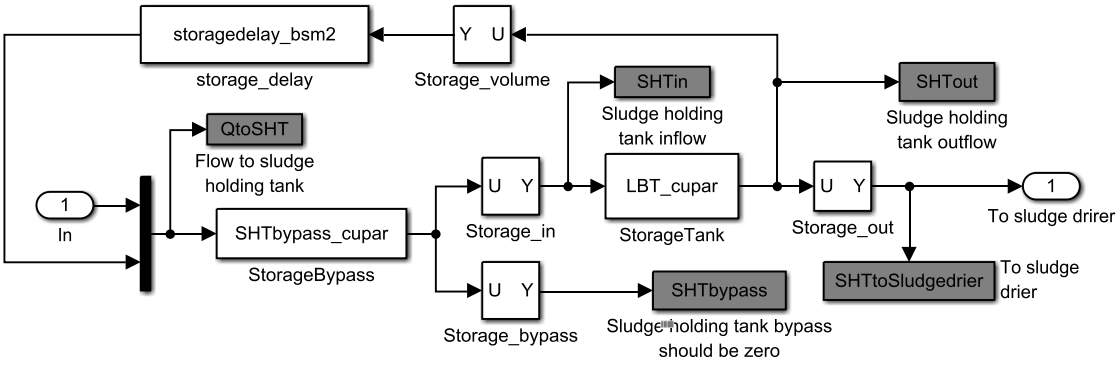

Figure 3-26: Simulink layout of the sludge holding tank model block

The sludge holding thanks is modelled as a storage tank model as of BSM2 model but with some modification with the Simulink model layout shown in Figure 3-26. The model 'SHTbypass_cupar' was used to determine the outflow from the sludge-holding tank to the centrifuge sludge thickener (referred here as sludge centrifuge) which depends on the time of the day and the day of the week, Eq. 3-28. If the simulation day is not Saturday or Sunday, the outflow from the sludge-

holding tank is modelled as shown below, as long as the simulation starts on a Monday. If simulation does not start on Monday, Eq. 3-28 can be modified just by adding the offset to the variable, day.

$$If \quad (day)\ or\ (day+1)\ are\ not\ divisible\ by\ 7, (i.e. weekday)\ \ and$$
$$If \qquad (t_{sim} - day) \geq t_{centrifuge,start} \qquad and$$
$$If \qquad (t_{sim} - day) \leq (t_{centrifuge,start} + t_{centrifuge,run}) \qquad then$$
$$Q_{centrifuge,t} = Q_{centrifuge}$$

Otherwise:

$$Q_{drier,t} = 0 \qquad \text{Eq. 3-28}$$

Where:

t_{sim}	=	Current simulation time [d]
day	=	Current simulation day [d]
$t_{centrifuge,start}$	=	Time the sludge centrifuge instigated manually (7:00 a.m.), expressed as a fraction of the day [d]
$t_{centrifuge,run}$	=	Time the sludge centrifuge runs in a day (6 hrs), expressed as a fraction of the day [d]
$Q_{centrifuge,t}$	=	Sludge flow rate to the centrifuge sludge direr at the current time step [$m^3\ d^{-1}$]
$Q_{centrifuge}$	=	Sludge flow rate to the centrifuge sludge centrifuge whenever the centrifuge is instigated (5.6 L s^{-1}) [$m^3\ d^{-1}$]

The liquor chamber block contains the BSM2 flow combiner model, ‘combiner_2’ the combines the supernatant return flow from the ‘dewatering’ and the ‘Thickener’ model block.

The Supernatant wet-well model block receives the combined flow from the liquor chamber. The supernatant wet-well control philosophy is modelled by modifying the inlet wet-well configuration to suit one pump operation and its set-points, see Table 3-3 and Figure 3-27. The ‘storagebypass_cupar_SRL’ model calculates the pump’s state based on the supernatant wet-well level and previous time-step pump’s state, calculates overflows if any. The calculation of the outflow rate from the supernatant wet-well to the liquor buffer tank is detailed in Section 5.2.1.4. Calculation of actual flow into the wet-well and update in the storage volume is done by modifying the BSM2 ‘storage’ model, presented here as ‘storage_cupar_SRL’.

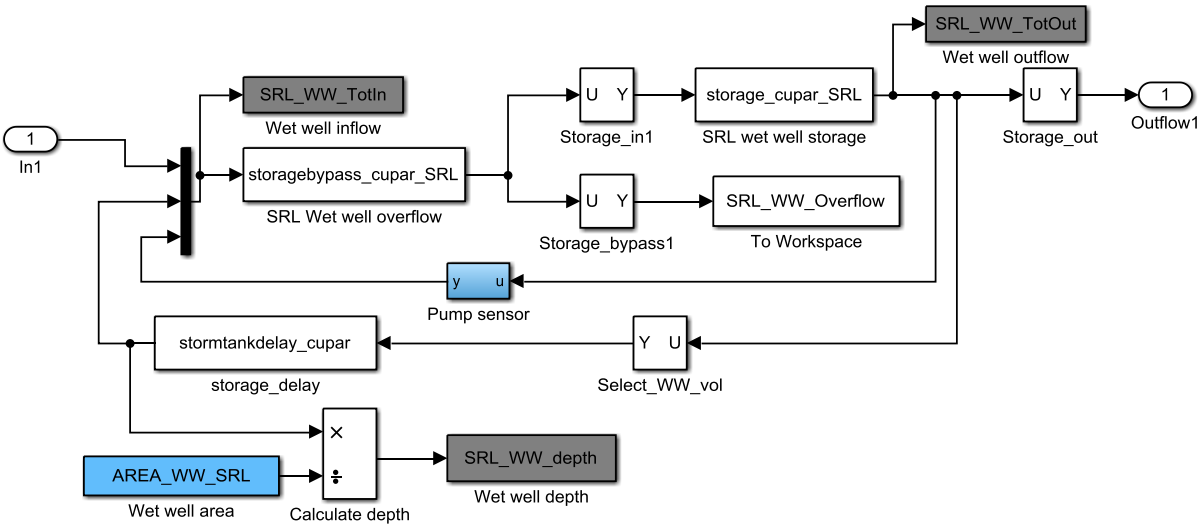

Figure 3-27: Supernatant wet-well model layout in Simulink

The liquor buffer tank is modelled using a modified version of the BSM2 'StorageTank' block, in which filling, emptying and bypass are determined based on the total flow to the tank, and volume/depth of liquor in the tank. In this instance, however, the return flow (calculated based on the height of liquor in the tank) and tank bypass are combined since both are passed to the inlet wet-well.

When the sludge buffer tank is empty, the return flow from the sludge buffer tank to the wet-well is zero. When the sludge buffer tank is either full or part full, return flow to the inlet wet-well is given by Eq. 3-29, where $Q_{out,buffer}$ is the outflow rate from buffer tank and $h_{water,buffer}$is hight of wastewater in buffer tank. The equation is developed using a simple energy balance approach by considering friction and energy losses at fittings, such as the half opened valve controllig flow from buffert tank to inlet wet-well. Flow into the buffer tank, and bypass flow is calculated using a simple water balance approach and the outflow rate from the supernatant wet-well. A diagram of the Simulink implementation of the liquor buffer tank model is given Figure 3-28.

$$Q_{out,buffer} = \left(11.31 \times \sqrt{h_{water,buffer} + 1}\right) \times 86.4 \qquad \text{Eq. 3-29}$$

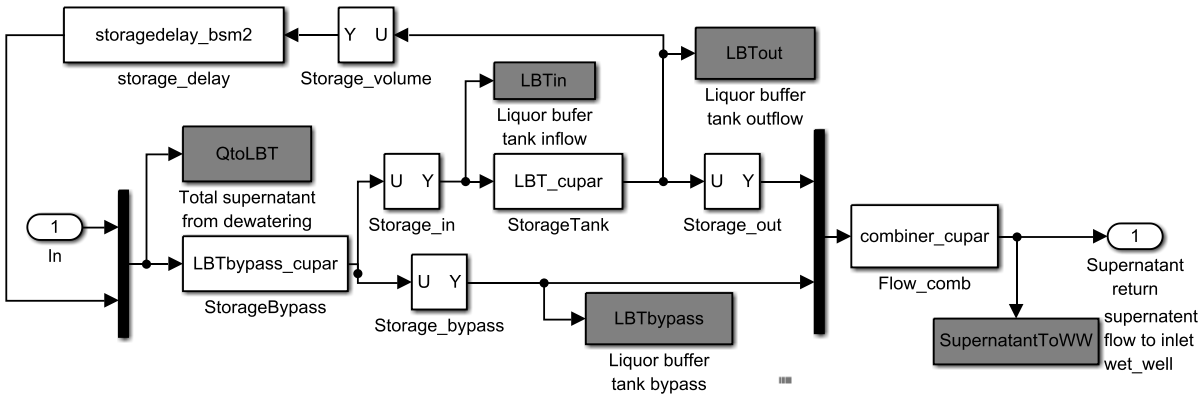

Figure 3-28: Liquor buffer-tank model layout in Simulink

4. Data Reconciliation

This chapter has three sections. The first section covers the influent wastewater characterisation and identification of parameters that should be monitored to accurately characterise influent wastewater with a focus on reducing model uncertainty. The second section deals with the identification of key points for hydraulic load measurement, validation of measured data by performing a simple hydraulic balance test at key points within the Cupar wastewater treatment plant (WWTP). The third section deals with the assimilation of measured physio-chemical characteristic indicators and interpolation of discrete data points to create a dataset with shorter timestep, currently 15 minutes time-step for model input.

Future demand for model based control of WWTP is expected to increase. In Europe, including the UK, models are mostly a research subject whereas in other parts of the world like North America WWTPs are predominantly used as an engineering tool in practice (Hauduc et al., 2009). This pattern is now changing in the UK, and water utilities have started to incorporate WWTP models in decision making, process control and optimisation. According to UKWIR (2013b), WWTP models are now being used for advanced process control and this practice is expected to increase significantly in the future due to tighter regulations and the potential of this approach to save energy and greenhouse gas (GHG) emissions. One of the challenges is the availability of data and their quality.

High quality data is crucial for the effective use of WWTP models. The reliability of the model results is strongly linked to the amount of the data used to set up and calibrate the model (Rieger et al., 2010). A carefully designed and collected dataset can reduce the time for the subsequent modelling study and can increase the confidence in using the model for the practical application. Conversely, data scarcity and low-quality data can reduce the accuracy of simulation results and even lead to wrong conclusions and serious consequences such as breaching of licenses.

Historical data can be used to understand the long-term behaviour of WWTPs. However, dynamic modelling for control purposes requires high resolution spatial and temporal data, which includes sub-daily monitoring of various parameters.

Stoichiometric/kinetic data can also be monitored to estimate the model parameters more accurately. However, this can be costly and demand experience to achieve all these datasets. Thus, it is important to determine what level is sufficient for the model-based study.

The importance of monitoring wastewater within the WWTP has been suggested to be crucial for both design and modelling purposes (Metcalf & Eddy, 2004; Melcer, 2003; Gernaey et al., 2006; Rosén et al., 2003). Nevertheless, the question lies in what level of data is sufficient to have reasonable confidence in the model to be used for active control purpose. Previous research showed the significance of characterising the influent wastewater to accurately model processes within the WWTP (Vanrolleghem et al., 2005; Vollertsen and Hvitved-Jacobsen, 2002; Benedetti et al., 2013). Sewer networks, WWTPs and receiving water bodies are interacting and are components of an integrated system. Hence, it is crucial that the wastewater charcterisation concepts and the description of microbial transformations used in the three systems be comparable. Ideally, the concepts and type of data collected in these three system components should be identical (Vollertsen and Hvitved-Jacobsen, 2002). The purpose of this chapter is to develop a step-by step guideline that can be used to identify data need in characterising the influent wastewater. It outlines steps used to monitor, analyse and validate measured data in the case study, Cupar WWTP. This chapter can be used as guidance in identifying the minimum data that would be required when the same modelling and control strategy design approach is used for other wastewater systems.

4.1. WWTP Influent Characterisation

The Activated Sludge Model No. 1 (ASM1) used in the WWTP modelling uses seven dissolved (S…) and six particulate (X…) components to characterise the influent wastewater and the activated sludge. These components include two forms of biomass (heterotrophic and autotrophic), seven fractions of COD (note that the biomass is fractions of the COD), four fractions of nitrogen, dissolved oxygen, and alkalinity (Gujer and Henze, 1991).

These components are listed below:

i. Soluble inert organic matter (S_I)
ii. Readily biodegradable substrate (S_S)

iii. Particulate inert organic matter (X^I)
iv. Slowly biodegradable substrate (X_S)
v. Active heterotrophic biomass ($X_{B,H}$)
vi. Active autotrophic biomass ($X_{B,A}$)
vii. Particulate products arising from biomass decay (X_P)
viii. Oxygen (S_O)
ix. Nitrate and nitrite nitrogen (S_{NO})
x. NH_4 + NH_3 nitrogen (S_{NH})
xi. Soluble biodegradable organic nitrogen (S_{ND})
xii. Particulate biodegradable organic nitrogen (X_{ND})
xiii. Alkalinity (S_{ALK})

It can be time consuming, and costly to directly measure some of the state variables required by the ASM1. Since wastewater composition varies significantly from location to location and direct measurement for each of the components is commonly not available/affordable, it is important to design the characterisation process based on available resources (Gujer and Henze, 1991; Melcer, 2003). Procedures are outlined below that can be used to characterise influent wastewater and can be used as a guideline for modelling other WWTPs like the case study in this study, Cupar WWTP.

4.1.1. COD Fractions

The COD fractions that are the active agent in the microbial transformations: the heterotrophic microbial biomass $X_{B,H}$, and the autotrophic biomass $X_{B,A,}$ which is responsible for denitrification process in the system, Figure 4-1. Other fractions are substrates for these biomasses (S_I, S_s, X_S, and X_S). Some of the substrates are readily biodegradable $S_{s,}$ and some are more slowly biodegradable X_S, i.e. they must be hydrolysed before the heterotrophic biomass can utilise them. Another part of the organic matter is not biodegradable at all; i.e. it is inert (S_I and X_I). Ideally, to reduce assumption and uncertainty all these components involved in the microbial transformation of wastewater organic matter should be determined explicitly at any time. However, no direct continuous method exists for the determination of all the COD components.

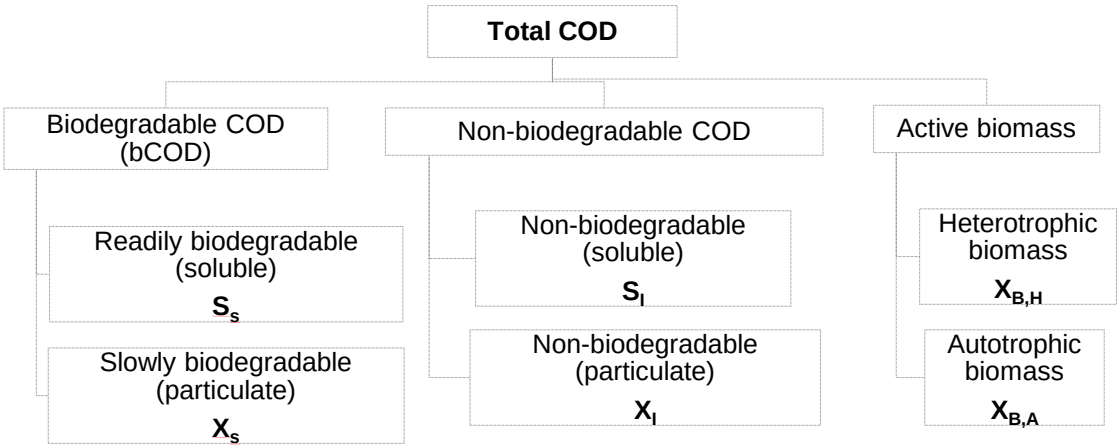

Figure 4-1: COD fractions adopted from Metcalf & Eddy (2004)

4.1.1.1. Soluble Inert Organic Matter (S_I)

The soluble inert organic matter is the soluble organic material that is unaffected by biological action in the activated sludge (Melcer, 2003). This fraction of COD can be estimated by assuming the residual soluble biodegradable COD in the final effluent is negligible, and there is no generation of soluble COD in the system. In this case, the soluble inert organic matter is equivalent to the soluble COD in the final effluent. The true soluble COD can be determined by directly measured filtered and flocculated COD, *Eq. 4-1*.

Thus;

$$S_I = COD_{ff,eff} \qquad \text{Eq. 4-1}$$

Where: $COD_{ff,eff}$ is the filtered and floculated COD concentration in the final effluent. Alternatively, if soluble COD is known, the inert soluble organic matter can be estimated using Eq. 4-2. In this instance, the readily bioderadebel substrate S_s, is calcualted based on Section 4.1.1.2, hence it is used in estmating S_I from the directly measured soluble influent COD, Eq. 4-2.

$$S_I = COD_{SOL} - S_s \qquad \text{Eq. 4-2}$$

Where: COD_{SOL}: *soluble influent COD which is equivalent to* $COD_{ff.Inf}$

4.1.1.2. Readily Biodegradable Substrate (S_s)

The soluble readily biodegradable COD is the material that can be absorbed easily by the microbial organisms and metabolised for energy and synthesis (Melcer, 2003). Oxygen uptake rate – respirometry or physiochemical methods can be used to determine this fraction of COD. The former can be time consuming

and requires experienced expertise skill (Sin et al., 2005). In the physiochemical method, S_S can be estimated either by measuring flocculated filtered COD (COD_{ff}). The COD_{ff} method suggested by Mamais et al. (1993) is easier compared to oxygen uptake rate approach, as it is not labour intensive and time consuming (Melcer, 2003).

The COD_{ff} method uses a physical separation by pre-flocculating the sample then followed by flocculation. The assumption is that the flocculation removes all the colloidal particles resulting in filtrate that contains only soluble material. The other assumption is all the readily biodegradable material is consumed in the activated sludge; thus, the difference between the soluble material of influent ($COD_{ff,Inf}$) and the soluble material of final effluent ($COD_{ff,eff}$) is the readily biodegradable COD (S_s).

$$S_S = COD_{ff,Inf} - COD_{ff,eff} \qquad \textit{Eq. 4-3}$$

Procedure (Mamais et al., 1993):

i. Samples are flocculated by adding 1ml of a 100 g L^{-1} zinc sulphate solution to a 100ml wastewater sample;
ii. Mix vigorously with a magnetic stirrer for approximately 1 minute;
iii. The pH of the mixed sample should be adjusted to about 10.5 with 6 M sodium hydroxide solution;
iv. The sample is then allowed to settle quiescently for a few minutes. (Standard Methods, (1985), Section 417B).
v. The clear supernatant of the sample (20-30 ml) should be withdrawn with a pipette and passed through a 0.45µm membrane filter.
vi. The COD of the supernatant filtrate is analysed. This COD is termed the flocculated and filtered COD

4.1.1.3. Slowly Biodegradable Substrate (X_S)

The slowly biodegradable COD (X_s) can be calculated using the soluble readily biodegradable COD concentration (S_s) and the biodegradable COD ($bCOD$). The $bCOD$ can be estimated according to Metcalf & Eddy (2004).

$$X_s = bCOD - S_s \quad \text{Eq. 4-4}$$

$$\frac{bCOD}{BOD} = \frac{{}^{UBOD}/_{BOD}}{1.0 - 1.42 f_d(Y_H)} \quad \text{Eq. 4-5}$$

Where f_d is the fraction of cell mass remaining as cell debris, g/g. Typical value of f_d for domestic wastewater is **0.15** (Metcalf & Eddy, 2004), which is adopted in this study. Y_H is the synthesis yield coefficient for heterotrophic bacteria [g VSS/g COD used] or [g cell COD formed/g COD oxidized]. Y_H at 15 °C is taken to be **0.67** similar to BSM2 (Jeppsson et al., 2007). BOD and UBOD are the Biochemical Oxygen Demand and Ultimate Biochemical Oxygen Demand, respectively. The ratio ${}^{UBOD}/_{BOD}$ for typical domestic wastewater is **1.5** (Metcalf & Eddy, 2004). This value was adopted in this study. Substituting these values into Eq. 4-5, $bCOD$ can be expressed in terms of BOD, see Eq. 4-6.

$$bCOD = 1.75 \times BOD \quad \text{Eq. 4-6}$$

4.1.1.4. Active Heterotrophic Biomass ($X_{B,H}$)

If modelling is performed downstream of the primary settlement tank, most of the active biomass in the activated sludge is generated from the activated sludge. The continuous seeding of biomass from wastewater influent can impact the behavior of the process. Accordingly, sometimes the process of quantifying the active biomass can be essential (Melcer, 2003).

No simple approach is found to be able to estimate this parameter. The mostly used method to determine this parameter is the use of batch test presented in Wentzel et al. (1995) and also suggested in Kappeler and Gujer (1992). A batch test uses a batch treatment on a lab scale in which the treatment process in a completely stirred reactor, is entirely concluded, and products discharged before more water sewage is taken in. The other approach that can be used to quantify these state variable is the oxygen uptake rate (OUR), which continuously monitored the oxygen uptake to calculate the growth rate and the presence of heterotrophic bacteria. Nitrate and nitrite concentration can be assessed to inform the presence of autotrophic bacteria.

These methods require lab space, expertise effort, and time (Vanrolleghem et al., 2003); thus, not considered to be used in this project.

Particulate COD is distributed over X_I, X_S, and $X_{B,H}$. In BSM2 X_I, X_S and $X_{B,H}$ are determined as a percentage of total suspended solid ($X_I + X_S + X_{B,H}$), i.e.;

$$X_{B,H} = X_{B,H\_fr} \times (COD_T - S_S - S_I) \qquad \textit{Eq. 4-7}$$

Where:

X_{B,H_fr} Fraction of the sum which is active heterotrophic biomass, assumed to be 10 %, (Gernaey et al., 2005b)

Hence, the active heterotrophic biomass concentration can be estimated from particulate COD which can be estimated as the difference between total COD and filtered COD (COD_T – COD_{ff}).

4.1.1.5. Particulate Inert Organic Matter (X_I)

The particulate unbiodegradable material is not registered in BOD. Thus, a high proportion of it affects the COD to BOD ratio of the wastewater. Hence, COD to BOD ratio can be used as an indicator of X_I. The higher the ratio is often an indication of a strong concentration of inert organic matter, X_I.

Colloidal slowly biodegradable COD (S_{COL}) is calculated by assuming active biomass concentration in the influent is zero, see Eq. 4-8. S_{COL} is not used in BSM2 since ASM2 uses only slowly biodegradable COD without fractionating it into soluble and particulate.

$$S_{COL} = COD_T - S_S - S_I - (X_I + X_S + X_{B,H}) \qquad \text{Eq. 4-8}$$

Many wastewater models including ASM1 and ASM2 assumed that the slowly biodegradable COD is in a particulate form as shown in Figure 4-1. Hence, the soluble colloidal concentration S_{COL} is assumed zero. Substituting this into and rearranging the equation the particulate inert organic matter concentration X_I can be estimated using Eq. 4-9.

$$X_I = COD_T - S_S - S_I - X_S - X_{B,H} \qquad \text{Eq. 4-9}$$

Where COD_T, the total COD of the influent, can be measured directly and where S_S, S_I, X_S, and $X_{B,H}$ can be estimated using Eq. 4-3, *Eq. 4-1*, Eq. 4-4, and **Error! Reference source not found.** Eq. 4-7 respectively.

4.1.1.6. Active Autotrophic Biomass ($X_{B,A}$)

Copp and Murphy (1995) listed down different approaches to estimate $X_{B,A}$ and they presented the in-situ nitrifier mass estimation technique which can be used to determine the nitrifier population within an activated sludge sample using dominant cultures of nitrifying organisms. The approaches require experience

and initial setup; hence not used in this study. Since the concentration of autotrophic bacteria is very few in ordinary wastewater (Henze, 2002), in this instance, it is assumed that their concentration is zero; similar to the original BSM2 model (Jeppsson et al., 2007).

4.1.1.7. Particulate Products from Biomass Decay (X_P)

There is no clear way presented in the literature to estimate this parameter, thus according to Jeppsson et al. (2007), X_P is assumed to be zero.

4.1.2. Oxygen (S_O)

The dissolved oxygen concentration in the influent wastewater can be readily determined by direct measurement using a dissolved oxygen probe. This parameter was assumed to be zero in BSM2. However, in this instance, the dissloved oxygen concentration is monitored during the monitoring campaign.

4.1.3. Nitrogen Fractions

In aerobic growth, heterotrophic microbial biomass consumes S_{NH}, Figure 4-2, and during the anoxic process, they absorb both S_{NH} and nitrates (S_{NO}). Autotrophic biomass plays a vital role in the reduction of S_{NH} in the wastewater during aerobic growth. The nitrogen compound in the form of slowly biodegradable particulate X_{ND} is hydrolysed to give biodegradable organic Nitrate (S_{ND}). These forms of nitrogen S_{ND}, from hydrolysis of X_{ND} or initially existing in the wastewater, are converted (through ammonification) to S_{NH} which is consumed by heterotrophic microbial biomass both in anoxic and aerobic growth or by autotrophic bacteria during the aerobic process. Thus, fractionating the total nitrogen is also necessary for characterising the wastewater.

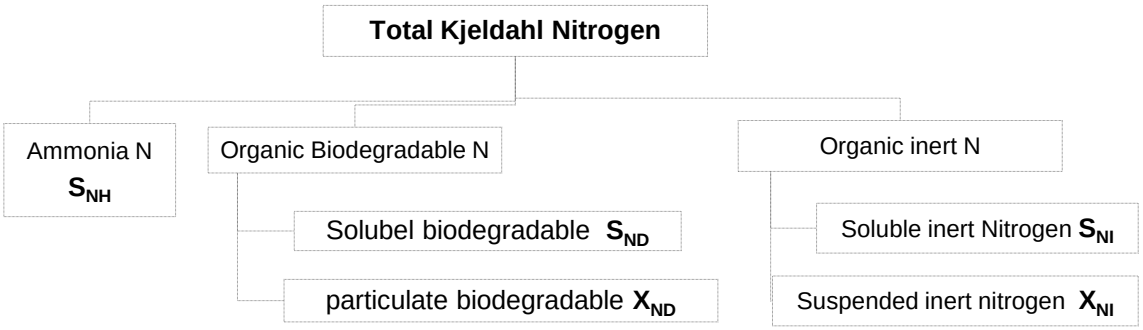

Figure 4-2: Nitrogen fractions

4.1.1.8. Nitrate and Nitrite Nitrogen (S_{NO})

Nitrates and nitrites (S_{NO}) are oxidised forms of nitrogen, commonly associated with fertilisers from agricultural fields (surface runoff), detergents in households and laundrettes (Butler et al., 1995; Braga and Varesche, 2014; Reeves, 1972). S_{NO} can easily be measured with sufficient accuracy either using standard methods or using online probes (Capelo et al., 2007; Drolc and Vrtovšek, 2010). Similar to that of the ammonia concentration determination, in this instance, a standard method was used to determine S_{NO}.

4.1.1.9. Ammonia (NH_4 + NH_3) Nitrogen (S_{NH})

Most of the nitrogen in domestic wastewater is in the form of ammonia mainly from household toilets (Butler et al., 1995), i.e. ammonia accounts for a major portion of influent Total Kjeldahl Nitrogen (TKN). Other forms of nitrogen may not be as significant as S_{NH} for modelling purpose, but if needed the estimation is neither sophisticated nor costly. S_{NH} can directly be measured by taking a sample of wastewater and filter it through a 0.45µm membrane filter and analyse the filtrate for ammonia concentration (Melcer, 2003). Alternatively, ammonia can also be monitored using online probes that showed an excellent accuracy compare to standard methods (Capelo et al., 2007). In this study, the standard method was found to be most convenient since monitoring was done for a short period and samples were already collected for analysing other pollutants.

4.1.1.10. Soluble Biodegradable Organic Nitrogen (S_{ND})

S_{ND} is the soluble biodegradable organic nitrogen which level can be estimated using measured filtered TKN and measured S_{NH} by assuming the inert form of TKN, S_{NI}, to be very small, see Sections 4.1.1.11 and 4.1.1.12. Since the inert nitrogen has no impact on the ASM2 model, this assumption may not significantly affect modelling performance (Melcer, 2003).

$$TKN_{Filtered} = S_{NH} + S_{ND} + S_{NI} \qquad \text{Eq. 4-10}$$

In this instance, for some unknown reason, the lab was not able to determine the filtered influent total Kjeldahl nitrogen ($TKN_{Filtered}$) for the samples collected during the campaign period. Pagilla et al. (2008) assessed the fraction of organic nitrogen as dissolved, colloidal, and partiuclte organic nitrogen for different WWTPs in the USA and Poland. The fraction of the particulate organic nitrogen (which is missing in the filterd TKN compared to the unfilted TKN) varies

signficantly from site to site, 11 % - 67 % of the total orgnaic nitrogen. In this instance, the particulated orgnig ntirogen is assumed to be 20 %; hence, filtered influent TKN is assumed to be 80 % of the unfiltered influent TKN.

$$TKN_{Filtered} = 0.8 \times TKN \quad \text{Eq. 4-11}$$

4.1.1.11. Soluble Unbiodegradable Organic Nitrogen (S_{NI})

The soluble unbiodegradable organic nitrogen (S_{NI}) is not directly used in the activated sludge model such as ASM2, i.e. it is not one of the model input parameters. However, it is necessary to estimate its concentration to calculate other model inputs such as the particulate biodegradable organic nitrogen, Section 4.1.1.12. S_{NI} is usually less than 3 % of the TKN (Melcer, 2003; Henze et al., 2000). Hence, S_{NI} can be estimated to be any value less than 3 % of the TKN without affecting model performance. Alternatively, it can also be determined using the filtered effluent TKN and assume $S_{ND,eff}$ is 0.4mg L^{-1}.

In this study, the influent soluble unbiodegradable organic nitrogen is assumed to be 2.5 % of the measured influent TKN.

4.1.1.12. Particulate Biodegradable Organic Nitrogen (X_{ND})

Particulate biodegradable organic nitrogen (X_{ND}) can be calculated using the mass-balance for Total Kjeldahl Nitrogen (TKN). TKN is the sum of ammoniacal, organic, and inert (reduced) nitrogen, see Eq. 4-12.

$$X_{ND} = TKN - (S_{NH} + S_{ND} + N_{Inert}) \quad \text{Eq. 4-12}$$

Where:

$$N_{Inert} = S_{NI} + X_{NI} \quad \text{Eq. 4-13}$$

X_{NI} is the particulate unbiodegradable influent nitrogen. X_{NI} can be estimated by assuming the TKN is equally distributed between particulate biodegradable and unbiodegradable COD (X_S and X_I respectively) (Melcer, 2003), see Eq. 4-14.

$$\frac{X_{NI}}{X_I} = \frac{TKN - TKN_{filtered}}{COD_T - COD_f} \quad \text{Eq. 4-14}$$

Solving the above equation for the measured average TKN, COD_T, COD_f, and the estimated filtered TKN (Eq. 4-11, gives the ratio X_{NI}/X_I to be equal to 0.022. For the detail on the estimation of X_I see the Section 4.1.1.4. Based on this approach, X_{NI} is 6 % of the TKN of the Cupar's influent wastewater. X_{NI} is a small fraction of the TKN, approximately 10 %, thus, the X_{NI}, calculated based on the above approach, will not give an undue error (Melcer, 2003).

For ammoniacal nitrogen (S_{NH}), and the soluble organic biodegradable nitrogen (S_{ND}) see Sections 4.1.1.9 and 4.1.1.10 respectively.

4.2. Flow Reaching the WWTP

In addition to the quality data requirements presented above, knowing some flow rates in the WWTP can immensely help to improve the model in simulating the hydraulics within the system.

Flow is proposed to be monitored at different points within the WWTP. These points are selected based on the need to complete the hydraulic balance for each possible subsystem within the WWTP, and the existing monitoring schemes. Existing data should always be assessed for potential error and uncertainty. Any existing monitoring point that faces uncertainty should be disregarded, and the new meter should be installed for comparison. Based on this approach, the following monitoring points were identified for Cupar WWTP. Monitoring points used in this study are shown in Figure 4-4 and Table 4-1:

- return flow rate from storm tanks to inlet wet-well, point 11
- spray bar return from final effluent chamber to oxidation ditch, point 30
- supernatant return flow, point 18**,** and
- scum return from the final settlement tanks to the wet-well, points 60 a, b, c

4.1.4. Frequency and Duration of Data Monitoring

Vanrolleghem et al. (2003) suggested that a time step of 2 – 4 hours samples taken for a week or two weeks can be sufficient to characterise influent wastewater. According to Petersen et al. (2002), for a plant scale dynamic modelling campaign should be done at least every one-fifth of the hydraulic retention time (HRT), and at least for a duration of 3 – 4 times HTR. For example, in the case of Cupar WWTP, the HRT is 18 hrs; hence, accordingly, sampling should be done at least every 3.5 hrs or 3 hrs for a minimum duration of 3 days. Based on these suggestions, cost of monitoring, and available fund the physio-chemical indicator parameters identified in the influent wastewater characterisation section were monitored every 2 hours for two weeks; with an attempt to catch one dry week and one wet week.

Monthly average rainfall data from 1981 – 2010 from the Met office data at Leuchars, 7.3 miles away from Cupar WWTP, is used. Data showed that the wettest month being October and the driest being February, March, April, and May. August is also dry compare to other months. Days of rainfall greater than or equal to 1mm are the least for the months February, and April. The months March, July, August, and September also have a lower number of days with rainfall greater than or equal to 1mm, see Figure 4-3.

Based on the trend below, August is the driest regarding average monthly rainfall and number of days with rainfall greater than 1mm until February 2016. The trend was used as a guidance to select dry and wet weeks. However, deploying sampling equipment for a week, removing them and then deploy them for another week was costly. Hence, by selecting the month with a low number of rainfall days, it is possible to maximise the chance of getting at least one dry week. Cupar WWTP is monitored for two weeks, 25/03/2016 – 10/04/2016, a period with relatively low rainfall days, April.

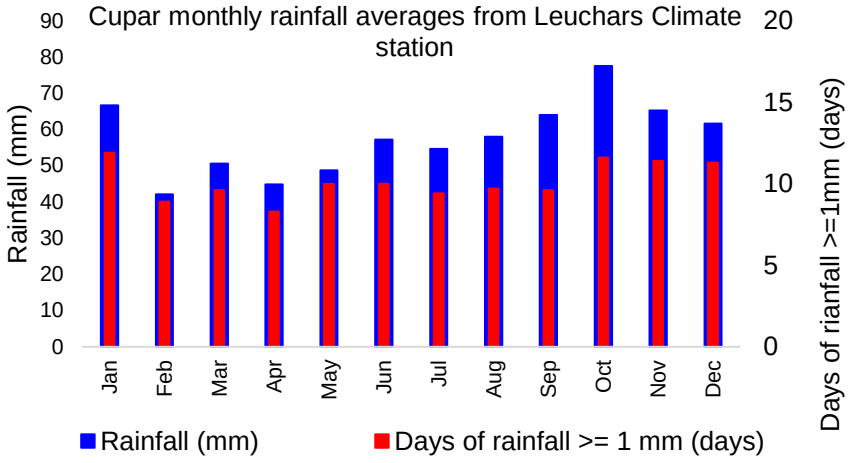

Figure 4-3 Cupar monthly rainfall and number of days with rainfall above 1mm

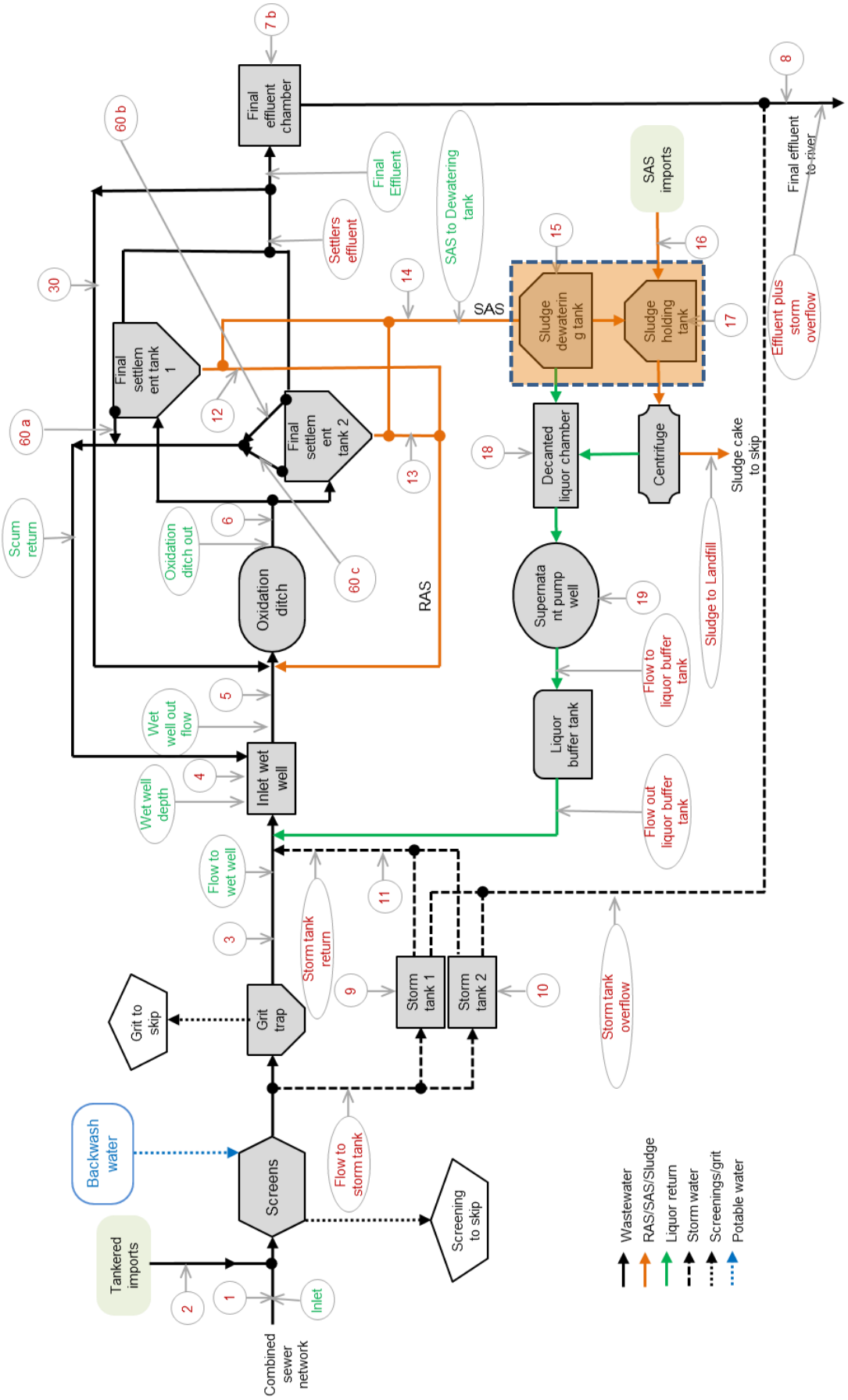

Figure 4-4: Cupar WWTP flow and wastewater quality monitoring points

Table 4-1 Cupar WWTP Sampling parameters and flow monitoring points details

Sampling point	Parameters monitored based on data need for wastewater characterisation	Time step	Period	Flow type
1	1. Total COD 2. Filtered COD 3. Flocculated filtered COD 4. BOD_5 5. TSS (Total suspended solids mg L^{-1}) 6. VSS (volatile suspended solids mg L^{-1}) 7. TKN (filtered total Kjeldahl nitrogen) 8. Total Nitrogen 9. Ammonia 10. Dissolved Oxygen 11. pH 12. Temperature 13. Nitrate (NO_3^-)	Time step for sampling for quality is 2 hours. First sample at 12:00 am.	Two weeks	Inlet (Influent)
7a	1. Total COD 2. Filtered COD 3. Flocculated filtered COD 4. BOD_5 5. TSS (Total suspended solids mg L^{-1}) 6. TKN (filtered total Kjeldahl nitrogen) 7. Total Nitrogen 8. Ammonia 9. Dissolved Oxygen 10. pH 11. Temperature 12. Nitrate (NO_3^-)	Time step for sampling for quality is 2 hours. First sample at 12:00 am.	Two weeks	Final effluent
18	1. Total COD 2. BOD5 3. TSS 4. Ammonia 5. TKN 6. pH 7. Temperature 8. Nitrate	Time step for sampling for quality is every 2 hours. First sample at 12:00 am	Two weeks	Supernatant return
60a, 60b, 60c,	Flow	2 minutes	Two weeks	Scum return
7a, 7b, 8	Flow	2 minutes	Two weeks	Final effluent
18	Flow	2 minutes	Two weeks	Supernatant return

4.3. WWTP Hydraulic Data Analysis

The hydraulic analysis for Cupar WWTP is first performed using existing data for the period 28/102012 – 11/07/2013 see Figure 4-5. First, the flow balance at the WWTP scale is analysed. The graphical analysis in Figure 4-6 shows, for the period 28/10/2012 – 26/04/2013 and 26/06/2013 – 11/07/2013, that the inlet flow to the WWTP is higher than the flow leaving (final effluent) it. This discrepancy can be because of either wastewater loss from the system, underestimation of flow by the final effluent flow meter, or over estimation of flow by the flow meters upstream of the wet-well. It has been checked on site if there was any water loss from the system, but no apparent loss is identified that could lead to a loss of over 28 L s^{-1} flow of wastewater. The most likely reason is, during high flow periods, backflow of wastewater from wet-well causing a high level of wastewater in inlet channel, upstream of wet-well, and hence over estimated flow to the wet-well and most probably the upstream flow meter located at the inlet point.

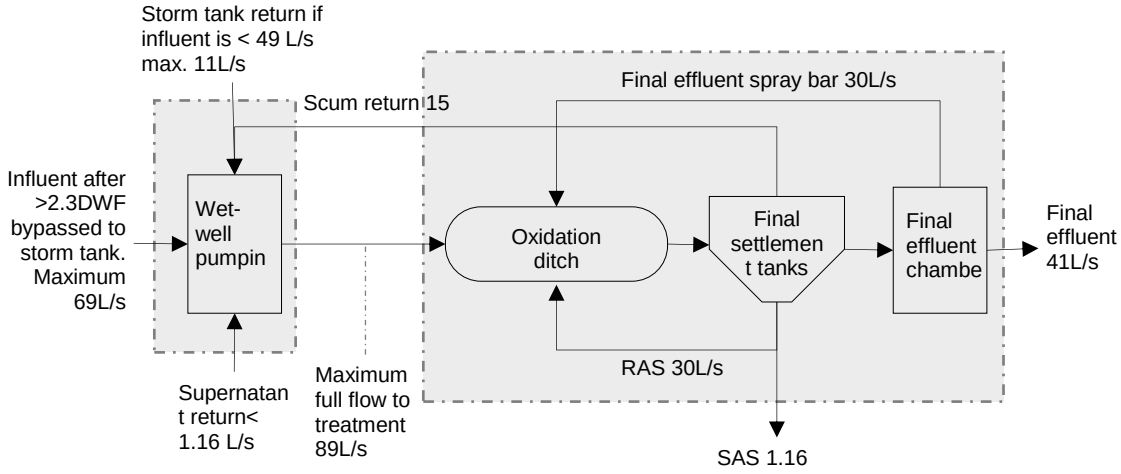

Figure 4-5: Flow balance at WWTP scale for Cupar

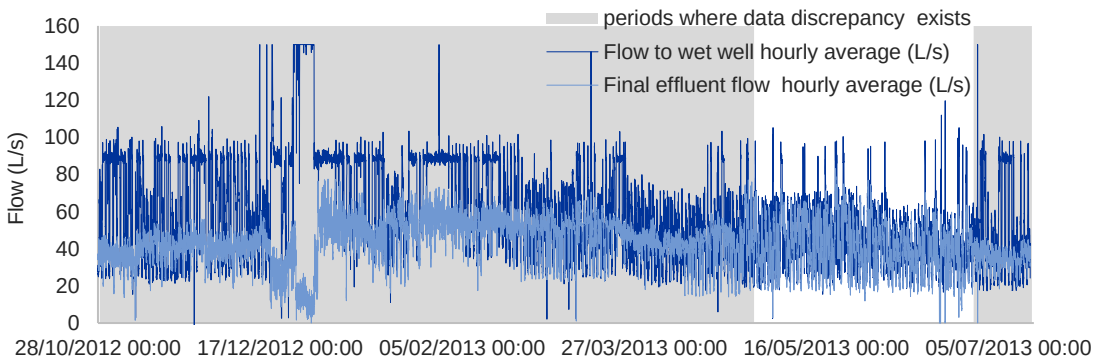

Figure 4-6: Graphical presentation of influent and final effluent flow at Cupar WWTP

Flow balance at the wet well was used to assess the uncertainty in existing dataset.

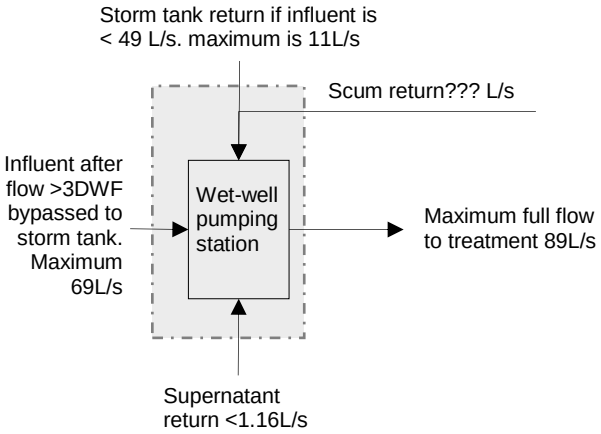

Figure 4-7: Flow balance at Cupar WWTP inlet wet well

The flowrates of all flows entering the wet-well are known except the scum return flow. Hence with the existing dataset, it is not possible to assess the hydraulic balance further. However, for the flow balance to work without any overflow or back flow in the inlet channel the scum return should not be higher than 20 L s^{-1}, on average. The scum return was calculated using the flow balance in Figure 4-7 at the wet-well by assuming zero storm tank return flow and 1.6 L s^{-1} supernatant return flow to the wet-well. The estimated scum return flow using this flow balance was compared to the one calculated using the flow balance at the secondary treatment level, see *Figure 4-8*. In other words, this is the comparison between scum return flow estimated using influent data*, Figure 4-7,* and scum return flow estimated using final effluent data *Figure 4-8***.** The comparison showed a good correlation for the period 26/02/2013 – 25/06/2013, see Figure 4-9. However, the flow comparison between 28/10/2012 – 25/02/2013 showed the scum return flow estimated using wet-well flow balance was much lower than the one estimated using the flow balance at the secondary treatment. Per this analysis, either the final effluent underestimates the flow for the period 28/10/2012 – 26/04/2013 and 26/06/2013 – 11/07/2013, or the inlet flow to the wet-well is overestimated.

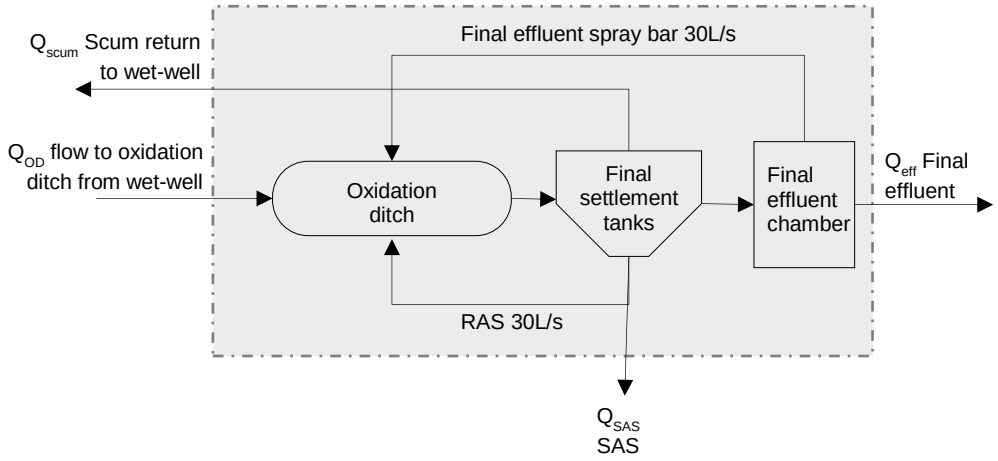

Figure 4-8: flow balance at secondary treatment at Cupar WWTP

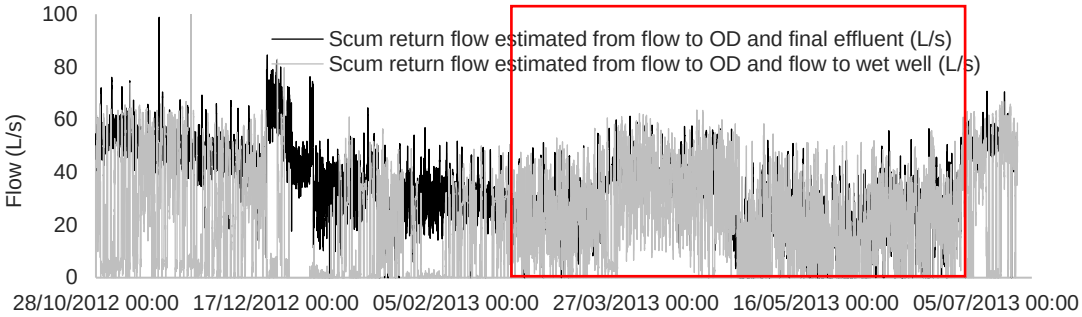

Figure 4-9: Scum return flow estimated using flow balance at wet-well and secondary treatment level

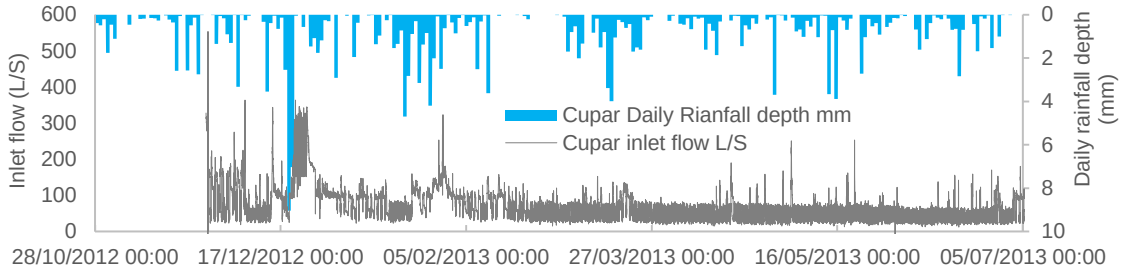

Figure 4-10: Cupar WWTP inlet flow and rainfall depth in mm d^{-1}

The above analyses showed that too much inlet flow is recorded for the observed rainfall and sometimes it was noisy. The flow data at the inlet point, measuring flow to wet well, overestimated flows when the wet-well level was high where backflow is expected. It is identified that the measured flow to the wet-well is not reliable. However, it is not possible to decide that this entirely the issue with the flow meter upstream of the wet-well or due to calculation error because of underestimation of the final effluent. The only way to identify the issue is to implement additional flow meter at the inlet, final effluent and measuring the scum return.

The hydraulic data collected during the campaign period was used together with the telemetry dataset to assess the discrepancy mentioned earlier. Using a flow balance at the wastewater treatment plant scale showed that the inflow to the WWTP (flow to wet-well) is higher than the final effluent by over 20 L s^{-1} in sometimes. For the campaign period, the flow to the wet-well, on average, was 48.9 L s^{-1} while the final effluent flow was 42.1 L s^{-1}, which shows an accounted sewerage loss at a flow rate of 6.8 L s^{-1}. Further to this, a flow balance assessment is done at secondary treatment scale (downstream of wet-well). This assessment showed that there is a consistent difference of, on average, 11.4 L s^{-1} between the estimated total scum-return flow and the measured ones, similar to the finding using only telemetry dataset, see Figure 4-20.

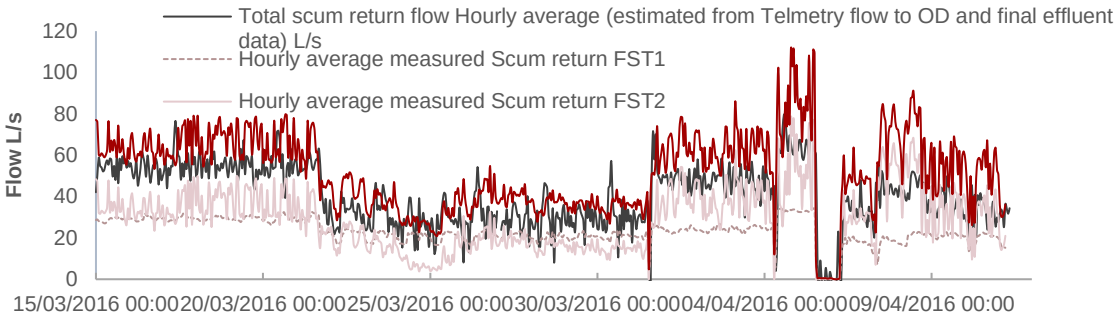

Figure 4-11: Scum return flow measured and estimated using flow to OD and final effluent flow

Adding the scum return flow calculated using the difference between the flow to oxidation ditch and the final effluent can give a general indication to justify the data quality of flow to wet-well logged into telemetry. The analysis showed that the high flows to the wet-well are overestimated, and once more this can be due to the backflow of water during a rising level of water in the wet-well which gives an incorrect water level in the inlet channel to the ultrasonic water level sensor. It is expected that the calculated flow to the OD to be more variable than the measured one due to the stability of flow by the inlet pumps in the succeeding one. However, the long-term average was expected to be similar. Unfortunately, the average flow to the OD for the period of the campaign was 82.4 L s^{-1} while the estimated flow to the OD, using final effluent flow and measured OD, was 89.1 L s^{-1}. There is, on average, a 6.6 L s^{-1} flow rate difference, which for the period 15/03/2016 – 11/04/2016 was 11,535 m^3 of wastewater. The significant storages available at the plant between the wet-well and the final effluent are; buffer tank 375 m^3, sludge holding tanks 544 m^3, oxidation ditch 2976 m^3, final settlement tanks 2916 m^3, and the wet-well 79 m^3. Hence, assuming no

wastewater initially, the highest storage capacity of the plant is around 6890 m^3 which are half of the difference between the estimated flow to OD and measured flow to OD. The analysis above showed that the discrepancy between these two flows was not due to storage at the wastewater treatment plant rather it is an indication that the measured flow to the wet-well is too high during high flow periods due to backflow.

4.1.5. Hydraulic Data from the Monitoring Campaign

4.3.1.1. Rainfall

The rainfall monitored in the campaign was not reliable since the measurements are zero, six or twelve, which is believed to be error in the rain gauge. This study has not used this information for any further analysis.

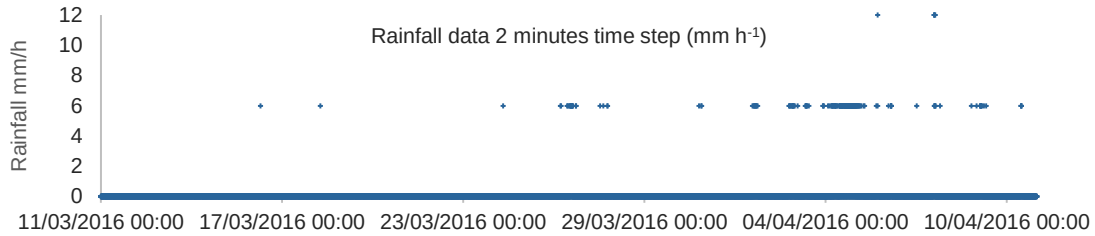

Figure 4-12: Rainfall data for Cupar WWTP

4.3.1.2. Inlet Flow Meter

The inlet flow meter has several missed data, and the result is not reliable through the monitoring period. This due to the kind of flow meter used and the nature of the utility hole. Due to the existence of a screen downstream whenever there is a high flow at the inlet point there is a backflow and the wastewater level in the utility hole raises significantly. This phenomenon results in a false reading of water depth and unreliable velocity. Hence, the inlet flow data monitored in this campaign was unsuitable to be used for any further analysis. This flow is compared with the existing online flow measurement already exists on site which shows a significant error in the measured flow at the campaign.

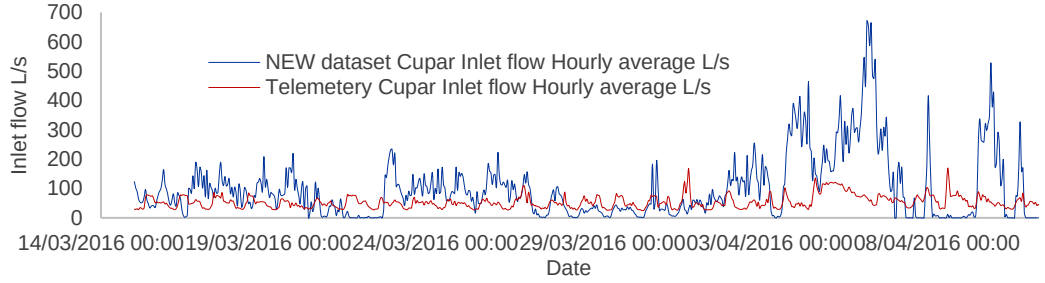

Figure 4-13: Cupar WWTP influent flow from campaign flow monitoring compared to data from telemetry

4.3.1.3. Scum Return Flow

The final settlement tanks at the Cupar wastewater has two scum boxes with variable depth which is manually controlled by the operators. The scum boxes' level is not set at a specific point, but they are let to be varied as needed by the WWTP operators. Controlling the scum boxes level as they would be set in a normal operation helps to identify how low and how high the return scum flow can go. Due to the way utility holes setup and due to the inconvenience of setting a flow meter for each scum box, the scum return flow from final settlement tank 1 (FST1) is measured downstream of the junction box where the flow from the two scum boxes combined. The scum return flow from final settlement tank 2 (FST2) is monitored by separately measuring return scum flow coming from the two scum boxes; scum box 1 and scum box 2.

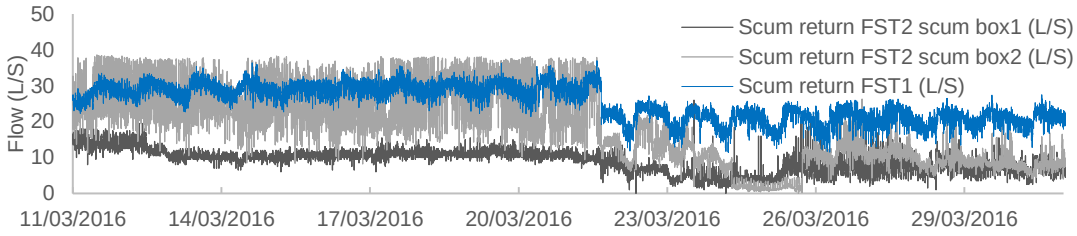

Figure 4-14: Scum return flows at Cupar WWTP without data screening

The data earlier 22/03/2016 has calibration issue and blockage of the channel by solids trapped by flow meter cables. The above issues are addressed on the 21/03/2016 around 15:00. For further analysis, the data starting from 22/03/2016 was used. The scum return flow from FST1 did not show any blockage issue since the flow passes through the utility hole at a higher velocity.

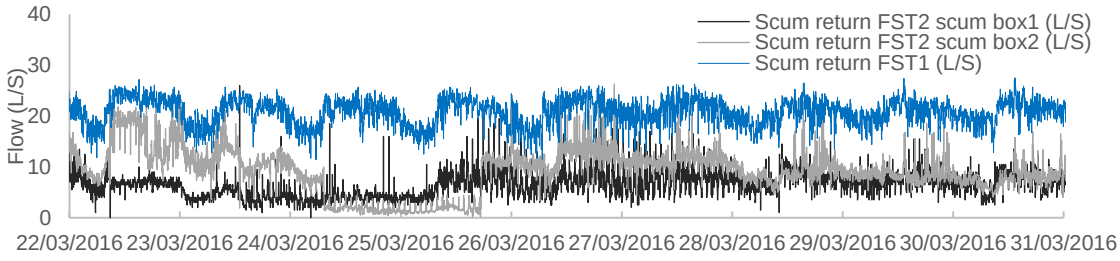

Figure 4-15: Scum return at Cupar WWTP after flow meter calibration and clearing blockage

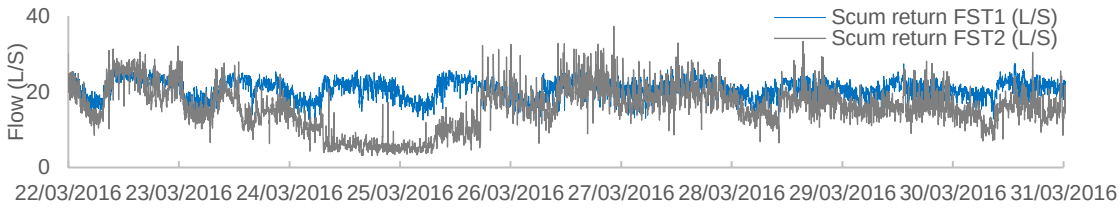

Figure 4-16: Scum return at Cupar WWTP from FST1 and FST2

For assessing the accuracy of the scum return flows, the flow to the oxidation ditch was estimated by adding the telemetry flow data to wet-well, and the scum return flows. The calculation is done with the assumption that there is no storage at the inlet wet-well, no return flow storm tanks and a constant supernatant return flow rate of 1.6 L s^{-1}. Averaging the flows reduces the variation of the flow to wet-well since outflow from the inlet wet-well has lesser temporal variation because the two pumps in operation control the flow to the OD. Hence hourly average is used.

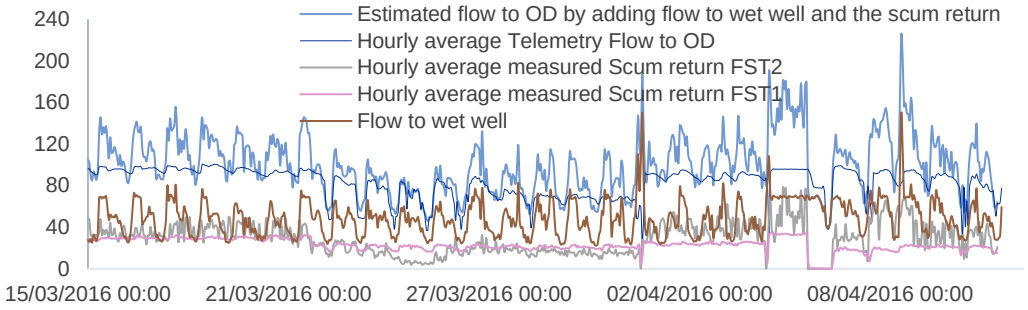

Figure 4-17: Flow to OD at Cupar WWTP estimated using flow to wet-well and measured scum return

Per Figure 4-17, the pattern of the flow data collected from telemetry and the campaign in this project are similar except some magnitude difference. The difference is either due to overestimation of scum return flow meters or due to an error in inlet flow (over estimation). To clarify this further scum return flow analysis using hydraulic balance is performed in the coming sections.

4.3.1.4. Final Effluent Flow

The final effluent monitored during the campaign showed a very close correlation with the one measured and logged in telemetry. This relationship can be taken as evidence showing that the telemetry final effluent flow meter data is reliable. However, during the campaign, there was no a significant rainy day to signify the reliability of the telemetry final effluent flow meter during high inlet discharges.

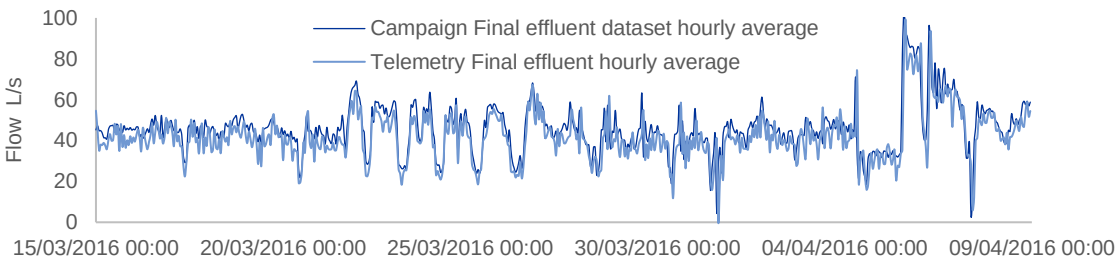

Figure 4-18: Final effluent flow at Cupar WWTP

4.3.1.5. Final Effluent Flows to Estimate Spray-bar Return Flow

The spray bar flow, pumped from a utility hole downstream of the final settlement tanks' outflow, was determined using the measured final-effluent flow before and after the spray-bar pump takeoff point. The data showed that this flow varies significantly, on average, from 4 L s^{-1} to 54 L s^{-1}. Although it was puzzling to identify how these variations occurred, on average, the spray bar return flow was found out to be 21.5 L s^{-1}.

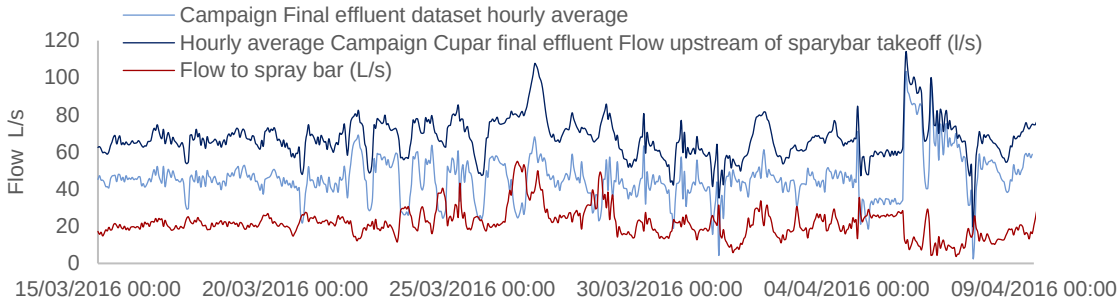

Figure 4-19: Spray bar return flow at Cupar WWTP

4.3.1.6. Supernatant Return Flow from Centrifuge Sludge Thickener

The supernatant return flow recorded during the period 15/03/2016 – 11/04/2016 showed that the flow is intermittent since the operation is manually started and stopped. This flow can go as high as 12 L s^{-1} with an average daily flow rate of 3.35 L s^{-1} in the first week of the campaign and 1.2 L s^{-1} for the other weeks. The flow pattern showed that the sludge centrifuge starts operating at 7:00 am and runs for six hours, on the next day they start at the same time and runs for one hour, or they may not operate at all. This cycle continues starting on Monday until Friday. Usually, the centrifuge sludge thickner is not running on Saturday and Sunday although the data showed that an hour of operations in some of the Saturdays. See Figure 4-20 with some typical daily patterns from each week and over the weekend. The cycle mentioned above doesn't always hold true since in some days the centrifuge had started at 6:00 and operated for eight hours, and in some cases, specifically the week 15/03/2016 – 18/03/2016, the supernatant return flow from the centrifuge was measured to be flowing overnight as well. According to the response from the plant operators, the sludge centrifuge did not run all night. Hence, the high average daily flow rate for the first week was perhaps due to backflow from the supernatant wet-well due to high liquor level in the liquor buffer tank.

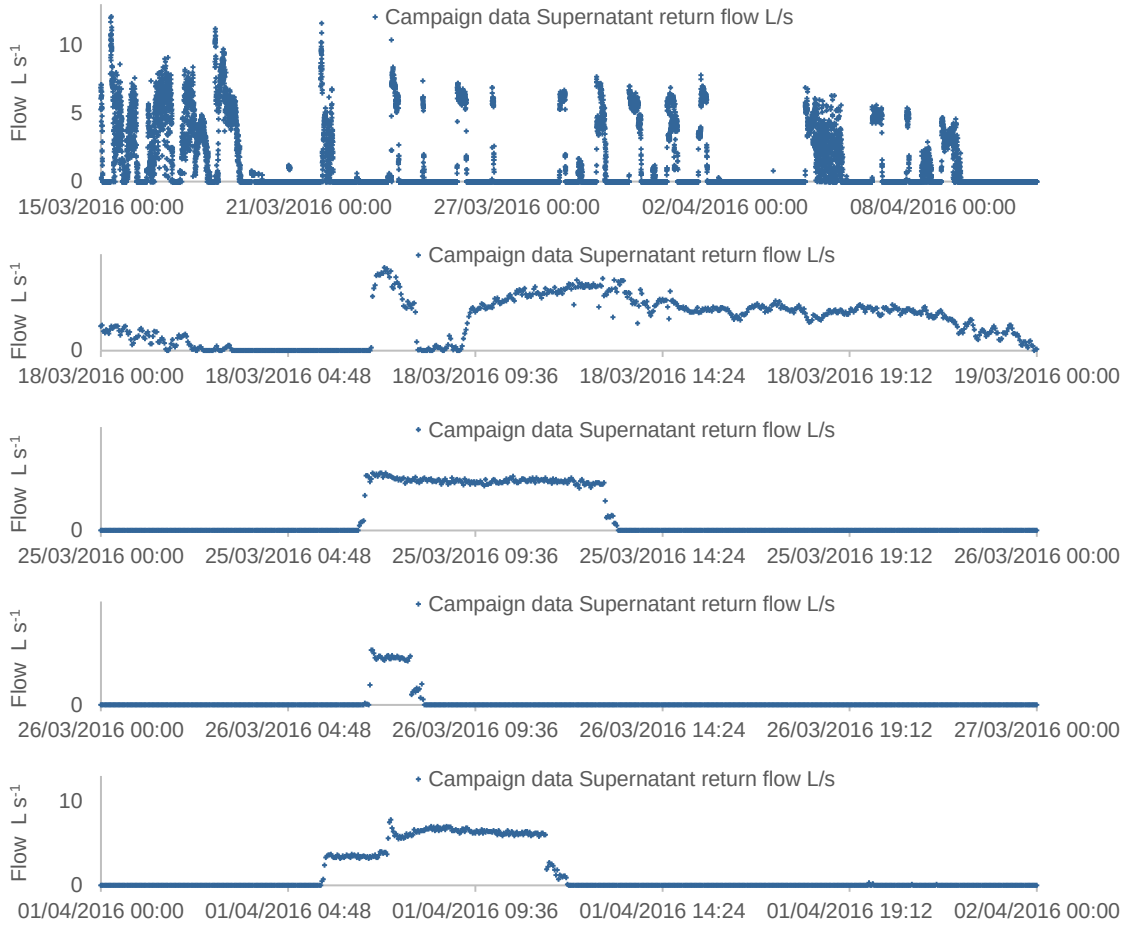

Figure 4-20: Supernatant campaign data

Table 4-2: Sludge centrifuge operational status and supernatant return flow:

Week starting on	14/03/2016		21/03/2016		28/03/2016		04/04/2016	
	Super-natant return flow (L s^{-1})	Sludge centrifuge status	Super-natant return flow (L s^{-1})	Sludge centrifuge status	Super-natant return flow (L s^{-1})	Sludge centrifuge status	Super-natant return flow (L s^{-1})	Sludge centrifuge status
Monday	-	-	1.2	Operating	1.1	Operating	2.2	Operating
Tuesday	3	Operating	0	Stopped	1.2	Operating	0.7	Operating
Wednesday	3.2	Operating	1.4	Operating	1.9	Operating	1.4	Operating
Thursday	3.2	Operating	0.2	*Operating**	1.3	Operating	0.6	*Operating**
Friday	4	Operating	1.6	Operating	1.3	Operating	1.4	Operating
Saturday	0.1	*Operating**	0.3	*Operating**	0	Stopped	0	Stopped
Sunday	0	Stopped	0	Stopped	0	Stopped	0	Stopped

* are for those days that operation was only for an hour or two

4.3.1.7. Summary

The rainfall data recorded during the campaign was not reliable and is not used for further analysis. The inlet flow to Cupar WWTP monitored during the campaign was compared against the one recorded in telemetry and showed a significant error in the campaign inlet flow data as the telemetry data showed a good correlation with downstream flows unlike the too high flow in the campaign data. Hence, this information would not be used for further analysis or model development procedures.

The measured scum return flow had shown a reliable pattern, but the first few days' data was too noisy to trust; it is observed that the measured scum return flow was overestimated by the flow meters due to utility hole blockage, especially at FST2.

Final effluent monitored during the campaign showed an excellent correlation with the one logged in telemetry which was crucial information needed in the hydraulic balance analysis. This dataset justified the accuracy of the existing final effluent flow meter. This final effluent was used together with the final effluent flow measured upstream of the spray-bar pump take-off point to calculate the spray bar return flow. These datasets showed that the average spray bar return flow is 21 L s^{-1} which is different from previous information from operatives, 30 L s^{-1}.

The supernatant return from the sludge centrifuge was used to show the operational pattern of the sludge centrifuge and to find out the average return flow which was 1.2 L s^{-1}. It should be noted that his flow does not include the decanted liquor from the sludge-holding tank.

The flow balance calculation together with the accurate final effluent showed that the inlet flow and the flow to the wet-well are not reliable, especially during rainy periods where the wet-well level is high and consequently the rise in sewage level in the inlet channels.

4.4. WWTP Campaign Quality-data Analysis

4.1.6. Influent and Final Effluent Measured Data Status

The quality parameters are monitored at every two-hour interval. Hence, 12 samples from one sampling point a day. Due to the need for sampling equipment and lab space to analyse these parameters, the monitoring work is commissioned to Scottish Water Scientific (SWS), an independent service provider such as analysitcal, and flow and load mearuements. Due to some forutunate logistic issues, the campaign period for the influent sampling point was longer than intended, 15/03/2016 - 10/04/2016. The final effluent sampling is taken for the period 15/03/2016 - 10/04/2016. Altohough the sampling period extended to three weeks only the weeks had a sampling frequency of two hours.

Out of the above listed parameters most of them were accurately monitored and measured, but some parameters suffered due to various reasons. For example, the total COD is expected to be higher than the flocculated COD, but in some cases, in the final effluent data, due to the less accurate procedure of estimating flocculated and fileted COD, the total COD was reported to be smaller. Similarly, the total Kjeldahl Nitrogen (TKN) is expected to be greater than or equal to the ammonia concentration, but again the less accurate method used in estimating this parameter resulted in data points with KTN less than ammonia concentration. Thus, data points with no such obvious error are referred to as ‘data suitable for use’, Table 4-3.

Some parameters were below the detection capacity of the sensors used for this monitoring. For example, in the final effluent, for most of the time, the ammonia concentration was below 0.5mg L^{-1}, which is below the detection capacity of the sensor and 80 % of the data resulted in not having a specific value.

Table 4-3 summarises the data monitored, and the actual data reported back to us from SWS and the data that are selected for the modelling and development of control strategies purposes.

Table 4-3 status of monitored data during the campaign period

	Cupar Influent			Cupar Final effluent		
	Data sampled for the intended period [%]	Data reported with specific value [%]	**Data suitable for use [%]**	Data sampled [%]	Data reported with specific value [%]	**Data suitable for use [%]**
Total COD	100	100	**100**	92	91	**91**
Flocculated and filtered COD	100	100	**100**	92	81	**75**
BOD	100	100	**100**	92	52	**52**
TSS	100	93	**93**	92	89	**89**
VSS	100	98	**98**	92	29	**29**
Total Nitrogen	100	99	**99**	92	74	**74**
Total Kjeldahl Nitrogen	100	98	**38**	92	26	**3**
Ammonia - N	100	98	**98**	92	10	**10**
Nitrite-N	100	34	**34**	92	81	**81**
Nitrate-N	100	18	**18**	92	92	**92**
Dissolved oxygen	100	92	**92**	92	88	**88**

On average, 96 % of the number of data points were monitored and analysed by the lab out of these data points 75 % of were reported by the lab with specific values and 71 % of the data were useful for further use for model setup and design of control strategies.

4.4.1.1. Influent Dataset

Table 4-4 below shows the parameters analysed for at the influent sampling point with their measured minimum, maximum and average values. Most of the parameters reported have a specific value. There are data points without specific values mainly because pollutant concentration was below the lowest level of the sensor or the analysis can measrue. For example, Nitrite and Nitrate data has specific value only for 34 % and 18 % of the time respectively.

Table 4-4 Summary of the influent dataset

	COD [mg L^{-1}]	BOD [mg L^{-1}]	COD_f [mg L^{-1}]	COD_{ff} [mg L^{-1}]	TSS [mg L^{-1}]	VSS [mg L^{-1}]	Nitrate [mg L^{-1}]	Nitrite [mg L^{-1}]	Ammonia [mg L^{-1}]	TKN [mg L^{-1}]	DO [mg L^{-1}]	pH
Minimum	71	19	28	11	25	16	0.5	0.06	1.3	1.82	0.1	6.4
Average	482	192	193	91	190	155	1.8	0.5	20	28	0.7	7.3
Maximum	2430	622	972	311.5	1366	1025	3.9	1.8	77.7	108.78	6	8.4

Different inter-dependant parameters are compared. For example, Ammonia versus total Kjeldahl Nitrogen, total COD versus flocculated and filtered COD, and total oxidised Nitrogen versus total Nitrogen.

COD and BOD

- Total COD: The total chemical oxygen demand was measured using the United Kingdom Accreditation Service (UKAS) certified approach which followed the procedure by Analysts (1986). Outliners are removed from the dataset, i.e. values higher than 2500 are considered to be errors.
- Filtered COD: Not measured directly
- Flocculated Filtered COD: The same procedure as that of the total COD but the sample was prepared using the procedures outlined by (Mamais et al., 1993)

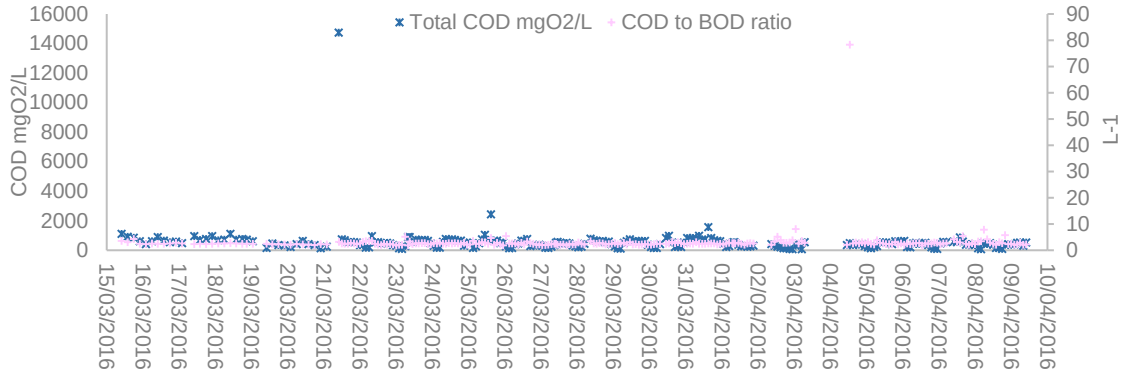

Figure 4-21 Cupar WWTP measured influent: total COD and COD/BOD ratio

The very high values of COD are accompanied by the high level of BOD which rules out analysis error. The reason why there is such a high COD level compared to other times is not clear to the author. Hence, the data is considered for the exceedance curve analysis of COD/BOD. Most of the very high values of COD occurred at 10:00 and some of them at 15:00. The COD to BOD ratio has an average value of 2.97, a median value of 2.17, a maximum value of 78.3, and a minimum value of 1.83. The data showed only 8 data points have COD/BOD ratio values higher than 10.

The data distribution curve shown above shows a flat slope for high values of COD/BOD ratio, see Figure 4-22. This showed that data points with high values of BOD/COD ratio are not frequent, specifically above 5. Hence, in the calculation of average values, the data points with a COD/BOD ratio higher than five are considered to be outliers. These data points are removed in further analyses, which also removes the very high COD values. This behaviour is not observed at the lower end of the data, and the raw data is left as it is.

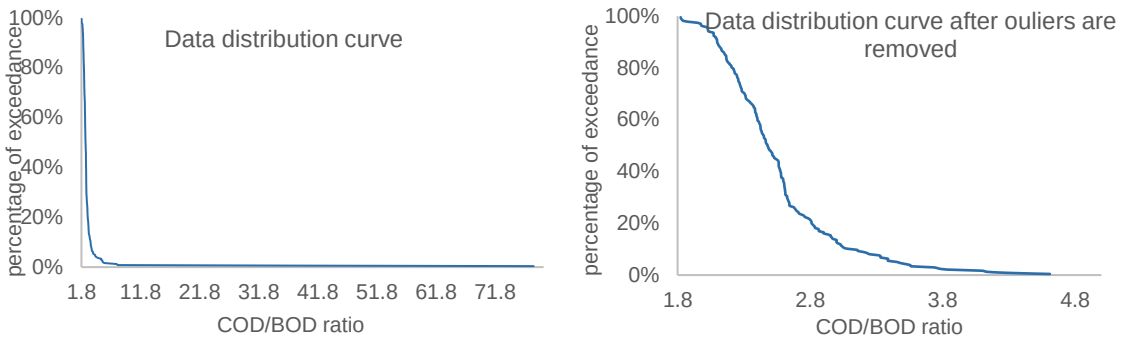

Figure 4-22 COD to BOD ratio distribution of measured data before outliers are removed (left) and after outliers are removed (right)

The COD data without outliers shows an average value of 2.56 and a median of 2.48. The closeness of the median and the average values in the distribution showed a very small skewness. The influent wastewater data have 9 data points with low COD to BOD ratio (1.5 – 2.5 mg of O_2 L^{-1}). 113 points have medium COD to BOD ratio (2.0 – 2.5), and 103 data points have high COD to BOD ratio (2.5 – 3.5). 18 data points are identified to have COD/BOD values higher than 3.5; the maximum suggested ratio for typical domestic wastewater (Henze et al., 2008). The ranges for COD/BOD ratio (low, medium, and high) of typical domestic wastewater is taken from Henze et al. (2008).

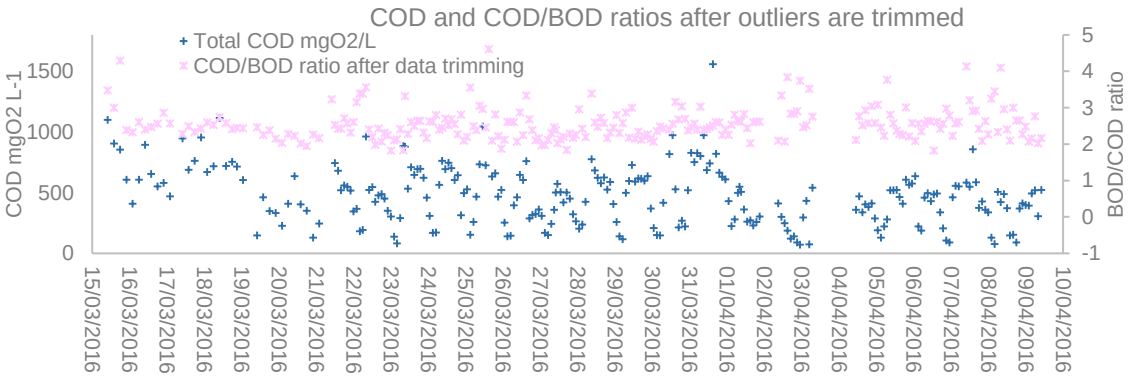

Figure 4-23 Cupar WWTP Measured influent COD and COD/BOD ratio after removing outliers

Filtered COD and flocculated and filtered COD:

Filtered COD is not analysed for any of the samples by the lab due to unknown reason. As a result, the filtered COD (COD_f) in this study was estimated based on the ratio of COD_f to total COD of typical domestic wastewater. The ratio of COD_f to total COD for domestic wastewater analysed in Melcer (2003) is suggested to be either 0.4 or 0.26 depending on the type of filter used. If the standard glass fibre filter is used the fraction would be 0.26 and if a 0.45 µm membrane filter is used the fraction would be 0.4. However, filter membrane filters

capture a considerable fraction of colloidal particles, which are the difference between the filtered COD and the flocculated and filtered COD (COD_{ff}). Therefore, to be consistent with the COD_{ff} analysis that uses a membrane filter, a typical fraction COD_f/COD value of 0.4 is used in this study.

Total suspended solids (TSS) and Volatile Suspended Solids (VSS)

The data showed that most of the values of the ratio of TSS and VSS fall between 0.75 and 0.9. There are six data points with TSS/VSS ratio higher than 0.95, and they are not used for further analysis. The data distribution curve showed that values under 0.54 are non-frequent and similarly they were not used for further analysis. The data showed an average value of 0.82 and a median of 0.85. After removing the outliers, the data showed an average of 0.83 and a median of 0.84.

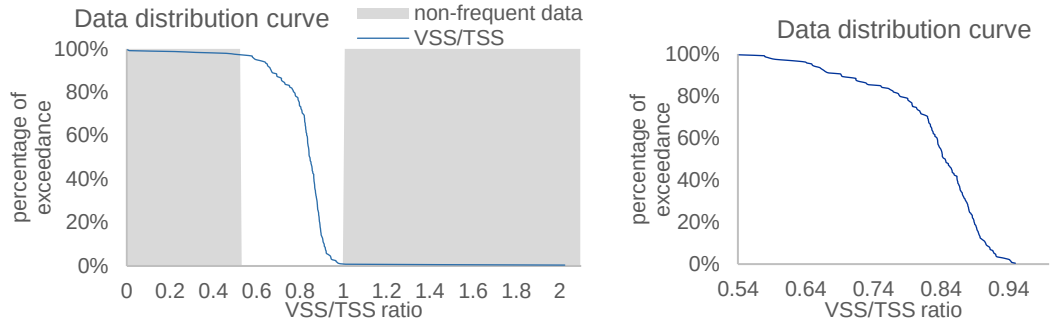

Figure 4-24 TSS to VSS ratio distribution of measured data before outliers are removed (left) and after outliers are removed (right)

Total Nitrogen (TN), Total Kjeldahl Nitrogen (TKN), Ammonia-N, Nitrite-N and Nitrate-N

Total Kjeldahl nitrogen is the sum of nitrogen concentration in the form of ammonia/ammonium and organic nitrogen. Total nitrogen in this campaign is calculated by adding the concentration of Nitrate-N and Nitrite-N to the total Kjeldahl nitrogen. The measured values for total nitrogen and total Kjeldahl nitrogen at Cupar WWTP reported being the same for all data points. In other words, the inorganic nitrogen concentration and nitrate are zero, which is not true. Hence, the measured TN data is not used further.

The main source of nitrate and nitrite (an oxidised form of nitrogen) are the fertilisers and manure applications when eroded by surface runoff. The measured data support this statement as it shows a high concentration of nitrate during mid-night (the time of the day where the main influent contributor being infiltration into the sewer network or the storm flow during rainfall events).

The Nitrate-N concentration monitored at the effluent was mostly, 88 % of the time, below 0.5 mg L^{-1}, the lowest the level the sensor can measure. Average value of Nitrate-N for those recorded accurately or above 0.5 mg L^{-1} were 1.84 mg L^{-1}. For further analysis, data points with values below 0.5 mg L^{-1} are assigned random values between zero and 0.5 mg L^{-1} of Nitrate-N.

The Nitrite-N concentration was recorded to be higher than 0.05 mg L^{-1} as N for 34 % of the time. Average value of Nitrite-N for those recorded accurately or above 0.5 mg L^{-1} were 0.51 mg L^{-1}. Since no strong correlation are observed between measured nitrate and nitrate N concentration, for further analysis, data points with Nitrite-N values below 0.05 mg L^{-1} were assigned random values between 0.01 and 0.05 mg L^{-1} of N.

Ammonia concentration was reported to be less than the total Kjeldahl Nitrogen (which is the sum of ammonia, ammonium ion and organic nitrogen) only for 38 % of the time which leave 62 % of the data in error, see Figure 4-25.

The reported ammonia-N concentration on average was 19.8 mg L^{-1} which is close to the suggested typical ammonia-N concentration of domestic wastewater 22mg L^{-1}, Manchester, UK (Horan, 1990). Also, the average ammonia-N concentration measured during this campaign is compared with the one measured during the Cupar WWTP baseline daily data collection in 2013. The average ammonia-N concentration in the baseline data was 20.6mg L^{-1}, which is slightly higher than the one monitored during the campaign. These two comparisons can be taken as an indication that the ammonia-N concentration measured during the campaign is reliable. Therefore, the data discrepancy between the measured TKN and Ammonia-N is due to the under estimation of the TKN measurement.

Further to comparing ammonia-N concentration with historical data, the COD to TN ratio for typical domestic wastewater (Henze et al., 2008) supports the above argument. In doing so, the COD/TN ratio is used as a comparison. Since the measured TN is not reliable, it is estimated by summing the measured nitrate-N, nitrite-N, and total Kjeldahl nitrogen. The ratio of COD to the TN was 25.2 which is much higher than the maximum COD/TN ratio of typical domestic wastewater; suggesting that the TN value is too low, and which might be because of its underestimated component, TKN. As a solution, at each time step, any TKN

values lower than the measured ammonia-N concentration by a factor of 1.05 were replaced by factoring the ammonia-N concentration with 1.14, which is the average of the ratio of measured TKN/Ammonia-N, data excluding points with TKN/ammonia-N ratio higher than 0.95. Recalculating the TKN from Ammonia-N using the ratio 1.14 increases the average TN and reduces the COD/TN ratio to 22; still higher than the maximum ratio of typical domestic wastewater.

Moreover, the typical ratio of ammonia-N to TKN for domestic wastewater (0.6 – 0.75) suggested by Melcer (2003) is considered for further investigation of the error in the dataset. The range is much lower than the one calculated using the campaign data, 0.88 excluding ammonia-N/TKN ratio higher than 0.95. The high ammonia-N to TKN ratio may be an indicator that the whole TKN data of the campaign was underestimating. A typical ammonia-N/TKN ratio of 0.7 is used to calculate TKN from measured Ammonia-N concentration. Hence, the TKN data is not further used and, instead, the TKN concentration was estimated according to Eq. 4-15. The new TN data from this calculation gave COD/TN ratio of 18.3 which is slightly higher than the maximum ratio, 16, see Table 4-5.

$$TKN = NH_x \times 1.4 \qquad \textit{Eq. 4-15}$$

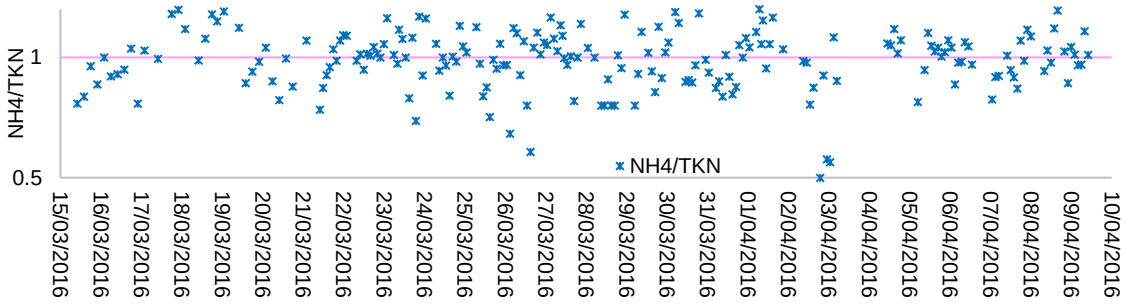

Figure 4-25 Ratio of measured influent ammoniacal nitrogen and underestimated TKN concentration

Comparison of Cupar influent wastewater to typical domestic wastewater

Cupar WWTP receives a significant amount of trade effluent from Fisher Services, industrial laundry and finishing of textile and garments such as dying and printing (Direction 14/04/D. Braga and Varesche (2014) showed that COD in industrial laundry wastewater could be as high as 4700 mg of O_2 L^{-1} with an average value of 1710 mg of O_2 L^{-1}. The same study showed that ammonia-N could be as high as 54.8 mg L^{-1} with an average value of 7 mg L^{-1}, and TKN as high as 136 mg L^{-1} with an average value of 32.4 mg L^{-1}. Similarly, Christova-Boal et al. (1996) showed that commercial laundary wastewater has a lower ammonia-N concentration (0.1 – 1.9 mg L^{-1}), slightly higher TKN (1 – 40 mg L^{-1}),

much higher COD, and nitrate and nitrite-N concentration varies between 0.1 and 0.31. Horan (1990) stated presented composition of wastewater from textiles to have a 5000 mg L^{-1} concentration of COD on average and very low concentration of TN. Hence, it is expected for wastewater with a high contribution of flow from laundrettes and textile industries to have higher COD/TN, and BOD/TN ratio.

The high COD/VSS ratio is again due to trade effluent characteristics with a very high COD concentration but relatively lower TSS or VSS concentration, see Table 4-4 and Table 4-5.

Table 4-5 Typical range of pollutant concentration in domestic wastewater and Cupar's influent wastewater

Ratio	High	Medium	Low	Cupar influent
COD/BOD	2.5 – 3.5	2.0 - 2.5	1.5 - 2.0	2.6
COD/TN	12.0 – 16.0	8.0 – 12.0	6.0 – 8.0	18.3
BOD/TN	6.0 – 8.0	4.0 - 6.0	3.0 – 4.0	8.2
COD/VSS	1.6 – 2.0	1.4 - 1.6	1.2 - 1.4	3.5
VSS/TSS	0.8 – 0.9	0.6 - 0.8	0.4 - 0.6	0.8

Source: Henze et al. (2008)

4.4.1.2. Final Effluent

The ammonia result has only 10 % with a specific value while 90 % of the data points were below the sensing threshold of the instrument, 0.5 mg L^{-1}. 48 % of the BOD data is reported without a specific value; mostly reported as less than 2 mg L^{-1}. 9 % of the COD and 19 % of the ffCOD data were reported to be less than 10 mg L^{-1} which is reported by the lab technicians that it is the minimum level that the COD can be estimated, using their standard method. The ffCOD and COD are compared. Since the ffCOD is a flocculated and filtered sample, it should be less than or equal to the total COD. However, the reported data showed that 25 % of the analyses for COD_{ff} resulted in values higher than the total COD.

74 % of the analyses for total Kjeldahl Nitrogen resulted in values below the sensing threshold of the analysis procedure, 2 mg L^{-1} as N. Similarly, 90 % of the Nitrite analyses resulted in values below the sensing threshold of the sensor, 0.05 mg L^{-1}. Total oxidised nitrogen (TON) was reported to be the sum of Nitrate and Nitrite. For points where the Nitrite concentration is below 0.05 mg L^{-1}, the total oxidised nitrogen is estimated to be equal to the Nitrate concentration. However, the reported oxidised nitrogen was reported to be above the total Nitrogen for 15 % of the time, which is an error in the estimation of the total Nitrogen, and those points are discarded from further analysis.

4.1.7. 15 Minutes Time-Step Data Development for Model Input

The main reason behind monitoring this dataset is to calculate the influent variables that are required by BSM2. The detail of the approach is given in Section 4.1. The method presented in Section 4.1 requires both the final effluent and the influent to be taken relatively at the same time. However, the samplers in the campaign took samples depending on at what time they start the sampling and may not be at the same time as the other samplers on site. Besides, ASM1 took input data at 15 minutes' time step. However, the data is monitored every 2 hours. Thus, to create a continous dataset of ASM1 input parameters, interpolation of the samples that are taken at 2 hours time-interval is required.

A cubic spline interpolation method is used (De Boor, 1978). As an example, the COD data monitored for influent and final effluent is presented, for example, in Figure 4-27 and Figure 4-30. The interpolation is done for each day of the week, see Figure 4-26, and averaged to create a typical daily variation of pollutants load, for example, see Figure 4-28. The details of how the continuous dataset for the campaign period (Figure 4-28, Figure 4-29, Figure 4-31) and the typical daily pattern (Figure 4-32) used in the model development is presented in Section 5.1.1. The details of the influent quality data points for each day of the week are presented in Appendix A. Similarly, the details of the final effluent data points for each day of the week are presented in Appendix B. Although there was data for the first week, 15/03/2015 – 21/03/2015, the data was not every 2 hours and lacks inconsistency. Hence, the data for the period 21/03/2016 – 10/04/2016 is used to generate the 15 minutes time-step dataset.

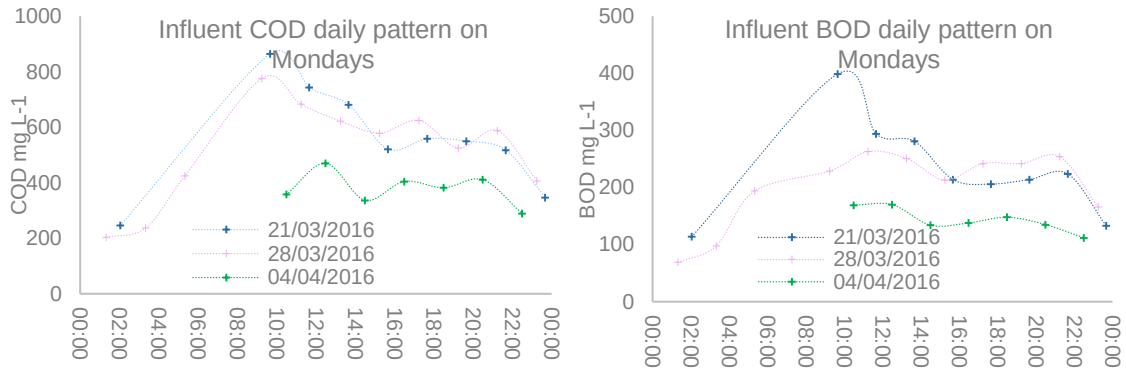

Figure 4-26 Measured influent COD and BOD concentration for Mondays

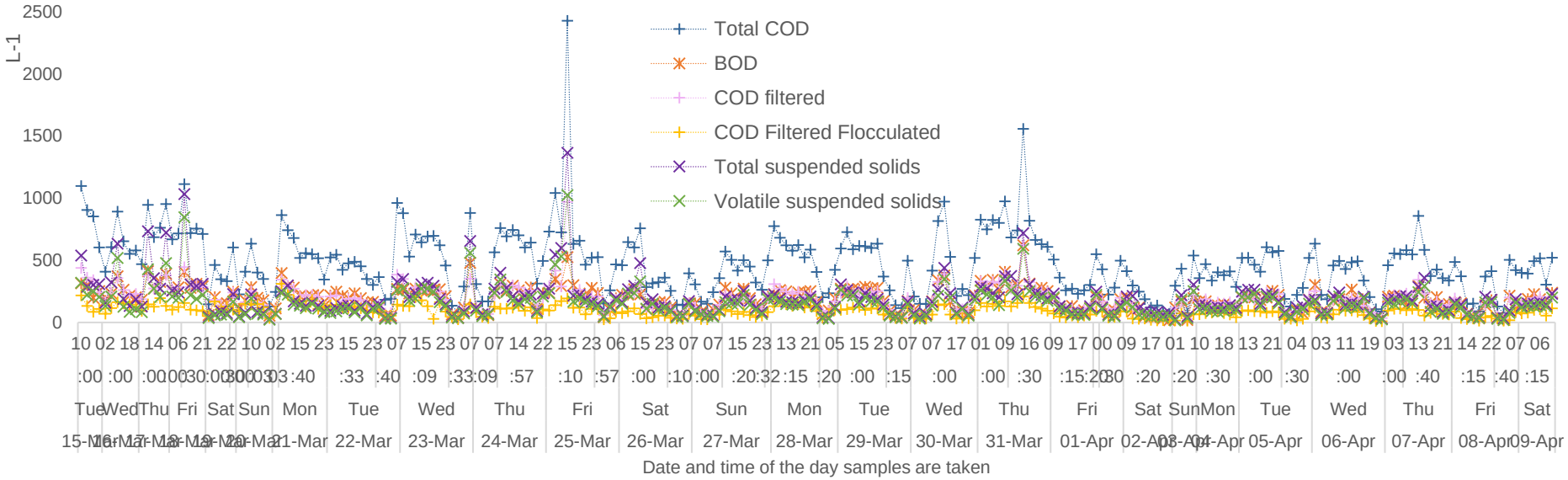

Figure 4-27 Influent pollutant concentration measured dataset after removing outliers

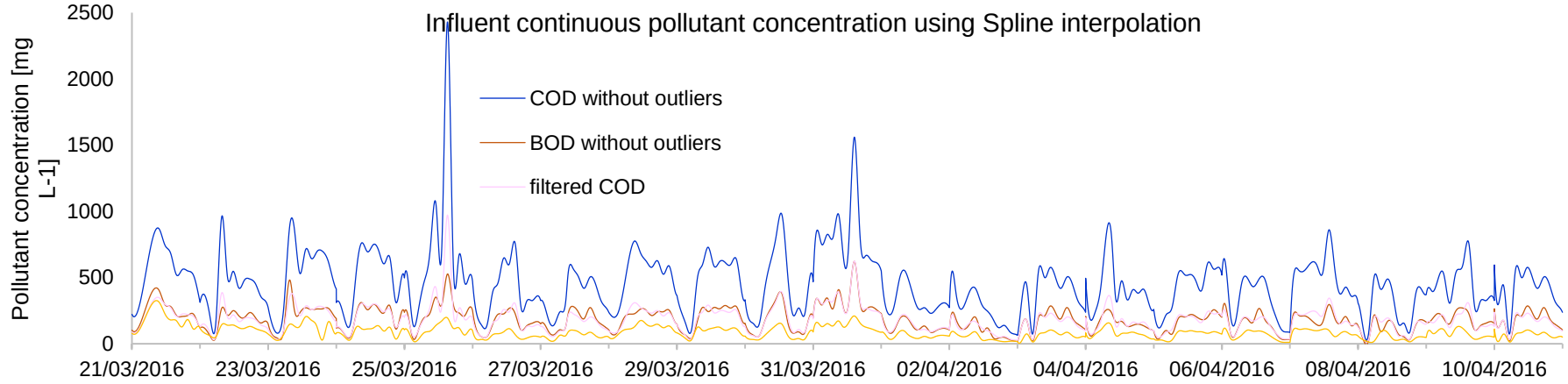

Figure 4-28 Continuous of influent pollutant concentration (COD, BOD, COD_f, and COD_{ff}) using Cubic Spline interpolation technique

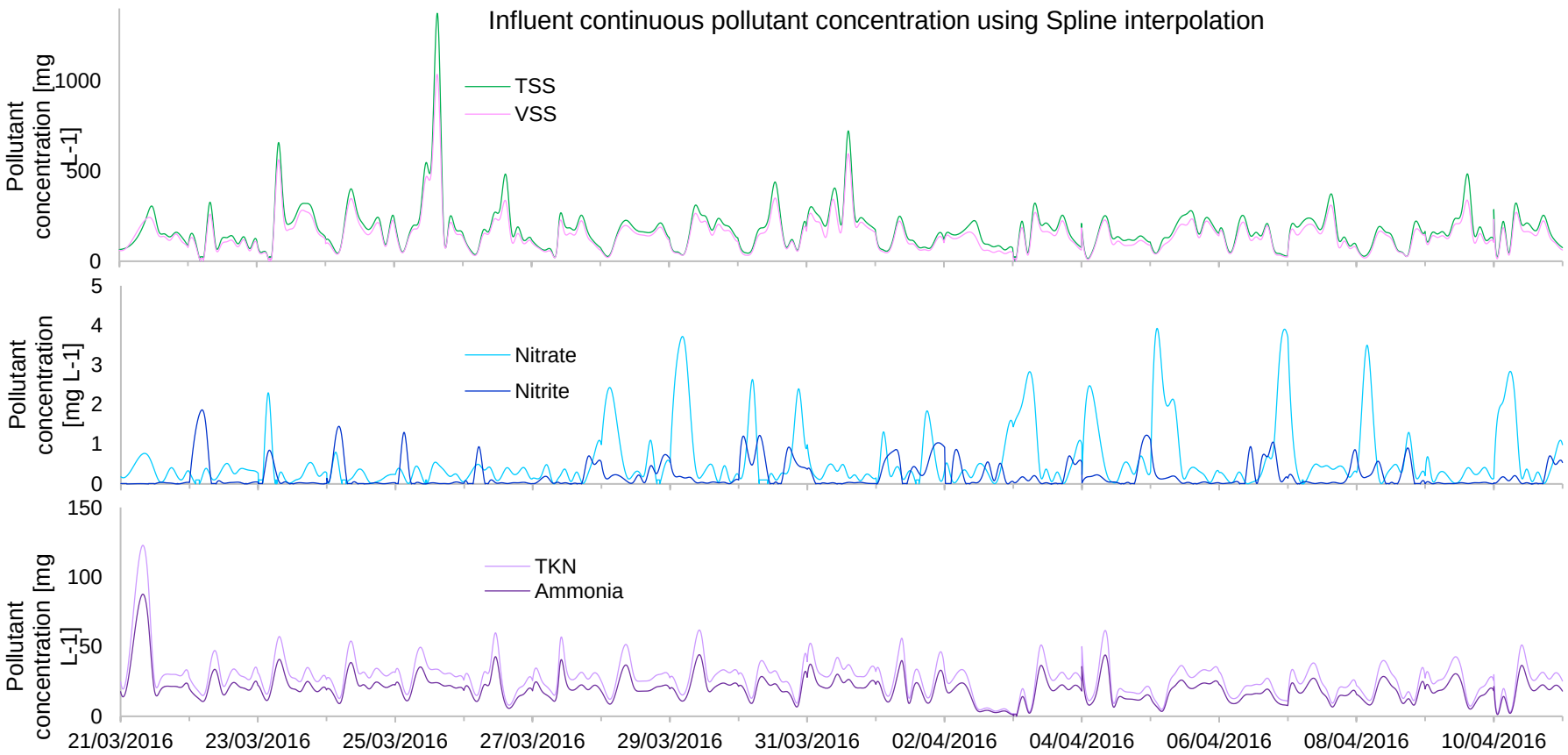

Figure 4-29 Continuous influent pollutant concentration (TSS, VSS, Nitrate, Nitrite TKN, and Ammonia) using Cubic Spline interpolation technique

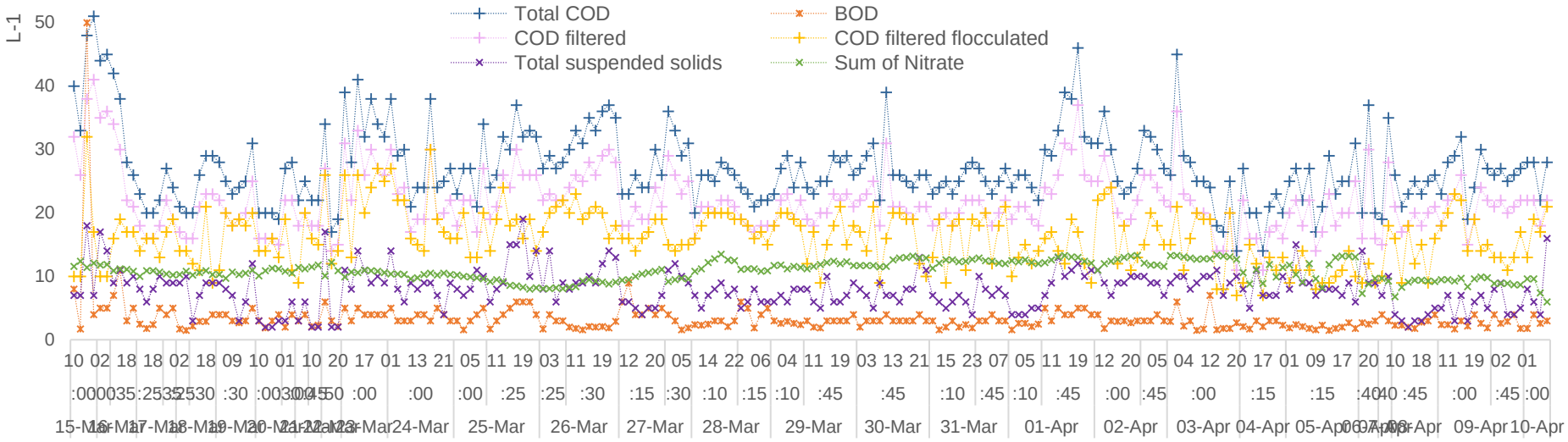

Figure 4-30 Final Effluent pollutant concentration measured dataset after removing outliers

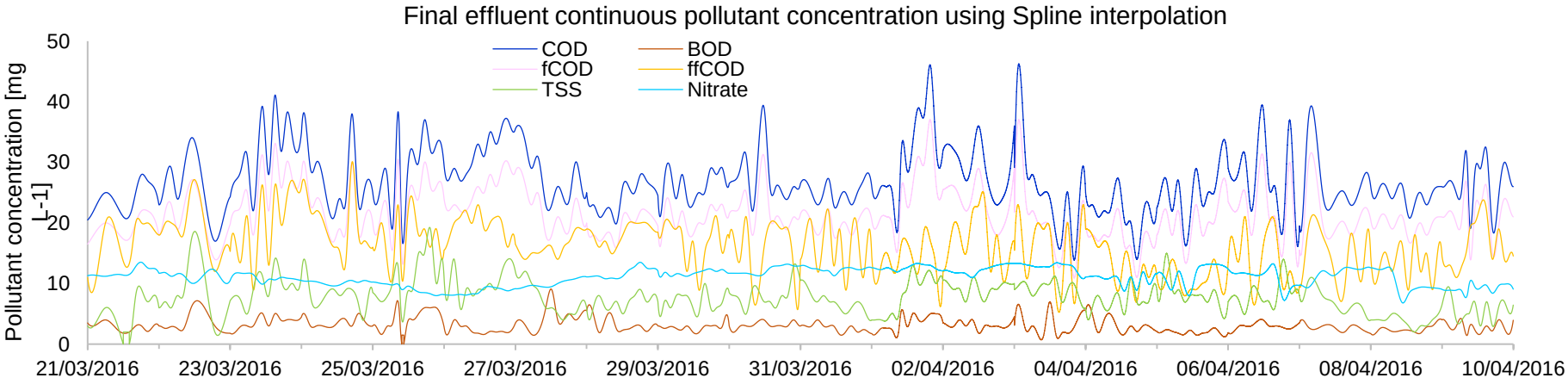

Figure 4-31 Continuous final effluent pollutant concentration (COD, BOD, filtered COD, flocculated and filtered COD, TSS, and Nitrate) using a cubic spline interpolation technique

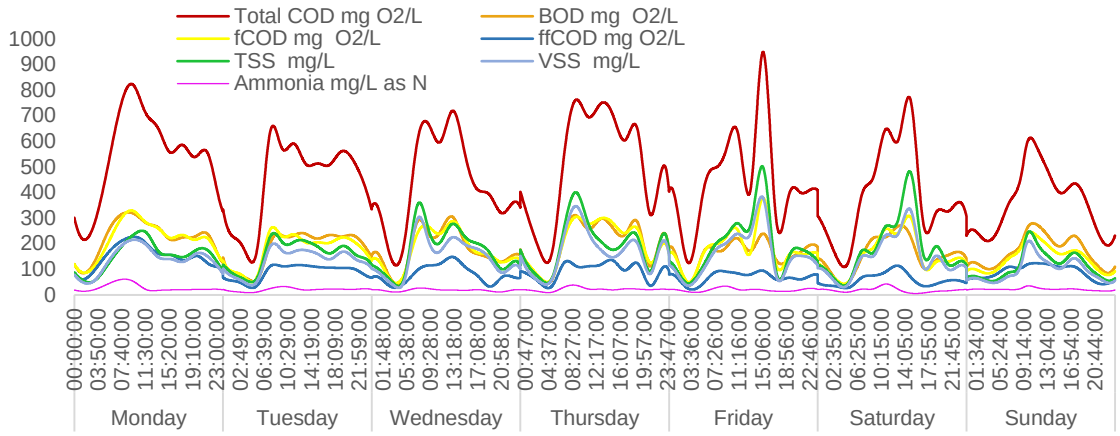

Figure 4-32: Typical daily pattern of COD load at Cupar WWTP for a typical week using cubic spline interpolation

5. WWTP Performance Assessment and Integrated Modelling Approach

The chapter covers the modelling approach used to represent the three major components of the urban wastewater systems; WWTP, the sewer network, and the receiving water flow and quality. The WWTP main processes and the modifications applied to the Benchmark Simulation Model No. 2 (BSM2) is presented in detail in Chapter 3, and only the overview of the model setup is discussed here. However, the next few sections will deal with the integration of WWTP model with an influent generator and receiving river model. The modelling approach used to simulate the flow and quality of the influent flow to WWTP from the sewer network is discussed in detail in Section 5.1.1. This section detailed the adoption of phenomenological wastewater generator model designed to generate dynamic input for BSM2 to simulate the influent wastewater to Cupar WWTP.

Later, the details of the modelling approach used to simulate and forecast flow and quality of receiving river, and its integration with the WWTP is presented in Sections 5.1.2 and 5.1.3 respectively. The river model uses rainfall data to forecast river flow and quality with the ability to simulate the impact of WWTP effluent and combined sewer overflow. The integration of this independently setup model with the WWTP and the aggregation of the WWTP model state variables is detailed as well.

Section 5.2 presents the WWTP performance assessment indices that are later used in Chapter 7 to evaluate different control strategies and innovative regulatory approaches. Section 5.2.1 describes the changes and the additional processes that are applied to the modified BSM2 (Jeppsson et al., 2007) to accurately simulate greenhouse gas (GHG) emissions enabling estimation of N_2O emissions, which is referred as BSM2-e (Sweetapple et al., 2016).

5.1. Integrated Modelling Approach

The WWTP model for Cupar is developed using existing blocks in the BSM-2 (Jeppsson et al., 2007) and the modified kinetic processes in the BSM2-e (Sweetapple et al., 2013), with modifications and additions. A diagram of the complete WWTP model is given in Figure 5-1. The figure is simplified by putting

the sub-models and blocks within the main one. The detail of the sub-models and blocks can be found in Chapter 3.

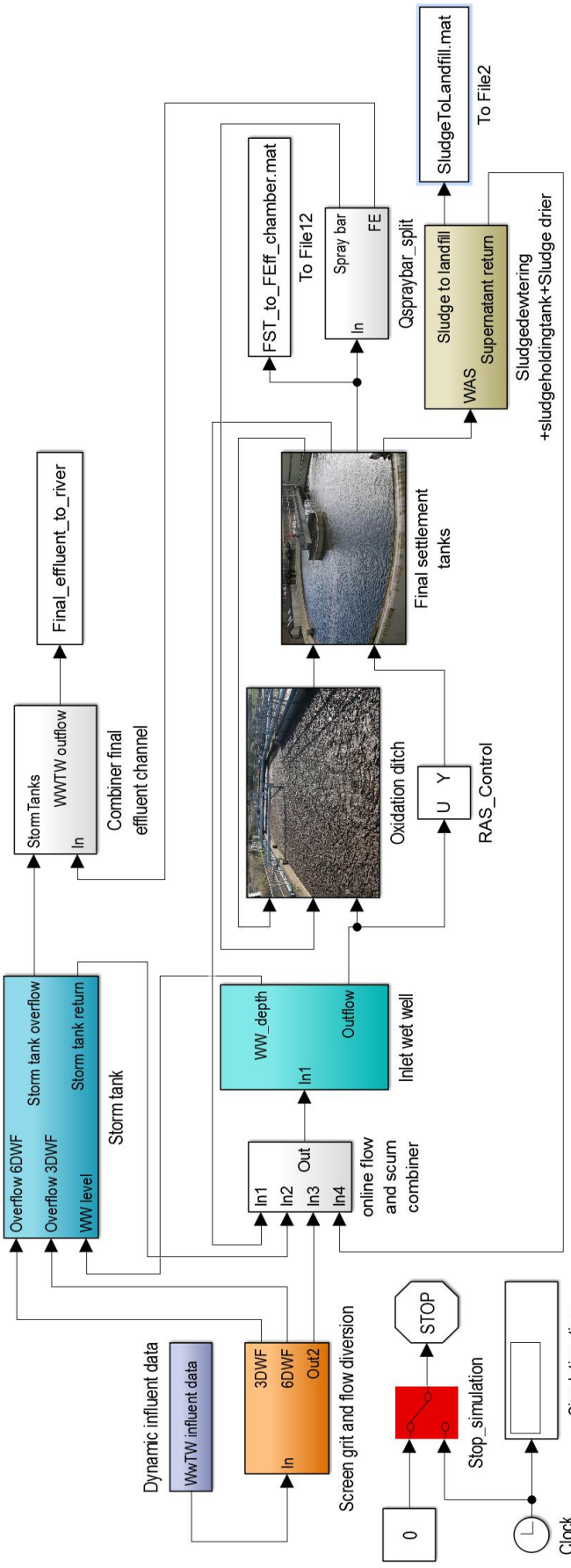

Figure 5-1 Cupar WWTP Simulink model without sewer and river model blocks

The WWTP model is setup using the 20 days data set from the campaign period, 20/03/2016 - 10/04/2016 with warming up period of 100 days, which helps to achieve pseudo steady state and allow controllers to adapt. This 120 days of simulation is used to assess the performance of the model and calibrate the model before using it for performance assessment. The details on the calibration of the model are detailed in Chapter 6. Once the WWTP is calibrated using campaign data, the model is linked to the influent generator model to simulate a total of 424 days; 04/11/2015 – 01/01/2017. This period is selected to match the period of simulation for the river model, which is developed outside this study but integrated later, see Section 5.1.2. The first 100 days are used for warming up the model and achieve a pseudo steady state. The integration of influent generator, WWTP, and river model are discussed in Section 5.1.3.

5.1.1. MATLAB/Simulink Phenomenological Modelling Approach for Generation of Dynamic WWTP Influent

Using two or three weeks data or simulation period is not sufficient to assess WWTP performance and provide a better control strategy (Foscoliano et al., 2016). Long-term periods consider seasonal variations of weather and influent characteristics, allowing a reliable approach to testing control strategies and intervention options (Vrecko et al., 2006; Magnus et al., 2016). Since it is costly to monitor all the necessary data to run the BSM 2 for long-term, it is required to use influent generator models instead. The phenomenological wastewater generator model presented in Gernaey et al. (2011) uses representative influent characteristics of wastewater reaching to WWTPs, rainfall data, temperature, and other characteristics of the sewer network to generate a long-term influent data. Since this model can easily be linked to BSM2, it was used in this study to generate wastewater influent for Cupar WWTP. A summary of the phenomenological model (Gernaey et al., 2011) is presented below.

The original model has the following six modules (Gernaey et al., 2005a):

- rainfall module
- soil module
- household wastewater generator module
- industrial wastewater module

- sewer and CSO module
- the temperature module

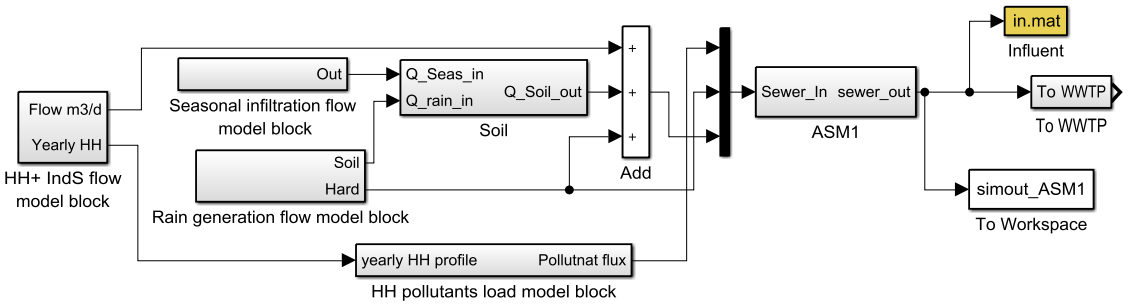

Figure 5-2 Layout of Influent generator model for Cupar WWTP

5.1.1.1. Rainfall Module

In the original model, the rainfall module used to generate rainfall (Gernaey et al., 2005b). However, if users have rainfall data, the rainfall generator can be replaced with measured data as used in Benedetti (2006). Since there are representative rainfall data that can be used for this instance, the rainfall generator is replaced with measured data.

The rainfall contributes flow to the sewer network in two ways; the first one is runoff generated from impervious surfaces which flows directly to the sewer network, and the second one is from pervious surfaces that the infiltrated water into the soil influences the groundwater level, and thus the infiltration into the sewer network. The percentage of impervious surface 'aHpercent' determines the portion of the total surfaces flow entering directly into the sewer network as a storm flow and the flow interring into the soil.

5.1.1.2. Soil Module

The soil module receives flow/input from rainfall module, and infiltration from the underlying layer (ground water) refereed here as seasonal filtration. The 'Soil' block estimates the amount of water entering the sewer network from the soil layer using a simple tank water balance. These flow from the soil block ('soil_total_flow_to_sewer'), represent both infiltration of water into the sewer network ('soil_inflitration_flow_to_sewer'), and surface runoff from the previous layer ('soil_overflow_to_sewer'). In addition, this module estimate flow from the soil layer into the aquifer below (ground water), 'soil_downward_flow_to_aquifer', whenever the seasonal infiltration low and the soil layer is full.

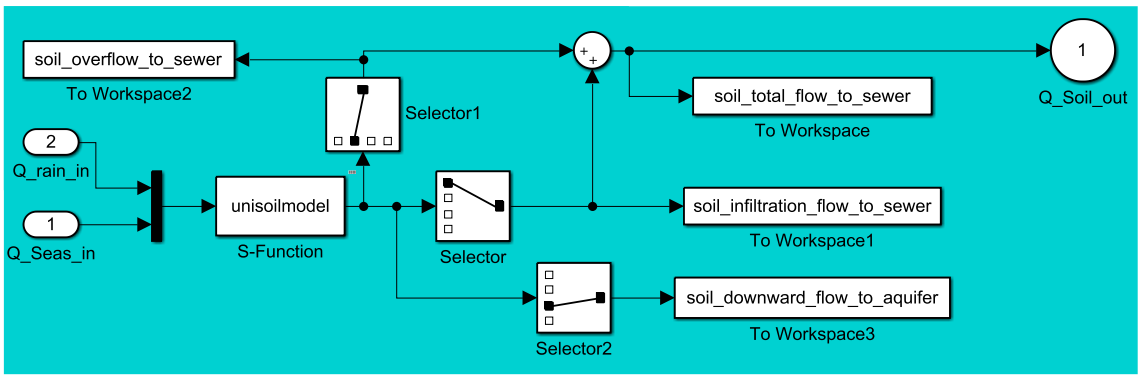

Figure 5-3 Layout of the Soil module

The seasonal infiltration flowrate is the flow entering the soil from the groundwater contribution. It reflects the typical effects of the rise in the ground water, i.e. increase in infiltration to the sewer network in the rainy season related to higher ground water levels compared to the dry season where groundwater level is low.

In the seasonal infiltration module (Gernaey et al., 2005a), a sine wave with an amplitude, Inf_{Amp}, of 1200 m^3 d^{-1}, average infiltration flowrate, Inf_{Bias}, of 7,100 m^3 d^{-1}, a sinewave frequency, Inf_{Freq}, of 2π/364 rad d^{-1}, and a phase shift, Inf_{Phase}, of –π*15/24 were used. If a constant value is preferred over a sine-wave, it can be done by turning the switch to constant, Inf_{cst}, 7,100 m^3 d^{-1}.

Considering the small size of the sewer distribution network of the Cupar WWTP initial values of Inf_{Amp}, and Inf_{Bias} were taken to be 800 m^3 d^{-1} and 1200 m^3 d^{-1}. The sinewave phase shift, Inf_{Phase}, is assigned a value of 0.5*π based on average monthly rainfall pattern of the area and the starting month of simulation, November, see Table 5-1. Inf_{cst} is not used in this study.

Table 5-1 Seasonal infiltration correction parameters

Seasonal correction parameters	Value	Description
InfAmp	800	Sine wave amplitude (m^3d^{-1})
InfBias	1200	Sine wave bias (m^3 d^{-1}) (average infiltration flow rate)
InfFreq	2*π/364	Sine wave frequency (rad d^{-1})
InfPhase	0.5*π	Sine wave phase shift
QSCIsatmin	0.001	Minimum flow rate to avoid error (division by zero) [m^3 d^{-1}]
QSCIsatmax	2*(InfBias+InfAmp)	Maximum infiltration flowrate to limit extreme noise
Q_SCI_ns	1000	noise seed
Q_SCI_nv	0.001*InfBias	Noise variance
Q_SCI_s	1	Noise sampling time

5.1.1.3. Household and Industrial Module

Gernaey et al. (2005b) use a separate approach for generating flow and pollutant from the industrial and the household wastewater. However, the wastewater characterisation presented in Chapter 4 is not done at source. Hence it is not possible to analyse these two sources separately. The separation of these two flows can be a source of uncertainty since the industrial effluent flowrate and quality were not monitored separately during the campaign. Therefore, the study combines these two flows and use the typical weekly pattern of pollutants reaching the WWTP for pollutant generation and the DWF pattern reaching the WWTP for generation of wastewater flow.

Hourly average of the flow reaching to the Cupar WWTP in the dry season, based on the analysis of a three weeks' dry weather data, is 4089 m^3 d^{-1}. The flow pattern for a typical day is estimated by averaging the dry weather flow to Cupar WWTP and reducing the infiltration from groundwater. The infiltration from groundwater is assumed to be constant over these dry periods and estimated considering various factors. These factors include leakage from household fittings (leakage from toilets, taps, shower fitting, and so on), actual use of water and flow from industrial flow balancing water tanks located at different industries within the Cupar sewer network. Studies showed that the leakage from household fittings varies between 10 % and 40 % of the night time flow (Britton et al., 2008; Mayer et al., 2004). Accordingly, for this study, it is assumed that the contribution of flow from these sources to be 20 % of the night time flow and the rest is due to infiltration from groundwater.

The night time flow is estimated through graphical observation of the dry weather flow pattern presented in Figure 5-4, and Figure 5-5. The night time flow is calculated to be 2000 m^3 d^{-1}. This flow a contribution of infiltration from ground water, 80 % (1600 m^3 d^{-1}), and the rest from household leakage, other water-use and industrial discharge (600 m^3). Based on this assumption the average dry weather flow without infiltration is 2490 m^3 d^{-1}.

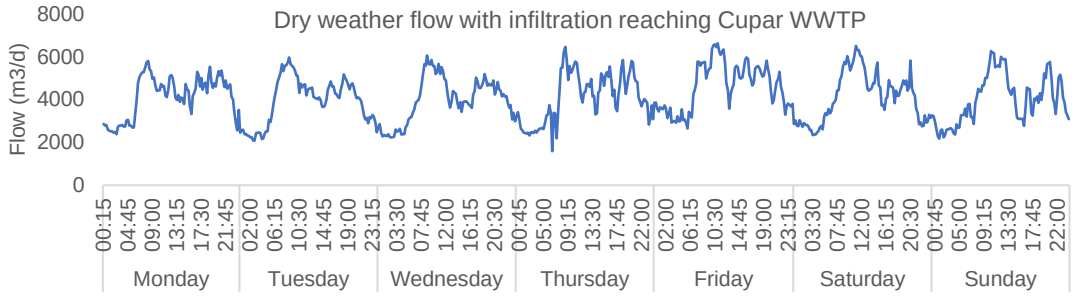

Figure 5-4 Dry weather flow with infiltration reaching Cupar WWTP

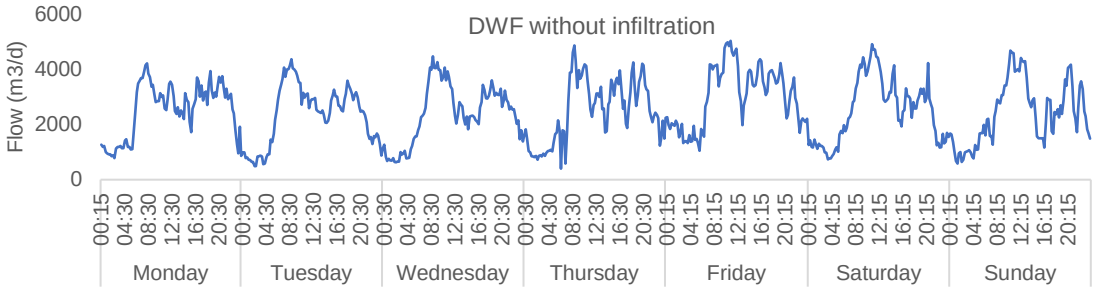

Figure 5-5 DWF without infiltration reaching Cupar WWTP

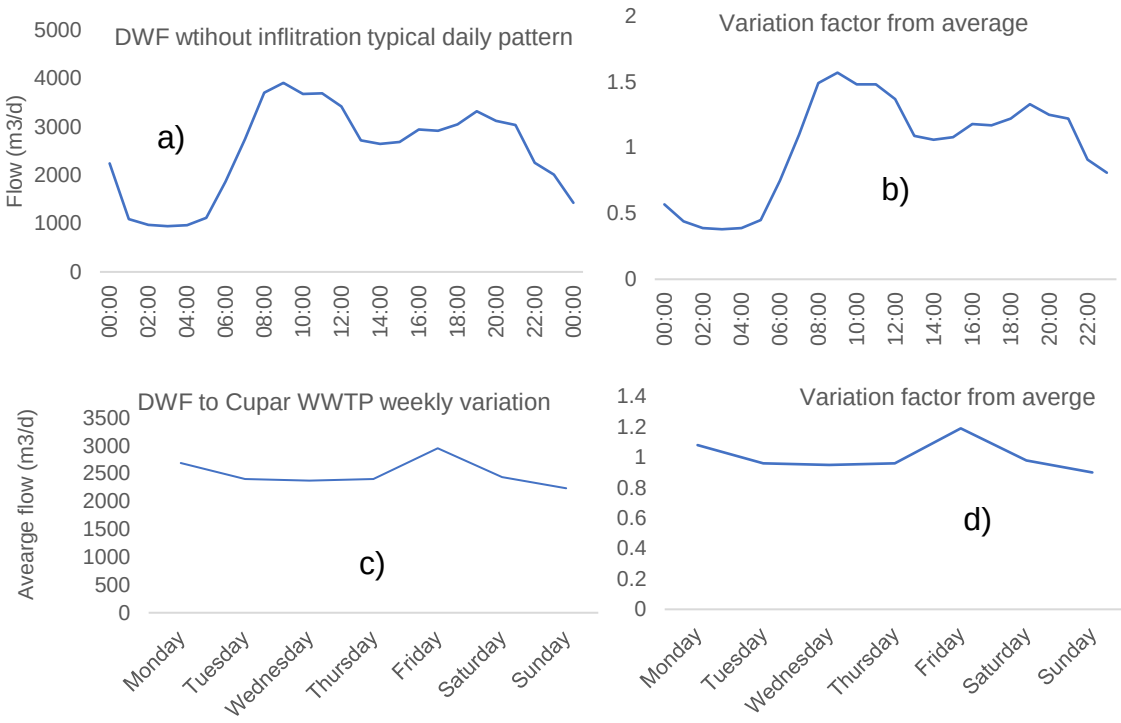

Figure 5-6 Typical patterns of DWF for Cupar WWTP a) Typical daily pattern in m^3 d^{-1} b) typical variation of DWF from the average c) Weekly variation of DWF at Cupar WWTP [m^3 d^{-1}] d) Weekly variation of DWF from the average

The household flowrate module generates sub-daily flow pattern by using a typical domestic daily flow pattern for each day of the week ('week_HS', Figure 5-6 (d)), variation of this over a year ('year_HS'), and using a typical daily flow pattern ('day_HS', Figure 5-6 (b)). Parameters used in the household flow model block is presented in Table 5-2.

Table 5-2 Parameters for combined household and industrial flow generator model block

Household model block (flow rate)	Value	Description
Model parameters		
QperPE	0.157	Wastewater flow rate per PE for municipal wastewater ($m^3\ d^{-1}$) per PE
PE	16000	Number of HH population equivalent connected to the WWTP
QHHsatmin	0.05	Minimum flow rate to avoid error (division by zero) [$m^3\ d^{-1}$]
QHHsatmax	QperPE*3	Maximum household flowrate to limit too high flowrate from noise
Noise parameters		
Q_HH_ns	5100	noise seed
Q_HH_nv	0.001	Noise variance
Q_HH_st	1/24	Noise sampling time
Switch functions		
Hhpopswitch	100	Switch the HH contribution on (100 %) or off (0 %)
Hhnoiseswitch	1	Switch the noise term in HH flow rate; on (1) or off (0)

Similarly, the household and industrial pollutant concentration are analysed without separating them unlike the phenomenological modelling approach used by Gernaey et al. (2005a). The pollutant concentration required is typical daily flux variation of soluble and particulate COD (CODsol_day_HS, CODpart_day_HS), Ammonia (SNH_day_HS), and total Kjeldahl Nitrogen (TKN_day_HS), for the details refer to Chapter 4. In addition to the typical sub-daily variation of pollutants, it is necessary to identify the daily average flux variation over a week (week_polHS). The daily average value of the soluble COD flux was estimated to be 234 kg d^{-1}, and the daily average value of the particulate COD flux was estimated to be 1026 kg d^{-1}, based on campaign data.

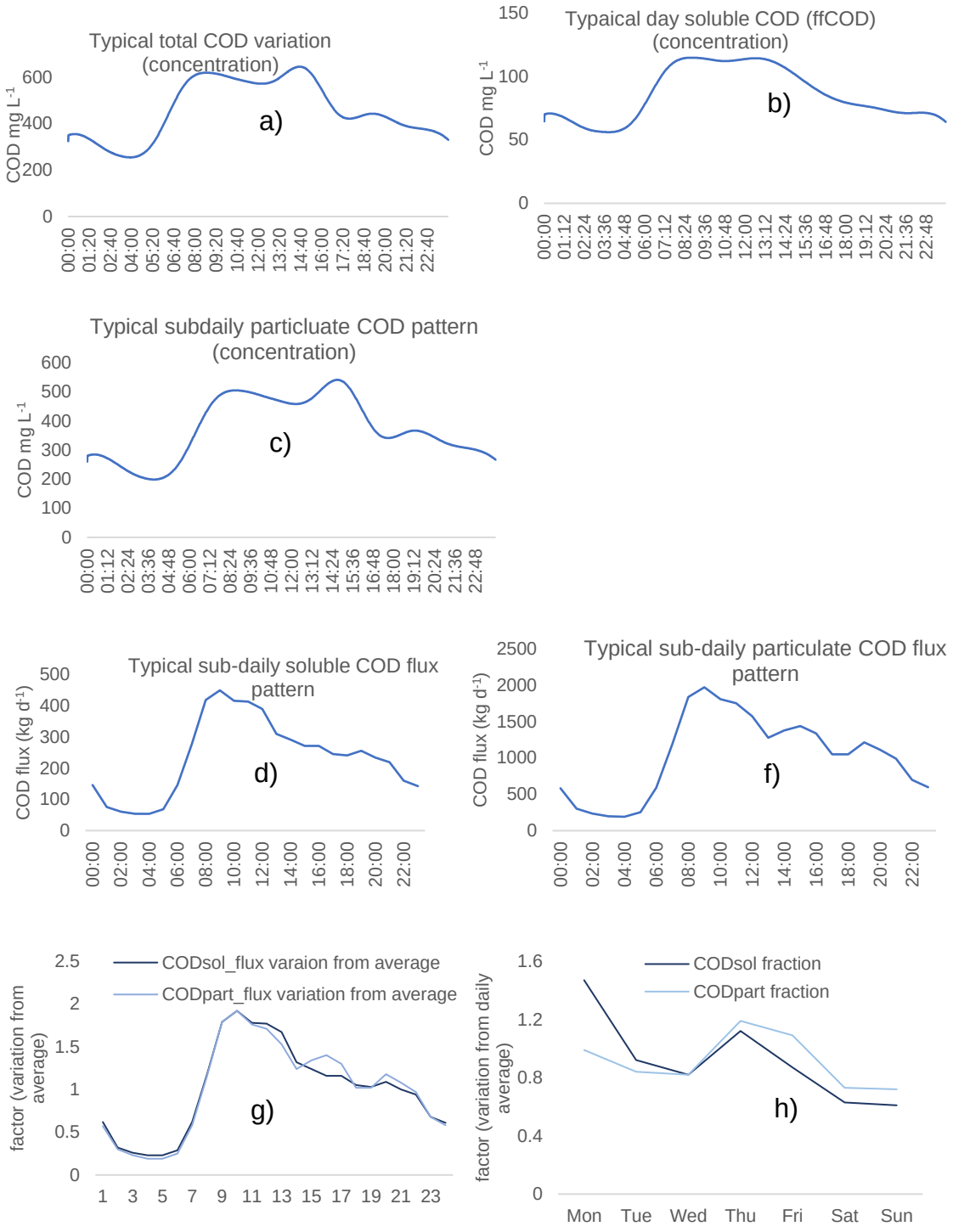

Figure 5-7 The pollutant concentration required is typical daily flux variation for Cupar WWTP a) total COD concentration variation in a day [g m^{-3}] b) soluble COD concentration variation in a day [g m^{-3}] c) particulate COD concentration variation in a day [g m^{-3}] d) Soluble COD flux pattern in a day [kg d^{-1}] f) Particulate COD flux variation in a day [kg d^{-1}] g) Sub-daily particulate and soluble COD flux variation from the daily average h) Particulate and soluble COD flux variation in a week compared to the daily average

Hence, the COD particulate and soluble fractions flux varies significantly from day to day on a significant level as shown in Figure 5-7, new parameters are introduced, i.e. instead of using one pollutant weekly variation input

(week_polHS), three different patterns were used; week_CODsol_HS (soluble COD weekly variation), week_CODpart_HS (particulate COD weekly variation), and week_N_HS (TKN and ammonia weekly variation) (Gernaey et al., 2005b). The soluble COD pattern is estimated from the filtered and flocculated COD which is monitored during the campaign, see Chapter 4. The particulate COD pattern is calculated as the difference between total COD and flocculated and filtered COD.

The typical sub-daily variation of ammonia and total Kjeldahl nitrogen flux was estimated from the directly measured ammonia and TKN during the data campaign. The two-hourly data that was collected during the campaign was interpolated using a cubic spline interpolation method to create data at a minute time step. This data is analysed to create the sub-daily variation and the variation in a daily average of these fluxes over a typical week similarly to the particulate and soluble COD. The average NH_4 flux was estimated to be 54 kg of N d^{-1} and TKN to be 75 kg of N d^{-1}.

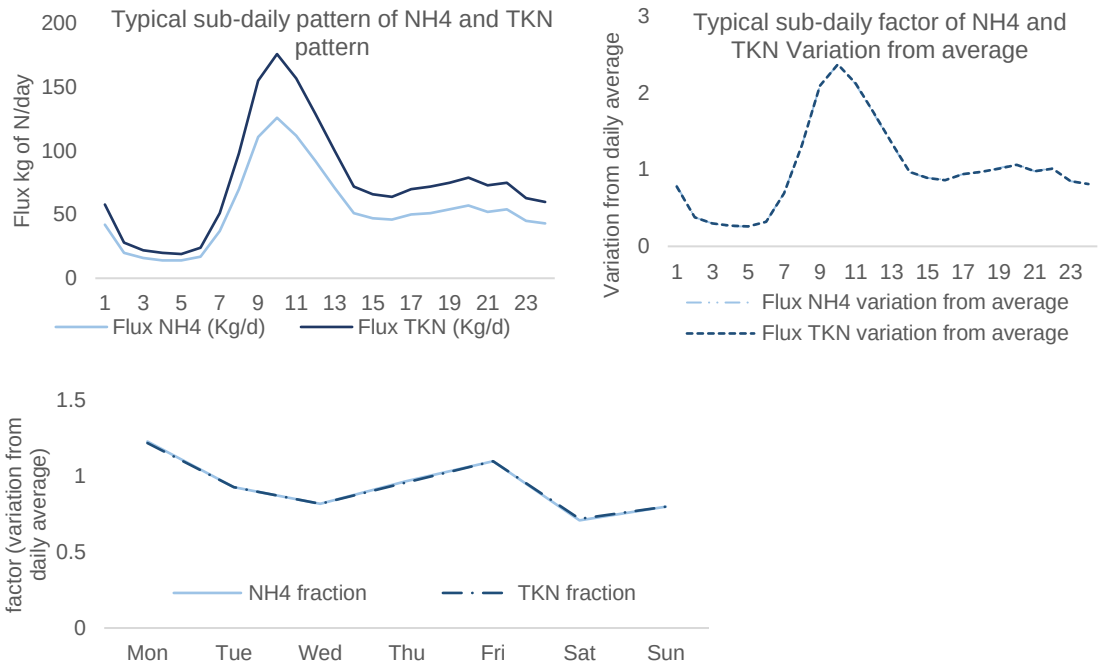

Figure 5-8 The pollutant concentration required is typical daily flux variation for Cupar WWTP a) Ammonia and TKN flux variation in a day [kg N d^{-1}] b) Variation of ammonia and TKN in a day from the average c) Ammonia and TKN flux variation in a week compared to the daily average

The typical sub-daily variation of NH_4 and TKN is similar since the TKN was estimated from the measured NH_4 based on a linear relationship. See Chapter 4 for the detail of TKN estimation from NH_4. For a similar reason, the variation of the daily average over a week for NH_4 and TKN appeared to be the same.

The household pollutant load is feed into the sewer network where the concentration of a pollutant is estimated based on total flow entering the sewer network and these pollutant loads. An S-function block, 'asm1_fractionation_cupar', is used to fractionate these pollutant loads into the state variables as discussed below. Although the 'asm1_fractionation_cupar' is within the sewer model block, it is more appropriate to discuss it here than later.

Measured data after cubic spline interpolation, Section 4.1.7, did not show a significant variation of non-biodegradable COD (S_I) (maximum 21.7 mg L^{-1} and a minimum of 8 mg L^{-1}). Hence, a constant value is used as an input, 15.7 mg L^{-1} which is the average over three weeks. The soluble biodegradable COD (S_S) was estimated as a difference between the total influent soluble COD and the soluble non-biodegradable COD, similar to the soluble COD in final effluent. The particulate COD was fractionated into biodegradable (X_S), non-biodegradable (X_I), and active heterotrophic biomass ($X_{B,H}$). The fractionation was done using factors that are determined from the three weeks monitoring and the wastewater characterisation in Chapter 4, f_{XS} (0.66) and f_{XI} (0.24) and $f_{XB,H}$ (0.1) respectively. Key parameters in representing COD load is presented in Table 5-3. The autotrophic bacteria flux is assumed to be 0.1 % (fr_{XBA}) of the total particulate COD. The active heterotrophic and autotrophic biomass is taken based on (Jeppsson, 2004) and (Henze, 1992) respectively. The particulate inert COD Xp is assumed to be zero, similar to that of BSM2 (Jeppsson et al., 2007). The Simulink representation of combined household and industrial pollutant load generation based on daily pattern, weekly pattern, yearly pattern, and average pollutant load [g d^{-1} or g d^{-1} PE^{-1}, see Table 5-3] is shown in Figure 5-9.

The ammonia concentration (S_{NH}) is taken directly from measured data during the campaign period. The organic nitrogen is estimated by using the measured Total Kjeldahl Nitrogen (TKN), ammonia flux (S_{NH}), influent heterotrophic biomass flux (X_{BH}) and the fraction of nitrogen in heterotrophic biomass (i_{XB}). The organic Nitrogen flux is obtained as the difference between TKN flux and the sum of S_{NH} flux and the Nitrogen flux corresponding to heterotrophic bacteria ($i_{XB} \times X_{BH}$). The organic Nitrogen flux is distributed between soluble and particulate organic nitrogen (S_{ND} and X_{ND}) (Gernaey et al., 2005a). Their respective fractions were estimated based the Cupar influent characterisation presented in Chapter 4, on average fr_{SND} (0.327) and fr_{XND} (0.672). The average organic flux, NO_X, is

calculated based on the average organic nitrogen concentration and the average household flow rate of 2512 m^3 d^{-1}, (QperPE × PE). Key parameters in representing TKN load is presented in Table 5-3.

The oxidised nitrogen flux is estimated based on the measured flux of nitrate and nitrite. Since the oxidised nitrogen concentration in the influent is relatively small, its sub-diurnal variation is not put into consideration for this influent generator. Hence, an average daily flux of 3.65 kg d^{-1} is used.

Table 5-3 Combined household and industrial pollutants model parameters

Parameter	Description	Value	Unit
CODsol_gperPEperd	Average soluble COD load	28.62	g COD d^{-1} PE^{-1}
CODpart_gperPEperd	Average particulate COD load	114.72	g COD d^{-1} PE^{-1}
SNH_gperPEperd	Average ammonium load	6.08	g N d^{-1} PE^{-1}
TKN_gperPEperd	Average TKN load	8.512	g N d^{-1} PE^{-1}
NOx*	Average inorganic N load (Nitrate + Nitrite)	1809	g N d^{-1}
CODsol_HH_min	Minimum soluble COD (saturation)	0.1*CODsol_gperPEperd*PE	g COD d^{-1}
CODsol_HH_max	Maximum soluble COD (saturation)	8*CODsol_gperPEperd*PE	g COD d^{-1}
CODpart_HH_min	Minimum particulate COD (saturation)	0.1*CODpart_gperPEperd*PE	g COD d^{-1}
CODpart_HH_max	Maximum particulate COD (saturation)	8*CODpart_gperPEperd*PE	g COD d^{-1}
SNH_HH_min	Minimum ammonium (saturation)	0.1*8*SNH_gperPEperd*PE	g N d^{-1}
SNH_HH_max	Maximum ammonium (saturation)	8*SNH_gperPEperd*PE	g N d^{-1}
TKN_HH_min	Minimum TKN (saturation)	0.1*TKN_gperPEperd*PE	g N d^{-1}
TKN_HH_max	Maximum TKN (saturation)	8*TKN_gperPEperd*PE	g N d^{-1}

* Direct Simulink block input

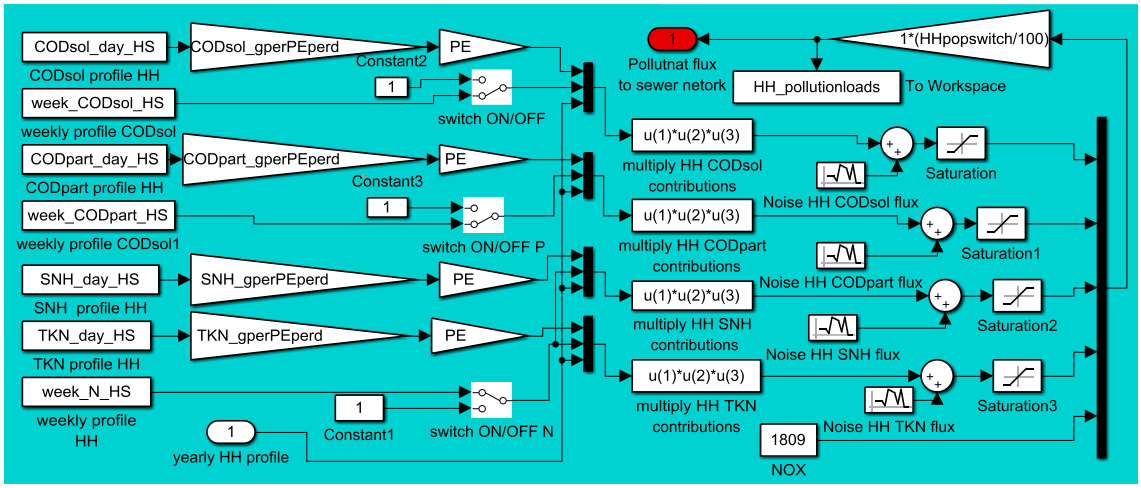

Figure 5-9 Combined household and industrial pollutants load model block

5.1.1.4. Sewer and CSO Module

The sewer model uses a simple water balance approach to estimate flow from sections of the sewer network. Depending on the size of the sewer, the sewer network can be divided into three or more sub-sections (sub-catchments). Each sub-section of the sewer network is considered as a simple tank where what comes in goes out using a simple rectangular weir equation. The total volume of the Cupar sewer network is estimated by sub dividing the network into gravity

pipes, connection pipes, rising pipes and chambers. The details on the length of pipes are collected from the spatial data of underground infrastructure from a Geographical Information System (GIS) database of Scottish Water. The diameter of each type of pipe is assumed based on discussion with asset managers and on-site sewer network team leaders, see Table 5-4.

Table 5-4 Rough estimations of the total volume of Cupar sewer network

Volume of sewer	Total length (m)	The assumed average diameter (m)	Total volume (m^3)
Cupar gravity pipes	73575	0.6	20803
Cupar connection pipes	5278	0.3	373
Cupar rising mains	1650.6	0.6	467
Cupar chambers (number)	1788		1788
The total volume of Cupar sewer network			**23431**

The total flow generated within the sewer network from the soil module, household influent generator, and storm flow is sub-divided into an equal number of sub-networks, 'subarea'. In this instance, the number of sub-networks was left for calibration, and based on calibration sub-area of four is found to be representative for Cupar area. Lower than four produced noisy influent flow and higher than four sub-networks produced a too-low noise compared to measured flow at the WWTP inlet point. The total flow is evenly distributed among the sub-networks, which are considered as a storage tank with an outflow rate estimated using Manning's equation of rectangular pipes. The outflow from each sub-network cannot exceed the pumping capacity of the pump allocated for it. The conceptual modelling approach is detailed in Figure 5-10, and the application into Simulink blocks is shown in Figure 5-11 and Figure 5-12.

Based on manual calibration, pumping capacity of 45 L s^{-1} is assigned for the most upstream sub-network, and 60 L s^{-1} and 90 L s^{-1} for the next two downstream sewer pumps. The calibration is done based on flow to the WWTP and it may not accurately simulate the frequency of CSO spills but can estimate the total volume of spill accurately. If the outflow estimated using the Manning's equation is greater than the pump capacity, the outflow from the sub-network will be limited to the pump's capacity of the sub-network. If the sub network is full and the outflow is less than the inflow, the difference of the two will be the spill, which is a similar approach used in estimating the flow balance of storage tanks in

BSM2. It is also similar to the approach used in simulating storage in WWTP in this study as well, see Section 3.1.4.

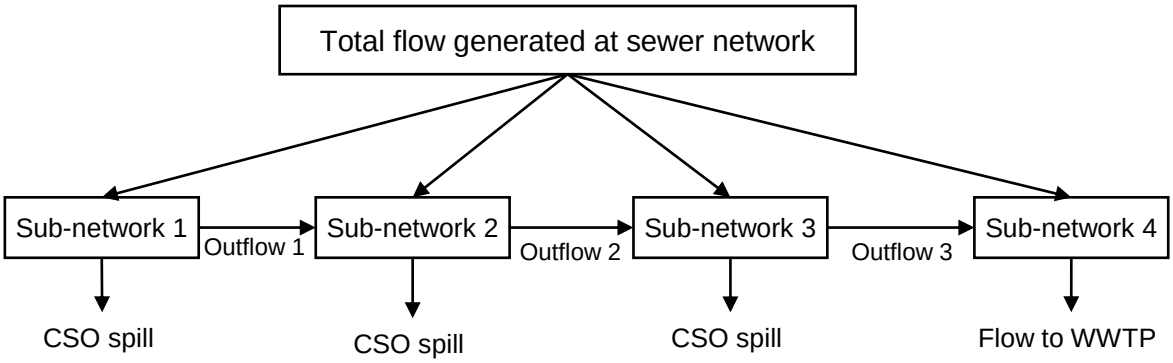

Figure 5-10 Conceptual framework of sewer network and CSO spill modelling

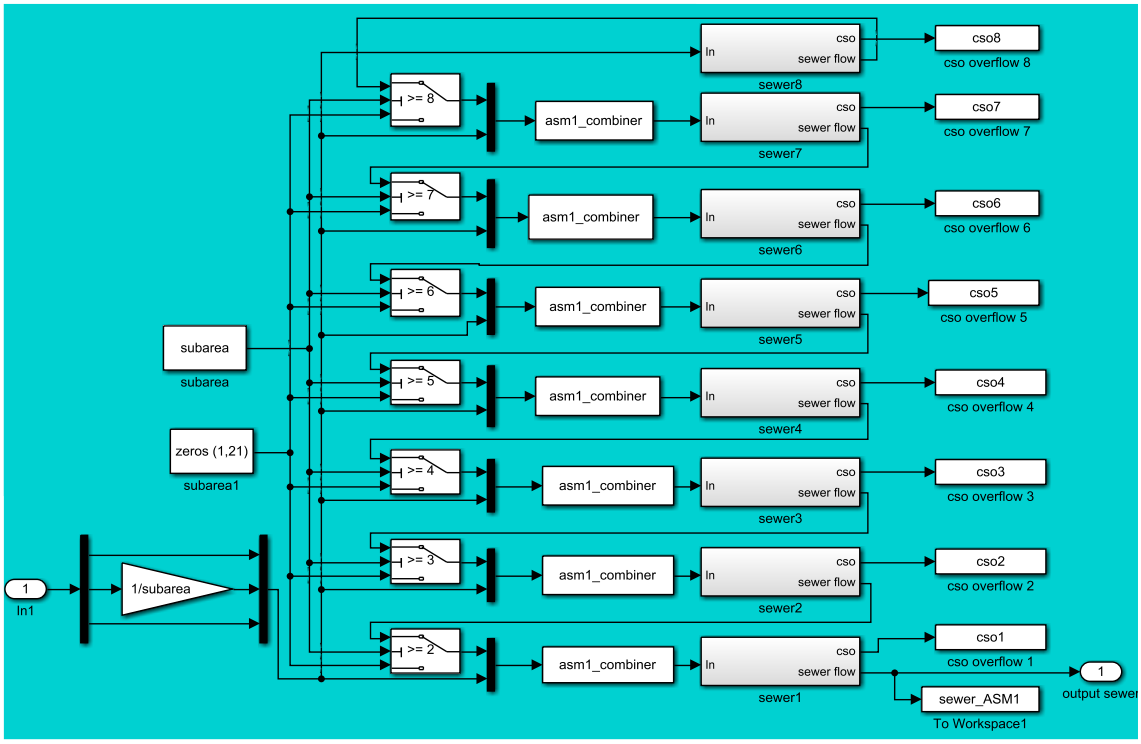

Figure 5-11 Sewer block showing the distribution of generated flow over sub-networks and CSO spill outputs

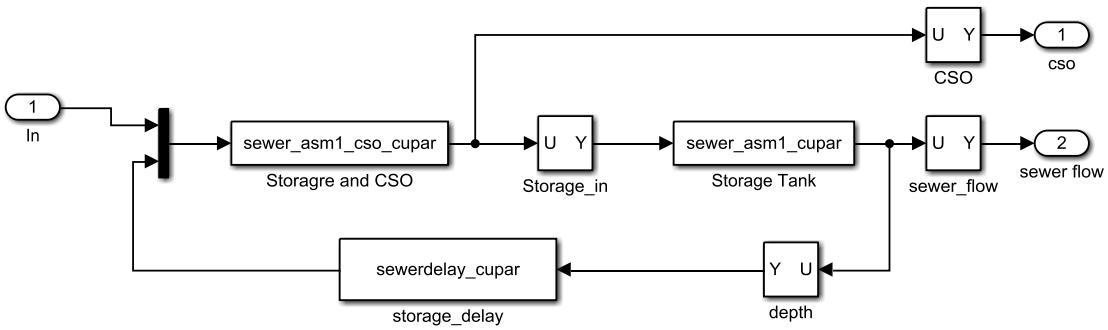

Figure 5-12 Sewer storage block with outflow calculator 'sewer_asm1_cso_cupar' and storage depth updater 'sewer_asm1_cupar'

5.1.1.5. Temperature Module

Temperature is generated based on the seasonal variation with a sine function and sub-daily variation with a sinusoidal wave. The seasonal variation of wastewater is estimated based on the variation in air temperature observed for a year. A moving-average of 10 days is used to assess the seasonal variation and reduce noise in the time-series shown in red in Figure 5-13. The simulation period for Cupar WWTP starts at the end of October. Thus, the sinusoidal curve, based on Figure 5-13, will have a phase shift ('TPhase') of 6 months, π.

The ten-days moving-average showed a maximum daily temperature of 21 °C and a minimum of 1.2 °C. However, influent wastewater temperature does not get as low or as high as the air temperature (Libhaber and Orozco-Jaramillo, 2012). The influent to constructed wetland wastewater treatment work in Minnesota showed that wastewater temperature gets not lower than 9 °C even if air temperature goes below -15 °C. Similarly, in Wallace (2007) cited in Libhaber and Orozco-Jaramillo (2012), although the air temperature on average went as high as 25 °C, the influent wastewater temperature stays below 18 °C. In this instance, the influent wastewater at Cupar WWTP is assumed to have a similar nature as the influent to the wetland treatment in Minnesota, and the maximum temperature of 18 °C is adopted. Since the air temperature at Cupar does not go as low as Minnesota, a minimum temperature of 12 °C is assumed. Hence, the sinusoidal seasonal variation of temperature represented by an amplitude of 3 °C and a bias of 15 °C.

Sub-daily variation of temperature also flows a sinusoidal variation with an amplitude ('TdAmp') of 0.5 °C, similar to Gernaey et al. (2005b). Observation sub-daily air temperature at Cupar showed maximum temperature occurs around 3:00 pm. Hence, a phase shift ('TdPhase') of 1.25π is taken for the sub-daily variation, see Table 5-5.

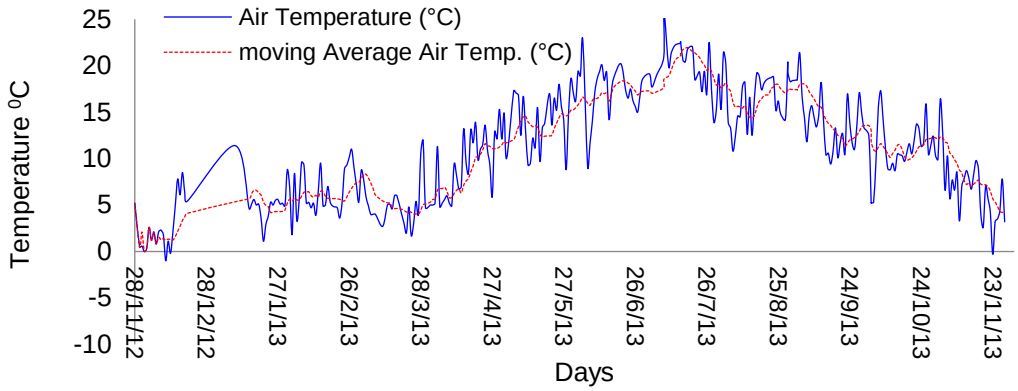

Figure 5-13 Air temperature - daily data with a moving average of 10 days

Table 5-5 Wastewater temperature model block parameters

Parameters for temperature model block	Value	Description
TAmp	3	Sine wave amplitude (deg. C)
TBias	15	Average temperature (deg. C)
TFreq	2*π/364	Sine wave frequency (rad d^{-1})
TPhase	π	Sine wave phase shift
TdAmp	0.5	Sine wave amplitude (deg. C)
TdBias	0	Sine wave bias (deg. C)
TdFreq	2*π	Sine wave frequency (rad d^{-1})
TdPhase	1.25*π	Sine wave phase shift

5.1.2. MATLAB/Simulink River Model

To assess intervention options and control strategies at WWTP in response to the assimilative capacity of receiving waters, an integrated model that links the WWTP, the sewer network, and the receiving water is essential (Benedetti et al., 2013). the WWTP model and the influent generator are integrated with the receiving water body model developed at the University of Sheffield (Dickinson, 2018). This model consists of a pragmatic and parsimonious hybridisation of artificial neural networks (ANN) and traditional mechanistic modelling components (Dickinson, 2018).

The receiving water body model proposed by Dickinson (2018) has three components; a combined sewer overflow (CSO) model, rainfall-runoff generation model, and surface water quality model. The CSO model is a simple single layer Artificial Neural Network (ANN) which deploys an adaptive linear neuron (ADALINE) networks to simulate the flow depth at CSOs based on rainfall. Whereas, the rainfall-runoff generation model uses a more complex non-linear autoregressive with exogenous input (NARX) networks, which are multi-layer ANN deployed in the modelling of rainfall-runoff and discharge in rivers

(Dickinson, 2018). Unlike these two model components, the surface water quality and routing model uses a simple mechanistic approach to routing the flow in rivers and model pollutants such as temperature, pH, dissolved oxygen (DO), Biochemical Oxygen Demand (BOD), and ammonia.

Since the objective of the study is not to represent the spatial variation of the sewer network, studies showed that a single layer ANN could be successfully used to simulate depth of stormflow at CSOs using measured rainfall (Mounce et al., 2014; Guo and Saul, 2011). Similarly, Dickinson (2018) uses a linear weighted approach of ADALINE to correlate the current flow depth at CSOs to previous time-step depth and rainfall rate using a moving time-window approach.

The rainfall-runoff process is modelled by using a NARX Network which can be used to simulate non-linear systems at discrete time-steps. This approach uses the open-loop form to train the network and then converted to a closed-loop form to give a predictive ability to the model with different lead-times. The details, development and application of NARX to Cupar WWTP's receiving water body, the Eden River, can be found in Dickinson (2018).

The receiving water body model consists of three sub-models; hydraulic sub-model that rout the flow in the river, a thermodynamic model for estimation of water temperature, and finally the water quality sub-model that simulate the physical (mixing) and chemical processes that affect three quality indicators: pH, DO, BOD, and NH_4. Dickinson (2018) developed the hydraulic routing using a variation of Manning's Equation together with conservation of mass and momentum. The water quality process model used by Dickinson (2018), and adopted in this study is based on the Streeter-Phelps simplified mass balance model (Streeter, 1925).

The receiving river, River Eden, is classified as a Type 5 river based on the Scottish River Basin Management Plan (SRBMP). Based on the chemical and physiochemical environmental standards, for the River Eden to be classified as 'good', the 10-percentaile DO level should be above 60 %, the total BOD should be below 5 mg L^{-1} or 11 mg L^{-1} for 90-percentile and 99-percentile respectively, and the 90-percentile ammonia concentration should not be above 0.6 mg L^{-1}. These environment quality indicators are used as a target to calculate the assimilative capacity of the river.

The assimilative capacity of the receiving water body is estimated within the surface water quality model, combining the modelled quality with known target values of the physicochemical quality indicators; DO, BOD, and ammonia. Thus, treating the optimisation as a constrained non-linear minimisation problem. This optimisation is achieved using one of the standard solvers provided with MATLAB/Simulink® based on an implementation of the Nelder-Mead simplex search algorithm which is well suited to minimisation or maximisation (minimax) problems in a multivariable space; the formulation is based on the work of Lagarias et al. (1998).

Table 5-6 lists down parameters used in the optimisation process, which currently uses the environmental quality standards as a target. The upstream river flow and quality are mixed with a minimum effluent flow and quality specified as a lower limit, and the model simulate the quality of the river after mixing. The concentrations of the final effluent quality indicators (flow, DO, TKN, and BOD) are simulated until the DO concentration in the river reaches the saturation level without violating the BOD and ammonia target. Further detail on the modelling, forecasting and assimilative capacity calculation can be found in Dickinson (2018).

Table 5-6 Parameters of WWTP final effluent for optimisation of the river's assimilative capacity (Dickinson, 2018)

Parameter	Description	
$\boldsymbol{Q_{eff}}$	WWTP final effluent	[$m^3\ s^{-1}$]
$\boldsymbol{S_{o,eff}}$	Dissolved Oxygen Concentration	[mg L^{-1}]
$\boldsymbol{BOD_{eff}}$	BOD_5 for estimating the Ultimate Carbonaceous BOD concentration $UCBOD = \boldsymbol{BOD_5} \Big/ (1 - e^{-k_1(5)})$; where k_1 is CBOD bottle test decomposition rate coefficient (Dickinson, 2018)	[mg L^{-1}]
$\boldsymbol{TKN}$	Total Kjeldahl Nitrogen for estimating Nitrogenous BOD Concentration; $NBOD = 4.57TKN$ (Dickinson, 2018)	[mg L^{-1}]
$\boldsymbol{N_o}$	Organic Nitrogen Concentration	[mg L^{-1}]
$\boldsymbol{S_{NH,eff}}$	Final effluent ammonia concentration	[mg L^{-1}]
$\boldsymbol{NO_{2,eff}}$	Final effluent nitrite concentration	[mg L^{-1}]
$\boldsymbol{NO_{3,eff}}$	Final effluent nitrate concentration	[mg L^{-1}]

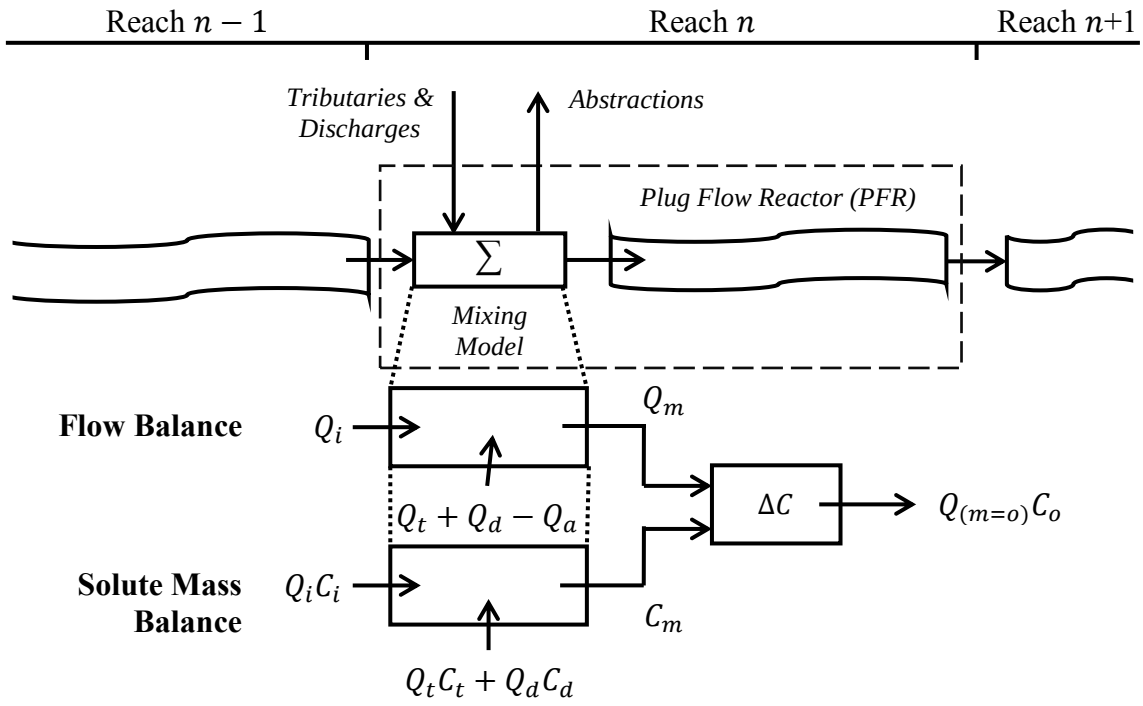

Figure 5-14 A conceptual layout of the water quality model Source: Dickinson (2018). Q and C represent flows and concentrations respectively. The subscripts i, t, d, a, m and o stand for inflow, tributary, discharge, abstraction, mixed and outflow. ∆C represents the change in concentration due to physiochemical processes.

Both the data-driven models and the mechanistic model are run using a one-year data monitored during the period 13/11/2015 – 31/10/2016. The implementation of receiving water body in MATLAB/Simulink is done by using an interpreted MATLAB function blocks; one upstream of WWTP model ('Cuparmodel.m') and the second one downstream of the WWTP ('DownstreamCuparModel.m'). The 'Cuparmodel.m' function consists of all the sub-models discussed in the paragraph above and estimate the assimilative capacity of the river using optimisation. The latter, 'DownstreamCuparModel.m', consists of only the water quality model that uses the mechanistic model to simulate mixing and determine pollutant concentration downstream of the WWTP, see Figure 5-15.

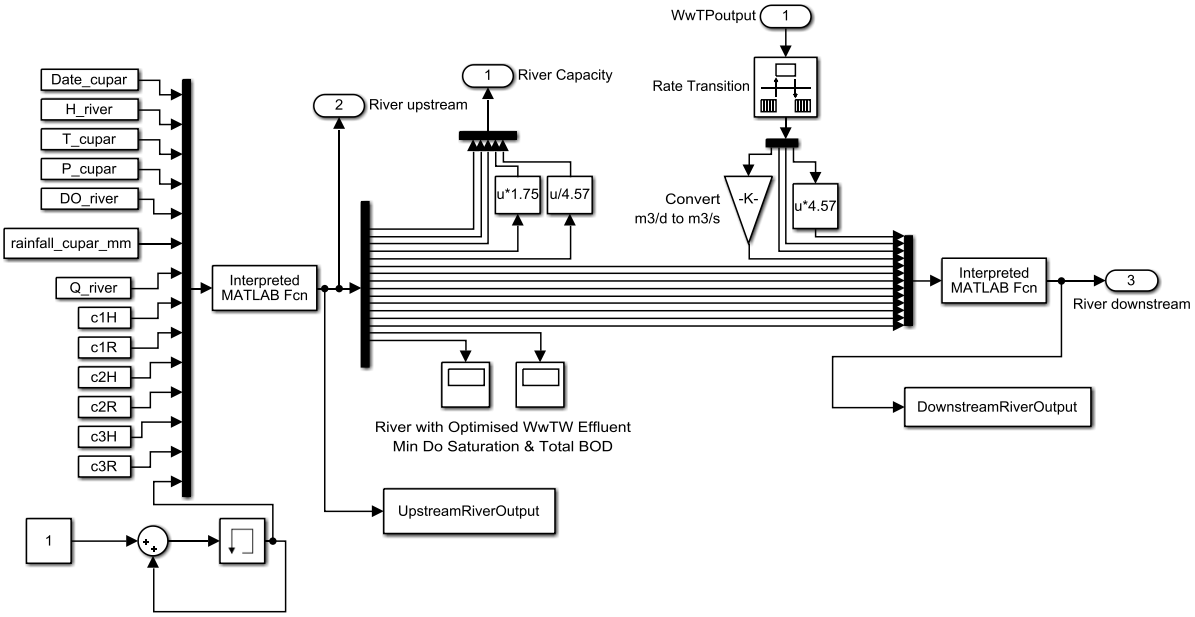

Figure 5-15 Implementation of River Model in MATLAB to link to the WWTP model: Source (Dickinson, 2018)

5.1.3. MATLAB/Simulink WWTP, Influent Generator and River Model Integration

Integrated wastewater management presents a great opportunity to minimise the impact on receiving water and can increase the efficiency of the system (Benedetti et al., 2013; Butler and Schütze, 2005). However, modelling of an integrated system can be challenging mainly due to the different sets of state variables from each model (Benedetti et al., 2013). In this instance, the integration of the influent generator and the WWTP model is straight forward since the state variables and simulation environment is the same. However, the integration of the WWTP model with the receiving water body model requires aggregation of the state variables from the WWTP. The state variables for the receiving water body is limited to the quality indicators that are commonly monitored by the regulatory bodies, DO, BOD and NH_4/TKN. The details of the integration of the three modelling components and system components are shown in Figure 5-16.

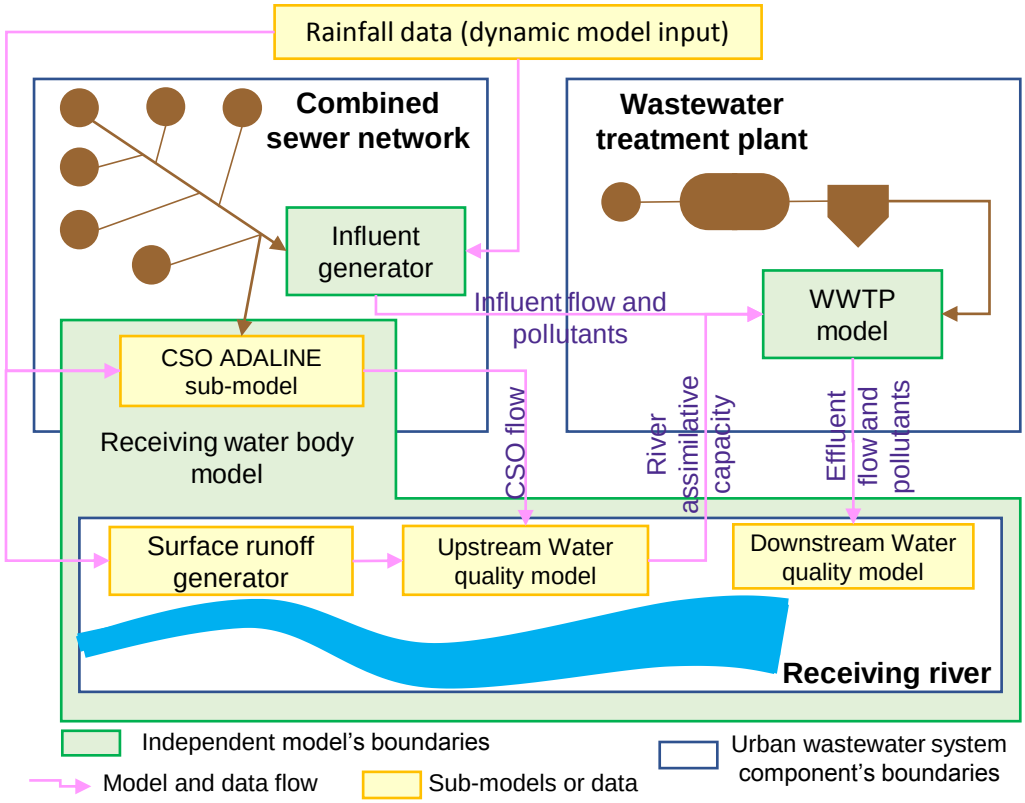

Figure 5-16 Summarized layout of the integrated wastewater modelling approach used in this study

The aggregation is required only to estimate BOD while the rest of the quality indicators in the river model are the state variables in the WWTP as well. The final effluent BOD is estimated based on the suggestion by Gernaey et al. (2014) and the approach used in the influent characterisation in Section 4.1. Hence, the BOD from WWTP to rivers ($BOD_{5,effluent}$) can be calculated by combining the BOD of final effluent from final settlement tanks from Eq. 5-46, and BOD of storm overflow from storm tanks from Eq. 5-47, see Eq. 5-1.

$$BOD_{5,effluent} = \frac{BOD_{5,eff} \times Q_{eff} + BOD_{5,ST} \times Q_{ST,spill}}{Q_{eff} + Q_{ST,spill}} \qquad \textit{Eq. 5-1}$$

The CSO flow is modelled both by the influent generator and by the receiving water body model. Although the influent generator can model both flow and pollutant load from CSOs, the complexity of linking this model with the receiving water body model justifies the use of the CSOs models within the receiving water body model.

The state variables from the WWTP model are selected and some converted to create compatibility with the BOD and nitrogenous-BOD (NBOD) based river model. The WWTP outputs or inputs state variables to the river model are

reduced from 21 to four; total Kjeldahl Nitrogen (TKN), BOD, DO, and flow rate. The TKN is estimated from the ammonia concentration of the final effluent assuming ammonia to TKN ratio in the final effluent is the same as the influent wastewater, Chapter 4, i.e. TKN = NH4 x 1.4. The BOD calculation from the COD components of the final effluent is done using Eq. 5-1. Dissolved oxygen is one of the state variables from the WWTP model and taken directly without any adjustment. The flowrate from the WWTP model has a unit $m^3\ d^{-1}$ while the river model runs at $m^3\ s^{-1}$; hence the unit conversion is done using a gain function in MATLAB/Simulink®.

The upstream river model that calculates river quality upstream of the WWTP and the assimilative capacity of the river has 16 state variables in its output. The first five variables are related to the WWTP allowable flow and pollutant concentrations. The variables are; forecast time-step, allowable WWTP flow rate, DO, BOD, and NBOD. The NBOD is converted to TKN using Eq. 5-2 (Chapra, 1997) cited in (Dickinson, 2018). The next nine state variables/outputs include upstream river flowrate, DO, BOD, NBOD, depth, temperature, AvD, Delta, and UDate. Calculated total BOD, and minimum DO saturation in percent are also outputs of the upstream model and just saved to the workspace and not needed further.

$$NBOD = 4.57 \times TKN \qquad \textit{Eq. 5-2}$$

The downstream river model combines flow from upstream river model and final effluent from WWTP, Figure 5-17. Its inputs, nine state variables from the upstream river model and four state variables from WWTP final effluent, are used for mixing and estimating further nitrification and biological assimilations. This model calculates output variables downstream of WWTP; river flowrate, DO concentration, BOD, NBOD, minimum DO, and minimum saturated DO.

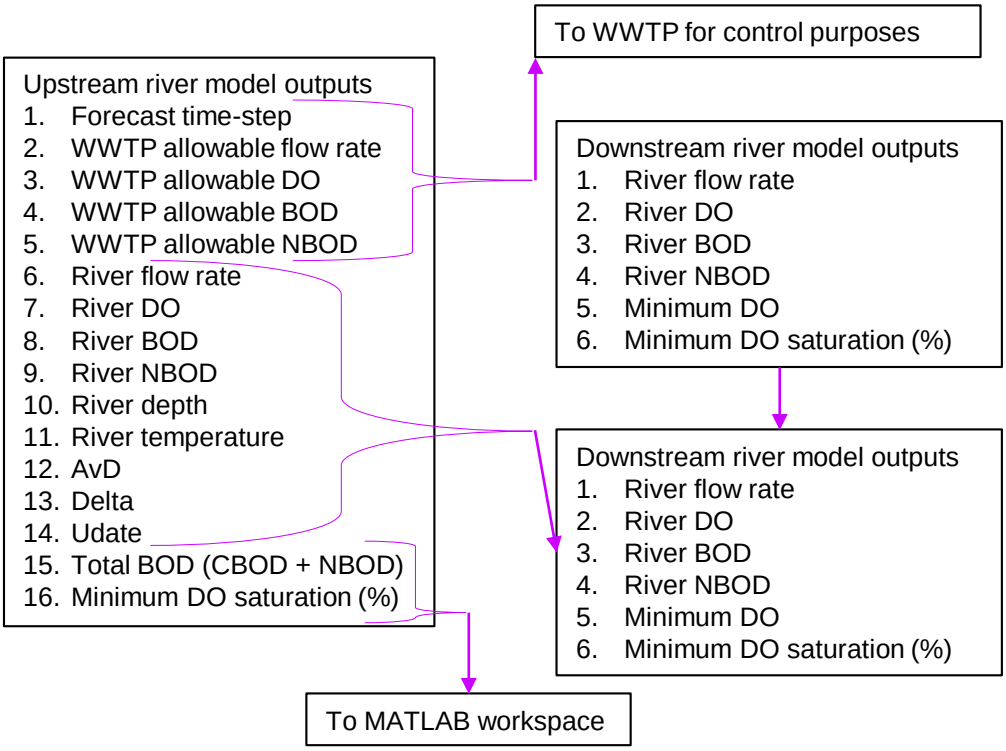

Figure 5-17 State variables interactions and conversions in the integrated model

5.2. WWTP Performance Assessment

5.2.1. Greenhouse Gas Emissions

The performance assessment for intervention options and control strategies is developed considering greenhouse gas (GHG) emissions, effluent quality, operational cost, receiving water quality and legislation compliance.

All GHG emissions from the WWTP are converted to CO_2 equivalent units to enable comparison of emissions magnitude from different sources. The emissions estimation in this study considered both direct emissions and indirect emissions as shown in Figure 5-18.

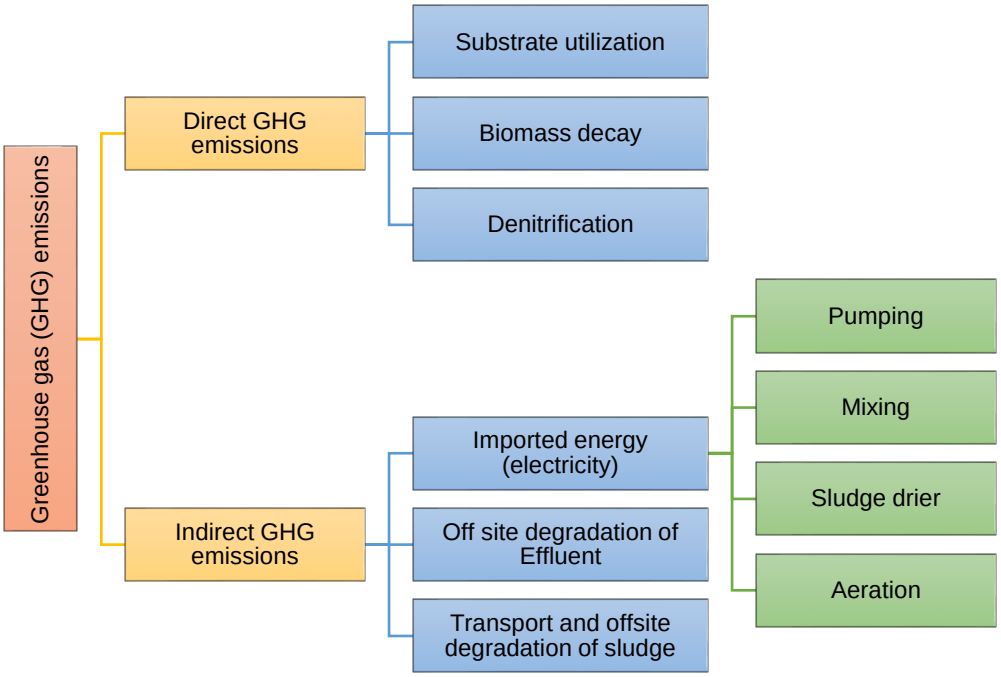

Figure 5-18 Greenhouse gas emission accounting and boundaries

5.2.1.1. Direct GHG Emissions – Substrate Utilisation

The direct GHG emissions from oxidation ditch that are considered in this study include emissions because of substrate utilisation, biomass decay, and denitrification processes, and are estimated using the methods suggested by (Sweetapple, 2014).

The major greenhouse gases, carbon dioxide (CO_2), methane (CH_4) and nitrous oxide (N_2O) can all be a direct emission from WWTWs. Their greenhouse impact is weighted based on their Global Warming Potentials (GWP). Nitrous oxide N_2O is a very potent GHG with a 100-year global-warming potential 298 times greater than that of CO_2, and CH_4 with GWP of 25 times that of CO_2 (IPCC, 2013).

Biological processes in ASM1 implemented in the original BSM2 model is based up on a cycle of death and regeneration biomass, which is different from the stoichiometric equation used to describe biomass decay and substrate utilisation for CO_2 emissions estimation. The stoichiometric equation used for CO_2 emission estimation in this study uses the growth and endogenous respiration detailed in Sweetapple (2014).

In an aerobic condition, two distinct processes are used by the bacteria to breakdown organic matter; biological oxidation, and biosynthesis. If oxygen is limited, auto-oxidation or endogenous respiration will occur (Henze et al., 2008; Gray, 2010; Monteith et al., 2005; Shahabadi et al., 2010; McCarty, 2012).

Oxidation of BOD to produce energy for growth:

$$2C_{10}H_{19}O_3N + 25O_2 \rightarrow 20CO_2 + 16H_2O + 2NH_3 + \text{Energy} \qquad \textit{Eq. 5-3}$$

Biosynthesis:

$$COHNS + O_2 + \text{Bacteria} \rightarrow C_5H_7O_2N \text{ (New cell tissue)} \qquad \textit{Eq. 5-4}$$

Auto-oxidation or endogenous respiration:

$$C_5H_7O_2N + 5O_2 \rightarrow 5CO_2 + NH_3 + 2H_2O + \text{Energy} \qquad \textit{Eq. 5-5}$$

Eq. 5-3 predicts that for every mole of oxygen consumed, 0.8 moles of CO_2 are released. The gram molecular weights of O_2 and CO_2 are 32 and 44 g, respectively, leading to a theoretical conversion ratio of 1.1 kg CO_2/kg O_2 (EF_{AerOxi}) (Monteith et al., 2005). There is no CO_2 emission during the biosynthesis process. Eq. 5-5 showed that 5 moles of CO_2 are released for every mole of biomass respired. The gram molecular weights of the biomass ($C_5H_7N0_2$) and CO_2 are 113 and 44, respectively, resulting in a conversion factor of 1.947 kg CO_2/kg EF biomass respired endogenously ($EF_{AerAutoOxi}$).

The oxygen consumed for growth is only the fraction of Vr_s (the substrate utilised for growth). The term r_s is based on BOD_5 rather than ultimate BOD (BODu). A typical value of the ratio of BOD_5/BOD_u (designated f) is 0.67 (Metcalf & Eddy, 2004). With appropriate unit conversions (for r_s and Y), the oxygen removal rate can be written as follows:

$$r_{O_2} = Vr_s\left(\frac{1}{f} - \left[f_{COD,VSS} \times Y\right]\right) \qquad \textit{Eq. 5-6}$$

Where

r_{O_2} = oxygen removal rate due to substrate oxidation [g of O_2 d^{-1}]

f = the ratio of BOD_5/BOD_u, for typical domestic wastewater, is **0.67** (Metcalf & Eddy, 2004)

$f_{COD,VSS}$ = conversion factor [g of COD per g of VSS] with a typical value of **1.42** (Henze et al., 2008)

A simple mass balance approach outlined in Monteith et al. (2005) and adopted by Sweetapple (2014) is used to enable calculation of CO_2 emissions from aerobic wastewater treatment based on the total theoretical mass of BOD converted into biomass.

$$V\frac{dX}{dt} = Q_{in}X_{in} - Q_{out}X_{out} + VYr_s - Vk_dX \qquad \textit{Eq. 5-7}$$

Where:

V = the volume of the section in the oxidation ditch [m^3]

dX/dt = the rate of change of biomass in the oxidation section [g VSS m^{-3} d^{-1}]

$Q_{in}X_{in}$ = biomass entering the oxidation ditch section [g VSS d^{-1}]

$Q_{out}X_{out}$ = biomass leaving the oxidation ditch section [g VSS d^{-1}]

Y = cell yield coefficient [g VSS/g BOD] has the value of Y_H for heterotrophic biomass and Y_A for autotrophic biomass similar to that of BSM2

r_s = aeration BOD removal rate [g BOD m^{-3} d^{-1}]

k_d = biomass endogenous decay coefficient (has the value of b_H for heterotrophic biomass and b_A for autotrophic biomass similar to that of BSM2)

Sweetapple (2014) uses the above equation to estimate the biomass formed in reactors from substrate utilisation (VYr_s) by calculating other parameters using ASM1 model outputs from BSM2. Eq. 5-7 can be rewritten as:

$$VYr_s = V\frac{dX}{dt} - Q_{in}X_{in} + Q_{out}X_{out} + Vk_dX \qquad \textit{Eq. 5-8}$$

The biomass simulated in ASM1 implemented in the BSM2 model considers only heterotrophic and autotrophic bacteria. Hence the total biomass can be estimated as the sum of heterotrophic bacteria concentration ($X_{B,H}$) and autotrophic bacteria ($X_{B,A}$). The rate of change of biomass in each reactor dX/dt can be estimated using a discrete time approach based on the current (t_j) and subsequent time steps (t_{j+1}).

$$\frac{dX}{dt} = \frac{\left(\frac{\left(X_{B,H} + X_{B,A}\right)_{j+1}}{f_{COD,VSS}} - \frac{\left(X_{B,H} + X_{B,A}\right)_j}{f_{COD,VSS}}\right)}{t_{j+1} - t_j} \qquad \textit{Eq. 5-9}$$

Biomass entering and leaving each reactor ($Q_{in}X_{in}$ and $Q_{out}X_{out}$) in Eq. 5-8 are estimated based on the concentration of heterotrophic and autotrophic bacteria in the section of the oxidation ditch.

$$biomass\ mass\ flow\ rate\ [g\ VSS/d] = Q\left(\frac{X_{B,H} + X_{B,A}}{f_{COD,VSS}}\right) \qquad \textit{Eq. 5-10}$$

The biomass decay rate (Vk_dX) in Eq. 5-8 is estimated using the biomass concentration from ASM1 in BSM2 model outputs and the reactor volume (Sweetapple, 2014).

$$rate\ of\ biomass\ decay\ [g\ VSS/d] = Vk_{d,T}\left(\frac{X_{B,H} + X_{B,A}}{f_{COD,VSS}}\right) \qquad \textit{Eq. 5-11}$$

$K_{d,T}$ is the endogenous decay coefficient at temperature T. Its temperature dependency is estimated similar to the decay coefficient (b_H) or (b_A) in BSM2 (Jeppsson et al., 2007). For b_H, based on the calibration value of **0.14** d^{-1} is used instead of 0.3 d^{-1}, a value used in Jeppsson et al. (2007) and Sweetapple (2014), see Chapter 6. The current activated sludge temperature (T_{as}) was taken from the BSM2 model output.

$$k_{d,T} = k_d exp\left(\left(\frac{ln\left(K_d/_{0.2}\right)}{5}\right)(T_{as} - 15)\right) \quad \textit{Eq. 5-12}$$

The rate of oxygen removal due to substrate oxidation can be estimated once the above parameters are calculated. Based on the oxygen removal rate from each section in the oxidation ditch, the CO_2 emission due to substrate oxidation ($CO_{2AS,BOD}$) (kg CO_2 d^{-1}) can be estimated (Sweetapple, 2014). A theoretical emission factor of 1.1 g of CO_2 per g of O_2 (EF_{AerOxi}) is adopted from Monteith et al. (2005).

$$CO_{2AS,BOD} = \sum_{i=1}^{12} EF_{AerOxi} \times r_{O2,i} \quad \textit{Eq. 5-13}$$

5.2.1.2. Direct GHG Emissions – Biomass Decay

The estimation of CO_2 emission from biomass decay was done by adopting the method outlined in Monteith et al. (2005). The theoretical conversion factor of 1.947 kg of CO_2 per kg of biomass respired endogenously ($EF_{AerAutoOxi}$) is used to calculate the rate of CO_2 production (kg CO_2 d^{-1}).

$$CO_{2AS,.VSS} = \sum_{i=1}^{12} EF_{AerAutoOxi} \times \left(Vk_{d,T}X\right)_i \quad \textit{Eq. 5-14}$$

5.2.1.3. Direct GHG Emissions – Denitrification

Denitrification process is one of the origins of N_2O production at WWTPs and at the same time CO_2 emissions due to nutrient removal in the anoxic zone. However, BSM2 uses a one step process to simulate the reduction of nitrate to nitrogen which makes it impossible to determine the intermediate product, N_2O. The four-step denitrification process detailed in Samie et al. (2011) adopted and modified by Sweetapple (2014) is used here. The single variable used in BSM2 for 'nitrate and nitrite nitrogen' (S_{NO}) is replaced with separate variables for nitrate (S_{NO3}), nitrite (S_{NO2}), nitric oxide (S_{NO}) and nitrous oxide nitrogen (S_{N2O}).

Denitrification is not the only source of N_2O. According to Foley et al. (2015), nitrification is also one of the processes that contribute to the production of N_2O in WWTPs. However, the production of N_2O from nitrification is not considered in this study. Modelling of nitrification stays similar to that of ASM1 (i.e. a single process without inhibition) instead of using two autotrophic processes (ammonia oxidation and nitrite oxidation) as in ASMN, and assimilative nitrite reduction to ammonia and biodegradation of specific organic components are not added (Sweetapple, 2014).

In addition to modelling N_2O production from the denitrification process, allowance is made for stripping of N_2O, which results in the emission of the gas to the atmosphere (Sweetapple, 2014). The rate of N_2O emissions [g N_2O m^{-3} d^{-1}] was estimated using temperature dependency of Henry's law constant in a similar manner as that of ASM1 methodology for stripping of CO_2. A base value of Henry's constant for N_2O $K_{H,N2O}$ in pure water was taken to be **0.0242** mol L^{-1} atm^{-1} in a temperature range of 20°C – 39°C with an uncertainty range of less than 10 % (Sander et al., 2006). The partial pressure of N_2O $(Pgas_{N2O})$ in atmospheric pressure is set to 3.2 10^{-7} atm (European Environmental Agency, 2011; Cole and Caraco, 2001). The N_2O gas transfer coefficient is set to 2 d^{-1} (Samie et al., 2011). Eq. 5-15 detailed the rate of N_2O emissions with conversion factors 3.14, 28, and 1000 g N to g N_2O [g N_2O per g N], g N mol^{-1} N_2O, and L m^{-3} respectively.

$$r_{N2Og} = 3.14 kLa_{N2O} \times max\left(0, \left(S_{N2Os} - 28 \times 1000 K_{H,N2O} Pgas_{N2O}\right)\right) \quad \textit{Eq. 5-15}$$

The total rate of N_2O emission from 12 sections of the oxidation ditch with volume V_i:

$$N2O_{AS,Deni} = \sum_{i=1}^{12} r_{N2Og,i} V_i \quad \textit{Eq. 5-16}$$

The CO_2 emissions associated with nutrient removal due to denitrification process are calculated using the stoichiometric relationship detailed in Shahabadi et al. (2010) quoted in Sweetapple (2014). Complete denitrification is assumed, and N_2 gas emission rate (r_{N2}) is used instead of nitrates. The yield factor of 2.83 g of CO_2 per g of N_2-N ($EF_{CO2Denit}$) was used considering that there is no additional carbon to the activated sludge process in this study.

$$r_{N_2} = \left(\frac{1 - Y_H \eta_Y}{0.571 Y_H \eta_Y}\right) procD \qquad \textit{Eq. 5-17}$$

Where Y_H = heterotrophic biomass yield adopted from calibrated BSM2 model [g COD/g COD]

η_Y = anoxic yield factor of heterotrophs, the value taken from calibrated BSM2 model

Hence, the CO_2 emission due to nutrient assimilation in the denitrification process is given in Eq. 5-18:

$$CO2_{AS,Deni} = \sum_{i=1}^{12} EF_{CO2Denit} \times r_{N2_i} \times V_i \qquad \textit{Eq. 5-18}$$

Where, $EF_{CO2Denit}$, 2.81 g of CO_2 per g of VSS, is emission factor for CO_2 emission from denitrification without external source addition (Shahabadi et al., 2010).

The total rate of direct GHG emissions from the activated sludge process in the oxidation ditch at each time step ($CO_{2AS,\ total}$) is given in Eq. 5-19:

$$CO2_{AS,total} = CO2_{AS,VSS} + CO2_{AS,BOD} + CO2_{AS,Deni} + 298 \times N2O_{AS,Deni} \qquad \textit{Eq. 5-19}$$

Where, Nitrous oxide N_2O is a very potent GHG with a 100-year global-warming potential (GWP) 298 times greater than that of CO_2 (IPCC, 2013).

5.2.1.4. Indirect GHG Emissions – Imported Energy

The indirect CO_2 emissions from a WWTP includes the use of imported energy such as electricity, use of chemicals, offsite degradation of effluent, and transport energy of sludge and its offsite degradation (Chai et al., 2015).

The rate of indirect emissions at each time step due to energy import is modelled using an emission factor ($EF_{electricity}$) of 0.4622 kg CO_2 kWh^{-1} as of 2015 suggested by (DEFRA, 2015).

$$CO2_{energy} = EF_{electricity} \times \left(E_{electricity}\right) \qquad \textit{Eq. 5-20}$$

Where $E_{electricity}$ is the total imported energy to the WWTP and $CO2_{energy}$ is the indirect GHG emissions due to the total imported energy. The above equation holds true only when there is no energy generation at the site. In situations where there are energy generation the net imported energy should be used hear, instead of the total.

The imported energy at a WWTP can be classified as net import energy for heating and electricity for pumping, mixing, aeration and other processes units. The earlier is not considered in this study since the need for heat due to digesters is not relevant since the case study do not have digesters.

$$E_{eletricity} = E_{pumping} + E_{aeration} + E_{mixing,AS} + E_{sludge,drier} \qquad \textit{Eq. 5-21}$$

Pumping Energy

The electricity energy required for pumping at WWTP can be calculated based on the BSM2 model outputs either as a function of flowrate or depth of wastewater in wet wells at the current time. The relationship is kept simple due to uncertainties involving pump capacity, efficiency, and operating conditions. This approach can be applied to different pumps operating at different conditions with different capacity. The energy consumption for each pump is estimated individually. Sweetapple (2014) assumes that pump efficiency is assumed to stay constant regardless of the operating condition. In this study, the variation of pump efficiency is put under consideration based on operational conditions and flow rate.

A generalised approach that can be applied to any pump in a WWTP is used. The parameters needed for each pump is shown in Table 5-7. The following paragraphs deal with the derivation of equations for each pump power requirement in kW and pump energy use in kWh d^{-1}. If it is a wet-well pump, the variation in wastewater level upstream of the pump is significant, and the upstream water height is considered. However, if it is not a wet well pump and the variation in upstream wastewater level (h_{ww}) is insignificant, (for example RAS/SAS pumps) the power is entirely dependent on discharge, and the upstream wastewater level assumed to be constant, see Table 5-7. The pump is assumed to be located at the bottom of the wet-well or tank upstream of the pump, i.e. h_{pump} is assumed to be zero. The power required to pump wastewater is calculated by using a simple conservation of energy approach, see Figure 5-18 and Eq. 5-22.

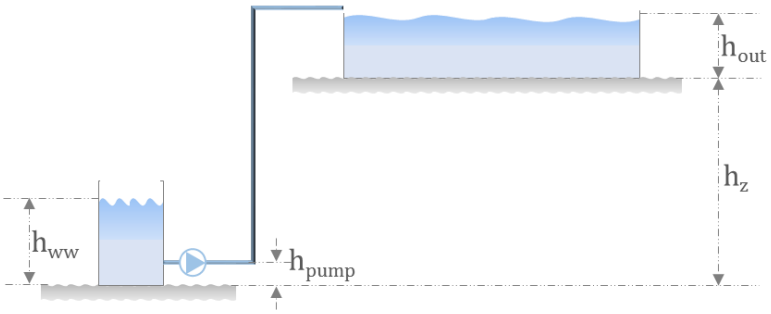

Figure 5-19 Typical pump layout showing the necessary heights

$$P_{PE_{abs}} = \frac{Q \times \rho \times g \times \left(h_z + h_{out} - h_{ww} + h_f + \frac{v^2}{2g}\right)}{1000} \qquad \textit{Eq. 5-22}$$

$$P_{PE} = \frac{P_{PE_{abs}}}{Eff_{.}} \qquad \textit{Eq. 5-23}$$

Where:

h_{out}	=	wastewater level in the receiving tank outlet point above the ground [m]
h_z	=	Static head or ground elevation difference between the bottom of wet-well and the bottom of receiving tank (outlet point) [m]
h_{ww}	=	wastewater level in the wet well or tank upstream of pump [m]
h_f	=	the frictional loss in pipes [m]
$P_{PE_{abs}}$	=	theoretical pump power required in KW
P_{PE}	=	actual pump power required in KW
$Eff_{.}$	=	the efficiency of the pump
$\frac{v^2}{2g}$	=	dynamic head where *v* is the velocity of flow in pipe and *g* is gravitational acceleration (9.81 $m^2\ s^{-1}$)
ρ	=	Density of wastewater; since difference between the density of wastewater and water is small (Henze et al., 2008), a constant density of 1000 kg m^{-3} is used for all types of wastewater
Q	=	Discharge at the outlet [$m^3\ s^{-1}$]

When the pump state (ON/OFF) is controlled based on the wet-well level, it is not straight forward to create a direct relationship between the discharge and the wet-well level. BSM2 model output for pump states, flow rate and wet-well level, can be used to calculate the power required at each time step. Whenever two or more pumps are operating together, pump's states are required to distinguish if pumps are running in parallel or if only a single pump is operating at a time. The energy consumed by the pumps is calculated as a time derivative of the power required

at each time step. Modelling and determining of pump states is detailed in Chapter 3.

$$E_{pump,i} = \int_{t_{start}}^{t_{end}} P_{PE,i}\, dt \qquad \textit{Eq. 5-24}$$

Where $E_{pump,i}$ is energy consumption by a pump that operates at a power of $P_{PE,i}$.

$$E_{pump} = \sum_{i}^{n} E_{pump,i} \qquad \textit{Eq. 5-25}$$

Where n is the total number of pumps under consideration.

The frictional loss in the pipes in the inlet wet well pumping system is calculated by using Reynold's number and relative roughness of the pipe. Moody's curve was used to estimate roughness coefficient (ε). It is assumed that the frictional loss is constant regardless of the variation in flow rate which helps to simplify the problem. The maximum flow rate from the wet well pumping station that was recorded on site is used for the calculation of Darcy–Weisbach's friction factor λ.

$$Re = \frac{V_{max} \times D}{v} \qquad \textit{Eq. 5-26}$$

Where: V_{max} is the expected or recorded maximum velocity

$$h_f = \frac{V^2}{2g} \times \frac{f}{D} \times L \qquad \textit{Eq. 5-27}$$

Where L is the pipe length, and V is the velocity of wastewater within the pipe. The velocity will be variable based on discharge which, in turn, is dependent on the operational head of the system.

$$h_f = \frac{\left(Q/_A\right)^2}{2g} \times \frac{f}{D} \times L \qquad \textit{Eq. 5-28}$$

Where A is a cross-sectional area of a pipe or channel

$$h_f = C_f \times Q^2 \qquad \textit{Eq. 5-29}$$

Where; C_f (s^2/m^7) is a coefficient introduced to estimate h_f as a function of discharge Q ($m^3\ s^{-1}$) once the Darcy-frictional factor f is calculated using the Haaland-equation described below.

Hence;

$$C_f = \frac{1}{2g} \times \frac{f}{D} \times L \times \frac{1}{A^2} \qquad \textit{Eq. 5-30}$$

For circular pipes, the above equation can be re-written as;

$$C_f = \frac{8}{g} \times \frac{f}{D^5 \pi^2} \times L \qquad \textit{Eq. 5-31}$$

Darcy-Weisbach friction factor, f, depends on the Reynolds number R_e, as defined in Eq. 5-26 and the relative wall roughness r = ε ÷ D. ε denotes wall roughness height, for old cast iron pipe a value of **3** mm is suggested by Hager (2010).

The value of f for turbulent flow, Reynolds number greater than 4000, can be estimated using the Colebrook-White equation. However, the Colebrook-White equation is not linear, and due to its implicit nature, it requires an iteration to solve for f. There are several suggested approximations of the Colebrook-White equations to reduce computational time with the required precision. The Haaland equation (Haaland, 1983) is one of the simplified version of White-Colebrook equation that solves f for a full-flowing circular pipe within an acceptable accuracy without iteration. To maximise computational speed, in this study, the Haaland equation is used to estimate f.

$$\frac{1}{\sqrt{f}} = -2log\left(\frac{\varepsilon}{3.7 \times D} + \frac{2.51}{Re\sqrt{f}}\right) \qquad \textit{Eq. 5-32}$$

Colebrook-White equation (Colebrook and White, 1937)

$$\frac{1}{\sqrt{f}} = -1.8log\left[\left(\frac{\varepsilon/D}{3.7}\right)^{1.11} + \frac{6.9}{Re}\right] \qquad \textit{Eq. 5-33}$$

Haaland equation (Haaland, 1983)

Table 5-7 Input parameters for calculation of pump energy use

Pump location	Inlet wet-well	RAS/SAS	Supernatant wet-well	Spray bar pump
Maximum discharge ($m^3 s^{-1}$)	0.12	0.035	0.03	0.03
Pipe diameter (m)	0.3	0.25	0.15	0.2
Depth (m)	-	-	-	-
Width (m)	-	-	-	-
Hydraulic radius (m)	-	-	-	-
Pipe length (m)	108	51	19	65
roughness coefficient	0.003	0.003	0.003	0.003
relative roughness (m)	0.01	0.012	0.02	0.015
Kinematic viscosity at 18°c (kg/m s^{-1})	0.00000115	0.00000115	0.00000115	0.00000115
Maximum velocity (m s^{-1})	1.7	0.71	1.7	0.95
Reynolds number (Re)	443478	154348	221739	165217
Friction factor using Haaland equation	0.038	0.041	0.049	0.044
C_f (s^2/m^7)	139.69	177.1	1014.05	739.23
h_f	$C_{f,ww} \times (Q)^2$	$C_{f,RAS} \times (Q)^2$	$C_{f,SRL} \times (Q)^2$	$C_{f,SB} \times (Q)^2$
h_z	5.6	6.8	3	5.6
h_{out}	4	4	6	4
h_{ww}	one pump operating *(Q-0.024)/0.018* two pumps operating in parallel *(Q-0.0488)/0.0145*	4.8	*(Q-0.00108)/0.0203*	2
Pump efficiency (Eff.)	*(84350Q^3 – 26277Q^2 + 2384.4Q)/100*	$(406501Q^3 - 78693Q^2 + 4022Q)/100$	$(406501Q^3 - 78693Q^2 + 4022Q)/100$	$(406501Q^3 - 78693Q^2 + 4022Q)/100$

Pump efficiencies for pumps at Cupar WWTP

Inlet wet-well pumps:

A polynomial correlation is derived from the pump manufacturer's data sheet, Figure 5-20.

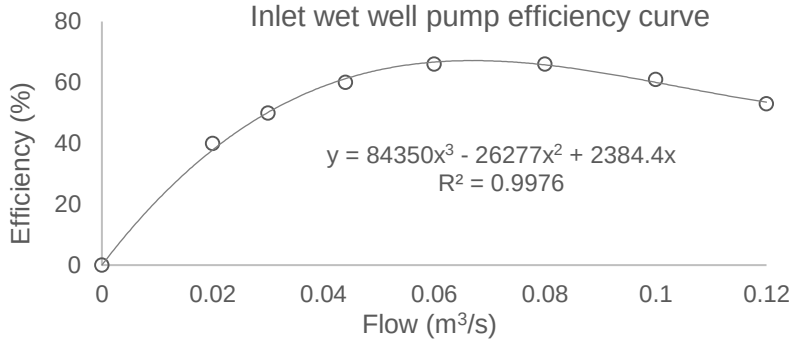

Figure 5-20 Inlet wet-well pumps' efficiency curve at different operational flow rates

$$Eff_{ww}\ (\%) = 84350Q^3 - 26277Q^2 + 2384.4Q \qquad \textit{Eq. 5-34}$$

Where Q is the wasteater flow rate in $m^3 s^{-1}$

RAS/SAS pumps, Supernatant return pump, Oxidation ditch spray pump:

There are two RAS/SAS pumps operating in parallel with an average flow rate of 35 L s^{-1} during returning and 30 L s^{-1} during removing sludge. The energy consumption of these pumps is estimated similarly to that of the rest of the inlet wet well pumps. Since the variation in final settlement tanks wastewater depths is insignificant, the upstream wastewater level (h_{ww}) is assumed to be constant, see Table 5-7. The detail of the pumps on site is not known, and a typical Flygt NP 3127 MT that is widely used in the sewer network is assumed to be similar to that of this pump. There is only one pump operates at a time for supernatant return pump and the oxidation ditch spray pump. Due to the lack of detail of these pumps, they are assumed to have the same pump efficiency curve like that of a Flygt NP 3127 MT pump. Pump efficiency curve from these pumps' datasheet using a polynomial interpolation is shown in Figure 5-21.

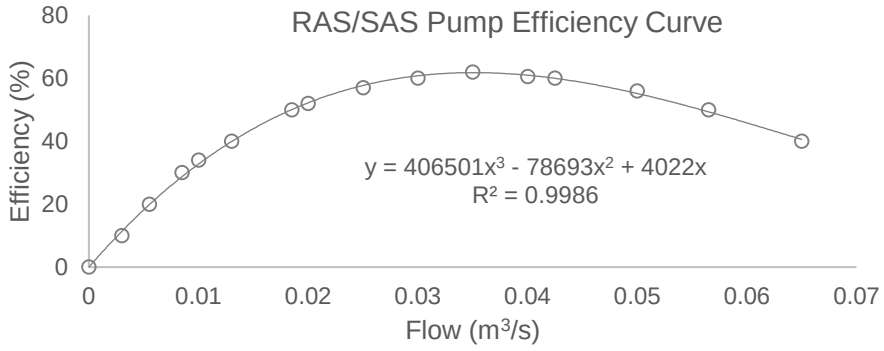

Figure 5-21 RAS and SAS pumps' efficiency curve at different operational flow rates

$$Eff_{otherpumps}\,(\%) = 406501Q^3 - 78693Q^2 + 4022Q \qquad \textit{Eq. 5-35}$$

Mixing Energy

A mixer with a rotating impeller is an open flow turbomachine that changes the stagnation enthalpy of the fluid moving through it. The enthalpy change is intimately linked to the pressure change in the fluid, wastewater (Khan, 2015). Euler's turbine equation attempts to connect the specific work, the geometry, and velocity of impellers. Using such equations require detailed information on the impellers geometry and other specifications. Due to the lack of this detailed information, in this study, a flow number and power number approach described in Alleyne et al. (2014). This approach uses a flow number, $N_{q,imp,}$ that measures the pumping capacity of impellers. This number is used to estimate the unknown

variable, the rotational speed of the impeller based on the total internal circulation (Q_{intr}), see Eq. 5-36 and Eq. 5-38.

$$N_{q,imp} = \frac{Q_{imp}}{N_{imp} \times (D_{imp})^3} \qquad \textit{Eq. 5-36}$$

Where Q_{imp} is flow rate produced by the impeller ($m^3\ s^{-1}$)

N_{imp} = impellers rotational speed [s^{-1}]

D_{imp} = impellers diameter [m]

An impeller power number $N_{P,imp}$ is a commonly used approach to characterise the performance of mixers (Skočilas et al., 2013; Deglon and Meyer, 2006) cited in (Alleyne et al., 2014), see Eq. 5-37.

$$N_{P,imp} = \frac{P_{mixer,abs}}{\rho_{liquor} \times \left(N_{imp}\right)^3 \times \left(D_{imp}\right)^6} \qquad \textit{Eq. 5-37}$$

Where $P_{mixer,abs}$ is the absolute power consumption [W]

$\rho_{liquor}$is the density of mixed liquor in the oxidation ditch ($kg\ m^{-3}$)

The value of N_P and N_q are estimated by several studies for different size of tanks and impeller diameter through computational fluid dynamics (CFD). For example, Alleyne et al. (2014) found that for a large-size tank the flow number, $N_{q,imp}$, is **0.76** and the power number, $N_{P,imp}$, is **1.21**. These values are adopted here to estimate the rotational speed of impellers based on flow rates and to estimate the power consumption by each mixer, see Eq. 5-38 and Eq. 5-37.

$$Q_{intr} = Q_{imp} \times n_{mixer} \qquad \textit{Eq. 5-38}$$

Where Q_{intr} is the total internal circulation flow rate ($m^3\ s^{-1}$) and n_{mixer} is the number of mixers in the oxidation ditch.

The theoretical power required by each impeller can be estimated by combining Eq. 5-35 and Eq. 5-36, and the actual power needed by each mixer is estimated using Eq. 5-40; where Eff_{mixer} is the efficiency of mixers, taken to be **0.6** in this instance.

$$P_{mixer,abs} = N_{P,imp} \times \rho \times \left(\frac{Q_{imp}}{N_{q,imp}}\right)^3 \quad \textit{Eq. 5-39}$$

$$P_{mixer} = \frac{P_{mixer,abs}}{Eff_{mixer}} \quad \textit{Eq. 5-40}$$

Energy use by sludge centrifuge

At Cupar WWTP, Hiller Decapress DP37E-422 centrifuge sludge thickener is used for dewatering the sludge and gives sludge with 18 – 20 % dry solid. Whenever the sludge centrifuge is operating, it works at a flow rate of, $Q_{actual,drier}$, 20 $m^3\ hr^{-1}$ (5.6 $L\ s^{-1}$) and a use of polymer solution at a flow rate of 0.28 $L\ s^{-1}$. According to the manufacturer's datasheet accessed from ESI-ENVIROPRO (2016), the energy-use by the centrifuge is estimated based on its output power rating, $P_{out,max,drier}$, 37.5KW with a maximum flowrate capacity, $Q_{max,drier}$, of 29 $m^3\ hr^{-1}$ (8 $L\ s^{-1}$). If a linear relationship is assumed for the actual output power and flowrate, the sludge centrifuge is working at its 69 %, $f_{acual/max}$, of its maximum capacity. Since the specific efficiency information couldn't not be found in the datasheet and other sources, a constant efficiency of, eff_{drier}, 75 % is assumed, based on a typical motor efficiency curve from IEC (2009). The actual input power required, $P_{input,actual,drier}$, can be estimated using Eq. 5-41 and Eq. 5-42.

$$f_{acual/max} = \frac{Q_{actual,drier}}{Q_{max,drier}} \quad \textit{Eq. 5-41}$$

$$P_{input,actual,drier} = \frac{f_{acual/max} \times P_{out,max,drier}}{eff_{drier}} \quad \textit{Eq. 5-42}$$

Aeration Energy

The energy required for aeration of the activated sludge reactors is calculated using a similar approach used in the BSM2, which is valid for Degremont DP230 porous disks at an immersion depth of 4 m (Alex et al., 2008). The diffusers in Cupar WWTP are fine-pore diffusers that might have a better performance than porous disks (Henze et al., 2008). However, due to the aging of the system, it is believed that the relation suggested by Alex et al. (2008) can represent the

energy use for aeration at Cupar WWTP. The approach estimates energy consumption at each time step based on the corresponding oxygen transfer coefficients, which can be altered throughout the simulation duration to control the aeration intensity in each tank. The total rate of energy consumption for aeration at each time step ($E_{aeration}$) is calculated using the equation below (Alex et al., 2008):

$$E_{aeration} = \sum_{i=1}^{12} \frac{S_o^{sat}}{1.8 \times 1000} V_i (KLa)_i \qquad \textit{Eq. 5-43}$$

Where:

S_o^{sat} = oxygen saturation concentration = 8 mg O_2 L^{-1}

1.8 = aeration oxygen transfer efficiency [kg O_2 kWh^{-1}]

1000 = unit conversion factor [(m^3 L^{-1}) × (mg kg^{-1})]

V = tank volume [m^3]

KLa = oxygen transfer coefficient [d^{-1}]

5.2.1.5. Indirect GHG Emissions – Offsite Degradation of Effluent

Although the water companies in the UK are not accounting degradation of effluent in their carbon foot print accounting, this study includes this source since it is the emission coming out from the WWTP regardless of where it is degraded. Sweetapple (2014) modelled offsite degradation of effluent using aerobic degradation stoichiometric equation given by Shahabadi et al. (2010), which is adopted in this study, see Eq. 5-44 and Eq. 5-45. Since BOD5 is not one of the state variables in BSM2, the final effluent BOD (BOD5,eff) is calculated based on the equation suggested by Gernaey et al. (2014), see Eq. 5-48.

$$CO2_{eff} = BOD_{5,eff} \times Q_{eff} \times EF_{AerBODreml} \qquad \textit{Eq. 5-44}$$

$$CO2_{ST,spill} = BOD_{5,ST} \times Q_{ST,spill} \times EF_{AerBODreml} \qquad \textit{Eq. 5-45}$$

$$BOD_{5,eff} = 0.25 \times \left(S_{s,eff} + X_{s,eff} + \left(1 - f_p'\right) \times \left(X_{B,H,eff} + X_{B,A,eff}\right)\right) \qquad \textit{Eq. 5-46}$$

The overflow from the storm tanks has a similar characteristic as the influent wastewater. Hence, the influent wastewater characterisation section is adopted here, and the BOD_5 calculation was done using a factor of $\frac{1}{1.75}$ (Metcalf & Eddy, 2004).

$$BOD_{5,ST} = \left(S_{s,ST} + X_{s,ST} + (1 - f_p') \times (X_{B,H,ST} + X_{B,A,ST})\right) / 1.75 \qquad \textit{Eq. 5-47}$$

Where:

$CO2_{eff}$	=	CO_2 emissions from final effluent from final settlement tanks [g CO_2 d^{-1}]
$BOD_{5,eff}$	=	Final effluent BOD_5 [g O_2 m^{-3}]
$EF_{AerBODreml}$	=	an emission factor of **0.33** adopted from Shahabadi et al. (2010) [g CO_2/g BOD]
$S_{s,eff}$ and $S_{s,ST}$	=	the readily biodegradable substrate in final effluent and storm tank overflow respectively [g m^{-3}]
$X_{s,eff}$ and $X_{s,ST}$	=	the slowly biodegradable substrate in final effluent and storm tank overflow respectively [g m^{-3}]
$X_{B,H,eff}$ and $X_{B,H,ST}$	=	active heterotrophic biomass in final effluent and storm tank overflow respectively [g m^{-3}]
$X_{B,A,eff}$ and $X_{B,A,ST}$	=	active autotrophic biomass in final effluent and storm tank overflow respectively [g m^{-3}]
$BOD_{5,ST}$	=	Storm tank overflow BOD_5 [g O_2 m^{-3}]
f_p'	=	a constant with a value of 0.2 (Gernaey et al., 2014), and should not be confused with the constant f_p in the ASM2 model
Q_{eff} and $Q_{ST.spill}$	=	Discharge final effluent and storm tank overflow respectively [m^3 d^{-1}]

Indirect N_2O emissions from WWTP effluent is calculated using the total nitrogen concentration (N_{eff} [g m^{-3}]) from the combined final effluent and storm tank overflow discharges and using an emission factor of **0.005** kg N_2O-N/kg N ($EF_{effluentN2O}$) (Eggleston et al., 2006).

$$N2O_{eff} = EF_{effluentN2O} \times {}^{44}/_{28} \times N_{eff} \times (Q_{eff} + Q_{ST.spill}) \qquad \textit{Eq. 5-48}$$

Where:

${}^{44}/_{28}$ = conversion factor [g N_2O/g N_2O-N]

5.2.1.6. Indirect GHG Emissions – Transport and Offsite Degradation of Sludge

Emissions resulting from the transport of sludge ($CO2_{sludge,trans}$) is estimated using Eq. 5-49, and Eq. 5-50. The emission factor ($EF_{sludge,trans}$) is estimated

using information on average distance travel, average sludge weight per trip, fuel economy of truck, energy generation rate for a diesel engine, and percentage solids of sludge.

$$EF_{sludge,trans} = \frac{EF_{diesel} \times d_{sludge} \times C_w}{FE_{truck} \times M_{sludge}} \quad \textit{Eq. 5-49}$$

Where:

$EF_{sludge,trans}$	=	Sludge emission factor [kg CO_{2e} per tonnes of TSS]
d_{sludge}	=	average distance to landfill [Km] (145Km in this instance)
C_w	=	sludge fraction of solids by weight [0.2]
FE_{truck}	=	fuel economy of the truck, for a typical medium to heavy duty truck [2.5 Km L^{-1}] (Nylund and Erkkilä, 2005)
M_{sludge}	=	total sludge mass per trip, based on the commonly used trucks capacity to transport sludge from Cupar WWTP [20,000 kg]
EF_{diesel}	=	Emission factor for diesel fuel [2.6 kg of CO_2 L^{-1} of diesel (average biofuel blend] (DEFRA, 2015)

This calculation for the case of Cupar results in sludge emission factor of 1.55 kg of CO_2 per tonnes of TSS. This value is small compare to the one given by Shahabadi et al. (2010) for long distance trips of Canadian sources, 24 kg of CO_2 per tonnes of TSS.

$$CO2_{sludge,trans} = EF_{sludge,trans} \times TSS_{sludge} \times Q_{sludge} \quad \textit{Eq. 5-50}$$

Indirect emissions resulting from the degradation of biosolids remaining in the sludge are modelled using the method presented in Sweetapple (2014).

$$CO2_{sludge} = EF_{AnaerVSSdecCO2} \times \frac{S_{s,sludge}}{1.42} \times Q_{sludge} \quad \textit{Eq. 5-51}$$

$$CH4_{sludge} = EF_{AnaerVSSdecCH4} \times \frac{S_{s,sludge}}{1.42} \times Q_{sludge} \quad \textit{Eq. 5-52}$$

$$N2O_{sludge} = EF_{sludge,N2O} \times \frac{44}{28} \times N_{sludge} \times Q_{sludge} \quad \textit{Eq. 5-53}$$

Where:

$EF_{AnaerVSSdecCO2}$	=	the theoretical CO_2 emission factor, set to 0.58 g CO_2 per g VSS (Shahabadi et al., 2010)
$EF_{AnaerVSSdecCH4}$	=	the theoretical CO_2 emission factor, set to 0.35 g CH_4 per g VSS (Shahabadi et al., 2010)

$EF_{sludge,N2O}$	=	N_2O emission factor of 0.01 kg of N_2O per kg of N suggested by Eggleston et al. (2006)
$S_{s,sludge}$	=	the readily biodegradable substrate in sludge [g m^{-3}]
N_{sludge}	=	total nitrogen concentration in sludge [g m^{-3}]
TSS_{sludge}	=	Total suspended solids in sludge to landfill [g m^{-3}]

The overall rate of emissions resulting from the disposal of sludge at each time step is therefore calculated using the equation below. Where, methane is a very potent GHG with a 100-year global-warming potential (GWP) 34 times greater than that of CO_2 with the inclusion of climate-carbon feedback (IPCC, 2013).

$$CO2_{sludge,total} = CO2_{sludge,trans} + CO2_{sludge} + 34(CH4_{sludge}) + 298\,(N2O_{sludge}) \quad \textit{Eq. 5-54}$$

5.2.2. Effluent Quality and Legislative Compliance

For analysis and selection of appropriate interventions and control strategies, it is crucial to consider the final effluent quality. The effluent quality can be assessed for each quality indicators such as TSS, COD, ammonia, nitrates and so on. However, having so many objectives (quality indicators) can be a challenge and time-consuming during designing or selection of control strategies through multi-objective optimisation. As a solution, An Effluent Quality Index (EQI) was first suggested by Jeppsson et al. (2007) and later modified by Nopens et al. (2010) to reflect the ecological impact of pollutants from the final effluent. The latter is successfully adopted by Sweetapple (2014) and also used in this study. The EQI is calculated by aggregating the commonly used quality indicators; TSS, COD, BOD, TKN, and NO_x, Eq. 5-55.

$$EQI = \frac{1}{1000.\,t_{obs}} \int_{t_{start}}^{t_{end}} \big[2 \times TSS_{eff} + COD_{eff} + 2 \times BOD_{eff} + 30 \times S_{TKN,eff} + 10 \times (S_{NO2} + S_{NO3} + S_{NO} + S_{N2O})\big] \quad \textit{Eq. 5-55}$$

$$S_{TKN,eff} = S_{NH,eff} + S_{ND,eff} + X_{ND,eff} + i_{XB}\big(X_{BH,eff} + X_{BA,eff}\big) + i_{XP}\big(X_{P,eff} + X_{I,eff}\big) \quad \textit{Eq. 5-56}$$

Where:

EQI	=	Effluent Quality Index [kg m^{-3}]
TSS_{eff}	=	total suspended solids in final effluent [g/ m^3]
COD_{eff}	=	Chemical Oxygen Demand in final effluent [g of O_2 m^{-3}]

BOD_{eff} = Biochemical Oxygen Demand in final effluent [g of O_2 m^{-3}]

$S_{TKN,eff}$ = Total Kjeldahl Nitrogen in final effluent equated using Eq. 5-56 [g of N m^{-3}]

S_{NO2} = nitrite ion in final effluent [g of N m^{-3}]

S_{NO3} = nitrate ion in final effluent [g of N m^{-3}]

S_{NO} = nitric oxide anion in final effluent [g of N m^{-3}]

S_{N2O} = nitrous oxide in final concentration [g of N m^{-3}]

$S_{NH,eff}$ = Ammoniacal nitrogen (NH_3 and NH_4) in the final effluent [g of N m^{-3}]

$S_{ND,eff}$ = soluble biodegradable organic nitrogen [g of N m^{-3}]

$X_{ND,eff}$ = particulate biodegradable organic nitrogen [g of N m^{-3}]

$X_{BA,eff}$ = active autotrophic biomass [g m^{-3}]

$X_{P,eff}$ = particulate products arising from biomass decay [g m^{-3}]

$X_{I,eff}$ = particulate inert organic matter [g m^{-3}]

i_{XP} = fraction nitrogen in particulate products [g N (g COD)$^{-1}$] a value of 0.06 adopted from Copp (2002)

t_{end} = time of in simulation that assessment finishes in days [d]

t_{start} = time in a simulation that assessment starts in days [d]

t_{obs} = total time of assessment in days [d]

In addition to EQI, during interventions and control strategies assessment, quality indicators that are used for compliance are included. Water environment and water services (Scotland) Act, 2003 issues the Controlled Activities Regulations (CAR) licenses for all WWTPs in Scotland. According to this regulation, final effluent BOD, ammoniacal nitrogen and total suspended solids in the final effluent at instantaneous sample should not exceed:

- BOD – 20 mg L^{-1}
- Ammoniacal nitrogen (expressed as N) – 10 mg L^{-1}
- Suspended solids – 30 mg L^{-1}

The limit of BOD and ammoniacal nitrogen may be exceeded 5 % of the time, but the TSS concentration limit should not be exceeded at any time.

5.2.3. Operational Cost

Operational costs are assessed using an operational cost index (OCI), as defined in BSM2 (Nopens et al., 2010), which provides a measure of the average energy demand for aeration, pumping, mixing, onsite sludge centrifuge and sludge production for disposal.

$$OCI = AE + PPE + 3 \cdot SP + ME + SC \qquad \textit{Eq. 5-57}$$

Where:

AE = aeration energy

PPE = pumping energy

SP = dried sludge production for disposal

ME = mixing energy

SC = sludge centrifuge energy demand

OCI has been used widely, but it doesn't reflect the variation of energy tariffs throughout the day (lower tariffs during off-peak hours), the week (lower tariffs over the weekend), and the year (such as lower tariffs on holidays). Using OCI only as a performance indicator may not show the benefit of optimising operations at WWTPs to maximise the benefit of lower tariffs. For example, in the UK, energy Demand Side Management (DSM) is the modification of consumers demand of energy through either financial incentivise or behavioural change through education (Chiu et al., 2013).

One of the financial incentives is the use of differential tariffs, such as the Economy 10 and Economy 7 electricity plan implemented in England and Wales or 'White meters' in Scotland, dynamic pricing schemes that have variable pricing rate per kWh of energy used during times of the day/week or year based on demand (Torriti et al., 2010). Such schemes are set out to balance electricity production and demand by setting the price per unit of energy variable throughout the day. For example, the most commonly used on in England, Economy 7, tariff provides a cheaper seven-hour night time pricing rate, varying between 20 % to 50 % depending on location and supplier, compared to that of the day-time rate.

There are other differential tariffs for business such as Economy 10 tariffs, Evening and Weekend tariffs, Evening Weekend and Night tariffs, or Seasonal time of day (SToD) tariffs. These differential tariff systems can be complex, for example, SToD can have up to 56 rates across the night, day, peak and other periods each measured separately by seasons usually suitable for Industrial and commercial consumer with extreme peaks and troughs. Similarly, variable evenings, weekends, and nights tariffs are mostly adopted by small and medium size enterprise (SME) and Industrial and Commercial professionals that use their energy during the evening and weekend. Due to the 24/7 use of electricity by the wastewater sector any of the above traffic can save energy cost at a various degree. For this study, the Evening, Weekend, and Night tariff are adopted, and the pricing rate is assumed to be 50 % cheaper during the night, 30 % cheaper during the evening and weekends. Since the tariff time is variable based on supplier and location, a commonly used time based on Economy 7 is adopted

here, i.e. the night time refers to 12:30am to 7:30am, and evenings refers to 8:00pm to 12:30am.

A new coefficient, Modified Operational Cost Index (MOCI), is introduced here to reflect the cost of operations based on variable tariffs.

$$MOCI = OCI \times f_{MOCI} \qquad \textit{Eq. 5-58}$$

Where;

$MOCI$	=	Modified Operational Cost Index [ ]
OCI	=	Operational Cost Index (Nopens et al., 2010)
f_{MOCI}	=	Factor based on DSM tariffs [ ]
	=	0.5; during night hours (00:30 −07:30)
	=	0.7; during evening hours (20:00 −24:00 and 00:00 −00:30)
	=	0.7; during weekend days (07:30 −20:00)
	=	1; during week-days day-time hours (07:30 −20:00)

6. Model Calibration and Validation

ASM-family models are popular and capable of representing most of the processes in activated sludge systems (Marquot et al., 2006), and they have been used at WWTP scale for various reasons such as assessing design scenarios (Devesa et al., 2009) or the impact of control strategies on the dynamic process (Foscoliano et al., 2016). In this instance, BSM2-e is selected to assess WWTP performances in response to different control strategies or operational changes based on different regulatory approach.

Although ASM-family models can represent most of the process in WWTPs, they inhibit uncertainty from several sources (Abusam et al., 2003; Sin et al., 2008; Vanrolleghem et al., 2005):

i. Uncertainty from model structure and underlying equations: although ASM-family models are mechanistic (process-based), these models are the simplification of the real world, and they have their own degree of accuracy in representing the actual processes (Hulsbeek et al., 2002; Sin et al., 2009)
ii. The non-linear relationship between model parameters and model output creating a high uncertain space, model parameter uncertainty.
iii. Uncertainty in measured data, which can be model input and output for model calibration purposes
iv. Uncertainty due to many model parameters (over-parameterisation) and dependency among parameters

It is challenging, costly, and time consuming to assess all these uncertainties. Determining ASM-family model parameters can be costly (Melcer, 2003; Abusam et al., 2001; Fronteau et al., 1997; Petersen, 2000). Hence, it is important to be selective and give emphasis on the most influential source of uncertainties and give a careful consideration to minimise error and uncertainty at every calibration step (Mannina et al., 2011; Sweetapple et al., 2013; Benedetti et al., 2008). In this instance, the uncertainty from measured parameters is reduced through a careful design and implementation of data monitoring campaign, see Chapter 4. Similarly, uncertainty around measured model outputs, for calibration purpose, such as TSS and NO_3 in the final effluent is reduced through a careful data

campaign implementation. However, model parameters that were not directly measured are further assessed and used in the calibration process.

There are several model calibration guidelines suggested in the past by Hulsbeek et al. (2002); Melcer (2003); Vanrolleghem et al. (2003), Langergraber et al. (2004), and Mannina et al. (2011). All of these guidelines emphasise on the need for sensitivity analysis to identify most influential parameters on model outputs. Mannina et al. (2011) and Vanrolleghem et al. (2003) emphasised on the benefit of sensitivity analysis in minimising efforts during model calibration and optimise calibration procedures (Liwarska-Bizukojc et al., 2011).

The general calibration procedure used in this study is shown in Figure 6-1. The methodology consists of three phases: the use of existing data set to set-up the model using existing data, and design and implementation of data monitoring campaign to collect more data. Phases two and three are an iterative process. Once model inputs and influent wastewater are characterised using the campaign data, phase two is repeated, i.e. sensitivity and model calibration. Initially, the second phase uses manual calibration of the WWTP hydraulics, which involves in changing values of uncertain parameters based on modeler experience in the feasible parameter space. The second phase later uses one of the simplest and most common one-at-a-time (OAT) approach to assess the effect of the change in the input to the model outputs or auto-calibration objectives. Initially, the model calibration using existing data runs for the period 28/10/2012 – 11/07/2013, the first 100 days for model warming up and the rest 156 days for model accuracy assessment. Upon identification of a further need for data, design and collection of campaign data, the second iteration on model calibration is done using campaign data for the period 20/03/2016 – 10/04/2016. A warming up period of 100 days with a non-dynamic dataset (average of the campaign data) helps models to achieve pseudo steady state and allow controllers to adapt. The model run with a dynamic dataset for three days then for 15 days. The last 15 days of simulation were used for sensitivity analysis and model calibration. The details in the sensitivity analysis and model calibration (phase two of Figure 6-1) using exciting data is not presented in detail here due to the similarity in the procedure. However, results are presented alongside the result of the model calibration using campaign data.

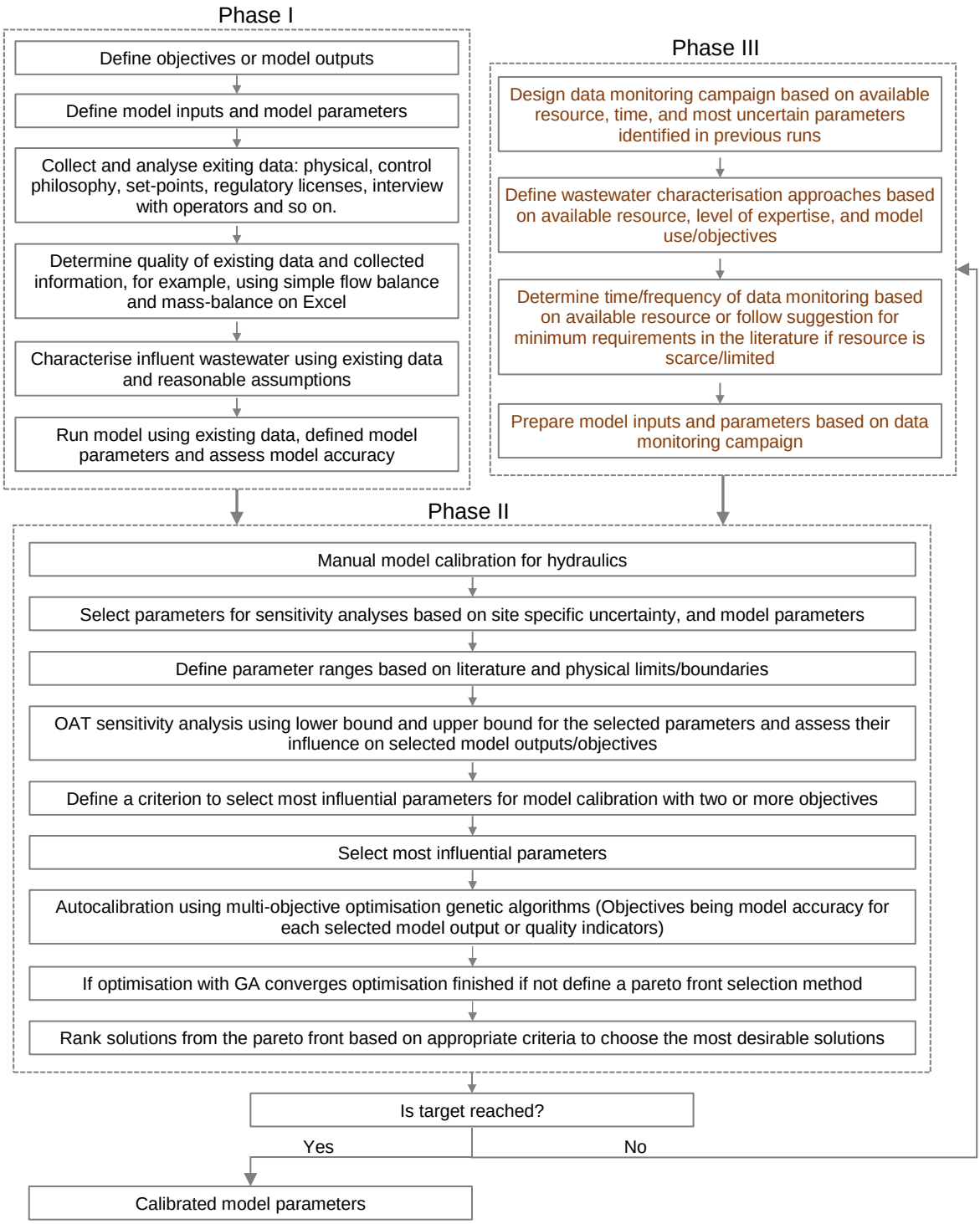

Figure 6-1 Flowchart of sensitivity analysis and model calibration procedures

6.1. Model Calibration Objectives (Model Accuracy)

The application of ASM-based models such as BSM2-e (Sweetapple, 2014), used in this study, introduces more parameters than the original ASM1. In addition, some physical and operational parameters are introduced to represent site specific processes and units. Hence a careful assessment and selection of these parameters and definition of calibration objectives are essential (Liwarska-

Bizukojc et al., 2011; Vanrolleghem et al., 2003). Model calibration, here, refers to the estimation of uncertain model parameters such as stoichiometric, kinetic and other site specific parameters to meet calibration objectives/targets (Gernaey et al., 2004). The objective of the model calibration thus includes fitting the simulated effluent quality (TSS, NO_3, NO_2 and NH_4), dissolved oxygen (DO) concentration and mixed-liquor suspended solid (MLSS) concentration with the measured dataset. The effluent quality indicators are selected based on current regulatory approaches and influence on GHG emissions. Although GHG emission is one of the interests of this study, due to lack of real GHG emissions data, model accuracy in the simulation of GHG emission could not be calibrated directly. However, the assumption is that if the model is calibrated for major bio-chemical processes, and adopt literature suggested values of GHG related parameters, the GHG emission estimation will fall into a reasonable range.

This study quantifies model-accuracy using various statistical goodness-to-fit measures for different quality indicators:

i. DO level in the oxidation ditch
ii. MLSS level in the oxidation ditch
iii. TSS concentration in the final effluent
iv. NH_4-N concentration in the final effluent
v. NO_3 and NO_2 of final effluent concentration

The evaluation criteria assess how close the model outputs are to measured data both in terms of pattern and residual error. This was represented by the use of statistical tests; coefficient of determination or the square of Pearson's coefficient (R^2), the Nash-Sutcliffe coefficient (NSE), and the Root-Means-Square-Error (RMSE).

6.1.1. Coefficient of Determination (R^2)

The R^2 (R-squared) is the square of the Pearson product moment correlation coefficient through data points in model output (predicted) and measured data (observed) as shown in Eq. 6-1 (Krause et al., 2005). The Pearson product-moment correlation coefficient is a dimensionless index, which is invariant to linear transformations of either predicted or observed dataset (Lee Rodgers and Nicewander, 1988).

$$R^2 = \frac{[\sum_{i=1}^{N}(O_i - \bar{O})(P_i - \bar{P})]^2}{\sum_{i=1}^{N}(O_i - \bar{O})^2 \times \sum_{i=1}^{N}(P_i - \bar{P})^2} \qquad \textit{Eq. 6-1}$$

Where:

O_i = Observed or measured data at the i[th] point in the time series [ ]
$\bar{O}$ = Average of measured data in the time series [ ]
P_i = Predicted or model output at the i[th] point in the time series [ ]
$\bar{P}$ = Average of model output in the time series [ ]
N = Number of data points in data series [ ]
R^2 = r-squared coefficient of determination

The value of R^2, lies between 0.0 and 1.0, can be interpreted as the proportion of the variance in model output, *P*, and the variance in measured data, *O* (Lee Rodgers and Nicewander, 1988). A value of 0 means that there is no correlation between predicted and observed time series, and a value of 1.0 means that the model outputs have the same pattern as the measured data (Moriasi et al., 2007; Krause et al., 2005). R^2 is a very good measure of pattern, but a model that under-predicts or over-predict all the time, and have a similar pattern as the measured data may have a very high R^2 value close to 1.0, i.e. it is insensitive to proportional differences between model prediction and measured data (Moriasi et al., 2007). Hence, R^2 should be supplemented by other statistical goodness-to-fit measures (Krause et al., 2005).

6.1.2. Nash-Sutcliffe Efficiency (NSE)

"The Nash-Sutcliffe efficiency (NSE) is a normalized statistic that determines the relative magnitude of the residual variance ('noise') compared to the measured data variance ('information')" (Nash and Sutcliffe, 1970). This widely used correlation coefficient can be calculated using Eq. 6-2.

$$NSE = 1 - \frac{\sum_{i=1}^{N}(P_i - O_i)^2}{\sum_{i=1}^{N}(O_i - \bar{O}_i)^2} \qquad \textit{Eq. 6-2}$$

NSE indicates how well the plot of observed versus simulated data fits the 1:1 line, i.e. the more scattered the plot is, the lower the NSE is and the closer the data points are to the 1:1, the higher the NSE (Moriasi et al., 2007). The value of NSE lies between -∞ and 1.0. A value of 1.0 means that the model output has the same value as the measured data at each data point (McCuen et al., 2006). Values below 0.0 indicate the residual variance is higher than the measured

variance, indicating that the mean of the mean of observed data is a better estimate than the model output. NSE is sensitive to model bias (McCuen et al., 2006), i.e. over-predication or under-prediction, which supplement the drawbacks of the R^2.

6.1.3. Root-Mean-Square-Error (RMSE)

The RMSE is the standard deviation of the differences between model output values and measured values, which is the prediction errors of a model compared to measured data (Willmott et al., 1985). It is a widely used statistical measure in hydrology and water quality models (Harmel et al., 2009). It aggregates the magnitudes of the errors at each data points and has the same unit as the model output (Hyndman and Koehler, 2006). Hence, care should be taken during the use of these test in multi-objective optimisation as it is scale dependent (Willmott et al., 1985). The RMSE can be calculated as shown in Eq. 6-3.

$$RMSE = \left[\frac{\sum_{i=1}^{N}(P_i - O_i)^2}{N}\right]^{1/2} \qquad \textit{Eq. 6-3}$$

6.2. Hydraulics – Manual Model Calibration

Unlike most hydrological or hydraulic models, WWTP models consist of both physical processes and biochemical processes. In most of the BSM2 model components, the complete mixing is assumed, and a simple flow-balance of a rectangular tan is used for flow routing. Outflow from each process unit is determined based on the inflow rate, and in some cases, the outflow is determined based on wastewater level in the tank or based on pump equation if it is wet-well. Details of this are given in Chapter 3 for each process unit. Otherwise, the outflow is the same as the inflow rate. Due to this simplification, it might not be possible to estimate flow propagation with high accuracy, but it is important to make sure that pump equations, outflow rate based on wastewater level, and any other assumptions are the close representative of the hydraulic process and flow-balance. The following flowchart shows the procedure taken for hydraulic model calibration of Cupar WWTP.

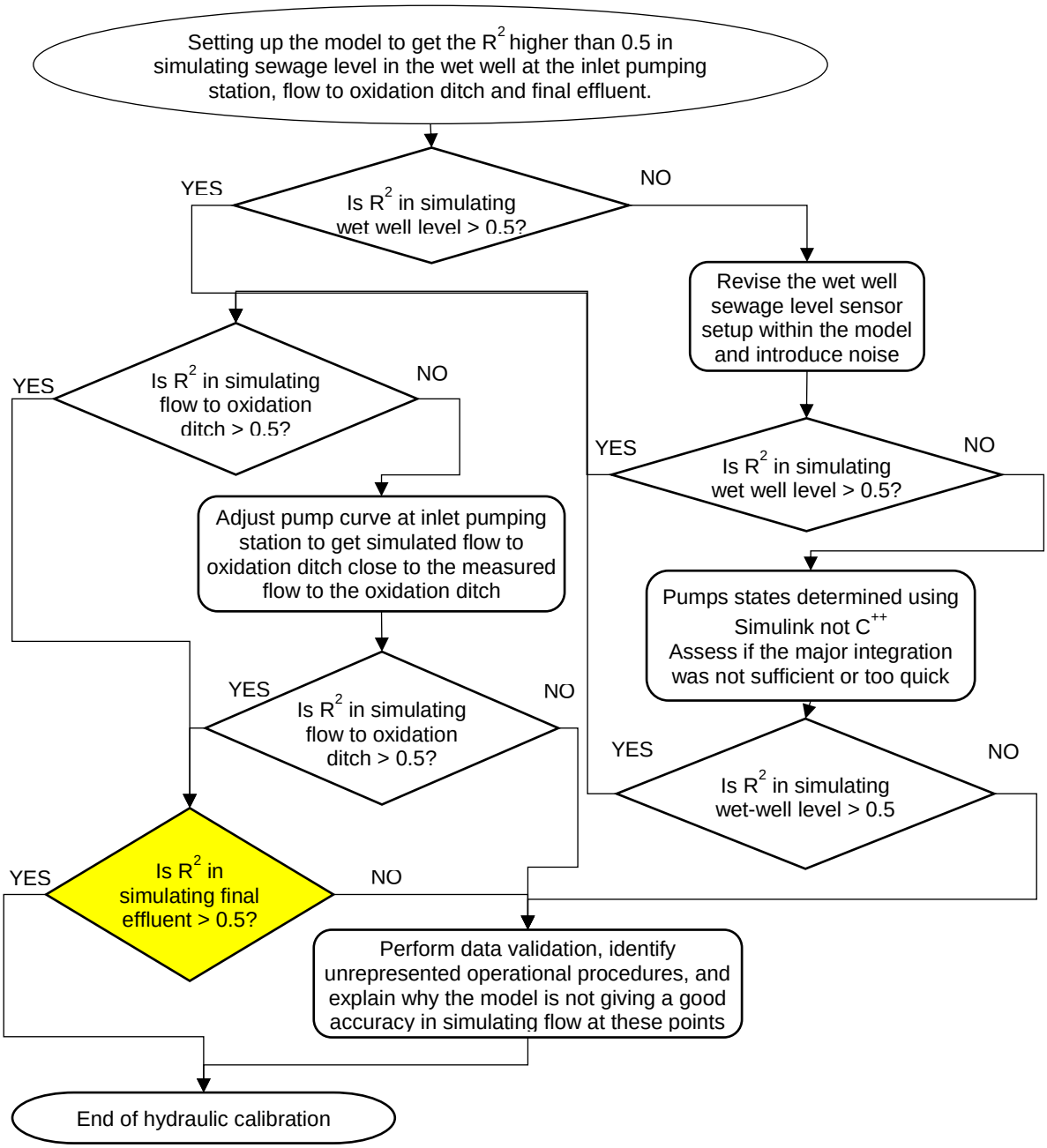

Figure 6-2 Hydraulic calibration procedures

6.2.1. Using Existing Dataset

The hydraulic model calibration is mainly focused on getting the flow balance right and make sure simulated flows have the same flow pattern and quantity as measured flows.

6.2.1.1. Inlet Flow

The flow from Cupar WWTP is bypassed to the storm tanks if the inlet flow is greater than 2.3 × DWF while any flow less than this set-point will pass to the inlet wet-well pumping station. The influent to the WWTP model is a measured dataset, but the flow to the wet-well pumping station is simulated using the bypass

procedure based on flow monitored at the inlet point and the bypass set point (2.3xDWF). This simulated flow to pumping station was compared to the measured flow to the pumping station.

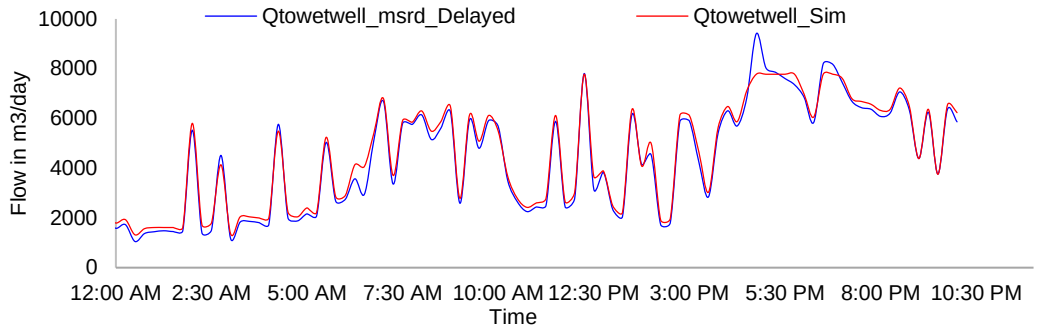

Figure 6-3 flow to inlet wet-well measured dataset forwarded by two hours and simulated flow to inlet wet-well at Cupar WWTP

By forwarding the measured flow at the inlet monitoring point by 2 hours, a more accurate correlation was observed between simulated flow to pumping station uisng Inet flow and measured flow to pumping station; having R^2 of 0.98 and Nash-sutcliff coefficient of 0.99.

6.2.1.2. Inlet Wet-well, Storm Tank Return, Scum Return and Supernatant Return

The inlet wet-well at Cupar WWTP receives wastewater from the inlet structure, and three return flows; storm tank return, scum return and supernatant return. Based on data analysis the storm return was observed start returning whenever the wet well level is below 2.7m. The valve opens and sewage flow through gravity to inlet wet-well at an average rate of 11 L s^{-1}; this is estimated using measured storm tank level data, see Figures Figure 6-4Figure 6-5Figure 6-6. Analysing the period 22/03/2013 – 27/03/2013 for rate of emptying (tank level reduction per minute) the tank 1 is found to be, on average, 0.00098m/minute the average of the slope of the trend lines for five storm water retuning events. Thus, using a surface area of 406 m^2, storm tank 1 starts returning, sewage flows at a rate of **6.63** L s^{-1}.

Repeating the same analysis for the period 22/03/2013 – 27/03/2013 for storm tank 2, the rate of storm water return is found to be 0.00172 m min^{-1}, i.e., sewage returns from storm tank-2 to wet-well at a rate of **11.64** L s^{-1}.

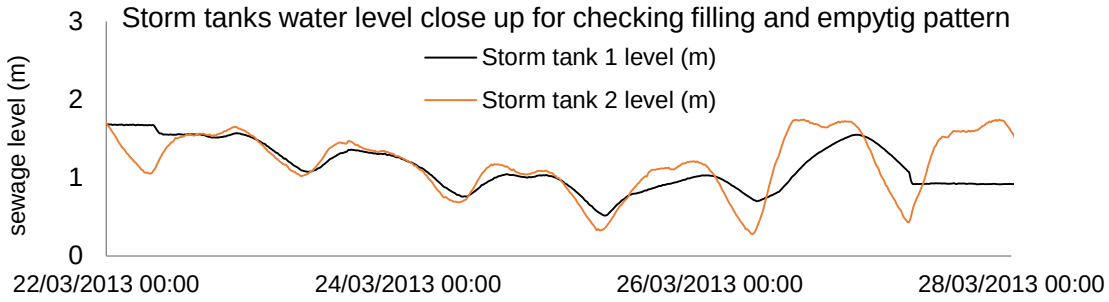

Figure 6-4 Storm tanks 1 and 2 sewage level for selected 6 days

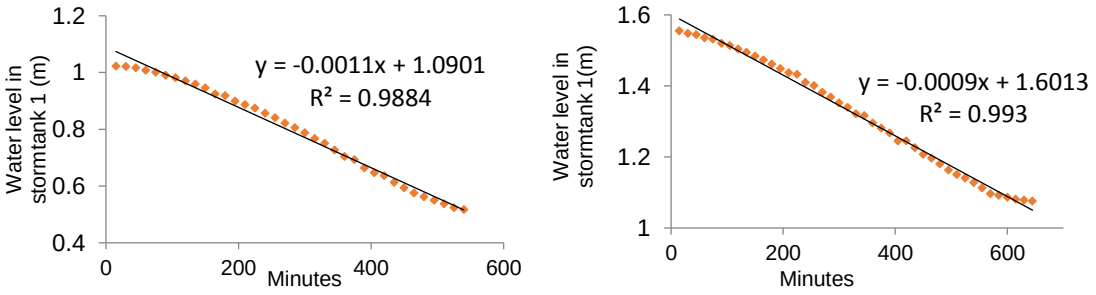

Figure 6-5 Regression analysis to calculate the rate of storm return flow from storm tank 1

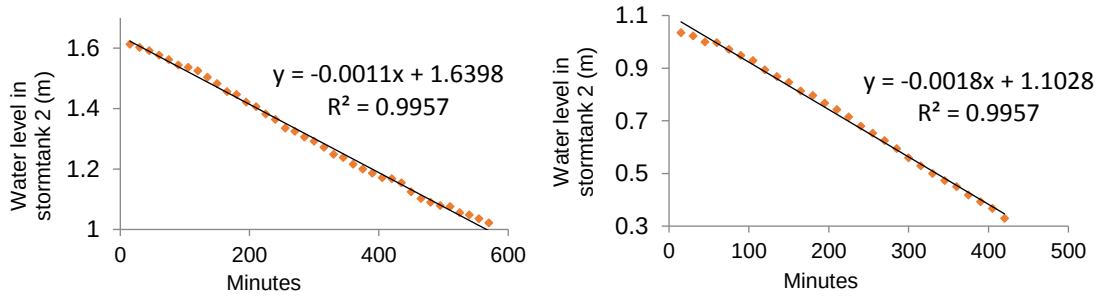

Figure 6-6 Regression analysis to calculate the rate of storm return flow from storm tank 2

The scum return from the final settlement tanks was observed on site and found out to be significant. This return flow is not monitored. However, the flow data downstream of the wet-well (referred here as wet-well outflow or flow to oxidation ditch) is used to estimate this flow. The scum return is calculated to be, on average, 28 % of the final settlement outflow.

The supernatant return is very small and is assumed not to have a significant impact in simulating the wet-well level and flow to the oxidation ditch.

The inlet wet-well pump operation is based on the sewage level in the wet-well, see Section 3.1.4. Two approaches were considered to simulate the discharge from the inlet wet-well pumping station to the oxidation ditch; one is by using manufacturers pump property curve, and the second one is by using the correlation between wet-well level and flow to OD monitored data. The discharge

estimated using wet-well level data showed less variation and a lower R^2. The discharge estimated from the pump curve and the use of simplified conservation of energy showed a good variation. Hence the discharge estimated from the pump curve is taken, but due to the algebraic loop, the discharge estimation using pump curves is simplified and converted into a linear empirical equation as shown in Figure 6-9.

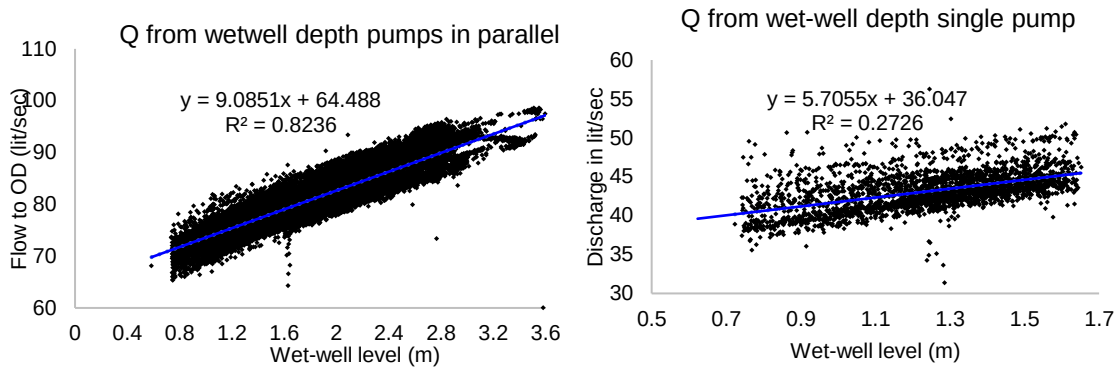

Figure 6-7 Correlation between measured wet-well depth and discharge from wet-well pumps

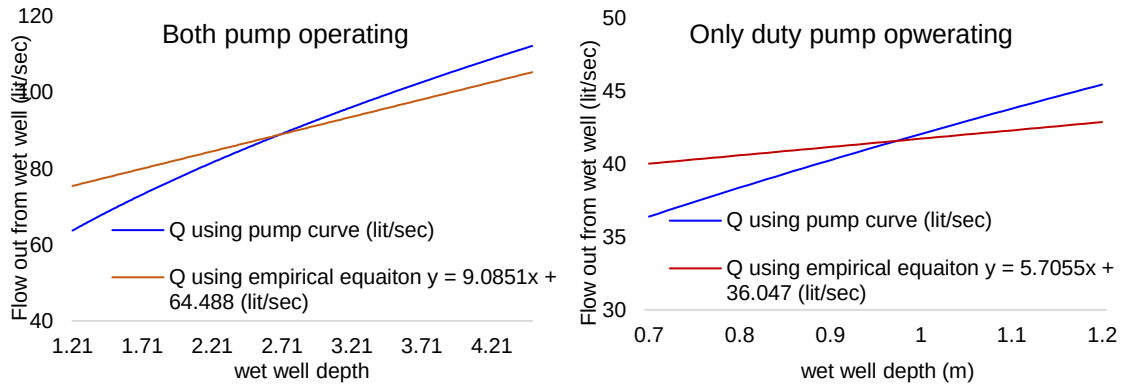

Figure 6-8 Comparison of flow vs wet-well depth for discharge estimated from pump curves and conservation of energy vs discharges from the correlation between measured wet-well depth and wet-well outflow

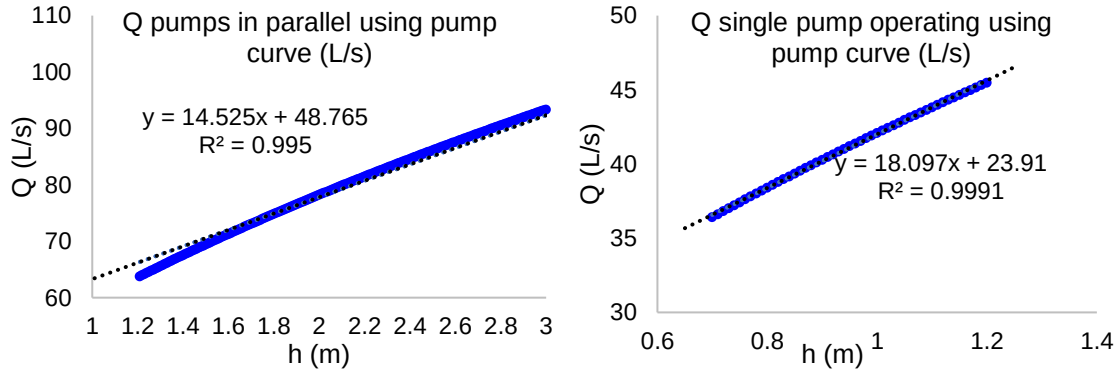

Figure 6-9 Surrogate equation to represent the estimation of discharge using pump-curve and conservation of energy

By using the above flow rates for storm tank return, scum return, and supernatant return (see chapter 3), the wet-well level and flow to the oxidation ditch was estimated.

$$Q_{ww} = 14.525h_{ww} + 48.765 \qquad if\ both\ pumps\ are\ operating$$
$$Q_{ww} = 18.097h_{ww} + 23.91 \qquad if\ only\ duty\ pump\ is\ operating \qquad \textit{Eq. 6-4}$$

Where:

Q_{ww} = Flow out from inlet wet-well to oxidation ditch [L s^{-1}]
h_{ww} = Inlet wet-well depth [m]

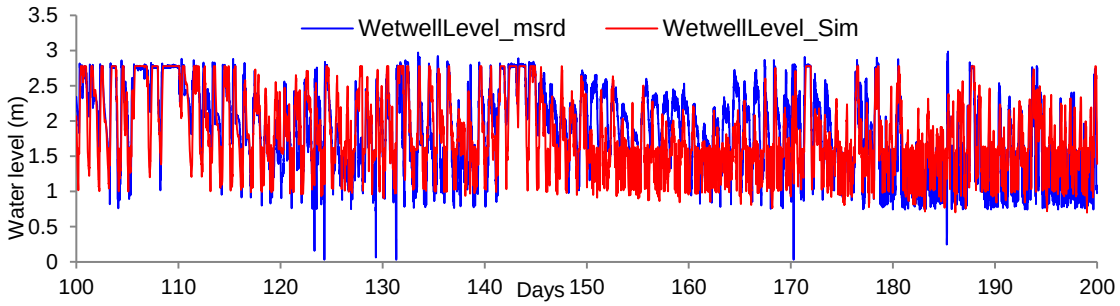

Figure 6-10 Wet-well level simulated and measured from existing dataset

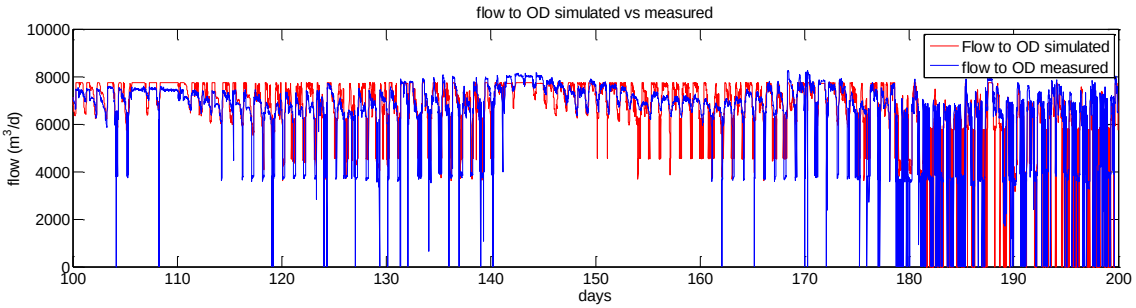

Figure 6-11 Flow to oxidation ditch simulated and measured using existing dataset

6.2.1.3. Spray-bar Return Flow to OD and Final Effluent

The spry-bar return flow to the oxidation ditch from the final effluent is not found to be significant in affecting the final effluent flow uncles there is a variation in the flow in a short period of time. The spray-bar return is reported to be 30 L s^{-1} based on an interview of the operators. Due to the uncertainty in the exact value of this flow, this flow is varied to improve model accuracy in simulating final effluent.

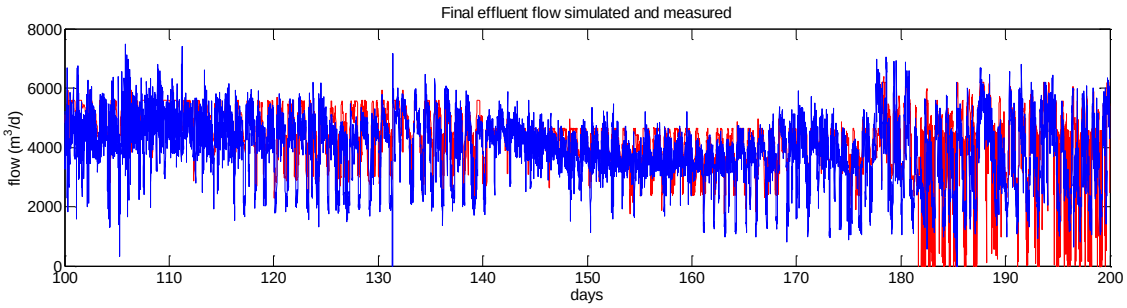

Figure 6-12 Final effluent flow rate simulate and measured using existing dataset

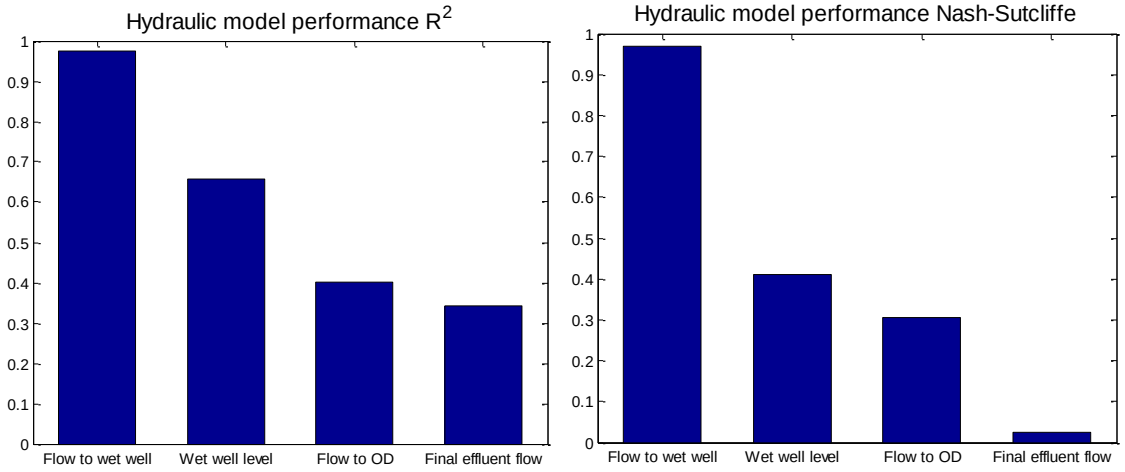

Figure 6-13 Hydraulic model accuracy at different points in the WWTP as measured by NSE and R^2

The R^2 value was 0.96, 0.63, 0.56 and 0.34 for flow to the wet-well, wet well level, flow to OD, and final effluent respectively. The NSE value for the whole calibration was 0.96, 0.42, 0.5, and 0.03 respectively, see Figure 6-13. Although the model accuracy is good upstream of inlet wet-well, due to uncertainty in return flows into wet-well and oxidation ditch, the hydraulic model accuracy gradually reduces as we proceed downstream of the WWTP. Further hydraulic data is measured during the campaign period to improve the model accuracy and reduce uncertainty.

6.2.2. Using Campaign Dataset

As detailed in Chapter 4, the campaign data measures important flow rates such as scum return, final effluent at various points, and spray bar return to the oxidation ditch. The model runs for 100 days in a steady state and then, using this new dataset, the model run for 20 days. By incorporating this information into the model, the following model performance is achieved, see Figure 6-14 and Figure 6-15. Due to the over-estimation of flow for the three days (102, 103, and 104), the accuracy of the model simulating the wet-well is lower than the one using existing dataset. To avoid the propagation of error, the flow from the wet

well is determined based on measured outflow instead of using the surrogate model; hence, the model has higher accuracy in estimating the final effluent, see Table 6-1.

Table 6-1 Hydraulic model accuracy using campaign dataset

	NSE	R^2	RMSE
Flow to wet well	0.79	0.8	796
wet well level	0.01	0.28	0.63
Final effluent flow	0.85	0.87	511

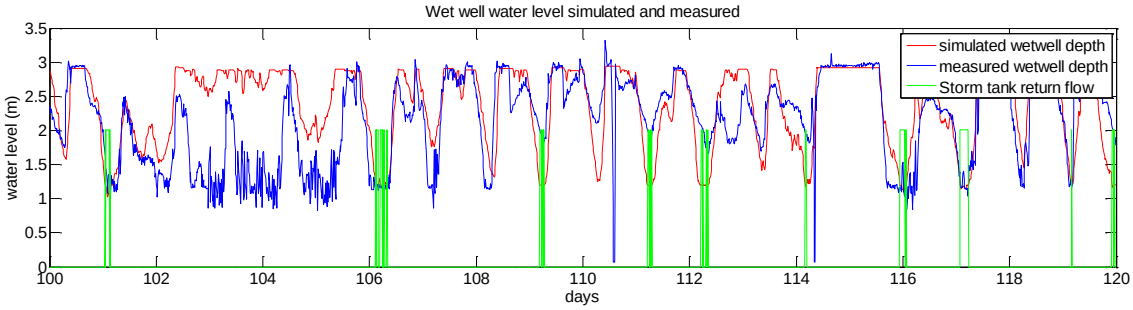

Figure 6-14 Wet-well level simulated and measured from campaign dataset over 20 days of the campaign period

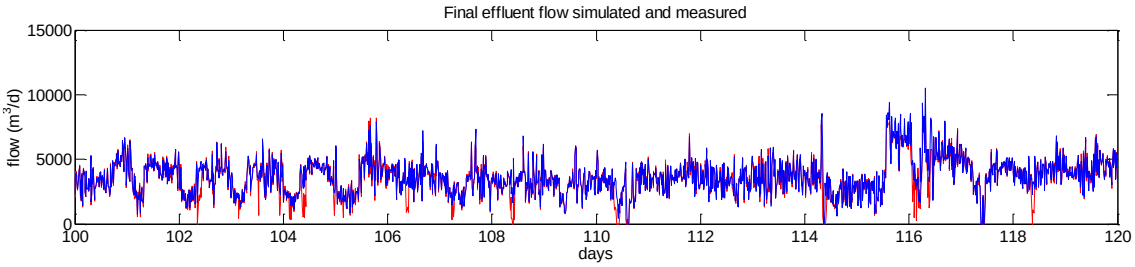

Figure 6-15 Final effluent flow rate simulated and measured using campaign dataset over 20 days of the campaign period

6.3. Sensitivity Analysis

Sensitivity analysis has been used for different purposes. For example:

- Sweetapple et al. (2013) use sensitivity analysis to identify the source of uncertainty in modelling greenhouse gas emissions from WWTPs.
- Identifying most critical parameters for a WWTP model-based studies and design of control strategies (Benedetti et al., 2008).
- Abusam et al. (2001) studied the influence of variations in stoichiometric, kinetic and operational parameters of an oxidation ditch simulation model through a sensitivity analysis. They used WWTP performance indices such as effluent quality index (EQI), aeration energy (AE), and total sludge production (TSP).

- Sensitivity analysis has also been used in understanding underlying processes. For example, Boiocchi et al. (2017) use a sensitivity analysis approach to understand the N_2O formation mechanisms in WWTPs.
- Benedetti et al. (2008) and Sweetapple et al. (2013) performed output parameter sensitivity analysis using the Benchmark Simulation Model 2 (BSM2) and BSM2-e respectively. Calibration can be a tedious process in complex process-based models the exact value of model parameters is unknown to the modeller, and sensitivity analysis can reduce calibration effort by identifying parameters that most influence the model output. Hence, reduce the number of parameters to consider for calibration purpose.

Commonly, sensitivity analysis is used in identifying parameters that significantly affect the model's output or the objective of the study. This study focuses on identifying most sensitive parameters for model calibration. Thus, the above Indexes may not directly indicate most sensitive parameters to improve the accuracy of the WWTP model to simulate effluent quality and pollutant concertation in the reactors as close as possible to the measured values.

One-factor-at-a-time (OAT) sensitivity analysis approach is used with the objectives being the goodness-to-fit measures that quantify the model accuracy by comparing model output to measured time-series. This was represented by the use of statistical tests, the Root-Means-Square-Error (RMSE), Eq. 6-1, Nash-Sutcliffe coefficient (NSE), Eq. 6-2, and coefficient of determination (R^2), Eq. 6-3. The evaluation criteria that indicate the WWTP model's performance in simulating final effluent TSS, NO_3-N, and NO_2-N were used in addition to oxidation ditch MLSS and DO concentration.

Relevant operational and design parameters are selected for Cupar wastewater treatment works. Wastewater treatment parameters list (kinetic and stoichiometric parameters) for ASM is adopted from (Jeppsson et al., 2007), see Table 6-2. Since Cupar WWTP doesn't have onsite anaerobic digester, AMD model parameters won't be the interest of this study. Default parameter values are taken from different literature. The same is done in finding out recommended upper and lower limit of parameters, Table 6-2. Parameters for which a specific minimum and maximum cannot be found, ±50 % of the literature average is used for minimum and maximum limit.

Table 6-2 Parameters used for sensitivity analysis

Para. No.	Para-meters	Description	Default value	Lower bound	Upper bound	Remark/ References
1	mu_H	Maximum specific growth rate for heterotrophic biomass [d^{-1}]	4.0	3.000	13	a, b, e
2	K_S	Half-saturation coefficient for heterotrophic biomass [g COD.m^{-3}]	10	5.000	120	Ks (mg L^{-1}) value varies from 5 - 120 for domestic waste (g, a)
3	K_{OH}	Oxygen Half Saturation Coefficient for heterotrophic biomass [g (-COD).m^{-3}]	0.2	0.100	2	K_OH value was reported 1mg L^{-1} (g, h, a)
4	K_{NO}	Nitrate NO_3-N half saturation coefficient for heterotrophic biomass [g NO_3-N.m^{-3}]	0.5	0.100	1.0	a
5	b_H	Decay coefficient for heterotrophic biomass [d^{-1}]	0.3	0.050	1.6	b_H without recycling was found to vary from 0.05 day^{-1} to 1.6 day^{-1} (a)
6	mu_A	Maximum specific growth rate for autotrophic biomass [d^{-1}]	0.5	0.340	0.65	mu_A is associated with the removal of ammonia nitrogen (a)
7	K_{NH}	Ammonia half-saturation coefficient for autotrophic biomass [g NH_3-N.m^{-3}]	1.0	0.500	1.5	c
8	K_{OA}	Oxygen Half Saturation Coefficient for autotrophic biomass [g (-COD).m^{-3}]	0.4	0.200	1.5	a, f
9	b_A	Decay coefficient for autotrophic biomass [d^{-1}]	0.05	0.010	0.15	a
10	ny_g	Correction factor for mu_H under anoxic condition [dimensionless]	0.800	0.600	1.2	b, a
11	k_a*	ammonification rate [m^3(gCOD.d)$^{-1}$]	0.050	0.025	0.075	b, c
12	k_h*	Maximum specific hydrolysis rate [g SBCOD. (g cell COD. d)$^{-1}$]	3.000	1.500	4.5	b, c, d
13	K_X*	Half-saturation coefficient for hydrolysis of slowly biodegradable substrate [g SBCOD. (g cell COD)$^{-1}$]	0.100	0.050	0.15	b, d
14	ny_h*	Correction factor for hydrolysis under anoxic condition [dimensionless]	0.800	0.400	1.2	b, d
15	Y_H	Yield for heterotrophic biomass [g cell COD formed.(g COD oxidized)$^{-1}$]	0.67	0.460	0.69	a
16	Y_A	Yield for autotrophic biomass [g cell COD formed. (g COD oxidized)$^{-1}$]	0.24	0.020	0.28	a
17	f_P*	Fraction of biomass leading to particulate products [dimensionless]	0.080	0.040	0.12	b, c
18	i_{XB}*	Mass of nitrogen per mass of COD in biomass [g N. (g COD)$^{-1}$ in biomass]	0.080	0.040	0.12	b, c
19	i_{XP}*	Mass of nitrogen per mass of COD in products from biomass [g N. (g COD)$^{-1}$ in biomass]	0.06	0.030	0.09	b, c
20	v_{0max}*	Secondary settlement maximum settling velocity [m.d^{-1}]	350	125	375	b, c
21	v_0*	Secondary clarifier maximum visilind velocity [m.d^{-1}]	474	237	711	b, c
22	r_h*	Secondary settlement hindered zone settling parameter [m^3(gSS)$^{-1}$]	0.0006	0.0003	0.0009	b, c
23	r_p*	secondary settlement flocculants zone settling parameter [m^3(gSS)$^{-1}$]	0.00286	0.00143	0.00429	b, c
24	f_{ns}*	Secondary clarifier non-settleable fraction [dimensionless]	0.00228	0.00114	0.00342	b, c
25	mu_{Hv2}*	Maximum specific growth rate for heterotrophic biomass [d^{-1}] (Added for nitrogen modelling (Sweetapple, 2014))	6.25	3.125	9.375	k, m

Henze et al. (2002) argue that most kinetic parameters value varies widely and very dependent on the nature of the wastewater being treated.

*Parameters whose upper bound (UB) and lower bound (LB) were taken ±50 % of the average literature value.

a - Henze (2002), b - Benedetti et al. (2008), c - Jeppsson et al. (2007), d - Sweetapple et al. (2013), e - Dold (1986), f - Picioreanu et al. (1997), g - Horan (1990), h - Henze et al. (2008)

Para. No.	Para-meters	Description	Default values	Lower bound	Upper bound	Remark
26	b_{Hv2}*	Decay coefficient for heterotrophic biomass [d^{-1}] (added for N modelling (Sweetapple, 2014))	0.408	0.204	0.612	k, m
27	Y_{Hv2}*	Yield for heterotrophic biomass [g cell COD formed. (g COD oxidized)$^{-1}$] (added for N modelling (Sweetapple, 2014))	0.6	0.3	0.9	k, m
28	K_{S2}*	Half-saturation constant for S_{NO3-} reduction [gN m^{-3}]	20	10	30	k, m
29	K_{S3}*	Half-saturation constant for S_{NO2-} reduction [gN m^{-3}]	20	10	30	k, m
30	K_{S4}*	Half-saturation constant for S_{NO} reduction [gN m^{-3}]	20	10	30	k, m
31	K_{S5}*	Half-saturation constant for S_{N2O} reduction [gN m^{-3}]	40	20	60	k, m
32	K_{NO3}*	Half-saturation constant for S_{NO3-} for heterotrophs [gN m^{-3}]	0.2	0.1	0.3	k, m
33	K_{NO2}*	Half-saturation constant for S_{NO2-} for heterotrophs [gN m^{-3}]	0.2	0.1	0.3	k, m
34	K_{NOv2}*	Half-saturation constant for S_{NO} for heterotrophs [gN m^{-3}]	0.05	0.025	0.075	k, m
35	K_{N2O}*	Half-saturation constant for S_{N2O} for heterotrophs [gN m^{-3}]	0.05	0.025	0.075	k, m
36	K_{OH2}*	O_2 inhibition of S_{NO3-} reduction [g O_2 m^{-3}]	0.1	0.05	0.15	k, m
37	K_{OH3}*	O_2 inhibition of S_{NO2-} reduction [g O_2 m^{-3}]	0.1	0.05	0.15	k, m
38	K_{OH4}*	O_2 inhibition of S_{NO} reduction [g O_2 m^{-3}]	0.1	0.05	0.15	k, m
39	K_{OH5}*	O_2 inhibition of S_{N2O} reduction [g O_2 m^{-3}]	0.1	0.05	0.15	k, m
40	K_{13NO}*	NO inhibition of S_{NO2-} reduction [g O_2 m^{-3}]	0.5	0.25	0.75	k, m
41	K_{14NO}*	NO inhibition of S_{NO} reduction [g O_2 m^{-3}]	0.3	0.15	0.45	k, m
42	K_{15NO}*	NO inhibition of S_{N2O} reduction [g O_2 m^{-3}]	0.075	0.0375	0.1125	k, m
43	ny_{g2}*	Anoxic growth factor for S_{NO3-} reduction [-]	0.28	0.14	0.42	k, m
44	ny_{g3}*	Anoxic growth factor for S_{NO2-} reduction [-]	0.16	0.08	0.24	k, m
45	ny_{g4}*	Anoxic growth factor for S_{NO} reduction [-]	0.35	0.175	0.525	k, m
46	ny_{g5}*	Anoxic growth factor for S_{N2O} reduction [-]	0.35	0.175	0.525	k, m
47	ny_{Y}*	Anoxic yield factor for heterotrophs [-]	0.9	0.45	1.35	k, m
48	$K_{Hnobase}$*	Henry's law constant for NO [mol L^{-1} bar^{-1}]	0.0019	0.00095	0.00285	k, m
49	$K_{Hn2obase}$*	Henry's law constant for N_2O [mol L^{-1} bar^{-1}]	0.025	0.0125	0.0375	k, m
50	kLa_{no}*	Gas transfer coefficient for NO [d^{-1}]	0	0	0	k, m
51	kLa_{n2o}*	Gas transfer coefficient for N_2O [d^{-1}]	2	1	3	k, m
52	$pgas_{no}$*	Partial pressure of NO in atmosphere [bar]	$2x10^{-7}$	$1x10^{-7}$	$3x10^{-7}$	k, m
53	$pgas_{n2o}$*	Partial pressure of N_2O in atmosphere [bar]	$3.2x10^{-7}$	$1.6x10^{-7}$	$4.8x10^{-7}$	k, m
54	$K_{NHadded}$*	Half saturation constant for NH_x for the growth of heterotrophs (added to prevent growth occurring when no NH_x is available (Sweetapple, 2014))	0.001	0.0005	0.0015	k, m
55	kLa1	Reactor 1 aeration intensity [d^{-1}]	180	100	240	c
56	kLa2	Reactor 2 aeration intensity [d^{-1}]	180	100	240	c
57	kLa3	Reactor 3 aeration intensity [d^{-1}]	180	100	240	c
58	kLa4	Reactor 4 aeration intensity [d^{-1}]	180	100	240	c
59	kLa10	Reactor 10 aeration intensity [d^{-1}]	180	100	240	c
60	kLa11	Reactor 11 aeration intensity [d^{-1}]	180	100	240	c
61	Q_{intr}	Internal recirculation within the oxidation ditch [m^3 d^{-1}]	904,672	120,336	922,384	operational

*Parameters whose upper bound (UB) and lower bound (LB) were taken ±50 % of the average literature value.
k - Sweetapple (2014), m - Samie et al. (2011)

The OAT approach changes model parameters and control handle to their literature or most possible minimum and maximum values and asses the changes on model outputs as measured by using goodness-to-fit measures (Sweetapple, 2014). Two simulations are done for each parameter; one using lower bound and another with its upper bound. The percentage change in each evaluation criteria with respect to the base (simulation using default parameter value) is calculated. The approach used by Sweetapple (2014) is modified to fit the criteria that can have negative values, see Eq. 6-5 and Eq. 6-6.

$$P_{j_{i,UB}} = 100 \times \frac{Y_{j_{i,UB}} - Y_{j_{base}}}{\left|Y_{j_{base}}\right|} \qquad \textit{Eq. 6-5}$$

$$P_{j_{i,LB}} = 100 \times \frac{Y_{j_{i,LB}} - Y_{base}}{\left|Y_{j_{base}}\right|} \qquad \textit{Eq. 6-6}$$

Where:

$Y_{j_{i,LB}}$ = $f(X_{1_{base}}, \ldots X_{i_{min}}, \ldots X_{n_{base}})$ The j[th] evaluation criteria for the i[th] parameter at its lower bound (minimum)

$Y_{j_{i,UB}}$ = $f(X_{1_{base}}, \ldots X_{i_{max}}, \ldots X_{n_{base}})$ The j[th] evaluation criteria for the i[th] parameter at its upper bound (maximum)

$Y_{j_{base}}$ = $f(X_{1_{base}}, \ldots X_{i_{base}}, \ldots X_{n_{base}})$ The j[th] evaluation criteria using default parameter values for all the parameters

$P_{j_{i,LB}}$ = Percentage change in the j[th] evaluation criteria with the i[th] parameter at its minimum compared to the base case

$P_{j_{i,UB}}$ = Percentage change in the j[th] evaluation criteria with the i[th] parameter at its maximum compared to the base case

The absolute value of the difference between the percentage change in evaluation criterial at the i[th] parameter lower bound and upper bound, $\left|P_{j_{i,UB}} - P_{j_{i,LB}}\right|$, is used for ranking the sensitivity results. The sensitivity result for each evaluation criteria is sorted in descending order based on this ranking criterion. The advantage of using the absolute value of the difference between the percentage change is that it gives higher priority to those parameters which tends to have a linear relationship to the evaluation criteria. The disadvantage is parameters with significant impact on evaluation criteria but if the change is in a similar direction, then these parameters get a lower priority. A manual search is done for parameters resulting in such behaviour and the decision to use them for calibration purpose is reinvestigated.

6.3.1. Sensitivity Analysis: Results and Discussions

The OAT sensitivity analysis results are presented in Figure 6-16 – Figure 6-25, showing the percentage change in model performance indicator with respect to the base case (average literature value) when each parameter was set to its respective upper and lower bounds. The variation of parameter values within the feasible range can have a significant effect in the model performance. The OAT sensitivity results showed that the model performance indicators R^2, NSE, and RMSE are highly sensitive to changes in b_H, r_h, Y_H, Y_A, V_0, f_{ns}, f_P, i_{XB}, K_S and K_{OH} which were also identified as sensitive parameters by Benedetti et al. (2008) and Sweetapple et al. (2013). Q_{intr} is one of the operation parameters that its variation has a significant impact on all the evaluation criteria assessed except on the OD concentration in the oxidation ditch.

Parameters identified as sensitive using NSE and RMSE are the same for each evaluation criteria; final effluent TSS, NO_3, NO_2, and oxidation ditch MLSS and DO. Hence, either the NSE or RMSE can be used for selection of the most sensitive parameters and for calibration purposes too. The parameters identified as sensitive based on R^2 are slightly different, showing the need to consider this goodness-to-fit measure together with either NSE or RMSE. This is mainly the fact that R^2 measures the variance from the mean while NSE and RMSE measure the residuals, i.e. they measure how the simulated results are far away or close to the measured values. For example, V0max is one of the parameters that affect the amount of TSS in the final effluent based on the OAT using NSE. However, this parameter does not have an impact on the pattern of the TSS variation over a period. Hence the reason why it is lower in the tornado plot, see Figure 6-16 and Figure 6-17.

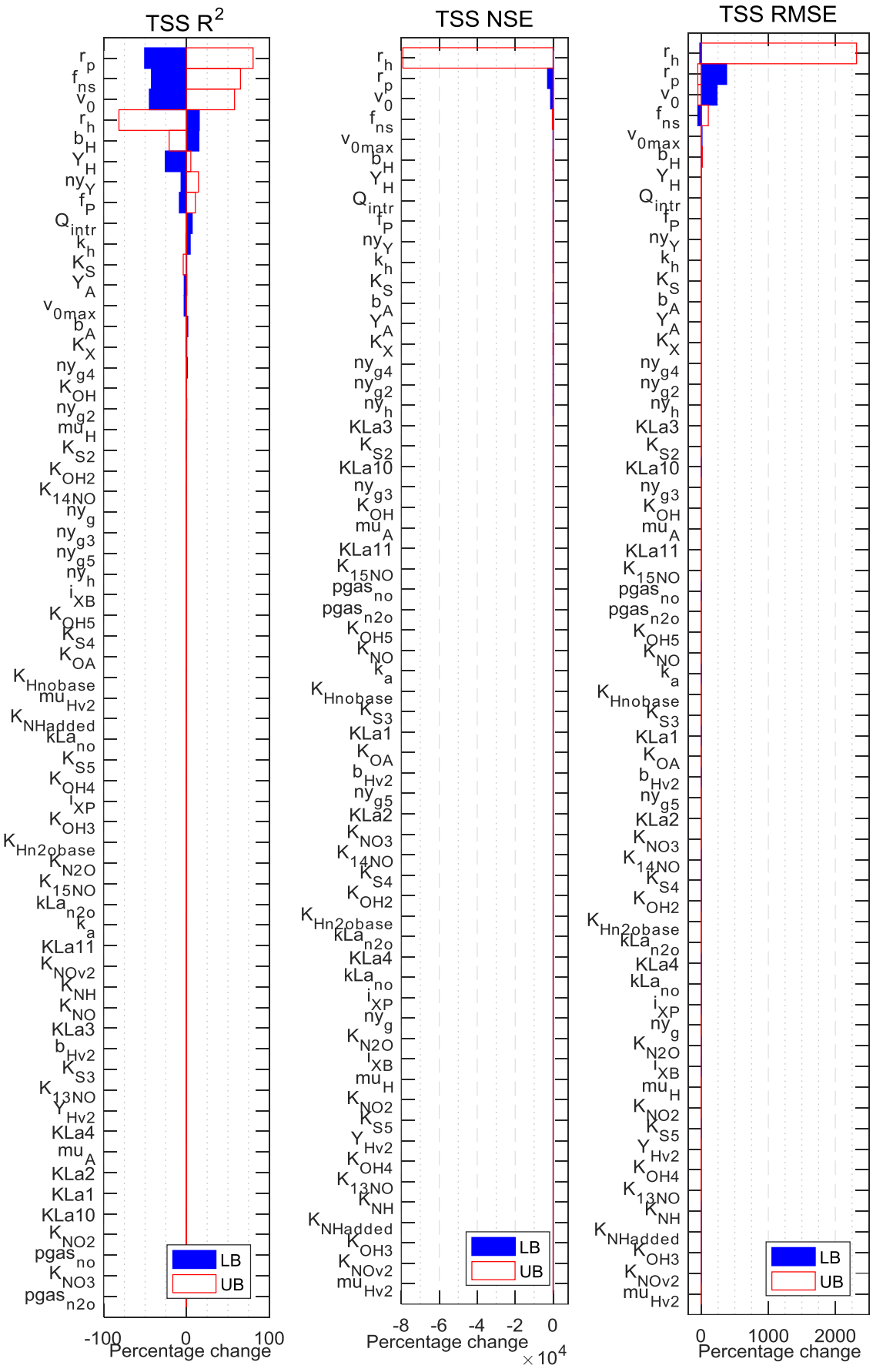

Figure 6-16 OAT results of final effluent TSS evaluated using R^2, NSE, and RMSE (left to right)

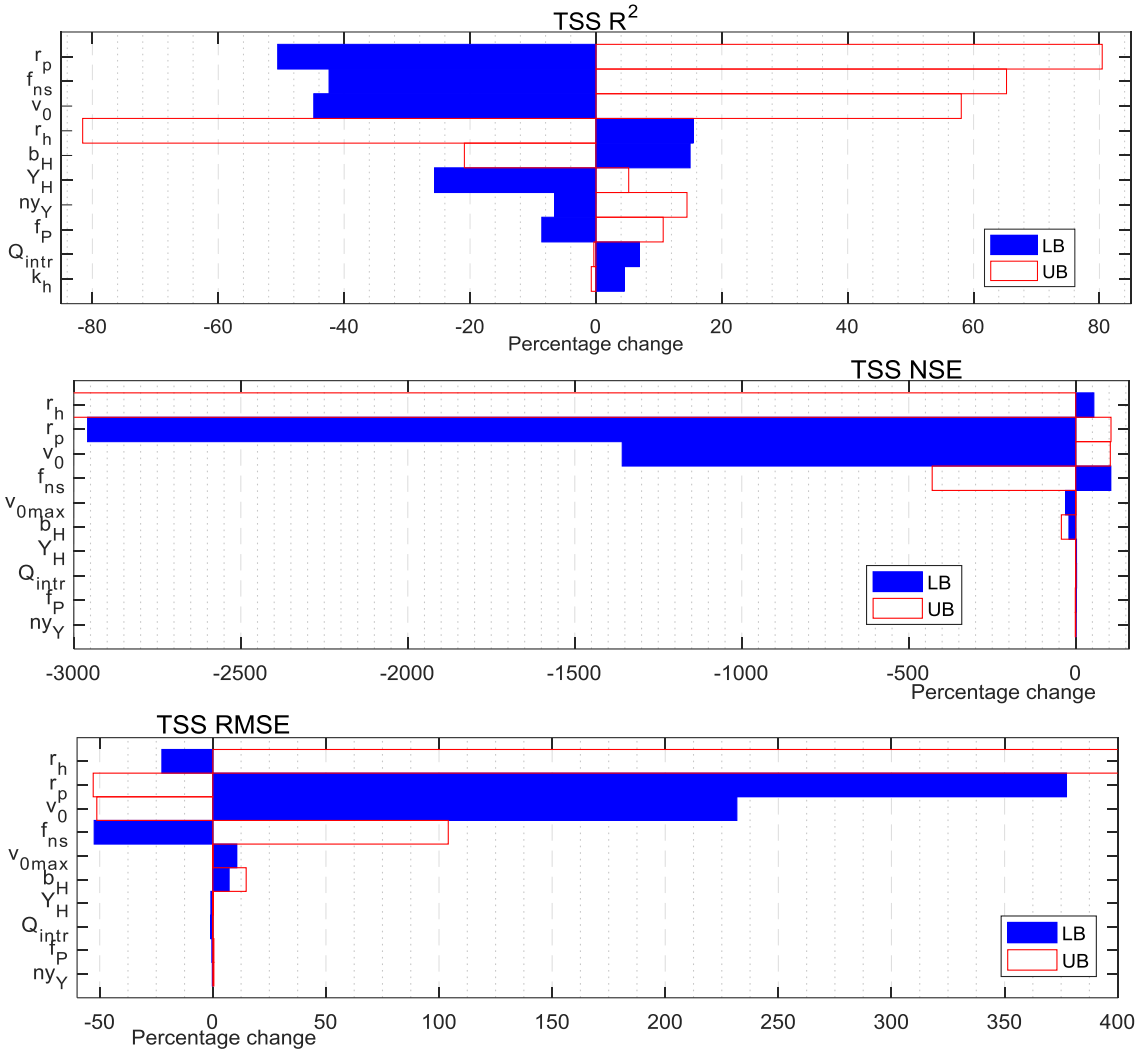

Figure 6-17 Top 10 OAT results of final effluent TSS evaluated using R^2, NSE, and RMSE (top to bottom)

The TSS in the final effluent is mainly affected by settler parameters r_p, f_{ns}, V_0, and r_h. The upper bound of r_h has the highest impact on the final effluent TSS concentration much higher than the other parameters as measured by NSE and RMSE, see Figure 6-16 and Figure 6-17. However, it does not have the same level of impact on R^2, showing that its influence on the variation of simulation from the average (noise) is not very high. Some of the stoichiometric parameters (Y_H, and f_p) show a slight sensitivity not more than 50 % change in the evaluation criteria. The operational parameter Q_{intr} showed a similar level of impact, not more than 50 % change in evaluation criteria. The kinetic parameters have an insignificant impact on final effluent TSS concertation except for n_{yY} and b_H.

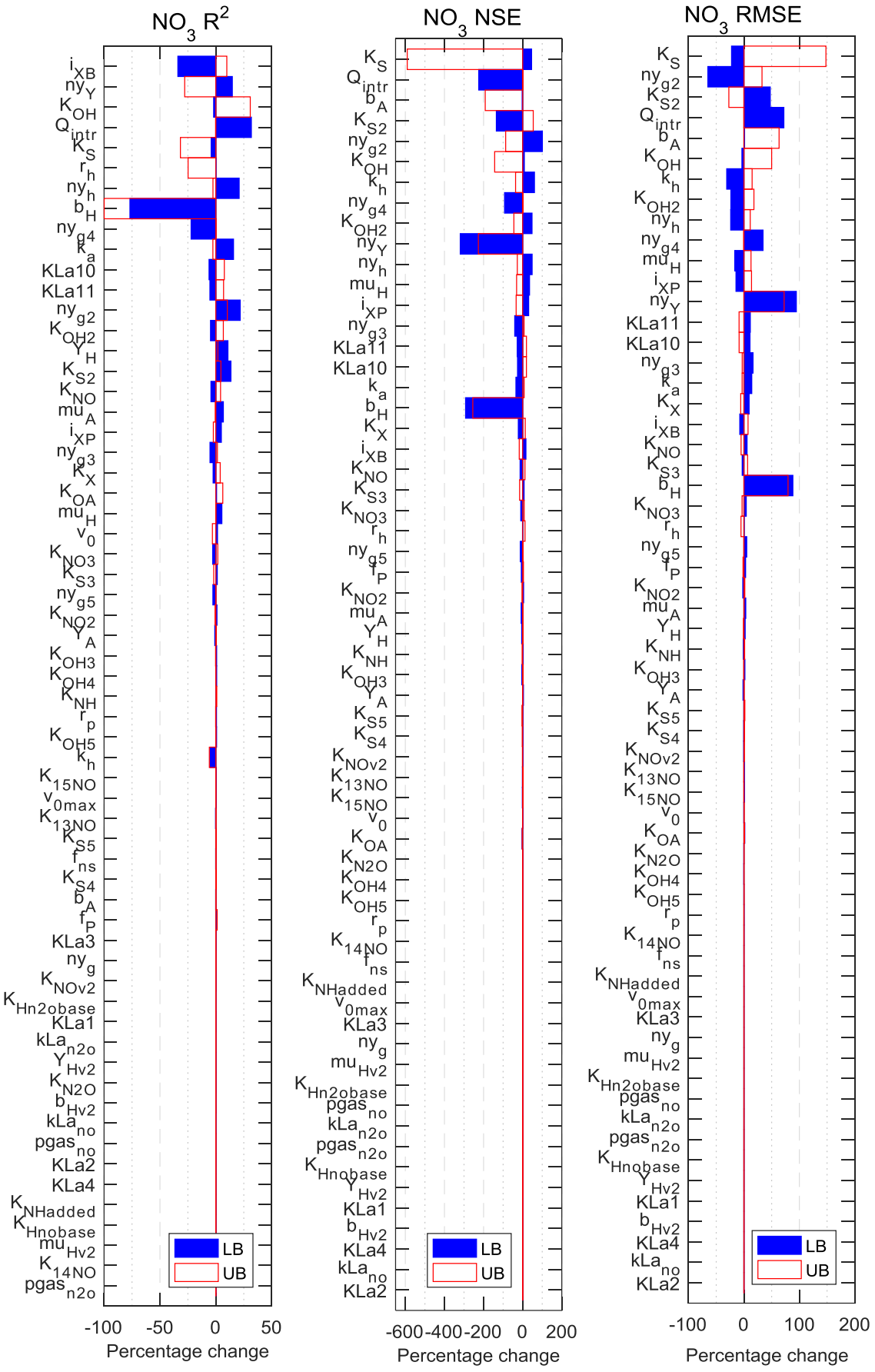

Figure 6-18 OAT results of final effluent NO_3 evaluated using R^2, NSE, and RMSE (left to right)

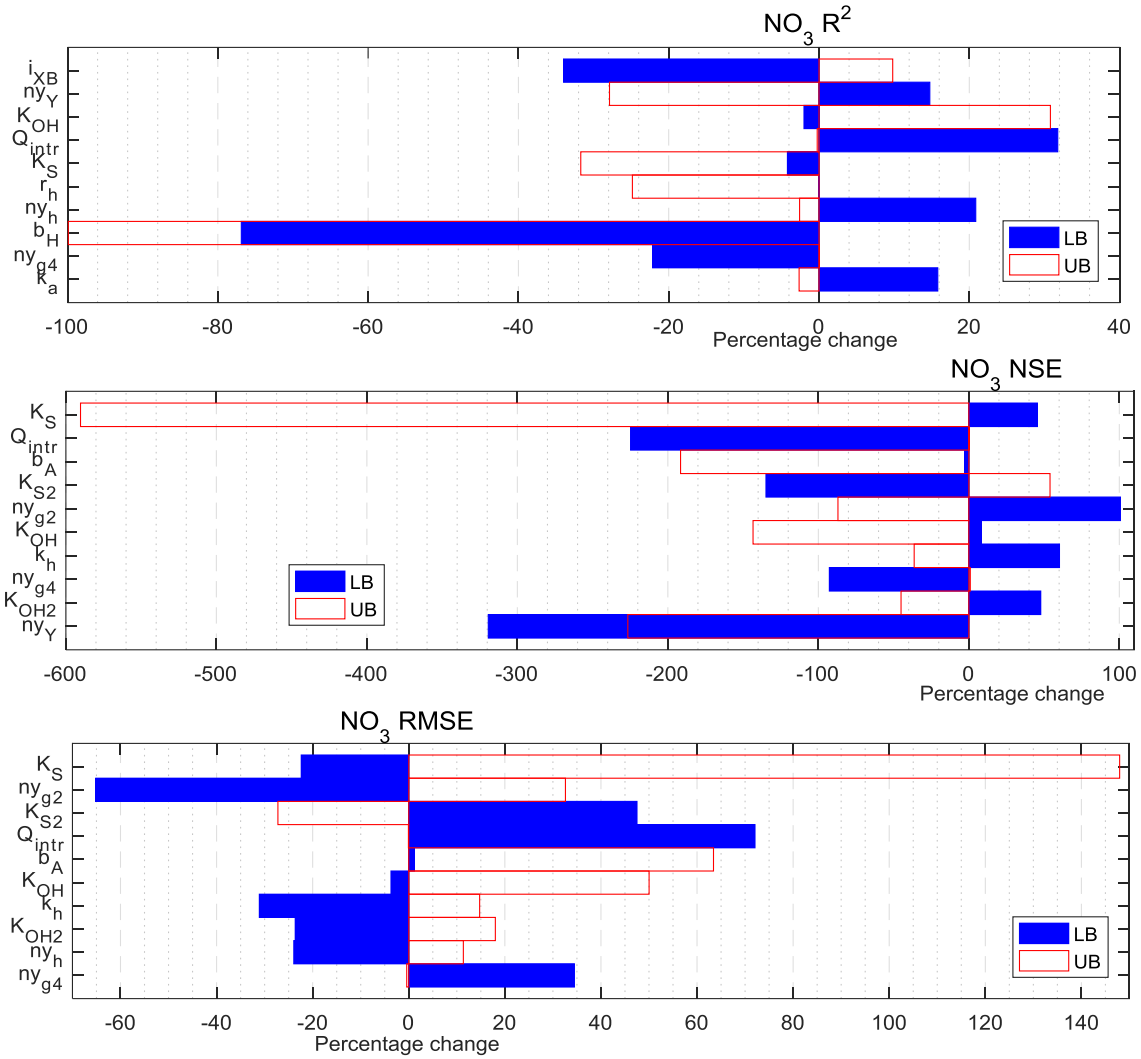

Figure 6-19 Top 10 OAT results of final effluent NO_3 evaluated using R^2, NSE, and RMSE (top to bottom)

The kinetic model parameters are the ones that have a significant impact on the NO_3 concentration in the final effluent; K_S, b_A, b_H, n_{yY}, K_{OH}, and K_{OH2}, see Figure 6-18 and Figure 6-19. The final effluent NO_3 showed sensitivity to stoichiometric parameter i_{XB} and the settler parameter r_h as measured by R^2, indicating that these parameters have more impact on the effluent diurnal pattern than changing its average value. Q_{intr} is the only operational parameter to affect all the evaluation criteria for NO_3 by causing, without considering direction of change, more than 30 %, 200 %, and 70 % change in R^2, NSE, and RMSE respectively, see Figure 6-19.

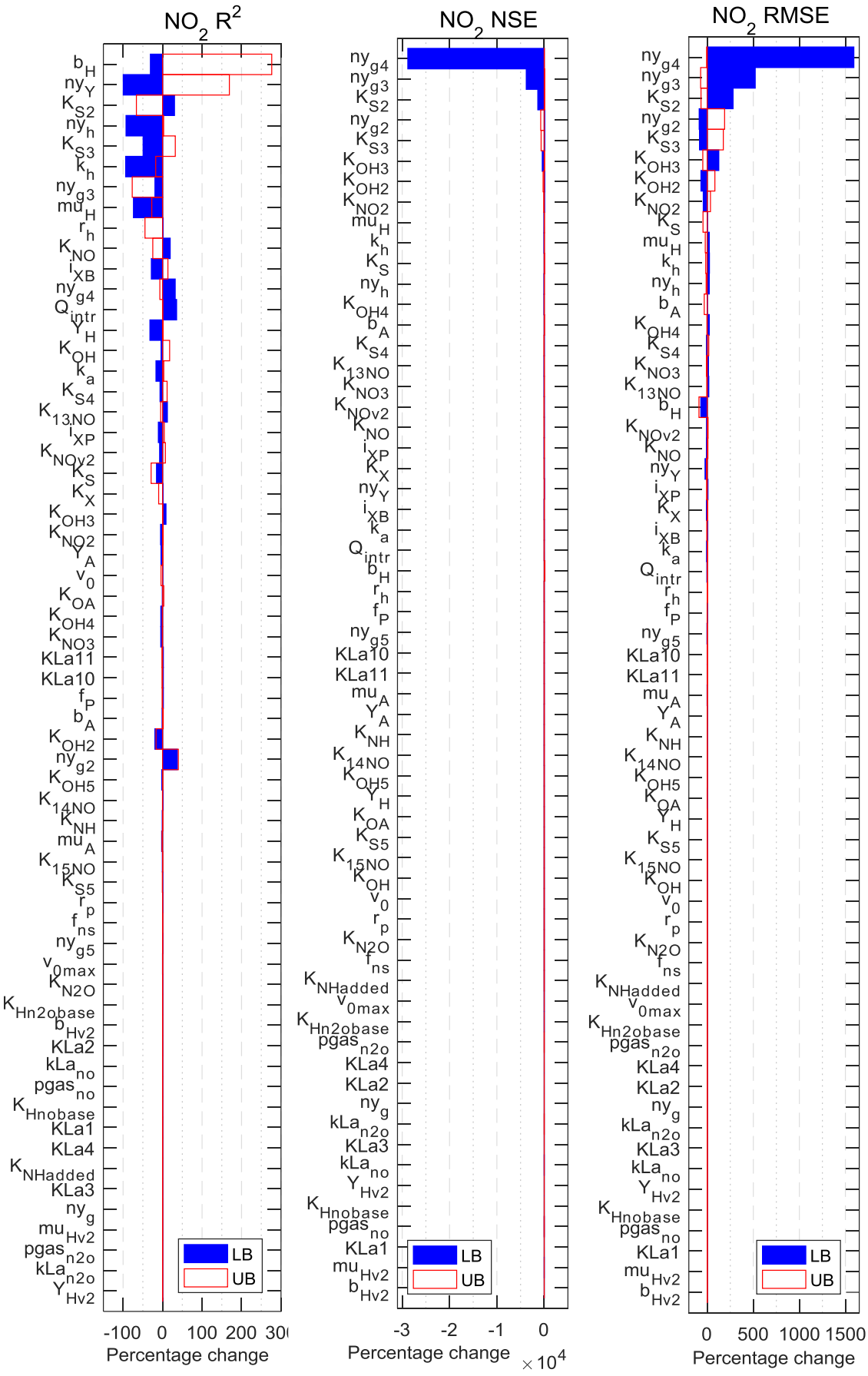

Figure 6-20 OAT results of final effluent NO_2 evaluated using R^2, NSE, and RMSE (left to right)

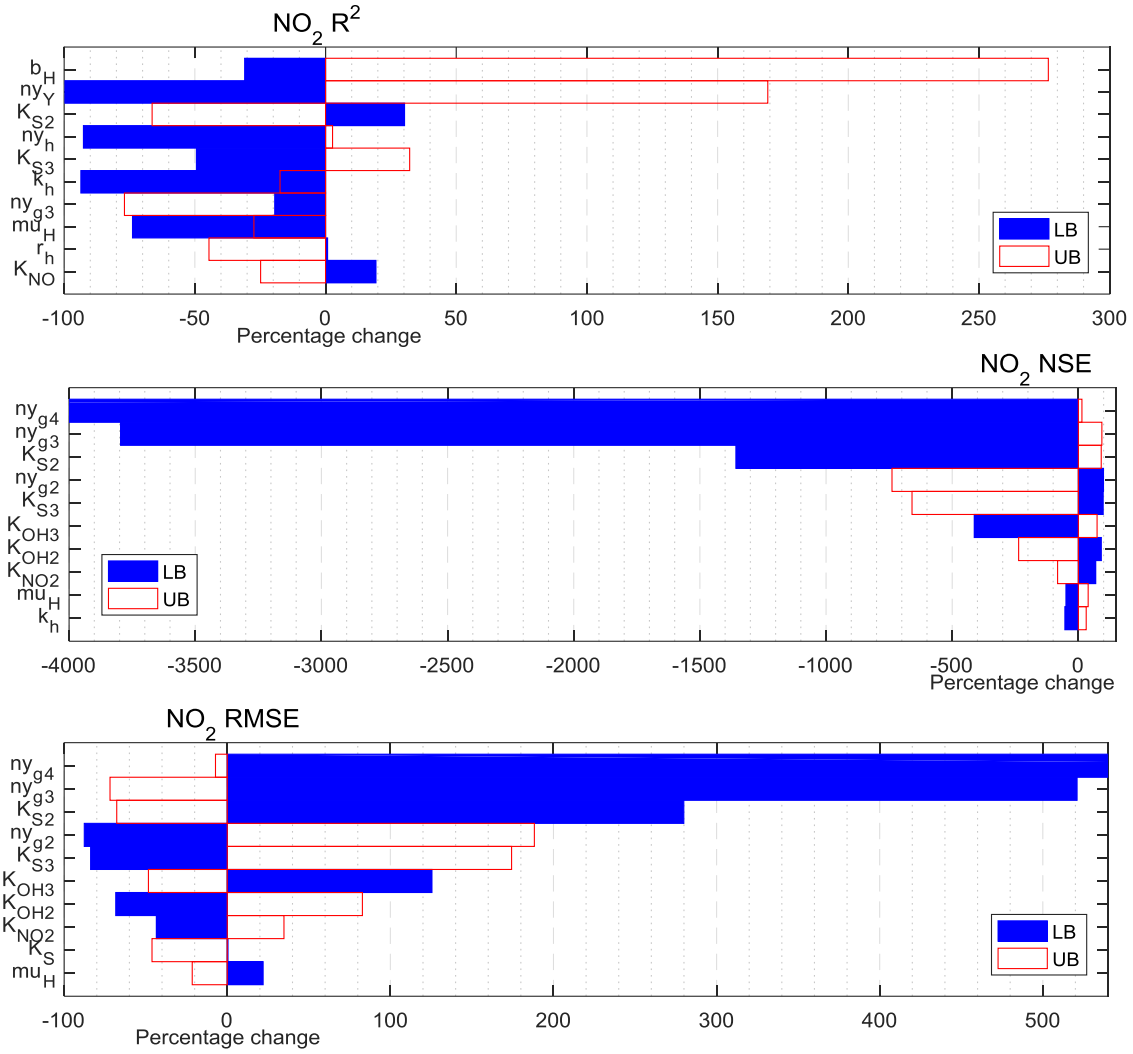

Figure 6-21 Top 10 OAT results of final effluent NO_2 evaluated using R^2, NSE, and RMSE (top to bottom)

The final effluent NO_2 concentration is sensitive to changes in a kinetic parameter such as ny_{g4}, ny_{g3}, K_{S2}, K_{S3}, K_{OH3}, K_{OH2}, and K_{NO2}, see Figure 6-20 and Figure 6-21. Unlike the other quality indicator assessed earlier (final effluent TSS and NO_3), final effluent NO_2 diurnal pattern (as measured by R^2) is mostly influenced by a set of parameters which do not appear in the NSE or RMSE based sensitivity analysis. For example, b_H, n_{yY}, n_{Yh}, and k_h have a very significant impact on the R^2 of the final effluent NO_2, but not on its average value as measured by NSE and RMSE. No stoichiometric parameters show a significant impact on the final effluent NO_2, as indicated by all the goodness-to-fit indicators.

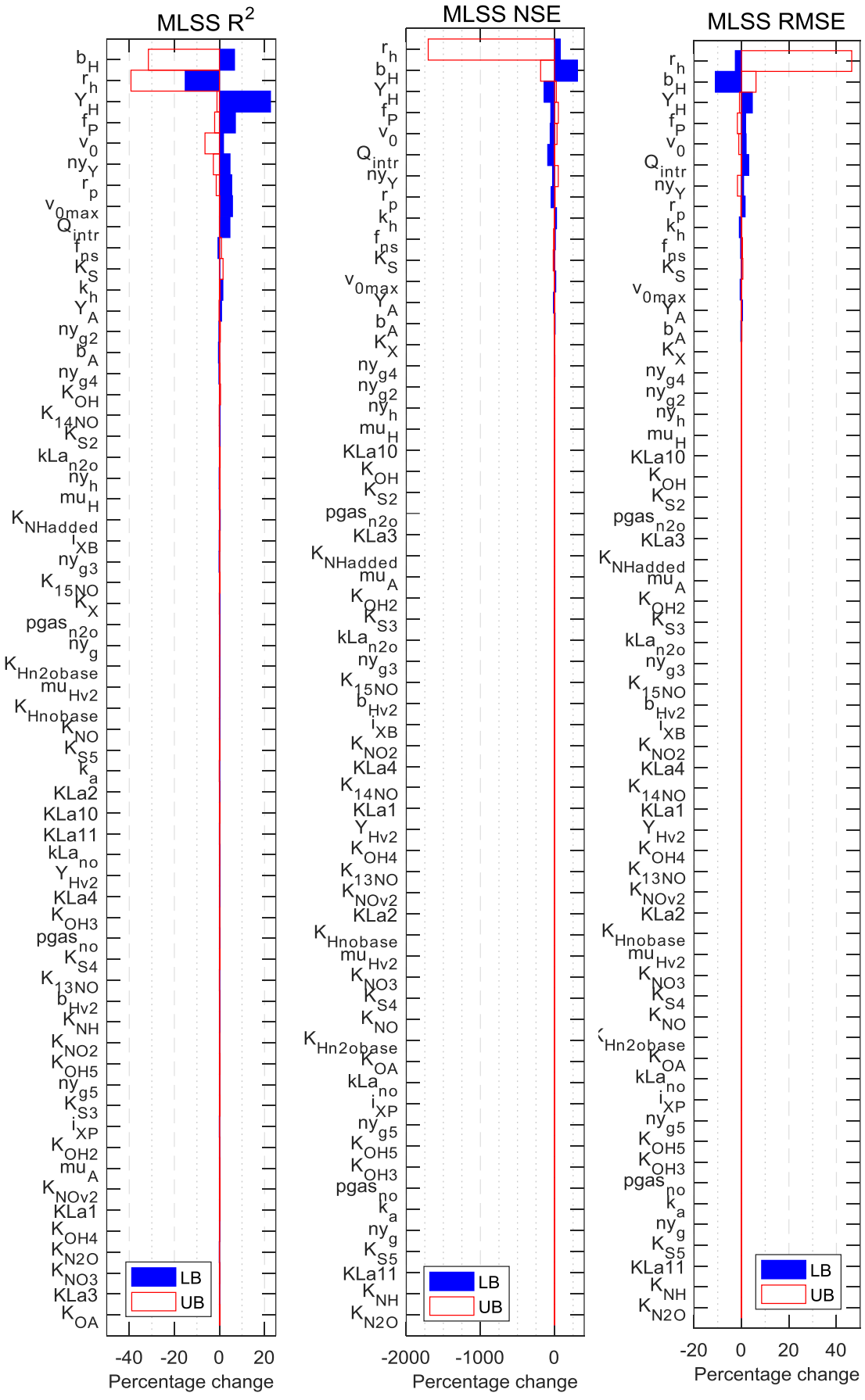

Figure 6-22 OAT results of MLSS in oxidation ditch: evaluated using R^2, NSE, and RMSE (left to right)

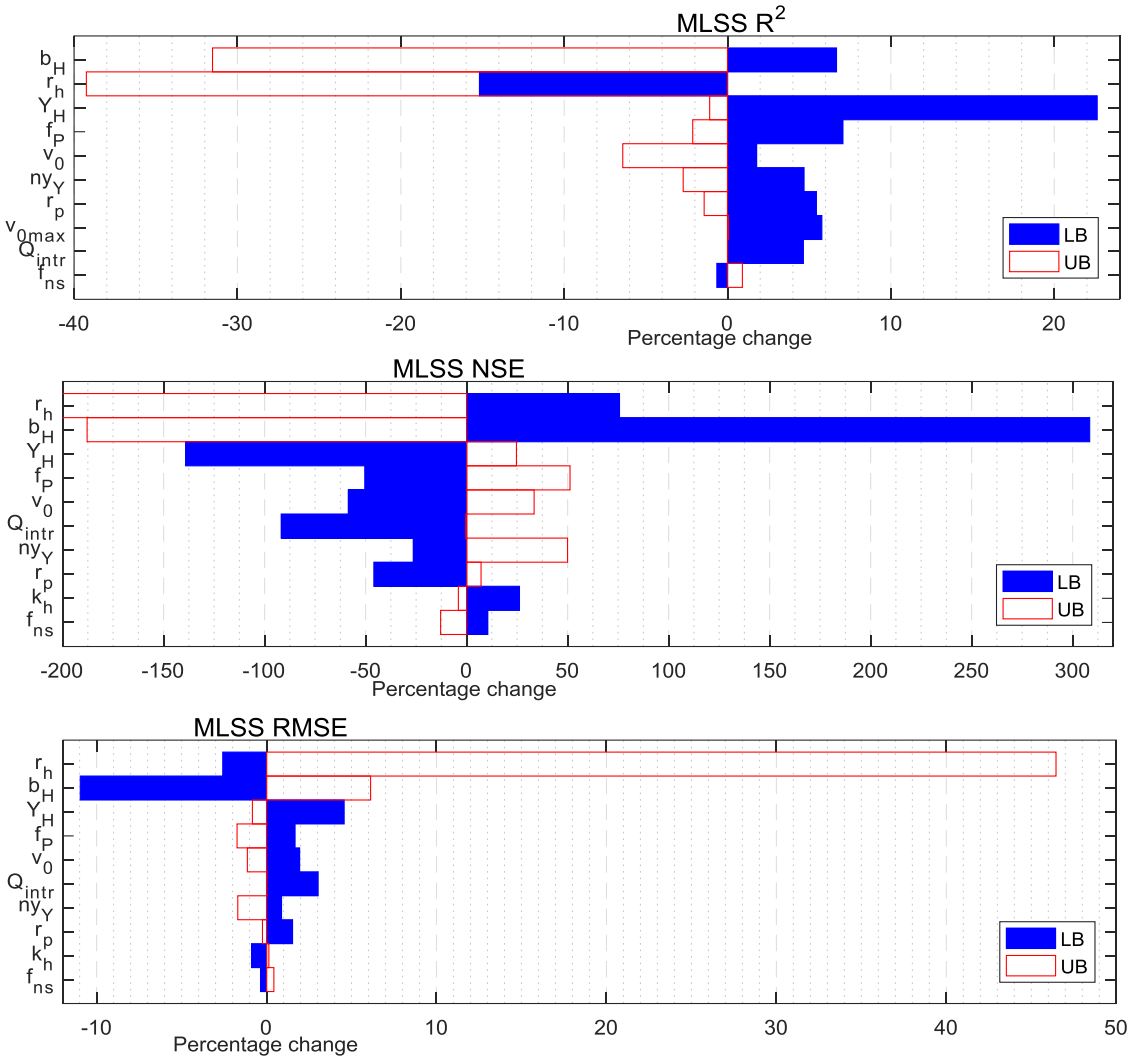

Figure 6-23 Top 10 OAT results of MLSS in oxidation ditch: evaluated using R^2, NSE, and RMSE (top to bottom)

Unlike the final effluent NO_2 concentration, the MLSS's noise and the average value are influenced by similar parameters, see Figure 6-22 and Figure 6-23. The variation in the settler parameter r_h causes the highest variation in MLSS concentration in as measured by all the goodness-to-fit measures. Other settler parameters such as V_0 and r_p show influence on the MLSS. The MLSS is sensitive to kinetic parameters, such as b_H and n_{yY}, and stoichiometric parameters, such as Y_H, f_p, and f_{ns}. The only operational parameter that has a significant impact in the simulation of MLSS is the Q_{intr}, which also has a significant influence on other model outputs such as final effluent NO_3. V_{0max} has a minor impact as measured by R^2, but it does not have a significant impact on the average value of MLSS in the oxidation ditch.

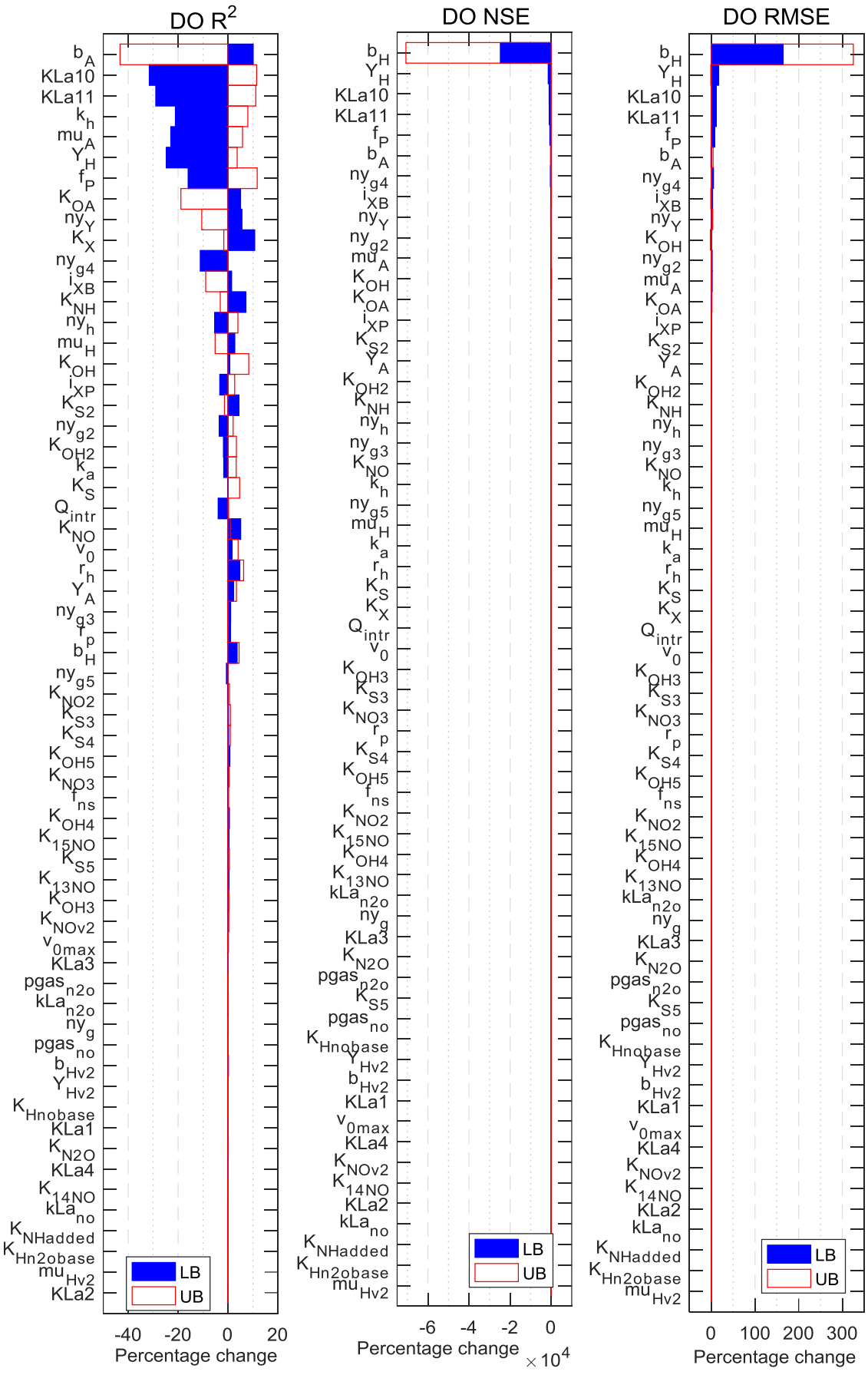

Figure 6-24 OAT results of DO in oxidation ditch: evaluated using R^2, NSE, and RMSE (left to right)

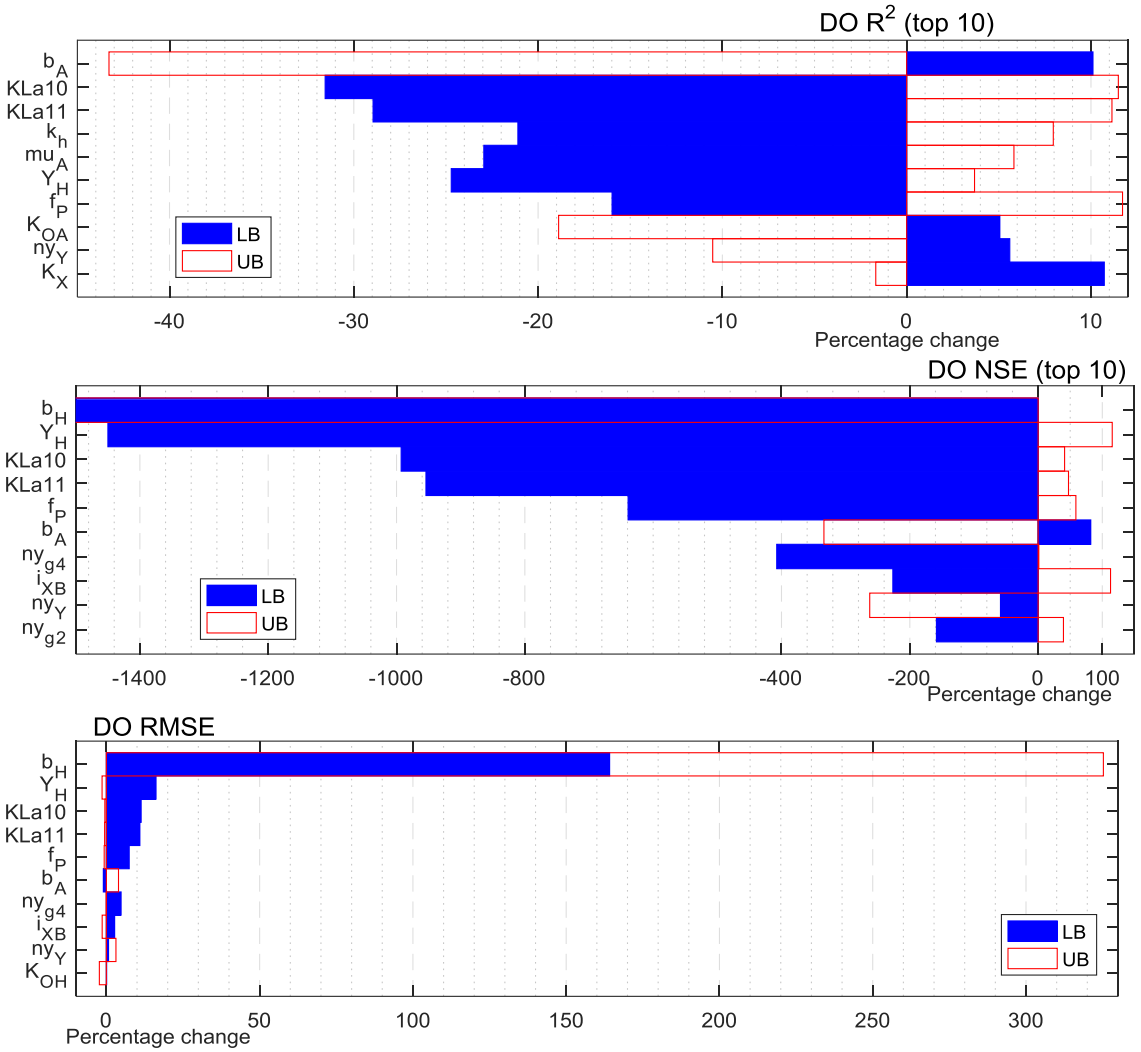

Figure 6-25 Top 10 OAT results of DO in oxidation ditch: evaluated using R^2, NSE, and RMSE (top to bottom)

The DO in the oxidation ditch is found to be sensitive to the kinetic model parameters b_H, b_A, n_{yg4}, and n_{yY} in terms of NSE, and RMSE, see Figure 6-24. The kinetic parameters k_h, m_{uA}, K_{OA}, and K_X affects the DO noise as measured by R^2 but not on the average value of the DO as they sit lower in the rank measured by NSE and RMSE, see Figure 6-25. Stoichiometric parameters Y_H, and f_P affects DO concentration significantly as measured by all the statistical tests. Some stoichiometric parameters such as i_{XB} has a significant impact on the overall DO level as measured by NSE and RMSE but has a less significant impact in terms of diurnal patter (R^2). The only operational parameters that affect the DO level are the kLa values of the last two zones in the oxidation ditch upstream of the DO sensor; kLa10 and kLa11. The settler parameters do not show significant impact on DO level.

6.3.1.1. Parameters Subset Selection for Calibration

In the above discussion, there is no clear boundary in identifying which parameter should be considered for calibration. The ranking was based on the percentage change, which can be very high for some and can be very small for some even if they are on the top of the rank (see the Tornado plots in Figure 6-16 – Figure 6-25). The parameters that cover larger space in the tornado plot are selected for calibration. The selection criteria are designed based on the total percentage difference in the evaluation criteria as shown in Eq. 6-7.

$$R_{j_i} = \left| P_{j_{i,UB}} - P_{j_{i,LB}} \right| \qquad \textit{Eq. 6-7}$$

Where:

- R_{j_i} = Rank based on the difference between percentage change in the j^{th} evaluation criteria with the i^{th} parameter at its lower and upper bound
- $P_{j_{i,LB}}$ = Percentage change in the j^{th} evaluation criteria with the i^{th} parameter at its minimum compared to the base case
- $P_{j_{i,UB}}$ = Percentage change in the j^{th} evaluation criteria with the i^{th} parameter at its maximum compared to the base case

If the parameter has a rank (R_{j_i}) more than 100 %, i.e. the difference in the evaluation criteria at lower and upper bound has more than 100 %; then the parameter is selected for calibration purposes. Based on these criteria the following 26 parameters are selected for calibration purposes, see Table 6-3. These significant parameters showed consistency with previous studies. For example, out of the 26 significant parameters selected here, 12 of them have been tested by Benedetti et al. (2008), out of which 11 of them showed consistency with the result, except K_S, which has a narrower range (5 – 15) in Benedetti et al. (2008). The result also showed consistency with Sweetapple et al. (2013), except the secondary settlement tank parameters, r_h and f_{ns}, mu_H and ny_{g4}. Similarly, the range of parameter values (lower limit and upper limit) are narrower in Sweetapple et al. (2013), and it is not possible to make a direct comparison. In addition, the significant parameters, in this study, are selected based on their influence on specific pollutants unlike the aggregated quality indicator EQI used both in Benedetti et al. (2008) and Sweetapple et al. (2013). Operational parameter Q_{intr} showed a significant influence on affecting the effluent quality and oxidation ditch MLSS level. Showing that it is also important to consider uncertain operational parameters in addition to model parameters.

Table 6-3 Influential model parameters selected for calibration

Para. No.	Parameters for calibration	Default	Lower bound	Upper bound	TSS		NO_3		NO_2		MLSS		DO		EQI	
					R^2	NSE	R^2	NSE	R^2	NSE	R^2	NSE	R^2	NSE	Benedetti et al. (2008)	Sweetapple et al. (2013)
1	mu_H	4	3	13					x	x					y	n
2	K_S	10	5	180			x	x							n	-
3	K_{OH}	0.2	0.1	2			x	x							y	y
5	b_H	0.3	0.05	1.6	x	x	x		x		x	x		x	*-	-
9	b_A	0.05	0.01	0.15				x					x	x	*-	y
12	k_h	3	1.5	4.5	x			x	x	x		x	x		y	y
14	ny_h	0.8	0.4	1.2			x		x			x			y	-
15	Y_H	0.67	0.46	0.69	x	x					x	x	x	x	y	y
17	f_P	0.08	0.04	0.12	x	x					x	x	x	x	y	-
18	i_{XB}	0.08	0.04	0.12			x							x	y	-
23	K_{S2}	20	10	30				x	x	x					-	y
24	K_{S3}	20	10	30					x	x					-	y
28	K_{NO2}	0.2	0.1	0.3						x					-	y
31	K_{OH2}	0.1	0.05	0.15				x		x					-	-
32	K_{OH3}	0.1	0.05	0.15						x					-	-
38	ny_{g2}	0.28	0.14	0.42				x		x				x	-	y
39	ny_{g3}	0.16	0.08	0.24					x	x					-	y
40	ny_{g4}	0.35	0.175	0.525				x		x				x	-	n
42	ny_Y	0.9	0.45	1.35	x	x	x	x			x	x	x	x	-	y
54	kLa10	180	100	240									x	x	-	-
55	kLa11	180	100	240									x	x	-	-
57	v_0	474	237	711	x	x					x	x			y	y
58	r_h	0.0006	0.0003	0.0009	x	x	x		x		x	x			y	n
59	r_p	0.00286	0.00143	0.00429	x	x					x	x			y	y
60	f_{ns}	0.00228	0.00114	0.00342	x	x					x	x			y	n
61	Q_{intr}	904,672	120,336	922,384	x	x	x	x			x	x			-	-

[x] influential model parameter
[n] not influential to EQI based on other studies
[y] influential to EQI based on other studies
[-] sensitivity analysis is not performed
[*-] sensitivity is not done directly but tested as a ratio of biomass growth rate to decay rate

6.4. Model Auto-calibration

However, due to the time-consuming nature of manual calibration especially dealing with many model parameters, automatic model calibration is suggested to fine-tune model accuracy by using uncertain model parameters.

In this auto-calibration exercise the 26 parameters that are identified to most affect the final effluent quality and DO, and MLSS in the OD were selected. The parameters cover all modelling sections; settlers, ASM1 stoichiometric parameters, and Nitrous oxide modelling related stoichiometric parameters, see Table 6-3.

Using all the evaluation criteria used in the sensitivity analysis will end up creating 15 objectives. Running a multi-objective optimisation for 15 objectives is computationally demanding, and the optimisation may not be able to reach to the optimal points easily. A careful investigation of the sensitivity analysis, TSS and MLSS are influenced by the same parameters. Similarly, NO_3 and NO_2 are influenced by the same parameters. Hence, it is possible to reduce the number of objectives without affecting the ultimate result. In addition, NSE and RMSE measure similar kind of variation, and it is possible to drop RMSE without affecting the goal. Therefore, the auto-calibration can run for objectives defined by final effluent TSS and NO_3, and oxidation ditch DO as measured by R^2 and NSE, i.e. a total of six objectives. Still, six objectives are too many for such a computational demanding, complex model with 25 number of parameters selected for calibration. Hence, three different auto-calibration optimisations are run; three objectives using NSE only, three objectives using a factor $R^2 \times$ NSE, and finally using RMSE for the three objectives.

6.4.1. Multi-Objective Optimization Using NSGA-II for Model Calibration

Genetic algorithms (GA) are a metaheuristic search and optimisation approach with a capability of producing high-quality solutions to optimisation and search problems using bio-inspired operators such as mutation, crossover and selection (Mitchell, 1998; Deb, 1999). Multi-objective optimisation using Non-dominated Sorting in Genetic Algorithms (NSGA) is first suggested by Srinivas and Deb (1994), but this approach is computationally demanding and complex, uses non-elitism approach, and it needs the user to specify sharing parameters (Deb et al., 2002). Deb et al. (2002) addressed these issues and proposed a faster and more efficient Non-dominated Sorting GAs (NSGA-II) (Jensen, 2003).

The effectiveness and efficiency of NSGA-II in solving multi-objective optimisation problems in the urban wastewater system have been demonstrated by Fu et al. (2008); Fu et al. (2009); Sweetapple et al. (2014), and Iqbal and Guria (2009). The capability of NSGA-II multi-optimisation approach applied to model auto-calibration has been demonstrated by Azari and Asadi (2017); Ercan and Goodall (2016), and Bekele and Nicklow (2007). Although NSGA-II is widely used in hydrological and catchment-based models auto-calibration, its application in the auto-calibration of WWTP is limited.

Based on its efficiency and ease to use, the NSGA-II multi-optimisation approach (Deb et al., 2002) is used in this instance. The MATLAB® implementation of the approach proposed by Seshadri (2009) is adopted in this study. The details on population initialisation, non-dominated sort, crowding distance, selection, genetic operators (such as simulated binary crossover and polynomial mutation), recombination and selection can be found in Seshadri (2009).

The auto-calibration problem is formulated by using *n* calibration parameters identified using sensitivity analysis, see Section 6.3.1.1 and Table 6-3.

$$X = [x_1, x_2, \ldots, x_n] \qquad \textit{Eq. 6-8}$$

The auto-calibration problem is formulated as a minimisation problem shown in Eq. 6-9.

$$Min\ F(X) = \{f_1(X), \ldots, f_m(X)\}, \quad X \in (\mathrm{L}, \mathrm{U}) \qquad \textit{Eq. 6-9}$$

Where x is the calibration parameter, and L and U are the vector of lower and upper bounds of x respectively. (L, U) defines the region restricted by $l_i \leq x_i \leq u_i$ where l_i, u_i, and x_i is the element of L, U, and X for $i = 1, 2, \ldots, n$. The assumption here is that the bounded region defined by the lower and the upper bounds has an intersection with the feasible solution space. The objective functions $f(X)$ are those objectives defined using the goodness-to-fit measures for the quality indicators, where m is the number of objectives. The goodness-to-fit measures, NSE and R^2, are modified to fit the minimization problem by multiplying them with a negative number because in effect we want to maximise NSE and R^2 (ideally near to one). In the case of RMSE, there is no need to multiply the objective by negative as the objective is to minimise RMSE.

NSGA-II is implemented as follows:

i. Population with random values for n individuals is initialised from the (L, U) array
ii. Objective values calculated for the initial population

iii. The initial population is sorted based on a fast non-domination algorithm (Deb et al., 2002)
iv. Since individuals are selected based on rank and crowding distance, once the sorting is completed, the crowding distance is assigned (Seshadri, 2009)
v. Individuals are selected using the non-domination rank and crowding distance
vi. Offspring population is generated using simulated binary crossover followed by polynomial mutation (Deb et al., 2002)
vii. Selection to form the next generation is performed once the offspring population is combined with the current generation population
viii. The above four procedures are repeated for the number of generations specified prior.

In this instance, 100 population size is chosen based on simulation speed and number of parameters for calibration. A crossover probability of 60 % is chosen, i.e. 60 % of the offspring in a population are made by crossover. A mutation probability of 20 % was used to determine part of the chromosome that will go under changes.

The solutions from the last generation from the NSGA-II may not be the true Pareto-front. Hence to aid the selection of best solutions from the last generation of the final population a simple hyper-grid-based scheme was used once optimisation runs are completed. The hyper-grid based selection in Pareto Envelope-based Selection Algorithm (PESA) (Corne et al., 2000) is adopted here. This selection is designed for two most desirable objectives which are determined based on the assessment of individual generation. The sorting is done in descending order of the values of the first objective in the last generation. The selection of Pareto-front is made based on the second objective in the assorted array as follows. If the second objective is greater than all the underneath second objectives in the array $\left(if\ f_2(X_j) \geq f_2(X_{j+1}), f_2(X_{j+2}), \ldots, f_2(X_t) \right)$, then solution j is dominant and will be selected, else solution j is not dominant and will be eliminated. t is the number of population in a generation, in this instance $t = 100$. The red dots in the final results show the solutions selected from the last generation using this hyper-grid-based selection algorithm.

6.4.2. Auto-calibration Results Using Three Objectives: NSE

In this auto-calibration, the simulated DO in the oxidation ditch, TSS, and NO_3 in the final effluent from the WWTP model were compared against the measured using NSE

as a goodness-of-fit measure. A population size of 100 and a total number of 62 generations were used in the NSGA-II auto-calibration runs. The following results are found. The red dots are the Pareto-front envelope selected based on the hyper-grid scheme using NSE for DO and NSE for NO_3. The two objectives are shown since the third objective, NSE of TSS has relatively a better performance than the two, i.e. majority of the NSE in simulating final effluent TSS are above zero. The top two figures showed the results from the last generation of auto-calibration results. The figure below them showed the top results (right corner of colour map chart) by avoiding very low values of NSE for final effluent NO_3, i.e. results are limited to NSE values between -1 and 0.5 for final effluent NO_3.

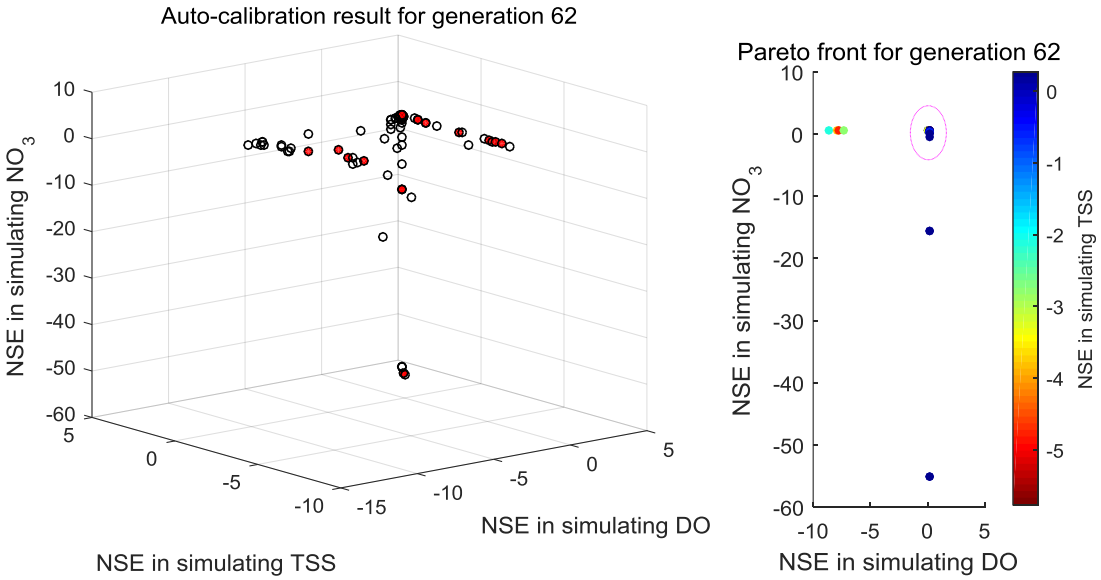

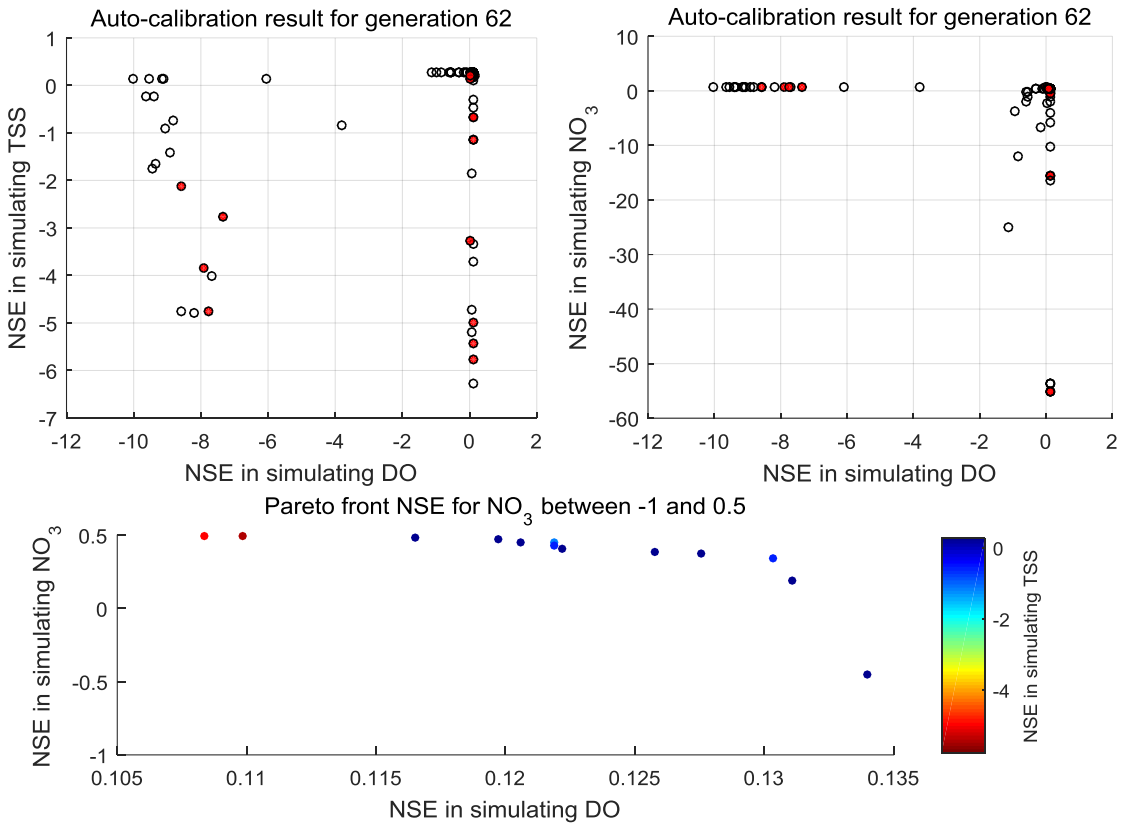

Figure 6-26 Auto-calibration results using three objectives: NSE of final effluent TSS, NO_3 and DO level of the oxidation ditch

The highest NSE values for the DO in the oxidation are mostly coupled with very low NSE values for NO_3 of the final effluent. Three solutions from the Pareto-front are selected with high NSE values for DO, and relatively higher NSE for NO_3 and TSS in the final effluent see Table 6-4. The twelfth solution, Table 6-4, has a better combination of parameter values to give a satisfactory model accuracy in most of the objectives.

Table 6-4 Parameter values and multi-objective optimisation objectives (NSE in simulating DO, TSS, and NO_3) from the Pareto-front selected using NSE in simulating DO and NO_3

																									NSE		
No.	Mu_H	K_S	K_{OH}	b_H	b_A	ny_h	Y_H	f_P	i_{XB}	K_{S2}	K_{S3}	K_{NO2}	K_{OH2}	K_{OH3}	ny_{g2}	Ny_{g3}	Ny_{g4}	Ny_Y	kLa_{10}	kLa_{11}	v_0	r_h	r_p	f_{ns}	Q_{intr}	DO	TSS	NO_3
1	8.9	85	0.71	0.87	0.103	0.7	0.52	0.083	0.058	16	20.2	0.22	0.09	0.1	0.29	0.19	0.37	0.66	185	179	461	0.00052	0.0032	0.0023	212327	-8.6	-2.1	0.63
2	8.9	107	0.74	0.87	0.103	0.86	0.54	0.083	0.055	15.7	19.8	0.22	0.09	0.14	0.28	0.21	0.44	0.7	168	178	459	0.00054	0.003	0.0024	211735	-7.9	-3.9	0.61
3	8.9	120	0.75	0.87	0.102	0.86	0.53	0.083	0.058	16	20.4	0.22	0.09	0.14	0.28	0.2	0.44	0.7	162	179	459	0.00054	0.0029	0.0024	211657	-7.8	-4.7	0.6
4	8.9	92	0.73	0.87	0.103	0.88	0.54	0.083	0.055	15.9	20.4	0.22	0.09	0.14	0.28	0.19	0.35	0.69	166	172	460	0.00052	0.003	0.0023	212108	-7.4	-2.8	0.6
5	3	84	0.65	0.3	0.106	0.83	0.66	0.071	0.086	13.7	24	0.19	0.08	0.09	0.23	0.18	0.37	1.24	226	163	506	0.00058	0.0037	0.002	596925	0	0.22	0.58
6	3	84	0.65	0.29	0.106	0.81	0.66	0.071	0.086	13.7	24	0.19	0.08	0.09	0.23	0.18	0.33	1.24	200	163	506	0.00058	0.0034	0.002	596925	0.03	0.15	0.58
7	5.5	84	0.55	0.31	0.108	0.55	0.65	0.075	0.091	17.4	20.9	0.19	0.08	0.09	0.25	0.18	0.4	1.32	230	169	575	0.00059	0.0025	0.0024	728417	0.03	-3.3	0.53
8	6.3	79	0.66	0.32	0.033	0.58	0.66	0.091	0.082	23	21	0.17	0.1	0.09	0.3	0.14	0.48	1.33	198	158	353	0.0007	0.0034	0.0023	587448	0.1	-5.8	0.53
9	4.6	92	0.64	0.32	0.032	0.9	0.63	0.093	0.081	18.3	19.9	0.16	0.1	0.09	0.23	0.19	0.32	1.34	194	183	359	0.00061	0.0034	0.0024	637504	0.11	-5	0.5
10	6.1	118	0.55	0.32	0.018	0.87	0.65	0.093	0.087	23	12.7	0.15	0.09	0.09	0.23	0.19	0.37	1.33	158	182	361	0.0006	0.0035	0.0025	594656	0.11	-5.4	0.5
11	4.4	92	1.08	0.33	0.031	0.85	0.63	0.091	0.085	18.3	19.6	0.16	0.1	0.11	0.26	0.18	0.34	1.35	192	183	482	0.00046	0.0035	0.002	637504	0.12	0.23	0.48
12	6.5	118	0.43	0.33	0.02	0.82	0.65	0.1	0.066	23	14.9	0.15	0.09	0.08	0.24	0.15	0.39	1.34	171	169	535	0.00044	0.0035	0.002	486231	0.12	0.25	0.47
13	4.7	107	0.86	0.34	0.031	0.85	0.63	0.088	0.085	18.3	19.3	0.17	0.1	0.11	0.23	0.18	0.33	1.34	208	183	516	0.00039	0.0034	0.002	637504	0.12	0.25	0.46
14	6.5	118	0.41	0.33	0.018	0.87	0.65	0.1	0.087	23	12.7	0.15	0.09	0.09	0.23	0.15	0.37	1.33	158	174	473	0.00044	0.0035	0.0025	486231	0.12	-1.2	0.45
15	4.4	92	1.08	0.3	0.032	0.9	0.63	0.091	0.097	17.3	19.1	0.16	0.09	0.1	0.2	0.18	0.33	1.34	186	179	472	0.00046	0.0033	0.0023	590207	0.12	-0.7	0.43
16	5	94	0.74	0.33	0.032	0.88	0.64	0.096	0.084	18.3	20.7	0.18	0.1	0.09	0.22	0.14	0.4	1.35	199	157	573	0.00046	0.0032	0.002	583450	0.12	0.27	0.41
17	5.1	109	0.58	0.33	0.018	0.87	0.64	0.1	0.087	19.7	23	0.15	0.1	0.09	0.22	0.13	0.32	1.35	184	154	492	0.00045	0.0034	0.002	582207	0.13	0.23	0.38
18	5.5	95	0.68	0.32	0.032	0.83	0.64	0.097	0.089	20.2	22.8	0.2	0.1	0.09	0.22	0.16	0.41	1.35	197	160	554	0.00049	0.0031	0.0021	600479	0.13	0.2	0.38
19	4.4	92	1.08	0.31	0.032	0.9	0.63	0.085	0.1	16.3	19.1	0.16	0.09	0.1	0.2	0.18	0.33	1.34	186	175	472	0.00046	0.0033	0.0023	445825	0.13	-0.7	0.34
20	5.4	96	0.74	0.33	0.025	0.86	0.64	0.095	0.089	20.8	25.6	0.18	0.1	0.09	0.23	0.14	0.39	1.35	196	154	566	0.00048	0.0032	0.002	431364	0.13	0.27	0.19
21	4.8	109	0.8	0.34	0.021	0.83	0.63	0.082	0.101	17.5	20.8	0.16	0.09	0.11	0.23	0.2	0.37	1.34	217	169	554	0.0004	0.0034	0.0021	607439	0.13	0.24	-0.5
22	7.8	109	1.07	0.34	0.03	0.83	0.6	0.078	0.093	19.9	20.8	0.21	0.1	0.11	0.24	0.21	0.37	1.34	217	169	554	0.0004	0.0034	0.0021	628182	0.14	0.24	-15
23	7.8	109	1.07	0.34	0.03	0.83	0.6	0.078	0.093	19.9	22.6	0.21	0.1	0.11	0.24	0.21	0.37	1.34	217	169	554	0.0004	0.0034	0.0021	628182	0.14	0.24	-16
24	7.4	126	1.44	0.6	0.014	0.82	0.59	0.103	0.06	16.4	22.8	0.22	0.1	0.13	0.24	0.21	0.38	0.68	190	181	517	0.0004	0.0034	0.0022	520401	0.14	0.17	-55
25	7.4	126	1.44	0.6	0.014	0.82	0.59	0.1	0.06	16.1	23.1	0.22	0.1	0.13	0.24	0.17	0.38	0.68	190	181	552	0.00046	0.0033	0.0022	601062	0.14	0.2	-55

6.4.2.1. Using Solution-12:

WWTP model runs using solution-12, and the model accuracy in estimating other objectives that are not used in the auto-calibration optimisation problems are assessed below. This includes MLSS, DO, TSS, NO_3 and NO_2. solution-5 and solution-17 didn't give a better result compare to solution-12 and are not discussed further.

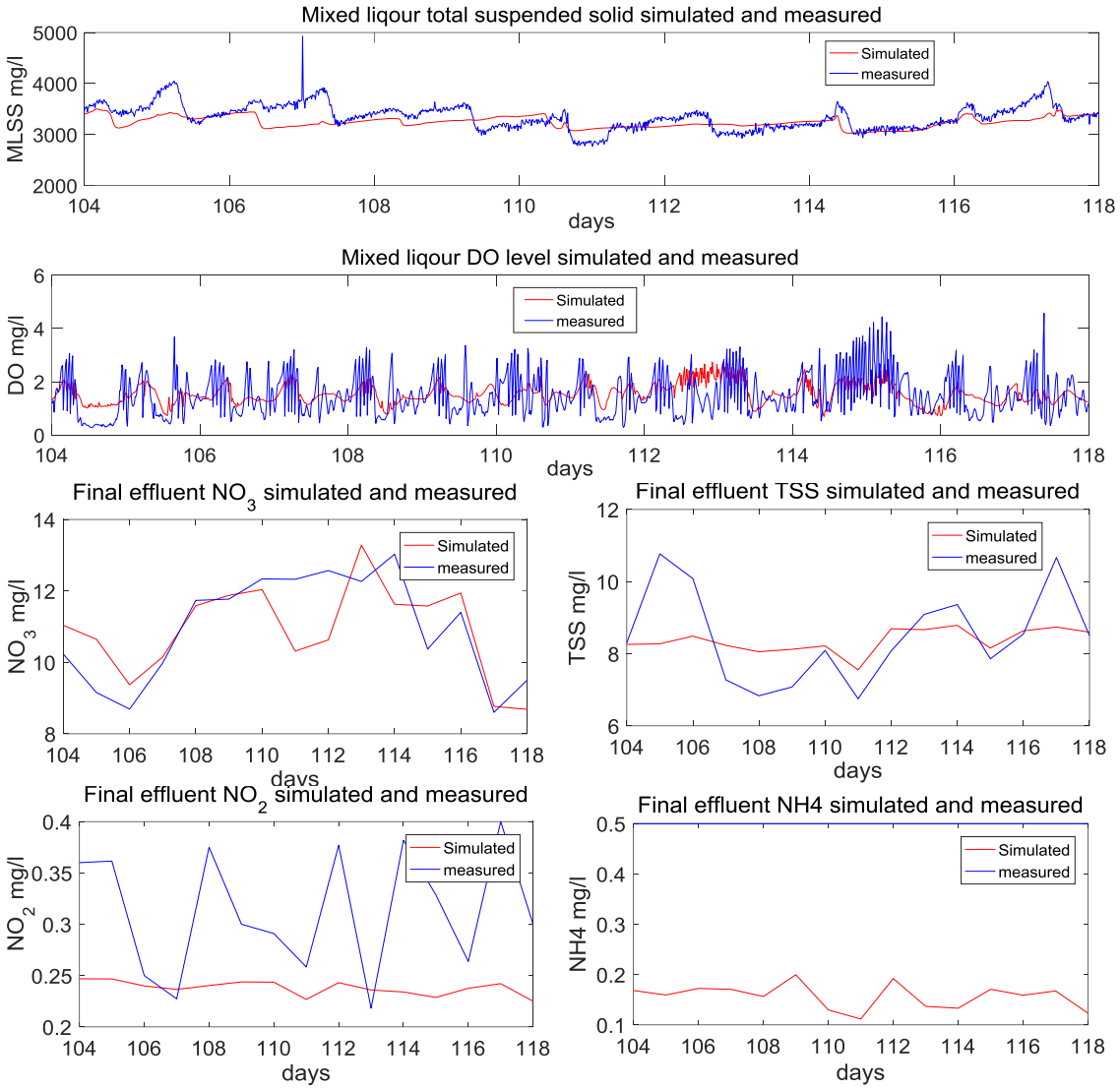

Figure 6-27 Comparison of simulated (NSE for calibration) and measured dataset during the calibration period: MLSS, DO, NO_3, TSS, NO_2 and NH_4 (top to bottom)

Table 6-5 Model accuracy using the twelfth solution of the pareto front (NSE for calibration)

Twelfth solution	R^2	NSE	RMSE
MLSS oxidation ditch	0.24	0.06	227
DO oxidation ditch	0.14	0.12	0.7
TSS final effluent	0.4	0.25	1.08
NO_3 final effluent	0.5	0.47	1.06
NO_2 final effluent	0.12	-1.56	0.09

6.4.3. Auto-calibration Results Using Three Objectives: NSE×R^2

In this auto-calibration, the DO in the oxidation ditch, TSS in the final effluent, and NO_3 in the final effluent were compared against the measured using statistical goodness of fit measure Nash-Sutcliffe coefficient (NSE) and the coefficient of determination (R^2). The product of this two goodness of fit measures was used to reduce number objectives from six to three, which will ultimately reduce the total auto-calibration time. A population size of 100 and a total number of 59 generations were used in the NSGA auto-calibration runs. The following results were found. The pareto-front, (red dots) for DO and NO_3 is used to select the good solutions from the last generation.

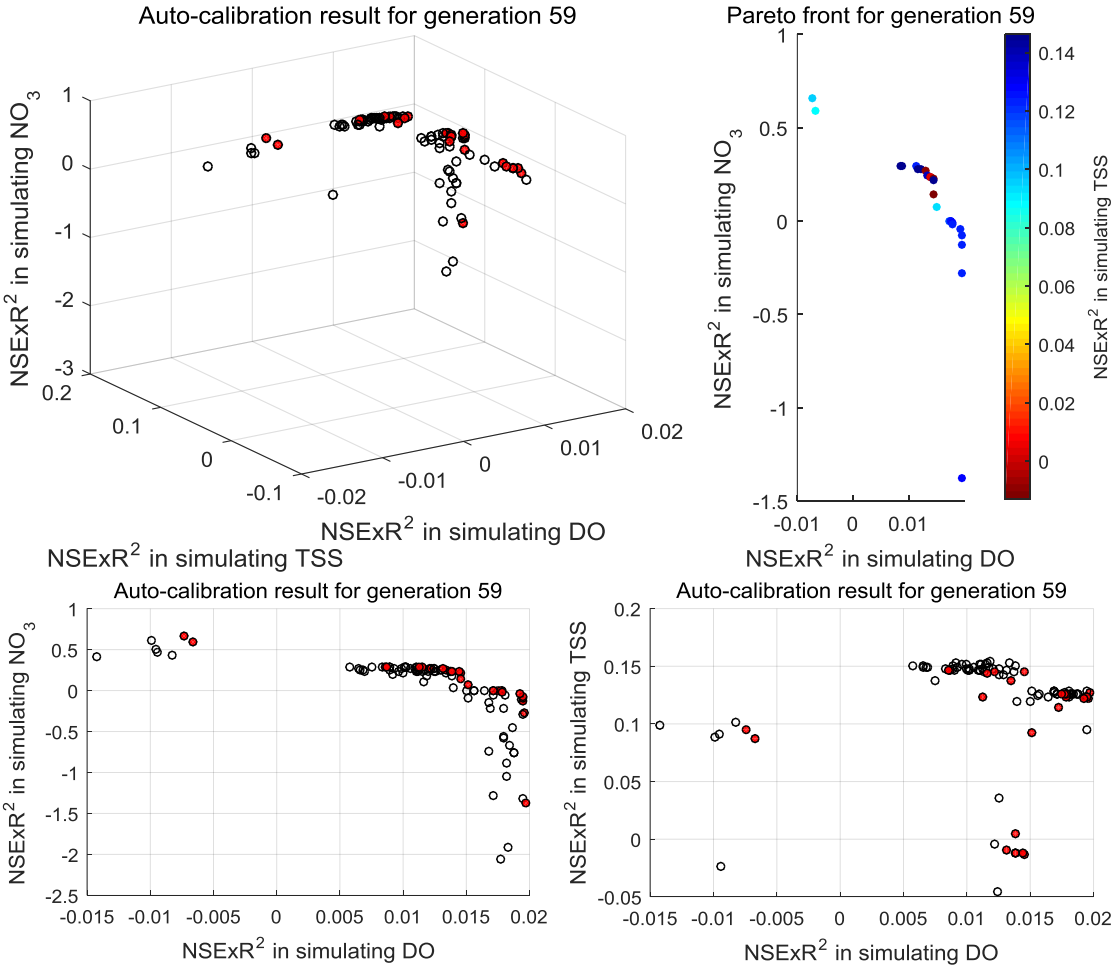

Figure 6-28 Auto-calibration results using three objectives: the product of NSE and R^2 of final effluent TSS, NO_3 and DO level of the oxidation ditch

The pareto-front selection showed that there are good model results in simulating the NO_3 with the expense of accuracy in DO, and a slight compromise in TSS simulation accuracy. The pareto-front selection gives 25 good answers, see Table 6-6. Solution 1, 3, 9, and 13 are assessed by calculating model accuracies of the other quality indicators. Solution 9 is presented in sec. 6.4.3.1.

Table 6-6 Parameter values and multi-objective optimisation objectives (the product of NSE and R^2 in simulating DO, TSS, and NO_3) from the Pareto-front selected using the product of NSE and R^2 in simulating DO and NO_3

																									NSE × R^2		
No.	Mu_H	K_S	K_{OH}	b_H	b_A	ny_h	Y_H	f_P	i_{XB}	K_{S2}	K_{S3}	K_{NO2}	K_{OH2}	K_{OH3}	ny_{g2}	Ny_{g3}	Ny_{g4}	Ny_Y	kLa_{10}	kLa_{11}	v_0	r_h	r_p	f_{ns}	Q_{intr}	DO	TSS	NO_3
1	6.4	104	1.23	0.69	0.148	0.73	0.58	0.088	0.055	14	15.3	0.17	0.08	0.12	0.27	0.17	0.35	1.35	140	134	572	0.00053	0.0033	0.0021	563961	-0	0.1	0.66
2	6.2	98	1.42	0.69	0.148	0.7	0.59	0.061	0.055	14.1	15.4	0.2	0.09	0.09	0.27	0.16	0.33	1.35	166	134	564	0.00053	0.0033	0.0021	554041	-0	0.09	0.59
3	8	109	1.38	0.34	0.034	0.76	0.67	0.093	0.076	17.7	14.9	0.17	0.1	0.11	0.2	0.2	0.32	1.35	162	136	596	0.00062	0.0035	0.0022	495065	0.01	0.15	0.3
4	8	110	1.48	0.34	0.038	0.73	0.67	0.093	0.076	14.9	14.7	0.18	0.09	0.11	0.19	0.2	0.32	1.35	168	138	605	0.00062	0.0035	0.0022	499507	0.01	0.15	0.29
5	6.6	110	1.24	0.33	0.027	0.75	0.67	0.094	0.072	13.7	15.3	0.2	0.09	0.09	0.22	0.2	0.32	1.35	163	143	606	0.00074	0.0037	0.0022	557292	0.01	0.12	0.29
6	8.1	109	1.4	0.34	0.025	0.82	0.67	0.094	0.065	16.3	15.1	0.16	0.09	0.11	0.2	0.2	0.32	1.35	168	128	611	0.00061	0.0036	0.0022	439325	0.01	0.14	0.28
7	8.2	109	1.34	0.34	0.031	0.8	0.67	0.093	0.067	15.4	15.5	0.16	0.1	0.11	0.19	0.2	0.31	1.35	164	143	595	0.00062	0.0035	0.0022	520365	0.01	0.15	0.28
8	7.9	108	1.38	0.34	0.012	0.77	0.67	0.087	0.063	14.6	15.8	0.18	0.09	0.11	0.22	0.2	0.31	1.35	164	143	607	0.00062	0.0035	0.0024	410157	0.01	-0	0.27
9	7.8	109	1.34	0.34	0.031	0.75	0.67	0.089	0.058	15	15.5	0.18	0.1	0.11	0.21	0.2	0.31	1.35	169	139	647	0.00062	0.0035	0.0022	579649	0.01	0.14	0.25
10	8.2	109	1.34	0.34	0.03	0.77	0.67	0.089	0.058	15.4	15.5	0.18	0.1	0.11	0.21	0.2	0.31	1.35	164	143	595	0.00062	0.0035	0.0024	579649	0.01	-0	0.24
11	8.2	109	1.25	0.34	0.028	0.77	0.67	0.09	0.056	15.5	15.3	0.18	0.1	0.11	0.21	0.2	0.32	1.35	165	142	603	0.00062	0.0035	0.0024	579649	0.01	0	0.23
12	8.2	108	1.34	0.34	0.03	0.77	0.67	0.089	0.056	15.4	15.5	0.18	0.1	0.11	0.21	0.2	0.31	1.35	164	143	595	0.00062	0.0035	0.0024	579649	0.01	-0	0.23
13	8.3	109	1.36	0.34	0.018	0.77	0.67	0.089	0.057	14.3	15.2	0.17	0.09	0.11	0.2	0.2	0.31	1.35	164	144	604	0.00062	0.0035	0.0022	598394	0.02	0.15	0.22
14	8.2	108	1.34	0.34	0.03	0.77	0.68	0.089	0.056	15.4	15.5	0.18	0.1	0.11	0.21	0.2	0.31	1.35	164	143	595	0.00062	0.0035	0.0024	579649	0.02	-0	0.15
15	7	110	1.5	0.35	0.011	0.76	0.67	0.092	0.05	13.6	14.6	0.16	0.07	0.1	0.26	0.2	0.35	1.35	170	122	609	0.00051	0.0032	0.0022	548772	0.02	0.09	0.08
16	7.2	126	1.48	0.39	0.01	0.76	0.67	0.091	0.051	15.6	16.1	0.17	0.08	0.09	0.28	0.19	0.32	0.75	174	130	600	0.0005	0.0036	0.0023	518124	0.02	0.12	0
17	7.7	120	1.5	0.39	0.014	0.8	0.68	0.096	0.045	15.1	15.4	0.17	0.08	0.11	0.27	0.2	0.31	0.8	176	117	612	0.00052	0.0036	0.0023	419866	0.02	0.13	0
18	7.8	110	1.63	0.38	0.021	0.73	0.67	0.094	0.046	14.9	13.7	0.17	0.07	0.11	0.27	0.2	0.3	0.79	173	128	611	0.00051	0.0036	0.0023	430861	0.02	0.13	0
19	7.8	111	1.77	0.38	0.01	0.76	0.67	0.096	0.045	15.9	13.6	0.17	0.08	0.1	0.27	0.2	0.3	0.86	167	130	616	0.00051	0.0036	0.0023	437964	0.02	0.13	-0
20	7.3	106	1.49	0.39	0.022	0.73	0.67	0.096	0.044	16.2	18.7	0.13	0.07	0.11	0.28	0.19	0.3	0.78	170	138	626	0.0005	0.0036	0.0023	534056	0.02	0.12	-0
21	7.1	106	1.49	0.39	0.015	0.73	0.67	0.096	0.041	15.9	18.8	0.15	0.07	0.1	0.28	0.19	0.3	0.78	170	138	626	0.0005	0.0036	0.0023	534056	0.02	0.12	-0
22	7.3	106	1.49	0.39	0.014	0.73	0.67	0.096	0.041	16.2	18.7	0.13	0.07	0.1	0.28	0.21	0.3	0.78	170	138	626	0.0005	0.0036	0.0023	534056	0.02	0.12	-0.1
23	7.3	106	1.49	0.39	0.014	0.73	0.67	0.096	0.041	16.2	18.7	0.13	0.07	0.1	0.28	0.21	0.3	0.78	170	138	626	0.0005	0.0036	0.0023	534056	0.02	0.12	-0.1
24	7.1	110	1.62	0.39	0.015	0.73	0.66	0.096	0.042	14.7	12.7	0.15	0.07	0.11	0.27	0.2	0.3	0.87	170	138	615	0.0005	0.0036	0.0023	425352	0.02	0.12	-0.3
25	7.7	108	1.52	0.38	0.014	0.8	0.67	0.096	0.043	15.9	15.4	0.17	0.07	0.11	0.27	0.2	0.28	0.87	173	137	598	0.00052	0.0036	0.0023	348333	0.02	0.13	-1.4

6.4.3.1. Using Solution 9:

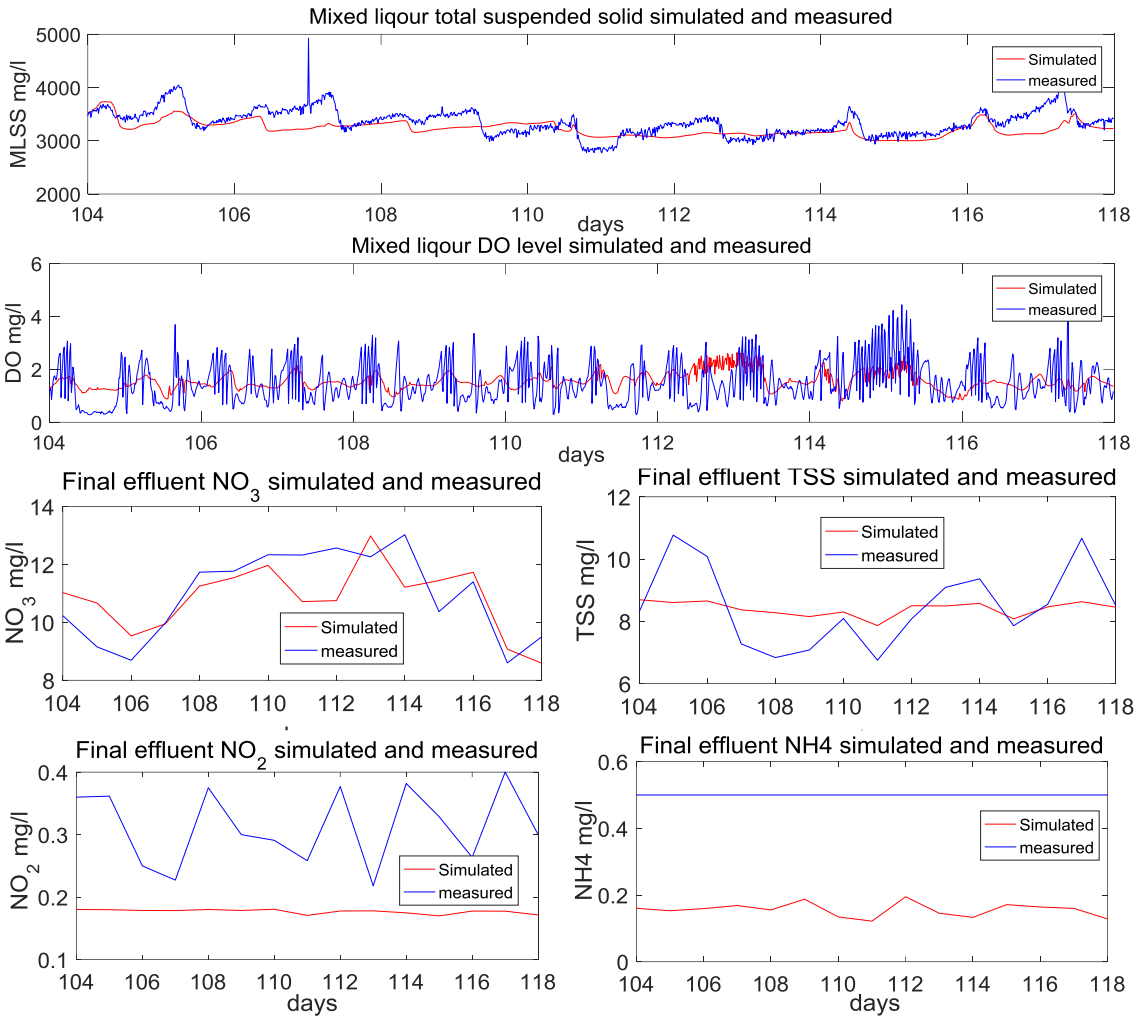

Figure 6-29 Comparison of simulated (the product of NSE and R^2 for calibration) and measured dataset during the calibration period: MLSS, DO, NO_3, TSS, NO_2 and NH_4 (top to bottom)

Table 6-7 Model accuracy using the 9th solution of the pareto front (the product of NSE and R^2 for calibration)

Ninth solution	R^2	NSE	RMSE
MLSS oxidation ditch	0.29	0.08	224
DO oxidation ditch	0.12	0.11	0.71
TSS final effluent	0.58	0.24	1.09
NO_3 final effluent	0.5	0.49	1.03
NO_2 final effluent	0.01	-5.35	0.15

The auto-calibration using the product of NSE and R^2 gave a better solution at a fewer number of generations compared to the auto-calibration using only NSE. Solution 9, for example, shown in Figure 6-29 and Table 6-7, have a better NSE and R^2 for final effluent TSS and NO_3, and MLSS in the oxidation ditch except a slight reduction in accuracy in simulating DO. Solution 9 stands to be the best solution based on its better estimation of final effluent concentration with minor compromise to DO compare solutions from Section 6.4.2.

6.4.4. Auto-calibration Results Using Three Objectives: RMSE

In this auto-calibration exercise, the DO in the oxidation ditch, TSS, and NO_3 in the final effluent were compared against the measured using statistical goodness of fit measure of Root-Mean-Square-Error (RMSE). A population size of 100 and a total number of 74 generations were used in the multi-objective genetic algorithm auto-calibration runs. The results are presented in Figure 6-30 show the calibration results with the red dots showing the pareto front based on final effluent NO_3 and DO level in the oxidation ditch. 24 solutions were found, which are presented in Table 6-8.

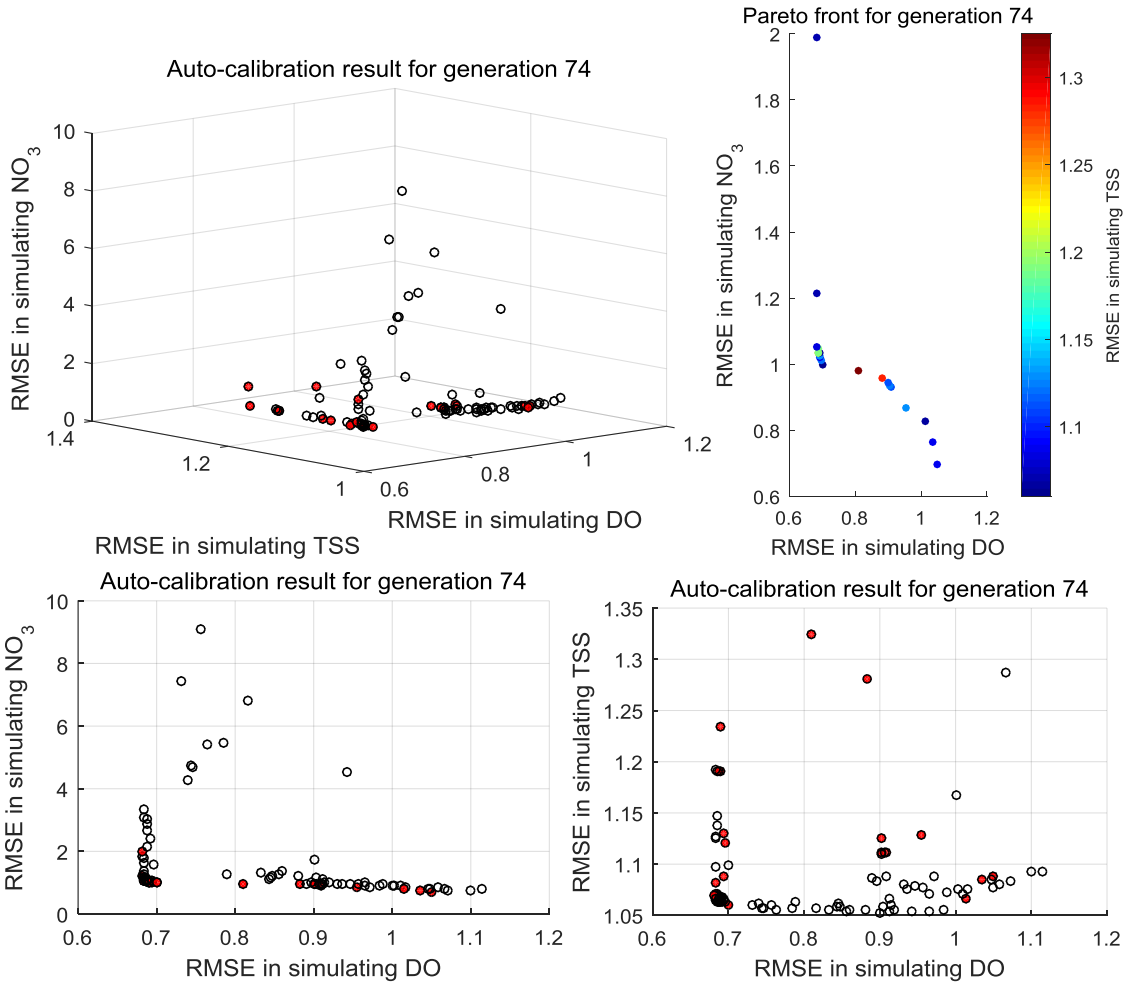

Figure 6-30 Auto-calibration results using three objectives: RMSE of final effluent TSS, NO_3 and DO level of the oxidation ditch

The Pareto-front envelop from the last generation is selected using RMSE of final effluent NO_3 and RMSE of DO in the oxidation ditch, red points in Figure 6-30. Most of the solutions with lower RMSE in simulating DO level in the oxidation ditch (below 0.7) are accompanied by lower RMSE both for TSS and NO_3 in the final effluent; some better than others. Some of the solutions in this space were selected and the model run further to assess accuracy in simulating other model

outputs using the rest of the goodness-to-fit measures. This auto-calibration gives the highest accuracy in simulating final effluent NO_3 and MLSS but with a compromise in accuracy in simulating the DO in the oxidation ditch. For example, solution-1 in Table 6-8, has given the highest NSE in simulating NO_3, 0.77 but the NSE in simulating DO is -0.95, which is unsatisfactory. Conversely, solution-14 and 18 give good accuracy in terms of simulating final effluent NO_3 and TSS, while having a satisfactory accuracy in simulating DO and MLSS in the oxidation ditch. The comparison of measured and simulated values and model accuracy using solution-18, the best solution from this auto-calibration, is presented in the next page.

Table 6-8 Parameter values and multi-objective optimisation objectives (RMSE in simulating DO, TSS, and NO_3) from the Pareto-front selected using RMSE simulating DO and NO_3

																									RMSE		
No.	Mu_H	K_S	K_{OH}	b_H	b_A	ny_h	Y_H	f_P	i_{XB}	K_{S2}	K_{S3}	K_{NO2}	K_{OH2}	K_{OH3}	ny_{g2}	Ny_{g3}	Ny_{g4}	Ny_Y	kLa_{10}	kLa_{11}	v_0	r_h	r_p	f_{ns}	Q_{intr}	DO	TSS	NO_3
1	9.2	54.3	1.17	0.74	0.112	0.8	0.54	0.067	0.051	26.6	17.2	0.22	0.1	0.09	0.25	0.17	0.33	1.08	159	132	479	0.45	3.8	0.0021	615411	1.05	1.09	0.7
2	9.2	63.9	1.17	0.74	0.112	0.79	0.54	0.068	0.053	25.7	19.4	0.14	0.1	0.09	0.26	0.15	0.37	1.15	159	132	479	0.45	3.8	0.0021	615411	1.04	1.09	0.77
3	9.3	51.7	0.97	0.74	0.104	0.77	0.56	0.081	0.043	24.1	17.7	0.2	0.09	0.1	0.26	0.17	0.39	1.03	162	143	502	0.57	3.9	0.0021	499801	1.01	1.07	0.83
4	9.3	51.4	0.57	0.74	0.102	0.8	0.57	0.087	0.054	23.6	13.9	0.23	0.09	0.1	0.26	0.16	0.4	1.12	166	140	487	0.45	3.6	0.0021	593981	0.95	1.13	0.87
5	9.1	36.5	0.78	0.74	0.1	0.77	0.59	0.086	0.047	23.6	16.4	0.2	0.11	0.1	0.3	0.19	0.39	1.15	162	145	515	0.51	4.0	0.0021	599845	0.91	1.11	0.93
6	8.9	59.6	0.37	0.74	0.102	0.73	0.57	0.087	0.046	23.6	13.9	0.27	0.09	0.09	0.26	0.16	0.4	1.12	160	136	504	0.52	3.6	0.0021	593981	0.9	1.13	0.94
7	9.1	36.5	0.78	0.74	0.1	0.77	0.59	0.086	0.04	23.6	16.4	0.2	0.12	0.1	0.3	0.19	0.39	1.15	162	145	515	0.51	4.0	0.0021	599845	0.9	1.11	0.94
8	8.1	59.6	0.8	0.71	0.101	0.73	0.57	0.086	0.058	23.6	17.2	0.26	0.09	0.1	0.26	0.17	0.39	1.14	160	139	455	0.53	3.6	0.0021	627795	0.88	1.28	0.96
9	6.7	106.4	0.44	0.83	0.036	0.68	0.68	0.076	0.088	21.9	16.5	0.11	0.09	0.11	0.23	0.14	0.36	1.18	205	178	513	0.44	3.5	0.0023	674559	0.81	1.33	0.98
10	3.5	74.9	1.06	0.27	0.03	0.8	0.68	0.092	0.068	22	22.6	0.2	0.09	0.1	0.24	0.14	0.36	1.27	157	126	558	0.47	3.5	0.0021	156727	0.7	1.06	1
11	6.4	75.8	0.65	0.35	0.041	0.83	0.68	0.095	0.069	22	22.1	0.22	0.1	0.09	0.23	0.15	0.39	1.27	175	181	565	0.44	3.5	0.0023	321668	0.69	1.12	1.01
12	6.4	75.8	0.53	0.35	0.041	0.83	0.68	0.095	0.065	22	22.1	0.19	0.1	0.1	0.23	0.15	0.39	1.27	175	181	566	0.43	3.5	0.0021	321668	0.69	1.09	1.02
13	6.4	76.1	0.66	0.35	0.04	0.83	0.68	0.094	0.069	22.3	22.1	0.22	0.1	0.09	0.23	0.15	0.4	1.27	173	181	565	0.44	3.5	0.002	321668	0.69	1.13	1.03
14	5.6	77.9	1.14	0.32	0.024	0.79	0.68	0.086	0.068	22.4	22.4	0.24	0.09	0.1	0.26	0.14	0.37	1.28	160	168	552	0.45	3.5	0.0021	273800	0.69	1.07	1.03
15	4.8	76.3	0.7	0.35	0.04	0.83	0.68	0.093	0.07	23.3	22.1	0.22	0.1	0.09	0.28	0.15	0.37	1.27	170	181	565	0.44	3.5	0.0019	399219	0.69	1.23	1.03
16	4.6	104.2	1.07	0.34	0.024	0.83	0.68	0.093	0.068	23.4	21.7	0.22	0.09	0.1	0.24	0.14	0.38	1.27	171	157	537	0.46	3.5	0.0023	310993	0.69	1.19	1.03
17	4.6	104.2	1.07	0.34	0.024	0.83	0.68	0.093	0.068	23.4	21.7	0.22	0.09	0.1	0.24	0.13	0.38	1.27	171	157	537	0.46	3.5	0.0023	310993	0.69	1.19	1.05
18	4.6	102.9	1.07	0.34	0.018	0.84	0.68	0.093	0.068	23.4	21.7	0.21	0.09	0.1	0.24	0.14	0.42	1.28	172	141	546	0.46	3.5	0.0022	310993	0.68	1.08	1.05
19	5.2	102.2	1.07	0.33	0.018	0.9	0.68	0.092	0.071	22.8	22.2	0.2	0.09	0.1	0.24	0.15	0.38	1.28	173	137	549	0.46	3.5	0.0021	580902	0.68	1.07	1.21
20	5.2	137	1.07	0.34	0.01	0.9	0.68	0.089	0.078	22.8	21.6	0.19	0.09	0.1	0.24	0.12	0.38	1.28	171	138	549	0.44	3.5	0.0021	511617	0.68	1.07	1.99

6.4.4.1. Using Solution 18:

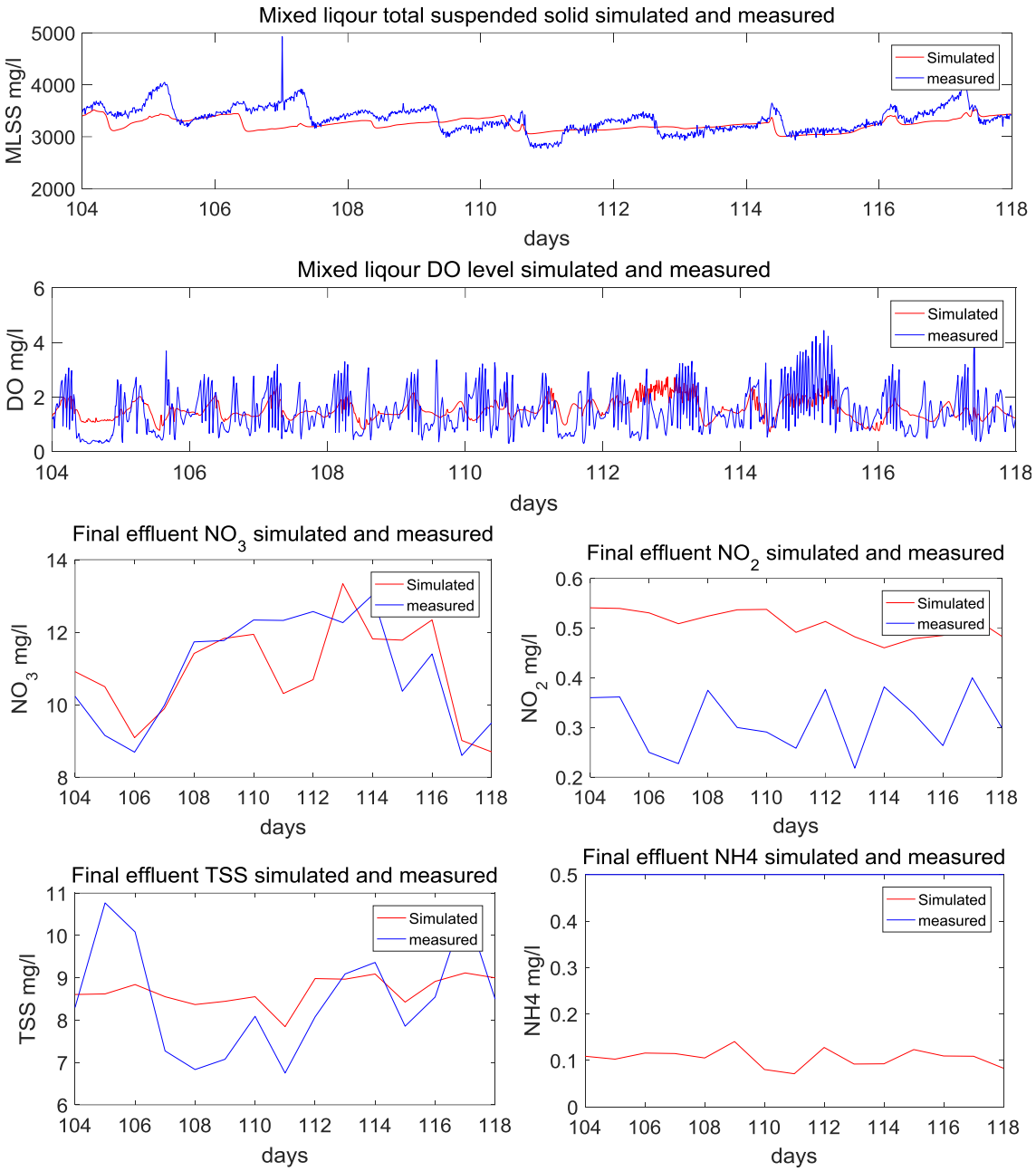

Figure 6-31 Comparison of simulated (RMSE for calibration) and measured dataset during the calibration period: MLSS, DO, NO_3, TSS, NO_2 and NH_4 (top to bottom)

Table 6-9 Model accuracy using the 18th solution of the pareto front (RMSE for calibration)

Eighteenth solution	R^2	NSE	RMSE
MLSS oxidation ditch	0.26	0.06	226
DO oxidation ditch	0.14	0.13	0.7
TSS final effluent	0.44	0.26	1.08
NO_3 final effluent	0.51	0.48	1.05
NO_2 final effluent	0.03	-11.23	0.21

The auto-calibration using RMSE in simulating DO in the oxidation ditch, and TSS and NO_3 of the final effluent gives a good solution in terms of simulating DO in the

oxidation ditch but with a slightly reduced accuracy in simulating final effluent TSS and NO_3. The other solutions highlighted; none of them gives a better solution than the one presented in Section 6.4.3.1.

6.4.5. Best Auto-calibration Result with Manual Calibration for NO_2

Solution 9 of the autocalibration using the product of NSE and R^2 in Section 6.4.3 gives the most accurate model in simulating final effluent TSS and NO_3, with NH_4 level of final effluent below 0.5mg L^{-1} (the minimum level the sensor can detect), and a reasonable accuracy in simulating the DO level in the oxidation ditch. However, the NO_2 was underestimated. To address the over estimation of NO_2, the K_{OH3}, O_2 inhibition of NO_2 reduction [g O_2 m^{-3}] is adjusted manually since the other quality indicators are not highly sensitive to this parameter, see Table 6-3.

After few trials, K_{OH3} is reduced from 0.109 (auto-calibration value) to 0.08 and using parameter values listed in Table 6-6, the following improvement in simulating NO_2 was found without affecting the other objectives.

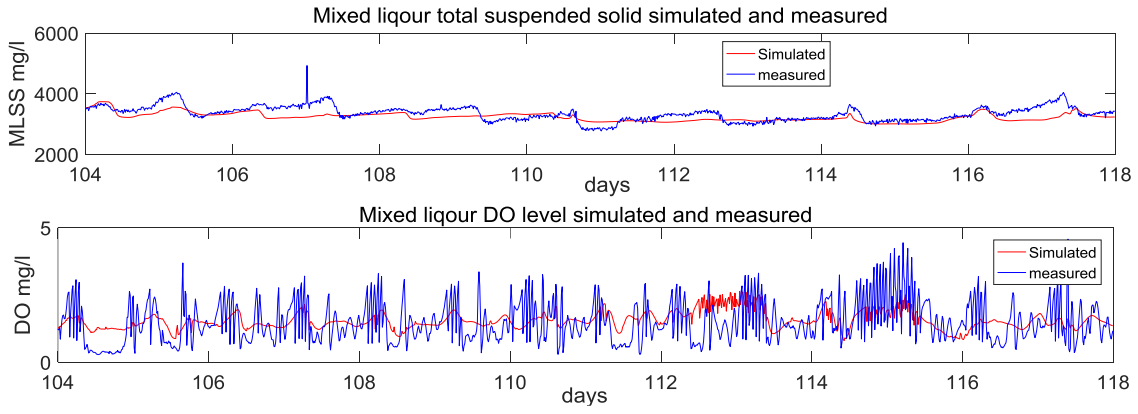

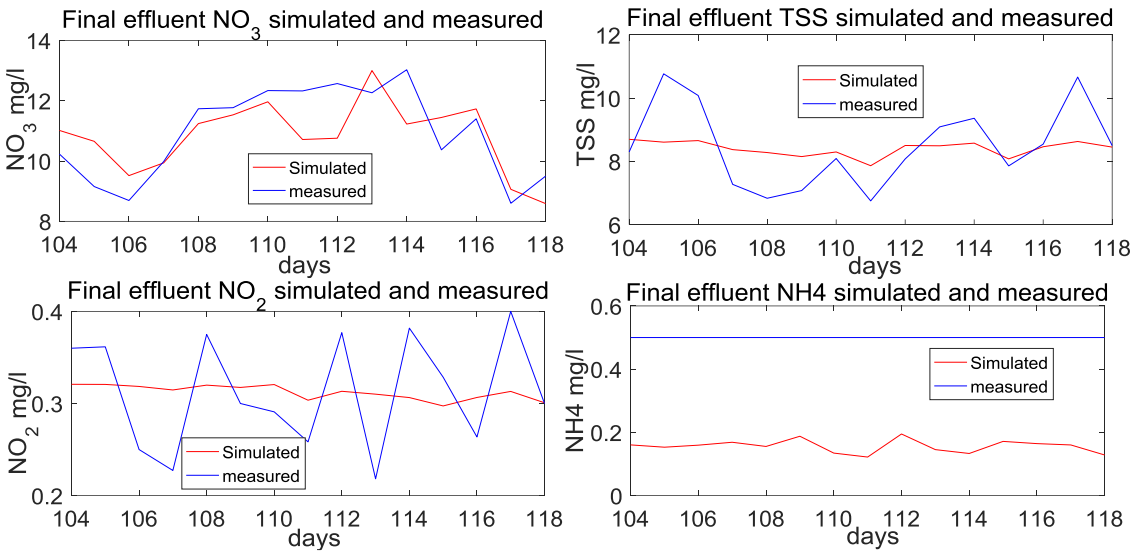

Figure 6-32 Comparison of simulated (the product of NSE and R^2 for calibration and further manual calibration for NO_2) and measured dataset during the calibration period: MLSS, DO, NO_3, TSS, NO_2 and NH_4 (top to bottom)

Table 6-10 Model accuracy using the 9th solution of the pareto front (the product of NSE and R^2 for calibration) after further manual calibration for NO_2

Ninth solution after manual calibration for NO_2	R^2	NSE	RMSE
MLSS oxidation ditch	0.29	0.09	224
DO oxidation ditch	0.12	0.11	0.71
TSS final effluent	0.57	0.24	1.09
NO_3 final effluent	0.51	0.5	1.03
NO_2 final effluent	0.03	0.02	0.06

6.4.6. Discussion

The three auto-calibration problems showed that with a careful selection of objectives it is possible to improve the WWTP model's accuracy in simulating the quality indicators of one's interest. There are model parameters that affect only a certain quality indicator, for example, final effluent NH_4 concentration, so it is necessary to consider each major model output in the definition and selection of objectives. However, in a situation where there is no measured data for all the major model outputs, the above analyses showed that it is possible to achieve a good model accuracy by performing auto-calibration for those where data is available and perform manual calibration for those which do not have accurate measured data. In this instance, by auto-calibrating the WWTP model for DO in the oxidation ditch, and TSS and NO_3 in the final effluent and performing manual calibration for NO_2, it is possible to find set of parameters values that can give a good model accuracy.

The use of the product of NSE and R^2 seems to find a better solution with a fewer number of generation compared to the use of RMSE or NSE alone. The model using solution-9 of the auto-calibration, which uses the product of NSE and R^2 as an objective function, with further manual calibration for NO_2 gives good accuracy in simulating TSS, NO_3, NO_2, and NH_4 with acceptable accuracy in simulating the DO and MLSS concentration in the oxidation ditch. Most importantly, this solution is not specifically optimised for simulation of NH_4 but gives a good accuracy without the need to reconsider further calibration.

The lower accuracy in simulating the DO is mainly due to the simplification of the intermittent nature of the DO control philosophy. As seen in most of the simulations, the DO control philosophy in the model has a quick response, and it does not have that huge fluctuation of DO level due to blowers turning ON and OFF, see Section 3.2.1. In other words, the DO control deployed in the WWTP model is more efficient and makes this simulation conservative. Specifically, the cost of baseline aeration cost from the model, due to more efficient DO control in the model, is expected to be lower than the actual cost.

The calibration of the WWTP model is run for a specific period. Some of the optimisations took longer than others which are reflected in the total number of generations that each auto-calibration run. Although this approach gives a near to an optimal solution, it should be noted that the accuracies can be improved by running the autocalibration for longer and by increasing population size. However, this is time demanding as a single simulation takes 2.5 minutes on average.

6.5. Validation of the Influent Generator

Once the auto-calibration for the WWTP model using the campaign data is performed, now we are confident to use this model for further investigations. However, the input data for the campaign is limited to only for three weeks, and there is a need to extend the inputs for at least a year. The influent generator is found to be the most feasible solution both in terms of its compatibility with the WWTP model and due to its convenient approach in the use of representative pollutant patterns to mimic the influent wastewater reaching the WWTP.

Since there is no data available to assess the modelling accuracy of the influent generator in terms of influent pollutants, there is no further model verification done once the influent generator is integrated with the WWTP. Most importantly, the

integrated model running using rainfall data for the period does not mean that we are trying to accurately estimate the pollutant load reaching at the WWTP in this period. Instead, we are trying to investigate the response of the WWTP to the seasonal variation of flow and pollutant load which is derived from the typical pollutant load pattern developed from the campaign dataset. However, the influent generator accuracy in generating flow is assessed, and a manual calibration is performed here.

The main calibration handles used in the influent generator is mainly at the routing stage. This specifically means the number of sub-catchments in the model, sewer overflow which is mainly influenced by sewer volumetric capacity and sewer pump capacity. There are major assumptions made in the influent generator are as follows:

- The sewer capacity is estimated from GIS asset database, and it is assumed whenever the wastewater in the sewer network is below 90 % of its capacity, the sewer can accept any flow without overflowing. When the sewer is holding wastewater at 90 % of its capacity or above, then it can only accept flow that is equivalent to outflow rate, and the excess is the CSO spill.
- To simplify sewer volume to depth relationship a rectangular cross section sewer pipes are assumed, and Manning's equation is used to estimate the outflow rate.
- The soil available water capacity is assumed to be constant all the time in the calculation of soil infiltration.
- Parameters involving the soil water-balance is left to be determined during calibration. This includes the maximum height of water (H_{max}) in the soil before the soil overflows, H_{inf}, and so on, see Section 5.1.1.2.
- It is assumed that the soil receives seasonal infiltration from upstream soil without a stopping condition.
- The surface area of the soil tank is assumed to be the area of Cupar catchment factored by the assumed available water capacity of 20 %.
- 45 % of the rainfall is assumed to be effective, i.e. either becomes surface runoff or infiltrate into the soil. The rest 55 % is assumed to be lost through evaporation.

The final calibrated-model result is shown in Figure 6-33, and the calibrated parameters that are used in the influent generator are presented in Section 5.1.1.

The influent generator simulated the influent flow patter to Cupar WWTP accurately although the level of noise within the simulated flow is not as exaggerated as the measured flow. The closeness in the pattern is maintained throughout the simulation period except in periods where there is a high rainfall over several days. The measured data during these high rainfall events are in error due to the back flow at the inlet structure, Section 4.3, suggesting the simulated flow being more reliable than the measured flow. Such errors in measured data make the use of statistical measures for model accuracy less informative. However, for the simulation period, between the 100th day and the 524th day, using 15-minutes time-step data without filtering errors, the model showed a reasonable accuracy in simulating the influent wastewater flow with a Nash-Sutcliffe coefficient (NSE) of 0.3 and a coefficient of determination (R^2) of 0.4.

The influent generator accuracy using statistical measures can be further improved by installing flow-meters in the sewer network in addition to the only one flow meter at the WWTP inlet. Doing so enables flow balance checks and helps to quantify and eliminate errors in measured data, in this case, the inlet flow data.

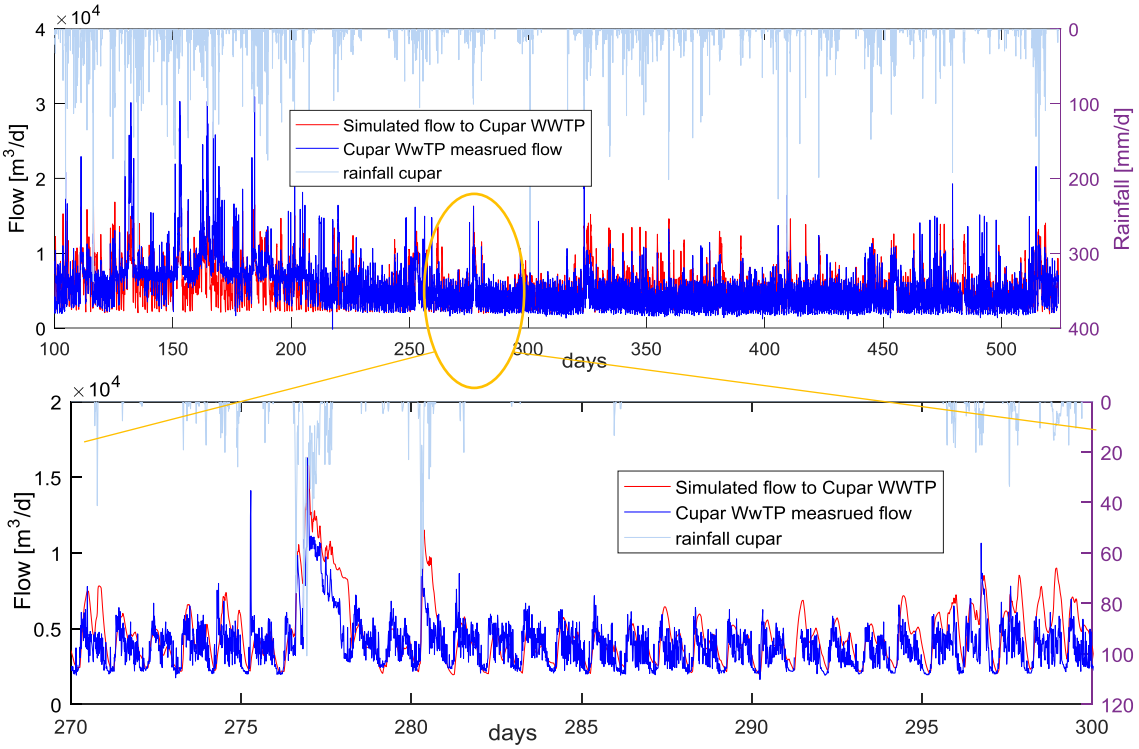

Figure 6-33 Measured (blue) and simulated (red) influent flowrates at Cupar WWTP for the 100 days model warming-up period and the 424 days plant performance assessment period

6.6. Simulation Results Using Calibrated Parameters

Once calibration parameters from WWTP and influent generator are identified, the best solution presented in Section 6.4.5 is used to assess the WWTP performance indicators; operational cost index (OCI), GHG emissions (CO_{2e}), and effluent quality index (EQI). The results are given in Table 6-11.

To make the appropriate intervention choice or to design control strategies at WWTPs, it is essential to understand the source of GHG emissions and the energy used by different process units within the WWTP (Wang et al., 2016; Guo et al., 2016; Flores-Alsina et al., 2011; Sweetapple, 2014; Mamais et al., 2015). Studies showed that the GHG emission from direct GHG is very variable from one WWTP to another, for example, GHG from N_2O can vary from 2 % to 90 % of the total GHG emissions (Foley et al., 2015). Similarly, the GHG from N_2O in this study varies from 4.6 % to 11.5 % of the total GHG. Figure 6-34 shows the source GHG emissions in the Cupar WWTP using calibrated parameters. The result shows that the biological assimilation being the highest contributor to GHG emissions (62 % of the total GHG emissions) followed by Nitrous Oxide (N_2O) emission from denitrification processes in the oxidation ditch (11.5 % of the total emissions). The aeration in the oxidation ditch is the highest indirect source of GHG emissions contributing 10.8 % of the total GHG emissions from the Cupar WWTP.

Table 6-11 WWTP performance indicators averaged for 15 days (calibration period using WWTP model) and averaged over 424 days (using integrated model)

Plant performance indicators	Based on the WWTP model for the calibration period	Based on the integrated model for 424 days
MOCI	3293	3446
OCI	3946	4095
CO_{2e}	7354	7221
EQI	3691	4342

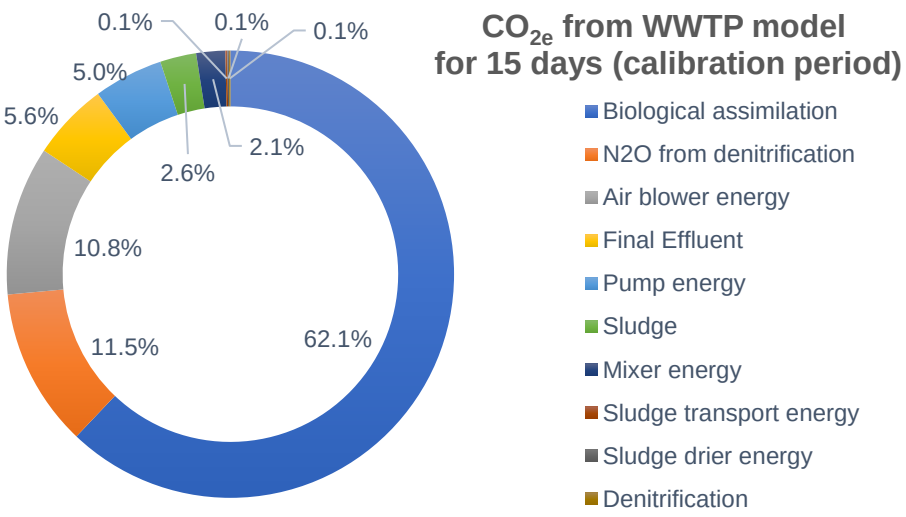

Figure 6-34 GHG emissions as CO_2 equivalent at Cupar WWTP based on calibrated WWTP averaged over 15 days

The calibrated model parameters are used in the integrated model that links the sewer network and the WWTP. The integrated model with influent generator and WWTP BSM2e model which covers a longer evaluation period (424 days) to consider variation in climatic conditions such as temperature and storm flow. The simulation showed that most of the quality indicators are close to results that are found by using the WWTP model for the calibration period (15 days), Table 6-11. The plant performance indicators averaged for the 424 days using the integrated model is presented in Table 6-11. There is a variation in the performance estimated using WWTP and the integrated model. This variation is mainly due to variation in wastewater constituent and temperature variations (mainly lower average temperature for the 424 days 14.4^{o}C compared to the higher average temperature for the calibration period 18^{o}C). The average concentration of pollutants in the influent wastewater is lower in the 424 days simulation due to higher storm water compare to the calibration period which was mostly dry, see

Table 6-12.

Table 6-12 comparisons of the average values of state variables at the influent from the campaign period for the WWTP model and influent generted from the integrated model

State variables	Calibrated WWTP influent state variables (average of 15 days) [mg L^{-1}]	Integrated model influent state variables (average of 424 days) [mg L^{-1}]
S_I	21.6	18.6
S_S	70.9	63.1
X_I	85.2	66.3
X_S	242.9	202.0
$X_{B,H}$	37.4	30.1
$X_{B,A}$	0.4	0.3
X_P	0.0	0.0
S_O	0.7	0.7
S_{NO}	0.8	0.8
S_{NH}	20.1	21.6
S_{ND}	1.7	2.2
X_{ND}	5.1	4.3
pH	7.4	7.0
TSS	234.2	191.2
Flow [m3 d^{-1}]	4766.8	5532.3
Temperature ^oC	18.5	14.4

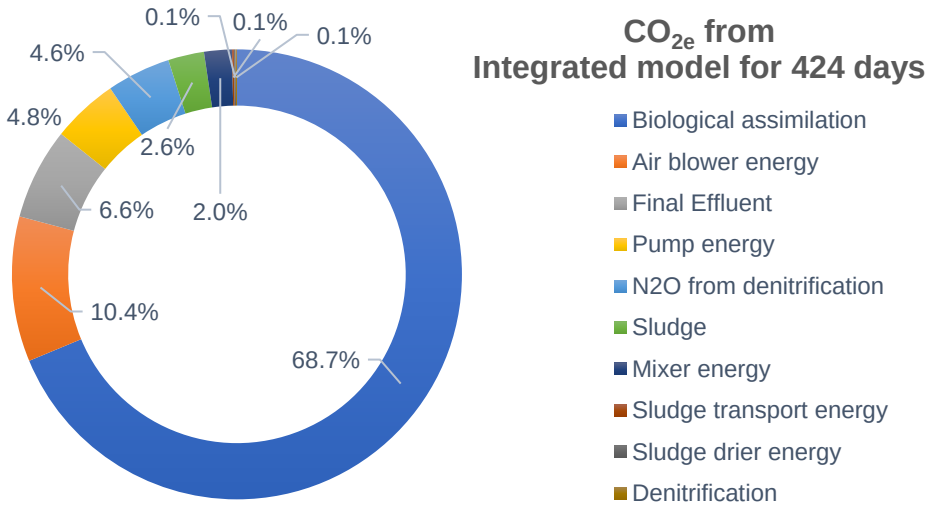

Figure 6-35 GHG emissions as CO_2 equivalent at Cupar WWTP based on integrated model averaged over 424 days

The GHG emissions sources estimated using the integrated model are identified as shown in Figure 6-35 showing a similar contribution from the WWTP model averaged for 15 days except for the N_2O emissions from denitrification. The N_2O emissions from the integrated model are only 4.6 % of the total and are not the second highest contributor, Figure 6-35. The average concentration of each state variable was increased one at a time to assess the cause for this difference. The test showed that the N_2O emission is very sensitive to temperature compared to other sources such as biological assimilation. The test was done by increasing the

average temperature in the integrated model from 14.4 to 16.4 by simply changing the ‘TBias’ from 15^{o}C to 17^{o}C, Section 5.1.1.5. Doing so increases the N_2O emission by 74 % without significantly affecting other emissions except for the biological assimilation, which increases by 10 %. Hence, the need to consider a long period (at least a year) to assess the performance of a WWTP, the feasibility of interventions, and the robustness of control strategies.

7 Interventions and Control Strategies

7.1 Introduction

Feedback process control design can be traced by as far as early third century BC (Stout and Williams, 1995). However the use of active feedback process control is still a topic that has not been yet fully utilised (Svrcek et al., 2014). The practical aspects of wastewater process control is a present-day topic (Olsson et al., 2005), mainly due to the need to improve process efficiency, regulations that requires reduction of GHG emissions from the system, licenses on the high standard effluent quality and the interest from the water industry to achieve these without high capital investments and operational costs.

This chapter investigates different interventions and control strategies within the WWTP using current licensing approaches. The impact of different control strategies on the reduction of GHG emissions, operational cost and effluent quality (Vivekanandan et al., 2017; Vivekanandan and Seshagiri Rao, 2016; Magnus et al., 2016; Sweetapple et al., 2014). Based on the results from the initial assessment of these control strategies, various intervention options and control handles are identified. Sections 7.3 and 7.4 cover the identification of interventions and through sensitivity analysis, their influence on the objectives, which are the reduction of GHG emissions, operational cost and effluent quality. Section 7.4 further explores the trade-off objectives based on the results from the sensitivity analysis, which is used as a springboard for modification of identified interventions, optimisation of the control strategies, Section 7.6.

Previous studies (Meng et al., 2016) show the current fixed licensing regulatory approach is not fully compatible with the holistic approach of the European Water Framework Directive (CEC, 2000) and, at the same time, addressing the Climate Change Act (CC-Act, 2008). Section 7.6.6 an alternative regulatory approach, dynamic licensing, is suggested that uses a variable licensing limit based on the assimilative capacity of the receiving river.

7.2 Interventions, Control Strategies and Implementation Complexity

Developing Interventions is part of a planning/management process. Existing problems and challenges need to be understood, and the degree of their complexity need to be perceived as accurately as possible to suggest the most efficient solutions. Hence, from systems management point of view, it is crucial to be able to make an informed decision in either understanding problems or in selecting the right solution. Tools and model-based studies can play a significant role here, i.e. supporting decisions. For example, in some cases, It is possible to have a complex problem, but the solution can be simple and practical, and in some cases, the problem can be simple, and the solution can be complex. This chapter is designed to investigate available solutions and their complexity to meet objectives such as reduction of operational cost, GHG emissions, and maintaining the quality of the water environment. Some suggested interventions are assessed based on a single objective and multiple objectives. In addition, the benefit of optimisation, integrated active control systems and a dynamic licensing regulatory approach, in meeting these objectives is explored.

There is no agreed specific definition for complexity in the literature. However, in this study complexity refers to the degree and ways of which parts of a system interact with each other, i.e. the more complex the system is the higher inter-dependence among the system parts. Similarly, the complexity of solutions or interventions can be defined as the degree of interaction of system parts needed, and the extent of the resulting disruption during installation. Simple interventions can be defined as those that require few system parts interaction and can be implemented easily without significant disruption of the processes.

Here, it should be noted that the level of complexity depends on the capacity of the company and its previous experience. For example, companies that have experience in handling technically complex solutions have a higher threshold in defining complexity and those with less experience, in handling technically complex solutions, their threshold in defining an issue/solution as ‘complex’ is lower. Hence, it should be noted that the level of complexity is not a clearly defined boundary, but rather it is a guideline for selecting an intervention and a control strategy.

Many of the urban wastewater systems in the UK and in the EU are operated with little automated control systems and very few of them with a sophisticated form of control (UKWIR, 2013a). Smart or active control strategies that use real-time information to adjust operations have been suggested by several studies, to deal with varying loads to WWTPs (Lacour and Schütze, 2011; Rieger et al., 2012; Ocampo-Martinez, 2010). Active control strategies should be considered as an intervention to create a system than can operate at its capacity whenever needed and increase performance through efficient operation (Butler and Schütze, 2005; Sweetapple et al., 2016).

In addition to managing to operate at system's capacity and increasing efficiency, active control strategies can help in achieving a stable removal of pollutants (Rieger et al., 2014; Vrečko et al., 2011). However, achieving stable removal of pollutants may not be the only objective in the UWWS. Hence, it is critical to assess the benefit of these strategies in terms of reducing operational cost and GHG emissions, and the trade-off among these objectives.

The following section covers the selection and identification of different control strategies and interventions that are hypothesised to help in achieving the three objectives; creating a stable effluent quality to the required standard and reducing operational cost and GHG emissions at the same time.

7.3 Identification of Interventions and Control Strategies

Different interventions that can potentially be applied within the WWTP in this study are presented in Table 7-1.

Table 7-1 Possible interventions and control strategies based on literature and site conditions

Category	Specific intervention options, hypothesis and expected outcome
1. Hydraulics, pumps and motors	i. Increase hydraulic capacity by building freeboard on open channels, distribution structures, and increasing storage of tanks by raising walls and weir levels. In combined sewer systems, where storm water is treated mixed with the municipality waste, the hydraulic retention time may reduce during high flow events. Reduction of retention time may reduce the efficiency in the reduction of BOD and is not favourable (Davies, 2005).
	ii. Increasing wet-well surface area. Increasing the surface area of the inlet wet-well pump can increase stability in the flow to the oxidation ditch. However, stabilising this flowrate may/may not have an impact in the biology in the OD, but one of the challenges in WWTP is variable flowrate and assessing stabilisation of this flowrate by increasing the surface-area (volume) of the inlet wet-well is justifiable.
	iii. Increasing capacity of pumps in the sewer network to reduce CSOs, i.e. increasing the maximum flow that can be discharged by each pump. This can increase the receiving capacity of the river downstream of the WWTP and may reduce GHG emission from the WWTPs by using a river quality-based control strategy, dynamic licensing.
	iv. Pumping systems upgrade: Increase the capacity of the pump in the wet inlet-well so as pumps operate at their highest efficiency. Brandt et al. (2012) estimate 5 - 10 % reduction in operational energy by upgrading existing pumps and 3 - 7 % through pump technology, specifically referring to replacing pumps with higher efficiency.
	v. Increasing the efficiency of pumps and motors by replacing them with more efficient pumps that can be operated at different flow rate without a significant lose in efficiency.
2. Possibilities to capitalise on demand side energy management schemes through control strategies	The urban wastewater system can schedule operations to capitalise on different energy demand management schemes provided by energy suppliers to encourage energy use in low demand times. The demand-side energy management schemes are usually designed by increasing energy tariffs during peak times (day times) and by reducing energy tariffs during low demand times (night times). WWTPs may benefit from these schemes by scheduling energy demanding tasks to take place in low energy-tariff periods. The possibility of varying DO set-point based on the time the day and delaying operation to take place during the night, such as sludge centrifuge, are investigated here.
3. Control strategies	i. Aeration systems control in oxidation ditch. Several stidies focus on the control of dissolved oxygen since aeration systems are one of the highest energy users within the sector. Hence, assessing a smarter control system that can reduce this cost without affecting the effluent quality and preferably reducing GHG emissions at the same time.
	ii. Control of scum return flow based on final effluent TSS with a limit on the maximum return flow. Return flows, if they can be minimised without affecting the bio-chemical process, they can reduce operational cost through reduction in energy use for pumping (Lemmer et al., 2000; Spellman, 2008).

	iii. Control of oxidation ditch internal circulation flow. The internal circulation in oxidation ditches is important for several reasons. A minimum horizontal velocity is required to avoid solids settlement, and the maximum flow rate is recommended not to be above 0.6 m s^{-1} to avoid hydraulic jumps and tank erosion (Babbitt and Baumann, 1958). Abusam et al. (2002a) recommend the use of horizontal velocity or internal circulation in an oxidation ditch as a control handle due to its impact on the denitrification process, especial if the reduction of total nitrogen is of interest.
	iv. Control of MLSS level in oxidation ditch to trade-off sludge production and TSS level in final effluent. MLSS can be controlled by altering the rate and frequency of surplus activated sludge (SAS). Increase the SAS and reduce the MLSS level in the oxidation ditch can reduce the sludge age (Von Sperling and Lumbers, 1989b) and potential reduce decay in aerators and associated GHG emissions (Iqbal and Guria, 2009).
	v. Control of RAS - Studies showed that 55 % of the RAS pumping energy could be saved through process optimisation (Abusam et al., 2002b). However directly controlling RAS flowrate may result in expected results especially in suspended solid variation (Olsson and Newell, 1999). Again, although the pump represents the energy demand, it is the whole system which needs attention to optimise gains (Brandt et al., 2012).
4. Upgrading aeration system	Improving the efficiency of blowers and diffusers can reduce operational cost through reduction of energy use, but the degree reduction depends on the current efficiency and available capital investment.
5. Selector zone	Aeration of selector zone. Selector zones are common in oxidation ditch WWTPs. Oxidation ditches are generally prone to bulking issue either due to low F/M ratio or filamentous bulking. Selector zones are provided as a solution for controlling filamentous bulking (Chudoba et al., 1973). These selectors can be aerobic, anoxic or anaerobic and their effectiveness varies from plant to plant. However, since the BSM2 is not capable of simulating the bio-chemical processes involving filamentous bacteria, the impact of optimal control of selector zones cannot be fully investigated in this study.
6. Final settlement tanks	Increasing volume of final settlement tank, or addition of final settlement tank. Increase the final settlement tanks volume either by introducing a board or building additional one. Since smaller particles settle slowly if total suspended solid in final effluent is a high increase in the volume the final settlement tanks may need to be considered. If TSS in final effluent is way below the required, reducing the volume of the final settlement tanks may need to be considered.
7. Sludge	Sludge centrifuge: Increasing energy use ==> Picket fence thickeners < Drum thickeners < Belt thickeners < Belt presses < Centrifuges. For WWTPs with less energy efficient sludge centrifuges, there might be a room for reduction in energy use. However, in this instance, the WWTP has a centrifuge sludge centrifuge, which is one of the energy-efficient sludge centrifuge system, and improving efficiency is not further assessed. Rather the optimal operation of the existing centrifuge sludge centrifuge is explored.
8. Decentralised source management	Reduction of the impervious area through interventions such as pervious car parks, pervious drive ways, collecting storm-water from roofs and directing to the ground to infiltrate (Campos et al., 2016).

In order to assess the potential of these interventions and the potential of control handles, in reducing operational cost, GHG emissions and final effluent pollutant load, a sensitivity analysis is performed. The sensitivity analysis varies the value of the control handles at their extremes and evaluate their influence on the objectives, which is used to select and redefine interventions and control strategies. The control handles that are not influencing the objectives are not further analysed, but those which are identified to have significant influence are further investigated either through optimisation of the control strategy or by using them as a baseline for testing other innovative control strategies and regulatory approaches, see Section 7.6. Section 7.4 presents the results from the sensitivity analysis and discusses the impact of intervention and control handles listed in Table 7-1.

7.4 Sensitivity Analysis

Sensitivity analysis in this section is used as a means of understanding how the variation of parameters that reflects the suggested interventions or control strategies can impact the plant-wide objectives. One-at-a-time (OAT) sensitivity analysis is used using the calibrated model of Cupar WWTP. The objectives here are the WWTP's operational cost index (OCI), effluent quality index (EQI), and GHG emission expressed as equivalent CO_2 emission (CO_{2e}). The parameters for the sensitivity analysis listed in

Table 7-2 are selected based on the suggested interventions in Table 7-1.

The lower and upper bound values, in this instance, are determined based on the possibility of alteration of infrastructure and/or literature values. Two simulations are done for each parameter, one using its lower bound (LB), and another one with its upper bound (LB). The percentage change using LB or UB values in each WWTP performance (objectives) with respect to the baseline (simulation using calibrated parameter value) is calculated. The OAT approach is detailed in Section 6.3.

The OAT sensitivity analysis results are presented in Table 7-3, showing the percentage change in WWTP performance indicators with respect to the baseline WWTP model. The variation of these parameters within the feasible range can have an impact on the WWTP performance, OCI, EQI and CO_{2e}. For example, the GHG emission is highly sensitive to the change in volume of the aerator (f_{VOL}), the return activated sludge (Q_r), and the oxygen transfer efficiency (KgO_2-kWh). These parameters have a significant impact on the operational cost as well. In addition to these parameters, the operational cost index (OCI) is highly sensitive to the waste activated sludge (Q_w), set-point to bypass flow to storm tanks (Qtostormtanks), and kLa value during the intermittent DO control phase (kLamin2). The third objective, EQI, is found to be sensitive to the inlet wet-well duty pump capacity (a1 and b1), storm tank bypass set-point (Qtostormtanks), the percentage of impervious area in the sewer network (aHpercent), and the WWTP influent flow set-point to instigate storm tanks return flow ($QFFTPS_{control}$).

Table 7-2 Sensitivity parameters for intervention and control strategy options

Para. No.	Parameters	Control handle description	Link to Table 7-1	Base-line	UB (%)	LB (%)
1	VOL_{ST}	Volume of storm tank [m3]	1.i, and 2	835.4	100	-50
2	$ReturnQ_{ST}$	Storm tank return flow rate [$m^3\ d^{-1}$]	1.i, and 2	1006	100	-50
3	$area_{WW}$	Wet well surface area [m^2]	1.i, 1.ii, and 2	17.11	100	-50
4	f_{VOL}	Volume of section zone in oxidation ditch (factor) [ ]	5	1	50	-25
5	Qintr	Internal circulation flow [$m^3\ d^{-1}$]	3.iii	6E+05	32	-83
6	Qr	RAS flow rate [$m^3\ d^{-1}$]	3.v	6048	29	-57
7	Qw	SAS flow rate [$m^3\ d^{-1}$]	3.iv	2592	50	-33
8	area	Surface area of final settlement tanks [m^2]	6	928	100	-50
9	a1	Wet-well duty pump outflow stage curve: slope of Eq. 6-4 [s^{-1}]	1.iv	14.53	50	-25
10	b1	Wet well duty pump outflow stage curve: intercept of Eq. 6-4 [$L\ s^{-1}$]	1.iv	48.8	50	-25
11	a2	Wet well standby outflow stage curve: slope of Eq. 6-4 [s^{-1}]	1.iv	18.1	50	-25
12	b2	Wet well standby outflow stage curve: intercept of Eq. 6-4 [$L\ s^{-1}$]	1.iv	23.9	50	-25
13	QtoStormTank	Limit for bypassing flow to the storm tanks [$m^3\ d^{-1}$]	2	5896	100	-50
14	SO4ref	DO set-point in aerators for PID controller [mg $O_2\ L^{-1}$]	2, and 3i	0.75	100	-40
15	DOset2	DO set-point for intermittent control phase [mg $O_2\ L^{-1}$]	2, and 3i	2.25	50	-33
16	kLamin2	kLa value when control is in the intermittent phase [d^{-1}]	2, and 3i	24	200	-100
17	kLa_{sz}	kLa value in selector zone (currently set to zero) [d^{-1}]	5	0	180	0
18	$MLSS_{ctrl}$	Maximum MLSS level to trigger SAS removal [mg L^{-1}]	3.iv	3250	25	-25
19	Qscum	Scum return flow rate [$m^3\ d^{-1}$]	3.ii	0.334	100	-50
20	$QFFTPS_{control}$	Influent flow set-point to instigate storm tanks return flow [$m^3\ d^{-1}$]	1.i, and 2	3024	95	-15
21	pump-capacity_1	Sewer pump 1 capacity (factor) [ ]	1.iii	∞	-	-
22	pump-capacity_2	Sewer pump 2 capacity (factor) [ ]	1.iii	7776	50	-25
23	pump-capacity_3	Sewer pump 3 capacity (factor) [ ]	1.iii	5184	50	-25
24	pump-capacity_4	Sewer pump 4 capacity (factor) [ ]	1.iii	3888	50	-25
25	aHpercent	Percentage of impervious area in the sewer network [%]	8	40	113	-38
26	eff_{pump1}	Inlet wet well pump 1 efficiency (factor) [ ]	1.vi	1	25	-25
27	eff_{pump2}	Inlet wet well pump 2 efficiency (factor) [ ]	1.vi	1	25	-25
28	eff_{RAS}	RAS/SAS pump efficiency (factor) [ ]	1.vi	1	25	-25
29	eff_{SRL}	Supernatant wet-well pump efficiency (factor) [ ]	1.vi	1	25	-25
30	eff_{SB}	SB/SAS pump efficiency (factor) [ ]	1.vi	1	25	-25
31	eff_{mixer_OD}	OD mixers efficiency [ ]	1.vi	0.6	58	-17
32	$eff_{centrifuge}$	Sludge centrifuge efficiency [ ]	1.vi	0.75	27	-33
33	KgO_2-kWh	Oxygen transfer efficiency [kg $O_2\ kWh^{-1}$]	4	0.8	225	-63

Sensitive parameters identification is performed using the total change in WWTP performance indicator indices, similar to Section 6.3.1.1, see Eq. 7-1. The impact of each control handle is considered to be significant if the total change, (TC_{j_i}), is

above 5 %. The shaded cells in Table 7-3 shows the parameters that have an impact on the WWTP performance indices.

$$TC_{j_i} = \left| P_{j_{i,UB}} - P_{j_{i,LB}} \right| \qquad \textit{Eq. 7-1}$$

Where:

TC_{j_i} = Total percentage change in the j[th] evaluation criteria with the i[th] parameter at its lower and upper bound

$P_{j_{i,LB}}$ = Percentage change in the j[th] evaluation criteria with the i[th] parameter at its minimum value (lower bound)

$P_{j_{i,UB}}$ = Percentage change in the j[th] evaluation criteria with the i[th] parameter at its maximum value (upper bound)

Table 7-3 Results of sensitivity analysis and influential parameters on WWTP performance indices

		Percentage change in performance indicators					
Parameter		CO_{2e}		OCI		EQI	
No.	Parameters	LB	UB	LB	UB	LB	UB
1	VOL_{ST}	0.0	0.1	-0.7	0.5	0.7	-0.3
2	$ReturnQ_{ST}$	0.1	-0.1	-0.1	0.9	3.0	-3.2
3	$area_{WW}$	0.0	0.0	0.0	0.0	0.0	0.0
4	f_{VOL}	-7.5	18.8	-3.6	12.6	-2.7	3.0
5	Qintr	3.6	0.0	-1.7	0.4	-4.0	0.1
6	Qr	0.71	-0.17	11.2	-4.8	29	0.1
7	Qw	-1.0	4.1	-11	21.3	-0.1	-0.1
8	area	-1.3	0.4	-1.8	1.0	6.3	-2.3
9	a1	-0.6	1.5	-2.8	1.1	8.4	0.0
10	b1	-1.2	4.8	-3.4	0.7	10.8	0.2
11	a2	0.2	-0.6	0.3	0.6	0.0	-0.1
12	b2	0.3	-0.5	0.5	0.3	0.0	-0.1
13	QtoStormTank	0.6	0.2	-13.1	1.3	47.5	-2.2
14	SO4ref	-1.1	1.2	0.1	0.3	-0.3	0.5
15	DOset2	0.8	-0.6	-1.9	4.6	-1.3	1.1
16	kLamin2	-1.2	2.7	-5.1	17.5	-0.4	1.6
17	kLa_{sz}	0.0	-5.2	0.0	3.7	0.0	4.0
18	$MLSS_{ctrl}$	-8.6	7.3	1.8	-0.6	-0.25	-0.2
19	Qscum	-3.9	2.2	-0.1	-3.8	-0.9	23.5
20	$QFFTPS_{control}$	0.0	0.1	-1.5	2.9	3.3	-9.2
21	pump-capacity_1	0.0	0.0	0.0	0.0	0.0	0.0
22	pump-capacity_2	-0.3	0.2	1.1	0.7	-4.7	0.0
23	pump-capacity_3	0.0	0.0	0.9	-0.2	-3.9	-0.4
24	pump-capacity_4	0.0	0.0	0.1	-0.4	0.3	-0.6
25	aHpercent	3.0	-4.7	2.9	-3.5	-11.3	16.6
26	eff_{pump1}	0.7	-0.4	2.3	-1.3	0.0	0.0
27	eff_{pump2}	0.6	-0.3	2.2	-0.9	0.0	0.0
28	eff_{RAS}	1.0	-0.6	3.3	-1.6	0.0	0.0
29	eff_{SRL}	0.0	0.0	-0.1	-0.1	0.0	0.0
30	eff_{SB}	0.4	-0.3	1.4	-0.7	0.0	0.0
31	eff_{mixer_OD}	0.1	0.0	0.6	-0.2	0.0	0.0
32	$eff_{centrifuge}$	0.2	-0.1	0.4	-0.2	0.0	0.0
33	KgO_2-kWh	24.2	-10.0	76.9	-31.8	0.0	0.0

Shaded cells show influential control handles to the corresponding performance indicator

The sensitivity analysis here only changes each parameter to its UB and LB values without altering the current operational procedures. Hence, the conclusion should not be drawn just based on this result. For example, the DO set-point in aerators for the PID controller (SO4ref) is indicated to have no influence on any of the objectives under the current operational procedure. It is true; since, under the current operation of Cupar WWTP, the blowers could not reduce their speed to zero, rather the intermittent phase is instigated which is linked to a minimum kLa value of 24 d^{-1}, i.e. the DO level could not be reduced to the required level due to this constraint. However, the result in Table 7-3 is further discussed in Section 7.4.1 through Section 7.4.10. In these sections, the different control strategies that are suggested in Table 7-1 are discussed based on the sensitivity result in Table 7-3. Based on these discussions more control strategies are suggested and the role of optimising some significant control handles are discussed through Sections 7.4.1 to 7.4.10, which include integrated active control and dynamic licensing approach.

7.4.1 Volume of Storm Tank

The volume of the storm tank was double and halved for this analysis. Operationally increasing storm tank volumes is directly associated with the amount and frequency of overflow into the receiving river. But, it is impact on the total volume returned to treatment plant depends on other control set-points, such as inlet flowrate level to instigate the storm tank return and the storm tank return flow rate itself.

The sensitivity analysis showed that the benefit of just increasing or reducing storm tank volume without altering the current operational procedure is insignificant in the reduction of CO_{2e}. It has a minor implication on operational cost and effluent quality, see Table 7-3. The reduction in storage volume increases the EQI and vice-versa; mainly since the reduction in the volume of storm tanks, increases the storm tank overflow contributing to the degradation of effluent quality (higher EQI).

Doubling the volume of the storm tank reduces overflow and improves final effluent by 0.3 %. The increase in storage volume increases the change of storm flow to be returned for full-treatment which has a slight impact on GHG emissions, 0.1 %. Similarly, due to more pumping to full-treatment, increasing storage volume results in a slight increase in operational costs OCI, 0.5 %. Generally, the impact of changing only the size of the storage tank does not show significant impact in any

of the performance indicators. However, it is important to assess this further by altering other control handles and operational procedures to explore the full potential of this intervention, see Section 7.6.1.

7.4.2 Surface Area of Wet-well

The main objective of the sensitivity test for the wet-well area ($Area_{ww}$) is to assess the impact of regulating full flow to treatment, i.e. the hypothesis is the higher the volume of the wet well, the more regulated flow to treatment, and avoid potential spill from the wet-well due to high influent coupled with high scum return flows. However, this can increase the total volume of wastewater treated because of avoiding spills. In contrast, the reduction in the volume can increase spill and unsmoothed flow to treatment, which might increase offsite CO_2 emission because of the increased spill to storm tank and ultimately to the receiving water whenever the storm tank is full. The sensitivity analysis showed an insignificant increase in CO_2 emission both for increasing and reducing the volume of the wet well. Regardless of the logical hypothesis, the impact of changing the wet-well volume on effluent quality and operational cost is insignificant. This change has less impact on the wet-well pumps' outflow, and the impact of just increasing the storage capacity without changing the operational procedures and pumping capacity cannot give the expected result since its impact on increasing/reducing the flow to full-treatment is insignificant.

7.4.3 Sewer Pumps Capacity and Sewer Catchment Impervious Area

These interventions can reduce the amount of CSOs with in the sewer network. However, their impact is not straight forward in terms of WWTP performances. In this instance, for Cupar WWTP, the sewer pumps in the influent generator model are represented by four pumps corresponding to each sub-catchment, see Section 5.1.1.4, Figure 5-10 and Figure 5-11. The sewer pumps play an insignificant role in reducing CO_2 emissions from WWTPs or improving the effluent quality index. However, there is a minor impact on operational cost. The change in the capacity of these pumps is not linear to that of the change in cost but generally, increasing the capacity of the sewer pumps further downstream in the sewer network increases operational cost. On the contrary, increasing pumps capacity near the upstream of the sewer network reduces operational cost, see Table 7-3. This is mainly due to the increase CSO spills because of increased flow from the upstream part of the sewer network. Reducing capacity of the sewer pumps adjacent to the

WWTP improves the EQI since it reduces the total flow during storm events reaching to the WWTP, i.e. less overflow at the WWTP. Hence, it is necessary to analyse the impact of these changes on CSO from the sewer networks and the trade-off with WWTP performances.

According to the sensitivity analysis, the percentage of impervious area (aHpercent) in the sewer catchment area has a significant impact on the performance of the WWTP, see Table 7-3. For example, reducing the impervious area in the sewer catchment area by 38 % (LB) improves the EQI by 11.3 %, and increases the OCI, and CO_{2e} by 2.9 % and 3 % respectively. This phenomenon is mainly due to the reduction of storm flows entering the sewer network which manifests itself in two ways; reduction of the spill in the WWTP hence better EQI, and reduction in dilution hence higher OCI and CO_{2e} from the WWTP.

These infrastructures are outside the WWTP, and their impact on river quality due to increased or reduced combined sewer overflow (CSO) occurs upstream of the WWTP. In other words, their impact on river quality is not captured by the EQI calculation. Hence, it is important to explore their impact on CSO.

Further analysis of the impact of the change in sewer pump capacity and percentage of impervious area in the sewer catchment area on CSO is done using OAT sensitivity approach. The pumps' capacity increased and decreased similar to

Table 7-2, but the objective being the CSO in the sewer network. The result showed that changing only one sewer pump capacity do not decrease CSO spill volume, see Figure 7-1. Increasing upstream pumps capacity without increasing downstream, either sewer storage capacity or pump capacity, results in more CSO. On the other hand, increasing the capacity of all sewer pumps at the same time by 50 % results in reducing the volume of CSO by 5 %. Similarly, reducing the capacity of all the sewer network pumps by 25 % showed an increase in CSO volume by 10 %.

The total change in the volume of CSO spill per percentage change in pumps' capacity is more pronounced due to the reduction in the pumps' capacity compared to change due to the increase in their capacity. This phenomenon showed that the current pump capacity is the critical (the bottle-neck) in reducing CSO. This simple test showed that, if the reduction of CSO is an interest, it is important to consider not only pump capacity but also sewer storage capacity as well.

The operational cost saving due to increased pump capacity, one pump at a time, didn't show a significant saving or reduction in WWTP operational cost, see Table 7-3. Although it is outside the scope of this study, considering upgrading all the sewer pumps and searching for the optimal capacity can play a significant role in reducing CSO spills, but with an increase in operational cost at the WWTP.

The increase or decrease in impervious area (aHpercent) showed a significant impact on the total volume of CSO. Reducing aHpercent by 38 % (LB) reduces the total CSO by 64 % and increasing aHpercent by 113 % (UB) increases the total volume of CSO per year by 302 %.

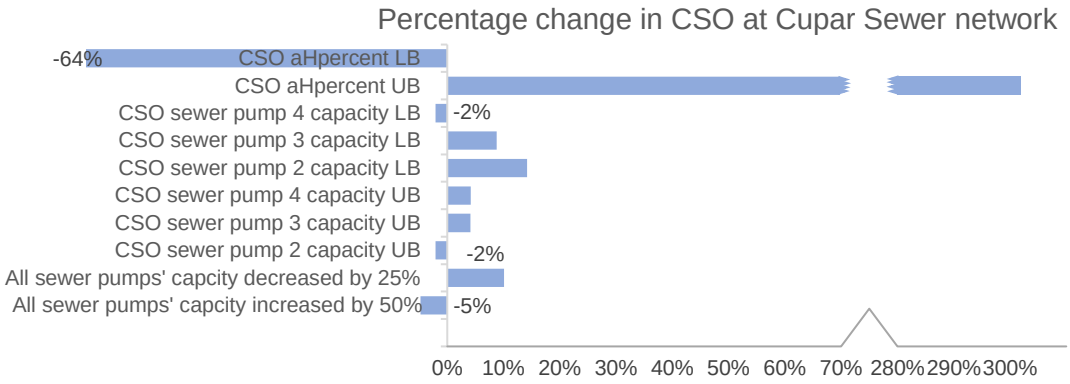

Figure 7-1 Percentage increase or decrease in CSO due to increase or decrease in sewer's pump capacity and percentage of impervious area in the sewer catchment

7.4.4 WWTP Inlet Wet-well Pump Capacity

Increasing the inlet wet well pumps' capacity by 50 % showed that the duty pump (capacity tested using discharge-depth curve variables a1 and b1) has a minor impact on effluent quality. However, reducing its capacity by 25 % has a significant impact on effluent quality, on average, an increase of EQI by 9 %, see Table 7-3. Although the percentage of change in OCI and CO_{2e} is not high, the increase in pump capacity results in an increase in CO_{2e} and OCI, i.e. due to the increase in the total volume of wastewater reaching to the OD. It should be noted that the sensitivity analysis is done based on current operational procedures and it is expected that if we alter operational procedures, these results may change. For example, if we increase the storm tank bypass ($Q_{storm,\ bypass}$) set-point as we increase inlet wet-well pump capacity, then we are reducing the bypass volume to storm tanks and potentially reducing storm tank overflow ($Q_{overflow}$) which has a role in reducing the EQI, see Figure 7-2.

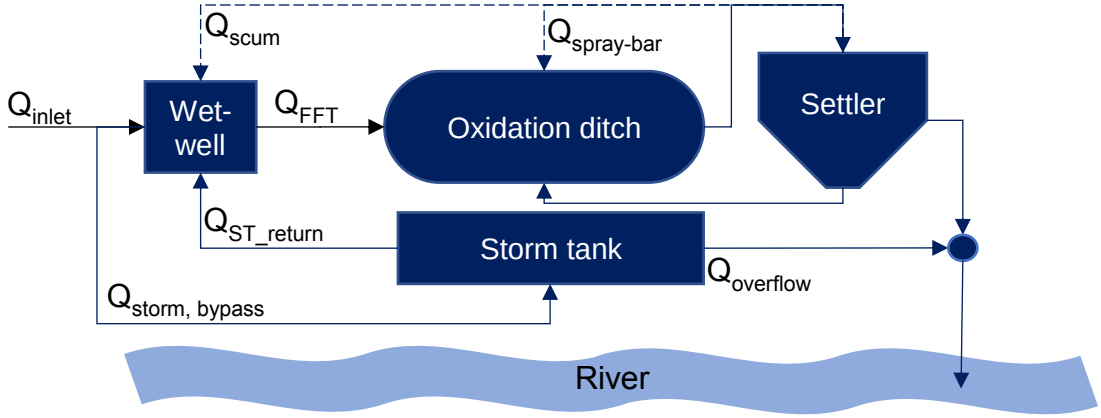

Figure 7-2 Simplified layout of Cupar WWTP showing the major flows

The sensitivity analysis for the assist pump showed a similar result except that the level of impact is much lower in this case. Again, the test is done only based on current operational procedures and the change in the capacity of this pump may be significant if operational procedures change.

7.4.5 Installing Pumps with Higher Efficiency

The efficiency of pumps is the ratio of the power drawn by the pumps and the power transformed for pumping wastewater, which also depends on the operational pressure head and flow rate (De Keyser et al., 2014). This ratio can be increased by replacing existing pumps with more efficient new pumps. In the sensitivity analysis, the efficiency of the pumps increased (UB) and reduced by 25 % (LB) from the exiting efficiency. Increasing pump efficiency reduces operational

cost and reduces GHG emissions as well. However, in this instance the impact on GHG reduction in not as pronounced as the reduction in operational cost, see Table 7-3. Improving pump efficiency can be a viable option to reduce CO_2 in a significant amount for WWTPs with higher carbon foot-print contributed from the use of electricity. In the case of Cupar WWTP where the highest CO_2 emission comes from biological processes, improving pump efficiency will not play a significant role in reducing CO_2 emission. The continuously operating pumps such as inlet wet-well pumps and RAS/SAS pumps has more impact in reducing operational cost compare to intermittent pumps such as return liquor pumps, see Table 7-3. In general, at Cupar WWTP a 25 % increase in pump efficiency can create a reduction in operational cost varying from 0.2 – 1.6 %, and a reduction in CO_2 emissions varying from 0.1 – 0.6 %. In addition, replacing pumps that have very low efficiency, may give a higher percentage of cost saving and CO_2 emission, i.e. the benefit of this intervention is expected to vary significantly from plant to plant.

So as to assess the benefit of improving the efficiency of all the pumps, mixers, and centrifuge, their efficiency is increased by 25 % similar to that of the sensitivity analysis. Improving efficiency of pumps, centrifuge, and mixer can reduce CO_{2e} up to 2.65 % and reduce operational cost index by 8.25 %. This intervention has no impact on effluent quality, see Table 7-4.

Table 7-4 Cupar WWTP performance indices of the intervention that install efficient pumps, mixers, and centrifuges

	Baseline	pumps, mixers, centrifuges efficiency increased by 25 %	Percentage change in Performance
CO_{2e}	7221	7030	-2.65
OCI	4087	3750	-8.25
EQI	4342	4342	0.00

7.4.6 Aeration Control

Aeration is one of the biggest energy consuming processes in activated sludge processes (Åmand et al., 2013; Stenstrom and Rosso, 2008; Foscoliano et al., 2016). This holds true for the case study in this research as well, see Section 6.6. Although the OCI for sludge is higher than aeration, the actual energy consumption is not comparable to that of the aeration. As a result, aeration is also the highest indirect CO_2 emission source in the WWTP, see Figure 6-35. The energy use of aeration within a WWTP can be as high as 45 - 75 % of the total onsite energy use

(Rosso et al., 2008). In addition to reducing their energy use, in the face of stringent regulations, control of the aeration systems for a reliable effluent quality is in the centre of creating an energy efficient and reliable system (Åmand and Carlsson, 2014).

The sensitivity analysis took several control handles on aeration and assessed their impact on OCI, EQI and CO_{2e}.Control handles include:

- DO set-point for the PID controller during continuous aeration phase (SO_{4ref})
- DO set-point to instigate the intermittent aeration phase (DOset2) and the associated minimum aeration intensity (kLamin2)

The variation in the DO set point for the continuous aeration phase (PID controller) does not show a significant impact on the performance indicators. In this case-study, there are two DO control phases; continuous and intermittent. The intermittent phase instigates when the DO level in the oxidation ditch cannot be reduced using the continuous aeration phase although blowers are operating at their minimum speed. This is implemented in the model, in the PID controller, by setting the minimum kLa value (kLa_min) to 72, see, Section 3.2.1. Hence, reducing the DO set-point in the continuous aeration phase, without altering the DO-set point that instigates intermittent phase and the kLa_min value, is not going to create a significant impact on any of the performance indicator.

On the other hand, DO set-point to instigate the intermittent aeration phase (DOset2) has a significant influence on OCI. Similarly, the aeration control in this case-study is the combined effect of both the intermittent and continuous aeration phase, just by changing only one of them at a time is was not possible to see a significant impact on the plant performance indices as expected. Different control strategies that target to overcome this practical limitation are presented in Section 7.6.2 through Section 7.6.4. Innovative DO control strategies that use the final effluent quality as a reference, and the assimilative capacity of the receiving river are explored in Section 7.6.5 and 7.6.6 respectively.

7.4.7 RAS Control

Reduction of RAS flowrate, Qr, from 70 L s^{-1} to 30 L s^{-1} results in the increase of operational cost (OCI) by 11.16 % although there was a reduction in pumping energy, which contributed a reduction of OCI by 2.2 %. However, the increase in cost due to more sludge drying and transportation outweighs the cost reduction

achieved through reduced RAS pumping. Reducing the RAS flow does not affect the GHG emissions significantly, but it increases the EQI by 29 % through increased TSS in the final effluent and associated increase in TKN.

On the other hand, increasing the RAS flow to 90 L s^{-1} reduces the operational cost through reduction in sludge production. The overall OCI reduction was 4.8 % although the reduction of OCI just due to reduced sludge treatment was 8.8 %. The increase in RAS pumping alone results in more energy use and an increase of OCI by 2.3 %. Similar to the reduction in Qr, the increase in Qr does not have a significant impact on the plants GHG emissions. However, unlike the reduction in Qr, it does not show significant impact on the on the final effluent quality.

By increasing the pumping costs, the system saves higher costs due to the resulting reduction in sludge production while not affecting the overall GHG emission and effluent quality. However, reducing RAS to save pumping cost can incur a higher cost due to the resulting higher sludge production and at the same time undesirable impact on the final effluent quality.

7.4.8 MLSS Control

To trade-off the sludge production and TSS concentration in the final effluent, it was hypothesised to consider, Table 7-1, the reduction of MLSS in the oxidation ditch by using the control handles; MLSS set-point, $MLSS_{ctrl}$, and the rate of surplus activated sludge (SAS) removal rate, Q_w. These handles are selected since the SAS removal operation is dependent on the $MLSS_{ctrl}$ and the MLSS concentration in the oxidation ditch. The SAS removal at Cupar WWTP is scheduled to take place every other day, and the operation will not take place at the scheduled day if the MLSS in the oxidation ditch is less than the MLSS set-point, $MLSS_{ctrl}$, see Eq. 3-27, in Chapter 3. On the scheduled day, the SAS removal takes place for two hours with a specified flowrate, Q_w. For example, increasing Q_w is expected to increase the total volume of SAS removed in the two hours, and increasing the $MLSS_{ctrl}$ is expected to interrupt the SAS removal as the set-point is higher and the chance of MLSS in the oxidation ditch to be higher than the increased $MLSS_{ctrl}$ value maybe lower.

To test this hypothesis, the sensitivity analysis increases the SAS flowrate, Q_w, by 50 % and reduces it by 33 %. The increase in Q_w, shows a slight impact on the CO_{2e}, increase by 4.1 %, but no significant impact on the final effluent quality (EQI).

The slight increase in GHG emissions is mainly due to increased sludge treatment. Similarly, it results in a significant increase in sludge treatment cost, which raises the overall OCI by 21.3 %. Generally, increasing the SAS removal does not show a favourable change from the point of management, and its impact on the biological processes within the WWTP was limited. Reducing the SAS removal rate has a minor impact on GHG emissions and no significant impact on effluent quality. However, it reduces the operational cost index by 11.1 % through the reduction of sludge treatment. Hence, the test showed that it is possible to reduce sludge treatment cost by manging the SAS removal rate without affecting the final effluent quality.

The other control handles tested in the management of MLSS and sludge production is the $MLSS_{ctrl.}$ A reduction in $MLSS_{ctrl}$ means SAS can be removed for the two hours period without interruption and increased $MLSS_{ctrl}$ can mean more interruption of SAS removal operation, see Eq. 3-27, in Chapter 3. Reducing the $MLSS_{ctrl}$ level results in a slight increase in SAS removal, resulting in a slight increase in sludge production and associated cost. This increases the overall OCI by 1.8 %. The slight increase in SAS and reduction of the MLSS in the oxidation ditch results in the reduction of decay (autoxidation), which contributes a significant reduction in GHG emission. Reducing the MLSS level in the oxidation ditch through $MLSS_{ctrl}$ reduces the GHG emissions by 8.6 %. The impact of this change on the final effluent is not significant. The increase in the MLSS set point does not have a significant impact on cost saving and effluent quality. However, it has a negative impact on GHG emissions by increasing the CO_{2e} by 7.3 %. The increase in $MLSS_{ctrl}$ results in an increase in MLSS concentration in the oxidation ditch with a small reduction in sludge production but increasing decay (autoxidation) in the oxidation ditch. The way the control setup and the fact that there are 100 days warming up period, the impact of increasing $MLSS_{ctrl}$ on operational cost was not significant.

7.4.9 Aeration of Selector Zone

In the baseline or current operation of Cupar WWTP, the selector zone is anoxic. Converting this zone into the aerobic zone by setting a kLa value of 180 reduces GHG emissions by 5.2 %. This reduction is due to the reduction in emission from biological assimilation and N_2O emissions, 4.7 % and 2.9 % respectively. The reduction in direct GHG emission from the oxidation ditch outweighs the increase

in indirect GHG emission due to increased use of energy for aeration. Although this operation reduces sludge production and associated cost, 2.7 % reduction in OCI, it is out weighted by the increase in aeration energy, 5.4 % increment in OCI. Due to increased aeration and reduction in the denitrification process, the nitrate concertation in the final effluent increases and as a result there was an overall increase in EQI by 4 %.

The test showed that that the performance indicators are sensitive to the aeration of the selector zone mainly effluent quality and GHG emissions. The OCI is increased by 3.7 %, but aeration of the selector zone results in a total reduction of GHG emission, 5.2 %. Although it shows a promising result, since the aim of installing selector zones upstream of oxidation ditches is to reduce filamentous bulking, it is essential to assess the impact of these operational change on filamentous bulking. The model used in this study is not capable of simulating the activity of filamentous bacteria, it was not possible to assess the overall benefit of this strategy. Hence, further modification or optimisation of this operation is not explored further in this study.

7.4.10 Aerator Volume

Sludge age is one of the fundamental parameters in WWTP design and control of nutrient removal (Ekama, 2010). The practical way of controlling sludge age is through hydraulic control that can reduce the volume of aerators through increased or reduced level of reactor overflow/outlet weirs (Samuelsson and Carlsson, 2002; Ekman et al., 2006; Ekama, 2010). Hence, in this section, the variation of aerator volumes and its impact on the WWTP indices are assessed.

The sensitivity analysis in Section 7.4 shows that the variation in the oxidation ditch volume has a significant impact on the average GHG emission from the WWTP. For example, reducing the volume of oxidation ditch by 25 % can reduce the CO_{2e} by 7.5 % while reducing operational cost (OCI) by 3.6 % and improving the effluent quality by 2.7 %, Table 7-3. This is a favourable result regarding meeting the three objectives. The system became more energy efficient with a reduction in the need for aeration. This phenomenon limits the volume needed for nitrifying bacteria to convert ammonia to nitrate resulting in less CO_{2e} from biological assimilation and N_2O emissions, Figure 7-3. Similarly, the concentration of Nitrate reduces in the final effluent with a slight increase in ammonia/TKN in the final effluent, Figure 7-3.

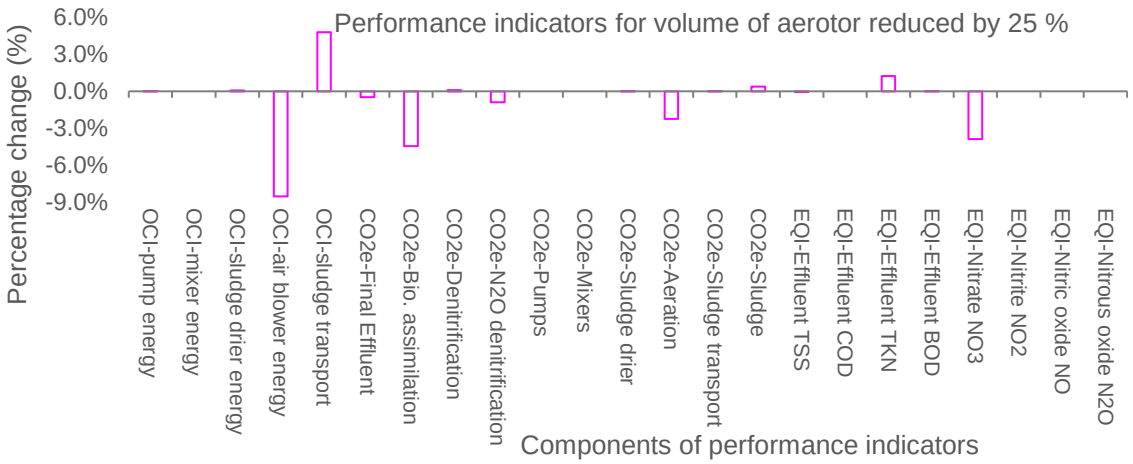

Figure 7-3 Percentage change in performance indicators' components for selected solutions from the reduction of oxidation ditch volume by 25 %

Studies showed that the use of variable aerator volume and automation of their control could reduce system disturbances and maintain effluent quality to the required standards; some using feedforward control (Brouwer et al., 1998; Ekman et al., 2006), and some using feedback loop (Samuelsson and Carlsson, 2002). Hence, the potential of this intervention can be maximised by automating the system, which is not further assessed in this study.

7.5 Capitalise on Demand Side Energy Management (DSM) Schemes through Control Strategies

In the UK, energy Demand Side Management (DSM) is the modification of consumers demand of energy through either financial incentivise or behavioural change through education (Chiu et al., 2013).

Referring to Section 5.2.3, One of the financial incentives is the use of differential tariffs, such as the Economy 10 and Economy 7 electricity plan. These plans put into effect dynamic pricing schemes that have variable pricing rate per kWh of energy use for different times of the day/week or year based on demand (Torriti et al., 2010). Such schemes are set out to balance electricity production and demand by setting the price per unit of energy variable throughout the day. For this study, the evening, weekend, and night tariff are adopted, and the pricing rate is assumed to be 50 % cheaper during the night, 30 % cheaper during the evening and weekends. The night time refers to the period 12:30am to 7:30am, evenings time refers to the period 8:00pm to 12:30am, and day-time refers to the period 7:30am to 8:00pm.

The Modified Operational Cost Index (MOCI), is introduced to reflect the cost of operations based on variable tariffs, see, Eq. 5-56 in Chapter 5, where $MOCI = OCI \times f_{MOCI}$. f_{MOCI} is the factor used to reflect DSM tariffs, it has a value of 0.5 during night hours and 0.7 during evening hours and weekend days. During day-time hours of week-days f_{MOCI} has a value of 1.

In order to capitalise on the energy DSM tariffs, four different scenarios are assessed here.

i. Sludge centrifuge operation rescheduled to be at night-time
ii. Variation of storm tank by-pass set-points
iii. Variable DO set-points
iv. Optimisation of storm tank by-pass set-points, inlet-pump capacity, and storm tank storage volume

7.5.1 Sludge Centrifuge Operating at Night

This scenario focuses on shifting sludge centrifuge operation from day-time towards the night-time when the energy tariff is cheaper. For this reason, this scenario is designed so as the sludge centrifuge operates only in the week-days during night hours. The operation starts (T_centrifuge_start) at 00:30 and runs at least for six hours (T_centrifuge_run) unless the sludge holding tank is empty. This duration of operation hasn't changed compared to the baseline. To synchronise the sludge centrifuge operation and availability of SAS in the sludge-holding tank, the SAS removal from the final settlement tanks is scheduled to start at the same time as the sludge centrifuge start-time, i.e. at 00:30. These changes are incorporated into the 'SHTbypass_cupar' model block.

Table 7-5 Cupar WWTP performance indices change by adjusting sludge centrifuge and SAS operations

Performance Indices	Baseline	Sludge centrifuge and SAS operation at night DSM	Percentage change in performance
CO_{2e}	7221	7225	0.06
OCI	4087	4113	0.64
EQI	4342	4350	0.18
MOCI	3439	3452	0.38

The plant wide OCI increases due to the increased sludge production. Looking at only the sludge centrifuge, the average kWh d^{-1} factored for MOCI showed a reduction from 18 kWh d^{-1} to 9.96 kWh d^{-1}. However, the change in the SAS

operation to favour the sludge centrifuge affects the total OCI, i.e. the amount of sludge entering the sludge-holding tank is increased. The SAS removal operation is controlled based on MLSS level in the oxidation ditch, i.e. the higher the MLSS is in the oxidation ditch, the more SAS will be removed. In this instance, due to the relatively higher MLSS level at night, more SAS is removed from the settlers, ultimately increasing sludge transport and associated cost and GHG emissions.

7.5.2 Storm Tank By-pass Set-Point

The Cupar license states that the flow to treatment should not be less than 69 L s^{-1} (5,962 m^3 d^{-1}) (2.3 × DWF). However, if day time flow to treatment is reduced through reduced storm tank by pass set-point, it is expected to reduce operational cost by reducing full flow to treatment in the day time. The hypothesis is the by-passed flow to the storm tanks will be returned to full treatment during night time, but this depends on the chosen set-point. If the new set-points chosen reduces the WWTP capacity, this will be reflected on the EQI and CO_2e plant performance indicators.

In this scenario, to maximise the DSM scheme, the full flow to treatment is reduced to 2xDWF during the day ($Q_{toStormTank}$), increased to 2.5xDWF during the evening hours ($Q_{toStormTank\_eveninig}$), and increased to 3xDWF during night hours ($Q_{toStormTank\_night}$).

Table 7-6 Cupar WWTP performance indices change by having variable set-point for storm tank by-pass

Performance Index	Baseline	Flow to full treatment variation DSM	Percentage change in performance
CO_{2e}	7221	7131	-1.25
OCI	4087	4037	-1.22
EQI	4342	4435	2.14
MOCI	3439	3389	-1.45

Reducing flow to full treatment set-point (storm bypass set-point) in the day-time and increasing it during the evening and the night time reduces both operational cost and CO_{2e}. However, this is not necessarily due to the maximising of the DSM scheme. The reduction in OCI and CO_{2e} shows that the total flow reaching to treatment is reduced because of increased overflow from the storm tanks in the day-time. The set-points chosen in this scenario reduces the Cupar WWTP capacity, i.e. current storm tank storage is not sufficient to accommodate this

control strategy, indicating that the control strategy in this scenario should be incorporated with the right storm tank capacity, see Section 7.6.1.

7.5.3 Variable DO Set-points

The aeration control is set up to have a variable DO set point at different times of the day. Cupar WWTP's DO control algorithm uses two operational phases; the continuous phase and the intermittent phase. In this scenario, the DO set-point that determine the instigation of the intermittent phase (DOset2) is interest due to its simplicity, and due to the insensitivity of performance indicators to the DO set-points in the PID controller alone (continuous phase), see Table 7-3. In the baseline, DOset2 is set to 2.25 mg L^{-1} of dissolved oxygen. In this scenario, the dissolved oxygen set point, DOset2, is given different values based of different times of the day; 1.5 mg L^{-1} during the day (DOset2), 2 mg L^{-1} during the evening ($DOset2_{evening}$), and 2.25 mg L^{-1} during the night ($DOset2_{night}$).

Table 7-7 Cupar WWTP performance indices change by varying intermittent phase DO set-point variation DSM

Performance Index	Baseline	Variable Doset2 for DSM	Percentage change in performance
CO_{2e}	7221	7247	0.36
OCI	4087	4053	-0.83
EQI	4342	4322	-0.46
MOCI	3439	3406	-0.96

The result showed that the operational cost as measured by MOCI showed a reduction of 1 % and so the EQI, by 0.5 %; however, the CO_{2e} is increased by 0.4 %. The reduction in MOCI is due to the reduction of aeration cost by 1.3 % but accompanied by increased sludge transportation cost, 0.3 %, see Figure 7-4. The increase in CO_{2e} is mainly due to increased denitrification resulting in higher N_2O and CO_2 from biological assimilation. Effluent quality is improved by reducing the NO_3 concentration in the final effluent due to increase denitrification in the OD.

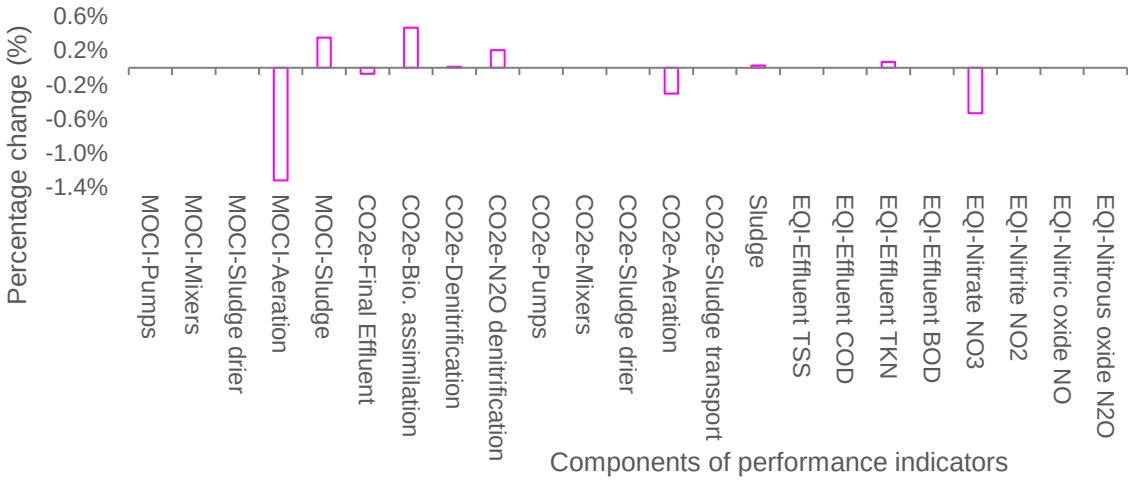

Figure 7-4 Performance indicators' components percentage change due to the variation of DOset2 in a day to maximise energy DSM scheme

This is a simple test using a random selection of set-points. Section 7.4.6 searches for the optimal setpoints for DOset2 and the DO set point for continuous phase.

7.6 Optimisation, Innovative Control Strategies and Regulatory Approaches

The sensitivity analysis and discussion in Section 7.5 showed that there are parameters that alter the objective functions significantly. And some do not, either their change could not alter the target process due to operational limitation or their complex interaction with other control handles. Sections 7.6.1 to 7.6.6 investigate the potential of these control handles either by considering more than two control handles at a time or by considering the necessary control procedure. Those interventions and control strategies that showed a significant impact on the objectives are further explored, and the benefit of multi-objective system optimisation is assessed. In addition, the benefit of innovative control strategies and dynamic licensing approaches are investigated.

7.6.1 Optimisation of Storm Tank By-pass Set-points, Inlet-pump Capacity, and Storm Tank Storage Volume

Three scenarios were considered in Section 7.5 to explore the benefits and possibilities of energy cost saving through DSM schemes. Further investigation is done by using a multi-objective optimisation by considering three control handles at a time; the storm tank by-pass set point, storm tank volume, and capacity of the inlet wet-well pump. The storm tank by-pass set-point ($Q_{tostormtank}$) that controls the full flow to treatment and the storm tank by-pass, Figure 7-2, is set to have three different set-points for various time of the day, see Section 7.5.2. In this instance,

unlike the scenario in Section 7.5.2, the inlet wet-well pumps' capacity and the volume of the storm tanks are varied at the same time and their optimal values for the different time of the day are assessed. A multi-objective optimisation is setup with objectives in reducing MOCI, CO_{2e}, and EQI, the number of population chosen to be 30 for each generation, and a total of 20 generations. The lower bound and upper bound of each parameter are given in Table 7-8.

Table 7-8 Lower bound and upper bound of parameters used in the optimisation

Parameters	**Description**	**Lower bound**	**Baseline**	**Upper bound**
$Q_{toStromtank}$	Day-time flow to full treatment set-point [m^3 d^{-1}]	1.15 × DWF	2.3 × DWF	2.5 × DWF
$Q_{toStromtank\_evening}$	Evening flow to full treatment set-point [m^3 d^{-1}]	2.3 × DWF	2.3 × DWF	3 × DWF
$Q_{toStromtank\_night}$	Night-time flow to full treatment set point [m^3 d^{-1}]	2.75 × DWF	2.3 × DWF	3.5 × DWF
VOL_{ST}	Volume of storm tanks in [m^3]	0.5 × 835.38	835.38	2 × 835.38
Pumpcapacity_1	Factor to change the capacity of the duty inlet wet-well pump [ ]	0.75	1	1.5
Pumpcapacity_2	Factor to change the capacity of the assist inlet wet-well pump [ ]	0.75	1	1.5

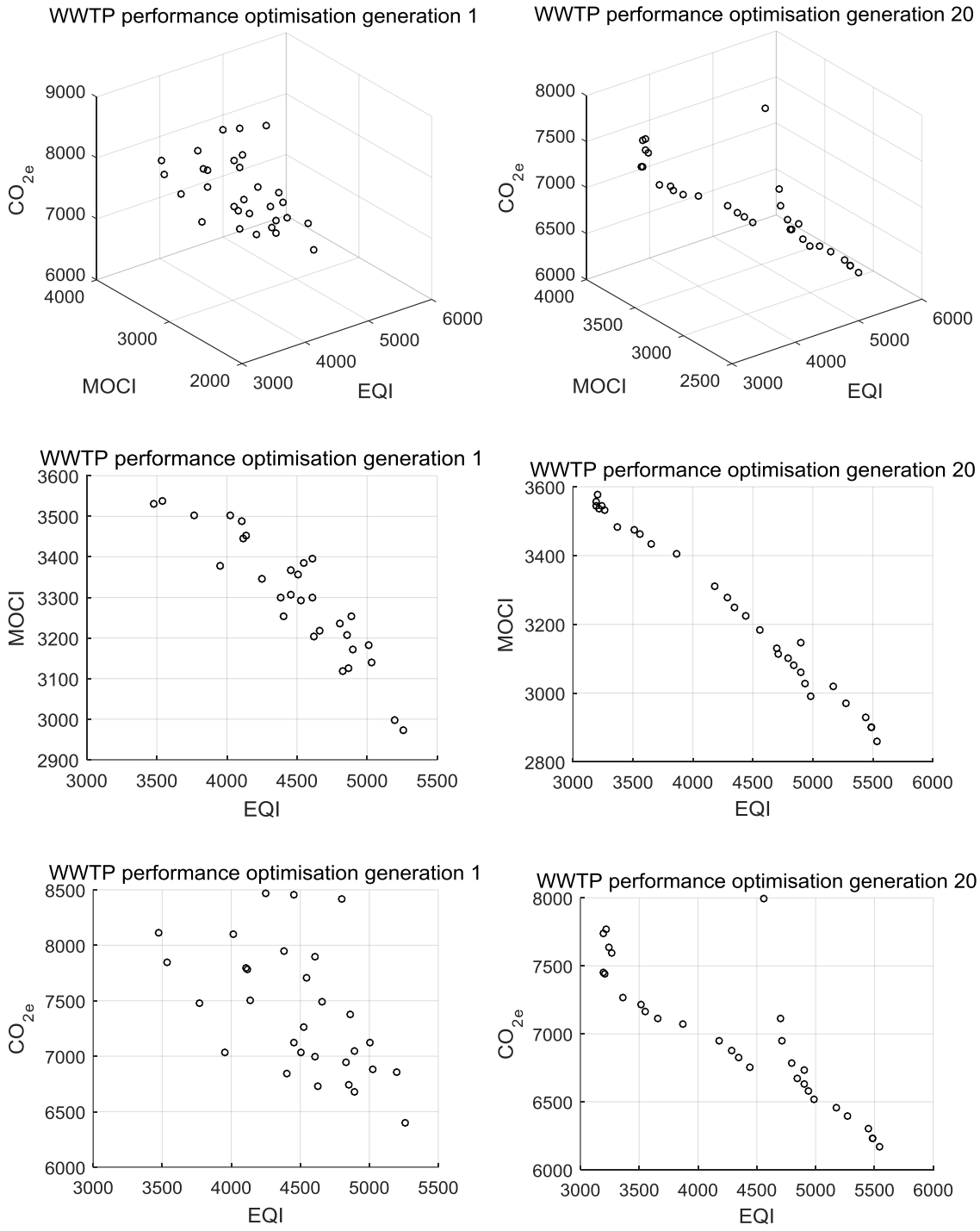

Figure 7-5 Optimisation results using storm tank by-pass set-points, inlet-pump capacity, and storm tank storage volume: First generation and last generation

Different combination of flow to full-treatment set-points, pumps' capacities, and storm tank storage volume gives rise to different solutions. The solutions have a negative linear pattern for EQI vs MOCI and EQI vs CO_{2e}, i.e. solutions with high MOCI and CO_{2e} are those with low EQI and vice-versa. To choose the most suitable solution in meeting the three objectives, the analysis is first started by assessing the solution that has the same EQI as the baseline, 4342.

Table 7-9 Optimisation solutions from the last generation showing parameters and objective values

Sol. No.	Pump 1	Pump 2	Qtostormtank as a fraction of DWF			as a fraction of the current volume			
			day	evening	night	VOL_ST	EQI	MOCI	CO_2e
1	0.76	1.07	1.22	2.92	3.12	1.74	5540	2858	6174
2	0.81	1	1.19	2.8	2.8	1.27	5489	2899	6235
3	0.81	1.02	1.19	2.8	2.8	1.23	5489	2900	6234
4	0.85	1	1.19	2.86	3.16	1.17	5446	2930	6298
5	0.96	1.11	1.19	2.77	3.36	1.8	5276	2969	6400
6	1.09	1.11	1.21	3	3.27	1.83	4987	2989	6513
7	1.01	1.12	1.21	2.99	3.36	1.7	5173	3018	6457
8	1.17	1.12	1.21	2.89	3.36	1.81	4933	3028	6580
9	1.1	0.97	1.26	2.95	3.2	1.52	4904	3059	6729
10	1.17	1.12	1.28	2.94	3.03	1.79	4842	3082	6669
11	1.18	1.09	1.33	2.86	3.16	1.78	4792	3100	6783
12	1.13	1.01	1.39	2.88	3.32	1.84	4714	3113	6948
13	1.19	1	1.39	2.9	3.04	1.84	4703	3131	7113
14	0.76	1.08	1.73	3	3.25	1.7	4904	3147	6627
15	1.15	0.92	1.5	2.9	3.2	1.46	4564	3182	7993
16	0.8	1.08	2.48	3	3.21	1.64	4444	3225	6752
17	0.82	1.12	2.5	2.99	3.15	1.76	4342	3251	6822
18	0.84	1.07	2.42	2.91	2.9	1.62	4287	3277	6874
19	0.87	0.99	2.5	2.85	2.75	1.37	4182	3310	6945
20	0.93	1.02	2.5	2.98	3.09	1.76	3867	3406	7067
21	0.97	1.12	2.5	2.98	3.15	1.66	3655	3435	7111
22	1	1.08	2.5	2.86	3.19	1.82	3556	3462	7164
23	1.03	1.06	2.47	3	3.11	1.73	3517	3474	7219
24	1.06	0.99	2.5	2.89	3.19	1.38	3367	3482	7266
25	1.13	0.9	2.5	2.89	3.17	1.62	3264	3533	7596
26	1.19	0.93	2.49	2.99	3.11	1.65	3217	3535	7768
27	1.19	0.93	2.5	2.98	3.11	1.65	3198	3543	7742
28	1.16	0.94	2.49	2.99	3.06	1.89	3239	3545	7637
29	1.19	1.15	2.5	2.99	3.15	1.78	3200	3556	7453
30	1.19	1.15	2.5	2.96	3.21	1.78	3209	3576	7440

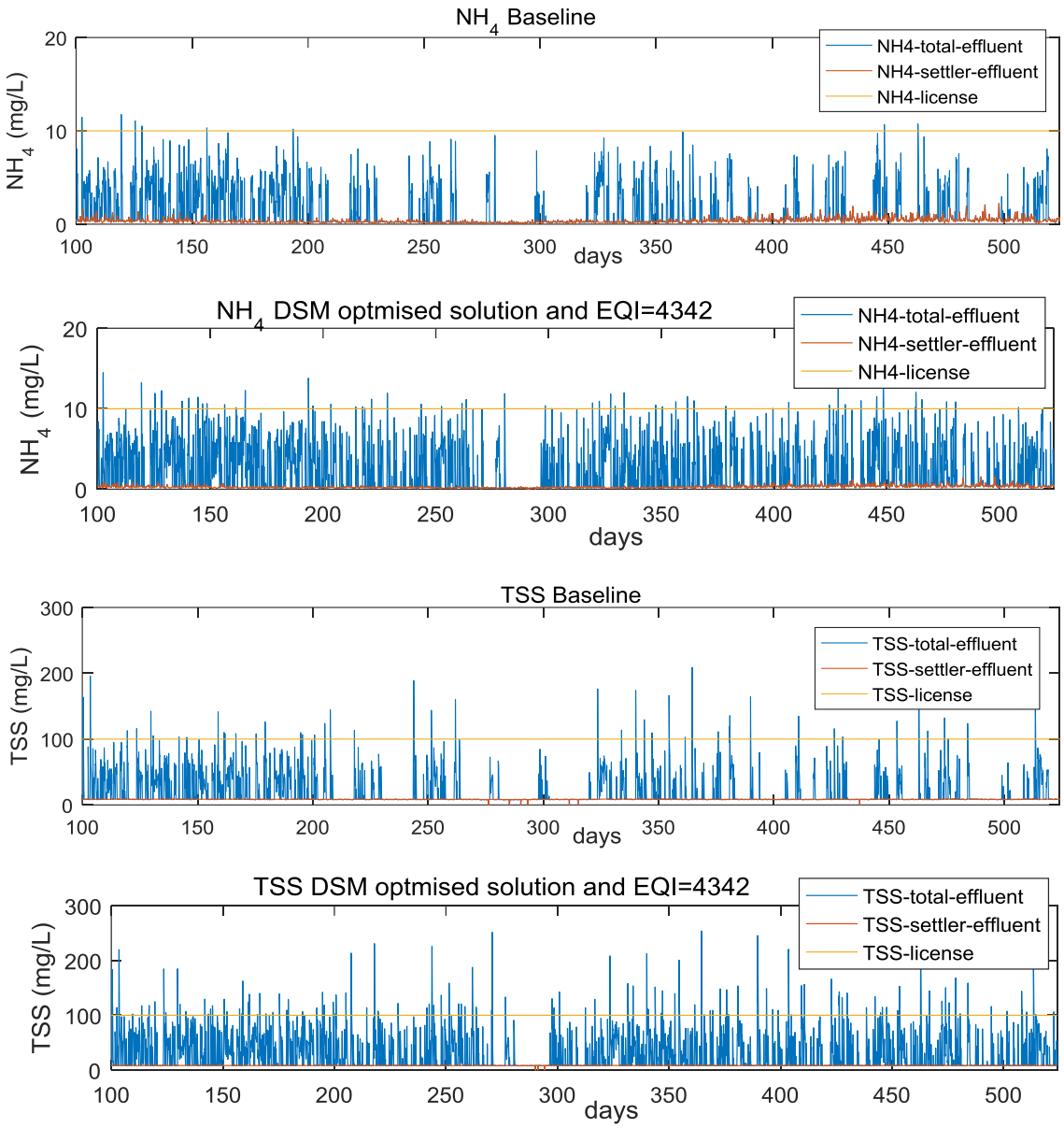

Figure 7-6 Final effluent pollutant concentrations compared to regulatory licenses: NH_4 and TSS Baseline vs Optimised Solution for inlet hydraulic capacity

The MOCI and CO_{2e} corresponding to the EQI value of 4342 (solution-17, Table 7-9) are both lower the baseline values; 3251 and 6822 respectively compared to the baseline values, 3439 and 7221 respectively. The lower MOCI and CO_{2e} are achieved because of the reduced capacity of the duty inlet wet-well pump by a ratio of 0.82, and by increasing the capacity of the WWTP as shown in Table 7-9.

In solution-17, although the capacity of the inlet of the WWTP is increased, the daily average flow reaching to the oxidation ditch (inlet wet-well outflow) is reduced due to the reduced capacity of the inlet wet-well pump. In the baseline scenario, the daily average flow to the oxidation ditch is 6524 m^3 d^{-1}, which is reduced to 6041 m^3 d^{-1} due to the overflow of sewage from the wet well because of the reduced capacity of the duty pump. similarly, the storm tank overflow is also

increased due to increased overflow from inlet wet-well. Regardless of the increase in the storm tank overflow, the EQI is similar to the baseline, but the proportion is different. In this scenario, the EQI due to TSS and TKN in the final effluent is increased by 3 % and 6.6 % respectively, but at the same time, EQI due to the COD and BOD in the final effluent is reduced by 3.2 % and 6.4 % respectively. Since EQI does not show whether effluent regulatory licenses are violated or not, Figure 7-6 shows that there is no violation of current licenses. The NH_4 license is 10 mg $L^{-1,}$ and the TSS license is 100 mg L^{-1}, see Section 5.2.2. The current license checks the quality of effluent from the final settlement before it mixes with the storm tank overflow, which is way below the license limit.

However, since the DSM approach with a variable set-point is suggesting a new licensing approach, it is necessary to look at the increase in violation after effluent is mixed with the storm tank overflow. The number of a license violation, after the final effluent is mixed with storm tank over flow, increases from 0 to 1 for NH_4 and from 1 to 3 for TSS, Table 7-10. Indicating that solution-17 can be used for reducing the cost of operation and CO_{2e} emission by 5 % and 6 % respectively, but with minor compromise in effluent quality.

Table 7-10 License conditions and violation for baseline scenario and DSM optimised solution-17

License violations in 424 days (40704 samples)	Effluent from settler			Effluent from settler mixed with storm tank overflow		
		DSM optimisation			DSM optimisation	
	Baseline	solution-17	solution-1	Baseline	solution-17	solution-1
Number of violation (NH_4)	0	0	0	16	326	4596
Number of violation (TSS)	0	0	0	294	1074	6577
of violation NH_4 license	0	0	0	0	1	11
of violation TSS license	0	0	0	1	3	16

On the other hand, solutions with high EQI values have low CO_{2e} and MOCI. For example, solution-1 in Table 7-9 has a reduction of MOCI by 19.2 % and reduction in CO_{2e} by 16.9 % but an increase in effluent pollutant load, EQI by 21.7 %. This is mainly due to the reduction of flow to full treatment through reduction of the storm by-pass set point during the day time ($Q_{tostormtank}$) and reduction of inlet wet-well duty pump's capacity. This increases the bypass flow to storm tanks which is, on average, 1899 m^3 d^{-1} compared to the baseline storm tank overflow, 711 m^3 d^{-1}.

The saving in operational cost is achieved mainly through the reduction of pumping, aeration and sludge transport. Since the total wastewater reaching the oxidation ditch is reduced to, on average, 5124 m^3 d^{-1} compared to the baseline,

6524m^3 d^{-1}, the CO_{2e} from biological assimilation is reduced. Due to high overflow from the storm tanks, the EQI due to TKN and TSS is increased by 16.7 % and 7.4 % respectively. However, unlike solution-17, the reduction in EQI from COD and BOD was not enough to counter balance this increase. The license violation of this scenario is shown in Figure 7-7. Not a suitable solution due to its high level of license violation and ultimately due to its impact on the quality receiving river.

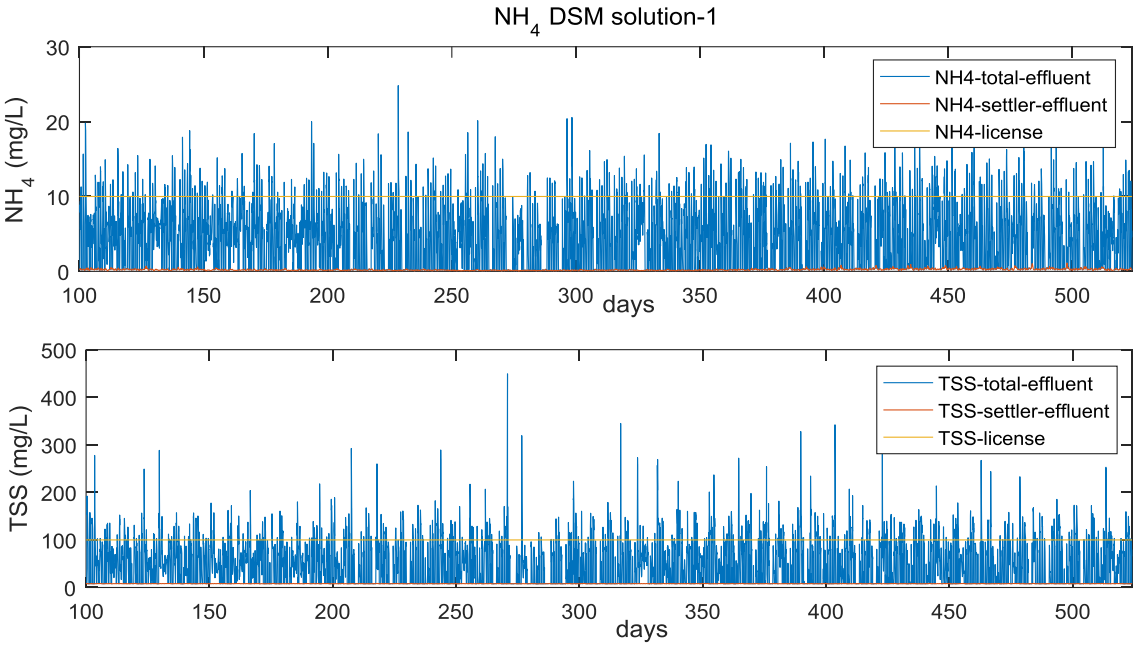

Figure 7-7 Comparison of license level and effluent quality of DSM optimisation solution-1: TSS and NH_4

7.6.2 Aeration Control Focusing on the Intermittent Phase

Commonly, intermittent aeration in single aerator is provided to accomplish the biological removal of nitrogen by creating an anoxic condition (Kimochi et al., 1998). The intermittent phase at Cupar WWTP is not designed to create an anoxic condition in the oxidation ditch (OD). Instead it is a mechanism to reduce the DO level if it is beyond the set-point, DOset2 (2.25 mg L^{-1}), see Chapter 3. Based on the sensitivity analysis in Section 7.4, variation of this set-point even without altering the continuous phase can have a significant impact on cost and a considerable impact on effluent quality and CO_2 emissions, see Table 7-3.

A simple test was used to assess the possibility of maximising the benefit of the energy tariff variation from energy DSM schemes, see Section 7.5.3, in which the intermittent DO set point is varied depending on the time of the day, see Table 7-11. However, this section considers more detail on the search for DOset2 values

and their best combination to trade-off and even optimise the aeration system to achieve the three objectives.

For this optimisation, the optimisation parameters are the three DO set-point, and the objectives are the thee performance indicators; MOCI, CO_{2e}, and EQI. The lower bound for the DOset2 point is set to be the same as the baseline DO set point for the continuous phase, 0.75 mg L^{-1}, see Table 7-11. The upper bound is offset from the values used during DSM by 0.25 mg L^{-1} for the day time and the night time Doset2 values used in the baseline scenario (2.5 mg L^{-1}). A population size of 30 and 20 generations are used.

Table 7-11 Intermittent DO set-points, upper and lower bound limits

Intermittent phase DO set-points	Baseline (mg L^{-1})	DSM (mg L^{-1})	Lower bound (mg L^{-1})	Upper bound (mg L^{-1})
DOset2 (day-time)	2.5	1.5	0.75	2
DOset2_evening	2.5	2	0.75	2.25
DOset2_night	2.5	2.25	0.75	2.5

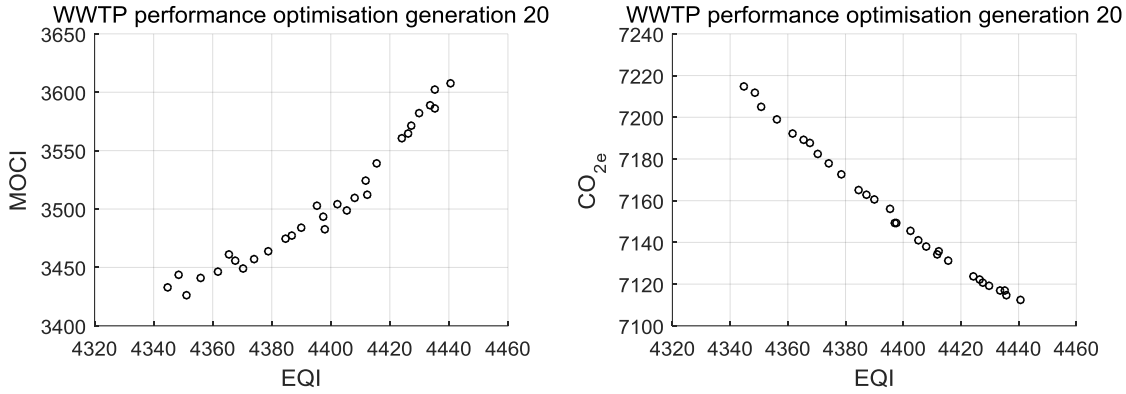

Figure 7-8 Optimisation results using intermittent-phase DO set-points: last generation

Searching for the optimal intermittent-phase DO set-points showed that with the current DO control strategy (continuous-phase with DO set point of 0.75 mg L^{-1}) it is not possible to trade-off all the three objectives, Figure 7-8. CO_{2e} increases when operational cost reduces and when effluent quality improves. However, comparing the optimisation result with the baseline, the solution with the highest CO_{2e} (Solution-1), 7215 kg CO_{2e} d^{-1}, is slightly lower the CO_{2e} from the baseline, 0.1 %, Table 7-12. The corresponding EQI is only 0.07 % higher than the baseline, and the MOCI is reduced by 0.2. The solution with the lowest CO_{2e} has the highest EQI and MOCI. Compared to the baseline, this solution with minimum CO_{2e} (Solution-30), has a reduction in CO_{2e}, 7112 kg CO_{2e} d^{-1}, 1.5 %, while having in increment both in EQI and MOCI, 4.9 % and 2.3 % respectively, Table 7-12. Hence, without

integrating the continuous-phase with the intermittent-phase, it is not possible to improve all objective and have a significant impact either.

Table 7-12 Optimisation solutions for DOset2, the last generation: parameters (intermittent-phase DO set-points) and objectives (performance indicators)

Sol. No.	Intermittent-phase DO set-points			WWTP performance indicators		
	Day	Evening	Night	EQI	MOCI	CO_{2e}
1	0.76	0.82	0.87	4345	3433	7215
2	0.76	0.96	0.93	4349	3444	7212
3	0.77	0.77	1.28	4351	3426	7205
4	0.92	1.06	0.93	4356	3441	7199
5	1	1.13	0.93	4362	3446	7192
6	0.97	1.1	1.26	4366	3461	7189
7	0.97	0.75	1.7	4368	3456	7187
8	1.07	1.1	1.26	4370	3449	7182
9	0.96	1.17	1.5	4374	3457	7178
10	1.08	1.1	1.62	4379	3464	7172
11	1.11	1.38	1.39	4385	3474	7165
12	1.1	1.26	1.7	4387	3477	7163
13	0.87	1.64	1.61	4390	3484	7160
14	1.41	0.98	1.9	4395	3503	7156
15	1.4	1.33	1.5	4397	3494	7149
16	1.24	1.27	1.89	4398	3482	7150
17	1.2	1.51	1.84	4403	3504	7145
18	1.3	1.45	1.9	4405	3499	7141
19	1.37	1.41	1.93	4408	3509	7138
20	1.36	1.56	1.91	4412	3525	7135
21	1.29	1.62	2.02	4413	3513	7136
22	1.57	1.6	1.67	4416	3539	7132
23	1.77	1.58	1.82	4424	3561	7124
24	1.67	1.83	1.71	4426	3564	7123
25	1.78	1.76	1.73	4427	3572	7121
26	1.75	1.77	1.89	4430	3582	7119
27	1.78	1.84	1.95	4434	3588	7117
28	1.9	1.87	1.8	4435	3602	7117
29	1.8	1.84	2	4435	3586	7115
30	1.98	1.82	2.04	4440	3607	7112

7.6.3 Continuous Aeration Control

The sensitivity analysis showed that the continuous DO set-point is not a sensitive parameter in the current operational procedure due to the high level of DO level in the oxidation ditch. In this section, it is assumed the blowers can be replaced so as the kLa values can be reduced to the required level by having a blower that can reduce the air flow to the minimum level required without entering an intermittent phase, unlike the current operational procedure. That is During intermittent-phase kLamin2 = 0 (in baseline operation it is 24), and in continuous-phase, the minimum kLa value can go as low as zero, i.e. kLa_min = 0. The baseline DO set-point for continuous-phase is used here.

Table 7-13 WWTP performance indicators using continuous DO control

Performance Index	Baseline	Continuous DO control	Percentage change in performance
CO_{2e}	7221	7608	5.36
OCI	4087	3809	-6.80
EQI	4342	4030	-7.19
MOCI	3439	3279	-4.65

Eliminating intermittent aeration and allowing continuous reduction or increment of the DO level in the oxidation ditch results in a better control of the DO, i.e. the DO level does not go as high as the DO level during the baseline control. The continuous DO control reduces operational cost index MOCI and OCI by 4.7 % and 6.8 % respectively through the reduction of energy use for aeration, see Table 7-13. The reduction in MOCI is higher than the reduction in OCI due to the need for aeration in the day-time (when pollutant load is higher) is much higher than the need for aeration during the night-time.

However, the lower DO level means higher death and more utilization of nitrates and resulting in higher GHG emission (5.4 %) from biological assimilation and N_2O from denitrification, which couldn't be counter balanced by the reduction in CO_{2e} from reduced energy use for aeration, see Figure 7-9.

The EQI is improved by 7.2 %, mainly due to the reduction of NO_3 concentration in the final effluent because of the increased denitrification process, Figure 7-9.

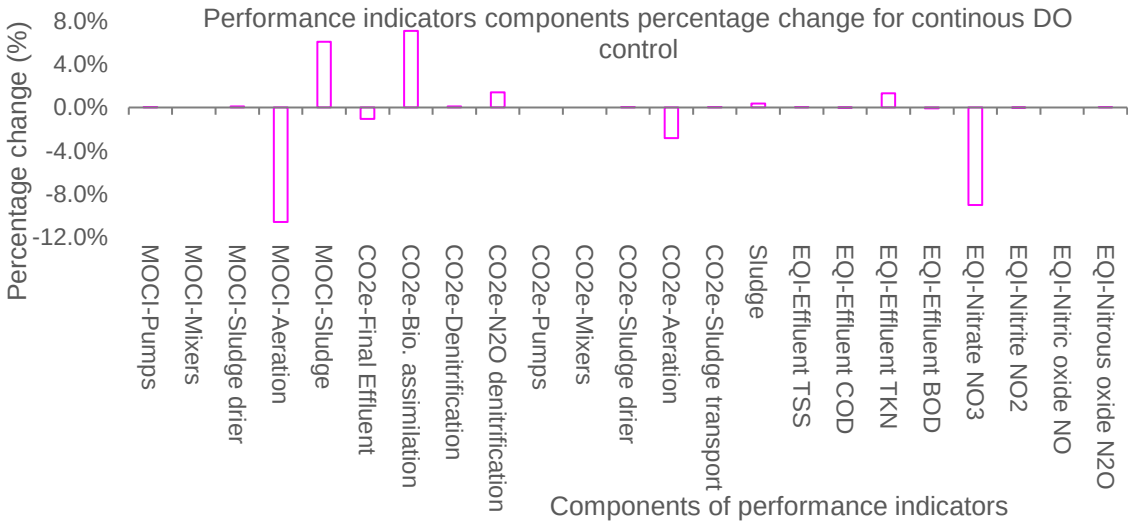

Figure 7-9 Performance indicators' components percentage change due to continuous DO control

7.6.4 Optimisation of the Continuous Aeration Control

In this scenario, the continuous DO control is from Section 7.6.3 is adopted, i.e. there is no intermittent phase. The day-time, the evening and the night-time DO set point, which was set to be 0.75 mg L^{-1} in the baseline scenario are used as optimisation variables. Their values vary from 0.05 mg L^{-1} (LB) to 2.25 mg L^{-1} (UB). The optimisation is setup with a population size of 30 and 20 generations, the objectives being the MOCI, EQI, and CO_{2e}.

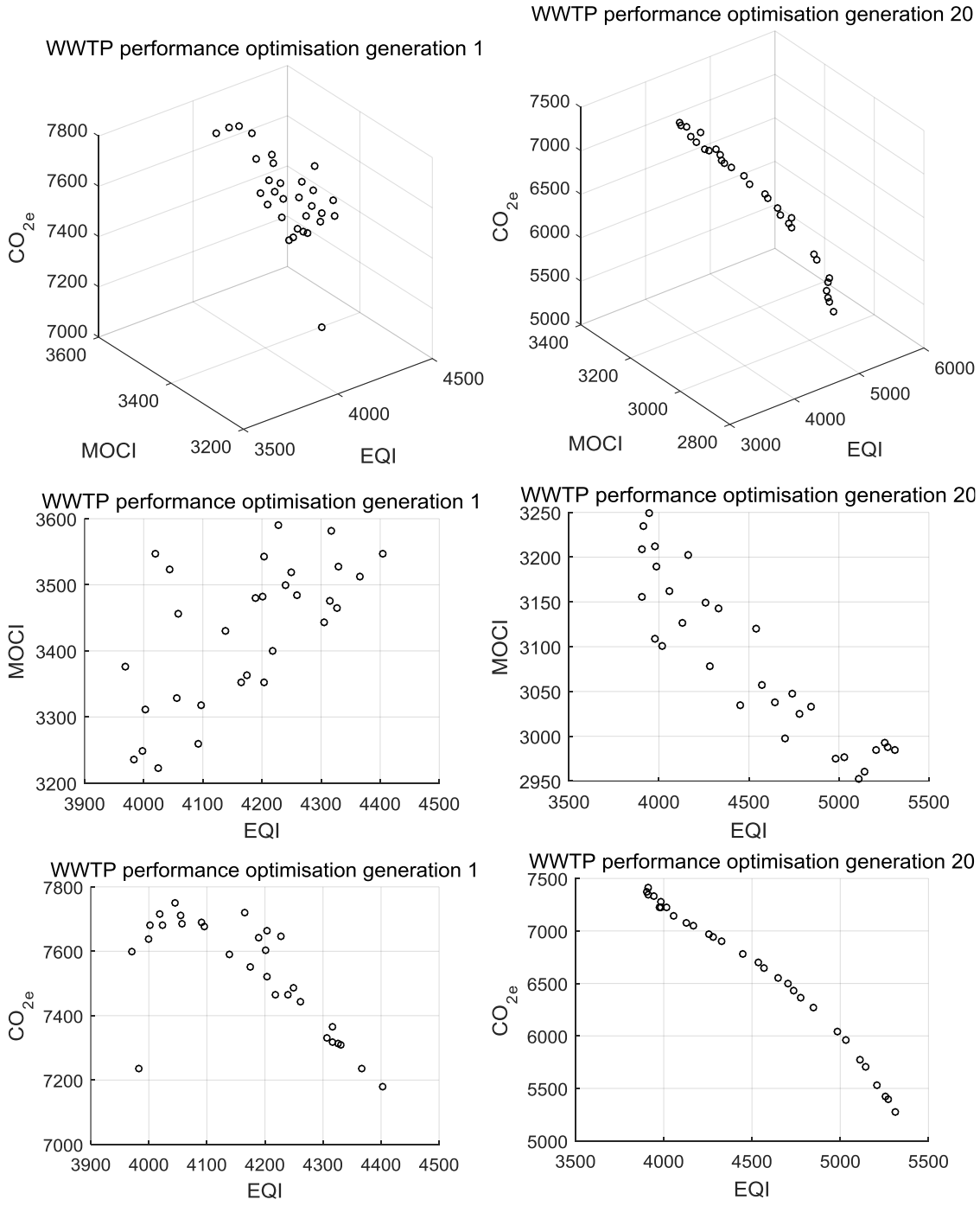

Figure 7-10 Optimisation results using continuous aeration control with variable DO set-points at different times of the day

The optimisation result, generation 20, presented in Figure 7-10 shows that generally, the CO_{2e} and the MOCI increases as the effluent quality improves. In other words, reduced CO_{2e} and MOCI can only be achieved by increasing the EQI. However, it is essential to compare the CO_{2e} and MOCI associated with the EQI value close to the baseline value. As a result, further assessment is done on solutions with the following objectives; minimum CO_2, minimum MOCI, minimum EQI, and EQI close to the baseline, see Table 7-14, in which the solutions are ranked in ascending order of the EQI.

Table 7-14 Continuous DO set-point optimisation solutions from the last generation showing parameters and objective values

Sol. No.	Intermittent-phase DO set-points			WWTP performance indicators		
	Day	Evening	Night	EQI	MOCI	CO_{2e}
1[i]	0.49	0.5	0.43	3903	3208	7377
2	0.4	0.48	0.62	3908	3156	7413
3	0.54	0.51	0.12	3911	3235	7346
4	0.65	0.15	0.39	3945	3250	7335
5	0.46	0.33	0.25	3980	3212	7228
6	0.06	0.21	0.67	3981	3109	7282
7	0.42	0.4	0.18	3983	3189	7220
8	0.15	0.05	0.61	4015	3101	7226
9	0.34	0.43	0.06	4057	3162	7148
10	0.23	0.45	0.17	4129	3126	7077
11	0.47	0.09	0.05	4164	3203	7056
12	0.36	0.17	0.24	4257	3149	6975
13[ii]	0.2	0.22	0.37	4283	3078	6945
14[iii]	0.35	0.21	0.17	4330	3143	6907
15	0.05	0.24	0.35	4449	3034	6778
16	0.34	0.16	0.06	4539	3120	6695
17	0.24	0.14	0.28	4569	3057	6648
18	0.24	0.23	0.18	4647	3038	6546
19	0.09	0.05	0.36	4705	2997	6496
20	0.26	0.17	0.18	4738	3047	6429
21	0.19	0.23	0.18	4779	3024	6366
22	0.24	0.17	0.14	4845	3034	6272
23	0.14	0.06	0.27	4983	2975	6041
24	0.14	0.05	0.26	5029	2976	5957
25[iv]	0.05	0.09	0.26	5114	2952	5775
26	0.1	0.09	0.22	5141	2961	5703
27	0.13	0.12	0.13	5211	2984	5536
28	0.13	0.05	0.13	5257	2994	5421
29	0.05	0.06	0.17	5268	2988	5392
30[v]	0.1	0.05	0.05	5312	2984	5269

i - Although solution-2 has the highest CO_2, it is dominated by solution-1 due to lower EQI and MOCI
ii - EQI close to the baseline EQI value. Solution-14 has closer EQI value to the baseline but dominated by this solution due to improved EQI, lower MOCI and a minor increase in CO_{2e}
iii - EQI close to the baseline EQI value.
iv - Minimum MOCI associated with near-to-minimum CO_{2e} and higher EQI
v - Minimum CO_2 emissions associated with higher EQI and near-to-minimum MOCI

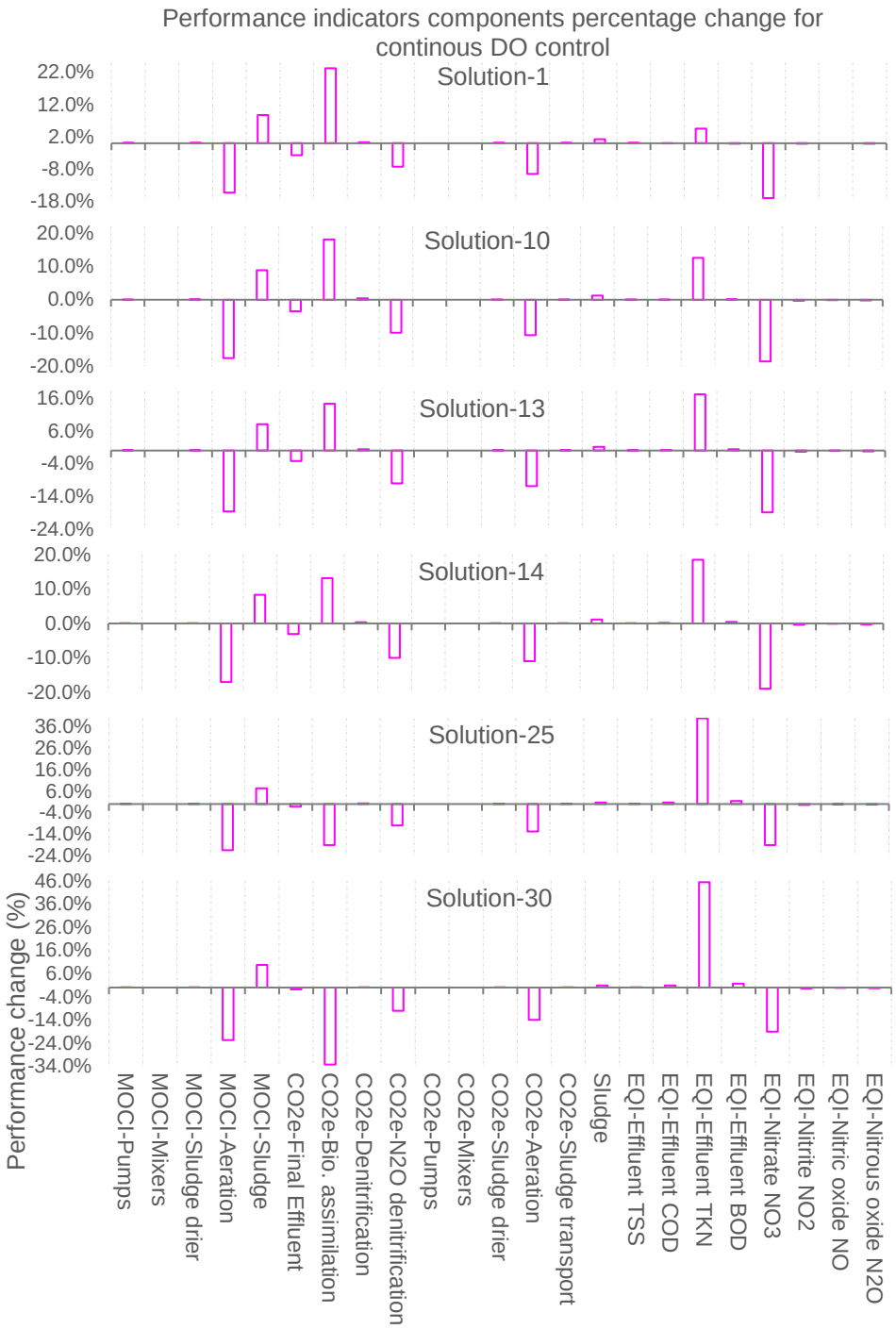

Figure 7-11 Percentage change in performance indicators' components for selected solutions from optimisation of continuous DO control

Table 7-15 Percentage change in WWTP performance indices from optimisation of continuous DO control strategy

WWTP Performance Index	Percentage change in performance indicator indices for optimisation of continuous DO control strategy					
	Solution- 1	Solution-10	Solution-13	Solution-14	Solution-25	Solution-30
CO_{2e}	2	-2	-4	-4	-20	-27
OCI	-10	-12	-13	-13	-17	-17
EQI	-10	-5	-1	0	18	22
MOCI	-7	-9	-10	-9	-14	-13

Solution 14 has an EQI value very close to the baseline EQI value of 4342, but it has lower operational cost and GHG emissions as well, Table 7-15. The operational cost OCI is reduced by 13 % but the MOCI only reduced by 9 % due to the time-insensitiveness of sludge transport cost, which is higher in this scenario, Figure 7-11 (Solution-14). Removing the intermittent phase of DO control and using continuous DO control at the original set-point (0.75 mg L^{-1}) only reduces cost but increase CO_2 as discussed in Section 7.6.3. In contrast, optimising this set-point can improve both operational cost and CO_{2e} to a higher degree without affecting the overall EQI. The overall EQI is not affected as the increase in TKN is counter balanced by the reduced NO_3 in the final effluent, Figure 7-11 (Solution-14). As shown in Figure 7-12, the ammonia concentration in the effluent from the settlers violates the license 3747 times, which is 9 % of the total data points. Hence, this solution violates the current fixed NH_4 license and, as it is, it cannot be considered as a potential solution.

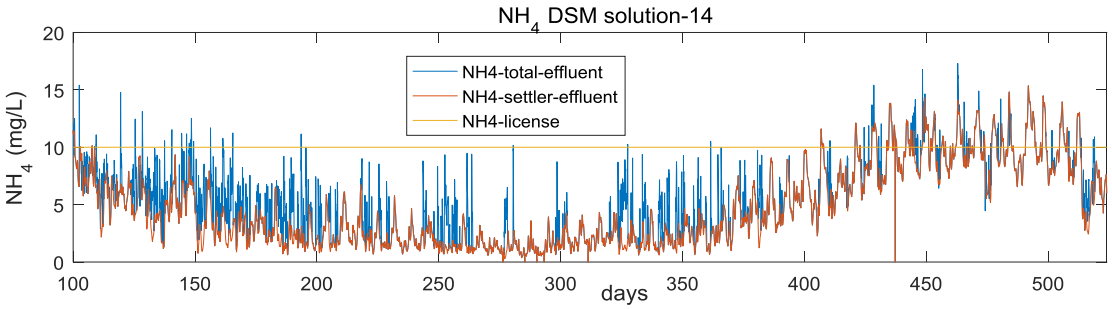

Figure 7-12 Final effluent ammonia concentration of Solution-14 compared to ammonia license

Solution-13 dominates Solution-14 due to its improved EQI and reduced operational cost, but again the ammonia limit in the final effluent is exceeded 6 % of the time, just below the license which allows 10 % exceedance. Moving up in Table 7-14, Solution-10 compared to the baseline shows a reduction in all the objectives (Table 7-15), and with no license violation with exceedance of 0.4 from the NH_4 limit (10mg L^{-1}), Figure 7-13. The seasonal variation of the NH_4 is driven

by temperature due to reduced DO level in the oxidation ditch, and if DO level does not increase as temperature increases, then the biomass decay rate will exceed the DO-deprived slow growth rate; hence, the increase in NH_4. Perhaps, increasing and DO set-points in relation to temperature might be a topic to investigate in future work as it is out of the scope of this project. Reducing the DO set-points below Solution-10 (solutions from 11 – 30) results in a high level of ammonia concentration in the final effluent and results in a violation of the license. Since this scenario is set-up with a hypothesis that there is no need for a new license the solutions with minimum CO_2 (e.g. Solution-30) and those with minimum MOCI (e.g. Solution-25) are not assessed further.

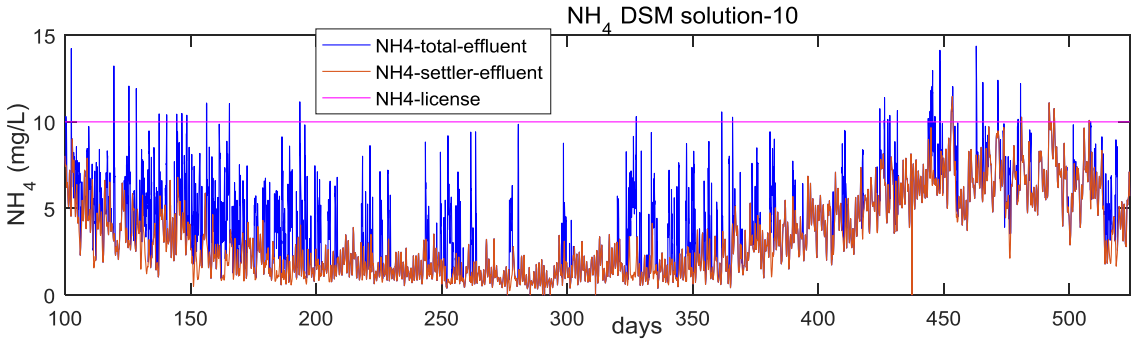

Figure 7-13 Final effluent ammonia concentration of Solution-10 compared to ammonia license

Solution-1 with the highest CO_{2e} is just 2 % more emissions than the baseline, but both EQI and OCI improved by 10 % and MOCI improved by 7 % (again improvement in MOCI is lower than OCI due to the higher cost of sludge transport in this solution, which is insensitive to time-of-day). The ammonia concentration increases from the baseline but no violation of the NH_4 limit. It is the safest solution but with an increased cost and GHG emissions compared to Solution-10.

7.6.5 Aeration Control Based on Final Effluent NH_4

In most WWTPs the objective of aeration control is to maintain DO level at a particular set point (Rieger et al., 2014). Similarly, the current DO control strategy at Cupar WWTP is designed to do the same. Such controls are used with the objective of achieving complete nitrification and making sure the effluent quality licenses such as ammonia limits are not violated. However, if the objective is to maintain final effluent ammonia level below the limit, the controller variable should be ammonia in the final effluent than the dissolved oxygen in aerators. There are many reasons why WWTPs still uses such control strategies such as simple DO control approach, but it is not the interest of this section to make the comparison.

Instead, this section will assess the benefit of controlling aeration in the oxidation ditch, in this instance, based on the ammonia concentration in the final effluent.

A feedback control loop presented in Chapter 2 which has the same structure as the baseline DO control strategy is used here but with variation in the controlled variable, Figure 7-14. The control variable or the feedback element is this control strategy is the final effluent NH_4 concentration. The controller action is done based on the difference between the feedback element and the desired value or set-point point, in this case, 90 % of the maximum ammonia license. The objective of the controller is to reduce this difference by the controller action, i.e. by adjusting the blowers' speed to determine the DO level in the oxidation ditch. This control strategy will create a variable DO set-point which is determined based on the difference between the final effluent NH_4 and the ammonia license limit. The gain factor, KSO_4, for controlling the oxygen supply in the oxidation ditch is modified to create a negative relationship with the change in ammonia concentration in the final effluent and the need for change in DO concentration. The gain factor, KSO4's value is taken to be similar to the baseline except for the negative relationship (-25) (Jeppsson et al., 2007).

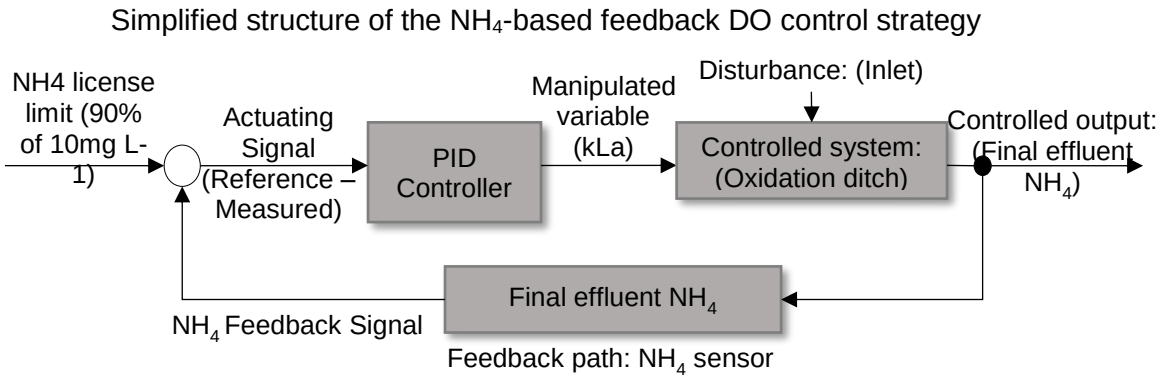

Figure 7-14 Simplified structure of the NH_4-based feedback DO control strategy

For Cupar WWTP, the aeration control is set-up assuming the same blowers can be used with this control strategy, i.e. the blowers won't be turned off completely if the reduction of DO is required. Instead, the blowers will enter an intermittent-mode similar to the baseline to give a minimum kLa of 24 h^{-1}, which is equivalent to the minimum kLa value for the baseline intermittent-phase (kLamin2). This control strategy can be implemented by placing ammonia sensor and connecting the signal to the existing controller or Supervisory Control and Data Acquisition (SCADA), which means it can be implemented with very low capital investment.

Table 7-16 Percentage change in WWTP performance indices from NH_4-based DO control strategy

Performance Index	Baseline	NH_4-based DO control	Percentage change in performance
CO_{2e}	7221	7279	0.80
OCI	4087	3674	-10.11
EQI	4342	3936	-9.35
MOCI	3439	3199	-6.98

Without the need to make major upgrades to infrastructures, this control strategy can reduce operational cost by 10.1 % and 7 % as measured by OCI and MOCI respectively, Table 7-16. The EQI is improved by 9.4 % while the CO_2 emission doesn't show improvement, a 0.8 % increment. The reduction in the operational cost is a result of the combination of the decrease in aeration cost (reduction of 20.8 % based on OCI and 15.7 % based on MOCI), and an increase in sludge transport cost, 8.6 %, Figure 7-1. Compared to the baseline the CO_{2e} from biological assimilation increases by 20.5 %, but the reduction in CO_{2e} due to the reduction in the production of Nitrous Oxide (7.4 %) and the reduction in energy use for aeration (9.6 %). The effluent quality is improved due to the reduction in Nitrite (NO_3^-) concentration in the final effluent (16.3 %) although there is an increase in TKN in the final effluent (4.8 %). The reduction or increase in other pollutants is insignificant, below 0.1 %, Figure 7-15.

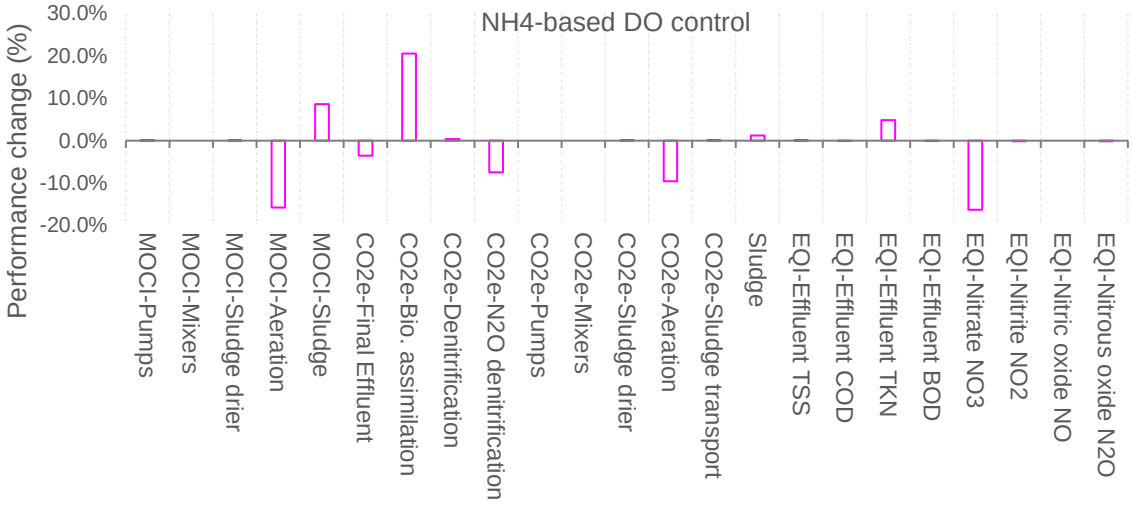

Figure 7-15 Percentage change in performance indicators' components for selected solutions from NH_4-based DO control

The NH_4-based DO control strategy reduces aeration and increases the ammonia concentration in the final effluent. However, the ammonia concentration in the final effluent is way below the target (90 % of the license limit, 10 mg L^{-1}), Figure 7-16; no exceedance. The reason that the NH_4 level in Figure 7-16 (red) is way below

the licence limit 10 mg L^{-1} since the blowers' speed cannot be reduced below their minimum speed during the continuous phase. In other words, similar to the baseline modelling, the kLa value in the aerated zones is not allowed to go below 72 h^{-1} and 24 h^{-1} in the continuous and intermittent phase respectively. This phenomenon results in more nitrification than needed.

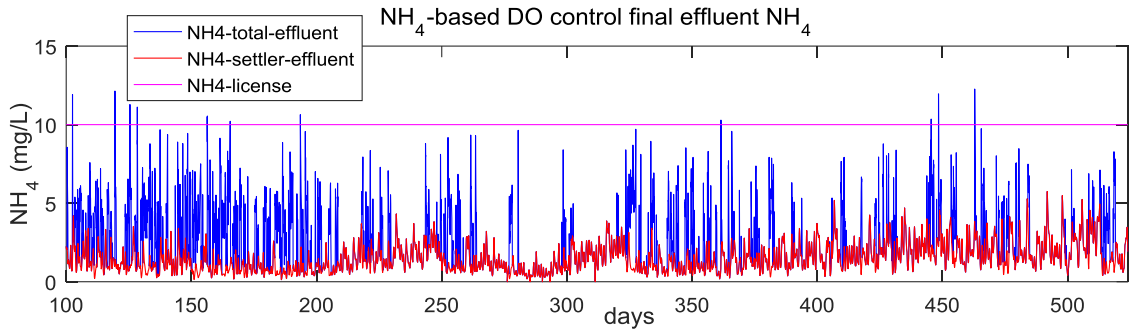

Figure 7-16 Final effluent ammonia concentration of NH_4-based DO control strategy compared to ammonia license

Further analysis is done by allowing the blowers to be turned off as long as needed, i.e. the kLa can be reduced to zero if required by the controller. Doing so increases the ammonia concentration in the final effluent to be close to the license limit, Figure 7-17. This control design results in the final effluent ammonia concertation exceeding the license limit (10 mg L^{-1}) only 1 % of the time (393 data points out of 40704), which is under the license limit that allows 10 of exceedance.

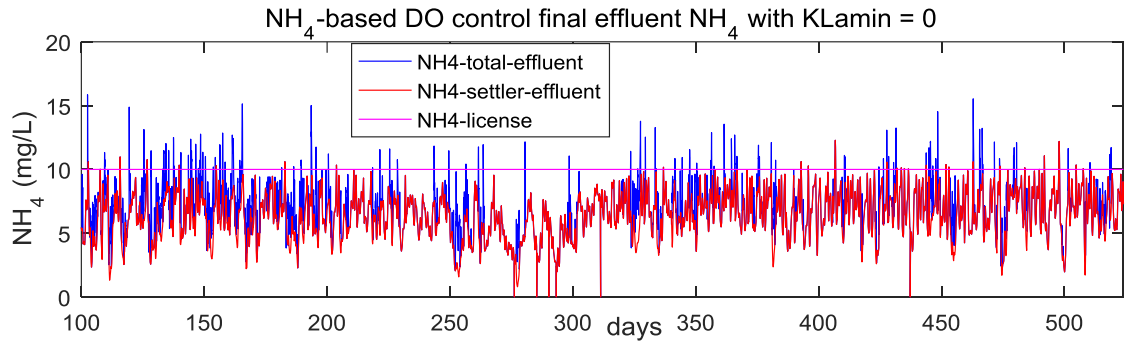

Figure 7-17 Final effluent ammonia concentration of NH_4-based DO control strategy (kLa allowed to be zero) compared to ammonia license

By allowing the kLamin to go as low as zero for as long as needed, the NH_4-based DO control strategy brings a good trade-off among the objectives. The control strategy reduces CO_2 emissions by 13.6 % and the operational cost by 12.7 % and 9 % as measured by OCI and MOCI, respectively, Table 7-17. The EQI is increased by 5.9 %.

Table 7-17 Percentage change in WWTP performance indices from NH_4-based DO control strategy (kLamin set to zero)

Performance Index	Baseline	NH_4-based DO control (kLamin = 0)	Percentage change in performance
CO_{2e}	7221	6236	-13.64
OCI	4087	3570	-12.65
EQI	4342	4597	5.87
MOCI	3439	3131	-8.96

Compared to the baseline the CO_{2e} from biological assimilation reduced by 3.3 %, and the production of Nitrous Oxide from denitrification, and CO_2 from energy use for aeration reduced by 4.5 % and 5.4 %, respectively. The pollutant load in the final effluent is increased due to an increase in TKN concentration (20.2 %) although there is a reduction of Nitrite (NO_3^-) concentration of 14.6 %. The reduction or increase in other pollutants is insignificant, below 0.4 %, Figure 7-18. Therefore, the NH_4-based DO control approach reduces both operational cost and GHG emissions without violating the license.

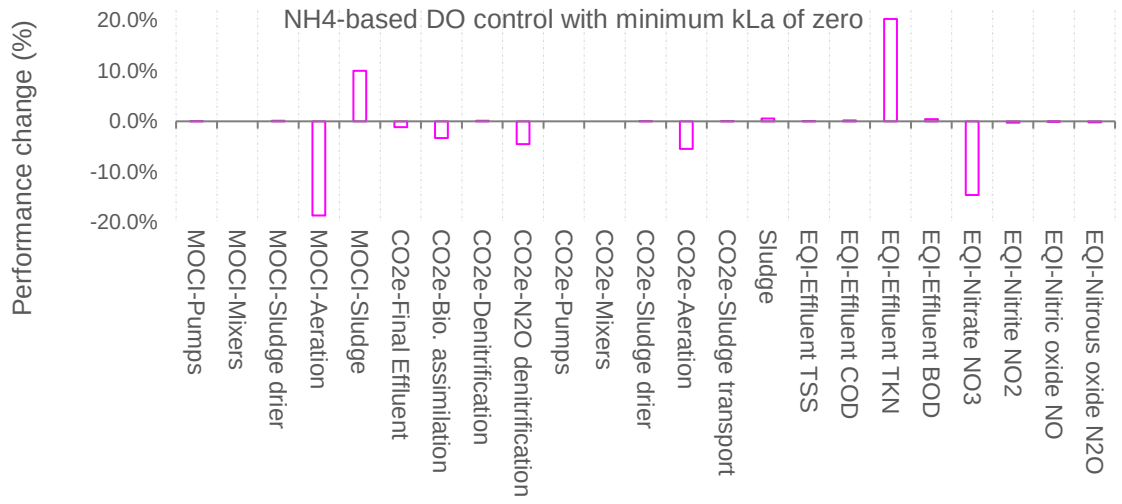

Figure 7-18 Percentage change in performance indicators' components for selected solutions from NH_4-based DO control (kLamin set to zero)

7.6.6 Dynamic Licensing: Receiving River's Assimilative-Capacity-Based DO Control

The current licensing or regulatory approach in place governing the WWTPs in the UK uses a fixed licensing approach. The fixed licensing approach uses a specific limit for a certain pollutant in the final effluent, i.e. the limit level will not change with time or the receiving water capacity. Such an approach can result over-treatment of the wastewater or unprecedent impact on the water ecosystem due to lower receiving/assimilative capacity of water bodies.

Dynamic licensing is a new licensing regime that uses variable final effluent pollutant limits, which are determined based on the assimilative capacity of the receiving water body. This variation can either be based on seasonal variation of the assimilative capacity, or even the real-time capacity, which can be used to determine the required standard on the effluent quality. In this study, dynamic licensing is tested for the latter case where a real-time capacity of the river is used to determine the effluent quality. In order to test this strategy, it is essential to integrate the WWTP and influent generator with the river model which is capable of calculating the assimilative capacity of the river. The details on how the river model estimates the assimilative capacity of the river and determine the maximum load available for wastewater discharges can be found in Dickinson (2018).

Control of the aeration in the oxidation ditch base on the assimilative capacity of the river is tested in this section. The assimilative capacity is calculated for ammonia, which is the current pollutant in the existing license. The control structure is shown in Figure 7-19. In the integrated, WWTP and influent generator model, the same control structure is applied as described in Section 7.6.5. the difference lies on the reference NH_4 concentration, which is determined as a maximum allowed NH_4 from the final effluent calculated by the river model using the assimilative capacity.

According to the Scottish River Basin Management Plan (SRBMP), the receiving river, River Eden, is classified as a type 3 river. For type 3 rivers to be classified as ‘good’ in terms of chemical and physiochemical environmental standards, they need to have a percentage oxygen saturation level as 10 percentile values to be above 60 %. The 90-percentile value of the BOD of the river should be above 5 mg L^{-1}, and the 99-percentile above 11 mg L^{-1}. In addition to these environmental standards, the Rive Eden is subjected to specific pollutant standards such as Ammonia. For River Eden to have a ‘good’ standard, the 90-percentile values of the total ammonia concentration in the river should be below 0.6 mg L^{-1}. The estimation of WWTP allowable load is estimated by through optimisation in the river model that uses these chemical and physiochemical environmental standards and simulated river flow and quality upstream of the WWTP, (Dickinson, 2018).

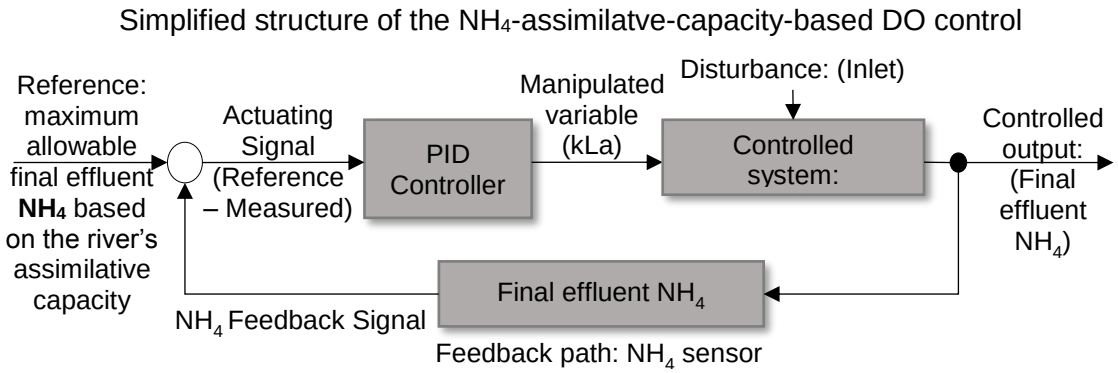

Figure 7-19 Simplified structure of the NH_4-assimilatve-capacity-based DO control

Sensor type B1 from the original BSM2 (Jeppsson et al., 2007)is adopted for sensing NH_4 in the final effluent, similar to Section 7.6.5. and the one used in the baseline scenario to control the dissolved oxygen in the oxidation ditch. The response time for this sensor was taken to be 5 minutes, 'T90_SO4'. The sensor uses the same sensor noise as that of the original BSM2 model (Jeppsson et al., 2007), see Section 3.2.1.2.

In the baseline scenario, the maximum DO level that can be sensed was limited to 10 mg L^{-1}. However, this maximum limit for NH_4 sensor after considering noise is revised to be 30 mg L^{-1}. The noise in the NH_4 sensor is generated randomly using a mean value of zero and a variance of 0.25 (Jeppsson et al., 2007). The standard deviation for the random noise is taken to be the same as the DO sensor, 0.025 mg L^{-1}.

The ammonia concentration is measured at immediately after the final settlement tanks before the final effluent is mixed with the storm tanks overflow. In order to avoid violating the maximum ammonia concentration target in the river as a result of not considering the storm overflow from the WWTP, a control mode switch is set up. Whenever there is an overflow the control of DO is switched from dynamic licensing to NH_4-based fixed licensing, described in Section 7.6.5, which is controlling aeration based on the concentration of NH_4 in the final effluent and its maximum allowable concentration in the license. The switch is implemented in the Simulink model by using a switch block to select the reference ammonia concentration, Figure 7-20. If the storm tank overflow is above 10 m^3 d^{-1}, control of aeration is based on fixed licensing; else it is controlled based on the assimilative capacity of the river, dynamic licensing. When control is based on fixed licensing, the reference NH_4 concentration is set to 9 mg L^{-1}, which is 90 % of the license limit (10 mg L^{-1}). This control structure is setup without altering the existing

infrastructure, for example, the blowers cannot reduce their speed below a certain level. In this case, the minimum oxygen transfer rate (kLamin2) at the lowest rotation of the blowers is taken to be 24, similar to the intermittent phase in the baseline DO control strategy.

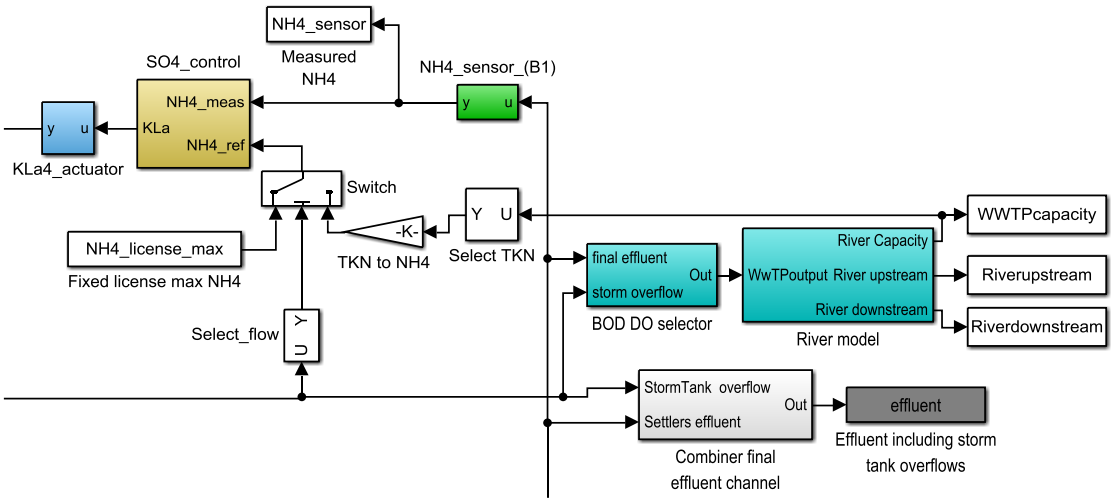

Figure 7-20 River assimilative-capacity-based aeration control structure implemented in Simulink

River assimilative-capacity-based DO control showed a reduction in operational cost and improvement in the final effluent quality, Table 7-1. However, the GHG emission increases by 4.3 due to increased emission from biological substrate assimilation and biomass decay. The reduction in operational cost is due to reduced aeration, OCI reduction of 11 % although there is an increase in sludge production of 5.3 %, Figure 7-21. The effluent quality improvement of 8.7 % is, compared to the baseline, mainly due to a reduction in NO_3 as a result of reduced nitrification, Figure 7-21.

Table 7-18 Percentage change in WWTP performance indices using rivers assimilative-capacity-based DO control

Performance Index	Baseline	River assimilative-capacity-based DO control	Percentage change in performance
CO_{2e}	7221	7566	4.78
OCI	4087	3913	-4.26
EQI	4342	3986	-8.20
MOCI	3439	3381	-1.69

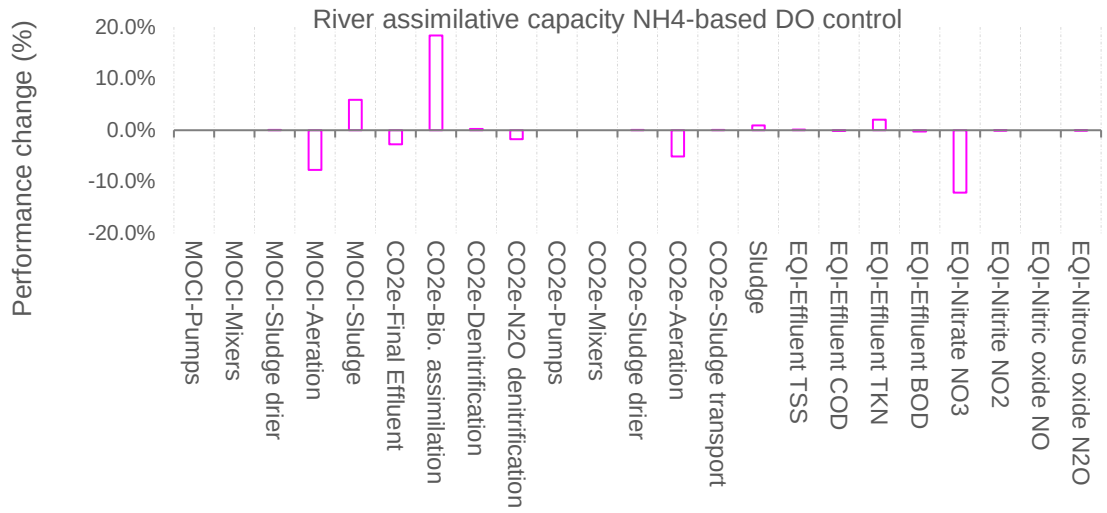

Figure 7-21 Percentage change in performance indicators' components for River's assimilative-capacity-based DO control

The improvements in WWTP performance is not as pronounced as those found using continuous DO control or using fixed licensing NH_4-based DO control. Initially, it was thought that the assimilative-capacity-based control strategy tested here uses the same infrastructure limitations as the baseline. However, tests showed that the WWTP performances in this control strategy are insensitive to these limitations. For example, the limitations on the blowers were removed to have a continuous reduction and increment of aeration can takes place. However, this does not improve or change any of the indicators. The switch to the fixed licensing setup was removed from the control structure but again did not show any change on the WWTP performance indicator.

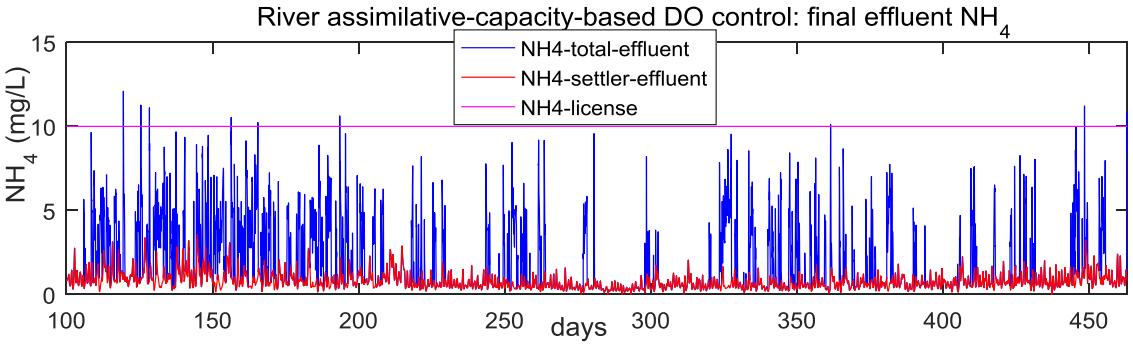

Figure 7-22 Final effluent ammonia concentration of river assimilative-capacity-based DO control strategy

Analysing the final effluent NH_4 concentration showed that the NH_4 concentration in the final effluent is way below the fixed licensing NH_4 limit, indicating that the river has a lower receiving capacity than anticipated, Figure 7-22. This leads to the need to investigate the allowable NH_4 concentration calculated by the optimisation

process in the river model. Figure 7-23 shows that the allowable final effluent NH_4 concentration (based on the assimilative capacity of the river) is much lower than the fixed licensing NH_4 limit (90 percentile of 10 mg L^{-1}). The assimilative capacity for NH_4 from the river model is very dynamic which is not common in river systems. The model estimate for allowable effluent flow rate is too high, with an average flow rate of 882,610 m^3 d^{-1}, compared to the average WWTP final effluent flow rate, 3,542 m^3 d^{-1}. This indicates that the lower allowable NH_4 is not actually due to low assimilative capacity of the river; rather it is due to the high allowable flowrate that requires a lower pollutant concentration.

Hence, the lower allowable NH_4 from the river model is associated with a high allowable flow rate which is much higher than the expected final effluent from the WWTP. The optimisation approach implemented in the river model to calculate the assimilative capacity of the river is not set for a specific flower rate, rather the flow rate is left to be searched for during the optimisation process. The optimisation tends to move to the high flow rate and low pollutant load solutions. However, a smaller flow rate with higher pollutant concentration may have the same impact on the river quality due to dilution. In other words, such optimisation process to search for a specific allowable flow rate, and simultaneously looking for the allowable pollutant concentration to come up with one solution is not a suitable approach for control purposes. Instead, pollutant load can be used for optimisation purposes that can have a different combination of flow rate and pollutant concentration. Once the allowable pollutant load is known, the allowable WWTP effluent pollutant concentration for a specified effluent flow rate can be calculated easily.

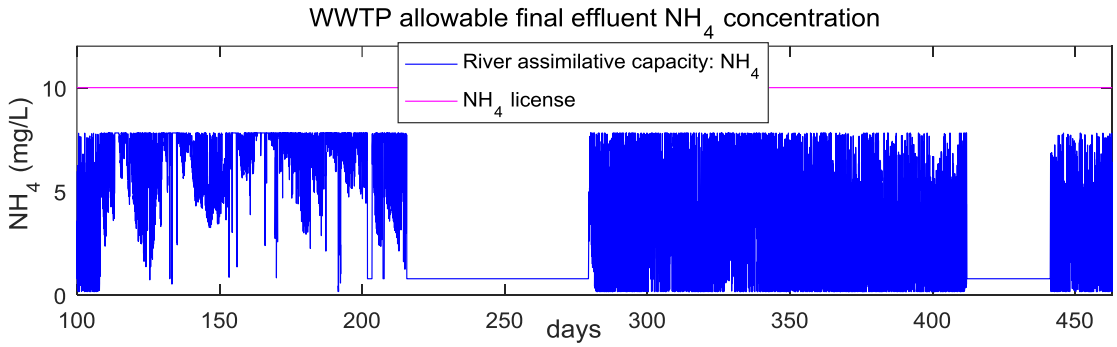

Figure 7-23 Allowable NH_4 concertation for WWTP final effluent (river model output)

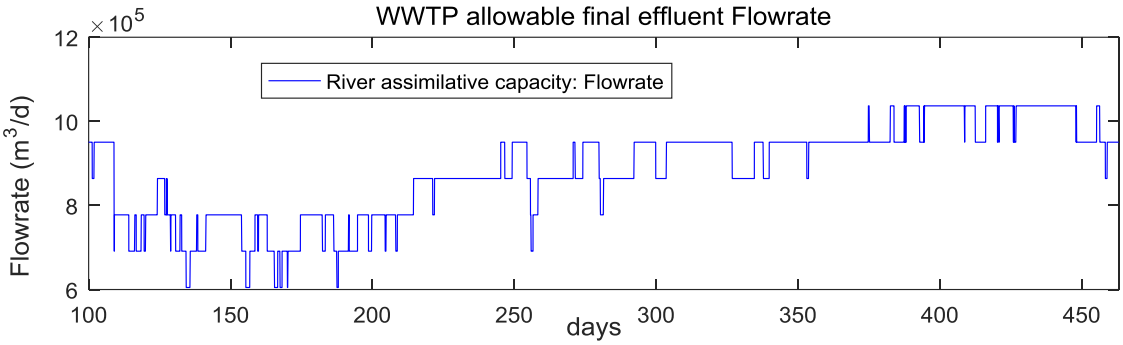

Figure 7-24 Allowable or maximum final effluent flow rate corresponding to the allowable pollutant concentration (River model output)

7.6.6.1 Assimilative-Capacity-Based DO Control: without Optimisation within the River Model

Although the optimisation approach for estimating the river assimilative capacity discussed in Section 7.5.9 put the major biochemical and physical processes in the river into consideration, the approach, as it stands, is not suitable for control purposes. In this section, the same river model without the optimisation part, to calculate river's assimilative capacity, is used. The river flow rate and pollutant concentration from the river model output are combined with the final effluent from the WWTP. The 'DownstreamCuparModel' interpreted MATLAB function (Dickinson, 2018) is modified to combine the final effluent (WWTP model output) with the river (river model output) to simulate flow and pollutant concentration in the river downstream of the WWTP.

The concentration of ammonia in the river downstream of the WWTP is estimated based on the Nitrogenous BOD level in the river, see Section 5.1.3. This ammonia level is used to control the DO level in the oxidation ditch based on the ammonia target for the river. For example, River Eden that receives effluent from the Cupar WWTP, to have a 'good' status, it should at least have ammonia concentration below 0.6 mg L^{-1} (SRBDD, 2014a; SRBDD, 2014b), Section 2.3. The control strategy using the integrated model is set up to meet the ammonia target (reference level) in the river by sensing ammonia level in the river downstream of the WWTP, see Figure 7-25.

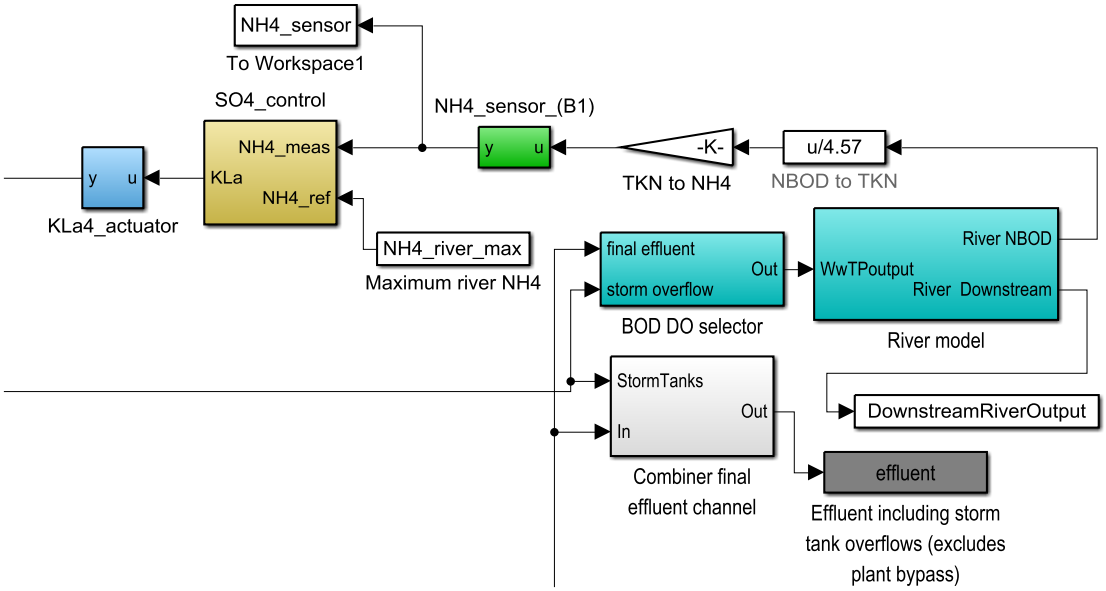

Figure 7-25 River assimilative-capacity-based aeration control structure implemented in Simulink: sensing ammonia concentration in the river to meet the reference ammonia (NH_4_river_max) which is determined based on the river classification standard and status (SRBDD, 2014a; SRBDD, 2014b)

The demerit of removing the optimisation section is that the capacity is only calculated from one parameter point of view and its impact on other quality indicator parameters is not considered. For example, the impact of increased NH_4 on DO concentration or Nitrates/Nitrites due to biochemical processes such as nitrification and denitrification in the river is overlooked.

Two setups are done in this test; one that uses the existing blower, and the second one uses new blowers with the ability to reduce their speed continuously until they stop. The first test uses the current intermittent blower operation phase whenever the DO level in the oxidation ditch is too high or in this case when the assimilative capacity of the river is very high. In other words, the minimum kLa value is set to 24 h^{-1}, similar to the baseline.

The plant performance in Table 7-19 shows that controlling the process in the WWTP using the available capacity of the river based on a simple mixing approach showed a reduction in operational cost (OCI) and improvement in the final effluent quality (EQI) by 9.84 % and 9.64 % respectively.

The main energy saving comes from the reduction of aeration resulting in a reduction of OCI by 16.7 %, see Figure 7-26. This control strategy results in increased in sludge production resulting in an increase in OCI of 6.7 %, which reduces the overall benefit of the strategy. The effluent quality is improved due to

a reduction in Nitrates concentration in the final effluent (reduced by 14.4 %) but accompanied by an increase in TKN load (increased by 4.1 %).

Although there is a significant saving and effluent quality improvement using this control strategy, the advantage in reducing GHG is not positive. The GHG emission shows a minor increase of 1.02 % due to increased emission from biological substrate assimilation and biomass decay. Even if the overall GHG emission shows an increase, the N_2O from the denitrification process and indirect emissions from the aeration process show a percentage reduction of 3.7 %, and 4.4 % respectively. However, this is counter balanced by the increase in GHG emission due to biological assimilation and decay within the oxidation ditch (increases by 9.9 %).

Table 7-19 Percentage change in WWTP performance indices using rivers assimilative-capacity-based DO control (No optimisation to calculate assimilative capacity)

Performance Index	Baseline	Assimilative capacity-based control with simple mixing	Percentage change in performance
CO_{2e}	7221	7295	1.0
OCI	4087	3685	-9.8
EQI	4342	3922	-9.7
MOCI	3439	3201	-6.9

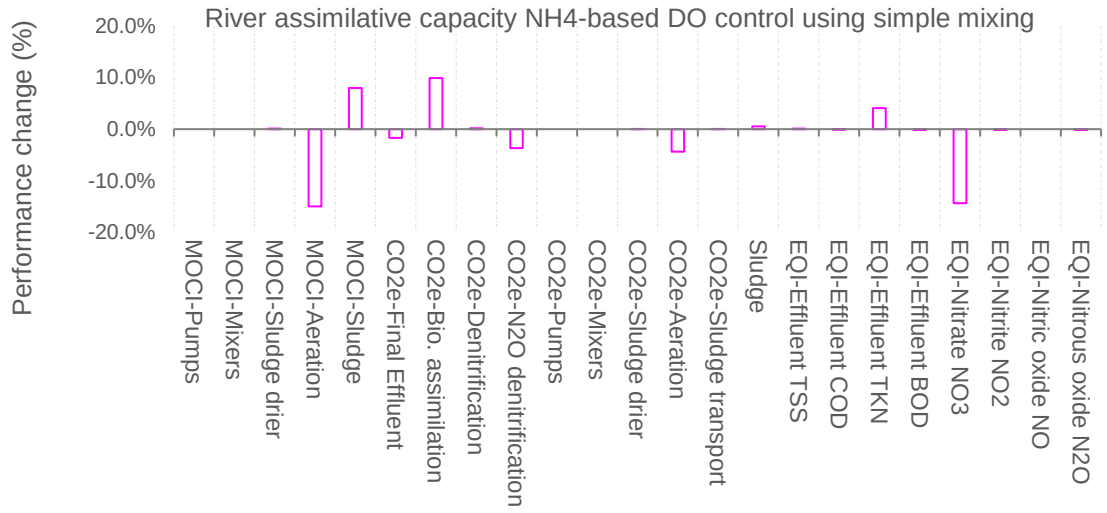

Figure 7-26 Percentage change in performance indicators' components for River's assimilative-capacity-based DO control (No optimisation to calculate assimilative capacity)

This control strategy is designed without altering the existing infrastructure, and the blowers' rotational speed cannot be reduced below a certain level.

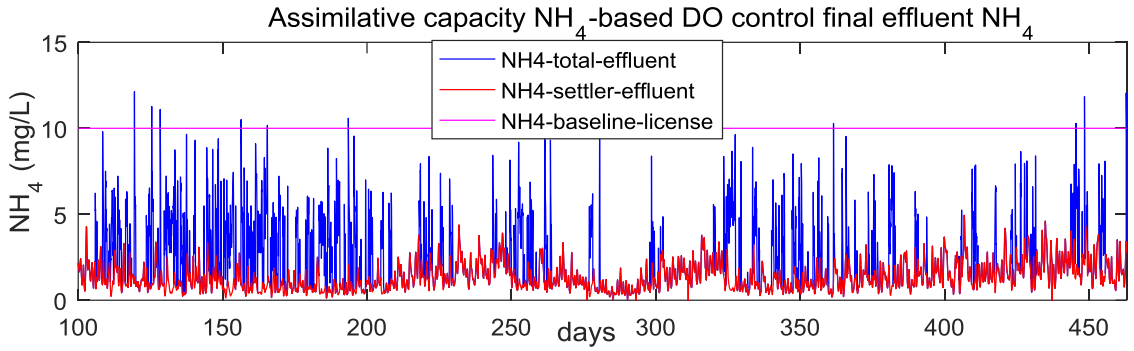

Figure 7-27 Time series of NH_4 concentration in settlers' effluent, settler effluent combined with storm tank overflow, and current licensing NH_4 limit (Using simple mixing approach for assimilative capacity)

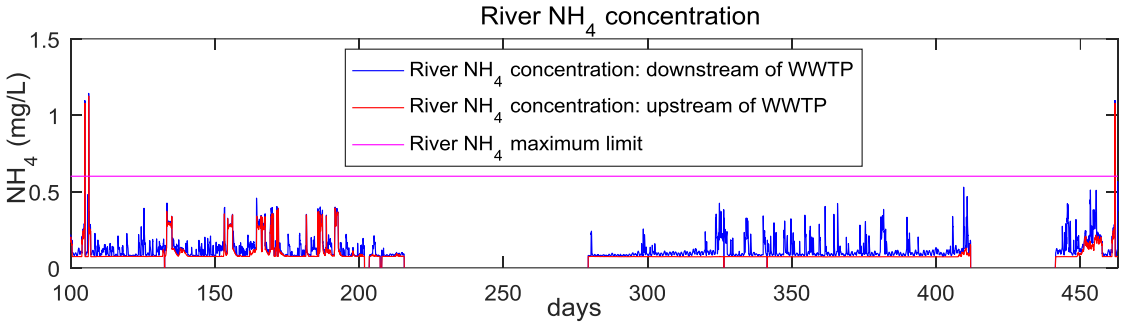

Figure 7-28 River Eden (receiving river for Cupar WWTP) model output for ammonia concentration upstream of Cupar WWTP (red) and downstream of WWTP (blue), and maximum ammonia limit based on (SRBDD, 2014a) and (SRBDD, 2014b) (Using simple mixing approach for assimilative capacity)

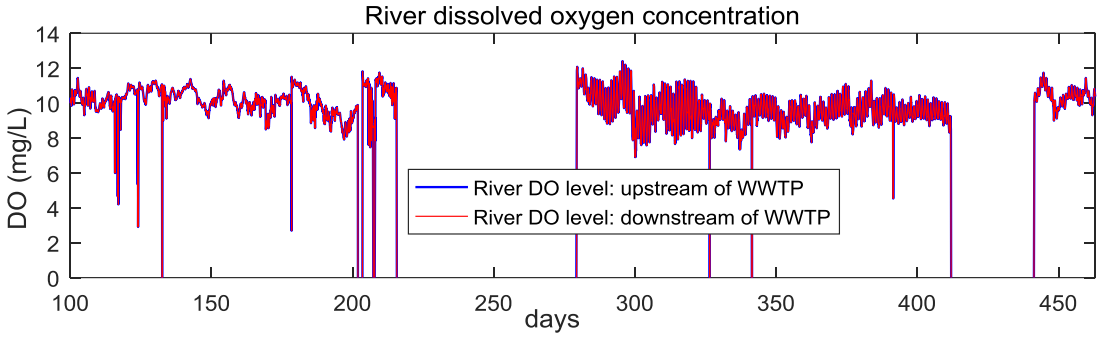

Figure 7-29 River Eden model output for dissolved oxygen concentration upstream of Cupar WWTP (blue) and downstream of WWTP (red)

Further by upgrading the blowers so that their speed can be reduced as low as needed, i.e. setting the minimum kLa value to zero, gives a very different result compared to the simulation with optimisation to calculate the river's assimilative capacity.

Removing the optimisation and replacing it with simple mixing and upgrading blowers to have continuous speed and minimum kLa of zero results in a significant reduction in CO_{2e} of **31.85** %. Operational cost as measured by OCI reduced by 16.39 %. However, the effluent quality (EQI) deteriorate by 22.8 %.

All the GHG emission contributors show a reduction. The N_2O from the denitrification process reduced to be zero which reduces the total GHG emissions by 4.8 %. There is a minor increase in GHG emission from the denitrification process, but the N_2O is significantly reduced indicating a complete denitrification process. The GHG emission from biological assimilation results in a reduction of the total GHG emission by 20.5 %. This reduction in CO_2 is mainly due to reduced decay (auto-oxidation) and a minor reduction in oxidation of organic matter. The GHG emissions because of reduction in aeration in the oxidation ditch contribute to the reduction of CO_{2e} by 6.8 %.

Reduced aeration contributed to 26 % of OCI reduction but accompanied by increase sludge production which contributed an increase in OCI by 9.5 %.

The scenario met the target of reducing operational cost and GHG emission significantly, but the effluent quality is deteriorated significantly. Due to the reduced O_2 level in the oxidation ditch, the aerobic ammonia oxidation is inhibited which results in reduced NO_3 and NO_2 in the reactor. In other words, the biological nutrient removal in this scenario is limited, and the final effluent ammonia concentration is much higher compared to previous scenarios (resulted in in EQI increase of 29.7 %). Due to complete denitrification in this scenario, the concentration of nitrates in the final effluent is reduced significantly contributing improvement of EQI by 12.3 %.

Figure 7-30 shows that the final effluent ammonia concentration both before and after mixing with the storm tank overflow. The final effluent ammonia concentration is higher than the current license limit. However, the impact of such high ammonia in the final effluent on the river quality is not very high, see Figure 7-31. This scenario (with upgraded aeration blower) results in the violation of the 0.6 mg L^{-1} river ammonia limit 106 times out of 44,448 samples. Out of the 106 violations, 39 of them are due to the upstream violation and are not associated with WWTP effluent. The violation is below 0.15 % of the time. For the river to have a ‘good’ status, at least, it should have ammonia concertation below 0.6 mg L^{-1} 90 % of the time. Such an approach for rivers with high assimilative capacity like the Eden River for Cupar WWTP can help in reducing operational cost and GHG emissions from WWT without affecting the biochemical status of the river. The results so far showed that by fine tuning the control design and by varying the set-point such an

approach it is possible to reduce GHG emissions and operational cost while keeping the river at the required status.

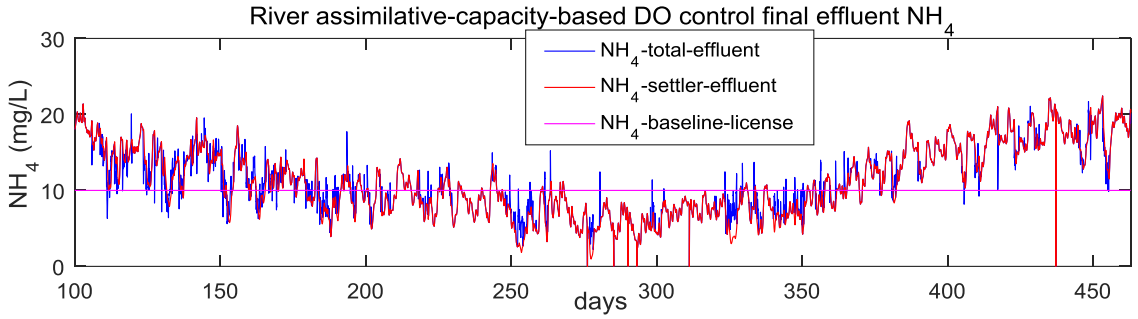

Figure 7-30 Time series of NH_4 concentration in settlers' effluent, settler effluent combined with storm tank overflow, and current licensing NH_4 limit (Using simple mixing approach for assimilative capacity and upgraded blower in WWTP)

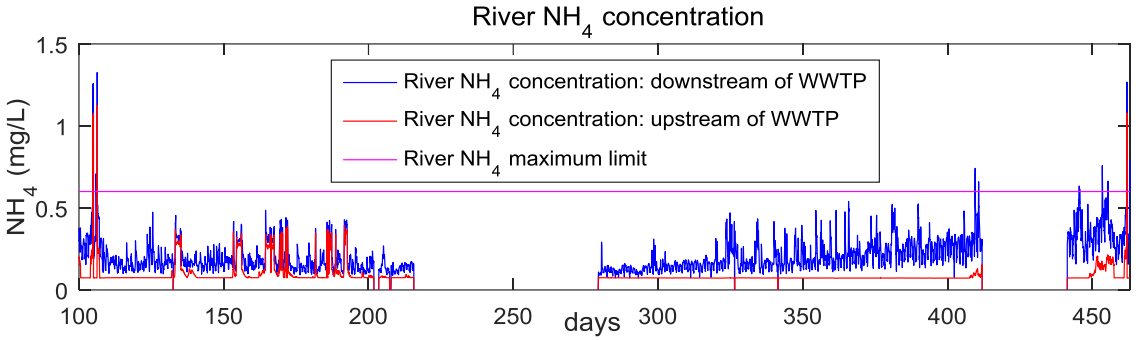

Figure 7-31 River Eden model output for ammonia concentration upstream of Cupar WWTP (red) and downstream of WWTP (blue), and maximum ammonia limit based on (SRBDD, 2014a) and (SRBDD, 2014b) (Using simple mixing approach for assimilative capacity and upgraded blower in WWTP)

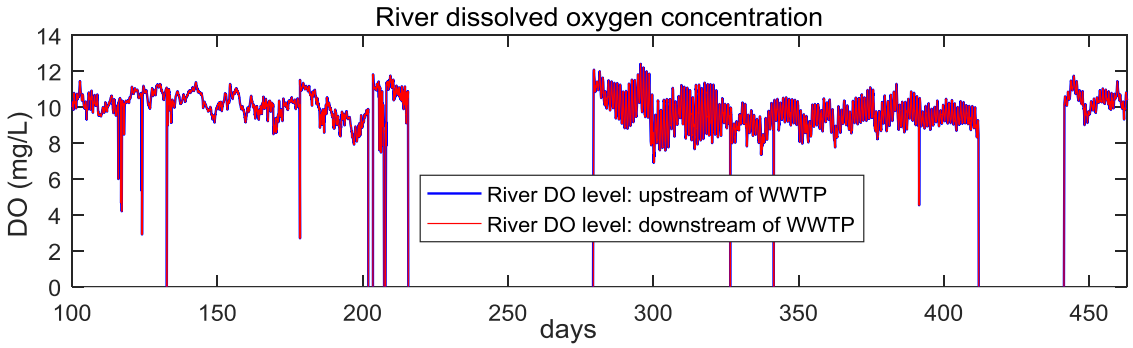

Figure 7-32 River Eden model output for dissolved oxygen concentration upstream of Cupar WWTP (blue) and downstream of WWTP (red) (Using simple mixing approach for assimilative capacity and upgraded blower in WWTP)

The dissolved oxygen level in the oxidation ditch reduced to 0.25 mg L^{-1} using this control strategy, see Figure 7-34. The reduction in dissolved oxygen in the oxidation ditch reduced the percentage reduction of ammonia due to reduced nitrification in the oxidation ditch, see Figure 7-33.

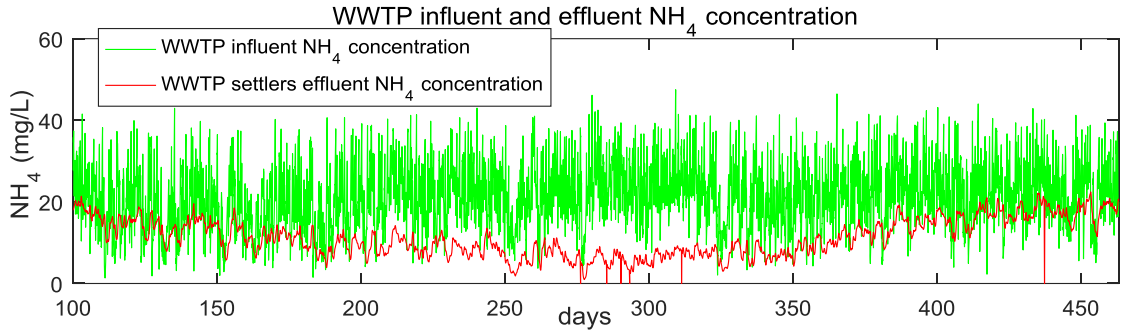

Figure 7-33 Time series comparison of WWTP influent and setters' effluent of ammonia concentration using simple mixing approach for assimilative capacity and upgraded blower in WWTP

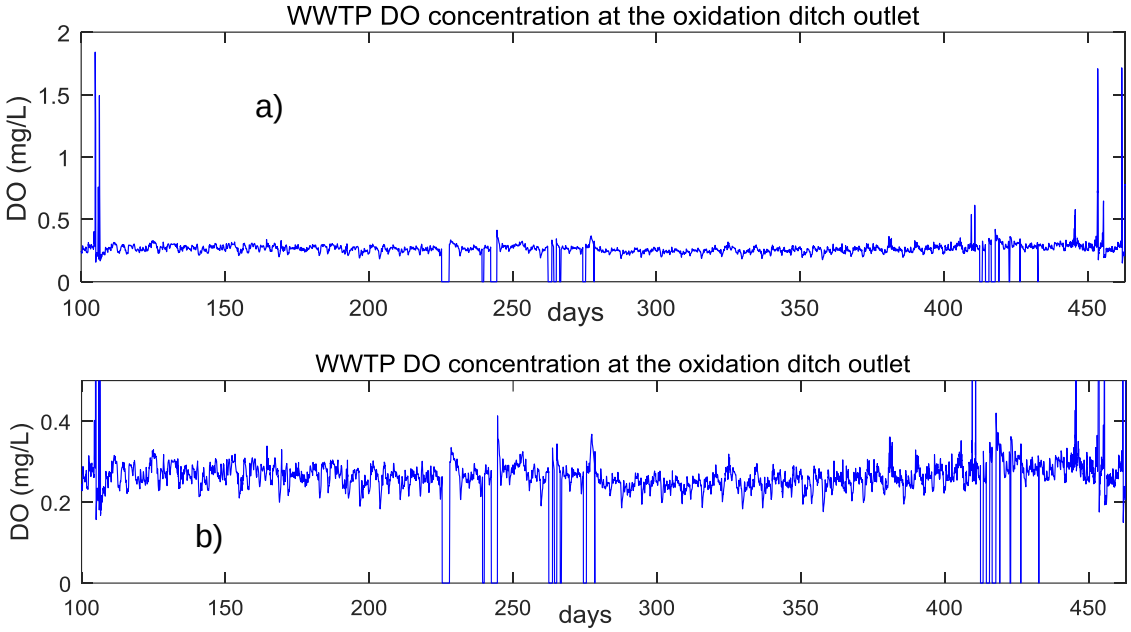

Figure 7-34 Oxidation ditch DO level using assimilative-capacity-based DO control (simple mixing for capacity estimation and upgraded aeration blowers): a) overall b) close up

7.7 Discussion

MOCI and OCI: the use of MOCI showed the benefit of energy use demand side management for the water industry. In scenarios related to controlling DO in the oxidation ditch, the oxygen demand generally drops during evening times and night times, the benefit in reduction of cost as measured by MOCI is not as pronounced as the of cost reduction as measured by OCI. In addition, some costs are not time dependent such as sludge transportation which can mislead the cost reduction as measured by MOCI to appear lower than OCI. Hence, it is important to use these two quality indices together.

The complexity of implementing the tested interventions is presented in Table 7-20. The trend showed the more integrated the solution is, the higher is the benefit. This is mainly because of the possibility offered by the integrated approach to utilise available capacity either within the WWTP or within the receiving river. Active control with the appropriate actuator, for example, variable speed blower with the capability to continuously reduce speed together with an active control with optimal set points, can help to meet objectives in reducing GHG emissions, reduce operational cost without violating current licenses.

By using a variable licensing approach (dynamic licensing) to utilise the environment quality-based directions of the WFDs, it is possible to reduce operational cost and GHG emissions. For dynamic licensing approaches to be benefited, it might be necessary to upgrade some of the WWTP components such as blower which might incur in capital investment. The wholistic approach that based on a dynamic licensing approach can be implemented easily, but prior to implementation, it is essential to develop an accurate model and understand the interaction of the UWWSs' components which can be complex and requires expertise.

Table 7-20 Complexity of control strategies and interventions

Interventions tested	Ability to meet the objective			Implementation Complexity			Remarks
	MOCI	CO_{2e}	EQI	simple	moderate	high	
Increase volume of Storm Tank	x	x	x		y		Requires capital investment and expansion of infrastructures in the WWTP. Requires a careful plan not to interrupt normal operations during upgrading. Possibility depends based on plant size, and foot print.
Increase surface Area of Wet-Well	x	x	x		y		Requires capital investment and expansion of infrastructures in the WWTP. Implementation complexity is similar to that of increasing volume of storm tanks.
Sewer Pumps Capacity and Sewer Catchment Impervious Area	y	y	y		y		Reducing the percentage of impervious areas in the sewer network is not in the hands of the water companies. It needs a collaborative effort from different stakeholders to implement SUDs and change the perception of society. Replacing existing pumps can be simple once the specification of the pumps for each station is identified.
WWTP Inlet Wet-Well Pump Capacity	x	x	y	y			Replacing existing pumps can be easy once the specification of the pumps required is identified.
Installing Pumps with Higher Efficiency	y	y	x	y			Replacing existing pumps can be easy once the specification of the pumps required for the pump station is identified.
Energy Demand-Side Management (DSM)							
Sludge centrifuge operating at night	x	x	x			y	It has high complexity since the SAS removal, and the sludge centrifuge operation is taking place at night, either operator should be assigned during night time which has its own cost implications or to avoid this, it will require full automation of the system, which can be complex.
Storm Tank By-Pass Set-Point	y	y	x	y			It is a matter of updating set points in the control system, which is a simple tax and with a very small or even no capital investment.
Variable DO set-points (intermittent phase)	y	x	y	y			It is a matter of updating set points in the existing control system, which is normally a simple task and with a very small or even no capital investment.
Optimisation of storm tank by-pass set-points and tank-volume, and inlet-pumps capacity,	y	y	y			y	Requires capital investment and expansion of infrastructures in the WWTP. Requires a careful plan not to interrupt normal operations during upgrading and the possibility of implementing and not affecting current procedure will vary based on plant size and foot print. This intervention also requires modelling and optimisation to find out suitable set-points which can sometimes be complex depending on the WWTP and availability of data.
Aeration Control							
Aeration Control (Intermittent phase optimisation)	y	y	x		y		The impact on the objectives is minor if EQI is put into consideration, but OCI and CO_{2e} can be reduced with a minor deterioration of the final effluent quality. It requires modelling and optimisation to find out optimal set-points. Implementation is simple and low or no capital investment.
Continuous Aeration Control	y	x	y		y		This is the replacement of blowers for a continuous reduction of speed until it comes to zero. Requires a significant capital investment but the implementation may not be complex.
Optimisation of the Continuous Aeration Control	y	y	y			y	This is the replacement of blowers for a continuous reduction of speed until it comes to zero. Requires a significant capital investment but the implementation may not be complex. In addition, to find out optimal set points modelling, and optimisation is required which can be complex.
Aeration Control Based on Final Effluent NH_4	y	y	y			y	This intervention requires ammonia sensor at the final effluent and implementation in the control system. If continuous reduction of DO is desired, there will be a need for replacement of blowers. This may result in a significant capital investment, but the implementation may not be complex. Also, to find out optimal set-points modelling, and optimisation is required which can be complex.
Dynamic Licensing:River's Assimilative-Capacity-Based DO Control	y	y	y			y	This intervention requires ammonia sensor in the final effluent and if continuous DO level reduction is desired there will be a replacement of blowers. This requires a significant capital investment, but the implementation may not be complex. In addition, to find out the optimal set-points of control variables models may be required.
Aerator volume	y	y	y	y			Reducing aerating volume can be achieved by lowering existing outflow weirs.

Although there is a general trend in the degree of complexity and ability of a solution to reach to objectives, Table 7-20 shows that it is not always the case. For example, reducing aeration volume is not a complex process, but it gives the possibility to meet all the three objectives. On the other hand, some operationally complex solutions, such as automating sludge centrifuge to maximise demand side energy management schemes, does not show much benefit. However, the more integrated the approach is, the more benefit is shown. For example, the highest benefit in reduction of GHG emissions and operational cost is demonstrated by integrated the WWTP process with the river assimilative capacity. These integrated approaches implementing dynamic licensing approach can give higher benefit when they are coupled with the right controller, such as continuous speed air blowers.

8. Business Case for Project Outputs

8.1. Introduction

This chapter covers the business case for the project outputs by analysing current issues in the wastewater sector in parallel with benefits from the project outputs. In order to tackle current challenges such as climate change, stricter regulation and increase in population, control strategies and innovative regulatory approaches suggested in this study. This chapter looks at how these suggestions can contribute to the water sector beyond trading-off objectives. The methodologies developed in this study and suggested solutions are discussed briefly to demonstrate a benefit to the sponsoring company's different business areas. Most of the discussion is done from the water company perspective and from an overarching view of the integrated UWWS in general. For example, Section 8.5 assess how integrated active control strategies and innovative regulatory approaches plays a role in creating a sustainable wastewater system.

This chapter uses a qualitative approach to demonstrate the economic benefit of research outputs and research methodologies to the sponsoring company. In a situation where there is sufficient data in valuing all possible economic benefits from such projects, a cost-benefit analysis can be beneficial. Cost-benefit analysis is commonly used to estimate the economic feasibility of a project or technology by comparing the cost associated with the implementation of it and the potential benefit. This approach is limited to economic benefit and overlooks societal benefits. Even in the application of such approaches in economic valuation of potential benefits such as improvement of the receiving water environment is challenging due to the complex interaction of the system and the wider impact on human and the water companies.

The commonly used method of cost-benefit analysis in most sectors is by expressing cost and benefit in monetary terms. Such methods include a net profit approach, benefit-cost ratio approach, cost-effectiveness and so on. For example, the net profit approach uses the sum of internal benefit to the company and external benefits outside the company (Stamatelatou and Tsagarakis, 2015). The internal benefit is the difference between the internal income and internal cost, and similarly, the external benefit is the difference between positive externalities and

negative externalities. Identifying and quantifying these benefits is the most complicated and uncertain part of this methodology. For example, internal impacts have a price determined by the market and therefore, can be quantified directly. However, the valuing the externalities is much more complex since they have not a price determined by the market (Stamatelatou and Tsagarakis, 2015). Monetization of non-market impacts and the inclusion of indirect impacts through the willingness to pay and opportunity cost is based on highly controversial value judgments, as it is based on assumptions of limited relevance (Djukic et al., 2016). Some attempts were done to use this approach but commonly for comparison of technologies or control strategies by expressing benefit per cost, for example, reduction in the volume of combined overflow from the sewer network per cost of investment (Dirckx et al., 2011).

Due to the controversial value judgments in the cost-benefit approaches and uncertainties in valuing non-market impacts, this chapter looks at the benefit of the project from a qualitative approach. In assessing the business case of the project and the implementation of it, a brief quantitative comparison is given, Section 8.3.

8.2. Implications of the Project

The water industry in the UK is facing several challenges arising from stricter regulations, variability in system load, and increase in storm flow due to urbanisation and climate change (Astaraie-Imani et al., 2012). The nature and scale of such challenges imply that the water industry faces complex and contradictory operational challenges and regulation. On the one hand, increased demand and uncertainties imply an increased capacity and reliability of systems on the other hand regulations requiring higher treatment level and at the same time reduction of operational energy. Several suggestions have been given to cope with these problems.

1. Greater operational efficiencies – greater operational efficiencies can address more than one objective, for example, by making sure WWTP effluent quality is meeting the standard and using much less energy.
2. Redeveloping existing processes – redeveloping existing processes through various interventions has potential in reducing energy use and delivering a reliable performance either through maximising the utilisation of available capacity or altering operational procedures.

3. The addition of least-carbon end-of-pipe solutions – This is technically replacing existing systems with a more least-carbon solution and commonly associated with a high capital investment.
4. Source control – source control is one of the most significant carbon saving mechanism but most of it out of the control of the water companies and it requires detailed source apportionment study and stakeholders' engagement and communication.
5. Energy generation – renewable energy generation is one of the sustainable ways of reducing operational cost, but it has its challenges; the common electricity generated from WWTPs is combined heat and power (CHP) which has a low ROC (Renewable Obligation Certificate) value of 0.5ROC/MWh which is not encouraging enough for most water companies (Georges et al., 2009).

The first two suggestions can be implemented within the boundary of the water industry with relatively smaller capital investment compare of source control, the addition of least-carbon solutions and energy generation. This study assesses the degree of benefit that can be achieved through increased efficiency and through redeveloping or optimising the existing system. The research attempts to develop a guideline where the wastewater sector can adopt to cope with operational challenges, mitigate climate change through a reduction of GHG emissions, and to maintain or even improve the quality of the receiving water bodies. By using an integrated active control approach, processes at the WWTPs are manipulated using information from sewer networks and assimilative capacity of the receiving water body so as WWTPs reach their maximum capacity and operate more efficiently with increased performance to meet multiple objectives.

The integrated modelling approach, GHG emissions modelling approach, and the step-by-step approach of assessing interventions and control strategies presented in this study can be adopted by water companies to assess the implication of strategic long-term investment projects, support decision making in the selection process of various intervention options and regulatory approaches. The outcomes from this study can be used both for design, managing existing assets, and improve operational performances.

In addition, this study provided a step-by-step approach to determining the minimum data required for integrated WWTP modelling. Since the use of WWTP

models became more common in the UK water companies for process control and optimisation UKWIR (2013b), such guidelines would be useful. Quality data is crucial for the effective use of these models since the reliability of the modelling results is strongly linked to data used to set up and calibrate the model (Rieger et al., 2010). This study, Chapter 4, showed that a carefully designed and collected dataset could reduce the time for the subsequent modelling study and can increase the confidence in using the model for the practical application, Chapter 6. This study comprehends and outlines a methodology than can be adopted to answer questions such as ‘what data to monitor’, ‘at what resolution’ and ‘How frequently and for how long’.

The integrated urban wastewater system (UWWS) model developed in this study can be adopted and applied to other activated sludge baseed WWTP to support decisions; for example, to evaluate various control strategies, intervention options, and innovative regulatory approaches for meeting financial performance indicators, reduce GHG emissions, make optimized asset management decisions, and maintain or even improve environmental quality indicators.

The project outlines a guideline that can be used by asset managers or operational team leaders to facilitate the assessment of a viable, innovative solution for operational, regulatory or efficiency related challenges. The guideline can be used for operational decision making to choose least-cost interventions being within the company’s strategic objectives. The fuideline can also be used to identify optimal long-term investment plans to achieve pre-defined operational or system wide objectives.

8.3. Cost-effectiveness of the Project to the Sponsoring Company

This section discusses and helps to compare whether the project is financially viable if it was done through other routes such as a consulting company or a Knowledge Transfer Programme (KTP). It assesses the magnitudes of externalities associated with the project, estimates the project's impact on the company framework and outside policies, identifies the incidence of costs, potential costs of other routes and its cost-effectiveness.

This project is part of the STREAM-IDC programme, which is an industrial based doctorate programme that brings together the water industry in the UK and water

focused research centres of five UK universities. The programme is supported by the Engineering and Physical Sciences Research Council (EPSRC) and a sponsoring company, which supports Research Engineers to peruse an EngD through applied research based on current and anticipated challenges that the water company is facing. Such programmes have advantages in so many ways, in addition to creating a cost-effective method for the sponsoring company to solve problems using scientific approaches and building a culture of evidence-based decisions and planning. Some of the advantages are listed below:

- A smoother innovation process and an efficient knowledge transfer through an easily accessible Research Engineer that can use problem solving skills, his/her wider knowledge of the sponsoring company's business framework, existing knowledge and state-of-the art tools within the research centres in the host university and generally in that discipline. This is mainly due to a coherent, collaborative partnership, the less formal interactions, and the exposure of the Research Engineer both to the company's latest issues and latest developments within the academia.
- The Research Engineer can be used as knowledge networks for wider dissemination of the research findings and outputs that can improve the industrial partner reputation
- Development of the next generation of science and technology (highly skilled human capital development) through the development of the Research Engineer's problem-solving and analytical skills
- Access to other project collaborations, scientific data bases (via the Research Engineer) and academic expertise and leading research at the host university

It is not easy to assign a monetary value on the above benefits. Traditional cost-benefit analysis such as the 'Pound Plus', commonly used by learning providers to analyse cost-effectiveness, cannot be used here since they massively depend on existing published data, which is not available for the wastewater sector. Since measuring these cost-effectiveness data is costly and time consuming as well, an opportunity benefit analysis is used to assess the benefit of the choice that sponsoring company (Scottish Water) took instead of the most common routes, such as contracting a consultant company or commissioning a KTP.

The original funding allocated to this project by the sponsoring company was £ 48,000 for four years, see Figure 8-1. Additional data monitoring was identified through this project required additional funding of £ 51,436.00 out of which the £ 5,000.00 was funded by the UoE. The extension of the project from September 2016 to June 2017 incurs an additional cost of £ 2,770 for the dissemination of project findings and outputs.

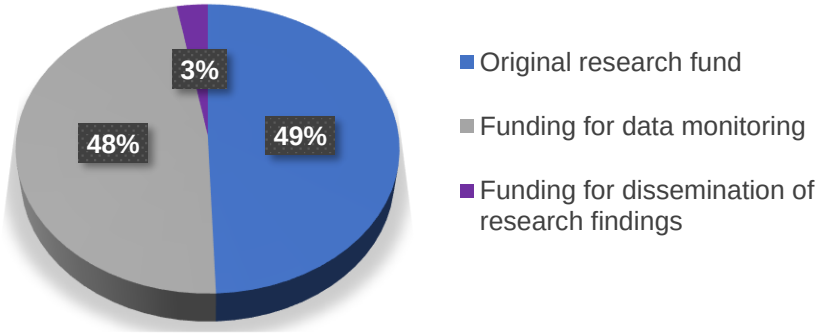

Figure 8-1 Percentage of cost distribution of the project

The consultant's fee to deliver a similar kind of project only for resource cost excluding material cost is estimated to range from £ 240,000 to £ 300,000 depending on the detail of work, see Table 8-1. This estimate has not included site visits, data collection, software costs, and other costs. The software costs are estimated based on what is used in this project, MATLAB® with Simulink® and other supporting tools such as optimization tool boxes, Infowroks ICM®, ArcGIS®, and AutoCAD®. This estimate does not consider the license cost for models that are free for educational purposes, for example, BSM_2 and Influent Generator models.

Table 8-1 project cost under EngD route compared to consultancy route

	Engineering Doctorate route	**Consultancy route**
Total resource cost	£50,770	£240,000 – £300,000
Software licenses cost	£0	£27,000 - £39,000
Events and conference fees (assume five events) *	£1,250 (student fee on average £250)	£3,750 (normal fee on average £750)
Data monitoring incur to company **	£46,436	£69,654
Total cost to sponsoring company	**£97,206**	**£340,404 - £412,404**

* Costs that are already covered by the fee

** Data monitoring cost was reduced with a thorough and detailed communication with the industrial partner. It is assumed that such cost reduction may not be achieved through consultancy due to a limited collaborative partnership

The other alternative route that the sponsoring company can take to achieve the objectives of this research project is through a Knowledge Transfer Partnership (KTP). KTP is designed to help the industry sector to improve their competitiveness and effectiveness by maximising the use of knowledge, technology and skills. It has a similar approach to that of EngD programmes regarding maximising the use of knowledge and helping to identify innovative solutions to the industry. Although this partnership is part-funded by a government grant, normally 40 % of the total KTP cost, it has a large cost in employing one or more KTP associates. The average annual cost of a long-term KTP project is £ 60,000, out of which £ 36,000 need to be met by the partner company. For a four-year project, the cost of achieving the research objectives through KTP, without transportation and data monitoring would be £144,000. The total cost including data monitoring, transport and accommodation would be £241,654. It is assumed that software licenses are covered by the host university. Ergo, the EngD is a cost-effective route with a total cost of £97,206 compared to the commensurate route KTP with a total cost of £241,000 and compared to a commonly used consultancy route with a total cost in a range of £340,404 - £412,404.

8.4. The Benefit to the Wastewater Sector: From a Water Company Perspective

Climate change has an impact on business in two ways. First through a direct impact because of climate change, which requires adaptation, and second through the regulations targeting to mitigate climate change, which requires a change in current practice. Accordingly, both climate change adaptation and mitigation require strategic planning to minimise the risk to service. Most water companies in the UK develop a Climate Change Adaptation Strategy, which for example, in the case of Scottish Water, includes:

- The development and use of robust in-house models for asset planning, understanding and managing available system capacity, informing investment planning and asset specification
- Integrating collected data so far and identify further data monitoring for evidence-based decisions and asset management
- Development of framework policies with regulatory bodies such as SEPA to maximise the net benefit to the environment, and ensure a sustainable treatment

This study was part of a proactive and more overarching attempt to design a pathway for the future than a response to just adopt climate change and regulatory challenges. In conjunction with other on-site trials, projects testing simpler dynamic licensing approaches (based on seasonal variation of the assimilative capacity of the receiving water, which is not presented in this thesis), this study has provided Scottish Water with a proof-of-concept which demonstrates that it is possible to operate with a variable effluent standard based on the assimilative capacity of the receiving river.

By combining a model-base study presented in this thesis and a trial with a simpler on-site trial to explore the practical realities, this project has demonstrated the additional benefits which can be realised through the application integrated active control systems and their optimisation, see Chapter 7. This study provided an evidence base, which allows Scottish Water and other interested water companies to support such innovative regulatory approaches and implement integrated active control systems to balance various drivers and performance goals.

The study can be considered as an enabler for further development of integrated active control systems and dynamic licensing approaches as it has explored various technical, theoretical, and to some extent practical challenges related to the UWWS and identified potential solutions. The benefit to the water company is not only the expansion of the concepts, tested in this study, to other sites, but the integrated UWWS modelling approach has the potential to offer additional value in other areas of the business. For example, they could be used to assess the response to future conditions such as population growth or climate change, assess future intervention strategies, and develop proactive maintenance scheduling tools.

Due to the advancement in, water quality indicators sensors, and remote sensing, and the advancement in data science it is likely that their use increased in the water companies in the UK (UKWIR, 2013a) thus expected to increase the amount of operational data available. Chapter 4 of this thesis detailed the type and amount of data required for such a model-based study; hence increasing the amount of available data will serve to increase the effectiveness of future applications. As these investments are likely to come not only from system optimisation or for the sake of model-based study, it is believed that they need to be made anyway, and

factoring in the data requirements presented in Chapter 4 will allow additional value to be realised.

Although there is an increasing trend in the use of active control systems, these approaches are yet to see more application in the UK water industry, possibly due to the relative complexity of these solutions and their need for expertise (UKWIR, 2013a). Considering this, pursuing this project will help to position the sponsoring company as an innovator and leader in the field with skills and expertise which have the potential to be offered throughout commercial and/or international ventures.

8.5. Research Outputs towards Creating a Sustainable System

The main purpose of the development of UWWS was the need for improvement of public health and sanitation, which consequently help in the reduction or even elimination of water borne diseases. Through time the UWWS objectives became beyond this due to increased understanding of the environment and greater need to develop more environmentally responsible systems whose performance is balanced by environmental, economic, and societal sustainability (Muga and Mihelcic, 2008). Although there is no consensus on the definition of sustainability especially in its scope, most authors (Balkema et al., 2002; Muga and Mihelcic, 2008; Molinos-Senante et al., 2014) agree that sustainability refer to maintenance of economic wellbeing, protection of the environment and prudent use of natural resources to meet both current and future demands, and equitable social progress which recognizes the needs of all individuals, communities, and the environment (Muga and Mihelcic, 2008).

The methodologies suggested has a significant role in addressing environmental sustainability in UWWS through minimization of energy consumption, reducing GHG emissions, and avoiding degradation of water resources (minimization of loss of nutrients and waste production. Some of the control strategies discussed in Chapter 7 showed potential in creating such a system by trading-off these objectives.

In addition to the benefit to the environment and playing a significant role in adapting and mitigating climate change, the research outputs can be used in maximising operational efficiencies, optimising existing system through integrated

active control, and implementing a variable licensing approach. These approaches can deliver an economic benefit to water companies through the reduction of operational cost which outweighs the necessary capital investment.

Although in some cases, the wastewater sector is overlooked when it comes to customer satisfaction, it plays a key role in delivering a cleaner and healthier water environment that the society benefit in so many ways; bathing water, fishing, and so on. In addition, WWTPs while treating wastewater and assure the quality of the water environment, there is associated GHG emission both due to energy use and direct emissions from biochemical processes within the plants. These impacts, whether an increase or reduction of the emission, greatly affect local and global sustainability both to the environment and to society (Muga and Mihelcic, 2008). Although, there is no attempt done in this study to quantify the impact of different control strategies and dynamic licencing approaches, the study demonstrated that it is possible to trade-off economic sustainability (through reduction of operational cost), environmental sustainability (through increase in percentage removal of pollutants and reduction in GHG emissions), and societal sustainability (by creating a healthier and hygienic environment).

The research outputs can contribute to societal sustainability through the development of framework policies with regulatory bodies that can maximise the net benefit to the environment using a dynamic licensing approach that considers both the environment and public health. However, there is still more work to be done to quantify and clearly define societal sustainability, but this output and methodologies in this study can be used as a baseline in creating a sustainable UWWS.

8.6. Conclusions

The short-term benefits from the project have been analysed for example the deployment of the data selection methodology to identify the kind of data to monitor, frequency and period of monitoring to create a robust integrated wastewater treatment tool, Chapter 4 and Chapter 6. The medium-term benefits are already realised, and sponsoring company is planning to implement trials to test suggested control strategies to optimise existing systems through an integrated active control. However, to realise the long-term benefit to the project it important for the water company to identify enabling conditions such as allocating

additional funding to integrated suggested methods into the company's decision-making framework.

Data is crucial for the development of such a model. Currently, the data requirements for implementing integrated active control systems with confidence are beyond what is currently gathered as a matter of course by most water companies. In the future, because of advancement in sensors, remote sensing, and data science, this issue will become less prominent.

Reducing operational cost and lowering environmental risk are key objectives of most water companies. Consequently, the benefit of integrated active control approaches for creating both environmentally and economically sustainable system can easily be realised as demonstrated in this study. Although the contribution of these approaches towards creating a sustainable system in these two dimensions is clear and somewhat straight forward, their contribution towards societal sustainability is rather not obvious and needs more study.

The STREAM EngD programme provides a cost-effective route in developing a guideline and tools that can be used to achieve the project objectives. It is the most cost-effective route compared to outsourcing the work through consultancy or through KTP programmes.

9. Conclusions and Recommendations

9.1. Summary

Stringent environmental water quality standards, on the one hand, require a higher level of wastewater treatment which results in a significant modification of operation or/and design. These changes usually have the potential to increase operational cost through higher energy use, chemical consumption, and capital investment. Such changes can increase GHG emissions both directly from treatment and indirectly due to increased use of energy and chemicals. On the other hand, the Carbon Reduction Commitment Energy Efficiency scheme requires the water industries to reduce their GHG emission significantly to meet the target of 80 % GHG emission reduction compared to the 1990 baseline by 2050. These stringent and contradicting standards together with an increase in urbanisation and climate change are one of the challenges that the wastewater sector, in the UK and Europe, is facing. There are emerging researches to show the benefit of improved control strategies at WWTPs to mitigate these challenges. However, there is no identified study that maximises the benefit of integrated active control using river's assimilative capacity to trade-off GHG emissions, operational cost and the quality of the receiving water body.

The aim of this research project is to assess the advantage of integrated active control of existing WWTPs and dynamic licensing approach to find the best trade-off among the reduction in energy use, GHG gas emissions and maintaining the quality of the water environment. The dynamic licensing approach focuses on the design of control strategies based on the receiving river's assimilative capacity by varying the currently used statistical-based fixed licensing and vary the license based on the assimilative capacity of receiving river.

The thesis used a simulation approach to test control strategies, interventions and dynamic licensing approaches. For that, it set up independent sub system models; WWTP, sewer network, and receiving river, which later is fully integrated to assess the advantage of integrated control strategies and dynamic licensing approach.

The first stage of the thesis was to set up an accurate integrated model that can be used with confidence to test different objectives. To set up an accurate model, the study characterises influent wastewater through identification of data needed

and collection of new data, and model calibration using the new dataset. Since the WWTP model has many parameters with uncertainty in their specific value and uncertainty in some physical and control parameters, the study performed an autocalibration. Due to the high number of parameters, to minimise effort and save computational time, a OAT sensitivity analysis is performed to identify the most influencing parameters. These influencing parameters are used to calibrate the model by comparing simulated effluent quality and measured effluent quality indicators.

By using the calibrated model, most influential control-handles are identified using the OAT sensitivity analyses based on the WWTP performance indicator indices. The possibility, advantages and drawbacks of the application of different control and licensing approaches are investigated using an index approach to quantify the performance of WWTP. Upon the results from this investigation, new control strategies and modification of licensing approaches are tested to analyse the benefit of multi-objective optimisation of WWTPs further.

9.2. Conclusions

Conclusions based on findings from each chapter are presented below. The findings are categorised into five main sections. Section 9.2.1, covers the main findings and conclusion related to the research needs identified in the literature review. Section 9.2.3 presents the main findings from the influent wastewater characterisation and data assimilation. Model development, integration and modelling approach are presented in Section 9.2.2. Section 9.2.4 covers the findings related to model calibration, model accuracy, and sensitivity analysis. The key findings and conclusions related to performance trade-off, control strategy optimisation, and dynamic licensing are presented in Section 9.2.5. Finally, a conclusion is drawn based on the cost-effectiveness analysis which is presented in Section 9.2.7.

9.2.1. Research Needs Associated with Integrated Urban Wastewater Control in the Face of Stricter and Contradicting Regulations

The literature review in chapter 2, carried out to identify research gaps in the urban wastewater system, points out the following key points:

- Control strategy development is one of the most challenging steps in the design of control systems of wastewater treatment plants. To evaluate these control strategies, it is essential to develop an accurate model of the system and performance criteria that should be designed carefully to represent objectives in hand.
- Previous studies were identified that aimed to trade-off effluent quality, GHG emissions, and operational cost using integrated active control systems, but none was identified focusing in the UK context. Also, most of these studies are done either on hypothetical or semi-hypothetical plants. And, those that use full-scale real-world case study failed to show their model accuracy before proceeding to the evaluation of control strategies.
- There are no research works identified that use the assimilative capacity of receiving water body as an objective (set-point) to control processes in wastewater treatment plants with the aim of trading-off GHG emissions and operational cost.
- To evaluate control strategies at WWTPs, it is essential to consider a seasonal variation of influent flow and quality; hence the need for simulation for an extended period, at least a year. Characterising influent wastewater for such a long time is costly, and the use of the influent generator is found to be the least costly approach without losing model accuracy.
- Similarly, for the purpose of optimisation, simplified data driven river (catchment) models are more suitable than process-based river (catchment) models as they significantly reduce computational cost and need for data.
- The UK water industry is under a strict regulation to improve effluent quality, which can increase GHG emissions from WWTPs. On the other hand, climate change driven regulations require the reduction of GHG emission from this industry. Some states like Scotland plan to introduce even more stringent intermittent carbon reduction targets than the one specified in the Climate Change Act (Scotland), 2009 in order to meet the 2050 emissions reduction target.

9.2.2. Integrated Modelling Approach and Application to a Real-world Case-study

Chapter 3 and 5 present the modelling approach used to simulate the case-study WWTP processes, influent to WWTPs, and the receiving river processes. The following conclusions are drawn based on the work in these two chapters.

- The hybrid model developed in this study can generate flowrates and pollutant loads (using a conceptual modelling approach) for an extended period using two or three weeks of onsite data collection and rainfall data for the extended period of simulation. It can mimic the sewer network with a capability of estimating CSO by considering sewer length, storage, and pumping capacity.
- Integrating the WWTP influent generator with WWTPs model with a capability of modelling GHG emissions (both direct and indirect) using a deterministic approach enables the application of the integrated model for real-world case study to evaluate control strategies in the reduction of GHG emissions over an extended period that covers seasonal variability of quality and quantity of the influent wastewater.
- The non-MATLAB/Simulink®-based hybrid data-driven river quality and quantity model integrated with the MATLAB/Simulink®-based WWTP model and influent generator creates a computationally efficient model that enables the evaluation of control strategies and regulatory approaches that targets in utilising the receiving river's assimilative capacity with a holistic view of keeping the water environment quality at the desired standard while meeting WWTP operational objectives.
- The BSM2 model blocks can be modified to model activated sludge processes in oxidation ditches and other hydraulic units with a complex control strategy, such as wet-wells. Oxidation ditches can be modelled as reactors in series, but in a loop, with an internal circulation flowrate that can be estimated based on onsite measurement of the velocity of the mixed liquor. The number of reactors can be determined by measuring dissolved oxygen level along the oxidation ditch and using other physical boundaries such as inflow and outflow points, the location of mixers, the location of diffusers and return sprays (if any).

- Modifying the BSM2-e (Sweetapple, 2014) model to include a variation of pump efficiency depending on operational conditions creates an opportunity to test the impact of both efficiency and operational conditions variation on GHG emissions.
- Operational cost indices such as the MOCI introduced in this study that can show not only the equivalent energy use per day but that can also consider variation of energy cost enables the opportunity to evaluate the impact of control strategies in situations where energy costs vary throughout the day to encourage the reduction of energy use during peak hours.

9.2.3. Step-by-step Procedure for Model Calibration and Design of Data Monitoring Campaign

Chapter 4 and Chapter 6 provided a step-by-step approach for model calibration procedures and steps in characterising influent wastewater. Chapter 4 listed out the minimum data required to set-up an ASM1 based WWTP model and required data monitoring. The following conclusions are drawn based on the findings of this chapter.

- In setting up WWTP models, it is crucial to characterise the systems before calibration of uncertain model parameters. The step-by-step procedure developed for the design of data monitoring campaign and model calibration was applied to Cupar WWTP and showed that following such guidelines and designing data monitoring campaigns based on the available resources can improve model accuracy significantly.
- Wastewater characterisation does not have to be expensive; Chapter 4 presented a procedure that only uses commonly and easily measured quality indicators and does not require expensive expertise. The suggested parameters to be measured are expected to be even cheaper in the future due to the advancement in online monitoring of wastewater quality and quantity, and progress in the simplification of complex tests such as TKN test. However, this does not mean that further lab scale analysis of influent wastewater characterisation, such as the use of oxygen uptake rate measurements, does not help in reducing uncertainties.
- It is essential to quantify the COD fraction that is involved in the microbial transformation of wastewater organic matter, but not all parameters need to be measured directly, and some parameters do not even need to be

calculated indirectly as they are not affected by biological actions. These state variables (fraction of COD or nitrogen) can be given a value based on reported values in literature, for example, soluble inert organic matter. However, reducing uncertainty around these parameters may be of interest depending on the problem in hand. Hence, measuring these parameters can be justified depending on site conditions and the problem in hand.

9.2.4. Sensitivity Analysis and Model Calibration to Improve Model Accuracy

Chapter six presents the details in model calibration that uses sensitivity analysis as a means of reducing calibration efforts. The key findings from this chapter are presented here.

- Quantifying model accuracy using different goodness-to-fit measures to determine how well the model outputs are close to the measured ones enables the use of auto-calibration processes to identify the value of uncertain parameters through a multi-objective optimisation approach.
- Selecting most sensitive parameters and performing auto-calibration per the guideline in Chapter 6, reduces computational time significantly. And, the auto-calibration process that deploys an NSGA-II multi-objective approach can improve WWTP model accuracy in simulating final effluent TSS, NO_3, and NO_2 concentration, and MLSS, and dissolved oxygen level in the oxidation ditch. Best auto-calibration result gave R^2 as high as 0.57 and NSE as high as 0.5.
- In multi-objective-based auto-calibration processes, combining two objectives, for example, R^2 and Nash-Sutcliffe coefficient (using their products), can reduce the number of generations to reach to the best solution. Hence, in multi-objective optimisation where simulation speed in an issue for using as many objectives as possible, combining objectives can be considered as one of the solutions.

9.2.5. Multi-objective Optimisation in Trading-off Operational or Strategic Objectives

The study tested, developed, and optimised different interventions, and control strategies. The following conclusion and key findings are drawn based on the work presented in Chapter 7.

- Optimisation coupled with replacing some assets to suit the strategy can trade of operational cost, GHG emissions and effluent quality. For example, based on the case-study in this project, by having a variable dissolved oxygen level at different time of the day, replacing blower to achieve continuous aeration reduction, and optimisation of these dissolved oxygen set-points can reduce GHG emissions by 4 % and operational cost by 13 % while maintaining the same effluent quality index.
- An integrated active control system can be used a way for trading-off cost, effluent quality, and GHG emissions. For example, controlling dissolved oxygen in aerators based on the final effluent ammonia concentration can reduce GHG emissions and operational cost by 13.6 % and 12.7 % respectively, only with a 1 % exceedance of the maximum ammonia limit.
- The benefit from DSM for WWTPs is not as pronounced as other sectors, as the need for aeration and pumping in the evening and at night are low when energy cost is lower. This is reflected in a lower reduction in MOCI from different control strategies as compared to OCI, which may not encourage system efficiency and implementation of automation and control at WWTPs.

9.2.6. Assimilative Capacity of Rivers and Dynamic Licensing Approach

The study uses an integrated modelling approach to assess the benefit of utilising the assimilative capacity of rivers and evaluated a dynamic licensing approach. The following conclusions and key findings are drawn based on the evaluation in Chapter 7.

- The dynamic licensing approach can enable the reduction of energy use without increasing GHG emissions. The control of oxygen level in the oxidation ditch based on the assimilative capacity of the receiving river can reduce operational cost through reduced aeration without increasing GHG emissions. Dynamic licensing approach tested for Cupar WWTP showed only a 0.15 % exceedance of river quality limit for ammonia, but still under the 10 % limit. This test is done on a river which has a ‘good’ status with a significant amount of assimilative capacity. In cases where there is limited assimilative capacity with rivers of ‘moderate’ or worse quality status, this approach can also be used not only to utilise assimilative capacity, but to

revise existing final effluent standards for WWTP. However, only chemical status is considered in this study and in future works it is beneficial to consider revising target chemical levels in the river based on the need to improve ecological status.

- Limiting oxygen to reduce operational cost can result in the reduction of final effluent NO_3, but can increase biomass decay in oxidation ditches, which can increase the direct GHG emissions due to auto-oxidation. Similarly, the reduction in operational cost in the dynamic licensing approach is not as low as expected due to the increase in sludge treatment because of increased biomass decay. Hence, to benefit from the dynamic licensing approach, it is essential to further optimise the control strategy to trade-off the reduction in effluent NO_3 concentration, sludge production and GHG emissions due to biomass decay.
- It can be concluded that it is essential to consider the complexity of interventions implementation in addition to the commonly used objectives. Some interventions such as improving aeration efficiency through replacement of diffusers can reduce both operational cost and GHG emission. However, their complexity in terms of installation and capital cost is high, and they might not be the first options to select. However, some interventions that focus on utilising existing system capacity are simple to implement and capable of improving all objectives. For example, reduction of aeration volume can improve effluent quality, reduce operational cost and GHG emissions. Hence, it is necessary to include implementation complexity as a criterion for selecting interventions, control strategies or licensing approaches.

9.2.7. Business Case for Outputs and Methods Developed in the Project

The following conclusions are drawn based on the discussion in chapter 6.

- The interventions, control strategies, and dynamic licensing approach investigated in this study can be in implemented within the boundary of the water industry and can play a significant role in creating a greater operational efficiency and utilising available capacity without the need for high capital investment.

- The study comprehends and outlines a guideline that attempts to answer questions such as “what data to monitor?”, “at what resolution?”, and “How frequent and for how long?”.
- The integrated modelling approach developed in this study can be used in another business area of the water company such as for assessing future interventions strategies, and perhaps in the development of proactive maintenance scheduling tools.
- The control strategies and dynamic licensing approach presented in this study can be considered as an option in creating a sustainable system as they contribute economic value to the water company, addresses environmental sustainability, mitigating climate change, and helps in creating a cleaner and healthier water environment that society benefits in so many ways.

9.3. Recommendations

The work presented here has identified a number of potential topics which can complement, follow on, expand, and build up on the findings and methodologies developed in this study.

9.3.1. Recommendations for Further Research

Consideration of filamentous bacteria activity

Although there is still no clear answer on the cause of foaming and scum formation in activated sludge systems, most studies identified that excessive filamentous hydrophobic bacteria are susceptible to floating and being the common cause of scum formation. The activity of filamentous bacteria is not considered in this study due to model in capability. However, the inclusion of such processes can help to quantify the impact of interventions that can potential affect scum formation. For example, the commonly used scum formation solutions are the provision of selector zones, spray final effluent over oxidation ditch, and removing scum from final settlement tank to be returned for full treatment, and so on. The impact of interventions and control strategies that can affect these unit processes or scum formation, in general, can be quantified through the inclusion of filamentous bacteria and the resulting scum formation in modelling practice. For further work, it is recommended that either use of alternative models with the capability of estimating scum formation due to the activity of these bacteria should be

considered or inclusion of this process in the existing BSM2-e (Sweetapple, 2014) should be considered.

Modelling and control strategies for other pollutants such as phosphorus

This study mainly focusses on the removal of nitrogen from wastewater as the current regulation for the chosen case-study only focuses on this nutrient and organic matter removal mainly due to the medium size of WWTP. However, other nutrients such as phosphorus (P), which occurs naturally both as inorganic and organic P, can deteriorate the water environment quality if too much of it inters in them. The Urban Wastewater Directive (CEC, 1991) sets a limit of 2 mg L^{-1} of P in wastewater effluent from large WWTPs, and the EU-Water Framework Directive (CEC, 2000), recommends limits of 0.5 – 1.0 mg L^{-1} of P in receiving water bodies. Rivers cannot achieve a 'good' status without appropriate control of P removal. Even though P removal is a big topic by itself, it is important to consider such nutrients along with the ammonia in the implementation/investigation of dynamic licensing approach for large WWTPs.

Control strategies at a catchment scale

The integrated approach presented in this work considers the integration of a single urban wastewater system (UWWS) shown in Figure 2-5. Integrated UWWS approaches have a significant benefit both to the water industry and the water-environment as outlined in Chapter 0, and they focus at managing urban wastewater system regardless of what is going on the upstream or downstream of the catchment. If the objective is to achieve a 'good' water environment quality, it is recommended to widen the scope from a single UWWS scale to a hydrologic catchment scale, where activities upstream and downstream of the WWTP can be put into consideration.

Through a catchment scale approach, Figure 9-1, it is possible to integrate diffuse and multiple point source pollution management to successfully achieve a good water-environment quality. For example, in Figure 7-8, there is a point where the ammonia concertation in the river upstream of the WWTP is already above the ammonia limit for the river to have a 'good' status. The approach presented here cannot address such issues; however, by using catchment scale approach, it is possible to address such issues. And, the dynamic licensing approach can be used as a starting point for implementing river quality-based control both at WWTPs and even in the management of diffuse pollution sources.

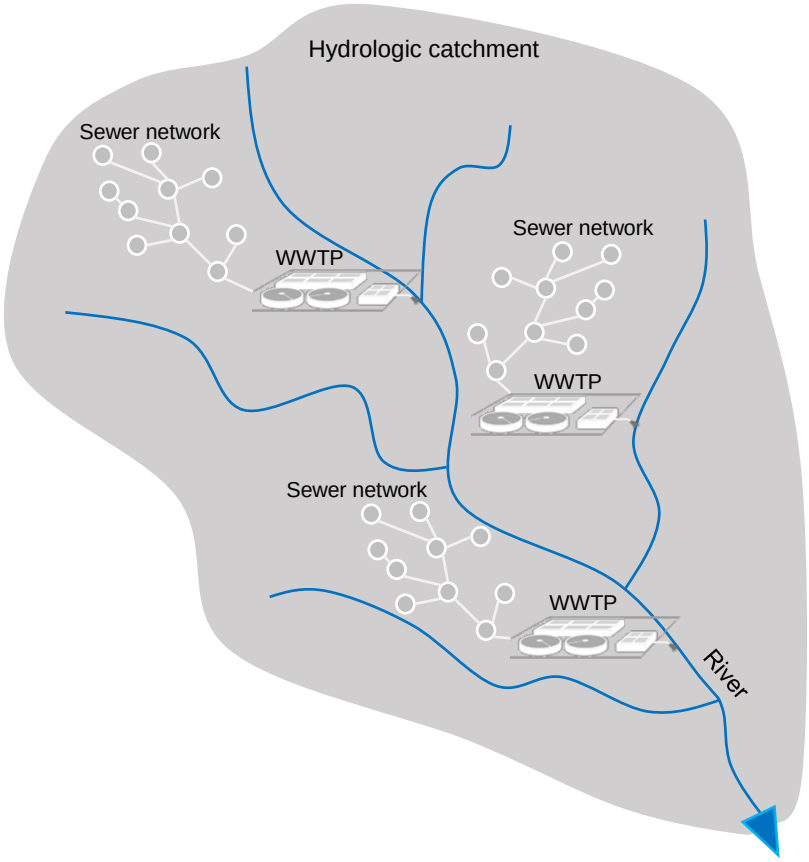

Figure 9-1 Scope of catchment scale management of UWWS

Model-based control of WWTPs and forecasting

The dynamic licensing approach tested in this study uses the river's ammonia concentration as set-point to control processes in WWTPs. The approach showed a promising result, but, in cases where the ammonia concentration in the river is very low compare to the maximum limit set by regulators based on EU-WFD, the control loop will continue to increase the ammonia concentration in the final effluent. Such a control loop can lead to, for example, a continuous deprivation of oxygen in reactors, and may give undesirable results such as increased direct GHG emissions. Hence, in such situation, it is recommended that the set-point for river ammonia concentration should be further assessed and a lower ammonia limit or a variable ammonia limit may need to be used, for example, based on river water level.

In addition, it is recommended to investigate the advantage of a model-based control approach to implement a dynamic licensing approach. Model-based control with a forecast capability can give the river quality ahead of time by considering diffusion and river quality processes. The modelling approach developed in this

study has a capability of using a forecast rainfall to estimate river quality and influent wastewater ahead of time, but further work is recommended to investigate the reliability of it and the benefit and feasibility of model-based control using real-world case study.

9.3.2. Recommendations for Application in the Water Industry

The work presented in this thesis shows the potential of integrated active control strategies and dynamic licensing approach. It also attempts to provide a guideline based on implementation complexity. Some recommendations related to their application are pointed out below.

- The key consideration that should be highlighted, in future deployment of such approaches, is to identify available data and the need for further data collection. A guideline for data collection is provided in this thesis, Chapter 4, which can be adopted to any other activated sludge bases WWTP. However, for a medium to long term plan, it is recommended to give emphasis in designing data collection strategies carefully for the utilisation of complex and spatially distributed integrated models. Through the identification of minimum data requirement and improved sensor technology, the water industry can benefit more from the use of integrated models to achieve operational and strategic benefits.
- The study uses a MATLAB® platform with Simulink® based models, and to further use the integrated model developed in this study, it is recommended to make such modelling platforms and tools are available. If such resources and required experts are not available, Knowledge Transfer Programmes (KTP) can be considered as a capacity building strategy.
- Based on this project and other partner projects outputs, the sponsoring water company is running real-world trials at two WWTP and performing further desk-study for further development of dynamic licensing approach-based control strategies. Such a strategy should be followed by interested water companies and the deployment of such an approach should be designed through the analysis of implementation needs, challenges, and feasibility through selected real-world trials.
- In addition, for integrated control and dynamic licensing approaches to work effectively, it is recommended for water companies to work closely with regulators and other stakeholders. And, the benefit of such approaches

needs to be realised equally both by the water companies and the regulatory bodies.

- Although the benefit of integrated active control design is not discussed here, previous studies showed that there is a considerable advantage in deploying them for new WWTPs. Hence, it is recommended to consider integrated active control systems for new WWTPs to efficiently achieve operational objectives.

Appendices

A. WWTP Influent Wastewater Quality Data Points for Each Day of the Week

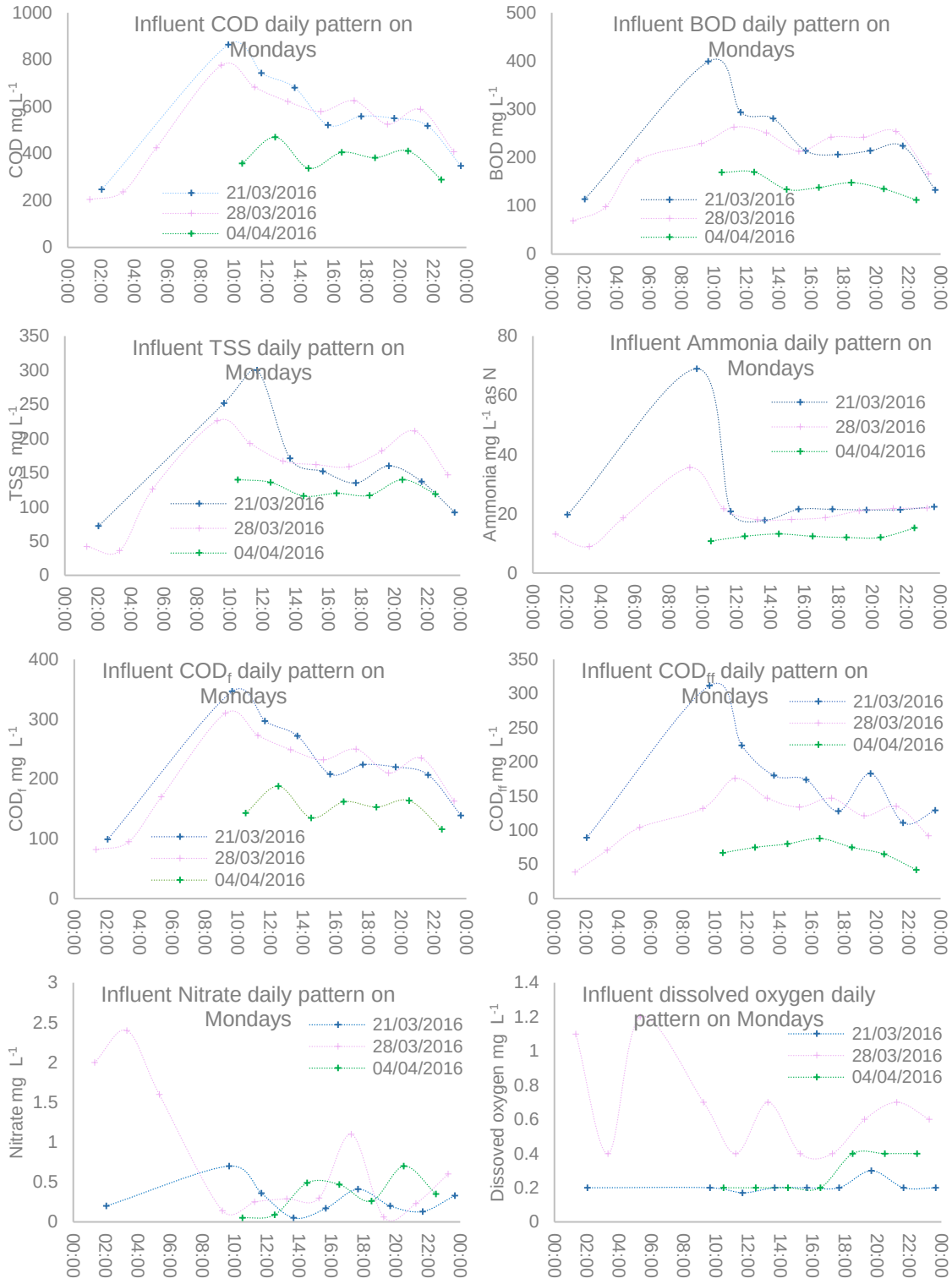

Figure A-1: Influent wastewater pollutants pattern from samples in the campaign period on Mondays

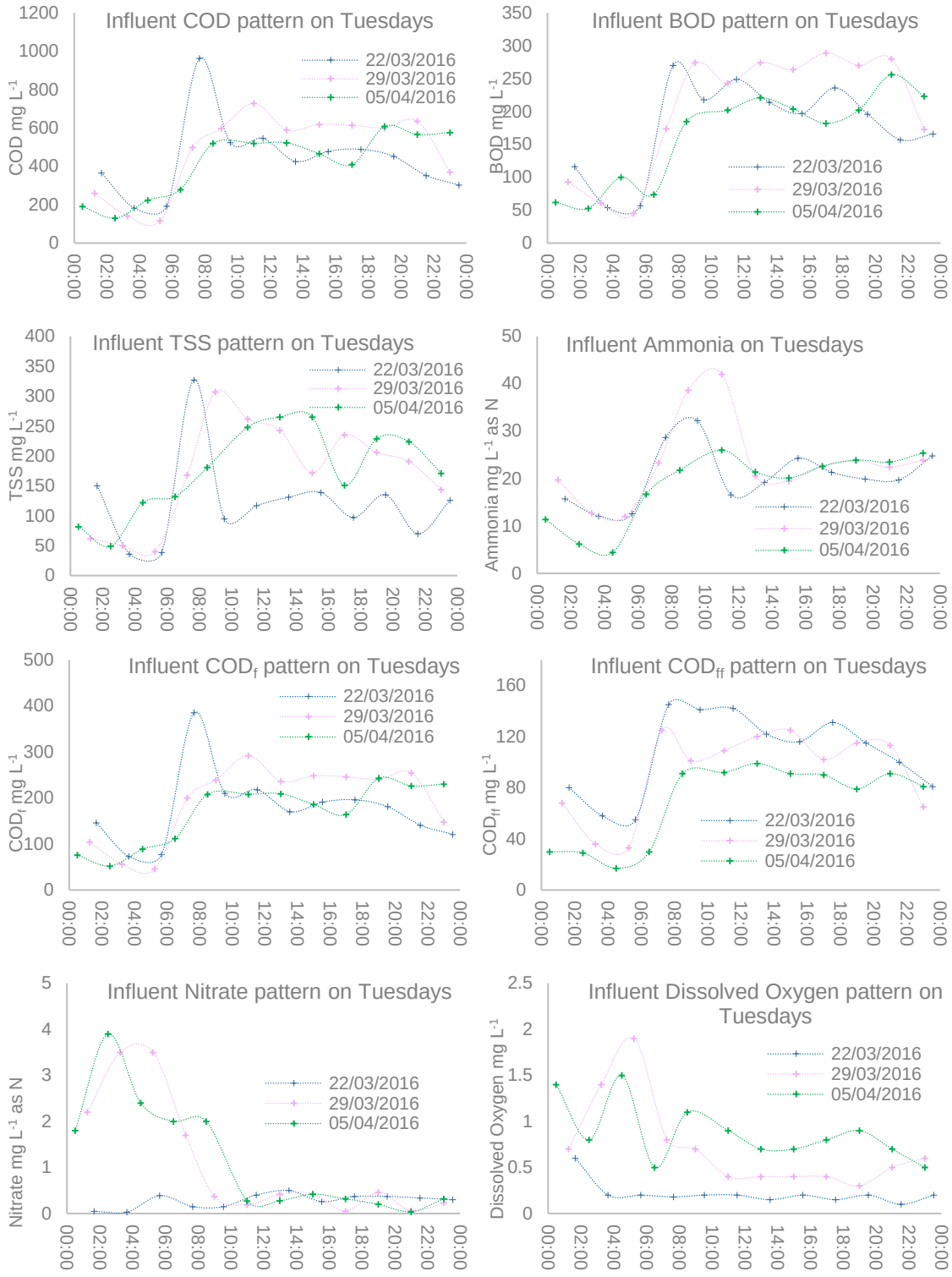

Figure A-2: Influent wastewater pollutants pattern from samples in the campaign period on Tuesdays

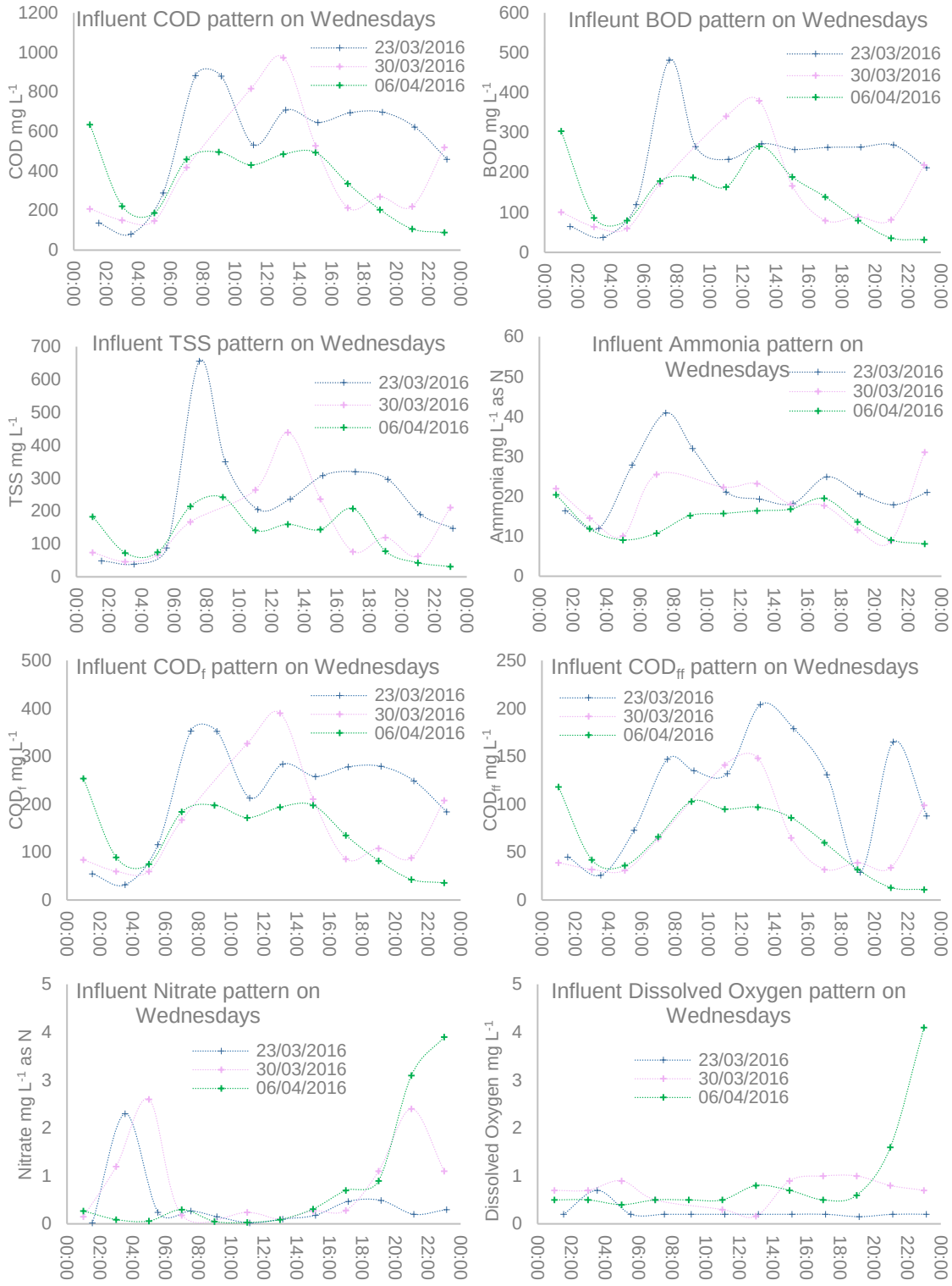

Figure A-3 Influent wastewater pollutants pattern from samples in the campaign period on Wednesdays

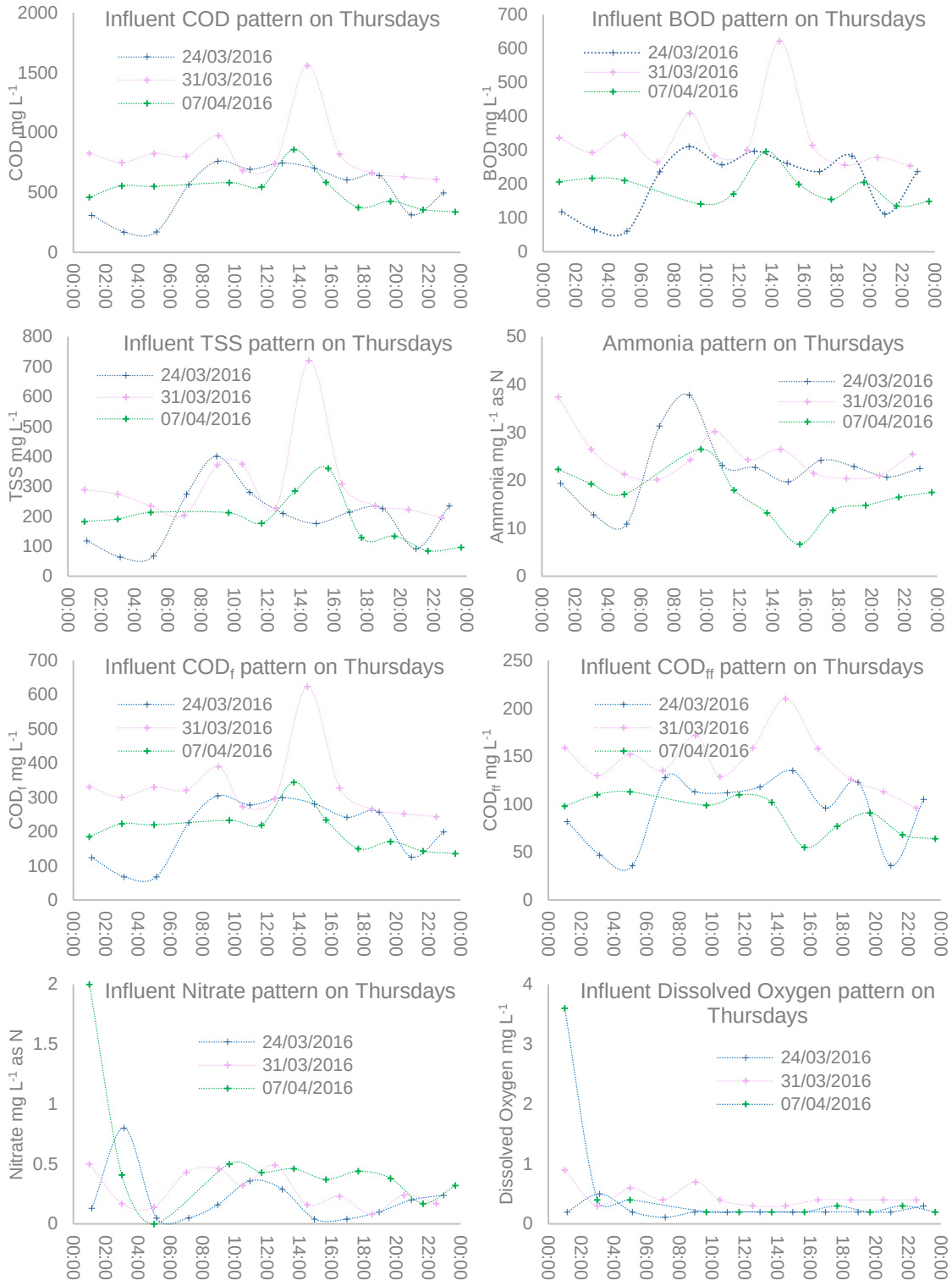

Figure A-4 Influent wastewater pollutants pattern from samples in the campaign period on Thursdays

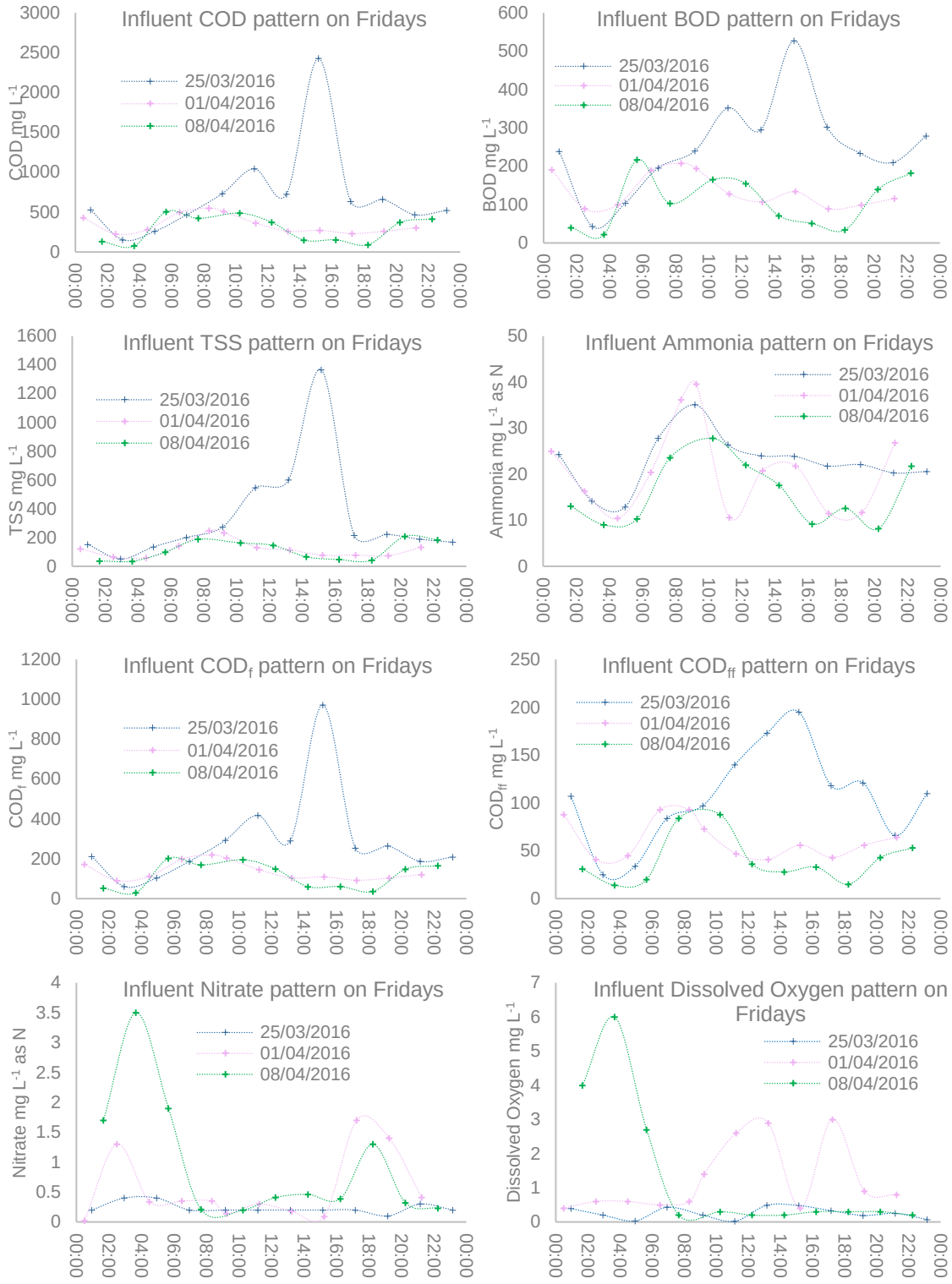

Figure A-5 Influent wastewater pollutants pattern from samples in the campaign period on Fridays

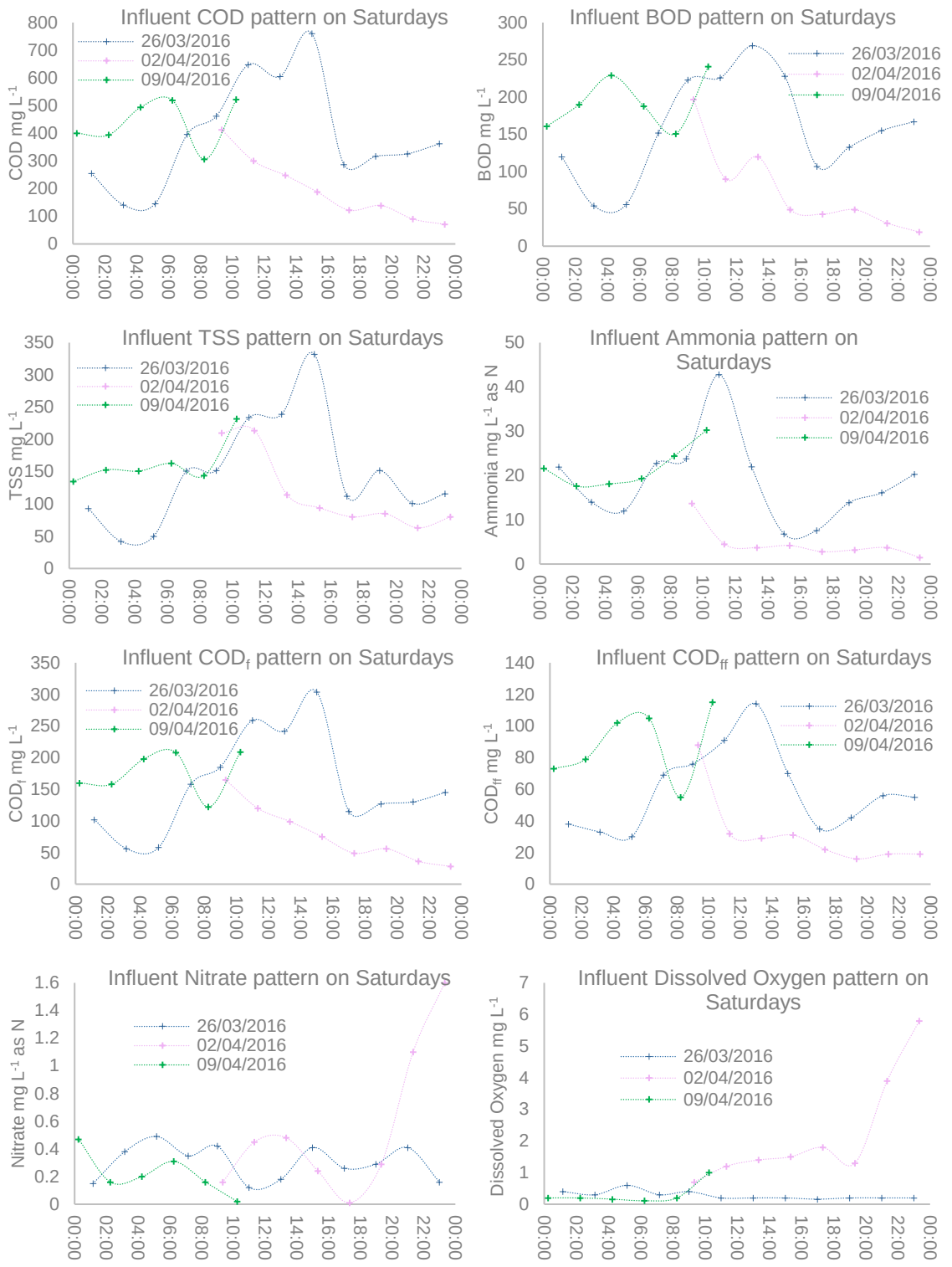

Figure A-6 Influent wastewater pollutants pattern from samples in the campaign period on Saturdays

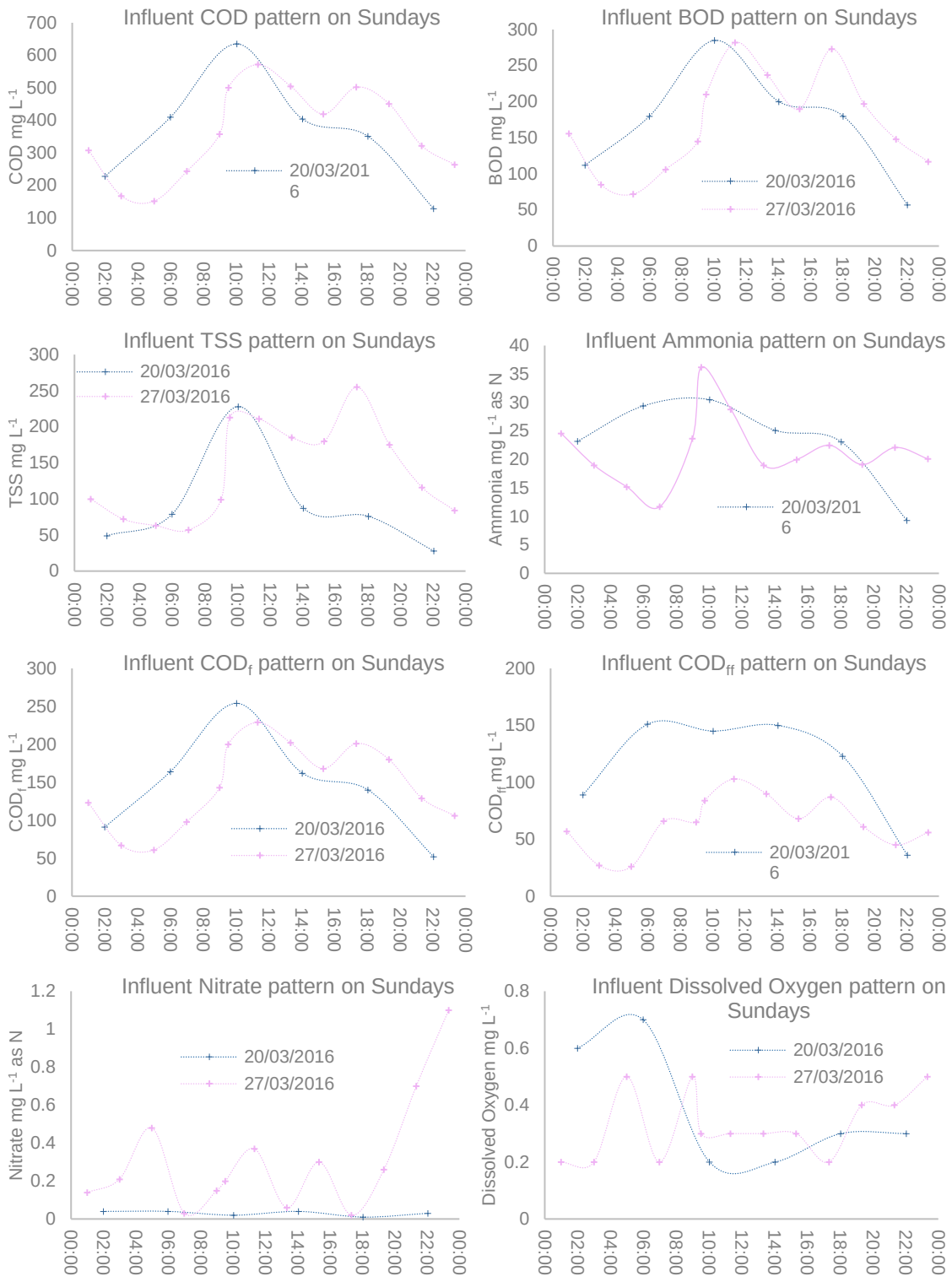

Figure A-7 Influent wastewater pollutants pattern from samples in the campaign period on Sundays

B. WWTP final effluent wastewater quality data points for each day of the week

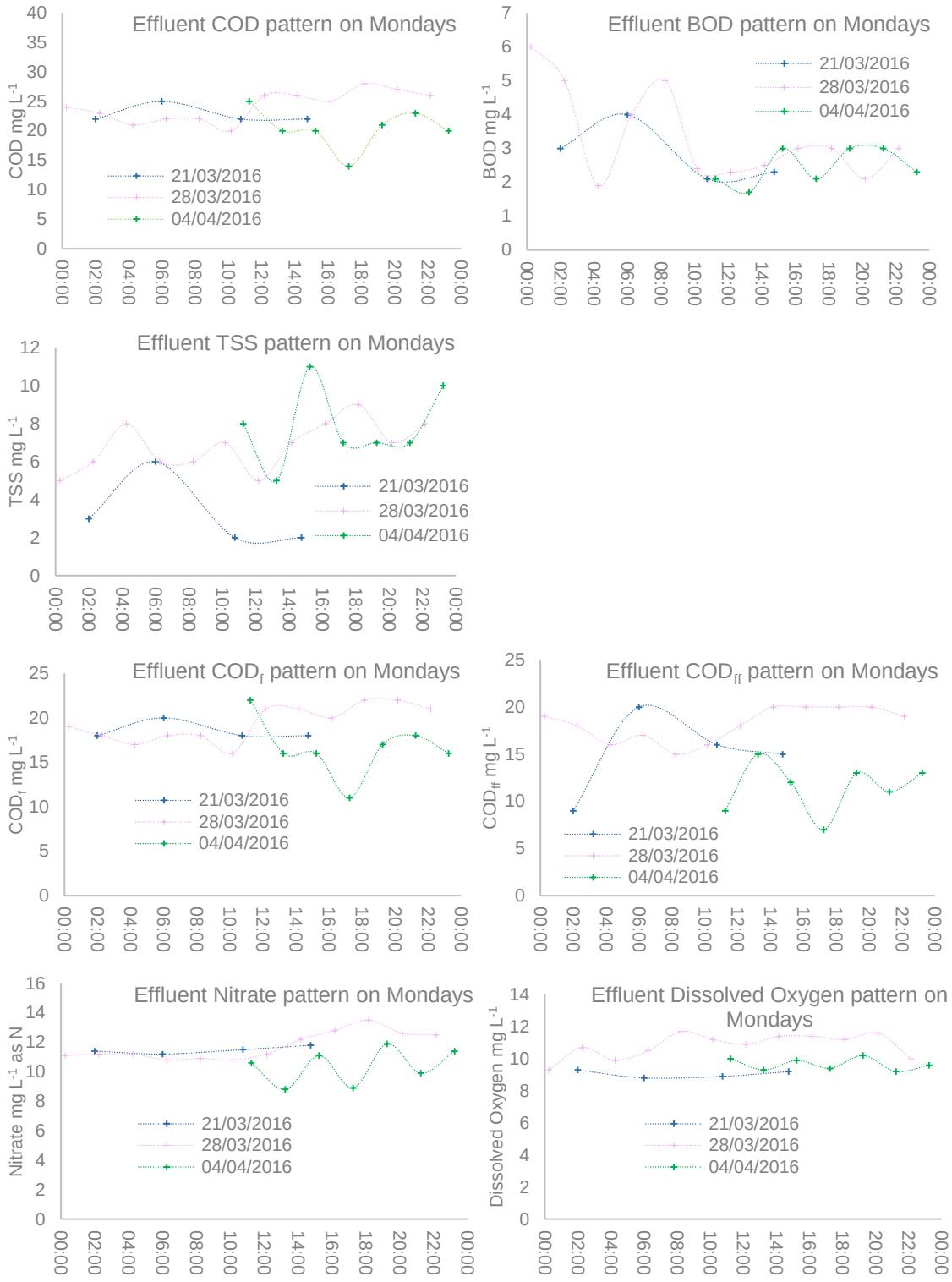

Figure B-1 Final effluent wastewater pollutants pattern from samples in the campaign period on Mondays

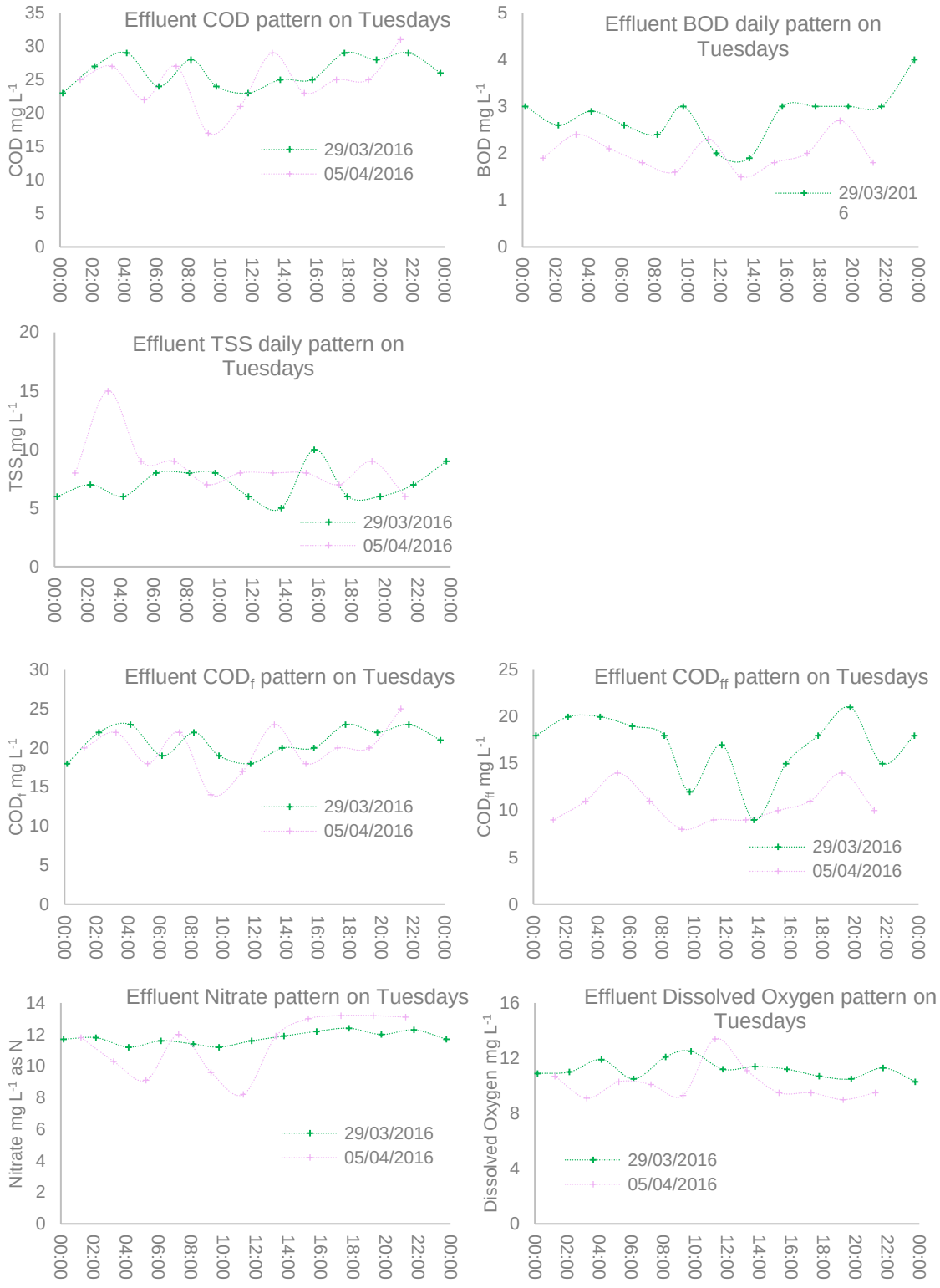

Figure B-2 Final effluent wastewater pollutants pattern from samples in the campaign period on Tuesdays

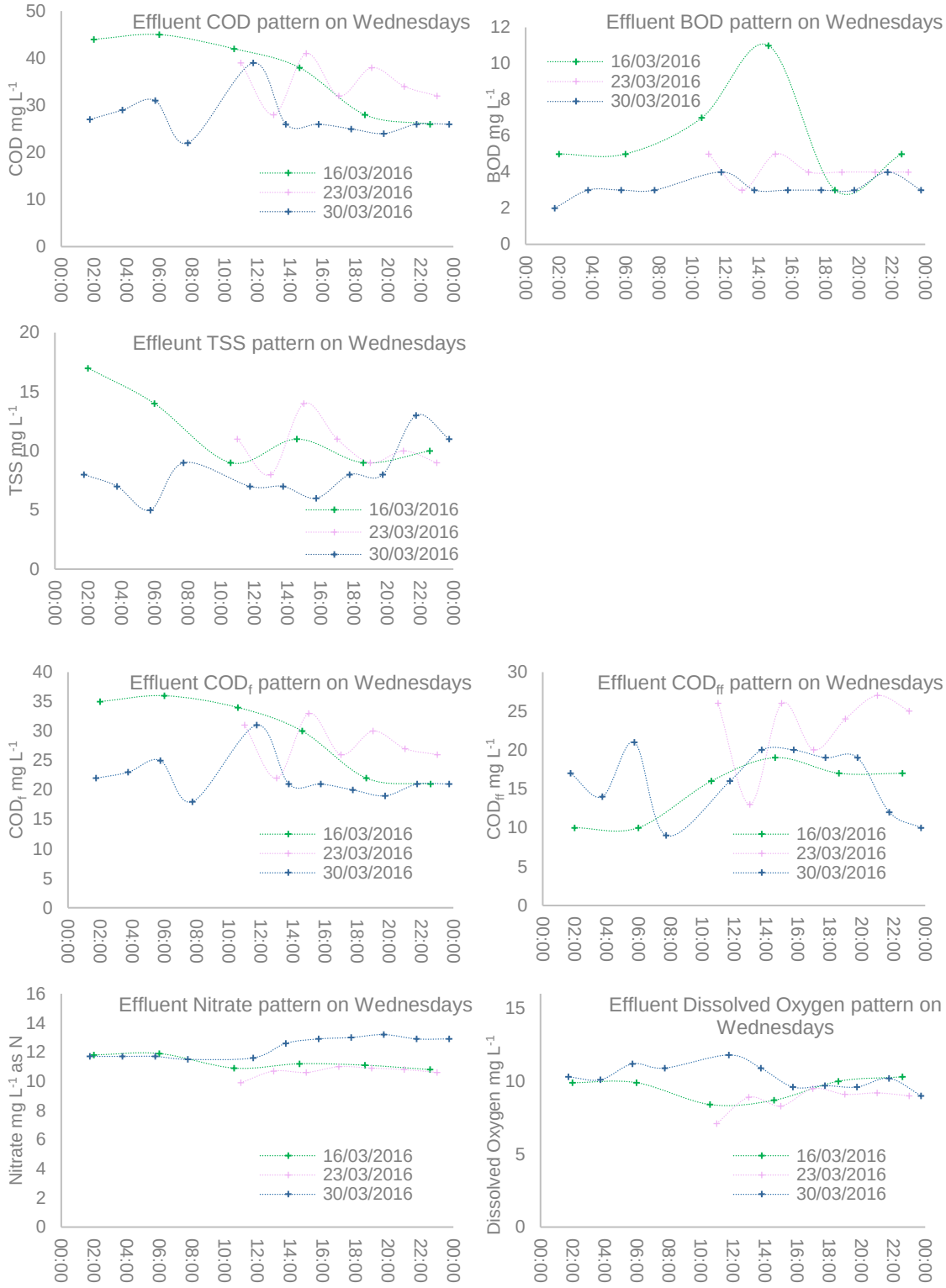

Figure B-3 Final effluent wastewater pollutants pattern from samples in the campaign period on Wednesdays

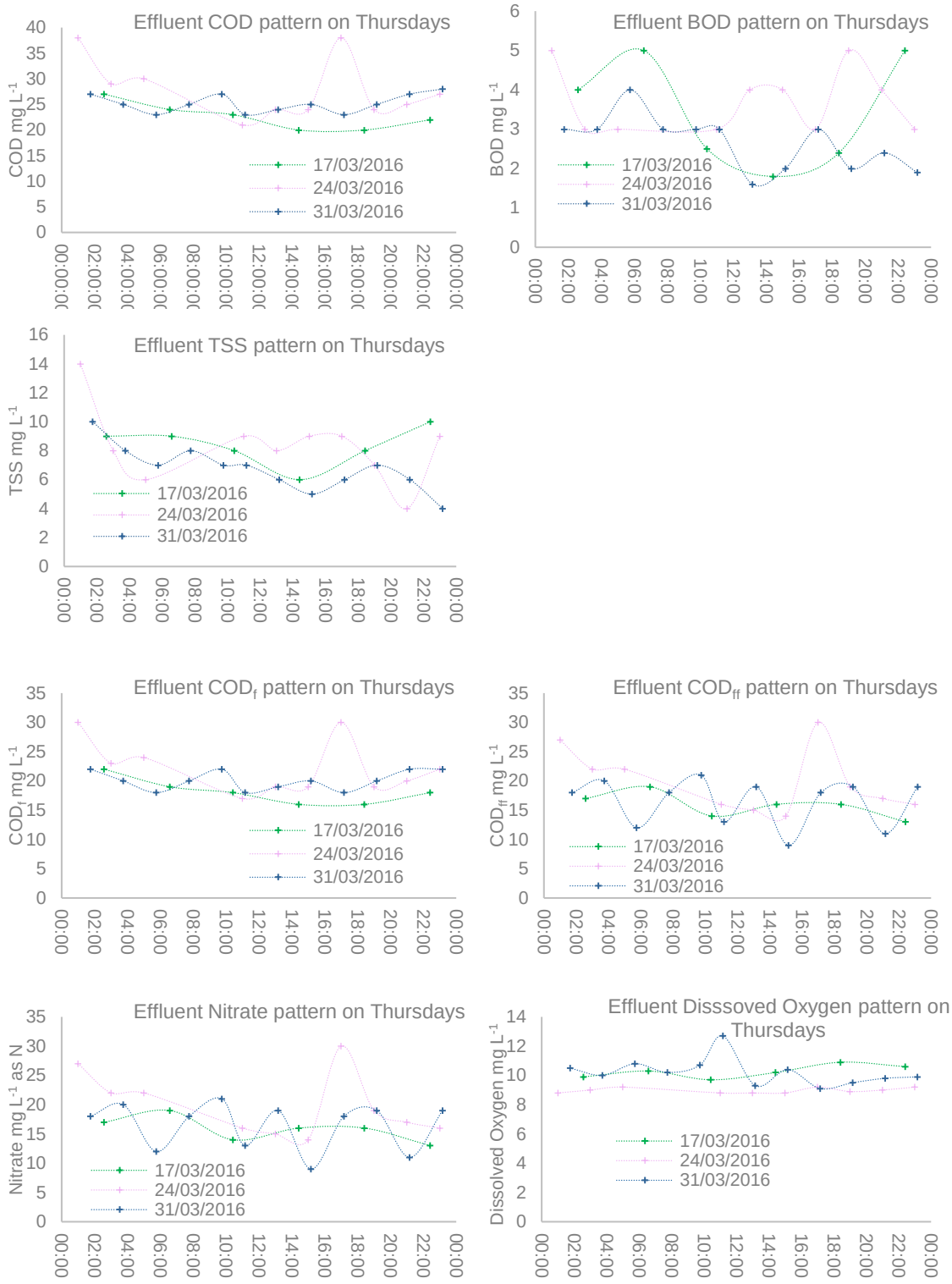

Figure B-4 Final effluent wastewater pollutants pattern from samples in the campaign period on Thursdays

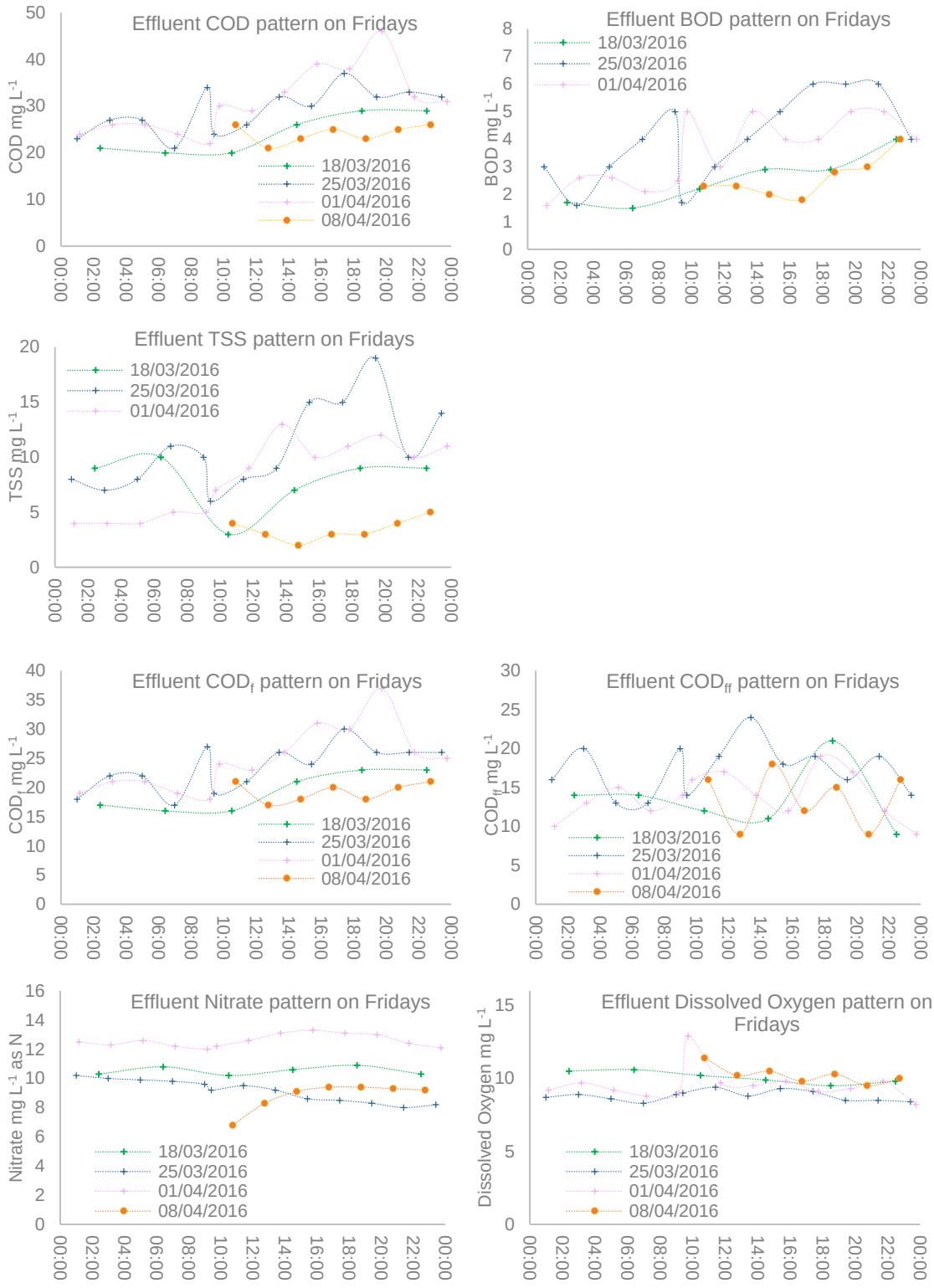

Figure B-5 Final effluent wastewater pollutants pattern from samples in the campaign period on Fridays

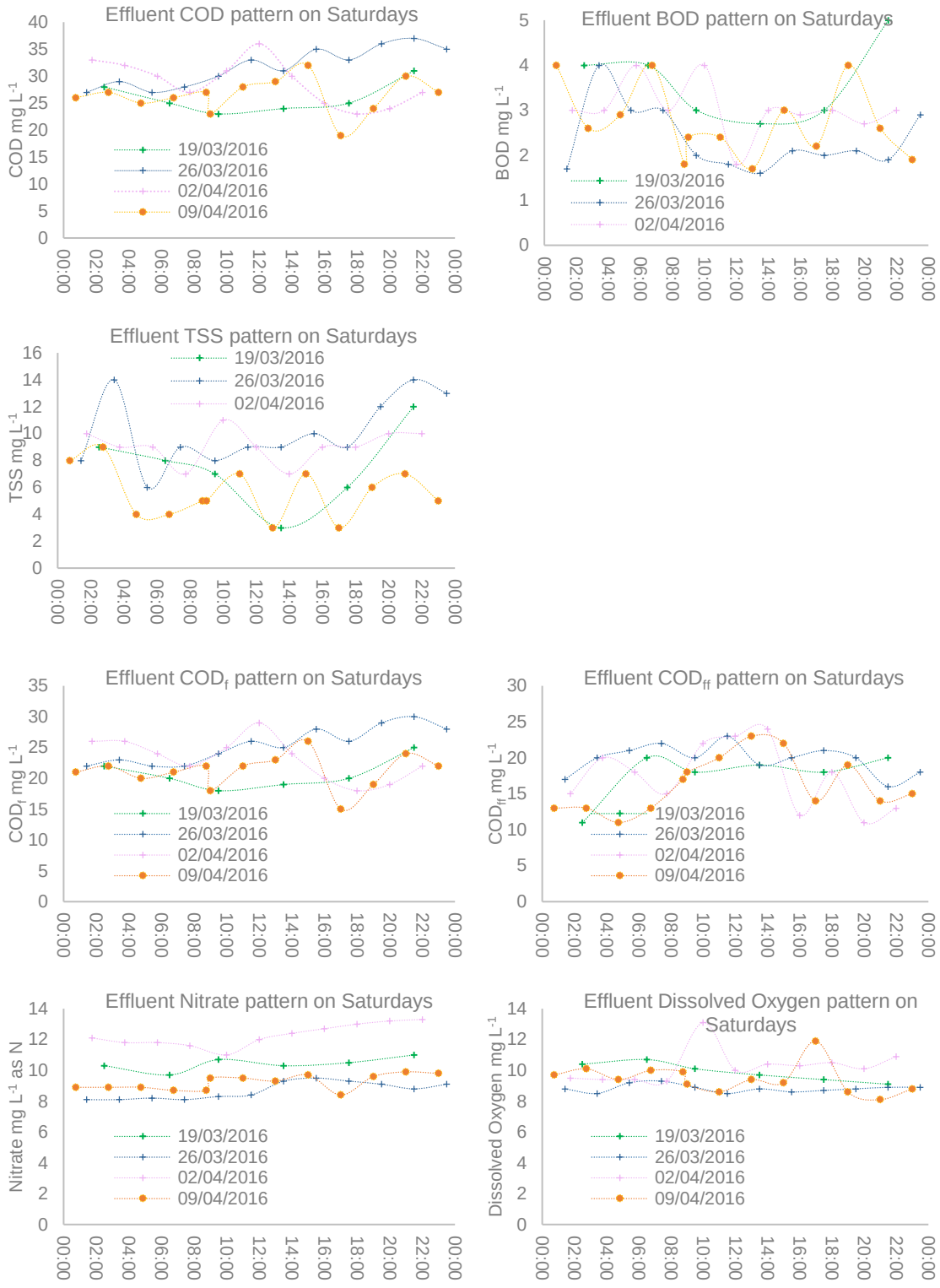

Figure B-6 Final effluent wastewater pollutants pattern from samples in the campaign period on Saturdays

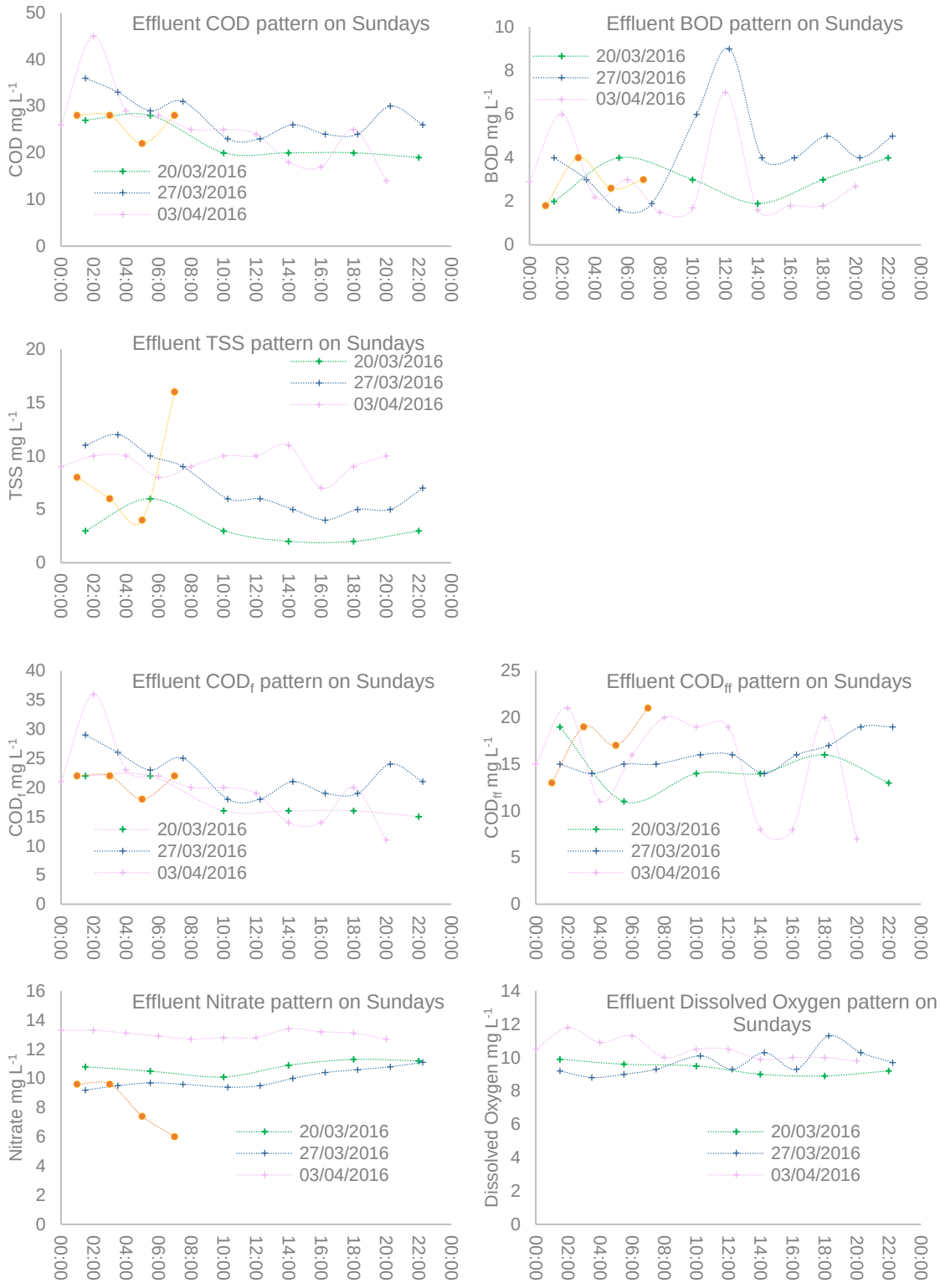

Figure B-7 Final effluent wastewater pollutants pattern from samples in the campaign period on Sundays

Bibliography

Abbasi, T. & Abbasi, S. A. 2011. Water quality indices based on bioassessment: The biotic indices. *Journal of Water and Health,* 9(2)**,** pp 330-348.

Abbasi, T. & Abbasi, S. A. 2012. *Water quality indices*: Elsevier.

Abusam, A. & Keesman, K. 1999. Effect of number of CSTR's on the modelling of oxidation ditches: steady state and dynamic analysis. *Mededelingen-Faculteit Landbouwkundige en Toegepaste Biologische Wetenschappen Universiteit Gent (Belgium)*.

Abusam, A., Keesman, K., Spanjers, H., van Straten, G. & Meinema, K. 2002a. Effect of oxidation ditch horizontal velocity on the nitrogen removal process. *Official Publication of the European Water Association (EWA),* 6(1-9.

Abusam, A., Keesman, K. J., Spanjers, H., Van Straten, G. & Meinema, K. 2002b. Evaluation of control strategies using an oxidation ditch benchmark. *Water Science & Technology,* 45(4-5)**,** pp 151-158.

Abusam, A., Keesman, K. J. & Van Straten, G. 2003. Forward and backward uncertainty propagation: An oxidation ditch modelling example. *Water Research,* 37(2)**,** pp 429-435.

Abusam, A., Keesman, K. J., Van Straten, G., Spanjers, H. & Meinema, K. 2001. Sensitivity analysis in oxidation ditch modelling: The effect of variations in stoichiometric, kinetic and operating parameters on the performance indices. *Journal of Chemical Technology and Biotechnology,* 76(4)**,** pp 430-438.

AERZEN. 2014. Rotary lobe blowers - Delta blowers genration 5.

Aguilar-López, R. 2008. Robust generic model control for dissolved oxygen in Activated Sludge Wastewater Plant. *Chemical and Biochemical Engineering Quarterly,* 22(1)**,** pp 71-79.

Ahn, J. H., Kim, S., Park, H., Rahm, B., Pagilla, K. & Chandran, K. 2010. N2O emissions from activated sludge processes, 2008− 2009: results of a national monitoring survey in the United States. *Environmental Science & Technology,* 44(12)**,** pp 4505-4511.

Alex, J., Benedetti, L., Copp, J., Gernaey, K., Jeppsson, U., Nopens, I., Pons, M. N., Rosen, C., Steyer, J. P. & Vanrolleghem, P. 2008. Benchmark Simulation Model no. 2 (BSM2). Unpublished manuscript.

Alex, J., Beteau, J. F., Copp, J. B., Hellinga, C., Jeppsson, U., Marsili-Libelli, S., Pons, M. N., Spanjers, H. & Vanhooren, H. Benchmark for evaluating control strategies in wastewater treatment plants. European Control Conference, ECC 1999 - Conference Proceedings, 1999. 3746-3751.

Alleyne, A. A., Xanthos, S., Ramalingam, K., Temel, K., Li, H. & Tang, H. S. 2014. Numerical investigation on flow generated by invent mixer in full-scale wastewater stirred tank. *Engineering Applications of Computational Fluid Mechanics,* 8(4)**,** pp 503-517.

Almeida, M. C., Butler, D. & Friedler, E. 1999. At-source domestic wastewater quality. *Urban Water,* 1(1)**,** pp 49-55.

Åmand, L. & Carlsson, B. 2014. Aeration Control with Gain Scheduling in a Full-scale Wastewater Treatment Plant. *IFAC Proceedings Volumes,* 47(3)**,** pp 7146-7151.

Åmand, L., Olsson, G. & Carlsson, B. 2013. Aeration control - A review. *Water Science and Technology,* 67(11)**,** pp 2374-2398.

Amita, J., Jain, S. S. & Garg, P. K. Prediction of Bus Travel Time Using ANN: A Case Study in Delhi. Transportation Research Procedia, 2016.

Analysts, S. C. o. 1986. *Chemical oxygen demand (Dichromate Value) of polluted and waste waters*: Methods for the Examination of Water and Associated Materials.

Andrews, J. F. 1974. Dynamic models and control strategies for wastewater treatment processes. *Water Research,* 8(5)**,** pp 261-289.

Andrews, J. F. 1993. Modeling and simulation of wastewater treatment processes. *Water Science and Technology,* 28(11-12)**,** pp 141-150.

Ashagre, B., Fu, G., Davidson, K. & Butler, D. The Impact of data availability on the predictive accuracy of wastewater treatment works models. 9th European Waste Water Management Conference, 12/10/2015 2015 Manchester, UK.

Asher, M., Croke, B., Jakeman, A. & Peeters, L. 2015. A review of surrogate models and their application to groundwater modeling. *Water Resources Research,* 51(8)**,** pp 5957-5973.

Astaraie-Imani, M., Kapelan, Z., Fu, G. & Butler, D. 2012. Assessing the combined effects of urbanisation and climate change on the river water quality in an integrated urban wastewater system in the UK. *Journal of Environmental Management,* 112(0)**,** pp 1-9.

Azari, A. & Asadi, M. 2017. Investigating the capabilities of the NSGA-II multi-objective algorithm in automatic calibration of the WEAP model for simulating Jareh Dam and network system. *Journal of Applied Research in Water and Wastewater,* 4(1)**,** pp 305-313.

Baban, A. & Talinli, I. 2009. Modeling of organic matter removal and nitrification in sewer systems - an approach to wastewater treatment. *Desalination,* 246(1-3)**,** pp 640-647.

Babbitt, H. E. & Baumann, E. R. 1958. *Sewerage and sewage treatment*, 8, New York: John Wiley and Sons.

Bach, P. M., Rauch, W., Mikkelsen, P. S., McCarthy, D. T. & Deletic, A. 2014. A critical review of integrated urban water modelling - Urban drainage and beyond. *Environmental Modelling and Software,* 54(88-107.

Balkema, A. J., Preisig, H. A., Otterpohl, R. & Lambert, F. J. D. 2002. Indicators for the sustainability assessment of wastewater treatment systems. *Urban Water,* 4(2)**,** pp 153-161.

Bekele, E. G. & Nicklow, J. W. 2007. Multi-objective automatic calibration of SWAT using NSGA-II. *Journal of Hydrology,* 341(3)**,** pp 165-176.

Benedetti, L. 2006. *Probabilistic design and upgrade of wastewater treatment plants in the EU Water Framework Directive context*: Citeseer.

Benedetti, L., Batstone, D. J., De Baets, B., Nopens, I. & Vanrolleghem, P. A. Global sensitivity analysis of biochemical, design and operational parameters of the Benchmark Simulation Model no. 2. Proceedings of iEMSs 2008: International Congress on Environmental Modelling and Software, 2008. 7-10.

Benedetti, L., Langeveld, J., Comeau, A., Corominas, L., Daigger, G., Martin, C., Mikkelsen, P. S., Vezzaro, L., Weijers, S. & Vanrolleghem, P. A. 2013. Modelling and monitoring of integrated urban wastewater systems: Review on status and perspectives. *Water Science and Technology,* 68(6)**,** pp 1203-1215.

Benedetti, L., Meirlaen, J., Sforzi, F., Facchi, A., Gandolfi, C. & Vanrolleghem, P. A. 2007. Dynamic integrated water quality modelling: A case study of the Lambro River, northern Italy. *Water SA,* 33(5)**,** pp 627-632.

Bermúdez, M., Ntegeka, V., Wolfs, V. & Willems, P. 2018. Development and comparison of two fast surrogate models for urban pluvial flood simulations. *Water Resources Management,* 1-15.

Bhattacharyya, S., Chapellat, H. & Keel, L. 1995. Robust control: the parametric approach. *Upper Saddle River*.

Boiocchi, R., Gernaey, K. & Sin, G. 2017. Understanding N2O formation mechanisms through sensitivity analyses using a plant-wide benchmark simulation model. *Chemical Engineering Journal*.

Bott, C. B. & Parker, D. S. 2011. WEF/WERF study quantifying nutrient removal technology performance.

Braga, J. & Varesche, M. 2014. Commercial laundry water characterisation. *American Journal of Analytical Chemistry,* 2014(

Brandt, M., Middleton, R. & Wang, S. 2012. Energy Efficiency in the Water Industry: A Compendium of Best Practices and Case Studies-Global Report. *Water Intelligence Online,* 11(9781780401348.

Brdys, M. A., Grochowski, M., Gminski, T., Konarczak, K. & Drewa, M. 2008. Hierarchical predictive control of integrated wastewater treatment systems. *Control Engineering Practice,* 16(6)**,** pp 751-767.

Brion, N., Verbanck, M. A., Bauwens, W., Elskens, M., Chen, M. & Servais, P. 2015. Assessing the impacts of wastewater treatment implementation on the water quality of a small urban river over the past 40 years. *Environmental Science and Pollution Research,* 22(16)**,** pp 12720-12736.

Britton, T., Cole, G., Stewart, R. & Wiskar, D. 2008. Remote diagnosis of leakage in residential households. *Journal of Australian Water Association,* 35(6)**,** pp 89-93.

Brouwer, H., Bloemen, M., Klapwijk, B. & Spanjers, H. 1998. Feedforward control of nitrification by manipulating the aerobic volume in activated sludge plants. *Water Science and Technology,* 38(3)**,** pp 245-254.

Brown, S. 1986. TOMCAT: A computer model designed specifically for catchment quality planning within the water industry.

Butler, D. 1991. A small-scale study of wastewater discharges from domestic appliances. *Journal of the Institution of Water and Environmental Management,* 5(2)**,** pp 178-185.

Butler, D. 1993. The influence of dwelling occupancy and day of the week on domestic appliance wastewater discharges. *Building and Environment,* 28(1)**,** pp 73-79.

Butler, D. & Davies, J. 2010. *Urban drainage*: Taylor & Francis.

Butler, D., Friedler, E. & Gatt, K. 1995. Characterising the quantity and quality of domestic wastewater inflows. *Water Science and Technology,* 31(7)**,** pp 13-24.

Butler, D. & Schütze, M. 2005. Integrating simulation models with a view to optimal control of urban wastewater systems. *Environmental Modelling and Software,* 20(4 SPEC. ISS.)**,** pp 415-426.

Cakir, F. & Stenstrom, M. 2005. Greenhouse gas production: a comparison between aerobic and anaerobic wastewater treatment technology. *Water research,* 39(17)**,** pp 4197-4203.

Campos, J., Valenzuela-Heredia, D., Pedrouso, A., Val del Río, A., Belmonte, M. & Mosquera-Corral, A. 2016. Greenhouse Gases Emissions from Wastewater Treatment Plants: Minimization, Treatment, and Prevention. *Journal of Chemistry,* 2016(

Candela, A., Freni, G., Mannina, G. & Viviani, G. 2012. Receiving water body quality assessment: An integrated mathematical approach applied to an Italian case study. *Journal of Hydroinformatics,* 14(1)**,** pp 30-47.

Capelo, S., Mira, F. & de Bettencourt, A. M. 2007. In situ continuous monitoring of chloride, nitrate and ammonium in a temporary stream: Comparison with standard methods. *Talanta,* 71(3)**,** pp 1166-1171.

Carlsson, B. & Milocco, R. H. 2001. A simple strategy for controlling the nitrate concentration in an activated sludge process using external carbon flow rate. *Latin American Applied Research,* 31(2)**,** pp 115-120.

Castro-Barros, C. M., Daelman, M., Mampaey, K., Van Loosdrecht, M. & Volcke, E. 2015. Effect of aeration regime on N2O emission from partial nitritation-anammox in a full-scale granular sludge reactor. *water research,* 68(793-803.

CC-Act. 2008. Climate Change Act 2008, Chapter 27. *In:* Parliament, U. (ed.). Her Majesty's Stationery office, London, UK.

CC-Scotland-Act. 2009. Climate Change (Scotland) Act 2009, (asp 12). *In:* Parliament, U. (ed.). Her Majesty's Stationery office, London, UK.

CCC. 2017. Meeting Carbon Budges: Closing the policy gap 2017 report to Parliament,

CCP. 2018. Climate Change Plan: The third report on proposals and policies 2018-2032,

CEC. 1991. Council of the European Communities Directive Concerning Urban Wastewater Treatment (91/271/EEC). *In:* Union, E. P. a. C. o. t. E. (ed.) *Official Journal of the European Union.*

CEC. 2000. Directive 2000/60/EC Establishing a framework for community action in the field of water policy. *In:* Union, E. P. a. C. o. t. E. (ed.) *Official Journal of the European Union.*

Cembrano, G., Quevedo, J., Salamero, M., Puig, V., Figueras, J. & Martí, J. 2004. Optimal control of urban drainage systems. A case study. *Control Engineering Practice,* 12(1)**,** pp 1-9.

Chai, C., Zhang, D., Yu, Y., Feng, Y. & Wong, M. S. 2015. Carbon footprint analyses of mainstream wastewater treatment technologies under different sludge treatment scenarios in China. *Water,* 7(3)**,** pp 918-938.

Chapra, S. 1997. Water quality modeling. New York: McGraw Hill.

Chen, J. & Beck, M. B. 2001. Operational control of storm sewage at an activated sludge process. *Water Science and Technology,* 43(7)**,** pp 131-137.

Chiu, W.-Y., Sun, H. & Poor, H. V. 2013. Energy imbalance management using a robust pricing scheme. *IEEE Transactions on Smart Grid,* 4(2)**,** pp 896-904.

Christova-Boal, D., Eden, R. E. & McFarlane, S. 1996. An investigation into greywater reuse for urban residential properties. *Desalination,* 106(1)**,** pp 391-397.

Chudoba, J., Grau, P. & Ottová, V. 1973. Control of activated-sludge filamentous bulking–II. Selection of microorganisms by means of a selector. *Water Research,* 7(10)**,** pp 1389-1406.

Cole, J. J. & Caraco, N. F. 2001. Emissions of nitrous oxide (N2O) from a tidal, freshwater river, the Hudson River, New York. *Environmental science & technology,* 35(6)**,** pp 991-996.

Colebrook, C. & White, C. 1937. Experiments with fluid friction in roughened pipes. *Proceedings of the royal society of london. series a, mathematical and Physical sciences,* 367-381.

Concepcion, H., Vrecko, D., Meneses, M. & Vilanova, R. Control strategies for removing nitrogen compounds in wastewater treatment plants. 2013 9th Asian Control Conference, ASCC 2013, 2013.

Copp, J. 2002. *The COST Simulation Benchmark: Description and Simulator Manual*, EC, Luxembourg: EC.

Copp, J. B. & Murphy, K. L. 1995. Estimation of the active nitrifying biomass in activated sludge. *Water Research,* 29(8)**,** pp 1855-1862.

Corne, D. W., Knowles, J. D. & Oates, M. J. The Pareto envelope-based selection algorithm for multiobjective optimization. International Conference on Parallel Problem Solving from Nature, 2000. Springer, 839-848.

Corominas, L., Flores-Alsina, X., Snip, L. & Vanrolleghem, P. A. 2012. Comparison of different modeling approaches to better evaluate greenhouse gas emissions from whole wastewater treatment plants. *Biotechnology and Bioengineering,* 109(11)**,** pp 2854-2863.

Corzo, G., Solomatine, D., Wit, M. d., Werner, M., Uhlenbrook, S. & Price, R. 2009. Combining semi-distributed process-based and data-driven models in flow simulation: a case study of the Meuse river basin. *Hydrology and Earth System Sciences,* 13(9)**,** pp 1619-1634.

Davies, P. S. 2005. The biological basis of wastewater treatment. *Strathkelvin Instruments Ltd,* 3(

De Boor, C. 1978. A practical guide to splines. Number 27 in Applied Mathematical Sciences. Springer, New York.

De Clercq, B., Coen, F., Vanderhaegen, B. & Vanrolleghem, P. A. 1999. Calibrating simple models for mixing and flow propagation in waste water treatment plants. *Water Science and Technology,* 39(4)**,** pp 61-69.

de Faria, A. B., Spérandio, M., Ahmadi, A. & Tiruta-Barna, L. 2015. Evaluation of new alternatives in wastewater treatment plants based on dynamic modelling and life cycle assessment (DM-LCA). *Water research,* 84(99-111.

De Gussem, K., Fenu, A., Wambecq, T. & Weemaes, M. 2014. Energy saving on wastewater treatment plants through improved online control: Case study wastewater treatment plant Antwerp-South. *Water Science and Technology,* 69(5)**,** pp 1074-1079.

De Keyser, W., Amerlinck, Y., Urchegui, G., Harding, T., Maere, T. & Nopens, I. 2014. Detailed dynamic pumping energy models for optimization and control of wastewater applications. *Journal of Water and Climate Change,* 5(3)**,** pp 299-314.

De Keyser, W., Gevaert, V., Verdonck, F., De Baets, B. & Benedetti, L. 2010. An emission time series generator for pollutant release modelling in urban areas. *Environmental Modelling and Software,* 25(4)**,** pp 554-561.

de los Reyes, F. L. 2010. Foam in Wastewater Treatment Facilities. *In:* Timmis, K. N. (ed.) *Handbook of Hydrocarbon and Lipid Microbiology.* Berlin, Heidelberg: Springer Berlin Heidelberg.

Deb, K. 1999. An introduction to genetic algorithms. *Sadhana,* 24(4-5)**,** pp 293-315.

Deb, K., Pratap, A., Agarwal, S. & Meyarivan, T. 2002. A fast and elitist multiobjective genetic algorithm: NSGA-II. *IEEE transactions on evolutionary computation,* 6(2)**,** pp 182-197.

DEFRA. 2008. Future Water: The government's water strategy for England, (Norwich, UK).

DEFRA. 2015. Greenhouse gas reporting - Conversion factors 2015 - Government emission conversion factors for greenhouse gas company reporting - Energy and climate change: evidence and analysis *In:* DECC (ed.).

Deglon, D. A. & Meyer, C. J. 2006. CFD modelling of stirred tanks: Numerical considerations. *Minerals Engineering,* 19(10)**,** pp 1059-1068.

Derco, J., Kralik, M., Hutnan, M., Bodik, I. & Cernak, R. 1994. Modelling of the Carrousel plant. *Water Science and Technology,* 30(6)**,** pp 345-354.

Devesa, F., Comas, J., Turon, C., Freixó, A., Carrasco, F. & Poch, M. 2009. Scenario analysis for the role of sanitation infrastructures in integrated urban wastewater management. *Environmental Modelling and Software,* 24(3)**,** pp 371-380.

Devisscher, M., Clacci, G., Fé, L., Benedetti, L., Bixio, D., Thoeye, C., De Gueldre, G., Marsili-Libelli, S. & Vanrolleghem, P. A. 2006. Estimating costs and benefits of advanced control for wastewater treatment plants - The MAgIC methodology. *Water Science and Technology.*

Dickinson, S. J. 2018. *Dynamic Wastewater Discharge Management: Surface Water Quality and Combined Sewer Overflow Modelling for Integrated Real-Time Control.* EngD Dissertation, University of Sheffield.

Dirckx, G., Schütze, M., Kroll, S., Thoeye, C., De Gueldre, G. & Van De Steene, B. 2011. Cost-efficiency of RTC for CSO impact mitigation. *Urban Water Journal,* 8(6)**,** pp 367-377.

Distefano, J. J., Stubberud, A. J. & Williams, I. J. 1997. *Schaum's Outline of Feedback and Control Systems*: McGraw-Hill Professional.

Djukic, M., Jovanoski, I., Ivanovic, O. M., Lazic, M. & Bodroza, D. 2016. Cost-benefit analysis of an infrastructure project and a cost-reflective tariff: A case study for investment in wastewater treatment plant in Serbia. *Renewable and Sustainable Energy Reviews,* 59(1419-1425.

Dochain, D. & Perrier, M. 1993. Control design for nonlinear wastewater treatment processes. *Water Science and Technology,* 28(11-12)**,** pp 283-293.

Dochain, D. & Vanrolleghem, P. A. 2001. *Dynamical modelling and estimation in wastewater treatment processes*: IWA publishing.

Dold, P. 1986. Evaluation of the general activated sludge model proposed by the IAWPRC task group. *Water Science & Technology,* 18(6)**,** pp 63-89.

Drolc, A. & Vrtovšek, J. 2010. Nitrate and nitrite nitrogen determination in waste water using on-line UV spectrometric method. *Bioresource Technology,* 101(11)**,** pp 4228-4233.

Dudley, J. 1995. Process testing of aerators in oxidation ditches. *Water Research,* 29(9)**,** pp 2217-2219.

Duncan, A., Chen, A. S., Keedwell, E., Djordjevic, S. & Savic, D. 2013. RAPIDS: Early warning system for urban flooding and water quality hazards.

ECN. 2005. *ECN Freshwater chemistyr data from Eden (Fife)* [Online]. The ECN Data Centre. [Accessed 10/02 2018].

Eggleston, H., Buendia, L., Miwa, K., Ngara, T. & Tanabe, K. 2006. IPCC guidelines for national greenhouse gas inventories. *Institute for Global Environmental Strategies, Hayama, Japan,* 2(48-56.

Ekama, G. 2010. The role and control of sludge age in biological nutrient removal activated sludge systems. *Water Science and Technology,* 61(7)**,** pp 1645-1652.

Ekman, M., Björlenius, B. & Andersson, M. 2006. Control of the aeration volume in an activated sludge process using supervisory control strategies. *Water research,* 40(8)**,** pp 1668-1676.

Erbe, V. & Schütze, M. 2005. An integrated modelling concept for immission-based management of sewer system, wastewater treatment plant and river. *Water Science & Technology,* 52(5)**,** pp 95-103.

Ercan, M. B. & Goodall, J. L. 2016. Design and implementation of a general software library for using NSGA-II with SWAT for multi-objective model calibration. *Environmental Modelling & Software,* 84(112-120.

ESI-ENVIROPRO. 2016. *DecaPress® DP37E-422 decanting centrifuge* [Online]. Environmental Standard Index. Available: http://cms.esi.info/Media/documents/Mobil_DP37E422_ML.pdf [Accessed 27/02/2017.

European Environmental Agency. 2011. *Atmospheric concentration of N2O (ppb)* [Online]. [Accessed 26/01/2017 2015].

Ferreira, F., Matos, J., Galvão, A. & Cardoso, M. A. 2011. Assessing the environmental performance of urban wastewater systems using the INSA model: Application to the Algés-Alcântara wastewater system, in Portugal. *Journal of Environmental Management,* 92(11)**,** pp 2944-2952.

Flores-Alsina, X., Arnell, M., Amerlinck, Y., Corominas, L., Gernaey, K. V., Guo, L., Lindblom, E., Nopens, I., Porro, J. & Shaw, A. 2014a. Balancing effluent quality, economic cost and greenhouse gas emissions during the evaluation of (plant-wide) control/operational strategies in WWTPs. *Science of the Total Environment,* 466(616-624.

Flores-Alsina, X., Arnell, M., Amerlinck, Y., Corominas, L., Gernaey, K. V., Guo, L., Lindblom, E., Nopens, I., Porro, J., Shaw, A., Snip, L., Vanrolleghem, P. A. & Jeppsson, U. 2014b. Balancing effluent quality, economic cost and greenhouse gas emissions during the evaluation of (plant-wide) control/operational strategies in WWTPs. *Science of the Total Environment,* 466-467(616-624.

Flores-Alsina, X., Corominas, L., Snip, L. & Vanrolleghem, P. A. 2011. Including greenhouse gas emissions during benchmarking of wastewater treatment plant control strategies. *Water Research,* 45(16)**,** pp 4700-4710.

Flores-Alsina, X., Saagi, R., Lindblom, E., Thirsing, C., Thornberg, D., Gernaey, K. V. & Jeppsson, U. 2014c. Calibration and validation of a phenomenological influent pollutant disturbance scenario generator using full-scale data. *Water Research,* 51(172-185.

Foley, J., Yuan, Z., Keller, J., Senante, E., Chandran, K., Willis, J., Shah, A., van Loosdrecht, M. C. & van Voorthuizen, E. 2015. *N2O and CH4 Emission from Wastewater Collection and Treatment Systems: State of the Science Report and Technical Report*: IWA Publishing.

Foscoliano, C., Del Vigo, S., Mulas, M. & Tronci, S. 2016. Predictive control of an activated sludge process for long term operation. *Chemical Engineering Journal,* 304(1031-1044.

Francisco, M., Skogestad, S. & Vega, P. 2015. Model predictive control for the self-optimized operation in wastewater treatment plants: Analysis of dynamic issues. *Computers and Chemical Engineering,* 82(259-272.

Freni, G., Mannina, G. & Viviani, G. 2011. Assessment of the integrated urban water quality model complexity through identifiability analysis. *Water Research,* 45(1)**,** pp 37-50.

Friedler, E. & Butler, D. 1996. Quantifying the inherent uncertainty in the quantity and quality of domestic wastewater. *Water Science and Technology,* 33(2)**,** pp 65-78.

Friedler, E., Butler, D. & Brown, D. M. 1996. Domestic WC usage patterns. *Building and Environment,* 31(4)**,** pp 385-392.

Fronteau, C., Bauwens, W. & Vanrolleghem, P. A. 1997. Integrated modelling: Comparison of state variables, processes and parameters in sewer and wastewater treatment plant models. *Water Science and Technology,* 36(5)**,** pp 373-380.

Fu, G., Butler, D. & Khu, S. T. 2008. Multiple objective optimal control of integrated urban wastewater systems. *Environmental Modelling and Software,* 23(2)**,** pp 225-234.

Fu, G., Khu, S. T. & Butler, D. 2009. Use of surrogate modelling for multiobjective optimisation of urban wastewater systems. *Water Science and Technology,* 60(6)**,** pp 1641-1647.

García, L., Barreiro-Gomez, J., Escobar, E., Téllez, D., Quijano, N. & Ocampo-Martinez, C. 2015. Modeling and real-time control of urban drainage systems: A review. *Advances in Water Resources,* 85(120-132.

Georges, K., Thornton, A. & Sadler, R. 2009. Transforming wastewater treatment to reduce carbon emissions. *Environment Agency*.

Gernaey, K., Rosén, C., Benedetti, L. & Jeppsson, U. Phenomenological modeling of wastewater treatment plant influent disturbance scenarios. 10th International Conference on Urban Drainage (10ICUD), 2005a. 21-26.

Gernaey, K., Rosén, C. & Jeppsson, U. 2005b. BSM2: A model for dynamic influent data generation,

Gernaey, K. V., Flores-Alsina, X., Rosen, C., Benedetti, L. & Jeppsson, U. 2011. Dynamic influent pollutant disturbance scenario generation using a phenomenological modelling approach. *Environmental Modelling & Software,* 26(11)**,** pp 1255-1267.

Gernaey, K. V., Jeppsson, U., Vanrolleghem, P. A. & Copp, J. B. 2014. Benchmarking of Control Strategies for Wastewater Treatment Plants. *Water Intelligence Online,* 13(

Gernaey, K. V., Rosen, C. & Jeppsson, U. 2006. WWTP dynamic disturbance modelling - An essential module for long-term benchmarking development. *Water Science and Technology.*

Gernaey, K. V., van Loosdrecht, M. C. M., Henze, M., Lind, M. & Jørgensen, S. B. 2004. Activated sludge wastewater treatment plant modelling and simulation: state of the art. *Environmental Modelling & Software,* 19(9)**,** pp 763-783.

Ghermandi, A., Bixio, D., Thoeye, C. & De Gueldre, G. 2005. Technical-economical evaluation of the operation of oxidation ditches.

Gray, N. D., Miskin, I. P., Kornilova, O., Curtis, T. P. & Head, I. M. 2002. Occurrence and activity of Archaea in aerated activated sludge wastewater treatment plants. *Environmental Microbiology,* 4(3)**,** pp 158-168.

Gray, N. F. 2010. *Water technology: an introduction for environmental scientists and engineers*: Butterworth-Heinemann.

Groves, K. P., Daigger, G. T., Simpkin, T. J., Redmon, D. T. & Ewing, L. 1992. Evaluation of Oxygen Transfer Efficiency and Alpha-Factor on a Variety of Diffused Aeration Systems. *Water Environment Research,* 64(5)**,** pp 691-698.

Guest, J. S., Skerlos, S. J., Barnard, J. L., Beck, M. B., Daigger, G. T., Hilger, H., Jackson, S. J., Karvazy, K., Kelly, L. & Macpherson, L. 2009. A new planning and design paradigm to achieve sustainable resource recovery from wastewater. ACS Publications.

Guisasola, A., de Haas, D., Keller, J. & Yuan, Z. 2008. Methane formation in sewer systems. *Water Research,* 42(6-7)**,** pp 1421-1430.

Gujer, W. & Henze, M. 1991. Activated sludge modelling and simulation. *Water Science & Technology,* 23(4-6)**,** pp 1011-1023.

Guo, J., Fu, X., Andrés Baquero, G., Sobhani, R., Nolasco, D. A. & Rosso, D. 2016. Trade-off between carbon emission and effluent quality of activated sludge processes under seasonal variations of wastewater temperature and mean cell retention time. *Science of The Total Environment,* 547(331-344.

Guo, N. & Saul, A. 2011. *Improving the operation and maintenance of CSO structures.* University of Sheffield.

Gupta, D. & Singh, S. K. 2012. Greenhouse gas emissions from wastewater treatment plants: a case study of Noida. *Journal of Water Sustainability,* 2(2)**,** pp 131-139.

Haaland, S. E. 1983. Simple and explicit formulas for the friction factor in turbulent pipe flow. *Journal of Fluids Engineering,* 105(1)**,** pp 89-90.

Haandel, A. v. & Lubbe, J. 2011. Handbook of biological wastewater treatment: Design and optimisation of activated sludge systems. *Handbook of*

biological wastewater treatment: Design and optimisation of activated sludge systems, Ed. 2)**,** pp.

Hager, W. H. 2010. *Wastewater hydraulics: Theory and practice*: Springer Science & Business Media.

Hamilton, R., Braun, B., Dare, R., Koopman, B. & Svoronos, S. A. 2006. Control issues and challenges in wastewater treatment plants. *Control Systems, IEEE,* 26(4)**,** pp 63-69.

Harmel, R., Smith, D., King, K. & Slade, R. 2009. Estimating storm discharge and water quality data uncertainty: A software tool for monitoring and modeling applications. *Environmental Modelling & Software,* 24(7)**,** pp 832-842.

Hauduc, H., Gillot, S., Rieger, L., Ohtsuki, T., Shaw, A., Takács, I. & Winkler, S. 2009. Activated sludge modelling in practice: an international survey. *Water Science and Technology,* 60(8)**,** pp 1943.

Hayakawa, T., Haddad, W. M. & Hovakimyan, N. 2008. Neural network adaptive control for a class of nonlinear uncertain dynamical systems with asymptotic stability guarantees. *IEEE Transactions on Neural Networks,* 19(1)**,** pp 80-89.

Henderson, K. J. & Reardon, D. J. 2004. How overdesign leads to high energy costs and simple techniques to optimize energy usage. *Proceedings of the Water Environment Federation,* 2004(9)**,** pp 368-374.

Henze, M. 1992. Characterization of wastewater for modelling of activated sludge processes. *Water Science and Technology,* 25(6)**,** pp 1-15.

Henze, M. 2002. *Wastewater treatment: biological and chemical processes*: Springer.

Henze, M., Gujer, W., Mino, T. & Van Loosdrecht, M. 2000. *Activated Sludge Models ASM1, ASM2, ASM2d and ASM3*, Cornwall: IWA Publishing.

Henze, M., Van Loosdrecht, M. C. M., Ekama, G. A. & Brdjanovic, D. 2008. *Biological wastewater treatment: principles, modelling and design*: IWA publishing.

Hiatt, W. C. & Grady, C. 2008. An updated process model for carbon oxidation, nitrification, and denitrification. *Water Environment Research,* 80(11)**,** pp 2145-2156.

Holubar, P., Zani, L., Hager, M., Fröschl, W., Radak, Z. & Braun, R. 2002. Advanced controlling of anaerobic digestion by means of hierarchical neural networks. *Water Research,* 36(10)**,** pp 2582-2588.

Horan, N. J. 1990. *Biological wastewater treatment systems: theory and operation*: John Wiley & Sons Ltd.

Hreiz, R., Roche, N., Benyahia, B. & Latifi, M. A. 2015. Multi-objective optimal control of small-size wastewater treatment plants. *Chemical Engineering Research and Design,* 102(345-353.

Huang, Z. & Liu, Z. 2009. Numerical study of a positive displacement blower. *Proceedings of the Institution of Mechanical Engineers, Part C: Journal of Mechanical Engineering Science,* 223(10)**,** pp 2309-2316.

Hulsbeek, J., Kruit, J., Roeleveld, P. & Van Loosdrecht, M. 2002. A practical protocol for dynamic modelling of activated sludge systems. *Water Science & Technology,* 45(6)**,** pp 127-136.

Hyndman, R. J. & Koehler, A. B. 2006. Another look at measures of forecast accuracy. *International Journal of Forecasting,* 22(4)**,** pp 679-688.

IEC. 2009. Rotary Electircal Machines - Part 31: Guide for the selection and application of energy-efficient motors including variable-speed applications

IPCC. 1990. Climate Change: The IPCC Scientific Assessment,

IPCC 2013. *Climate Change 2013: The Physical Science Basis. Contribution of Working Group I to the Fifth Assessment Report of the Intergovernmental Panel on Climate Change*, Cambridge, United Kingdom and New York, NY, USA: Cambridge University Press.

Iqbal, J. & Guria, C. 2009. Optimization of an operating domestic wastewater treatment plant using elitist non-dominated sorting genetic algorithm. *Chemical Engineering Research and Design,* 87(11)**,** pp 1481-1496.

Jacobs, O. L. R. 1974. *Introduction to control theory*: Clarendon Press Oxford.

Jensen, M. T. 2003. Reducing the run-time complexity of multiobjective EAs: The NSGA-II and other algorithms. *IEEE Transactions on Evolutionary Computation,* 7(5)**,** pp 503-515.

Jeppsson, U. 2004. A general description of the Activated Sludge Model No 1 ASM1.

Jeppsson, U. & Pons, M.-N. 2004. The COST benchmark simulation model—current state and future perspective. *Control Engineering Practice,* 12(3)**,** pp 299-304.

Jeppsson, U., Pons, M. N., Nopens, I., Alex, J., Copp, J. B., Gernaey, K. V., Rosen, C., Steyer, J. P. & Vanrolleghem, P. A. 2007. Benchmark simulation model no 2: General protocol and exploratory case studies.

Jing, L., Chen, B., Zhang, B. & Li, P. 2015. Process simulation and dynamic control for marine oily wastewater treatment using UV irradiation. *Water Research,* 81(101-112.

Johnson, M. A. & Sanchez, A. Process control loop tuning and monitoring using LQG optimality with applications in wastewater treatment plant. International Conference on Control and Automation, 2003. 922-926.

Jonelis, K., Brazauskas, K. & Levišauskas, D. Mathematical model for adaptive control of dissolved oxygen concentration in biological wastewater treatment process. 4th International Conference on Electrical and Control Technologies, ECT 2009, 2009. 121-124.

Kalantar, B., Pradhan, B., Naghibi, S. A., Motevalli, A. & Mansor, S. 2017. Assessment of the effects of training data selection on the landslide susceptibility mapping: a comparison between support vector machine (SVM), logistic regression (LR) and artificial neural networks (ANN). *Geomatics, Natural Hazards and Risk,* 1-21.

Kandare, G., Viúdez-Moreiras, D. & Hernández-Del-Olmo, F. 2012. Adaptive control of the oxidation ditch reactors in a wastewater treatment plant. *International Journal of Adaptive Control and Signal Processing,* 26(10)**,** pp 976-989.

Kannel, P., Kanel, S., Lee, S., Lee, Y.-S. & Gan, T. 2011. A Review of Public Domain Water Quality Models for Simulating Dissolved Oxygen in Rivers and Streams. *Environmental Modeling and Assessment,* 16(2)**,** pp 183-204.

Kappeler, J. & Gujer, W. 1992. Estimation of kinetic parameters of heterotrophic biomass under aerobic conditions and characterization of wastewater for activated sludge modelling. *Water Science & Technology,* 25(6)**,** pp 125-139.

Katebi, M. R. & Graells, F. P. 2005. A FRAMEWORK FOR MODELLING, SIMULATION AND CONTROL OF INTEGRATED URBAN WASTEWATER SYSTEMS. *IFAC Proceedings Volumes,* 38(1)**,** pp 49-54.

Khan, M. K. 2015. *Fluid Mechanics and Machinery*: Oxford University Press.

Kimochi, Y., Inamori, Y., Mizuochi, M., Xu, K.-Q. & Matsumura, M. 1998. Nitrogen removal and N2O emission in a full-scale domestic wastewater treatment plant with intermittent aeration. *Journal of Fermentation and Bioengineering,* 86(2)**,** pp 202-206.

Kishida, N., Tsuneda, S., Sakakibara, Y., Kim, J. & Sudo, R. 2008. Real-time control strategy for simultaneous nitrogen and phosphorus removal using aerobic granular sludge.

Kokash, N. 2005. An introduction to heuristic algorithms. *Department of Informatics and Telecommunications,* 1-8.

König, M., Escher, B. I., Neale, P. A., Krauss, M., Hilscherová, K., Novák, J., Teodorović, I., Schulze, T., Seidensticker, S., Kamal Hashmi, M. A., Ahlheim, J. & Brack, W. 2017. Impact of untreated wastewater on a major European river evaluated with a combination of in vitro bioassays and chemical analysis. *Environmental Pollution,* 220(1220-1230.

Krause, P., Boyle, D. & Bäse, F. 2005. Comparison of different efficiency criteria for hydrological model assessment. *Advances in Geosciences,* 5(89-97.

Lacour, C. & Schütze, M. 2011. Real-time control of sewer systems using turbidity measurements. *Water Science and Technology,* 63(11)**,** pp 2628-2632.

Lagarias, J. C., Reeds, J. A., Wright, M. H. & Wright, P. E. 1998. Convergence properties of the Nelder-Mead simplex method in low dimensions. *SIAM Journal on optimization,* 9(1)**,** pp 112-147.

Landau, I. D., Lozano, R., M'Saad, M. & Karimi, A. 2011. *Adaptive control: algorithms, analysis and applications*: Springer Science & Business Media.

Langergraber, G., Alex, J., Weissenbacher, N., Woerner, D., Ahnert, M., Frehmann, T., Halft, N., Hobus, I., Plattes, M. & Spering, V. 2008. Generation of diurnal variation for influent data for dynamic simulation. *Water science and technology,* 57(9)**,** pp 1483.

Langergraber, G., Rieger, L., Winkler, S., Alex, J., Wiese, J., Owerdieck, C., Ahnert, M., Simon, J. & Maurer, M. 2004. A guideline for simulation studies of wastewater treatment plants. *Water Science & Technology,* 50(7)**,** pp 131-138.

Langeveld, J. G., Clemens, F. H. L. R. & van der Graaf, J. H. J. M. 2002. Increasing wastewater system performance – the importance of interactions between sewerage and wastewater treatment. *Water Science and Technology,* 45(3)**,** pp 45-52.

Law, Y., Ni, B.-J., Lant, P. & Yuan, Z. 2012. N2O production rate of an enriched ammonia-oxidising bacteria culture exponentially correlates to its ammonia oxidation rate. *Water research,* 46(10)**,** pp 3409-3419.

Lee Rodgers, J. & Nicewander, W. A. 1988. Thirteen ways to look at the correlation coefficient. *The American Statistician,* 42(1)**,** pp 59-66.

Lemmer, H., Lind, G., Müller, E., Schade, M. & Ziegelmayer, B. 2000. Scum in Activated Sludge Plants: Impact of Non-filamentous and Filamentous Bacteria. *Acta hydrochimica et hydrobiologica,* 28(1)**,** pp 34-40.

Lens, P., Zeeman, G. & Lettinga, G. 2001. *Decentralised sanitation and reuse*: IWA publishing.

Li, S. & Zheng, Y. 2015. *Distributed Model Predictive Control for Plant-wide Systems*: John Wiley & Sons.

Libhaber, M. & Orozco-Jaramillo, Á. 2012. *Sustainable Treatment and Reuse of Municipal Wastewater: For Decision Makers and Practicing Engineers*: Iwa publishing.

Lin, M. J. & Luo, F. 2015. An adaptive control method for the dissolved oxygen concentration in wastewater treatment plants. *Neural Computing and Applications,* 26(8)**,** pp 2027-2037.

Lindberg, C.-F. 1997. *Control and estimation strategies applied to the activated sludge process*: Uppsala University Stockholm, Sweden.

Lindblom, E., Arnell, M., Flores-Alsina, X., Stenström, F., Gustavsson, D., Yang, J. & Jeppsson, U. 2016. Dynamic modelling of nitrous oxide emissions from three Swedish sludge liquor treatment systems. *Water Science and Technology,* 73(4)**,** pp 798-806.

Liwarska-Bizukojc, E., Olejnik, D., Biernacki, R. & Ledakowicz, S. 2011. Calibration of a complex activated sludge model for the full-scale wastewater treatment plant. *Bioprocess and Biosystems Engineering,* 34(6)**,** pp 659-670.

Logist, F., Houska, B., Diehl, M. & Van Impe, J. F. 2011. Robust multi-objective optimal control of uncertain (bio)chemical processes. *Chemical Engineering Science,* 66(20)**,** pp 4670-4682.

Lukasse, L. 1999. *Control and identification in activated sludge processes.* PhD PhD, Landbouwuniversiteit Wageningen.

Luo, T., Yang, M., Han, J. & Sun, P. 2014. A novel model-based adaptive control strategy for step-feed SBRs dealing with influent fluctuation. *Bioresource Technology,* 167(476-483.

Maere, T., Neethling, J., Clark, D., Pramanik, A. & Vanrolleghem, P. A. 2016. Wastewater Treatment Nutrient Regulations: An International Perspective with Focus on Innovation. *WEF/IWA Nutrient Removal and Recovery.* Denver, Colorado, USA.

Magnus, A., Magnus, R., Felipe, O. & Jeppsson, U. 2016. Evaluating Environmental Performance of Operational Strategies at Wastewater Treatment Plants. *IWA 10th World Water Congress and Exhibition (WWC2016).* Brisbane, Australia.

Mahmoud, M. S. & Xia, Y. 2012. *Applied Control Systems Design*: Springer Science & Business Media.

Makinia, J. 2010. *Mathematical modelling and computer simulation of activated sludge systems*: Iwa Publishing.

Mamais, D., Jenkins, D. & Prrr, P. 1993. A rapid physical-chemical method for the determination of readily biodegradable soluble COD in municipal wastewater. *Water research,* 27(1)**,** pp 195-197.

Mamais, D., Noutsopoulos, C., Dimopoulou, A., Stasinakis, A. & Lekkas, T. D. 2015. Wastewater treatment process impact on energy savings and greenhouse gas emissions. *Water Science and Technology,* 71(2)**,** pp 303-308.

Mampaey, K., Beuckels, B., Kampschreur, M., Kleerebezem, R., Van Loosdrecht, M. & Volcke, E. 2013. Modelling nitrous and nitric oxide emissions by autotrophic ammonia-oxidizing bacteria. *Environmental technology,* 34(12)**,** pp 1555-1566.

Mannina, G., Butler, D., Benedetti, L., Deletic, A., Fowdar, H., Fu, G., Kleidorfer, M., McCarthy, D., Steen Mikkelsen, P., Rauch, W., Sweetapple, C., Vezzaro, L., Yuan, Z. & Willems, P. 2018. Greenhouse gas emissions from integrated urban drainage systems: Where do we stand? *Journal of Hydrology,* 559(307-314.

Mannina, G., Cosenza, A., Vanrolleghem, P. A. & Viviani, G. 2011. A practical protocol for calibration of nutrient removal wastewater treatment models. *Journal of hydroinformatics,* 13(4)**,** pp 575-595.

Mannina, G., Ekama, G., Caniani, D., Cosenza, A., Esposito, G., Gori, R., Garrido-Baserba, M., Rosso, D. & Olsson, G. 2016. Greenhouse gases from wastewater treatment — A review of modelling tools. *Science of The Total Environment,* 551–552(254-270.

Marquot, A., Stricker, A. & Racault, Y. 2006. ASM1 dynamic calibration and long-term validation for an intermittently aerated WWTP. *Water Science & Technology,* 53(12)**,** pp 247-256.

Martin, C. & Vanrolleghem, P. A. 2014. Analysing, completing, and generating influent data for WWTP modelling: A critical review. *Environmental Modelling & Software,* 60(188-201.

Mayer, P., DeOreo, W., Towler, E., Martien, L. & Lewis, D. 2004. Tampa water department residential water conservation study: the impacts of high efficiency plumbing fixture retrofits in single-family homes. *A Report Prepared for Tampa Water Department and the United States Environmental Protection Agency*.

McCarty, P. L. 2012. *Environmental biotechnology: principles and applications*: Tata McGraw-Hill Education.

McCuen, R. H., Knight, Z. & Cutter, A. G. 2006. Evaluation of the Nash–Sutcliffe efficiency index. *Journal of Hydrologic Engineering*.

McDougald, S., Imrie, B. & Cole, B. 1974. An Investigation of the Volumetric. Efficiency of a Roots Blower.

Mcgee, M. & Pearson, G. 1999. Wastewater Technology Fact Sheet, Fine Bubble Aeration. *Epa. org. US Environmental Protection Agency*.

Meirlaen, J., Van Assel, J. & Vanrolleghem, P. A. 2002. Real time control of the integrated urban wastewater system using simultaneously simulating surrogate models. *Water Science and Technology.*

Mekonnen, B. A., Nazemi, A., Mazurek, K. A., Elshorbagy, A. & Putz, G. 2015. Hybrid modelling approach to prairie hydrology: fusing data-driven and

process-based hydrological models. *Hydrological sciences journal,* 60(9)**,** pp 1473-1489.

Melcer, H. 2003. *Methods for wastewater characterization in activated sludge modeling*: IWA publishing.

Meng, F., Fu, G. & Butler, D. 2016. Water quality permitting: From end-of-pipe to operational strategies. *Water Research,* 101(114-126.

Metcalf & Eddy, I. 2004. *Wastewater engineering: treatment and reuse. Metcalf & Eddy*, 4th: Inc., McGraw-Hill, New York.

Mhlanga, F. T. & Brouckaert, C. J. 2013. Characterisation of wastewater for modelling of wastewater treatment plants receiving industrial effluent. *Water SA,* 39(3)**,** pp 403-408.

Mitchell, M. 1998. *An introduction to genetic algorithms*: MIT press.

Molinos-Senante, M., Gómez, T., Garrido-Baserba, M., Caballero, R. & Sala-Garrido, R. 2014. Assessing the sustainability of small wastewater treatment systems: A composite indicator approach. *Science of The Total Environment,* 497-498(607-617.

Monroy, O., Alvarez-Ramirez, J., Cuervo, F. & Femat, R. 1996. An adaptive strategy to control anaerobic digesters for wastewater treatment. *Industrial and Engineering Chemistry Research,* 35(10)**,** pp 3442-3446.

Monteith, H., Kalogo, Y. & Louzeiro, N. 2007. Achieving stringent effluent limits takes a lot of energy! *Proceedings of the Water Environment Federation.* Water Environment Federation.

Monteith, H. D., Sahely, H. R., MacLean, H. L. & Bagley, D. M. 2005. A rational procedure for estimation of greenhouse-gas emissions from municipal wastewater treatment plants. *Water Environment Research,* 77(4)**,** pp 390-403.

Moriasi, D. N., Arnold, J. G., Van Liew, M. W., Bingner, R. L., Harmel, R. D. & Veith, T. L. 2007. Model evaluation guidelines for systematic quantification of accuracy in watershed simulations. *Transactions of the ASABE,* 50(3)**,** pp 885-900.

Mounce, S., Shepherd, W., Sailor, G., Shucksmith, J. & Saul, A. 2014. Predicting combined sewer overflows chamber depth using artificial neural networks with rainfall radar data. *Water science and technology,* 69(6)**,** pp 1326-1333.

Muga, H. E. & Mihelcic, J. R. 2008. Sustainability of wastewater treatment technologies. *Journal of Environmental Management,* 88(3)**,** pp 437-447.

Muschalla, D. 2008. Optimization of integrated urban wastewater systems using multi-objective evolution strategies. *Urban Water Journal,* 5(1)**,** pp 59-67.

Nash, J. E. & Sutcliffe, J. V. 1970. River flow forecasting through conceptual models part I—A discussion of principles. *Journal of hydrology,* 10(3)**,** pp 282-290.

Nejjari, F., Dahhou, B., Benhammou, A. & Roux, G. 1999. Non-linear multivariable adaptive control of an activated sludge wastewater treatment process. *International Journal of Adaptive Control and Signal Processing,* 13(5)**,** pp 347-365.

Ni, B.-J., Ruscalleda, M., Pellicer-Nacher, C. & Smets, B. F. 2011. Modeling nitrous oxide production during biological nitrogen removal via nitrification and denitrification: extensions to the general ASM models. *Environmental science & technology,* 45(18)**,** pp 7768-7776.

Ni, B. J., Yuan, Z., Chandran, K., Vanrolleghem, P. A. & Murthy, S. 2013. Evaluating four mathematical models for nitrous oxide production by autotrophic ammonia-oxidizing bacteria. *Biotechnology and Bioengineering,* 110(1)**,** pp 153-163.

Nopens, I., Benedetti, L., Jeppsson, U., Pons, M.-N., Alex, J., Copp, J. B., Gernaey, K. V., Rosen, C., Steyer, J.-P. & Vanrolleghem, P. A. 2010. Benchmark Simulation Model No 2: finalisation of plant layout and default control strategy. *Water Science and Technology,* 62(9)**,** pp 1967-1974.

Nylund, N.-O. & Erkkilä, K. Heavy-duty truck emissions and fuel consumption simulating real-world driving in laboratory conditions. DEER Conference, 2005 Chicago, Illinois, USA.

Ocampo-Martinez, C. 2010. *Model predictive control of wastewater systems*: Springer Science & Business Media.

Olsson, G. 2006. Instrumentation, control and automation in the water industry–state-of-the-art and new challenges. *Water science and technology,* 53(4-5)**,** pp 1-16.

Olsson, G. 2012. ICA and me–a subjective review. *Water research,* 46(6)**,** pp 1585-1624.

Olsson, G. & Newell, B. 1999. *Wastewater treatment systems: modelling, diagnosis and control*: IWA publishing.

Olsson, G., Nielsen, M., Yuan, Z., Lynggaard-Jensen, A. & Steyer, J.-P. 2005. Instrumentation, control and automation in wastewater systems. *Water Intelligence Online,* 4(9781780402680.

Ort, C., Schaffner, C., Giger, W. & Gujer, W. 2005. Modelling stochastic load variations in sewer systems. *Water Science and Technology.*

Pagilla, K. R., Urgun-Demirtas, M., Czerwionka, K. & Makinia, J. 2008. Nitrogen speciation in wastewater treatment plant influents and effluents—the US and Polish case studies. *Water Science and Technology,* 57(10)**,** pp 1511-1517.

Peña-Guzmán, C. A., Melgarejo, J., Prats, D., Torres, A. & Martínez, S. 2017. Urban water cycle simulation/management models: A review. *Water (Switzerland),* 9(4)**,** pp.

Peters, C., Keller, S., Sieker, H. & Jekel, M. 2007. Potentials of real time control, stormwater infiltration and urine separation to minimize river impacts: dynamic long term simulation of sewer network, pumping stations, pressure pipes and waste water treatment plant. *Water Science and Technology,* 56(10)**,** pp 1-10.

Petersen, B. 2000. *Calibration, identifiability and optimal experimental design of activated sludge models calibratie, identificeerbaarheid en optimale proefopzet voor actief-slib modellen.* UNIVERSITEIT GENT.

Petersen, B., Vanrolleghem, P., Gernaey, K. & Henze, M. 2002. Evaluation of an ASM1 model calibration procedure on a municipal–industrial wastewater treatment plant. *Journal of Hydroinformatics,* 4(15-38.

Petre, E. & Selişteanu, D. 2013. A multivariable robust-adaptive control strategy for a recycled wastewater treatment bioprocess. *Chemical Engineering Science,* 90(40-50.

Petre, E., Selişteanu, D. & Şendrescu, D. 2013. Adaptive and robust-adaptive control strategies for anaerobic wastewater treatment bioprocesses. *Chemical Engineering Journal,* 217(363-378.

Petre, E., Selişteanu, D., Şendrescu, D. & Ionete, C. 2010. Neural networks-based adaptive control for a class of nonlinear bioprocesses. *Neural Computing and Applications,* 19(2)**,** pp 169-178.

Picioreanu, C., Van Loosdrecht, M. & Heijnen, J. 1997. Modelling the effect of oxygen concentration on nitrite accumulation in a biofilm airlift suspension reactor. *Water Science and Technology,* 36(1)**,** pp 147-156.

Piotrowski, R., Brdys, M. A., Konarczak, K., Duzinkiewicz, K. & Chotkowski, W. 2008. Hierarchical dissolved oxygen control for activated sludge processes. *Control Engineering Practice,* 16(1)**,** pp 114-131.

Qiao, J. F., Bo, Y. C., Chai, W. & Han, H. G. 2013. Adaptive optimal control for a wastewater treatment plant based on a data-driven method. *Water Science and Technology,* 67(10)**,** pp 2314-2320.

Răducan, O., Woinaroschy, A. & Lavric, V. 2006. Optimal control of a wastewater activated sludge system. *UPB Scientific Bulletin, Series B: Chemistry and Materials Science,* 68(2)**,** pp 3-14.

Ragazzo, P., Falletti, L., Chiucchini, N. & Serra, G. 2013. Management optimisation and technologies application: a right approach to balance energy saving needs and process goals. *Water Practice and Technology,* 8(2)**,** pp wpt. 2013028.

Rauch, W., Aalderink, H., Krebs, P., Schilling, W. & Vanrolleghem, P. 1998. Requirements for integrated wastewater models - Driven by receiving water objectives. *Water Science and Technology,* 38(11)**,** pp 97-104.

Rauch, W., Bertrand-Krajewski, J.-L., Krebs, P., Mark, O., Schilling, W., Schütze, M. & Vanrolleghem, P. A. 2002. Deterministic modelling of integrated urban drainage systems. *Water science and technology,* 45(3)**,** pp 81-94.

Reeves, T. G. 1972. Nitrogen removal: a literature review. *Journal (Water Pollution Control Federation),* 1895-1908.

Repšyte, J., Čebatoriene, I. & Wenzel, A. Adaptive control system for dissolved oxygen concentration in Kaunas wastewater treatment plant. 4th International Conference on Electrical and Control Technologies, ECT 2009, 2009. 125-130.

Riechel, M., Matzinger, A., Pawlowsky-Reusing, E., Sonnenberg, H., Uldack, M., Heinzmann, B., Caradot, N., von Seggern, D. & Rouault, P. 2016. Impacts of combined sewer overflows on a large urban river – Understanding the effect of different management strategies. *Water Research,* 105(264-273.

Rieger, L., Jones, R. M., Dold, P. L. & Bott, C. B. 2014. Ammonia-based feedforward and feedback aeration control in activated sludge processes. *Water Environment Research,* 86(1)**,** pp 63-73.

Rieger, L., Takács, I. & Siegrist, H. 2012. Improving nutrient removal while reducing energy use at three Swiss WWTPs using advanced control. *Water environment research,* 84(2)**,** pp 170-188.

Rieger, L., Takács, I., Villez, K., Siegrist, H., Lessard, P., Vanrolleghem, P. A. & Comeau, Y. 2010. Data reconciliation for wastewater treatment plant simulation studies—planning for high-quality data and typical sources of errors. *Water Environment Research,* 82(5)**,** pp 426-433.

Rodríguez, J. P., McIntyre, N., Díaz-Granados, M., Achleitner, S., Hochedlinger, M. & Maksimović, Č. 2013. Generating time-series of dry weather loads to sewers. *Environmental Modelling and Software,* 43(133-143.

Rosén, C., Röttorp, J. & Jeppsson, U. 2003. Multivariate on-line monitoring: challenges and solutions for modern wastewater treatment operation. *Water Science & Technology,* 47(2)**,** pp 171-179.

Rosso, D., Larson, L. E. & Stenstrom, M. K. 2008. Aeration of large-scale municipal wastewater treatment plants: state of the art. *Water Science and Technology,* 57(7)**,** pp 973-978.

Samie, G., Bernier, J., Rocher, V. & Lessard, P. 2011. Modeling nitrogen removal for a denitrification biofilter. *Bioprocess and biosystems engineering,* 34(6)**,** pp 747-755.

Samuelsson, P. 2005. *Control of Nitrogen Removal in Activated Sludge Processes.* Dissertation/Thesis, Uppsala : Acta Universitatis Upsaliensis.

Samuelsson, P. & Carlsson, B. 2002. Control of the aeration volume in an activated sludge process for nitrogen removal. *Water Science and Technology,* 45(4-5)**,** pp 45-52.

Sanchez, E. N., Beteau, J. F. & Carlos-Hernandez, S. Hierarchical fuzzy control for a wastewater anaerobic treatment plant. Proceedings of the IEEE International Conference on Systems, Man and Cybernetics, 2001. 3285-3290.

Sander, S., Golden, D., Kurylo, M., Moortgat, G., Wine, P., Ravishankara, A., Kolb, C., Molina, M., Finlayson-Pitts, B. & Huie, R. 2006. Chemical kinetics and photochemical data for use in atmospheric studies evaluation number 15,

Santín, I., Pedret, C., Meneses, M. & Vilanova, R. Process based control architecture for avoiding effluent pollutants quality limits violations in wastewater treatment plants. 2015 19th International Conference on System Theory, Control and Computing, ICSTCC 2015 - Joint Conference SINTES 19, SACCS 15, SIMSIS 19, 2015a. 396-402.

Santín, I., Pedret, C., Vilanova, R. & Meneses, M. 2015b. Removing violations of the effluent pollution in a wastewater treatment process. *Chemical Engineering Journal,* 279(207-219.

Sasaki, T., Hanakuma, Y., Nakaya, K., Adachi, H. & Nakanishi, E. 1994. An application of simple adaptive control to level control loop of wastewater tank. *Kagaku Kogaku Ronbunshu,* 20(5)**,** pp 636-641.

Schaper, C., Mellichamp, D. & Seborg, D. Robust control of a wastewater treatment system. Proceedings of the IEEE Conference on Decision and Control, 1990. 2035-2040.

Schilling, W., Andersson, B., Nyberg, U., Aspegren, H., Rauch, W. & Harremoës, P. 1996. Real time control of wastewater systems. *Journal of Hydraulic Research,* 34(6)**,** pp 785-797.

Schilperoort, R. P. S. 2011. *Monitoring as a tool for the assessment of wastewater quality dynamics*: TU Delft, Delft University of Technology.

Schütze, M., Butler, D. & Beck, B. M. 2011. *Modelling, simulation and control of urban wastewater systems*: Springer Science & Business Media.

Schütze, M., Campisano, A., Colas, H., Schilling, W. & Vanrolleghem, P. A. 2004. Real time control of urban wastewater systems - Where do we stand today? *Journal of Hydrology,* 299(3-4)**,** pp 335-348.

Schütze, M., To, T., Jumar, U. & Butler, D. Multi-objective control of urban wastewater systems. International Federation of Automatic Control 15th IFAC World Congress, 2002.

Scottish-Water. 2008. Cupar wastewater treatment works operating manual. Scottish Water.

Serhani, M., Raissi, N. & Cartigny, P. 2009. Robust feedback control design for a nonlinear wastewater treatment model. *Mathematical Modelling of Natural Phenomena,* 4(5)**,** pp 128-143.

Seshadri, A. 2009. NSGA-II: A multi-objective optimization algorithm. *MAT-Lab Central, Implementierung*.

Shahabadi, M. B., Yerushalmi, L. & Haghighat, F. 2010. Estimation of greenhouse gas generation in wastewater treatment plants–Model development and application. *Chemosphere,* 78(9)**,** pp 1085-1092.

Shammas, N. K. & Wang, L. K. 2009. Oxidation Ditch. *In:* Wang, L. K., Pereira, N. C. & Hung, Y. (eds.) *Biological Treatment Processes. Handbook of Environmental Engineering.*

Sharma, A. K., Guildal, T., Thomsen, H. R. & Jacobsen, B. N. 2011. Energy savings by reduced mixing in aeration tanks: Results from a full scale investigation and long term implementation at Avedoere wastewater treatment plant. *Water Science and Technology,* 64(5)**,** pp 1089-1095.

Sharma, D. & Kansal, A. 2012. Assessment of river quality models: a review. *Reviews in Environmental Science and Biotechnology,* 1-27.

Sin, G., De Pauw, D. J., Weijers, S. & Vanrolleghem, P. A. 2008. An efficient approach to automate the manual trial and error calibration of activated sludge models. *Biotechnology and bioengineering,* 100(3)**,** pp 516-528.

Sin, G., Gernaey, K. V., Neumann, M. B., van Loosdrecht, M. C. & Gujer, W. 2009. Uncertainty analysis in WWTP model applications: a critical discussion using an example from design. *Water Research,* 43(11)**,** pp 2894-2906.

Sin, G., Van Hulle, S. W., De Pauw, D. J., Van Griensven, A. & Vanrolleghem, P. A. 2005. A critical comparison of systematic calibration protocols for activated sludge models: A SWOT analysis. *Water research,* 39(12)**,** pp 2459-2474.

Skočilas, J., Fořt, I. & Jirout, T. 2013. A study of CFD simulations of the flow pattern in an agitated system with a pitched blade worn turbine. *Chemical and Process Engineering,* 34(1)**,** pp 39-49.

Smith, P. G. 2005. *Dictionary of water and waste management*: Butterworth-Heinemann.

Snip, L., Boiocchi, R., Flores-Alsina, X., Jeppsson, U. & Gernaey, K. 2014. Challenges encountered when expanding activated sludge models: a case study based on N2O production. *Water Science and Technology,* 70(7)**,** pp 1251-1260.

Snip, L. J. P., Flores-Alsina, X., Aymerich, I., Rodríguez-Mozaz, S., Barceló, D., Plósz, B. G., Corominas, L., Rodriguez-Roda, I., Jeppsson, U. & Gernaey, K. V. 2016. Generation of synthetic influent data to perform (micro)pollutant

wastewater treatment modelling studies. *Science of the Total Environment,* 569-570(278-290.

Soddell, J. & Seviour, R. 1990. Microbiology of foaming in activated sludge plants. *Journal of Applied Microbiology,* 69(2)**,** pp 145-176.

Solomatine, D. P. & Ostfeld, A. 2008. Data-driven modelling: some past experiences and new approaches. *Journal of hydroinformatics,* 10(1)**,** pp 3-22.

Song, X. L., Zhao, Y. B., Song, Z. Y. & Liu, C. Y. 2012. Dissolved oxygen control in wastewater treatment based on robust PID controller. *International Journal of Modelling, Identification and Control,* 15(4)**,** pp 297-303.

Spellman, F. R. 2008. *Handbook of water and wastewater treatment plant operations*: CRC Press.

SRBDD. 2014a. Environmental protection: The Scotland River Basin District (Standards) Directions, SRBDD

SRBDD. 2014b. Environmental protection: The Scotland River Basin District (Status) Directions, SRBDD

Srinivas, N. & Deb, K. 1994. Muiltiobjective optimization using nondominated sorting in genetic algorithms. *Evolutionary computation,* 2(3)**,** pp 221-248.

Srivastava, D. & Singh, R. M. 2014. Breakthrough Curves Characterization and Identification of an Unknown Pollution Source in Groundwater System Using an Artificial Neural Network (ANN). *Environmental Forensics,* 15(2)**,** pp 175-189.

Stamatelatou, K. & Tsagarakis, K. P. 2015. *Sewage Treatment Plants: Economic Evaluation of Innovative Technologies for Energy Efficiency*: IWA Publishing.

Stamou, A. I. 1997. Modelling of oxidation ditches using an open channel flow 1-D advection-dispersion equation and ASM1 process description.

Stenstrom, M. & Rosso, D. 2008. Aeration and mixing. *Biological Wastewater Treatment: Principles, Modelling, and Design,* 245-272.

Stout, T. M. & Williams, T. J. 1995. Pioneering work in the field of computer process control. *IEEE Annals of the History of Computing,* 17(1)**,** pp 6-18.

Streeter, H. W. 1925. A study of the pollution and natural purification of Ohio River. *Health Bulletin, Department of Health Education and Welfare,* 146(

Suescun, J., Ostolaza, X., Garcia-Sanz, M. & Ayesa, E. 2001. Real-time control strategies for predenitrification - Nitrification activated sludge plants biodegradation control. *Water Science and Technology.*

Svrcek, W. Y., Mahoney, D. P. & Young, B. R. 2014. *A real-time approach to process control*: John Wiley & Sons.

Sweetapple, C. 2014. *Developing strategies for the reduction of greenhouse gas emissions from wastewater treatment.* PhD, University of Exeter.

Sweetapple, C., Fu, G. & Butler, D. 2013. Identifying key sources of uncertainty in the modelling of greenhouse gas emissions from wastewater treatment. *Water Research,* 47(13)**,** pp 4652-4665.

Sweetapple, C., Fu, G. & Butler, D. 2014. Multi-objective optimisation of wastewater treatment plant control to reduce greenhouse gas emissions. *Water Research,* 55(52-62.

Sweetapple, C., Fu, G. & Butler, D. Reliable, robust and resilient system design framework with application to wastewater treatment plant control. 2016. American Society of Civil Engineers.

Takács, I., Patry, G. G. & Nolasco, D. 1991. A dynamic model of the clarification-thickening process. *Water Research,* 25(10)**,** pp 1263-1271.

ten Veldhuis, J. & Tait, S. Data-driven urban drainage analysis: an alternative to hydrodynamic models? International conference on urban drainage, Porto Alegre/RS-Brazil, 11-16 September 2011, 2011. Internaional Water Association.

Thornton, A., Sunner, N. & Haeck, M. 2010. Real time control for reduced aeration and chemical consumption: a full scale study. *Water Science and Technology,* 61(9)**,** pp 2169-2175.

Toro, R., Ocampo Martínez, C. A., Logist, F., Impe, J. v. & Puig Cayuela, V. Tuning of predictive controllers for drinking water networked systems. 2011. International Federation of Automatic Control.

Torres Zúñiga, I., Queinnec, I. & Vande Wouwer, A. 2012. Observer-based output feedback linearizing control strategy for a nitrification-denitrification biofilter. *Chemical Engineering Journal,* 191(243-255.

Torriti, J., Hassan, M. G. & Leach, M. 2010. Demand response experience in Europe: Policies, programmes and implementation. *Energy,* 35(4)**,** pp 1575-1583.

Traoré, A., Grieu, S., Puig, S., Corominas, L., Thiery, F., Polit, M. & Colprim, J. 2005. Fuzzy control of dissolved oxygen in a sequencing batch reactor pilot plant. *Chemical Engineering Journal,* 111(1)**,** pp 13-19.

UKWIR. 2013a. Factors Limiting the Use of Active System Control (ASC) on Sewerage Systems in the UK, (Queen Anne's Gate, London).

UKWIR. 2013b. Role of Wastewater Process Control in Delivering Operating Efficiencies, Limited, U. W. I. R. (London).

US-EPA. 2003. Wastewater technology fact sheet: Screening and Grit removal,

Vanrolleghem, P. A., Benedetti, L. & Meirlaen, J. 2005. Modelling and real-time control of the integrated urban wastewater system. *Environmental Modelling & Software,* 20(4)**,** pp 427-442.

Vanrolleghem, P. A., Insel, G., Petersen, B., Sin, G., De Pauw, D., Nopens, I., Dovermann, H., Weijers, S. & Gernaey, K. 2003. A comprehensive model calibration procedure for activated sludge models. *Proceedings of the Water Environment Federation,* 2003(9)**,** pp 210-237.

Venkat, A. N., Hiskens, I. A., Rawlings, J. B. & Wright, S. J. 2008. Distributed MPC strategies with application to power system automatic generation control. *Control Systems Technology, IEEE Transactions on,* 16(6)**,** pp 1192-1206.

Vivekanandan, B., Rao, A. S. & Saravananae, R. 2017. Enhanced control of activated sludge process using predetermined set-points. *International Journal of Environmental Science and Technology,* 14(3)**,** pp 487-496.

Vivekanandan, B. & Seshagiri Rao, A. 2016. Evaluation of control strategies in activated sludge process for biological wastewater treatment. *Chemical Product and Process Modeling,* 11(4)**,** pp 279-289.

Vollertsen, J. & Hvitved-Jacobsen, T. 2002. Biodegradability of wastewater - A method for COD-fractionation. *Water Science and Technology.*

Von Sperling, M. & Lumbers, J. P. 1989a. Control objectives and the modelling of MLSS in oxidation ditches. *Water Science and Technology,* 21(12)**,** pp 1621-1622.

Von Sperling, M. & Lumbers, J. P. 1989b. Control objectives and the modelling of MLSS in oxidation ditches. *Water Science and Technology,* 21(10-11 -11 pt 4)**,** pp 1173-1183.

Vrecko, D., Gernaey, K. V., Rosen, C. & Jeppsson, U. 2006. Benchmark Simulation Model No 2 in Matlab-Simulink: Towards plant-wide WWTP control strategy evaluation. *Water Science and Technology,* 54(8)**,** pp 65-72.

Vrečko, D., Hvala, N., Stare, A., Burica, O., Stražar, M., Levstek, M., Cerar, P. & Podbevšek, S. 2006. Improvement of ammonia removal in activated sludge process with feedforward-feedback aeration controllers. *Water Science and Technology,* 53(4-5)**,** pp 125-132.

Vrečko, D., Hvala, N. & Stražar, M. 2011. The application of model predictive control of ammonia nitrogen in an activated sludge process. *Water Science and Technology,* 64(5)**,** pp 1115-1121.

Wahab, N. A., Katebi, R., Balderud, J. & Rahmat, M. F. 2011. Data-driven adaptive model-based predictive control with application in wastewater systems. *IET Control Theory and Applications,* 5(6)**,** pp 803-812.

Wallace, S. 2007. The wetland wastewater alternative. *Water 21,* 38-39.

Wang, H., Yang, Y., Keller, A. A., Li, X., Feng, S., Dong, Y.-n. & Li, F. 2016. Comparative analysis of energy intensity and carbon emissions in wastewater treatment in USA, Germany, China and South Africa. *Applied Energy,* 184(873-881.

Wang, X., Kvaal, K. & Ratnaweera, H. 2017. Characterization of influent wastewater with periodic variation and snow melting effect in cold climate area. *Computers and Chemical Engineering,* 106(202-211.

Warn, A. 1987. SIMCAT-A catchment simulation model for planning investment for river quality. *Systems Analysis in Water Quality Management. Pergamon Press New York. 1987. p 211-218, 10 ref.*

Weast, R. 1972. *Handbook of Chemistry and Physics 53rd edn (Cleveland, OH: Chemical Rubber Company)*.

Wentzel, M., Mbewe, A. & Ekama, G. 1995. Batch test for measurement of readily biodegradable COD and active organism concentrations in municipal waste waters. *WATER SA-PRETORIA-,* 21(117-117.

Wik, T., Fransson, C. M. & Lennartsson, B. Feedforward Feedback Controller Design for Uncertain Systems. Proceedings of the IEEE Conference on Decision and Control, 2003. 5328-5334.

Willmott, C. J., Ackleson, S. G., Davis, R. E., Feddema, J. J., Klink, K. M., Legates, D. R., O'donnell, J. & Rowe, C. M. 1985. Statistics for the evaluation and comparison of models. *Journal of Geophysical Research: Oceans,* 90(C5)**,** pp 8995-9005.

Woodman, B. & Mitchell, C. 2011. Learning from experience? The development of the Renewables Obligation in England and Wales 2002–2010. *Energy Policy,* 39(7)**,** pp 3914-3921.

Wu, J. & Luo, J. Aeration control of activated sludge wastewater treatment process using optimal control. Proceedings of the World Congress on Intelligent Control and Automation (WCICA), 2012. 4969-4973.

Xu, Z. & Cheng, X. Study on control method of activated sludge sewage treatment system. Proceedings of 2016 2nd International Conference on Control Science and Systems Engineering, ICCSSE 2016, 2016. 154-158.

Yan, Z., Di, T., Ye, Y. & Han, W. 2013. The modeling of petrochemical wastewater activated sludge system and water quality forecast based on neural network. *Advanced Materials Research.*

Yang, O., Hu, Z., Wang, C., Wu, H., Xu, M. & Takashi, S. 2016. Domestic wastewater treatment by A/O process with an intelligent aeration control system. *Chinese Journal of Environmental Engineering,* 10(11)**,** pp 6255-6260.

Ye, H. T., Li, Z. Q. & Luo, W. G. Dissolved oxygen control of the activated sludge wastewater treatment process using adaptive fuzzy PID control. Chinese Control Conference, CCC, 2013. 7510-7513.

Yong, M., Yong-zhen, P., Xiao-lian, W. & Shu-ying, W. 2006. Intelligent control aeration and external carbon addition for improving nitrogen removal. *Environmental Modelling & Software,* 21(6)**,** pp 821-828.

Yu, R., Kampschreur, M. J., Loosdrecht, M. C. v. & Chandran, K. 2010. Mechanisms and specific directionality of autotrophic nitrous oxide and nitric oxide generation during transient anoxia. *Environmental Science & Technology,* 44(4)**,** pp 1313-1319.

Zacharof, A., Butler, D., Schütze, M. & Beck, M. 2004. Screening for real-time control potential of urban wastewater systems. *Journal of hydrology,* 299(3-4)**,** pp 349-362.

Zhang, P., Yuan, M. & Wang, H. 2008. Improvement of nitrogen removal and reduction of operating costs in an activated sludge process with feedforward–cascade control strategy. *Biochemical Engineering Journal,* 41(1)**,** pp 53-58.